

Bulletin 296

DEPARTMENT OF COMMERCE
BUREAU OF MINES

IRON OXIDE REDUCTION EQUILIBRIA

A CRITIQUE
FROM THE STANDPOINT OF
THE PHASE RULE AND THERMODYNAMICS



UNITED STATES
GOVERNMENT PRINTING OFFICE
WASHINGTON : 1929

ADDITIONAL COPIES
OF THIS PUBLICATION MAY BE PROCURED FROM
THE SUPERINTENDENT OF DOCUMENTS
U. S. GOVERNMENT PRINTING OFFICE
WASHINGTON, D. C.
AT
60 CENTS PER COPY

CONTENTS

	Page		Page
Introduction.....	1	The system ferric oxide-magne-	
Scope of bulletin.....	1	tite.....	41
Importance of subject.....	2	Heating and cooling curves..	42
Ferric oxide.....	5	Magnetic properties.....	43
Characteristics.....	5	Oxygen pressure.....	45
Methods of preparation.....	6	Reduction isotherms.....	52
Chemical behavior.....	7	Optical properties.....	52
Specific gravity and specific		Magnetite.....	53
volume.....	9	Characteristics.....	53
Behavior on heating.....	10	Methods of preparation.....	54
Thermal coefficient of expan-		Chemical properties.....	57
sion.....	10	Crystal system.....	57
Electrical conductivity.....	12	Polymorphism.....	58
Thermal conductivity.....	13	Behavior with temperature	
Melting point.....	15	change.....	58
Boiling point.....	16	Melting point.....	59
Dissociation pressure.....	16	Dissociation pressure.....	59
Crystal system.....	20	Electrical conductivity.....	59
Polymorphism of ferric oxide..	20	Magnetic properties.....	62
678° C. transition.....	21	Thermal electromotive force..	65
360° C. transition.....	23	Thermal emissivity.....	66
Sintering.....	23	Specific heat.....	68
Glow effect.....	24	Entropy.....	71
Magnetic ferric oxide.....	24	Heat of formation.....	72
Properties.....	25	Mixer's value.....	72
Ferromagnetic ferric oxide..	26	Ruff and Gersten's values..	73
Conversion of ferromagnetic		Berthelot's value.....	74
to paramagnetic ferric		Baur and Glaessner's value	74
oxide.....	28	Wöhler and Günther's value	74
Curie point.....	29	Yermilov's value.....	74
Specific heat.....	29	Treadwell's value.....	75
Entropy.....	31	Eastman and Evans's values	75
Heat of formation.....	32	Summary.....	76
Free energy.....	35	Free energy.....	77
Higher oxides of iron, ferrites,		Iron-oxygen complexes interme-	
and ferrates.....	37	diate between magnetite	
Ferrites.....	37	and ferrous oxide.....	81
Ferrates (or peroxyferrites)..	38	Surface coatings on metallic	
Perferrates (or peroxyfer-		iron.....	81
rates).....	39	Work of Mosander.....	82
Iron ferrites.....	40	X-ray investigations of	
Iron perferrates.....	40	Bozorth.....	82

	Page		Page
Iron-oxygen, etc.—Con.		The system iron—Continued.	
Surface coatings, etc.—Con.		Strengths of iron at different	
X-ray investigations of		temperatures.....	130
Groeblor and Oberhoffer..	83	X-ray spectrographic work...	131
Work of Merwin and Fedot-		Allotropy and polymorphism	
jeff.....	83	of iron.....	132
Melting points.....	84	Pyrophoric iron.....	134
Magnetization.....	84	Transformation points.....	135
Reduction-equilibrium dia-		Heating and cooling curves..	136
grams.....	87	A ₂ transformation range.....	138
Solubilities from reduction		A ₂ by heating and cooling	
isotherms.....	88	curves.....	139
Discussion of Figure 25....	88	A ₂ by calorimetric methods..	140
Discussion of Figure 26....	91	A ₂ by magnetic methods....	141
Wüstite field.....	93	A ₂ by thermoelectric meth-	
Adjustments.....	94	ods.....	143
Ferrous oxide.....	95	A ₂ by electrical resistance	
Characteristics.....	95	methods.....	145
Field of stability.....	96	A ₂ by dilatometer.....	147
Splitting and recombination		A ₃ transformation range.....	148
of ferrous oxide.....	97	A ₃ by thermal methods....	149
Analysis of mixtures of FeO,		A ₃ from specific heat	
Fe ₃ O ₄ , and Fe.....	100	curves.....	149
Preparation of pure FeO....	101	A ₃ by magnetic methods....	150
Work of Wöhler, Balz, and		A ₃ by thermoelectric meth-	
Günther.....	101	ods.....	151
Work of other investigators..	102	A ₃ by electrical resistance	
Preparation of FeO by reduc-		methods.....	152
ing magnetite with iron..	104	A ₃ by dilatometer.....	152
Work of Millar.....	105	Other changes at A ₃ point..	154
Work of Groeblor and Ober-		A ₄ transformation range.....	155
hoffer and of Hilpert and		Melting point.....	157
Beyer.....	105	Boiling point and vapor pres-	
Work of other investigators	106	sure.....	157
Miscibility of FeO and Fe ₃ O ₄ ..	108	Other supposed points.....	159
Miscibility of FeO and Fe....	108	370° C. point.....	159
Melting point.....	108	830° C. point.....	160
Stability in air.....	109	Thompson and Goffey	
Heat of formation.....	109	points.....	162
Free energy.....	110	Other investigations.....	164
Specific heat.....	111	Magnetism of iron.....	164
Entropy.....	112	Electrical resistance.....	166
Dissociation pressure.....	113	Thermoelectric phenomena of	
Supplementary note.....	113	iron.....	169
Iron-oxygen complexes having		Thermal conductivity.....	171
less oxygen than FeO.....	115	Specific volume and density..	172
Metallic iron phase containing		Compressibility.....	172
carbon and oxygen.....	126	Thermal dilatation.....	175
Summary.....	128	Expansion coefficients of	
The system iron.....	129	gamma and delta iron...	177
Introduction.....	129	Effect of extremely low	
Atomic weight.....	129	temperatures.....	179
Crystal system.....	129	Change of transformation	
		temperature with pressure..	180

The system iron—Continued.	Page	The system iron-carbon—Con.	Page
Effect of alloying elements on transitions.....	182	Cementite—Continued.	
Mechanical and physical properties.....	183	Free energy.....	231
Emissivity of iron.....	185	Identification of quenched phases.....	232
Specific heat and total heat....	186	Specific volumes and densities of iron-carbon system....	232
Early calorimetric investigations.....	187	Volume change at A° point....	235
Summary of work.....	189	Volume change at eutectic....	236
Heats of transition.....	191	Pressure and the iron-carbon diagram.....	236
Latent heat of evaporation....	194	Heat content of steels.....	238
Total heat of iron.....	194	Results of rapid quenching....	239
Entropy of iron.....	196	Precipitation of cementite in hypereutectoid steels..	243
Allotropy and thermodynamics of iron.....	197	Results of tempering martensite to $200^{\circ}C$	244
The system iron-carbon.....	199	Heat changes at pearlite composition.....	244
Constituents on surface of iron-carbon alloys.....	201	Heat changes at $A_1, A_2,$ and A_3 points.....	245
Delta ferrite.....	201	Uncertainty of heats at A_1	247
Austenite.....	201	Other thermal data in iron-carbon system.....	247
Boydenite.....	202	Other equilibria involving iron carbide.....	249
Cementite.....	202	Oxyaustenite.....	250
Ledeburite.....	203	Work of Schenck.....	251
Pearlite.....	203	Work of other investigators....	252
Alpha ferrite.....	203	Oxyferrite-oxyaustenite equilibrium.....	253
Martensite.....	204	Effect of pressure on carburization equilibria.....	254
Troostite.....	206	Cementite in high-temperature equilibria.....	254
Sorbite.....	206	Equilibrium between austenite and carbon oxides....	255
Epsilon and eta phases of Hanemann.....	207	Discussion of Figure 81....	255
Definitions.....	209	Discussion of Figures 82 and 83.....	256
Critical points in iron-carbon alloys.....	211	Work of Johansson and von Seth and of Takahashi.....	257
Discussion.....	213	Variations with temperature	260
Cementite.....	215	Carbon pressures of carbon and cementite.....	260
Preparation.....	216	Discussion of Figure 84....	261
Crystal system.....	217	Discussion of Figure 85....	262
Density.....	217	Carbon-oxygen-iron equilibria in liquid steel.....	264
Action toward reagents....	219	Discussion of Figure 86....	265
Cementite at various temperatures.....	219	Discussion of Figures 87 and 88.....	266
Curie or magnetic transition point.....	220		
Cementite in molten iron....	221		
Interfacial tension between cementite and ferrite....	222		
Specific resistance.....	222		
Thermal conductivity.....	222		
Magnetic susceptibility....	223		
Heat capacity.....	223		
Entropy.....	226		
Heat of formation.....	226		

	Page		Page
Other equilibria, etc.—Con.		The system iron-oxygen—Con.	
Determination of oxygen in iron and steel.....	269	Smits and Bijvoet's pressure-temperature diagram.....	293
Schenck's space model.....	269	Pressure-composition phase diagram.....	295
Carburization equilibria involving methane.....	271	Oxidation-reduction systems for iron oxides.....	297
Discussion of Figure 98....	273	Baur and Glaessner's diagram	297
Discussion of Figure 99....	279	Matsubara's diagram.....	297
Missing equilibria.....	281	Ideal reduction-oxidation isotherm.....	300
Iron carbonyls.....	283	Schenck's diagram.....	302
Formation of carbonyls.....	284	Hydrogen-reduction system..	304
Properties of carbonyls.....	285	Stability field for ferric oxide..	305
The system iron-oxygen.....	287	Ternary diagram, Fe-O-C....	306
Discussion of Figure 100.....	287	Reinders's triangular diagrams	307
Placing of wüstite area....	288	Summary of important thermal data.....	311
Discussion of Figure 101.....	289	Index.....	313
Benedicks and Löfquist's temperature-composition diagram.....	291		

ILLUSTRATIONS

Fig.	Page
1. Electrical conductivity of hematite rods.....	12
2. Thermal conductivity of ferric oxide.....	14
3. Dissociation of ferric oxide.....	18
4. Lowering of 678° C. transition point of ferric oxide by Al ₂ O ₃ and Cr ₂ O ₃	22
5. Magnetic susceptibility of hematite as a function of temperature and thermal history.....	26
6. Specific heat of ferric oxide.....	30
7. Entropy and free energy of ferric oxide.....	32
8. Thermal points of the Fe ₂ O ₃ —Fe ₃ O ₄ system (Kohlmeyer).....	43
9. Temperature of magnetic anomalies v. composition in the Fe ₂ O ₃ —Fe ₃ O ₄ system (Huggett and Chaudron).....	44
10. Oxygen pressures of the Fe ₂ O ₃ —Fe ₃ O ₄ system (Sosman and Hostetter).....	46
11. Derived thermal data (dissociation) of the Fe ₂ O ₃ —Fe ₃ O ₄ system (after Sosman and Hostetter).....	48
12. Oxygen pressure v. temperature for the Fe ₂ O ₃ —Fe ₃ O ₄ system (derivations by Tigerschöld).....	50
13. Dynamic experiments with Fe ₂ O ₃ —Fe ₃ O ₄ system; residues after heating in air (Ruer and Nakamoto).....	51
14. Reduction isotherms of Matsubara.....	51
15. Electrical resistance of magnetite (Königsberger).....	60
16. Electrical conductivity of magnetite (Veil).....	61
17. Intensity of magnetization v. temperature for magnetite (Weiss and Beck).....	62
18. Reciprocal magnetic susceptibility v. temperature for magnetite (Weiss and Foex).....	63
19. True temperature of iron under a layer of oxide (roll scale).....	67
20. True specific heat of magnetite.....	68
21. Free energy of magnetite.....	78
22. Magnetic characteristics of Fe ₃ O ₄ —FeO system (Hilpert and Beyer).....	85
23. Magnetism-temperature anomalies in the Fe—Fe ₂ O ₃ system.....	87
24. Equilibrium constants of system FeO : Fe ₃ O ₄ :: H ₂ : H ₂ O (Eastman).....	89
25. Gas-reduction isotherms at slow rate (Eastman, Matsubara, and Schenck).....	90
26. System Fe ₃ O ₄ —FeO conjugate solid solutions.....	92
27. Splitting and recombination of FeO (Ferguson).....	97
28. Splitting and recombination of FeO (Chaudron and Forestier).....	98
29. Specific heat of ferrous oxide (83 per cent) (Millar).....	112
30. System Fe—FeO (Tritton and Hanson).....	116
31. System Fe—FeO, modified (after Schönert).....	117
32. Solubility of FeO in molten iron (Herty).....	119
33. Isothermal slow reduction of Fe ₂ O ₃ with CO (Matsubara and Schenck).....	121
34. Isothermal oxidation of iron by water vapor at 772° C. (Eastman and Evans).....	122

Fig.	Page
35. Equilibrium data of Schenck at 1 atmosphere and 0.33 atmosphere total pressure with mixtures of CO and CO ₂ acting on iron oxide systems.....	126
36. Body-centered cubic packing, alpha iron.....	132
37. Face-centered cubic packing, gamma iron.....	132
38. Lattice constant of iron.....	133
39. Cooling and heating curve of electrolytic iron (Ruer and Bode).....	137
40. Differential cooling and heating curves of electrolytic iron (Wever).....	138
41. Magnetic susceptibility v. temperature; large units (Honda).....	142
42. Magnetic susceptibility v. temperature; magnified vertical scale (Honda).....	142
43. Iron: Reciprocal susceptibility v. temperature (Weiss and Foex).....	144
44. Electrical resistance of Kahlbaum iron (Honda and Ogura).....	146
45. Increase of resistance of iron compared to platinum (Burgess and Kellberg).....	146
46. Differential dilatation, iron-gold (Benedicks).....	148
47. Magnetic changes at A ₃ point (Terry).....	150
48. Thermoelectric power of iron against platinum (Burgess and Scott).....	152
49. A ₃ point by electrical resistance (Burgess and Kellberg).....	153
50. Upper and lower limits of A ₃ transformation range, Fe-Ni alloys (Honda and Miura).....	154
51. Magnetic susceptibility near A ₄ point (Ishiwara and Terry).....	156
52. Electrical resistance of electrolytic iron (Broniewski).....	161
53. Torsional elastic limit v. temperature (Goffey and Thompson).....	162
54. Pure iron: Inner friction v. temperature (Ishimoto).....	163
55. Electrical resistance of iron (Burgess and Kellberg).....	167
56. Thermoelectric power of electrolytic iron (Broniewski and Harrison).....	170
57. Thermoelectric power of platinum v. iron (Schneider).....	171
58. Density of armco iron after tensile test.....	174
59. Change in density on annealing hammered armco iron (Ishigaki).....	175
60. Dilatation of electrolytic iron (Broniewski).....	176
61. Dilatation of electrolytic iron (Sato).....	176
62. Coefficient of thermal expansion.....	177
63. Effect of chromium on A ₃ and A ₄ transitions.....	182
64. Tensile strength of iron as a function of temperature.....	184
65. Physical properties of cold-rolled electrolytic iron.....	184
66. Pyrometric corrections for iron surfaces.....	187
67. Specific heat of iron.....	188
68. Total heat-temperature curve for iron.....	195
69. Free energy of alpha and delta forms of iron as a function of temperature.....	197
70. Iron-carbon temperature-composition phase diagram.....	200
71. Hanemann's proposed addition to iron-carbon diagram.....	208
72. Magnetization curve of a steel near A ₀	221
73. True specific heat of cementite.....	225
74. Proportionate change in volume during freezing of cast iron with 4.1 per cent of total carbon (Honda and Endo).....	237
75. Total heats of steels (Meuthen).....	239
76. Mean specific heats of steels (Umino).....	240
77. Heat changes in steels.....	241
78. Heats of A ₁ , A ₂ , and A ₃ transformations (Umino).....	246
79. Iron-oxygen-carbon reduction system, 1 atmosphere (Schenck).....	252

Fig.	Page
80. Carburization of iron v. temperature pressure, 0.4 atmosphere (Johansson and von Seth).....	253
81. Isotherms in austenite stability field (Takahashi).....	255
82. Lines of constant gas composition in equilibrium with austenite (Takahashi).....	257
83. Trivariant equilibria of austenite.....	258
84. Ratio of carbon pressures, austenite to carbon (Johansson and von Seth).....	261
85. Ratio of carbon pressures v. temperature (Johansson and von Seth).....	263
86. Equilibrium constants in carbon-oxygen-liquid iron (Herty and others).....	266
87. Equilibrium concentrations of carbon and oxygen in liquid iron at various temperatures (Herty and others).....	267
88. Relation between carbon in metal and FeO in slag; basic open hearth (Herty and others).....	268
89. Schenck's space model of the iron-carbon-oxygen system.....	270
90. Schenck's space model of the iron-carbon-oxygen system.....	271
91. Schenck's space model of the iron-carbon-oxygen system.....	272
92. Schenck's space model of the iron-carbon-oxygen system.....	273
93. Schenck's space model of the iron-carbon-oxygen system.....	274
94. Schenck's space model of the iron-carbon-oxygen system.....	275
95. Schenck's space model of the iron-carbon-oxygen system.....	276
96. Schenck's space model of the iron-carbon-oxygen system.....	277
97. Schenck's space model of the iron-carbon-oxygen system.....	278
98. Equilibria for methane (Schenck).....	279
99. Equilibria for methane-hydrogen-steel (Sykes).....	280
100. Iron-oxygen composition-temperature diagram (Schenck).....	288
101. Possible interpretation of Schenck's oxyferrite.....	290
102. Composition-temperature phase diagram for iron-oxygen.....	292
103. Pressure-temperature phase diagram for iron-oxygen.....	294
104. Equilibrium diagram of Baur and Glaessner.....	298
105. Equilibrium diagram of Matsubara, showing equilibria involving Fe ₃ C.....	298
106. Reciprocal temperature v. logarithm equilibrium constant, $k = \frac{\text{CO}_2}{\text{CO}}$ (Eastman).....	299
107. Ideal reduction-oxidation isotherms.....	300
108. Equilibria between oxides of carbon and iron.....	303
109. Hydrogen equilibria with iron oxides (after Eastman).....	304
110. Hydrogen reduction-equilibrium diagram (corrected hypothetically).....	305
111. Isotherm in gamma iron range for system C-Fe-O (Iwase).....	306
112. Portion of pressure-temperature diagram in alpha iron range (Reinders).....	308

IRON OXIDE REDUCTION EQUILIBRIA: A CRITIQUE FROM THE STANDPOINT OF THE PHASE RULE AND THERMODYNAMICS¹

By OLIVER C. RALSTON

INTRODUCTION

A study of the variables affecting the rate of reduction of iron ore in a blast furnace can not logically be made until the stages through which the iron ore may pass during its reduction to metal are known. In other words, a study in dynamics must necessarily be preceded by a study in statics. Therefore the more obtruse aspects of the rate of iron ore reduction in the blast furnace have been more or less recessed, as far as their study by the Bureau of Mines was concerned, until the following study of existing information could be made.

The reduction equilibria, when studied, supply data on the composition of gases in equilibrium with the various solid and liquid iron-oxygen compounds that can be formed, but, of course, equilibrium data can be obtained only after sufficient time to approach equilibrium has elapsed. Equilibrium data do not have immediate value to the operator of the blast furnace and do not deal with rates of reduction. Their value lies in setting the limits beyond which no one can hope to go. A reducing gas at a certain temperature will react only until the products of reaction stop further reduction and equilibrium is approached. The blast-furnace engineer is interested in knowing how nearly he has exhausted the reducing power of the gas in the furnace at each elevation. The equilibrium value is the limit beyond which it is foolish to attempt to utilize reducing power and with which values actually attained must be compared when estimations of efficiency are made.

SCOPE OF BULLETIN

This bulletin, therefore, presents the properties of the common oxides of iron, their combinations with each other, and the reduction-equilibrium diagrams by which the investigator passes from one to

¹ Work on this manuscript completed May, 1928.

the next; the end point is not pure iron but the carburized iron of the blast furnace, cast iron. The energy quantities involved are discussed at length, due to their intimate relation to the equilibria and to the other physical properties of iron-oxygen systems. The thermal data are also of great importance in dealing with heat balances.

The iron-oxygen system has not proved as simple as might be expected. In fact, it is amazingly complex; although there are only three authenticated oxides of iron, they dissolve in each other in several series of solid solutions, so that the pure oxides are rarely found. Sosman ² has described the situation very aptly:

The chemist is amazed by the facile transformations of iron from ferric to ferrous, beholding the two states of oxidation acting like two absolutely different elements. The physicist stands appalled before the spectrum of iron, realizing the many unknown quantities hidden behind its thousands upon thousands of lines. Even the layman can get a vivid realization of the complexity of the problems involved; he has but to walk through the country * * * and note the bewildering play of inorganic colors everywhere about him, ranging from deep brown-black through various shades of drab, brown, purple, maroon, and through many tints of pink, ocher, and rose to the most brilliant reds and orange-yellows, and then realize that almost every one of these hundreds of colors is due to an oxide or hydrated oxide of iron.

The body of this bulletin is a critical discussion of existing scattered data, but also includes occasional new data which have been collected by the Bureau of Mines. None of the encyclopedic texts on inorganic chemistry have yet included iron and its compounds. The subject has been too complex to give any satisfaction to the ordinary reviewer. Only careful critical inspection of data, especially the use of thermodynamics in interconnection between various physical data, has allowed partial unraveling of the puzzle. This paper, better than any other means, will indicate the surprising lack in our knowledge concerning the properties of one of the most important metal-oxide systems known to man. Unsolved problems are mentioned in almost every paragraph and unsatisfactory data discussed.

IMPORTANCE OF SUBJECT

Why an oxide system of such immense industrial importance has received so little attention from the scientist is difficult to comprehend. A few enthusiastic workers can be named, such as Sosman, Chaudron, Schenck, Eastman, and Ferguson, but all of them have been much diverted by other matters and are only occasional contributors to the literature on the subject. The Geophysical Laboratory of the Carnegie Institution of Washington, of which Sosman is

²Sosman, R. B., Some Problems of the Oxides of Iron: Jour. Washington Acad. Sci., vol. 7, 1917, pp. 55-72.

a staff member, has done more work on the oxides of iron than any other institution, but of course from the standpoint of the mineralogist and geologist. Schenck has been interested from the standpoint of the metallurgist, while the other workers have been interested as pure scientists.

When a lump of hematite ore is introduced into the top of an iron blast furnace it comes in contact with reducing gases, and the popular conception has been that it is reduced successively through the stages Fe_2O_3 , Fe_3O_4 , FeO , and Fe . While this is in general true, the fact that only limited time is available causes each lump to be reduced rapidly at the surface and to contain a core of less-reduced material. All four of the above materials can exist in a single lump, the exterior being completely reduced to metal and the interior containing a core of unreduced Fe_2O_3 with intermediate layers of Fe_3O_4 and FeO . However, these last two constitute only a small proportion of the intermediate layers. In fact, the layers which consist entirely of pure Fe_3O_4 and FeO are almost imperceptibly small. They dissolve in each other, and Fe_3O_4 dissolves in Fe_2O_3 in all proportions at higher temperatures, so that the bulk of the partly reduced oxide shell is composed largely of solid solutions. Just how the oxygen from the centers of the iron oxide lumps is abstracted by reducing gases is a question of mechanism important to the student of reaction rates, but one which will not be considered in connection with the present study in chemical statics. The present project is to paint as carefully as possible the picture of the phases that can exist in the iron-oxygen system in order to clear the ground for those who must later study means of controlling the rates of deoxidation.

If metallic iron could be the end point in the reduction, all would be well, but unfortunately the reduction by carbon monoxide usually overshoots the mark, and a part of the metallic iron is converted into carbide, Fe_3C , which dissolves in the hot metal but separates and sometimes decomposes on cooling. The conditions causing carburization must be understood when the reduction system is studied. The iron-carbon system is the foundation of all steel metallurgy, but only enough of it will be considered here to clear up the oxide reduction equilibria.

FERRIC OXIDE

CHARACTERISTICS

Ferric oxide, Fe_2O_3 , in various forms is one of the most conspicuous coloring agents in inorganic nature and needs very little description to those interested in this paper. In its hydrated forms it varies from light yellow to deep brown, and in the dehydrated forms it can be found in all shades of red through brown to black. The yellow color of certain bricks has been thought to be due to a colloidal yellow modification of anhydrous ferric oxide made stable by alumina.³ On the other hand, the degree of agglomeration is probably an important factor,⁴ because fine grinding of the darker varieties always gives a powder of lighter color.

Yoe⁵ has studied the subject extensively and states that the true color of masses of fine particles of ferric oxide is yellow and the usual red appearance is due to agglomeration, which can be prevented by stabilizing agents. Alumina, when present to the extent of 10 per cent or more, functions as a stabilizing agent, as does barium sulphate, although 84 per cent of the latter is necessary. An attempt was made to stabilize a mass of ferric oxide with alumina and then dissolve out the alumina with caustic soda solutions. Most of the alumina could be removed, but the ferric oxide changed in color to a dark reddish brown, indicating agglomeration. From the standpoint of colors, therefore, if ferric oxide is polymorphic, it must have many different forms. Probably most of the color differences are not due to polymorphism.

The natural forms of ferric oxide are known as hematites and occur in numerous forms, although roughly classed merely as massive (amorphous) and crystalline. The red hematites are massive and cryptocrystalline, while macroscopic crystals go under the name of "specular iron" or specularite, which occurs as rhombohedra and scalenohedra. One form of crystals is micaceous flakes, that can be translucent when less than 0.1 millimeter thick, although the usual color of crystalline ferric oxide is black.

Hedvall⁶ has made a study of the color of iron oxides, and concludes that the tint of the preparation depends on the temperature

³ Scheets, F. H., Ferric Oxide and Alumina: Jour. Phys. Chem., vol. 21, 1917, p. 570.

⁴ Wöhler, L., and Condrea, C., Die verschiedenen Farben des Eisenoxys, eine Erscheinung der Korngrösse: Ztschr. angew. Chem., Jahrg. 21, 1908, p. 481.

⁵ Yoe, John H., Anhydrous Yellow Ferric Oxide: Jour. Phys. Chem., vol. 25, 1921, pp. 196-200.

⁶ Hedvall, J. A., Über die Farbe des Eisenoxys: Ztschr. anorg. u. allgem. Chem., Jahrg. 121, 1922, pp. 217-224.

of formation and the duration of heating. The colors may in general be divided into two groups, the bright orange-red and the darker colors. The first can be made by heating ferric sulphate at a temperature below 650° C. The differences in color were compared with microscopic appearance for 27 different samples prepared by different methods. The material prepared by heating ferric sulphate was found to consist of plates and scales, while all the other materials were granular. Hedvall concluded that the difference in the reflection of light from the crystals of different shapes accounted for most of the difference. Later he studied them by the X-ray diffraction pattern method⁷ and found that they gave identical patterns, indicating that all known forms of ferric oxide consist at room temperatures of the same ultimate crystals.

This last generalization needs at least one modification, as Bohm⁸ has studied the glow effect noticed when freshly precipitated and dehydrated Fe_2O_3 , Sc_2O_3 , Cr_2O_3 , TiO_2 , ZrO_2 , Ta_2O_5 , and Cb_2O_5 are heated to dull redness; the material glows brightly for a short time. The temperature of glowing depended to some extent on the method of preparation of the oxide. By an X-ray study of the fresh and glowed forms it was found that the fresh material was mostly amorphous while the glowed form was crystalline. The transition evidently released energy. On the other hand, the above could easily describe phosphorescent phenomena, and the subject deserves study.

The transition from the amorphous to the crystalline state was also observed by Chaudron and Forestier,⁹ who prepared rods of ferric oxide by various methods for study of the thermal coefficient of expansion over a range of temperatures. When prepared by desiccating the precipitated hydroxide at low temperature the rods underwent a transformation above 400° and below 600° C. whereby heat was liberated so that they glowed, and usually compressed rods of the substance were ruptured during the transition. An estimate of the energy involved in the change has been made by Mixer, and is discussed later in this paper.

METHODS OF PREPARATION

In the laboratory, crystalline ferric oxide can be made by fusing the amorphous ferric oxide under borax and then dissolving the borax with dilute hydrochloric or nitric acid.¹⁰ Friend states that accord-

⁷ Hedvall, J. A., Studien über die durch verschiedene Herstellungsweise hervorgerufene Eigenschaftsänderungen einiger glühbeständigen Metalloxyde mit Hilfe von Roentgenstrahlen-Interferenz: *Arkiv. Kemi. Mineral. Geol.*, Jahrg. 8, No. 11, 1921-1923, 18 pp.

⁸ Bohm, J., Über das Verglimmen einiger Metalloxydes: *Ztschr. anorg. u. algem. Chem.*, Jahrg. 149, 1925, pp. 217-222.

⁹ Chaudron, G., and Forestier, H., Allotropie des sesquioxides de fer, de chrome, et d'aluminium: *Compt. rend.*, t. 179, 1924, pp. 763-766.

¹⁰ Friend, J. N., *Iron and Its Compounds*: London, 1922, pp. 115-132.

ing to the method of H. St. Claire Deville crystals can be made by passing gaseous hydrogen chloride over ferric oxide at red heat or by passing steam containing ammonium fluoride over the massive oxide at 600° C. or over ammonium chloride vapor at 700° C. Micaceous flakes can be made by heating solutions of copper and ferrous sulphates in sealed tubes for 10 hours¹¹ at 210° C. Friend also states that an exceptionally pure form (crystalline condition not specified) can be made by extracting purified ferrous chloride with ether, treating the extract in water solution with SO₂, and precipitating it as ferrous oxalate which can be calcined to ferric oxide.

Gay-Lussac¹² is reputed to have produced crystalline Fe₂O₃ in 1823 by action of steam on ferric chloride.

Arctowski¹³ treated ordinary amorphous ferric oxide at a high temperature with vapors of ammonium chloride and obtained crystalline ferric oxide, and many other experimenters have used variations of this method, which really originated with St. Clair Deville in France in 1860.

Nearly all complete analyses of natural and artificial forms of ferric oxide show a slight deficiency in oxygen below that necessary to make Fe₂O₃ and the presence of a small amount of ferrous iron. Many of the so-called hematites contain 0.4 to 5.0 per cent of FeO. When such a product is heated in air for long periods of time it slowly takes up oxygen and approaches Fe₂O₃ in composition, but anyone who has burned an iron precipitate to Fe₂O₃ in the laboratory will appreciate the extreme slowness of taking up the last traces of oxygen. One hour heating at 1,200° C. is sufficient, but at lower temperatures the necessary time increases so that 100 hours are necessary at 1,000° C., according to Greulich.¹⁴

CHEMICAL BEHAVIOR

The best-known characteristics of ferric oxide are its reduction by hydrogen or carbon monoxide to lower oxides or even to metal at temperatures above about 300° C., the lowest temperatures of noticeable reaction varying with the mode of preparation of the material. Crystallized specimens are much less reactive than the massive forms and are frequently described in the literature as polymerized. This term may not be justified, although ignition

¹¹ de Senarmont, M. H., *Experiences sur la formation des minéraux par poie humide dans les gites métallifères concrétionnés*: *Ann. chim. phys.*, t. 32, 1851, p. 144.

¹² Gay-Lussac, M., *Réflexions sur les volcans*: *Ann. chim. phys.*, t. 22, 1823, p. 415.

¹³ Arctowski, H., *Über die kunstliche Darstellung von Haematit*: *Ztschr. anorg. Chem.*, Jahrg. 6, 1894, pp. 377-379.

¹⁴ Greulich, Erich, *Über die chemischen Veränderungen des Magnetits beim Erhitzen an der Luft*: *Ztschr. anorg. u. allgem. Chem.*, Jahrg. 159, 1926, pp. 65-77.

of the massive forms causes progressive blackening and recrystallization with a temperature rise, and the resulting product is more sluggish in reduction and more difficult to dissolve in acids. The major portion of the ferric oxide in the first stage of reduction becomes magnetite; and this step requires almost a negligible proportion of hydrogen or carbon monoxide in comparison to the water vapor or carbon dioxide formed, being, in practical effect at least, an irreversible reaction. Only about 1 volume of hydrogen to 1,000,000 of water vapor is necessary.

Ferric oxide dissolves in various mineral acids with varying degrees of rapidity; hydrochloric acid is probably the best, although sulphuric acid is satisfactory if given enough time. Hematite, unlike magnetite, dissolves very slowly in hydrofluoric acid. The effect of previous ignition was mentioned above.

Heated with sulphur vapor, hematite yields ferrous sulphide, sulphur dioxide, and hydrogen (?). With sulphur dioxide at 700° to 800° C., it forms¹⁵ magnetic oxide, Fe_3O_4 , and sulphur trioxide, SO_3 . Friend states that chlorine attacks it at high temperatures, giving ferric chloride and oxygen, while ammonia gas at high temperatures gives water and nitride of iron.

Ferric oxide can be hydrated by boiling it with a 70 per cent solution of NaOH at 100 to 120° C., as determined by Estelle.¹⁶ This fact is of importance in connection with one of the proposed electrolytic iron processes in which a strong solution of caustic soda containing sodium ferrite is electrolyzed. By virtue of the fact that a strong caustic solution dissolves a certain amount of ferric hydroxide to form sodium ferrite the electrolysis results in secondary reduction of iron at the cathode. The actual mechanism of the hydration by the strong caustic solution is probably the formation of ferrite, which is decomposed into sodium hydroxide solution and ferric hydroxide on cooling and diluting the pulp. During the action 20 parts of Fe_2O_3 are taken up by 80 of caustic soda, and the heating must be continued several hours. If the ferric oxide has been previously calcined, the water in the caustic solution may require evaporation until the melt contains nearly anhydrous NaOH and the temperature rises to as much as 320° C. Magnetite can likewise be hydrated in this manner, and the precipitate remains black if not overheated.

When ferric oxide is heated above about 1,175° in vacuo or above about 1,348° in air it loses oxygen, giving products intermediate between ferric oxide and magnetite in composition and approaching

¹⁵ Hammick, D. L., The Action of Sulphur Dioxide on Metal Oxides; Part 1: Trans. Chem. Soc., vol. 111, 1917, p. 379.

¹⁶ Estelle, T. C., Process of Electrolytically Producing Iron: British Patent 159906, Mar. 17, 1921.

magnetite as the heating continues and the temperature rises, as will be discussed later. The dissociation pressures are discussed below.

SPECIFIC GRAVITY AND SPECIFIC VOLUME

The specific volume and specific gravity of ferric oxide are known only imperfectly. Mineralogists have many data on densities of various natural products, but as a rule they are not pure ferric oxide. Rammelsberg¹⁷ states that the crystallized forms have a specific gravity of 5.16 to 5.30, with 5.24 as a safe average. Schröder¹⁸ says that the massive forms have a density from 5.04 to 5.17, with 5.12 as an average. Kohlmeyer¹⁹ gives 5.187 to 5.193 for a sample of quite pure ferric oxide, but the thermal history of his samples makes it probable that they had been heated sufficiently to drive off part of their oxygen and leave some magnetite in the sample, as they are described as being strongly magnetic. Dana²⁰ gives 5.20 to 5.25 for the natural crystallized forms, a result in good agreement with Rammelsberg's figure of 5.24. On the other hand, the International Critical Tables²¹ give Schröder's figure of 5.12, which in view of the age of the data and the lack of knowledge of the properties of ferric oxide in 1878 seems too low to be acceptable at present except for lack of better data. The subject merits attention.

In references, especially in the earlier literature, too numerous to mention, the density of artificial preparations of ferric oxide seems to vary between 5.04 and 5.17, the higher value being for samples that have been ignited to the higher temperatures. Blanc and Chaudron²² prepared ferric oxide by heating ferric nitrate and ferric sulphate to 500° C. The density of this material after it is heated to various higher temperatures was then recorded as follows:

Density of ferric oxide at various temperatures

Microscopic appearance	Temperature in ° C.	Density
Large grains.....	500-600	4.910
Very fine grains.....	620-700	5.040
Grains of increasing size.....	750	5.110
Do.....	850	5.175

¹⁷ Rammelsberg, —, ————: Handbuch krystallogr. u. phys. Chem., Abt. 1, Leipzig, 1881.

¹⁸ Schröder, H., Beiträge zum Sterengesetz: Wiedemann's Annalen Physik u. Chemie.

¹⁹ Kohlmeyer, E. J., Über Bleioxyd und Eisenoxydulferrierte; Metall u. Erz. Jahrg. 1, 1913, pp. 447-462; Versuche über das Schmelzen von Eisenoxyd: Metallurgie, Jahrg. 6, 1909, pp. 323-325.

²⁰ Dana, E. S., A Textbook of Mineralogy: 3d ed., revised and enlarged by W. E. Ford, 1922, p. 415.

²¹ International Critical Tables, New York: Vol. 1, 1926, p. 128.

²² Blanc, L., and Chaudron, G., Étude magnetique de la forme stable des sesquioxides et de chrome: Compt. rend., t. 180, 1925, pp. 289-291.

They interpreted the decrease of size between 600° and 700° as being due to evolution of gas and accompanying disintegration, but as will be seen below there is a reversible polymorphic transition at 678° which could cause this change. However, gas evolution is a possible explanation, as the description of the preparation of the samples of these investigators and their failure to record analyses do not allow one to judge whether the original nitrate or sulphate had been completely decomposed and whether the 500° C. ferric oxide was pure. Giving them the benefit of the doubt, due to the general experience of others, there is apparently an increase in density as ferric oxide formed at low temperatures is heated to higher temperatures, with signs of recrystallization.

Martite, the natural pseudomorph of ferric oxide after magnetite, is described by Joannis²³ as having a low density. A Brazilian sample of this substance had a density of 4.82, and a sharply crystallized Peruvian sample had a density of only 3.86 and a dull fracture. No more recent determinations of the density of martite have been noted. It is not ferromagnetic, except where unoxidized magnetite is present.

Taking the mineralogists' average figure for the specific gravity of hematite as 5.24, the specific volume is 0.191. If the specific gravity is taken as 5.12, the specific volume is 0.1954. The corresponding values of the molecular volume are 30.5 and 31.2. In the face of such uncertainty it is time for new, accurate determinations, and as there is probably some polymorphism involved in ferric oxide accurate density determinations on different suspected polymorphic forms will be worth while.

BEHAVIOR ON HEATING

Ferric oxide has received desultory study at the temperature of boiling liquid air (about 80° K.) to about 1,600° C., at which it is no longer stable and is dissociated, as mentioned above. Its melting point is not well known, as it is above the temperature at which oxygen begins to be evolved rapidly by thermal dissociation. Heating and cooling curves and the change of various physical properties with rise or drop of temperature show discontinuities, indicating several polymorphic forms of Fe_2O_3 or other physical changes. The glowing of the massive form when transformed to the crystalline form at 400° to 600° C. has been mentioned above.

THERMAL COEFFICIENT OF EXPANSION

The linear coefficients of expansion parallel and perpendicular to the principal crystallographic axis of hematite have been measured by

²³ Joannis, M., Fremy's Encyclopedie Chimique; III, Metaux: 9th ed., Paris, 1884.

two observers, Fizeau²⁴ and Bäckström. The two data published by Fizeau were the linear data and apply to a sample from the Island of Elba. They are:

Parallel to axis (40° C.): $\alpha = 0.000\ 008\ 29$, $\Delta\alpha/\Delta t = 0.000\ 000\ 0119$.
 Perpendicular to axis: $\alpha' = .000\ 008\ 36$, $\Delta\alpha'/\Delta t = .000\ 000\ 0262$.

From these data the cubical coefficient of expansion is derived; at 40° C. it is 0.000 025 01, and its temperature coefficient is $\Delta\alpha/\Delta t = 0.000\ 000\ 0643$.

TABLE 1.—Resistance of hematite rods

Parallel to main axis		Perpendicular to axis	
Temperature	Resistance	Temperature	Resistance
° C.	Ohms	° C.	Ohms
16.25	927.4	17	1,280
68	339	47.75	634
72	320	117	238
98.75	227.4	153	165.3
161	115.6	180.5	135.5
265	52	205	112.3
11.75	1,000	258	82.6
15	938		

On another sample of Elba hematite Fizeau collected the following figures:

Parallel to principal axis: $\alpha = 0.000\ 007\ 81$, $\Delta\alpha/\Delta t = 0.000\ 000\ 0059$.
 Perpendicular to axis: $\alpha' = .000\ 007\ 31$, $\Delta\alpha'/\Delta t = .000\ 000\ 0131$.

From these figures one can calculate that the two expansions are equal at 34.7° C., and above this temperature the linear expansion perpendicular to the axis is greater while below it the linear expansion parallel to the axis is the greater.

Bäckström's²⁵ results on hematite from Langö (a Norwegian locality) were as follows:

Parallel to axis:

$$L_t = L_o (1 + 7.6109 \cdot 10^{-6}t + 0.4901 \cdot 10^{-8}t^2) \text{ (tem. range, } 5^\circ \text{ to } 80^\circ \text{ C.)}$$

Perpendicular to axis:

$$L_t = L_o (1 + 7.6918 \cdot 10^{-6}t + 1.2000 \cdot 10^{-8}t^2) \text{ (tem. range, } 4^\circ \text{ to } 82^\circ \text{ C.)}$$

No extrapolation out of the observed range is allowable. According to these equations the two rates of expansion are equal at -5.7° C. and the expansion parallel to the axis is greater at temperatures below this, as was observed by Fizeau. The data of Bäckström and Fizeau on magnitude are in reasonable agreement as far as magnitude is concerned.

²⁴ Fizeau, R., Memoire sur la dilatation des corps solides par la chaleur: Ann. chim. phys., t. 8, 1866, p. 335.

²⁵ Bäckström, H., Bestimmung der Ausdehnung durch die Wärme und des elektrischen Leitungsvermögens des Eisenglanzes: Ztschr. Kryst., Jahrg. 26, 1896, p. 93.

The volume coefficient will of course be in the order of three times the average of the linear coefficients.

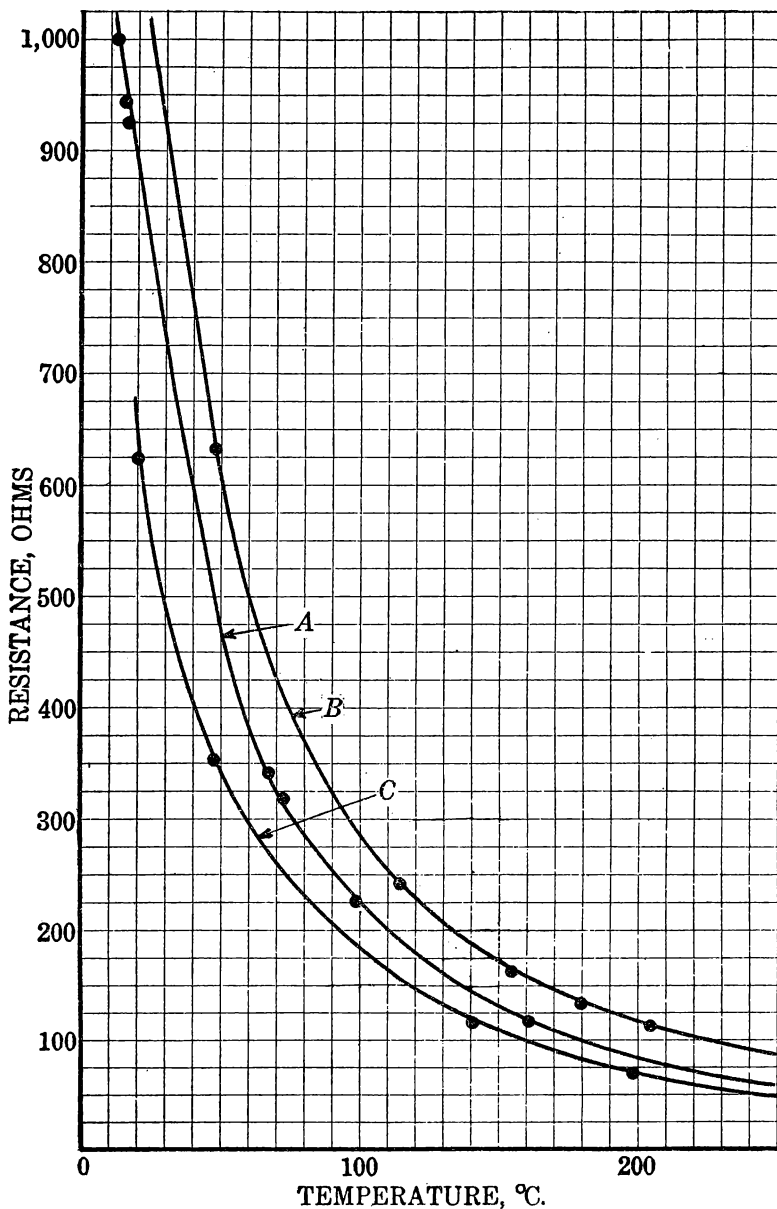


FIG. 1.—Electrical conductivity of hematite rods: A, Parallel to main crystallographic axis; B and C, perpendicular to axis

ELECTRICAL CONDUCTIVITY

Ferric oxide is a good conductor of electricity as compared with many other metal oxides, and data on Swedish hematite have been

reported by Bäckström²⁶ and on Elba hematite by Königsberger and Reichenheim.²⁷

They found approximately the same conductivity in hematites of widely different sources. Hematite from Norway and from the Island of Elba in the southern Atlantic were investigated. One good crystal was cut so that a rod of material 7.285 square millimeters in cross section by 16.25 millimeters in length came from a direction parallel to the principal crystallographic axis. For this sample the resistance per centimeter cube at 19.9° C. was 38.4 ohms. It contained about 3.01 per cent of moisture. The data collected on the rod and similar data collected on a rod cut from the same crystal but perpendicular to the axis are contained in Table 1. Unfortunately the latter rod broke during manipulation, so data were collected on the two pieces. These data are plotted in Figure 1 and show that the shape of a resistance curve as a function of temperature is quite consistent but not exactly reproducible.

Heating to 1,000° C. and then cooling rapidly gave a sample which was a poor conductor, while slow cooling of the reheated sample gave a much better conductor. No conclusions were drawn, but evidently the conductivity will be a good property to use when one engages in a study of heat treatment of hematite as a factor in changing its physical characteristics.

After heating to 1,000° C. the resistance of the Elba hematite was 0.63 ohm and of a Norwegian sample 0.70 ohm.

Bäckström summarized his results on the effect of temperature on the electrical conductivity of hematite between 0° and 80° with two empirical equations which allow no extrapolation:

Parallel to axis:

$$R_t = R_o(1 - 0.014\ 178t + 0.000\ 125\ 33\ t^2 - 0.000\ 000\ 516\ 21\ t^3).$$

Perpendicular to axis:

$$R_t = R_o(1 - .012\ 796t + .000\ 111\ 08\ t^2 - .000\ 000\ 464\ 64\ t^3).$$

Such electric conductivity data as the above are of only general value, as more modern work has shown that endless precautions are necessary for getting at precise true values.

THERMAL CONDUCTIVITY

The thermal conductivity of powdered ferric oxide has been measured by Furnas²⁸ over the temperature range 20° to 650° C., and his

²⁶ Bäckström, H., Elektrisches und thermisches Leiternogen des Eisenglanzes: Öfv. af Ak. Forh. Stockholm, 1888, p. 533; also in Ztschr. Kryst., Jahrg. 17, 1890, p. 424.

²⁷ Königsberger, J., and Reichenheim, O., Über die Elektrizitätsleitung einiger natürlich kristallisierter Oxyde und Sulfide und des Graphites: N. J. B. Min., pt. 2, 1906, p. 29.

²⁸ Furnas, C. C., Heat Conduction of Solids: Trans. Am. Inst. Chem. Eng., vol. 18, 1926, pp. 295-307; Thermal Properties of Ferric Oxide: pp. 309-346; also dissertation, Univ. of Michigan, 1926.

data are given in Table 2 and in Figure 2. Because the specific heats simultaneously derived in Furnas's experiments were not consistent

TABLE 2.—*Thermal conductivity of powdered ferric oxide*

Temperature, °C.	Calorie per second per square centimeter per centimeter ° C.	Temperature, ° C.	Calorie per second per square centimeter per centimeter ° C.
125	0.000918	500	0.00113
150	.000925	550	.00117
175	.000930	600	.00122
300	.000940	650	.00127
350	.000980	650	.00128
400	.00108	700	.00133
450	.00113	750	.00138
450	.00109		

with other thermodynamic data, these data must be used conservatively until checked further.

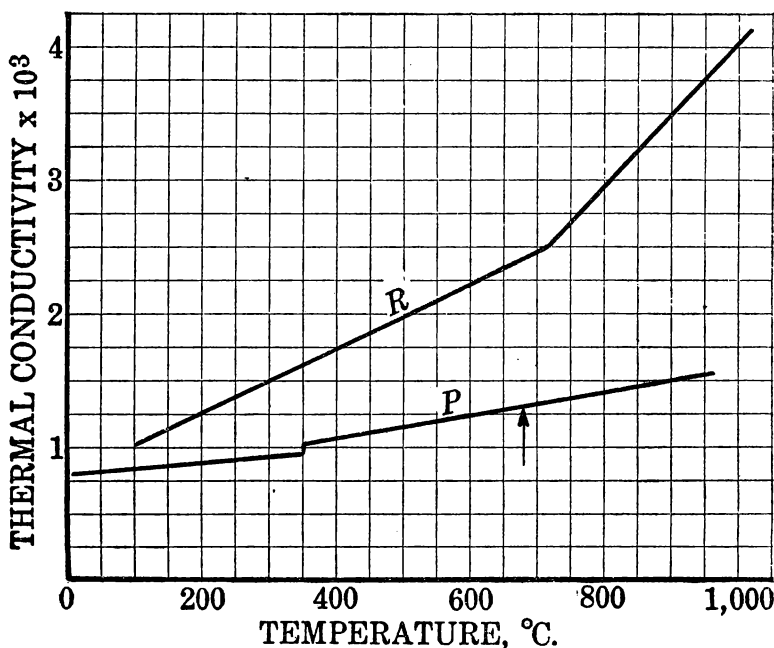


Fig. 2.—Thermal conductivity of ferric oxide: P, Powdered Fe₂O₃ (Furnas); R, prepared rods of Fe₂O₃ (Bidwell). Arrow indicates 678° C. transition temperature

Another set of doubtful data comprises those of Bidwell,²⁹ whose work was done on a rod of what he thought was magnetite, although

²⁹ Bidwell, C. C., Electrical and Thermal Properties of Iron Oxide: Phys. Rev., vol. 10, 1917, pp. 756-766.

later he reported that it had oxidized in the air to ferric oxide during the experiments, so that his data should be regarded as applying to Fe_2O_3 instead of Fe_2O_4 . These data, given for what they are worth and probably representing a mixture of Fe_2O_4 and Fe_2O_3 , are included with those of Furnas in Figure 2.

The 678° C. transition does not show in the Furnas curve, which is an extrapolation above 650° C., but Bidwell's curve shows a change in direction at about 728°, which is possibly associated with it.

MELTING POINT

Due to the tendency of Fe_2O_3 to dissociate into magnetite and oxygen at high temperatures its melting point has not been precisely determined. The so-called melting points have always been proved to be those of mixtures of Fe_2O_3 and Fe_3O_4 . The accepted figure is that of Hilpert and Kohlmeyer³⁰ at 1,565° C., if the freezing point of palladium is 1,541°. The sample used was analyzed after melting and found to contain 3.1 per cent of FeO (10 per cent of Fe_3O_4), and therefore probably melted at a lower temperature than the melting temperature of the pure substance. The present value of the palladium point is 1,555° C. \pm 2, which changes the above observation from 1,565° to 1,579°, plus the lowering caused by solution of 10 per cent of magnetite, an unknown quantity. The care with which this work was apparently done has always given it credence in spite of the later statement by Kohlmeyer³¹ that the point has no significance, as it falls on the melting curve of mixtures of magnetite and ferric oxide.

Ruer and Nakamoto state³² that if the melting point is 1,550°, the material must be melted under a pressure of 10 atmospheres of oxygen. However, their work consisted mainly in determining dissociation pressures at lower temperature, and their melting point is not a direct determination. A direct determination of the melting point of ferric oxide under enough oxygen pressure to prevent dissociation remains to be made.

Another recent rough determination worth recording is that of Fink and Mantell.³³ Pure ferric oxide powder was molded into a cone with a small amount of carbonaceous binder, which was burned off in an open muffle. Heating above 800° was continued at the rate of 5° to 10° per minute; at 1,492° the cone showed softening and at

³⁰ Hilpert, S., and Kohlmeyer, E. J., *Über Calciumferrit*: Ber. Deut. chem. Gesell., Jahrg. 42, 1909, p. 4581.

³¹ See footnote 19, p. 9.

³² Ruer, Rudolf, and Nakamoto, Minoru, *Über Eisen- und Kupferoxyde*: Rec. trav. Chem., Jahrg. 42, 1925, pp. 675-682.

³³ Fink, C. G., and Mantell, C. L., *Thermic Reduction with Metals of Bolivian Tin Concentrates*: Eng. and. Min. Jour., vol. 125, 1928, pp. 325-328.

1,497° initial deformation, and it became fluid and flattened out at 1,503° C. No analysis of the final (probably partly dissociated) product is given, and no precautions or corrections of the thermocouple are mentioned. The reading is, therefore, doubtless too low, but the value of the data consists in giving an idea as to what to expect in ordinary practical treatment of ferric oxide without regarding closely its ultimate chemical composition or the precise determination of the temperature at which it melted.

BOILING POINT

Volatilization of ferric oxide is said by Friend³⁴ to take place between 2,500° and 3,000° C., but this is undoubtedly an error, as what volatilizes is either magnetite or more probably ferrous oxide resulting from dissociation of the higher oxides. Extrapolations from observed dissociation pressures, discussed in the following section, show that ferric oxide reaches 1,000 atmospheres dissociation pressure at 1,900°, and at 2,500° the dissociation pressure will be of the order of 400,000 atmospheres. Even magnetite should reach 1 atmosphere dissociation pressure at 2,500° C.

DISSOCIATION PRESSURE

Although ferric oxide is known to dissociate thermally, its dissociation pressures have been studied by only a few observers and at only a few temperatures. The available data are summed up in Table 3 and Figure 3 in which the common logarithms of the pressure, in atmospheres, are plotted against the reciprocals of the absolute temperatures. Such data should give a straight-line plot as long as the same crystalline substance is involved and no solution of other materials is present. The 10 data of Walden³⁵ have commonly been thought to be the least precise of the data available, although they are the most numerous. However, disregarding his three lower-temperature data, the other seven are in reasonable agreement with those of the other observers. Walden failed to report the amounts of ferric oxide used and of oxygen liberated, so his points are open to some suspicion but may nevertheless be good. The most precise work is that of Sosman and Hostetter,³⁶ while more recent work was done by Ruer and Nakamoto,³⁷ and these observers report two data.

³⁴ See footnote 10, p. 6.

³⁵ Walden, P. T., On the Dissociation Pressures of Ferric Oxide: *Jour. Am. Chem. Soc.*, vol. 30, 1908, pp. 1350-1355.

³⁶ Sosman, R. B., and Hostetter, J. C., The Oxides of Iron, I; Solid Solution in the System Ferric Oxide-Magnetic Oxide: *Jour. Am. Chem. Soc.*, vol. 38, 1916, pp. 807-833.

³⁷ See footnote 32, p. 15.

The two points accorded to Sosman and Hostetter above are the ones at the Fe_2O_3 end of a series of oxygen pressures measured with a series of mixtures of ferric oxide and magnetic oxide, Fe_3O_4 , at two temperatures in very carefully designed and operated apparatus. They are for a mixture which is very nearly pure Fe_2O_3 (97.1 per cent), although it lacks a small amount of oxygen necessary to satisfy that formula. The ferric oxide and magnetic oxide were shown by them to form a continuous series of solid solutions. The dissociation pressure of the ferric oxide fell off rapidly as the amount of Fe_2O_3 in the mixture decreased, and the oxygen pressure of the pure substance is therefore probably somewhat greater than that shown by the two data quoted here.

TABLE 3.—*Ferric oxide-oxygen pressures*

Observers	Temperature			Pressure		
	° C.	° K.	1/T	Millimeter	Atmosphere	Log P
Walden.....	1, 100	1, 373	0. 000728	5	0. 00657	-2. 182
	1, 250	1, 523	. 000657	20	. 0263	-1. 58
	1, 320	1, 593	. 000628	90	. 1191	-. 924
	1, 340	1, 613	. 000620	138. 5	. 1822	-. 739
	1, 360	1, 633	. 000612	202	. 265	-. 575
	1, 380	1, 653	. 000605	297	. 391	-. 408
	1, 400	1, 673	. 000597	454	. 698	-. 156
Sosman and Hostetter 97.1 per cent Fe_2O_3 , 2.9 per cent Fe_3O_4 , 85.43 Fe_2O_3 +14.37 per cent Fe_3O_4 .	1, 100	1, 373	. 0007283	. 37	. 000487	-3. 313
	1, 200	1, 473	. 0006789	5. 00	. 00657	-2. 182
	1, 100	1, 373	. 000728	. 13	. 000171	-3. 767
	1, 200	1, 473	. 000678	2. 6	. 003430	-2. 466
Ruer and Nakamoto.....	1, 385	1, 658	. 000603	-----	. 207	-. 6985
	1, 455	1, 738	. 000575	-----	1. 00	. 000
Tigerschiöld calculations Sosman and Hostetter, 97.1 per cent Fe_2O_3 .	527	800	-----	-----	1.86×10^{-10}	-16. 270
	727	1, 000	. 001000	-----	1.20×10^{-10}	-10. 080
	1, 127	1, 400	. 000714	. 828	. 00109	-2. 902
	1, 227	1, 500	. 000686	13. 75	. 0181	-1. 742
	1, 327	1, 600	. 000625	166. 4	. 219	-. 659
	1, 527	1, 800	. 000555	-----	16. 03	+1. 205
	1, 727	2, 000	. 000500	-----	578. 0	+2. 762
	1, 927	2, 200	-----	-----	2.56×10^3	+3. 408
10.37 per cent Fe_2O_3	1, 227	1, 500	. 000666	-----	. 00317	-2. 499
	1, 327	1, 600	. 000625	-----	. 0429	-1. 367
	1, 527	1, 800	. 000555	-----	3. 76	+ . 575
	1, 727	2, 000	. 000500	-----	165. 0	+2. 218

Ruer and Nakamoto worked with pure ferric oxide and found that when heated in a stream of pure dry nitrogen for one hour only a very small amount of oxygen was lost at 1,150° C. (as determined by loss in weight of the sample held on a boat), and at 1,125° no change occurred in that time. Evidently the method is not as sensitive as that of Sosman and Hostetter, as the latter measured the dissociation pressure at 1,100° with satisfactory precision. Heated to 1,425° in air the ferric oxide lost enough weight to be converted into magnetite, but on lowering the temperature to 1,370° and waiting one-half hour oxygen was taken up again. Therefore

the temperature at which the dissociation pressure is equal to the oxygen content of air is chosen as $1,385^{\circ}$, which is 40° higher than

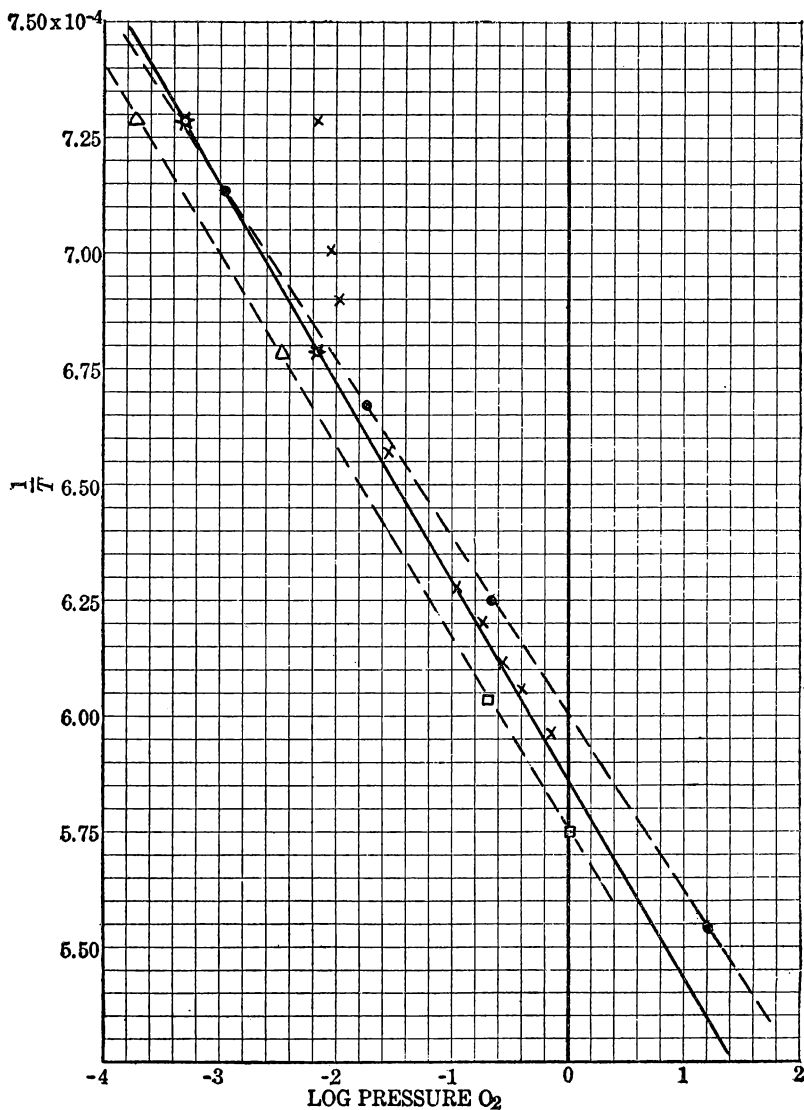


FIG. 3.—Dissociation of ferric oxide: ☆, Sosman and Hostetter, 97.1 per cent Fe_2O_3 ; △, Sosman and Hostetter, 85.4 per cent Fe_2O_3 ; □, Ruer and Nakamoto; ●, Tigerschild; ×, Walden

the point observed by Walden. The description of their work does not allow one to ascertain whether or not the magnetite was completely reoxidized to Fe_2O_3 at $1,370^{\circ}$ or during quick cooling of the boat in air in preparation for weighing, and one must know this before it is certain that their pressures were not too low. The prod-

uct measured might have been a solid solution of ferric oxide containing some magnetic oxide when it was taken from the furnace. The above work of Sosman and Hostetter had shown a great drop in dissociation pressure with only a slight loss of oxygen from Fe_2O_3 . The data of Sosman and Hostetter and of Walden are, with the exception of Walden's three obviously poor data, all on a reasonably straight line, while the data of Ruer and Nakamoto show lower pressures than would correspond to the straight line through the work of the other two sets of investigators.

Ruer and Nakamoto further determined that in pure dry oxygen Fe_2O_3 lost weight at $1,470^\circ \text{C}$. and took it up again at $1,440^\circ$, and they chose $1,455^\circ$ as the point at which ferric oxide has a dissociation pressure of 1 atmosphere. This point suffers from similar uncertainty, and the pressure is probably too low, or what is equivalent—the temperature corresponding to a definite pressure is too low.

A thermodynamic study of the Sosman and Hostetter data was made by Tigerschiöld.³⁸ Writing the dissociation equation: $6 \text{Fe}_2\text{O}_3 = 4 \text{Fe}_3\text{O}_4 + \text{O}_2$, he uses the Sosman and Hostetter data, the heat capacities of the reactants, and other data to set up an equation for the equilibrium constant, which in this case is also the oxygen pressure, in terms of absolute temperature—

$$\log k = \log p = -20,946/T + 3.5 \log T + 0.001157 T - 0.6332.$$

The heat-capacity terms introduced were approximations, and the equation as written does not allow exact reproduction of both of Sosman and Hostetter's data, as can be seen from the dotted line in the figure representing Tigerschiöld's equation. While the Tigerschiöld equation very nearly fits the data, it is, therefore, not quite correct, but the deviation is in the proper direction to give more nearly the thermal data for absolutely pure Fe_2O_3 . However, it is reasonably close, and the heat of dissociation indicated when combined with the heat of formation of magnetite gives a heat of formation of 197,100 calories at 17°C . for ferric oxide as derived from the two Sosman and Hostetter data for a mixture containing 97.1 per cent of Fe_2O_3 . This compares favorably with the Le Chatelier heat of formation of 197,700 calories, quoted later. If the Ruer and Nakamoto data were allowed to influence the position of the line in Figure 3, too great a discrepancy in the heat of reaction with other data would be found.

A line drawn through the two Ruer and Nakamoto points, when extended down to the temperature employed by Sosman and Hostetter, passes through points corresponding to the oxygen pressures of a sample with 85.4 per cent of Fe_2O_3 and the remainder magnetite.

³⁸ Tigerschiöld, Magnus, *Jarnets Oxider Från Termodynamisk Synpunkt: Avtryck ur Jernkontorets Annaler För Ar, 1923, pp. 67–105.*

It is doubtful if the Ruer and Nakamoto samples were as deficient in oxygen as this, and it is probably a coincidence that a line passing through both of their points should pass through both points for the above-mentioned solid solution. Nevertheless, this fact constitutes an additional justification for disregarding the Ruer and Nakamoto data.

The equation for the line through the two Sosman and Hostetter data on 97.1 per cent of Fe_2O_3 and the Walden data for pure Fe_2O_3 is, therefore, the only one which can be accepted at present and reads as follows:

$$\log p = -23,550/T + 13.83.$$

From this we can derive the temperature $1,348^\circ \text{C.}$, at which ferric oxide has an oxygen pressure of 0.207 atmosphere. This is the temperature up to which ferric oxide is stable in air and above which it would lose oxygen. Similarly, the temperature at which ferric oxide could exert 1 atmosphere pressure is $1,430^\circ$. This is the temperature to which it could be heated in pure oxygen without decomposition and is the temperature above which pure ferric oxide placed in a muffle vented at 1 atmosphere would continuously generate oxygen gas. The fact that the resulting magnetite would dissolve in some of the unreacted ferric oxide and lower its oxygen pressure will be discussed in a later section.

CRYSTAL SYSTEM

Hematite crystallizes in ditrigonal scalenohedrons (hexagonal system) and rhombohedrons. It is found in columnar to granular, in botryoidal, and even in lamellar variations of these forms, the latter being the flaky specularite. The axial ratios are $a:c=1:1.36557$ to $1:1.3654$. It is isomorphous with corundum and the analogous titanates. The hardness is from 5 to 6. The refractive coefficients are quoted by Doelter,³⁹ who states that it has strong negative double refraction.

POLYMORPHISM OF FERRIC OXIDE

Ferric oxide probably exists in several different crystalline forms, although conclusive evidence to prove this is lacking. P. J. Holmquist⁴⁰ states that two crystalline forms of ferric oxide exist, the alpha form at low temperatures and beta form at high temperatures. No evidence supporting this claim is given in the abstract which was available to the writer. Unless Holmquist has studied the

³⁹ Doelter, C., *Handbuch der Mineralchemie*: Dresden and Leipzig, Jahrg. 3, part 2, 1926, p. 629.

⁴⁰ Holmquist, P. J., Communication without title on Några artificiella mineralbildningar: Geologiska Föreningens i Stockholm, vol. 47, 1925, pp. 142-144.

X-ray diffraction patterns at high and low temperatures, the X-ray work remains to be done. The 678° C. transition seems well established; others are not.

678° C. TRANSITION

The earliest reference to this point is by Keppler and d'Ans,⁴¹ who state that a polymorphic change takes place at 640° C., the temperature where maximum SO₃ formation took place and where there seemed to be a rather sharp intersection of two curves (one for high and one for lower temperature) thought possibly to be connected with polymorphism of the Fe₂O₃ catalyst. Due to the complications of other reactions involved the point may have no significance.

Sosman and Hostetter⁴² carried out differential heating curves with pure ferric oxide and found a sharp reversible inversion with heat absorption at 678° and a slight irregularity between 775° and 785° C.

The same point is indicated in a thermal expansion curve of Chaudron and Forestier,⁴³ in which a maximum thermal expansion per degree is observed at 680° C.

Ferric oxide is normally a paramagnetic substance, and a drop in its magnetic susceptibility is quoted at 678° by Sosman.⁴⁴

Blanc and Chaudron⁴⁵ also state that there is a drop in susceptibility in the neighborhood of 600°, but Huggett and Chaudron⁴⁶ later studied the whole Fe₂O₃-Fe system from the magnetic standpoint and found the Curie point of ferric oxide to be 675° C. In view of the precise work of Sosman it seems wise to accept his figure of 678° C. for a polymorphic change in ferric oxide.

The heat change involved at this point has been measured by Furnas,⁴⁷ who has been able to estimate it only in combination with the small additional change in the range 755° to 785° C. and finds that the combined heat in the two changes, most of which is ascribable to the 678° change, is 41.8 calories per gram, which corresponds to 6,690 calories per mol.

⁴¹ Keppler, G., and d'Ans, J., Die thermische Dissociation der wasserfreien Eisensulfate: Ztschr. phys. Chem., Jahrg. 62, 1908, p. 89.

⁴² See footnote 36, p. 18.

⁴³ See footnote 9, p. 6.

⁴⁴ Sosman, R. B., The Common Refractory Oxides: Jour. Ind. Eng. Chem., vol. 8, 1916, pp. 985-990.

⁴⁵ See footnote 22, p. 9.

⁴⁶ Huggett, J., and Chaudron, G., Temperatures de transformations magnetiques dans le system ferresquioxide de fer: Compt. rend., t. 184, 1927, pp. 199-201.

⁴⁷ See footnote 28, p. 13.

The temperature of this transition is lowered by the presence of aluminum or chromium oxides, as shown by Forestier and Chaudron,⁴⁸ and by magnetite, as shown by Huggett and Chaudron. Mixtures of

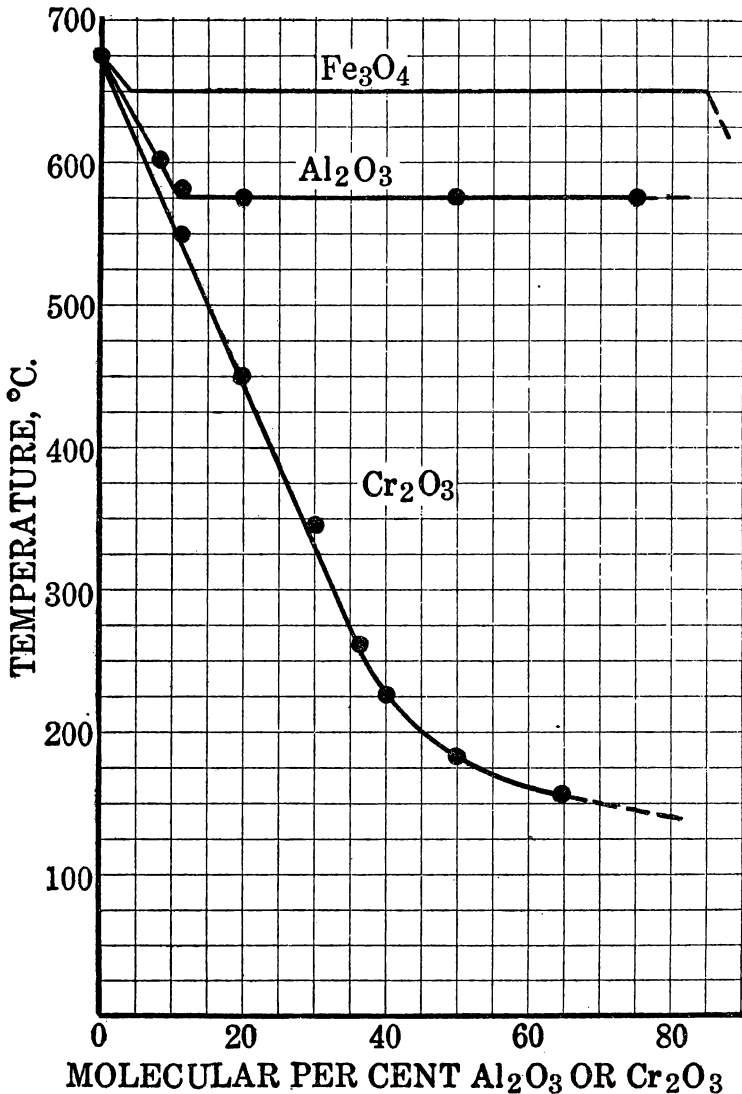


FIG. 4.—Lowering of the 678° C. transition point of ferric oxide by Al₂O₃, Cr₂O₃, and Fe₂O₄

ferric with aluminum or chromium hydroxides were precipitated together, dried, shaped into rods, and baked for two hours at 900° C.

⁴⁸ Forestier, H., and Chaudron, G., Points de transformation des solutions solides d'alumina ou de sesquioxyde de chrome dans le sesquioxyde de fer: *Compt. rend.*, t. 180, 1925, pp. 1264-1266.

Just what happened to these mixtures during the baking is not known, but with the help of a Chévenard dilatometer a discontinuity was determined at 675° C. for the pure ferric oxide. The point was lowered by the presence of alumina in linear proportion to the amount added until it became constant at 12 molecular per cents of alumina at 575° C. This is shown graphically in Figure 4. The transition of chromic oxide was also lowered in linear proportion to 230° at 40 molecular per cents and from there on with decreasing magnitude. The curve for mixtures with magnetite is also given in Figure 4 and shows that 10.35 molecular per cents of Fe_3O_4 lower the transition of Fe_2O_3 to 650°, after which it remains at this temperature. These facts may be interpreted as showing that ferric oxide forms solid solutions with alumina, chromic oxide, or magnetite, and the lowering of the transition temperature is one result. Only 12 per cent of alumina is soluble in ferric oxide at 900°, but ferric oxide and chromic oxide are soluble in all proportions.

360° C. TRANSITION

Furnas has reported another transition temperature at 360° C. found when studying the specific heat of ferric oxide at higher than room temperatures. A discontinuity exists in his specific heat curve and his thermal conductivity curve at this temperature. He was able to measure the heat absorption, which amounted to 4.85 calories per gram or 775 calories per mol. No work has yet been done to determine whether the transition at 360° is a polymorphic one, but the thermal change is large enough to lead one to believe that there are probably at least three forms of ferric oxide, as indicated by the above work, one stable up to 360°, one stable between 360° and 678°, and a third at temperatures above 678°.

SINTERING

Finely powdered ferric oxide on heating through 920° to 950° sinters and shrinks in volume, as evidenced by the work of Kohlmeier. Kohlmeier⁴⁹ noticed a kink in the heating curve of ferric oxide during this sintering phenomenon. This may correspond to a heat absorption accompanying a polymorphic change, or it may be the energy corresponding to transition from small crystals to large crystals. The point deserves study.

C. C. Furnas has noticed that powdered ferric oxide becomes very active just before reaching the sintering temperature, tending to flow like water and assuming practically a zero angle of repose, although

⁴⁹ See footnote 19, p. 9.

every minute particle is still present unaltered in dimensions and no true liquids are present. The phenomenon could be caused by accumulation of similar electric charges on the particles or by evolution of gas. The writer has noticed it during the roasting of powdered sulphide ores, when the whole mass is permeated with gas being evolved from the particles and the interstices between the powdered material are not large enough to allow exit of the gas through them as rapidly as it is evolved. If there is gas evolution at this temperature or if there is an accumulation of electric charges, the phenomenon is worth scientific investigation.

GLOW EFFECT

The glow effect when amorphous ferric oxide crystallizes at about 400° has already been described earlier in this chapter and might well be called a polymorphic change. It is, of course, accompanied by a change in color of the material. A study of the thermal effect accompanying the glow or the crystallization of amorphous ferric oxide has been made by Mixter,⁵⁰ who has determined that it amounts to roughly 9,000 calories per mol. His method consisted in measuring the heat change when calcined ferric oxide and freshly precipitated and desiccated ferric oxide reacted in a calorimeter with sodium peroxide. The difference he called "heat of polymerization."

MAGNETIC FERRIC OXIDE

As mentioned above, ferric oxide is normally a paramagnetic substance and most of its mineral forms are paramagnetic. However, it is also known to exist in a ferromagnetic form, as magnetic as magnetite (about 100,000 times as susceptible as natural hematite), both as a laboratory preparation and as a natural mineral. Both forms have been described by Sosman and Posnjak.⁵¹ The natural mineral has not been named, but the X-ray diffraction pattern of the iron atoms is similar to that of magnetite. X-ray work by others has also shown that the magnetic form of ferric oxide has an identical X-ray pattern with that of magnetite, indicating in connection with the methods of preparation described below that it is derived by low-temperature oxidation of magnetite. Its color is chocolate brown. Precipitated magnetite, on standing in air, is altered to the brown ferromagnetic Fe_2O_3 . Ferric oxide occurs in nature also as a pseudomorph after magnetite, called martite, but not ferromagnetic.

⁵⁰ Mixter, W. G., Heat of Formation and Polymerization of Some Oxides and Determination of the Heat of Combustion of Water by Fusion with Sodium Peroxide: *Am. Jour. Sci.*, vol. 40, 1915, pp. 23-32.

⁵¹ Sosman, R. B., and Posnjak, E., Ferromagnetic Ferric Oxide, Artificial and Natural: *Jour. Washington Acad. Sci.*, vol. 15, 1925, pp. 329-342.

PROPERTIES

The magnetic properties of ordinary ferric oxide as a function of its temperature have been studied by Forestier and Chaudron.⁵² Fe_2O_3 has a very low coefficient of magnetization and is ordinarily classed as paramagnetic. However, as in the case of ferromagnetic substances, the value of the coefficient varies with the thermal and magnetic treatment to which it has been subjected. A recording thermomagnetic instrument was used in which samples of Fe_2O_3 were slowly heated or cooled. The resulting curves showed that the coefficient of the completely unmagnetized oxide increases to a maximum at about 600° and then drops sharply to 675° C. (the Curie point). Above 675° it remains constant. When the oxide is cooled the curve retraces itself to the maximum at 600° C., but the coefficient continued to increase at lower temperatures down to room temperature, where it had a much greater value than at the beginning. When the experiment is repeated with this polarized sample the cooling curve from the previous experiment was traced reversibly either during heating or cooling. Heating and cooling through 675° in a magnetic field is sufficient to polarize the material quite perceptibly. However, heating and cooling the polarized material through 675° C. in a nonmagnetized field destroyed the acquired magnetism.

Earlier work of the same kind was done by Honda and Sone,⁵³ whose curve of magnetic susceptibility as a function of temperature and past history is given in Figure 5. This curve contains more information than is given by Forestier and Chaudron, who did not cover the temperature range between room temperature and liquid-air temperatures. When ordinary paramagnetic ferric oxide is cooled, the susceptibility falls off rapidly to about -40° C. and thereafter very slowly. From -40° to -185° C. the curve is reversible, but when the material is warmed above -40° , if in a magnetic field, it becomes ferromagnetic, so that at room temperature the susceptibility is nearly twice that of the original sample. With further warming the susceptibility increased irreversibly (in the magnetic field) to about 600° C. and then fell off rapidly to the original value at about 690° C. Above this temperature not much change could be detected and the change was reversible, but on cooling below 690° in an excited field the susceptibility increased

⁵² Forestier, H., and Chaudron, G., Caractères ferromagnétiques du sesquioxyde de fer stable: *Compt. rend.*, t. 183, 1926, pp. 787-789.

⁵³ Honda, K., and Sone, T., Magnetic Investigation of Structure Changes in Iron and Chromium Compounds at Higher Temperatures: *Sci. Reports Tohoku Imperial University*, 1st Ser., vol. 3, 1914, pp. 223-234.

as the temperature dropped to room temperatures, where the experiment ended. The susceptibility induced by this type of heat treatment was much below that of magnetite, but evidently during a change of temperature from -40° to $+600^{\circ}$ C., if carried out in a magnetic field, the material becomes increasingly ferromagnetic. It would be interesting to hold a sample of paramagnetic Fe_2O_3 at about 500° C. in a magnetic field for a period of time to see if the thermal agitation was sufficient to cause a continuous increase in the susceptibility until the value of the material made from magnetite might be approached. On the other hand, the material made from magnetite may be unstable and would tend to lose with time some of its susceptibility in a nonmagnetized field.

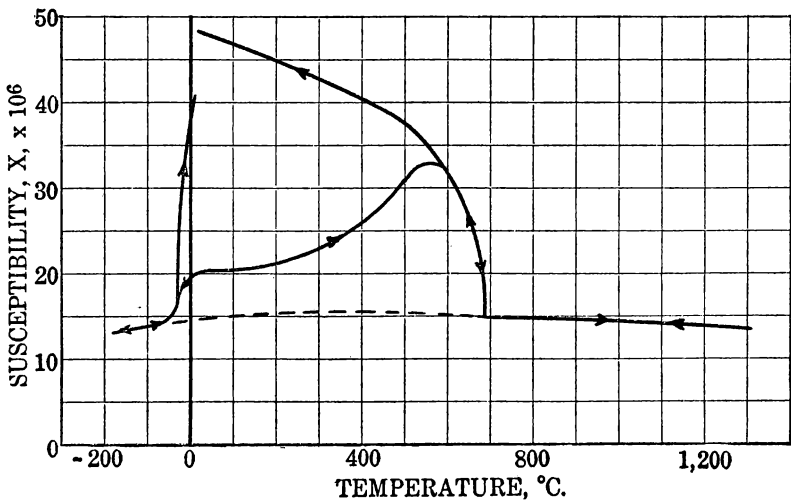


FIG. 5.—Magnetic susceptibility of hematite as a function of temperature and thermal history

FERROMAGNETIC FERRIC OXIDE

The work of the geologists and mineralogists on the known deposits of ferromagnetic hematite⁵⁴ has led to the conclusion that this mineral forms only under restricted oxygen supply and temperatures up to 320° , while ordinary hematite forms at the lower temperatures. However, the evidence is none too satisfying and should not yet be accepted as a point in the geological thermometer. Most of the occurrences of this mineral seem to be in association with the oxidation of iron sulphides.

⁵⁴ Frebold, G., and Hesemann, J., Über magnetischen und nichtmagnetischen Eisenglanz und seine Bedeutung für die Erzlagertstättenkunde: Central. Mineral. Geol., 1926A, pp. 314-331.

Perhaps the most extensive work on ferromagnetic ferric oxide has been done by Welo and Baudisch,⁵⁵ who have been interested in the catalytic effects of the ferromagnetic form on certain biological processes. Their method of preparation consists in precipitating a hydrated Fe_3O_4 by dissolving equivalent amounts of ferrous and ferric sulphates in water and pouring the mixture into an excess of hot, strong, sodium hydroxide solution. The black precipitate can be washed and dried and oxidized at 220° to 330° C. in air, giving a yellowish-red ferromagnetic ferric oxide.

Another method of preparation is that of Chevallier,⁵⁶ who heats commercial black magnetic iron oxide powder (probably roll scale) containing some free iron to 350° C. in air. Abraham and Planiol⁵⁷ reduced ferric oxide with hydrogen or carbon monoxide at 500° to give magnetite, which on rapid reoxidation at high temperatures gives red paramagnetic Fe_2O_3 , but on slow oxidation in air at 200° to 250° gives yellowish-brown strongly magnetic ferric oxide. Still another method of preparation was discovered by Sosman and Posnjak, who dehydrated lepidocrocite, one of the two crystal forms of the monohydrate of ferric oxide, $\text{Fe}_2\text{O}_3 \cdot \text{H}_2\text{O}$. Dehydration of the other form, goethite, yields only the paramagnetic form of ferric oxide. Sosman and Posnjak's method of preparing ferromagnetic ferric oxide from a hydrated ferric oxide mineral agrees with the observations of Wedekind and Albrecht,⁵⁸ who have studied the magnetic susceptibility of several hydrated oxides, including those of iron, and have drawn the following conclusions as to the magnetic behavior of ferric oxide hydrates: (1) The hydrates are always more strongly magnetic than the corresponding oxides; (2) in the range of 22 to 43 per cent of water content the magnetic susceptibility decreases as the hydrate water content increases; and (3) oxyhydrates, such as the artificial form of goethite, $\text{FeO}(\text{OH})$, precipitated in the usual manner and heated in an autoclave at various pressures, are ferromagnetic.

When ferric oxide functions as an acid, as it does in ferrites of strong bases, the products are frequently ferromagnetic. It therefore seems probable that in the oxidation of magnetite (ferrous ferrite)

⁵⁵ Welo, Lars A., and Baudisch, Oskar, The Two-Stage Transformation of Magnetite into Hematite: *Phil. Mag.*, vol. 50, 1925, pp. 299-408; The Catalytically Active and Inactive Forms of Ferric Oxide: *Jour. Biol. Chem.*, vol. 65, 1925, pp. 215-227; Neue Anschauungen über das Wesen der Katalyse; Aktives und inaktives Eisenoxyd: *Chem. Ztg.*, Jahrg. 49, 1925, pp. 661-662.

⁵⁶ Chevallier, Raymond, Sur l'oxyde ferrique ferromagnétique: *Compt. rend.*, t. 180, 1925, pp. 1473-1475.

⁵⁷ Abraham, Henri, and Planiol, Rene, Magnetic Iron Sesquioxide: *Nature*, vol. 115, 1925, p. 930; Sur le sesquioxyde de fer magnétique: *Compt. rend.*, t. 180, 1925, pp. 1328-1329.

⁵⁸ Wedekind, I. E., and Albrecht, W., Kennzeichnung der verschiedenen Arten von Eisen (III)-Oxygen und Eisen (III)-Oxyhydraten durch ihre unterschiedlichen magnetischen Eigenschaften (I): *Ber. Deut. chem. Gesell.*, Jahrg. 59, 1926, pp. 1726-1730.

the only change is the production of ferric ferrite which is still magnetic.

Another so-called new form of magnetic ferric oxide has been reported by Chevallier.⁵⁹ Strong solutions of ferrous sulphate and sodium hydroxide were used, and the resulting ferrous hydroxide was to be oxidized by hydrogen peroxide. Excess soda was used, but Chevallier does not say whether the hydrogen peroxide was added simultaneously with the other reagents or afterwards. Washing of the ferric oxide precipitates is also not mentioned, although they were dried several weeks in vacuo. The stronger the soda and the greater its excess the more highly magnetic the resulting ferric oxide. An optimum temperature of 45° to 50° for the precipitation was observed, and above that the ferric oxide produced was much less magnetic. Also, all of the samples of ferric oxide lost most of their magnetism when raised to 100° C. for one hour or to 200° C. for a few minutes, whereas the previously known forms were quite stable up to about 600° C. To one familiar with the commercial production of caustic soda the presence of sodium ferrites in strong soda solutions under Chevallier's conditions is well known, and the amount of ferric iron dissolved increases with the strength of the solution, while on dilution of the strong solutions the iron is thrown out again as hydrate. One can not help but feel that Chevallier must have been unconsciously producing ferrites or ferrates of sodium under his imperfectly described conditions and that the magnetism of his products was associated either directly with these compounds or with their decomposition products. Certainly their behavior with variation of temperature would support this explanation. Chevallier merely suggested that his precipitate was possibly a special micellular colloidal precipitate of ferric oxide which was incidentally ferromagnetic and which was destroyed by gentle heating. His explanation does not seem so probable as that of the writer.

CONVERSION OF FERROMAGNETIC TO PARAMAGNETIC FERRIC OXIDE

When heated to about 700° C. the ferromagnetic ferric oxide having the cubic crystal lattice of magnetite or martite is transformed to paramagnetic hematite which, of course, has rhombohedral crystallization. The unit cube of magnetite may be written $\text{Fe}_{24}\text{O}_{32}$, and after oxidation has the formula $\text{Fe}_{24}\text{O}_{36}$, there seemingly having been enough room in the unit cube to allow entrance of 4 extra oxygen atoms. It would be interesting to know whether on recrystallization to paramagnetic hematite at higher temperature the specific volume of the resulting product is identical with that of crystalline ferric oxide produced by the usual methods.

⁵⁹ Chevallier, Raymond, Sur un nouvel oxyd ferrique ferromagnetique: *Compt. rend.*, t. 184, 1927, pp. 674-676.

The exact temperature of conversion from ferromagnetic to paramagnetic ferric oxide is not well established. Welo and Baudisch say 550° C. Chevallier says that on calcining to different temperatures the ferromagnetism falls off with temperature, decreasing rapidly between 600° and 700°, but is not completely removed even at 745° C. Abraham and Planiol state that the temperature is 650° C. Sosman and Posnjak follow the lead of Hilpert⁶⁰ and distinguish between reversible and irreversible loss of ferromagnetism. They say the irreversible change is slow but noticeable at 500° and becomes rapid at 650° C. It is doubtless associated with the permanent rearrangement of the less stable ferromagnetic molecule to form a more stable (hematite) arrangement of atoms (paramagnetic) and should not be confused with the Curie point. The 678° transition of ferric oxide, involving probable recrystallization, should give excellent opportunity for the magnetism to be lost and is probably the critical point after heating above which very little ferromagnetism will return on cooling in absence of a magnetic field.

CURIE POINT

Reversible loss of ferromagnetism is probably not associated with any molecular rearrangement. It is called the Curie point. The Curie point has been observed for all ferromagnetic substances and is the temperature below which the substance becomes increasingly ferromagnetic with drop of temperature and above which the substance is only paramagnetic. The Curie points of iron and magnetite are definitely known not to be associated with any change in the space lattice of their crystals. The magnetic change is probably associated with the electrons in one of the first three shells of the iron atoms. It is interesting to note that the Curie point of ferromagnetic ferric oxide, slightly above 500°, is considerably lower than the Curie point of magnetite, which occurs at 593.5° C.

The energy change involved in the irreversible polymorphic transformation from ferromagnetic to paramagnetic form has not been measured.

SPECIFIC HEAT

Reliable measurements of the specific heat of ferric oxide exist only in the range from room to liquid-air temperatures. Russel⁶¹ collected three data at the temperatures of ice, carbon dioxide snow, and liquid air by the method of mixtures, and recently Parks and Kelley,⁶² using

⁶⁰ Hilpert, S., Über Beziehungen zwischen chemischer Konstitution und Magnet: Eigenschaften bei Eisenverbindungen: Ber. Deut. phys. Gesell., Jahrg. 7, 1909, pp. 293-299.

⁶¹ Russel, A. S., Messungen von spezifischen Wärmen bei tiefen Temperaturen: Physikal. Ztschr., Jahrg. 13, 1912, p. 59.

⁶² Parks, G. S., and Kelley, K. K., Heat Capacity of Magnetite and Ferric Oxide: Jour. Phys. Chem., vol. 30, 1926, pp. 47-55.

an aneroid calorimeter, collected several data between room temperature and liquid-air temperatures. These data are plotted in Figure 6 and are extrapolated to zero specific heat at 0° K. in accordance with the third law of thermodynamics. Except for work in the tempera-

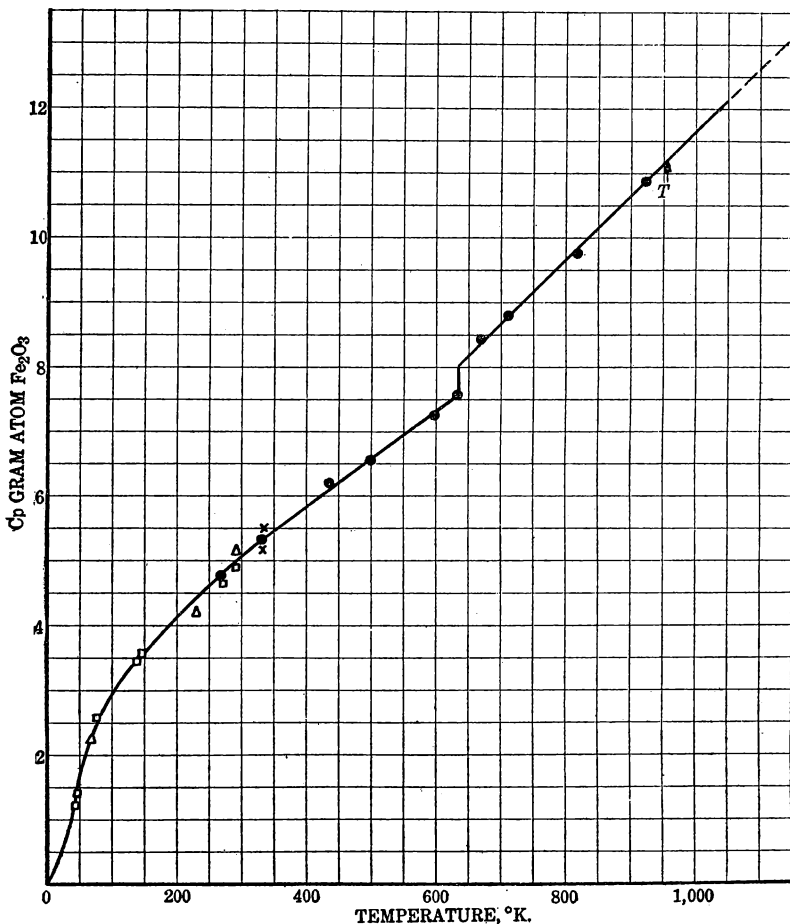


FIG. 6.—Specific heat of ferric oxide: □, Parks and Kelley; ●, Furnas; △, Russel; ×, Regnault, Joly, Oeberg, Abt

ture interval between liquid air and liquid hydrogen, there is little left to be asked on specific heat data below room temperature.

For temperatures above room temperature four older experimenters⁶³ have each obtained a single datum by the method of mix-

⁶³ Oeberg, ———: *Ofs. Stockh.*, vol. 42, 1885, No. 8, p. 43. Joly, J., *On the Specific Heats of Minerals*: *Proc. Roy. Soc.*, vol. 41, 1886, pp. 250–274. Abt, ———: *Sitzungsber. d. Liedenburger-Museums Ver. II, Med. nature*, vol. 42, 96. Regnault, V., *Recherches sur la chaleur spécifique des corps simples et des corps composés*: *Ann. chim. phys.*, t. 3, part 1, 1841, p. 129.

tures, heating the ferric oxide to about the boiling temperature of water and dropping it into a calorimeter at room temperature. The most extensive series of figures has been collected by Furnas, who worked from room temperatures to slightly above 650° C. Representative points from his data are given in the chart, Figure 5. This curve should be accepted only tentatively and needs to be checked because Furnas's method of measurement was entirely new. It consisted in measurement of the thermal diffusivity of ferric oxide, which is a function depending on the thermal conductivity and the specific heat. Furnas's data on the thermal conductivity are given earlier in this paper. He felt that his data were probably accurate to within 10 per cent but had no real comparison of the precision of his method with accepted methods. His data can be summed up by two equations:

$$\text{From } 298^\circ \text{ to } 633^\circ \text{ K., } C_p = 14.13 + 0.0378T \text{ (per mol).}$$

$$\text{From } 633^\circ \text{ to } 951^\circ \text{ K., } C_p = 9.16 + .0491T.$$

His data above 951° K. (678° C.) are disregarded in this paper.

However, from room temperatures up, the specific heat of ferric oxide still needs to be measured by an accepted method.

ENTROPY

Using the specific heat data given above and plotting C_p against the logarithm of the absolute temperature and taking the area under the curve from absolute zero to 298° K. this area is a measure of the absolute entropy of ferric oxide at 298° K. Parks and Kelley performed this operation with their data and arrived at the figure 21.5 calories per degree mol Fe_2O_3 as the absolute entropy of ferric oxide at room temperature. Expressed in the accepted mathematical symbols, this reads, $S_{298} = 21.5$. For the formation of ferric oxide from its elements according to the reaction $2\text{Fe} + 3/2\text{O}_2 = \text{Fe}_2\text{O}_3$, the change of entropy at room temperature is $21.5 - 2 \times 6.87 - 3 \times 24.0 = -64.24 = \Delta S_{298}$. The entropy figure of Parks and Kelley could easily be in error by 0.5 entropy unit, because they had no data between liquid air and absolute zero. The same is true of the entropy figure for iron which is derived later in this paper,⁶⁴ so the above change of entropy estimate for the formation of ferric oxide, due to multiplication, might be in error as much as two units.

Table 5 gives the absolute entropy of Fe_2O_3 and the change in entropy, ΔS , during the formation of Fe_2O_3 at various temperatures. These data were derived from the specific heat data of Furnas, already mentioned. The values for oxygen were computed from the

⁶⁴ The entropy of $1/2 \text{ O}_2$ is the figure given by Lewis and Randall in their text on Thermodynamics of Chemical Substances: 1923, p. 467.

datum of Lewis and Randall, and those for iron were derived from a specific heat plot in which the low-temperature data of Rodebush and Michalek⁶⁵ were used and the high-temperature specific heats data of Oberhoffer and Grosse.⁶⁶

These data are plotted in Figure 7. It is unfortunate that there are no data above 678° C., the temperature of the second transition. Industrially, the interesting temperature range is above 678°, and

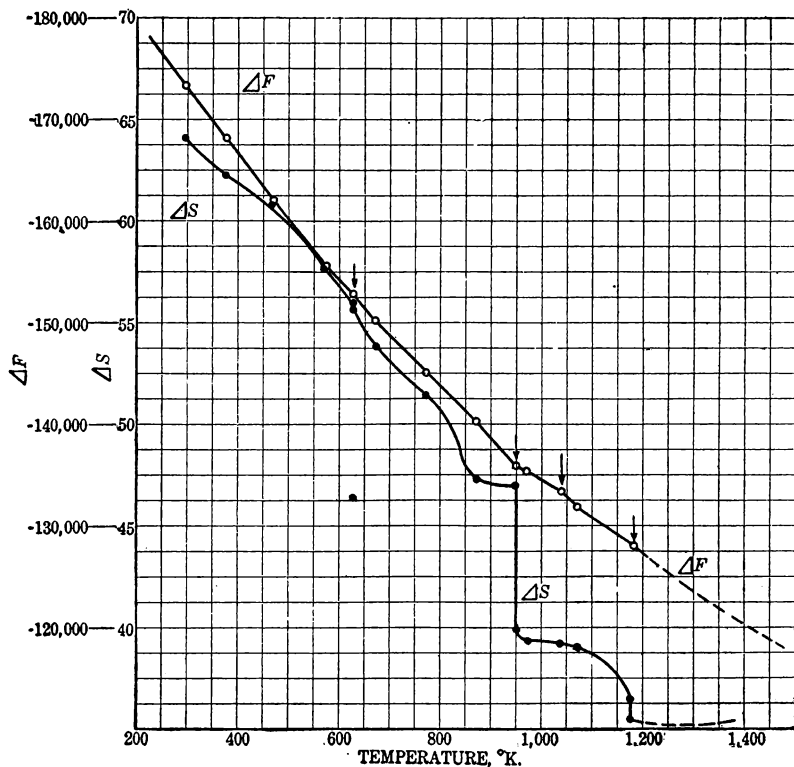


FIG. 7.—Entropy and free energy of ferric oxide: ΔS , Entropy; ΔF , free energy

if the free energy, mentioned later, is to be used to predict the behavior of ferric oxide, the specific heat must be measured through this range.

HEAT OF FORMATION

The value of the heat change when 1 mol of ferric oxide is formed by chemical union of its elements is somewhat doubtful because there are only two determinations available and they differ considerably.

⁶⁵ Rodebush, W. H., and Michalek, J. C., The Atomic Heat Capacities of Iron and Nickel at Low Temperatures; Jour. Am. Chem. Soc., vol. 47, 1925, pp. 2117-2121.

⁶⁶ Oberhoffer, P., and Grosse, W., Die spezifischen Wärme des Eisens: Stahl u. Eisen, Jahrg. 47, 1927, pp. 576-582.

The one most accepted is that of Le Chatelier,⁶⁷ $-197,700$ at 17° C. (When converted to 25° C. the figure used has been $-197,500$ calories per mol. The minus sign is used to signify heat liberated, and a plus sign would mean heat absorbed.) The value determined by Mixter⁶⁸ 20 years later is $-192,200$ calories. For some reason Le Chatelier's older value has gained almost universal acceptance, and Mixter's value has been ignored. One reason for this is that the sodium peroxide calorimetry of Mixter was not so well worked out as the method of acid dissolution used by Le Chatelier; also, Mixter had several corrections to make, such as that due to incomplete reaction. The Le Chatelier datum, however, did not receive the corrections that would be applied to it in modern calorimetry. For instance, no correction was made for the evolution of hydrogen when iron metal is dissolved.

The choice of data has too frequently involved consideration only of the methods and tools used and has often neglected the use of thermodynamics in comparing data from widely differing sources. On the other hand, Tigerschiöld, in his thermodynamic calculations on oxides of iron already mentioned, assumed some specific heats for ferric oxide and magnetite which could be used in connection with the dissociation-pressure data of Sosman and Hostetter and thereby calculated that ferric oxide should have a heat of formation somewhere between $-197,100$ and $-197,900$ calories. However, the Fe_2O_3 specific heat data of Furnas, even though of undetermined precision, have since become available and allow a repetition of Tigerschiöld's calculations with greater, although none too satisfactory, certainty. The calculation gives a figure much closer to that of Mixter and justifies abandoning the old Le Chatelier datum. The equations for his data are as follows:

⁶⁷ Le Chatelier, H., Sur la chaleur de formation de quelques composés du fer: *Compt. rend.*, t. 120, 1895, p. 623.

⁶⁸ See footnote 50, p. 24.

TABLE 4.—Heat capacity of ferric oxide

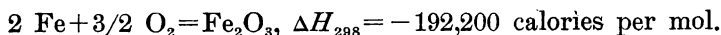
[Molecular weight equals 159.68]

Observers	Temperature		Heat capacity per—			
	° C.	° K.	Gram	Milli-gram atom	Gram molecule	
Parks and Kelley.....		89. 8	0.0404	1. 29		
		273. 3	.0414	1. 32		
		300. 5	.0410	1. 31		
		355. 5	.0445	1. 42		
		148. 4	.0827	2. 64		
		186. 9	.1082	3. 46		
		192. 8	.1109	3. 54		
		196. 3	.1128	3. 60		
		275. 9	.1477	4. 72		
		278. 1	.1488	4. 75		
		289. 1	.1534	4. 90		
		291. 9	.1539	4. 92	24. 60	
	C. C. Furnas.....	0	273	.150	4. 79	23. 95
		20	293	.158	5. 046	25. 23
40		313	.164	5. 238	26. 19	
60		333	.1695	5. 414	27. 07	
80		353	.175	5. 588	27. 94	
100		373	.180	5. 798	28. 74	
160		433	.1935	6. 18	30. 90	
200		473	.2025	6. 47	32. 34	
260		533	.216	6. 90	34. 49	
300		573	.225	7. 186	35. 93	
320		593	.2295	7. 35	36. 65	
340		613	.234	7. 474	37. 37	
360		633	.2385	7. 616	38. 08	
380		653	.2525	8. 064	40. 32	
400		673	.2645	8. 448	42. 24	
450		723	.280	8. 942	44. 71	
500	773	.2955	9. 44	47. 19		
550	823	.311	9. 93	49. 66		
600	873	.326	10. 41	52. 06		
650	923	.342	10. 92	54. 61		
A. S. Russell.....	44 to 3. 7	296. 7	.1600	5. 12	25. 60	
	-74 to 0	236	.1320	4. 22	21. 10	
	-192 to -81	136	.0730	2. 33	11. 65	

TABLE 5.—Ferric oxide, entropy, and free energy

[$2\text{Fe} + 3/2 \text{O}_2 = \text{Fe}_2\text{O}_3$. Based on Parks and Kelley, and Furnas's specific heat data]

Temperature		Absolute entropy			ΔS Calories ° mol	ΔF Calories mol
° C.	° K.	2Fe	3/2 O ₂	Fe ₂ O ₃		
25	298. 1	13. 74	72. 0	21. 5	-64. 27	-173, 050
100	373	16. 56	73. 53	27. 7	-62. 39	-168, 380
200	473	19. 72	75. 19	35. 0	-60. 91	-162, 192
300	573	22. 62	76. 54	41. 6	-57. 56	-156, 230
360	633	24. 07	77. 25	45. 3	-55. 97	-152, 892
360	633	24. 07	77. 25	45. 5	-55. 77	-152, 892
400	673	25. 04	77. 68	48. 8	-53. 92	-150, 688
500	773	27. 42	78. 68	54. 5	-51. 60	-145, 450
600	873	30. 10	79. 58	60. 5	-47. 18	-140, 542
678	951	31. 76	80. 20	64. 96	-47. 00	-136, 868
678	951	31. 76	80. 20	71. 98	-39. 98	-136, 868
700	973	32. 42	80. 37	73. 24	-39. 55	-136, 004
785	1, 041	36. 30	80. 90	77. 68	-39. 52	-133, 282
800	1, 073	36. 32	81. 110	78. 3	-39. 12	-132, 038
906	1, 179	37. 96	81. 81	84. 3	-35. 47	-128, 060
906	1, 179	39. 40	81. 81	84. 3	-36. 91	-128, 060
1, 000	1, 273	By extrapolation of ΔF				-124, 200
1, 100	1, 373	- T plot				-121, 200
1, 200	1, 473					-117, 700



FREE ENERGY

The corresponding free energy change in the formation of 1 mol of ferric oxide is then easily derived from the entropy change and the heat of formation by the relation, $\Delta F = \Delta H - T\Delta S$, $\therefore \Delta F_{298} = -192,200 - 298 \times (-64.24) = -173,050$ calories. (If the Le Chatelier heat of formation is used, the result would be $-178,350$ calories.) Until satisfactory high-temperature specific heat work has been done on ferric oxide and magnetic oxide estimates of free energy at higher temperatures will be only approximate.

Using the entropy data derived from Furnas's specific heats given above and the thermodynamic equation $d\Delta F/dT = -\Delta S$, the free energy at higher temperatures can be calculated. The integral of this last equation can be written:

$$\int_{298}^T \delta\Delta F = - \int_{298}^T \Delta S \delta T$$

Plotting the values of the change in entropy, ΔS , against the absolute temperature and performing the integration mechanically by taking the areas between the desired temperatures with a planimeter, the values of the free energy at the desired temperatures up to 906° C., referred to the above derived free energy datum at 298° as a basis, were derived. They are included in Table 5 and Figure 7. Until better values of the high-temperature specific heats of ferric oxide have been obtained these data can be used for rough calculations.

Although the table of free energies given is based on the Mixer heat-of-formation datum, the free energies as based on the Le Chatelier datum can be obtained by adding $-5,300$ calories to each of the figures in Table 5 or Figure 7.

An interesting comparison with other data is possible. The work of Sosman and Hostetter on the dissociation pressure of ferric oxide can be compared at $1,200^\circ$ C. by use of the well-known thermodynamic relation, $\Delta F = -RT \ln k = -RT \ln p_{O_2}$, for the reaction $6Fe_2O_3 = 4Fe_3O_4 + O_2$. If the free energy of magnetite and the above free energy of the dissociation reaction are known, the free energy of ferric oxide is directly derivable by subtraction (providing the free energy change on dissolving magnetite in a solid solution is not too great). Plotting the author's data on the free energy of ferric oxide and extrapolating to $1,200^\circ$ C. ($1,473^\circ$ K.), one obtains the value, Fe_2O_3 , $\Delta F_{1473} = -117,700$ calories per mol. A figure derived from Eastman's⁶⁹ data on free energy of magnetite can be compared with

⁶⁹ Eastman, E. D., Equilibria in the Systems Iron; Carbon; Oxygen and Iron; Hydrogen; Oxygen and the Free Energies of the Oxides of Iron: Jour. Am. Chem. Soc., vol. 44, 1922, pp. 975-998.

this by likewise extrapolating Eastman's data to 1,200° C., and the result is Fe_2O_3 , $\Delta F_{1473} = -103,425$ calories. The specific heat data of Parks and Kelley at low temperatures and of Weiss, Piccard, and Carrard ⁷⁰ at temperatures up to 670° C. are also available; from these the free energy of magnetite has been calculated. By also extrapolating from 670° to 1,200° C. the value for the free energy of ferric oxide is Fe_2O_3 , $\Delta F_{1473} = -114,525$. This agrees much better with the author's figure than that of Eastman but is thought to be less accurate and illustrates the uncertainty of the present thermal data on the oxides of iron, due to poor data, the long extrapolations necessary, and lack of knowledge of the heat of solution of ferric oxide and magnetite in their solid solutions.

⁷⁰ Weiss, P., Piccard, A., and Carrard, A., *Calorimétrie des substances ferro-magnétiques*: *Arch. sci. phys. nat.*, t. 43, 1917, pp. 113-130.

HIGHER OXIDES OF IRON, FERRITES, AND FERRATES

Oxides with more oxygen than ferric oxide, Fe_2O_3 , have not been formed spontaneously but by decomposition of compounds like ferrites and ferrates in which ferric oxide functions as an acid anhydride.

FERRITES

Ferrites are the most important of the compounds in which iron is present in the acid radical. The minerals magnetite, franklinite, and magnesio-ferrite are among the natural compounds of this nature, and many ferrites of bases have been prepared in the laboratory, although their physical properties are not known in detail. These ferrites are salts of ferrous acid, HFeO_2 or $\text{H}_2\text{Fe}_2\text{O}_4$, an acid difficult to prepare in the free condition, as it tends to split into H_2O and Fe_2O_3 . However, Van Bemmelen and Klobie⁷¹ state that careful hydrolysis of sodium ferrite will give HFeO_2 , which they describe as having the same crystal form and transparency as sodium ferrite and as losing water at temperatures below 100°C .

Most of the ferrites are prepared by heating ferric oxide with more basic oxides to temperatures between 500° and $1,000^\circ\text{C}$. Calcium ferrite is formed by heating lime and ferric oxide together but tends to decompose if heated too near its melting point.⁷² It is deep red to black and crystalline. Several more basic ferrites have been described, but their existence is disputed.⁷³ Lead ferrite has been described by Kohlmeyer.⁷⁴ Ferrites of cobalt, copper, nickel, and zinc are also well known.

The ferrites of zinc⁷⁵ and copper, formed during roasting of their sulphide ores in metallurgical furnaces, cause trouble in hydrometallurgy of the respective metals due to their resistance to dilute sulphuric acid leaching solutions. The oxides of copper and iron, if heated in contact to about 650° , combine to form cupric ferrite, most of which remains undissolved by the ordinary 5 to 10 per cent H_2SO_4 solutions used in the copper-leaching plant. The oxides of zinc

⁷¹ van Bemmelen, J. M., and Klobie, E. A., Ueber das amorphe, wasserhaltige Eisenoxyd, das krystallinische Eisenoxydhydrat, das Kallumferrit, und das Natriumferrit: Jour. prakt. Chem., Jahrg. 154, 1892, p. 497.

⁷² Sosman, R. B., and Merwin, H. E., Preliminary Report on the System, Lime: Ferric Oxide. Jour. Washington Acad. Sci., vol. 6, 1916, p. 532.

⁷³ Campbell, E. D., On the Function of Ferric Oxide in the Formation of Portland Cement Clinker: Jour. Ind. and Eng. Chem., vol. 7, 1915, p. 835; Some Mix-Crystals of Calcium Ferrite and Aluminate: Vol. 11, 1919, p. 116.

⁷⁴ See footnote 19, p. 9.

⁷⁵ Ralston, O. C., Electrodeposition and Hydrometallurgy of Zinc: New York, 1921.

and iron, if heated in close association in a roasting furnace whose temperature is always over 600° C. and frequently over 200° higher, will form zinc ferrite which is dissolved with difficulty and is therefore the cause of considerable loss in zinc-leaching plants.

Zinc ferrite can be decomposed by treatment with stronger acid solutions (20 to 30 per cent of H_2SO_4) at a temperature near boiling (process of U. C. Tainton) or by a hot dilute solution with a longer time of contact (method of Anaconda Copper Mining Co. at Great Falls, Mont.). Being ferromagnetic it can be concentrated magnetically from the remainder of the calcine and treated separately (process of Tainton). During roasting, if the finished product before removal from the furnace is treated with a gas high in sulphur dioxide, the zinc ferrite is decomposed and most of the zinc sulphated. This latter fact was worked out at the zinc-leaching plant of the Consolidated Mining & Smelting Co., Trail, British Columbia. Any carbonaceous reducing agent such as coal dust, on admixture with the hot calcine just before its discharge from the roasting furnace, reduces the zinc ferrite so that the zinc dissolves easily in dilute acid.

Ferrites of the alkali metals are formed by interaction between fused or very concentrated solutions of caustic alkalies and ferric oxide, such as iron rust. In caustic alkali evaporators conditions are always good for the formation of ferrites, and their removal from the caustic constitutes one of the important operations in finishing commercial caustic. Here again the use of reducing agents is the usual method. The sprinkling of sulphur over the top of a pot of molten caustic at the finish of the evaporation is an example of a convenient method of reducing ferrites. The resulting iron oxides settle at the bottom of the caustic pot. Other reducing agents are used, practice varying in different plants, and frequently the exact reducing agent and method of its application are important plant secrets. Not only are there ferrites present in the caustic, but further oxidation by air tends to form higher oxidized compounds like ferrates or perferrates, so that a whole series of brilliant colors from these various compounds, including shades of green, blue, red, brown, and yellow, can be seen frequently in the layers of caustic that creep over the edges of the caustic evaporating pot and come in contact with the air. Dilution of caustic containing ferrites until the solution contains less than 40 per cent of NaOH will precipitate most of the iron as ferrous acid or as ferric hydroxide, depending on the conditions.

FERRATES (OR PEROXYFERRITES)

Ferrates are salts of the hypothetical acid H_2FeO_6 . They are very rare and known only in the anhydrous condition, as they are decom-

posed by water. Barium or strontium ferrates are formed by heating their oxides with ferric oxide in a current of oxygen at about 600° C. Barium ferrate is friable, black, amorphous, and stable up to at least 650° C. Its formation is probably due to the known tendency of barium oxide to form barium peroxide, BaO_2 , which on uniting with ferric oxide would form not barium ferrite but barium ferrate. On treatment with water it decomposes into the oxides and oxygen.

PERFERRATES (OR PEROXYFERRATES)

Perferrates are compounds of the hypothetical acid H_2FeO_4 . They are misnamed and called ferrates by most writers. Three usual methods of forming perferrates are known:

1. The Fremy method is to throw iron filings into molten potassium nitrate, KNO_3 . This has been found by Losana⁷⁶ to give a very poor yield.

2. Calcium perferrate solution can be made by adding ferric chloride solution to a solution of calcium hypochlorite, CaOCl_2 , and boiling.⁷⁷ It can then be used to form other salts such as barium perferrate, which is a purple substance precipitated when barium chloride is added to a solution of the calcium salt. The barium salt is also formed when barium chromate is added to sodium perferrate solution.

3. Sodium perferrate, Na_2FeO_4 , gives an intensely red solution when ferric hydroxide is suspended in caustic soda solution and acted on by chlorine, ozone, or sodium hypochlorite.⁷⁸ The potassium salt can be crystallized into black needles resembling permanganate, and the solution keeps for several days without decomposition.

Losana's studies on perferrates show that the perferrates of silver, barium, strontium, calcium, copper, lead, zinc, nickel, and cobalt can be prepared and dried without decomposition. On the other hand, it was impossible to dry without decomposition the perferrates of aluminium, thorium, ferric, and ferrous iron. All of the perferrates decomposed when raised to the proper temperatures, the barium salt losing water at 108° C. and decomposing at 144° C., the strontium and calcium salts decomposing at progressively lower temperatures, and the nickel and cobalt salts decomposing at 30° C. The vacuum desiccator at room temperatures was used for dehydrating most of the salts, although some of them did not release their water of crystallization under these conditions.

⁷⁶ Losana, L., *Acido ferrico e ferrati*: Gazz. chim. Ital., vol. 55, 1925, pp. 468–497.

⁷⁷ Bloxam, C. L., *Lecture Experiment—the Ferrates*: Chem. News, vol. 54, 1886, p. 43.

⁷⁸ Mailfert, M. l'abbé, *Recherches sur l'ozone*: Compt. rend., t. 94, 1882, p. 860.

IRON FERRITES

Ferrous ferrite, $\text{FeO}\cdot\text{Fe}_2\text{O}_3$ or Fe_3O_4 , is the well-known compound, magnetite, which is quite stable under a wide variety of physical conditions. Ferric ferrite, $\text{Fe}(\text{FeO}_2)_3$, Fe_4O_6 , or Fe_2O_3 , is probably formed when magnetite is heated in air at temperatures not over about 400°C . Enough oxygen is taken up to correspond to the oxidation of the ferrous iron to the ferric state, and yet the product is as strongly magnetic as magnetite. When heated to about 600°C . the magnetism is lost, and the product is then ordinary ferric oxide, which has the same ultimate composition as ferric ferrite, but doubtless a different inner arrangement of the oxygen and iron atoms and their valence electrons.

IRON PERFERRATES

As already mentioned, neither the ferrous nor the ferric perferrates can be formed by interaction of iron salts with solutions of sodium perferrate and subsequent drying, due to decomposition. They are therefore known only in hydrated forms. These perferrates, however, are equivalent to higher oxides than Fe_2O_3 . For instance, ferrous perferrate, $\text{Fe}(\text{FeO}_4)$, is equivalent to 2FeO_2 . Ferric perferrate, $\text{Fe}_2(\text{FeO}_4)_3$, is equivalent to Fe_5O_{12} . Means will doubtless be found ultimately for preparation of these "higher oxides."

THE SYSTEM FERRIC OXIDE-MAGNETITE

Although the properties of ferric oxide and of magnetite are fairly well known and are discussed separately in this publication, the mixtures intermediate between the two are not well understood. There is considerable physicochemical evidence, especially in the work of Sosman and Hostetter,⁷⁹ discussed later, that they form a series of solid solutions at the higher temperatures, but at room temperatures and up to about 1,000° C. their condition is more doubtful. Hematite crystallizes in the hexagonal and magnetite in the regular system and might therefore be suspected of not forming an unlimited series of solid solutions, especially at lower temperatures, although at temperatures nearer their melting points they might do so.

Martite is the natural mineral which approximates the composition of ferric oxide, is pseudomorphic after magnetite, and has doubtless been formed by oxidation of magnetite. It is usually somewhat magnetic and seems to contain some residual unoxidized magnetite. As a result of their high-temperature work indicating a continuous series of solid solutions, Sosman and Hostetter carried out some magnetic studies of various natural iron oxide minerals and decided that martite was magnetic, due to magnetite in solid solution in the hematite. (A ferromagnetic form of ferric oxide is known both as a laboratory product and as a mineral but is extremely ferromagnetic as compared to the faint magnetism exhibited by martite.)

Broderick,⁸⁰ who personally studied natural iron oxide minerals from most of the important districts, has objected to these conclusions. In some of the mineral specimens examined by Sosman and Hostetter and assumed by them to contain solid solutions Broderick finds by microscopic examination of polished surfaces that there is residual magnetite present in free state. The Elba hematite, in which Sosman and Hostetter found zonal distribution of magnetism, and the martite samples all showed residual magnetite. Broderick does not deny that a solid solution of ferric oxide and magnetite might occur in natural minerals but feels that only after the free magnetite has been accounted for and optical homogeneity shown in

⁷⁹ Sosman, R. B., and Hostetter, J. C., The Ferrous Iron Content and Magnetic Susceptibility of Some Artificial and Natural Oxides of Iron: *Trans. Am. Inst. Min. Eng.*, vol. 58, 1918, pp. 409-444.

⁸⁰ Broderick, T. M., Some of the Relations of Magnetite and Hematite: *Econ. Geol.*, vol. 14, 1919, pp. 353-366.

a material containing both Fe_2O_3 and Fe_3O_4 can solid solutions in natural products be established. He has observed certain phenomena which may support the existence of solid solutions of this kind, such as variations of color of reflected light from adjacent grains similarly oriented, apparent lack of enough magnetite to account for all of the magnetic property of the material, and differences in behavior of grains on etching.

HEATING AND COOLING CURVES

While studying the behavior of ferric oxide on heating Kohlmeier⁸¹ found that when sufficiently heated ferric oxide lost oxygen, and the residue was a mixture of ferric oxide and magnetite, depending on the temperature and the time of heating. His cooling curves, therefore, differed considerably from his heating curves and from each other, depending upon the percentage of decomposition that had taken place.

On heating ferric oxide he noticed pauses in the heating curve which are tabulated below, together with the probable explanation of each pause:

- 650° to 700° C. Polymorphic change in Fe_2O_3 .
- 920° to 950° C. Sintering and formation of larger crystals of Fe_2O_3 .
- 1,370° C. Beginning of thermal decomposition of Fe_2O_3 .
- 1,430° to 70° C. First melting phenomenon, unknown compounds of Fe_2O_3 and Fe_3O_4 .
- 1,525° to 75° C. Second melting phenomenon, another unknown compound.

On cooling, pauses were noticed at 1,580° to 1,525°, 1,470°, 1,425°, 1,370°, 1,350° to 1,250° (?), and 1,030° C. At the end of the first pause, near a temperature of 1,525° C., remelting occurred, the surface crust which had formed broke, and liquid welled out from the interior of the mass. The material which did this had approximately the composition $3\text{FeO}\cdot 4\text{Fe}_2\text{O}_3$. The melt which gave the longest pause at 1,470° C. had the composition $3\text{FeO}\cdot 5\text{Fe}_2\text{O}_3$, and the melt which gave the longest pause at 1,370° C. had a composition $\text{FeO}\cdot 3\text{Fe}_2\text{O}_3$. Kohlmeier therefore drew up a temperature-constitution diagram, shown in Figure 8, based on these phenomena and omitting the 1,030° C. point.

Kohlmeier's diagram, while it could explain his heating and cooling curves and lend support to the probability of existence of the three intermediate compounds assumed by him, is not entirely consistent. It assigns a melting point of 1,370° C. to Fe_2O_3 , which is entirely too low, as it probably melts nearer to 1,550° C. One of Kohlmeier's own preparations was heated rapidly to 1,430° C. before

⁸¹ See footnote 19, p. 9.

appreciable decomposition set in, and it did not melt. Also, the melting point of pure magnetite is placed at 1,600° C., whereas the more precise data of Sosman, quoted later, place it at about 1,580° C. The jogs in his cooling curves are certainly significant, but later study of his supposed compounds by Sosman and Hostetter did not lend support to their existence. Instead, at 1,100° to 1,200° C. they found only a continuous series of solid solutions and admit the possibility that $2\text{FeO}\cdot 3\text{Fe}_2\text{O}_3$ is present.

MAGNETIC PROPERTIES

The most complete series of mixtures of iron oxides which has so far been investigated magnetically is that of Huggett and Chaud-

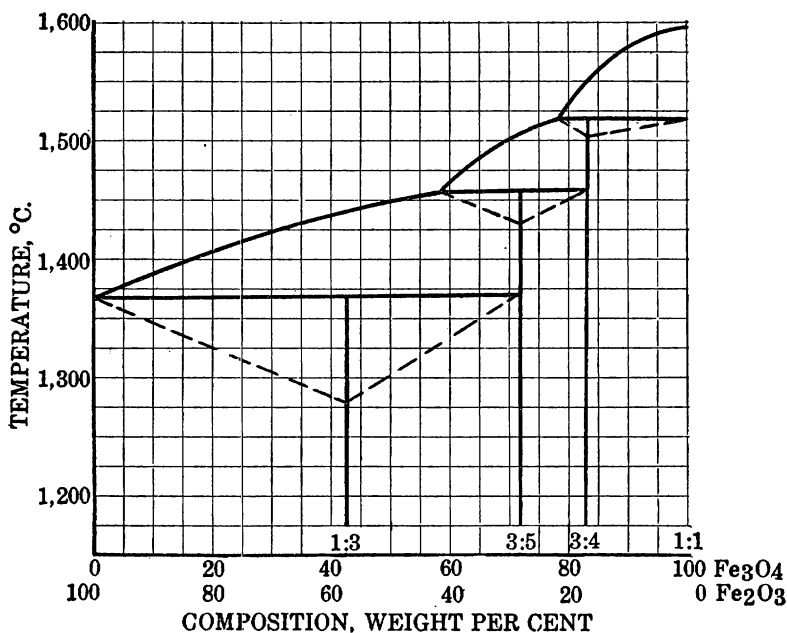


FIG. 8.—Thermal points of the Fe_2O_3 - Fe_3O_4 system (Kohlmeyer)

ron.³² They used ferric oxide, treating it at 500° C. with hydrogen to reduce it partly, weighing the water produced, and stopping at the desired iron-oxygen ratios. The preparations were then homogenized by holding them at 700° C. in vacuo for over 30 hours and then chilling quickly to room temperature. The samples were placed in a recording magnetometer, quickly raised in temperature through 800° C., and cooled again to room temperature. The magnetometer recorded sudden changes in magnetic susceptibility with temperature. The portion of the resulting diagram of temperature of mag-

³² See footnote 46, p. 21.

netic changes as a function of composition is given for the mixtures of Fe_2O_3 and Fe_3O_4 in Figure 9. The regular magnetic transformation of magnetite (Curie point) at 570°C . is observed in all the mixtures up to about 90 per cent of Fe_2O_3 . Moreover, a magnetic anomaly was observed at 670°C . for pure Fe_2O_3 and at 650°C . for mixtures having 10.35 per cent of Fe_3O_4 or more up to 80.54 per cent by weight of Fe_3O_4 , beyond which the anomaly could only be faintly traced but was thought to be further lowered.

About the only way that this curve of Huggett and Chaudron can be interpreted is that up to 10.35 per cent of magnetite the substance is a solution of Fe_3O_4 dissolved in excess Fe_2O_3 , whose

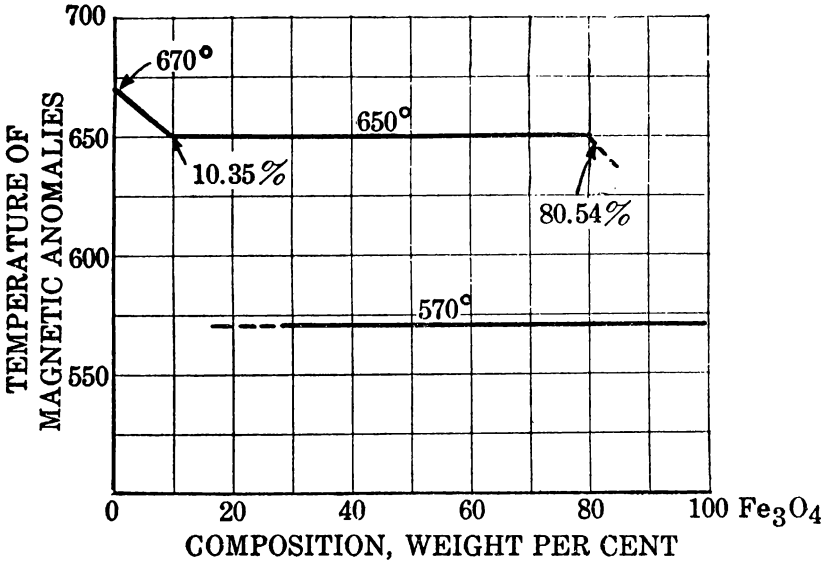


FIG. 9.—Temperature of magnetic anomalies v. composition in Fe_2O_3 — Fe_3O_4 system (Huggett and Chaudron)

transformation point is lowered by increasing amounts of magnetite, until at 10.35 per cent of Fe_3O_4 the solid solution is saturated. Any further addition of magnetite will remain as a new solution of ferric oxide in magnetite, which does not mix with the solid solution of Fe_3O_4 in ferric oxide. When a mixture containing 80.54 per cent of magnetite is reached this is the analysis of a solid solution of Fe_3O_4 which is saturated with Fe_2O_3 , all of the Fe_2O_3 solid solution will be dissolved, and further addition of Fe_3O_4 merely produces solutions of magnetite that are not saturated with ferric oxide. Apparently in the range of compositions tested, the magnetic transformation of magnetite is not altered in temperature by the magnetite being in solid solutions. However, the temperature of

the polymorphic change of Fe_2O_3 is definitely lowered by solution of increasing amounts of Fe_3O_4 in the Fe_2O_3 .

Whether magnetite retains its identity in these solid solutions is questionable. No points were taken with materials containing less than 10.35 per cent of Fe_3O_4 , but it is possible that when magnetite dissolves in ferric oxide it loses its identity, as seems to be the case when magnetite is dissolved in ferrous oxide. Work needs to be done with mixtures containing less than 10.35 per cent of Fe_3O_4 , not only to check this point but to determine more definitely the solubility of magnetite in ferric oxide at 650° to 670° C.

In one experiment ferric oxide was ignited (probably in a gas flame) at $1,100^\circ$ C. for six hours, and the sample was then found to have had its polymorphic transition temperature lowered from 670° to 655° C. The analysis of the sample was not reported. Present knowledge of the properties of ferric oxide indicates that it would lose an extremely small amount of oxygen at $1,100^\circ$ C. in six hours, especially if heated over a gas flame, and would become a solution of magnetite in ferric oxide, the magnetite lowering the transition temperature as reported above.

Sosman and Hostetter, in quantitative magnetic measurements on their samples of solid solutions, found the susceptibility proportional to the FeO (Fe_3O_4) content.

There was no indication of the presence of intermediate compounds in the magnetic work of Huggett and Chaudron or Sosman and Hostetter.

OXYGEN PRESSURE

The oxygen pressure of a series of mixtures of Fe_2O_3 and Fe_3O_4 has been measured at $1,100^\circ$ and $1,200^\circ$ C. in a very painstaking and

TABLE 6.—Oxygen pressure of system Fe_2O_3 - Fe_3O_4

FeO, weight per cent	Fe ₃ O ₄ , weight per cent	Fe ₃ O ₄ , molecular per cent	Oxygen pressure, mm.		Log P_1 , 1,100° C.	Log P_2 , 1,200° C.	ΔH , 1,423° K.
			1,100° C.	1,200° C.			
0.90	2.90	2.01	0.37	5.0	-0.432	0.699	+103,300
1.80	5.80	4.07	.22	3.6	-.658	.557	+111,000
2.71	8.73	6.18	.17	3.0	-.770	.477	+113,900
4.52	14.57	10.50	.13	2.60	-.886	.415	+117,900
9.09	29.30	22.22	.10	2.15	-1.000	.333	+121,700
13.70	44.15	35.25	.092	1.80	-1.036	.255	+118,000
18.37	59.2	50.00	.085	1.55	-1.070	.190	+115,100
23.07	74.4	66.8	.069	1.27	-1.161	.104	+115,600
27.83	89.7	85.9	.052	.85	-1.284	-.070	+111,000
(31.03)	(100.0)	(100.00)	(<.005)	(<.04)	(-2.3)	(-1.4)	+85,200

precise manner by Sosman and Hostetter.⁸³ Ferric oxide was placed in a platinum container in a tube furnace in high vacuum and heated

⁸³ See footnote 36, p. 13.

to a constant temperature. Oxygen was pumped out and the pressure for each step measured. The pressure gradually fell off as more and more ferric oxide was dissociated to magnetite, and on pumping in oxygen again the pressures were measured reversibly.

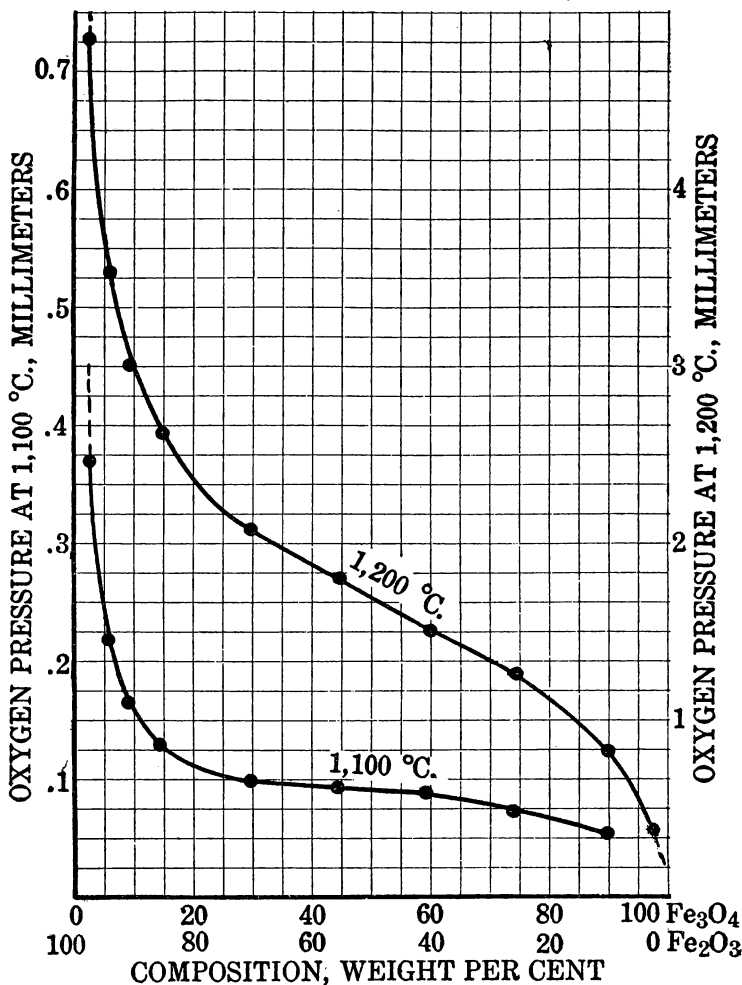


FIG. 10.—Oxygen pressures of the Fe_2O_3 — Fe_3O_4 system (Sosman and Hostetter)

The two isotherms as measured are given in Figure 10. Nearly 50 points were measured on each curve, and great care was taken to reach equilibrium in each case. Representative data from the smoothed curves are given in Table 6, from which Figure 10 was plotted. No evidence, thermal or otherwise, was obtained of the existence of compounds of the two constituents at temperatures above 1,000° C. The shapes of the curves in Figure 10 were interpreted

as showing the existence of a continuous series of solid solutions from Fe_2O_3 to 90 per cent of Fe_3O_4 and indicating the same result for the remaining mixtures. The steeper ends of the curves and the flatness of the central portion of the $1,100^\circ\text{C}$. curve as compared with that of the central portion of the $1,200^\circ\text{C}$. curve, especially when the logarithms of pressures instead of pressures are plotted, lead one to suspect that at some lower temperature a pressure isotherm with a horizontal central portion might be found. Such an isotherm would mean that along the horizontal portion two immiscible solid solutions would be in equilibrium with each other, one being mainly Fe_2O_3 with Fe_3O_4 dissolved in it and the other being the conjugate solution in which Fe_3O_4 predominates. The two sloping ends of the curve would be for a series of unsaturated solid solutions. The magnetic curves of Figure 9 illustrate the type of curve that might be expected for these lower temperature-pressure isotherms. However, the actual magnitudes of the pressures to be measured are so small that they are beyond the range of practical measurement, and other means of studying the system at temperatures below $1,100^\circ\text{C}$. will have to be used. Sosman and Hostetter's work is of such precision that no successful criticism has been leveled against it, although the interpretation of the exact meaning of the curves is subject to debate.

Interpreting their curves as a continuous series of solid solutions of Fe_2O_3 and Fe_3O_4 at $1,100$ and $1,200^\circ\text{C}$., which on investigation at lower temperatures might be found to split into two series of solutions of limited miscibility, it is of interest to deduce thermodynamically any thermal evidence that the data seem to justify.

Using the Clausius-Clapeyron equation so familiar in thermodynamics in the form

$$\frac{d \ln P}{d \left(\frac{1}{T} \right)} = - \frac{\Delta H}{R},$$

where $\ln P$ is the natural logarithm of the oxygen pressure resulting from the reaction $6\text{Fe}_2\text{O}_3 = 4\text{Fe}_3\text{O}_4 + \text{O}_2$, ΔH is the heat of the reaction and will vary according to the composition of the solid solutions of Fe_2O_3 and Fe_3O_4 , and R is the gas constant expressed in calories per mol, 1.985. The use of this equation results in the column of values of ΔH for the absolute temperature, $1,423^\circ\text{K}$., intermediate between $1,100^\circ$ and $1,200^\circ\text{C}$. These are plotted in Figure 11, each calculated point being represented by a circle.

For comparison, the heats of formation of Fe_2O_3 , $6(-192,200)$, and Fe_3O_4 , $4(-265,700)$, are used in the reaction to calculate its heat at room temperature, and if the change in specific heat of the

system is assumed as about -1.6 calories per mol of oxygen, the heat of the reaction at $1,423^\circ \text{K.}$ is calculated as $+88,480$ calories, when 6 mols of pure Fe_2O_3 decompose to give 4 mols of pure magnetite and 1 mol of oxygen gas. This hypothetical point for pure Fe_2O_3 is represented on the plot by a cross, to which the curve for the solid solutions can be easily extended by extrapolation. A similar calculation for the heat of dissociation of pure Fe_3O_4 decomposing to give oxygen and FeO , on the assumption that their heats of forma-

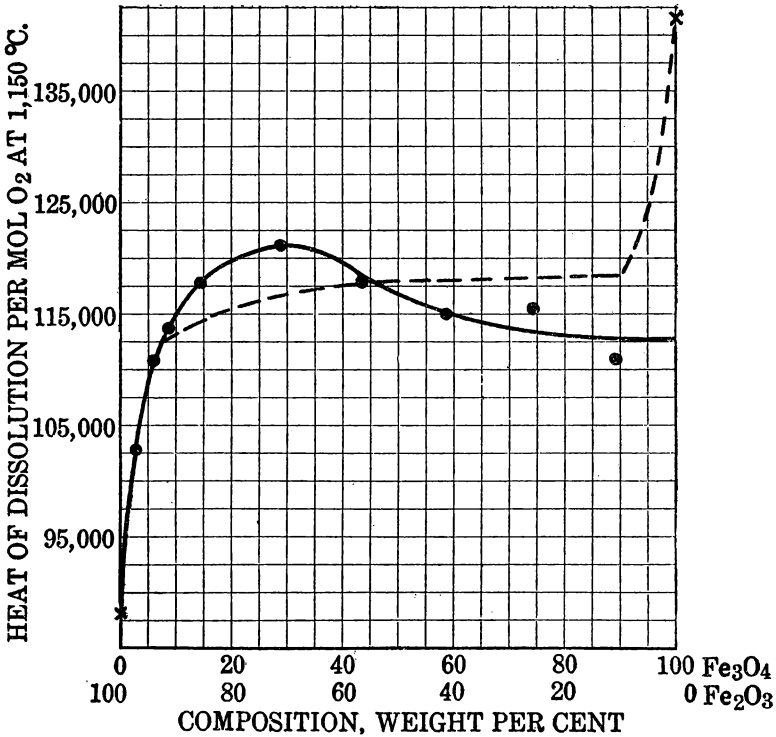


Fig. 11.—Derived thermal data (dissociation) of the Fe_2O_3 — Fe_3O_4 system (after Sosman and Hostetter)

tion are $-265,700$ and $-63,825$ calories per mol, and the change in specific heat of the system with temperature, $C_p = -4.6$, yields the value $+141,950$ calories per mol of oxygen gas for pure Fe_3O_4 . Extrapolation of the plot to this point is not easily justified by the shape of the solid curve drawn through the circles of Figure 11. Small errors in temperatures or pressures make large errors in the calculated heats of reaction. Although the series of points in Figure 11 seems to fall on a fairly smooth curve, the one exception, combined with the knowledge of the limitations in accuracy of this method of calculation, might better justify the dotted curve as a

rough average. It could, of course, then be extrapolated upward to +141,950 calories for pure magnetite. Other thermal work on the mixtures of Fe_2O_3 and Fe_3O_4 would be very instructive. For instance, a series of such samples might be dissolved in acid in a calorimeter and the heats of solution of Fe_2O_3 and Fe_3O_4 in each of their respective solid solutions calculated therefrom. Cooling curves of the various mixtures prepared at high temperatures should also be taken and microscopic examination of polished surfaces of slowly cooled preparations made.

To avoid confusion it should be pointed out that the values of ΔH discussed above are heat absorbed when 1 mol of oxygen gas is evolved by thermal dissociation of Fe_2O_3 in an infinite amount of a solid solution of Fe_2O_3 and Fe_3O_4 , an infinite amount being assumed so that the composition of the solid solution will not change with evolution of 1 mol of oxygen.

Using the Sosman and Hostetter dissociation-pressure data and the values for the heat of formation of Fe_2O_3 and Fe_3O_4 previously accepted ($-197,700$ and $-270,700$ calories) and assuming certain values of specific heats, Tigerschiöld⁸⁴ has derived the equations for oxygen pressure of two series of solid solutions of Fe_2O_3 and Fe_3O_4 at other temperatures. For the solid solutions with 97.1 per cent of Fe_2O_3 the equation reads:

$$\text{Log } P = -20946/T + 3.5 \log T + 0.001157 (T - 600) + 0.061.$$

The solid solutions containing 10.31 per cent of Fe_2O_3 give the following equation:

$$\text{Log } P = -22080/T + 3.5 \log T + 0.001157 (T - 600) + 0.061.$$

These equations would be somewhat modified if the fundamental thermal values chosen by the present writer were to be used but not sufficiently so to make the calculation worth repetition. Tigerschiöld's calculated pressures are therefore used to plot the curves in Figure 12, giving the approximate boundaries of the oxygen pressures of the series of solid solutions of Fe_2O_3 and Fe_3O_4 . The field of stability of pure Fe_2O_3 , as far as oxygen pressure and temperature are concerned, is thereby outlined as well as the field for Fe_3O_4 or its decomposition products.

One other series of data on the solid solutions of Fe_2O_3 and Fe_3O_4 deserves consideration but must be discarded. Ruer and Nakamoto⁸⁵ prepared pure ferric oxide and passed nitrogen gas over it in a heated combustion tube with gradually rising temperature, periodically removing the boat to be weighed. Their product lost no weight

⁸⁴ See footnote 38, p. 19.

⁸⁵ See footnote 32, p. 15.

until 1,150° C. was reached (see fig. 13) and then suddenly lost weight until a product consisting of about 98 per cent of Fe_3O_4 and 2 per cent of Fe_2O_3 remained. This required further heating in the stream of nitrogen, and the temperature-composition curve is shown in Figure 13, weight continuing to be lost even after the product was completely converted to Fe_3O_4 and part of the Fe_3O_4 was decomposed, leaving FeO . Ruer and Nakamoto take their flat curve at 1,150° C. to mean that there are no solid solutions until the product with 98 per cent of Fe_3O_4 is reached and consider that they have disproved Sosman and Hostetter's continuous series of solid solutions. Trans-

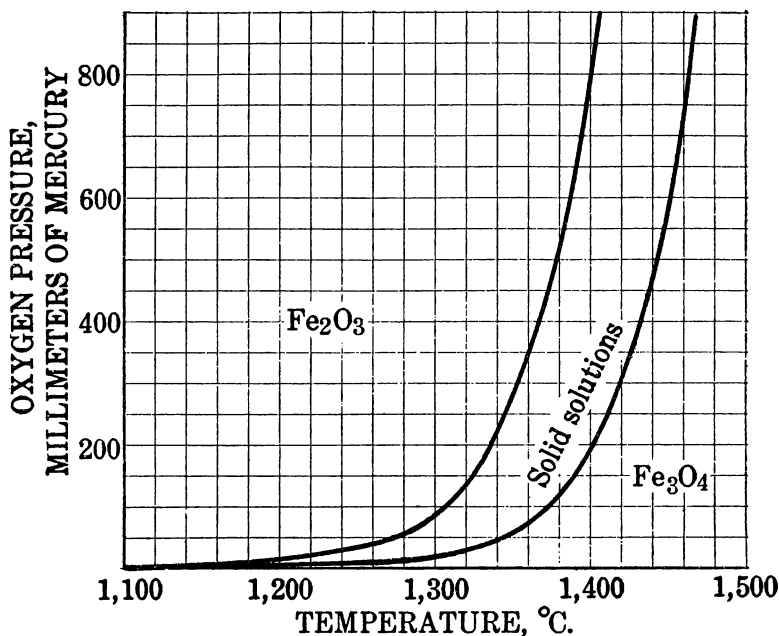


Fig. 12.—Oxygen pressure v. temperature for the Fe_2O_3 — Fe_3O_4 system (derivations by Tiggerschiöld)

formation of ferric oxide into magnetite was almost complete in 12 hours at 1,200° C. and took 50 hours at 1,175°. No effect whatever was noticed at 1,100° C. This fact, contradicting the results obtained by all other observers, who have found increase in magnetism and other signs of decomposition at 1,100° C., together with the fact that Sosman and Hostetter have actually measured the oxygen pressures at 1,100°, makes the Ruer and Nakamoto data rather than those of Sosman and Hostetter of doubtful value. The fact that more heat was needed to break up the last traces of Fe_2O_3 seems to support the probability at least of the existence of solid solutions of Fe_2O_3 in Fe_3O_4 , because the 2 per cent Fe_2O_3

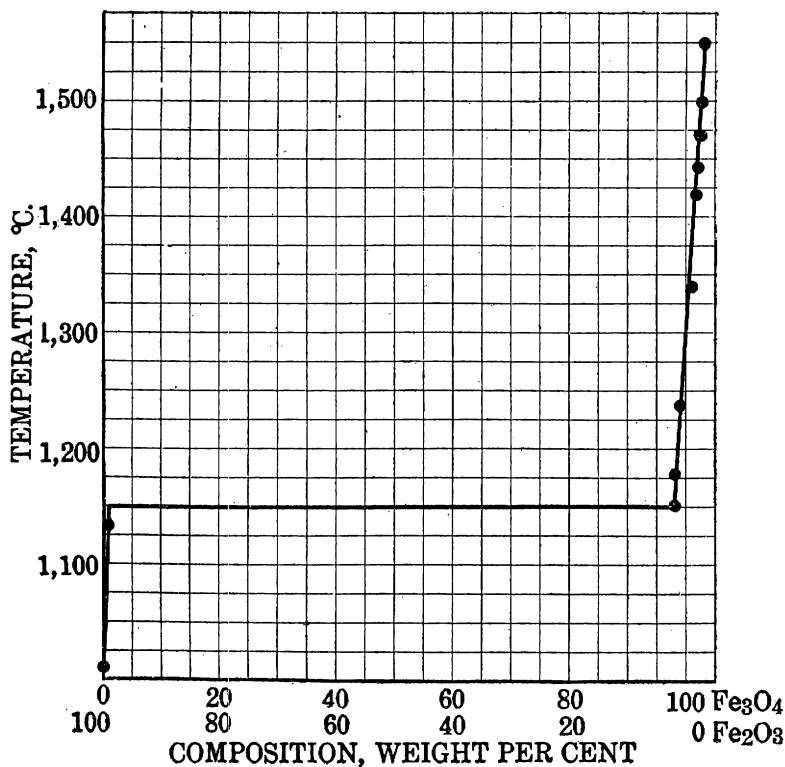


FIG. 13.—Dynamic experiments with Fe_2O_3 — Fe_3O_4 system; residues after heating in air (Ruer and Nakamoto)

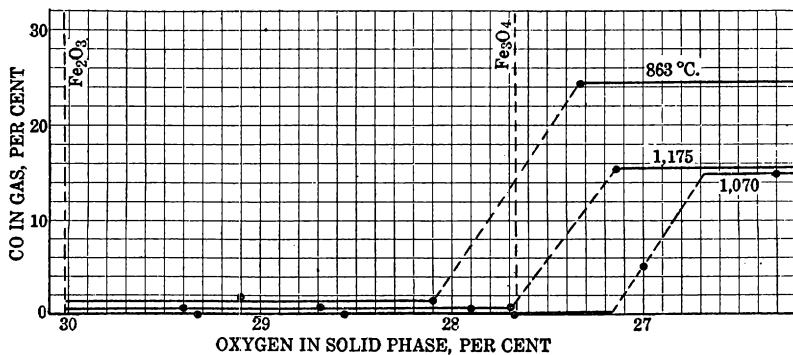


FIG. 14.—Reduction isotherms of Matsubara. Insufficient number of points between 27 and 28 per cent oxygen to permit drawing any conclusions

analysis at 1,150° C. is in reasonable agreement with the observation of Sosman and Hostetter that the oxygen pressure was falling off rapidly at this composition.

REDUCTION ISOTHERMS

Starting with pure ferric oxide, a number of experimenters, whose work is to be discussed in detail later, have treated it at various constant temperatures with successive amounts of reducing gas, allowing the gas and solid to come to equilibrium after each addition and periodically analyzing the gas. Using carbon monoxide Matsubara⁸⁶ found that it was practically quantitatively converted to CO₂ and that apparently the reaction was irreversible. The point at which all of the free ferric oxide was converted to magnetite might be expected to show a certain amount of CO in the gases, and from there on removal of oxygen from the solid would demand increasing proportions of CO in the equilibrium gases. Neither Matsubara nor any experimenter who followed him took enough points on their isotherms to show any such point; therefore, while the method might yield valuable results to date, it has been inconclusive. The portions of Matsubara's isotherms of interest in this chapter are given in Figure 14.

OPTICAL PROPERTIES

Sosman and Hostetter also studied the optical properties of their chilled solid solutions, determining the index of refraction with proper liquids for comparison. The index seemed to vary continuously, without indication of breaks, up to the point where the opacity due to high Fe₃O₄ content (about 50 per cent) prevented further observation, thus supporting their claim of a continuous series of solid solutions.

⁸⁶ Matsubara, A., Chemical Equilibrium Between Iron, Carbon, and Oxygen: Trans. Am. Inst. Min. and Met. Eng., vol. 67, 1922, pp. 3-55.

MAGNETITE

CHARACTERISTICS

The mineral magnetite, Fe_3O_4 , is one of the most stable oxides of iron. It occurs in many terrestrial rocks and in meteorites, being formed under a very wide variety of circumstances. The natural forms are rarely hydrated, although hydrates with one and with one and one-half molecules of water of crystallization have been prepared in the laboratory. Magnetite ores are found in commercial quantities in many different localities and are worked especially in Sweden and the United States.

The formula Fe_3O_4 does not properly describe the compound, as it really consists of a ferrite of ferrous iron, $\text{FeO}\cdot\text{Fe}_2\text{O}_3$ or $\text{Fe}^{++}(\text{Fe}_2\text{O}_4)^{-}$. It has been variously called ferrous ferrite, ferrosferric oxide, and magnetic iron oxide, but all of these names are cumbersome in comparison with the name magnetite, which has come to mean not only the natural mineral but is quite generally understood to include the artificially prepared Fe_3O_4 . The name magnetite is quite naturally associated with the most prominent physical property of the mineral, that of being ferromagnetic, and is connected with the history of its discovery. The Greeks found it in Asia Minor in a region called Magnesia and the word magnet therefore had this origin, the early specimens noticed having been strongly magnetic lodestone. The magnetic quality seems to be associated with ferric oxide, which is frequently magnetic when it acts as an acid in a salt, other ferrites also being ferromagnetic. Magnetite constitutes one of the steps in the reduction of ferric oxide to metal.

As a mineral magnetite is rarely known in the pure state, but usually either part of the ferrous oxide is replaced by some other base like MgO , NiO , MnO , or CaO , or the acid end of the compound, Fe_2O_3 , is replaced in part by Al_2O_3 , Cr_2O_3 , or even TiO_2 . Magnetite therefore shades off into other spinel minerals like franklinite, ilmenite, and chromite. The octahedral crystals are well known, and the other physical characteristics by which the mineralogist identifies it are discussed below.

Color.—Magnetite, even in a finely divided or freshly precipitated condition, is always black. It is so opaque that little is known of its optical characteristics, although when found in very thin flakes in mica it permits passage of a little light.

Cleavage.—The well-crystallized forms sometimes cleave along planes parallel to the octahedral crystal faces, but this is not a pronounced tendency. Usually the break is uneven.

Hardness.—On the Mohs scale the hardness varies from 5.5 to 6.5, according to texts on mineralogy.

Specific gravity.—The density of magnetite varies considerably with its state of agglomeration or crystallization. The finely divided material formed at low temperatures has a specific gravity⁸⁷ as low as 4.86, but the well-crystallized material⁸⁸ shows a specific gravity of 5.168 to 5.18.

Compressibility.—No data on the elastic properties such as compressibility or tensile and compressive strength of magnetite are available.

METHODS OF PREPARATION

To form a compound of the exact formula Fe_3O_4 is somewhat difficult, as it forms solid solutions with FeO and probably with Fe_2O_3 , and slight errors in some of the methods of preparation will result in one of the solid solutions.

According to Doelter,⁸⁹ synthesis of magnetite in silicate melts is quite common, although no mention is made of the purity of the Fe_3O_4 formed. The writer has also noticed that when air gains access to the surface of an otherwise clear melt of a ferrous silicate, blackening results, due to formation of a cloud of magnetite particles. Mineralogically the substance formed in this manner is magnetite, but it probably has some silicate in solid solution. Doelter also states that the heating of double ferrous ammonium chloride to red heat, presumably in the presence of water vapor, leaves crystallized magnetite. F. Kuhlmann⁹⁰ heated calcium chloride and ferrous sulphate in a closed crucible and obtained magnetite. Gorgeu⁹¹ heated metallic iron with ferric sulphate until gas evolution ceased and the iron was converted to magnetite.

Many products resulting from the surface oxidation of pieces of iron are called magnetite, especially the roll scale from rolling mills, but these products are of variable composition, their outer surfaces frequently being altered almost completely to ferric oxide and the inner layers having an excess of FeO , ratios as high as $6\text{FeO}\cdot\text{Fe}_2\text{O}_3$ being reported. Oxygen seems to penetrate the surface of metallic iron at the grain boundaries first, and the corroded spaces then grow bigger.

⁸⁷ See footnote 23, p. 10.

⁸⁸ See footnote 20, p. 9.

⁸⁹ See footnote 39, p. 20.

⁹⁰ des Cloizeaux, M., Sur la forme des cristaux artificiels de fer oligiste produits dans les fours de M. Kuhlmann: Compt. rend., t. 52, 1861, p. 1325.

⁹¹ Gorgeu, A., Sur le ferrite de fer—production artificielle de la magnétite: Bull. Soc. Min., t. 10, 1887, p. 174.

The surface layer of oxidized iron has been examined by means of reflected X-rays by Bozorth.⁹² He found that the layer adjacent to unaltered iron gave almost entirely the diffraction pattern of ferrous oxide, with only a few faint lines suggesting the spectrum of magnetite, but that magnetite was present near the outer surface and the very skin gave the spectrum of ferric oxide.

A more reliable method of preparation is to heat finely divided iron at any temperature above 500° C. in a stream of water vapor or carbon dioxide. The treatment must be prolonged to convert all the FeO to Fe₃O₄. Friend⁹³ recommends the use of steam and strips of sheet iron at 820° C., avoiding contamination with carbon, which might result from splitting of the oxides of carbon if CO₂ were used. Joannis also recommends heating FeCO₃, ferrous carbonate, in a stream of CO₂ at over 400° C., but Friend's suggestion to use water vapor instead of CO₂ might be of value even here.

Mosander⁹⁴ obtained magnetite by heating ferric oxide to 1,500° C. in a stream of nitrogen. This method has a good theoretical background, as ferric oxide should have several atmospheres dissociation pressure at this temperature, and although the oxygen pressure of the solution of Fe₂O₃ in Fe₃O₄ falls off as the composition of the solid or liquid solution approaches that of pure magnetite, the stream of nitrogen should ultimately carry off all the necessary oxygen. However, magnetite has a dissociation pressure of its own, and prolonged heating is likely to cause further loss of oxygen and formation of the solid solution of magnetite and FeO. Probably the best procedure is to heat such a sample of ferric oxide until it has lost enough weight to leave the proper ratio of oxygen to iron, irrespective of whether the surface layers may have some free ferrous oxide and the centers of the particles some undecomposed ferric oxide. Standing in vacuo for several days at about 1,000° C. should allow homogenizing of this product and the travel of oxygen from a place of high oxygen pressure to one of low oxygen pressure until the whole system is equalized. Huggett and Chaudron, in work discussed later in this paper, introduced the idea of homogenizing their product and kept all of their iron oxide preparations at 650° in vacuo for 30 hours. Their low temperature would avoid sintering and sealing up of portions of the mass, so that readjustment of its oxygen content could take place with ease.

⁹² Bozorth, R. M., Structure of the Protective Coating of Iron Oxides: Jour. Am. Chem. Soc., vol. 49, 1927, pp. 969-976.

⁹³ Friend, J. N., Hull, T. E., and Brown, J. H., The Action of Steam on Iron at High Temperatures: Trans. Chem. Soc., vol. 99, 1911, p. 969.

⁹⁴ Mosander, C. G., Untersuchungen des sogenannten Eisen-Hammerschlags: Pogg. Annalen, Jahrg. 6, 1826, p. 35.

On the other hand, higher temperatures should encourage diffusion through the solid, and certainly a more definitely crystalline product should form. Further study of homogenizing temperatures for systems of this type would be useful.

Thompson⁹⁵ states that if ferric oxide is strongly heated for 12 hours at about 1,169° with excess sodium chloride it is converted into black crystals of magnetite. Strong heating probably means a temperature above 1,100° C., at which point the dissociation pressure of ferric oxide becomes appreciable and the sodium chloride would be molten and would act more or less as a solvent, permitting solution and splitting of Fe_2O_3 , and crystallization of Fe_3O_4 . One must certainly keep the oxygen pressure of the space above the melt lower than the oxygen pressure of the melt, and therefore vacuum operation or passage of a stream of nitrogen would be advisable.

Direct reduction of ferric oxide with a stream of hydrogen saturated with water at 30° to 50° C. is reported by Hilpert and Beyer,⁹⁶ the proper temperature or reaction being 400° C. This method is also attractive from a theoretical standpoint because the ferric oxide is easily reduced by even a small percentage of hydrogen in the reducing gas, and at all temperatures below 570° C. ferrous oxide is metastable and not likely to form. Therefore, if enough water vapor is maintained in the mixture to prevent reduction of any magnetite to iron metal, the final product should approximate closely the analysis of magnetite.

Wet methods of producing magnetite have two disadvantages: Water of hydration is difficult to eliminate and the products always oxidize somewhat during drying, so that the usual final product contains ferric oxide and rarely exceeds 90 per cent of magnetite.⁹⁷ The usual wet method of preparation is to mix ferrous and ferric sulphates in proper proportions and then to pour the resultant solution into an excess of strong caustic soda solution. The two hydroxides precipitate simultaneously and form a black magnetite hydrate. Ferrous hydroxide prepared in the same manner can be fractionally oxidized by air to magnetite, but the method is not quantitative. Baudisch and Welo found nitric oxide gas a good reagent for oxidizing precipitated ferrous hydroxide to hydrated magnetite by bubbling through the freshly prepared pulp.

⁹⁵ Thompson, H. V., *The Dissociation of Salt*: Trans. Ceram. Soc., vol. 17, pt. 2, 1918, p. 340.

⁹⁶ Hilpert, S., and Beyer, J., *Über Eisenoxyduloxylde und Eisenoxydul*: Ber. Deut. chem. Gesell., Jahrg. 44, 1911, pp. 1608-1619.

⁹⁷ Baudisch, O., and Welo, L. A., *Studies on Precipitated Magnetite*: Phil. Mag., vol. 3, 1927, pp. 396-410.

CHEMICAL PROPERTIES

The behavior of magnetite differs greatly according to its method of preparation. The low-temperature preparations are all very reactive and will react with acids or gases toward which the crystallized forms prepared at high temperatures are almost inert. Moissan⁹⁸ noticed that nitric acid would easily dissolve the low-temperature form but not the high-temperature form into which it is convertible by heating. Most forms of magnetite are completely soluble in hydrochloric acid, although the higher temperature forms are dissolved with more difficulty. Hydrofluoric acid will dissolve a powdered sample only with a long time of contact. Bisulphate fusion converts it into ferric oxide slowly.

Magnetite weathers to hematite, and the product is often pseudomorphic after magnetite (martite) and is magnetic. On heating in air⁹⁹ active oxidation does not begin until about 400° C., but the Fe₂O₃ formed seems to act as a protective skin and retards the reaction. The oxidation is only 95.6 per cent complete even after 100 hours at 1,000° C. Above that the rate increases more rapidly, as it is nearly complete in two hours at 1,100° C. and in one hour at 1,200° C. Above 1,380° no further reaction can be caused to take place, and when heated above 1,450° the ferrous iron content of the final product was about the same as that of the original magnetite. At 1,500° and 1,550° the product formed had excess FeO as though part of the magnetite had decomposed, lost oxygen, and been converted to FeO.

The loss of oxygen at higher temperatures was reported by Sosman and Hostetter,¹ who found that when held in platinum containers at high temperatures magnetite loses oxygen and the resulting iron dissolves in the platinum. Under low oxygen pressures this took place at as low as 1,400° C. Platinum acted as a reducing agent to this extent, the activity of metallic iron in a dilute solution with platinum being much lower than the activity of pure iron toward oxygen.

The precipitated hydrated forms of magnetite are quite active and even on standing in dry air² alter slowly to the chocolate-brown ferromagnetic ferric oxide.

CRYSTAL SYSTEM

Magnetite forms characteristic octahedrons in the regular system, with minor occurrences of other crystal faces recorded in the miner-

⁹⁸ Moissan, H., Sur les oxydes métalliques de la famille du fer: Ann. chim. phys., t. 21, 1880, p. 199.

⁹⁹ See footnote 14, p. 7.

¹ See footnote 36, p. 18.

² See footnote 51, p. 24.

alogy texts. No other crystal lattice for magnetite is reported at ordinary temperatures, and there seems to have been no X-ray studies at other temperatures. The X-ray data are given by Wyckoff³ and by Bozorth,⁴ who state that the edge length of the unit cube in the crystal lattice is 8.374 Å. O. Claasen,⁵ in a more recent determination, gives 8,400 Å. U.

POLYMORPHISM

Little reliable evidence of any polymorphism of magnetite exists. It has some strange transitions in several curves with which energy is associated, but they remain to be studied by the X-ray method. For instance, Parks and Kelley⁶ and R. W. Millar (results unpublished) in their specific heat curves found a sharp peak at about 117° K. (−156° C.). The magnetite might have a different crystal form below this point. Also, on heating through 593.5° C., Weiss, Piccard, and Carrard⁷ found a similarly shaped peak in the specific heat curve and a contemporaneous change in the magnetization (transition from ferromagnetic to paramagnetic substance) which has been proved to have no association with a change in crystal structure in the case of iron. On the other hand, during some work on electrical conductivity of magnetite as a function of temperature Königsberger and Schilling found that their test pieces of crystalline magnetite tended to break and split in the temperature range between 500° and 600° C. Such splitting and breakage usually occur at a polymorphic transition, as in the case of quartz, which crumbles like cube sugar when a crystal is heated above its 573° C. transition and then quenched.

BEHAVIOR WITH TEMPERATURE CHANGE

The two discontinuities in the specific heat curve mentioned above are the most prominent results of heating magnetite. The facts that rapid oxidation in air begins at about 400° C. and that the chemically active forms produced at low temperatures sinter or agglomerate at about red heat into much less active but more definitely crystalline forms are important. The calcined form of magnetite is probably the most definite molecular condition. Changes in the electrical conductivity and other properties of magnetite, including its melting point and dissociation pressure, are discussed below.

³ Wyckoff, R. W. G., and Crittenden, E. G., *The Preparation and Crystal Structure of Ferrous Oxide*: Jour. Am. Chem. Soc., vol. 47, 1925, pp. 2876–2882.

⁴ See footnote 92, p. 55.

⁵ Claasen, A. A., *The Scattering Power of Oxygen and Iron for X Rays*: Proc. Phys. Soc. London, vol. 38, 1926, pp. 482–487.

⁶ See footnote 92, p. 29.

⁷ See footnote 70, p. 36.

MELTING POINT

The only thing certain about the melting point of magnetite is that it falls above $1,500^{\circ}$ C. Sosman⁸ has the most definite and probably the most accurate statement about its melting point. He says that magnetite melts to a mobile liquid at $1,580^{\circ}$ C. Hilpert and Kohlmeyer⁹ in earlier and less precise work found it to be $1,527^{\circ}$ C. if palladium melts at $1,541^{\circ}$ C., but $1,527^{\circ}$ must be corrected to $1,541^{\circ}$, due to the melting point of palladium now being given as $1,555^{\circ}$ C. Kohlmeyer¹⁰ later published a melting diagram of the system $\text{Fe}_3\text{O}_4\text{-Fe}_2\text{O}_3$, in which the melting point of magnetite is given as $1,600^{\circ}$ C. This is in quite reasonable agreement with the datum of Sosman, which is therefore chosen herein as the best available. Magnetite has been fused in industrial quantities to produce fused magnetite electrodes for anodes in electrodeposition of copper. It was used in the copper-leaching plant at Chuquicamata,¹¹ Chile, during 1913 and 1914, the brittle slabs of cast magnetite being made in Germany.

DISSOCIATION PRESSURE

Although the "reduction" of magnetite by platinum indicates an appreciable dissociation pressure, no measurable dissociation pressure has been observed. If satisfactory values of the free energy of magnetite at higher temperatures were available, it could be calculated. However, the fact that on heating to $1,550^{\circ}$ C. as much as 3 per cent excess FeO was found in the resulting mass shows that the oxygen pressure at this temperature is appreciable and explains the uncertainty in the melting-point determinations, doubtless caused by lowering of the melting point of the magnetite through contaminations by ferrous and ferric oxide. Experimental difficulties have to date prevented direct measurement of the oxygen pressure at these high temperatures.

ELECTRICAL CONDUCTIVITY

Data on the conductivity of magnetite and its reciprocal resistance are conflicting and very unsatisfactory. At ordinary temperatures magnetite is not as good a conductor as copper, Weintraub¹² giving the conductivity as 0.0116×10^4 reciprocal ohms per

⁸ Sosman, R. B., Some Problems of the Oxides of Iron: Jour. Washington Acad. Sci., vol. 7, 1917, pp. 55-72.

⁹ See footnote 30, p. 15.

¹⁰ See footnote 19, p. 9.

¹¹ Smith, E. A. C., Leaching and Electrolytic Treatment of Copper Ores at Chuquicamata, Chile: Trans. Am. Electrochem. Soc., vol. 25, 1914, pp. 193-206.

¹² Weintraub, E., The Conductivity of Solids: Trans. Am. Electrochem. Soc., vol. 21, 1912, pp. 49-67.

centimeter as compared to 64×10^4 reciprocal ohms per centimeter for copper. Data on the temperature coefficient are exceedingly conflicting, as will be shown later. Common experience, however, shows that the conductivity increases considerably with rise of temperature.

Brown¹³ became interested in magnetite as a resistance thermometer and prepared shapes of fused magnetite. (Most fused magnetite will not have exactly the ratio of oxygen to iron given by the chemical formula Fe_3O_4 but will be deficient in oxygen.) The specific electrical resistance at 20° C. was 562.5 ohms per cubic centimeter, and over the range -3° to $+365^\circ$ C. the following interpolation formula can be used: $R_t = R_{20} (1.82 - 0.0524 t - 0.00057 t^2)$. The 20° C. datum

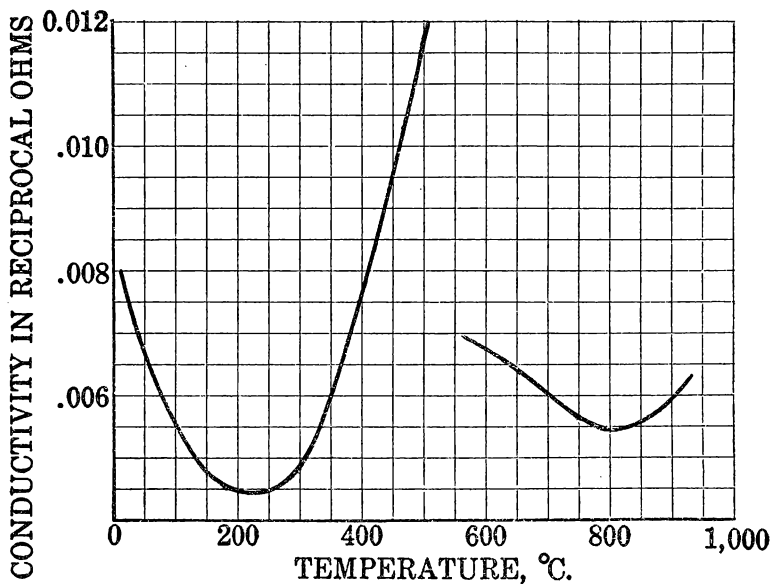


FIG. 15.—Electrical resistance of magnetite (Königsberger)

corresponds to a specific conductivity of 0.00178 reciprocal ohm per cubic centimeter, which is an entirely different magnitude from the figure quoted by Weintraub, but agrees in magnitude with the work of Königsberger and Schilling,¹⁴ who found a minimum in the conductivity-temperature curve at 220° C. (See fig. 15.) This does not agree well with the Brown equation given above, which, if rewritten in reciprocal, shows no maxima or minima in the interpolation range but would indicate a minimum in conductivity at about -5° C., which may be entirely due to the limitations of the quadratic

¹³ Brown, S. L., A New Form of Resistance Thermometer: *Phys. Rev.*, vol. 5, 1915, pp. 126-135.

¹⁴ Königsberger, J., and Schilling, K., Über Elektrizitätsleitung in festen Elementen und Verbindungen, I: *Ann. Phys.*, Jahrg. 32, 1910, pp. 179-230.

equation during extrapolation. Königsberger and Schilling's data were carried to almost 500°C . and then skipped to a higher temperature range from 550° to 905°C . A second minimum is shown in this higher temperature range at 815°C . (See fig. 15.) The investigators concluded that there was a discontinuity at about 530°C . because a number of their samples broke on passing through this temperature, a phenomenon attributed to a polymorphic change. This work was done on rods of magnetite cut from large natural crystals in the Moriah mine near Port Henry, N. Y. The data above 500°C . are to be accepted with caution, in view of the work of Mlle. Veil.¹⁵ The conductivity-temperature curve of Mlle. Veil given in Figure

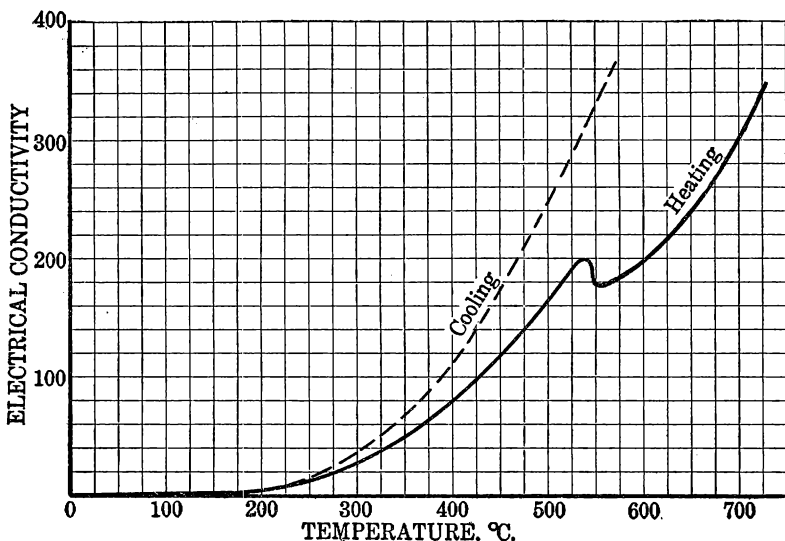


FIG. 16.—Electrical conductivity of magnetite (Veil)

16 covers a longer temperature range, but her conductivity units are in doubt. Her interest was in the possible revelation of allotropism by the curve, hence absolute units of conductivity are to be ignored. Her curve shows an anomaly beginning at about 500°C ., causing a sharp drop in conductivity at about 550°C ., but it is of much less magnitude than the drop found by Königsberger and Schilling. The curve then continues to rise, although the effect of the anomaly is shown as far up as 575°C . on her curve.

Apparently these irregularities in electrical conductivity are to be associated with the loss of ferromagnetism and the Curie point and with the abnormal specific heat of magnetite through this same range.

¹⁵ Veil, S., Variétés allotropiques d'oxydes: *Compt. rend.*, t. 172, 1921, pp. 1405-1407.

MAGNETIC PROPERTIES

Mention has already been made of the Curie point at 530° to 593° C., according to the observer consulted, below which magnetite is ferromagnetic and above which it is only paramagnetic. The Curie point is therefore frequently called the magnetic inversion temperature. It was originally supposed to be a sharp discontinuity in the curve of the susceptibility or permeability plotted against the temperature, but on close examination it has been found that the

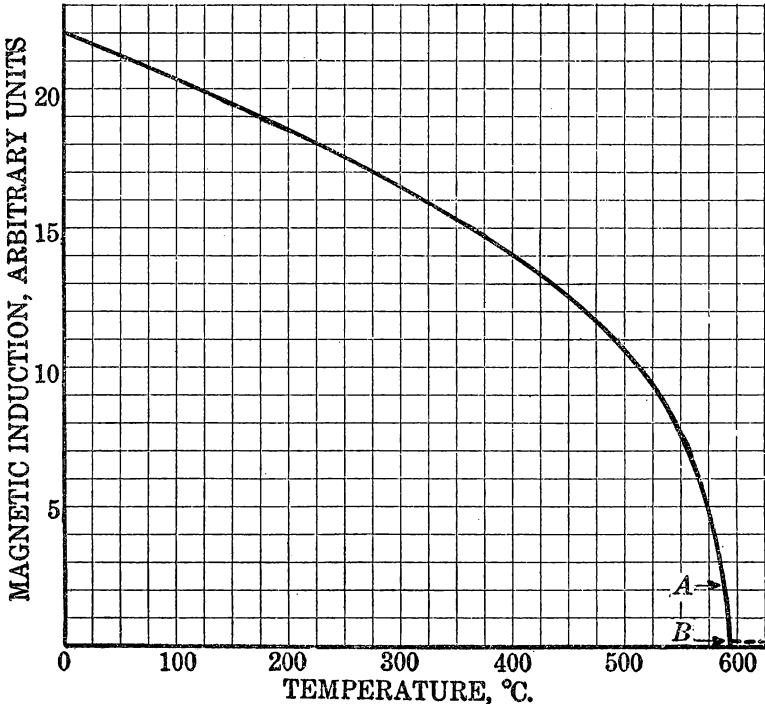


FIG. 17.—Intensity of magnetization v. temperature for magnetite (Weiss and Beck). Curie point at 588° C.

apparent sharp change of direction is not real and there is a continuous transition from the ferromagnetic to the paramagnetic state. Figure 17 gives a collection of data derived from Weiss and Beck¹⁶ of the intensity of magnetization I in arbitrary units as a function of temperature for magnetite up to the Curie point, which in this particular case was estimated at 588° C. Actually, the intensity does not fall off completely to zero but to a low nearly constant value such as that indicated by the dotted line for higher temperatures.

¹⁶ Weiss, P., and Beck, P. N., Chaleur spécifique et champ moléculaire des substances ferromagnétiques: Arch. sci. phys. nat., t. 25, 1908, pp. 529-548.

Data at higher temperatures have been collected by Weiss and Foex.¹⁷ The reciprocal of magnetic susceptibility, when plotted against absolute temperature, frequently gives a straight line, and since $\alpha (T-\theta) = C$, in which susceptibility is represented by the symbol α , absolute temperature by T , temperature of Curie point by

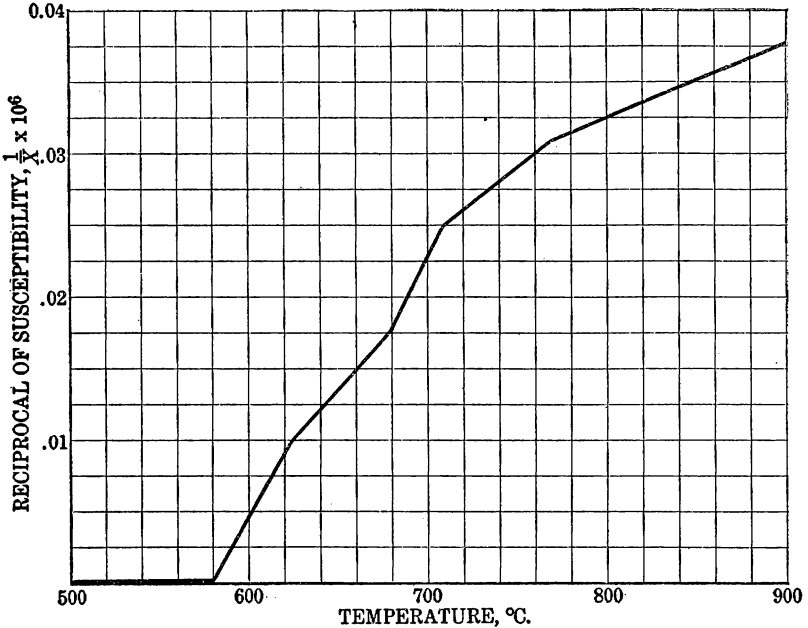


Fig. 18.—Reciprocal magnetic susceptibility v. temperature for magnetite (Weiss and Foex)

θ , and the Curie constant by C , the Curie points and Curie constants of the various forms of a substance can be derived from the equations of these straight lines. The reciprocal susceptibility plot for magnetite given in Figure 18 shows four straight lines with an intermediate range (680° to 710°) for which the corresponding theoretical Curie point and constants are as follows:

Theoretical Curie points and constants

Interval, ° C.	Curie point, ° C.	Curie constant
581-622	581+273	0.00445
622-680	558	.00682
680-710	-----	-----
710-770	433	.0105
770-900	194	.0180
900-1360+	0	.028

¹⁷ Weiss, Pierre, and Foex, G., Étude de l'aimantation des corps ferromagnétiques au-dessus du point de Curie: Arch. sci. phys. nat., t. 31 (1911), pp. 5-19 and 89-117; Jour. physique, vol. 1, 1911, pp. 274-287.

Only the first Curie point, 581° C., is important in this paper, the remaining ones being mainly of importance to the Weiss theory of magnetism, which is not universally accepted. The inference from Weiss's work is that whenever his curve changes direction either a new form of magnetite is responsible or some other physical change takes place. Weiss deduces that the different forms of magnetite differ by the number of (Weiss) magnetons that they contain. No other experimenters have noticed changes in other physical properties of magnetite in the same temperature range to correspond to the magnetic changes discussed. The specific heat curve might be expected to show changes in energy content if accurately enough determined.

The original determination of the Curie point was made by Curie,¹⁸ who found it to be 535° C. for magnetite, a temperature considerably lower than that of most other observers. Curie's thermometry was undoubtedly in error, as all of his other observed points fall below those of other observers. He places the melting point at $1,377^{\circ}$ C. Also the curve plotted by Curie shows no sharp change in direction, and at 535° C. the susceptibility actually seemed to be falling off almost vertically with temperature and was not the point where the last traces of ferromagnetism were lost. Huggett and Chaudron observe the Curie point at 570° C. and du Bois¹⁹ gives 555° C.

The work by Curie does not include suitable temperature-magnetization curves for magnetite over as wide a temperature range as desired. Magnetization down to liquid-air temperatures should be undertaken with magnetite to see what connection there is, if any, with the -156° C. point observed by Parks and Kelley and by Millar. Honda and Sone²⁰ published a temperature-susceptibility curve for magnetite from -150° to $+1,300^{\circ}$ C. Unfortunately, they started out by heating powdered pure magnetite in air to $1,300^{\circ}$ C., raising the temperature by intervals and measuring the magnetic properties at each step. The magnetite was then cooled by degrees to room temperature and chilled to liquid-air temperature. Their curve for magnetite is almost identical in shape and only slightly higher in magnitude than the one taken by them for hematite and shows that nearly all their determinations were vitiated by the oxidation of heated magnetite by air, until their sample consisted almost entirely of ferric oxide. At first the ferric oxide, formed at temperatures below 600° C., was ferromagnetic, as is possible when ferric oxide is formed by air oxidation from magnetite at low temperatures.

¹⁸ Curie, P., *Propriétés magnetiques des corps à diverses temperatures*: Ann. chem. phys., t. 5, 1895, pp. 289-405.

¹⁹ du Bois, H. E. J. G., *Discussion on Note upon the Magnetic and Nonmagnetic Qualities of Iron Alloys*: Trans. Faraday Soc., vol. 8, 1912, p. 211.

²⁰ See footnote 53, p. 25.

It loses this ferromagnetism irreversibly at about 700° C. (probably 678° C.) and on cooling can never again take on the same amount of ferromagnetism.

The saturation intensity of a sample of magnetite was determined by du Bois²¹ to be 350 gaussess attained in all magnetic fields of over 1,000-gauss strength. His data, containing H, the field strength used; I, the intensity of magnetization; B, the induced magnetism, and μ , the permeability, are given in Table 7.

TABLE 7.—Magnetization of magnetite (du Bois)

H	I	B	μ
500	325	8,361	16.7
1,000	345	9,041	9.0
2,000	350	10,084	5.0
12,000	350	20,084	1.7

With another sample of magnetite Weiss²² has found that the saturation intensity at 16.2° C. is 476.5 gaussess. Evidently magnetites from different sources vary as much as do iron and steel samples.

The temperature of the Curie point is not raised or lowered by the presence of ferric oxide or of ferrous oxide in solid solution in the magnetite, as shown by the work of Huggett and Chaudron.²³ They prepared a series of such products and observed the "magnetic transformation point" at 570° C. on their recording magnetometer. This point is 23° lower than the Weiss, Piccard, and Carrard calorimetric datum, but the thermometry was probably not as precise and there was probably some difference in temperature, due to two different methods of observing the point.

Compton and Rogney²⁴ found that magnetization and demagnetization had no effect on the crystal structure of magnetite.

THERMAL ELECTROMOTIVE FORCE

The thermoelectric power of magnetite toward iron has been measured by Brown and Shuddemagen.²⁵ The magnetite was made by fusing the higher oxide, relying on thermal decomposition to release all of the oxygen necessary to leave a residue of magnetite. As mentioned above, this is not likely to leave a product of exactly the composition of magnetite. No analyses of the product were reported, and the data will therefore have to be accepted only as

²¹ du Bois, H. E. J. G., On Magnetization in Strong Fields at Different Temperatures: *Phil. Mag.*, vol. 29, 1890, p. 293.

²² Weiss, Pierre, Mesure de l'intensité d'aimantation à saturation in valeur absolue: *Jour. physique*, t. 9, 1910, pp. 373-393.

²³ See footnote 46, p. 21.

²⁴ Compton, A. H., and Rogney, O., Is the Atom the Ultimate Magnetic Particle?: *Phys. Rev.*, vol. 16, 1920, pp. 464-476.

²⁵ Brown, S. L., and Shuddemagen, L. O., Thermal Electromotive Forces of Iron and Copper Oxides: *Phys. Rev.*, vol. 5, 1915, pp. 385-389.

approximations until more careful work has been done. The thermo-electric force against iron was 427 microvolts per degree rise in temperature and was nearly constant to 725° C. Metallic iron is positive toward magnetite. Magnetite was also negative toward cuprous oxide, the E. M. F. temperature curve being reported by Brown and Shuddemagen. The results for Fe:Fe₃O₄ in the range zero to 700° C. can be summed up in the equations $e=0.427(t-20)$ and $de \div dt=0.427$.

THERMAL EMISSIVITY

The rate at which a unit of magnetite surface can radiate heat is important, because in most industrial operations involving high-temperature treatment of iron and steel the surface of the hot metal becomes coated quickly with a layer whose outer surface is essentially magnetite. Kahanowicz²⁶ has published results of his own measurements in the form of an equation, where E stands for the emissivity.

$$E = 1.30 \times 10^{-10} T^4 e^{-380.5/T}$$

This equation is claimed to agree well with earlier measurements of Lummer.

Burgess and Foote²⁷ have measured monochromatic emissivity (equals 0.65) and total emissivity from 500° to 1,050° C., and extrapolated their results upward to 1,200° C. Their equation for monochromatic emissivity for the wave length used was

$$\frac{l}{T} - \frac{l}{S_\lambda} = \frac{\lambda}{0.4343 \times 14450} \log E_\lambda,$$

where S is the observed absolute temperature and T the true absolute temperature. Tabulating the value observed gives:

True temperature, °C-----	800	900	1,000	1,100	1,200
Emissivity, monochromatic----	0.98	0.97	0.95	0.93	0.92

The corresponding corrections for an optical pyrometer vary from 0° to 10° C.

The total emissivity was measured by use of a radiation pyrometer and the equation used was $E=(S/T)^4$. The tabulated values of emissivity are:

True temperature, °C----	500	600	700	800	900	1,000	1,100	1,200
Total emissivity-----	0.85	0.85	0.87	0.87	0.87	0.88	0.88	0.89

From these data was prepared Table 8, embodying corrections for optical and radiation pyrometers sighted on surfaces of iron oxide consisting mostly of magnetite, as follows:

²⁶ Kahanowicz, M., Potere emissivo di alcuni metalli ed ossidi: Atti della acad. Lincei, Series 5, vol. 30, pt. 2, 1921, pp. 132-137.

²⁷ Burgess, G. K., and Foote, P. D., The Emissivity of Metals and Oxides, IV. Iron Oxide: U. S. Bureau of Standards Sci. Paper 249, 1915, 7 pp.; U. S. Bureau of Standards Bull. 12, 1915-16, pp. 83-89.

TABLE 8.—*Corrections for pyrometers sighted on surfaces of iron oxide*

Observed temperature	True temperature	
	Optical pyrometers	Radiation pyrometers
° C.	° C.	° C.
500	-----	530
600	600	630
700	700	735
800	801	835
900	902	940
1,000	1,004	1,040
1,100	1,106	1,145
1,200	1,210	-----

The temperature drops somewhat through the layer of oxide, so the true temperature of the metal beneath the oxide layer is higher than that at the outside of the oxide layer. A plot of the true

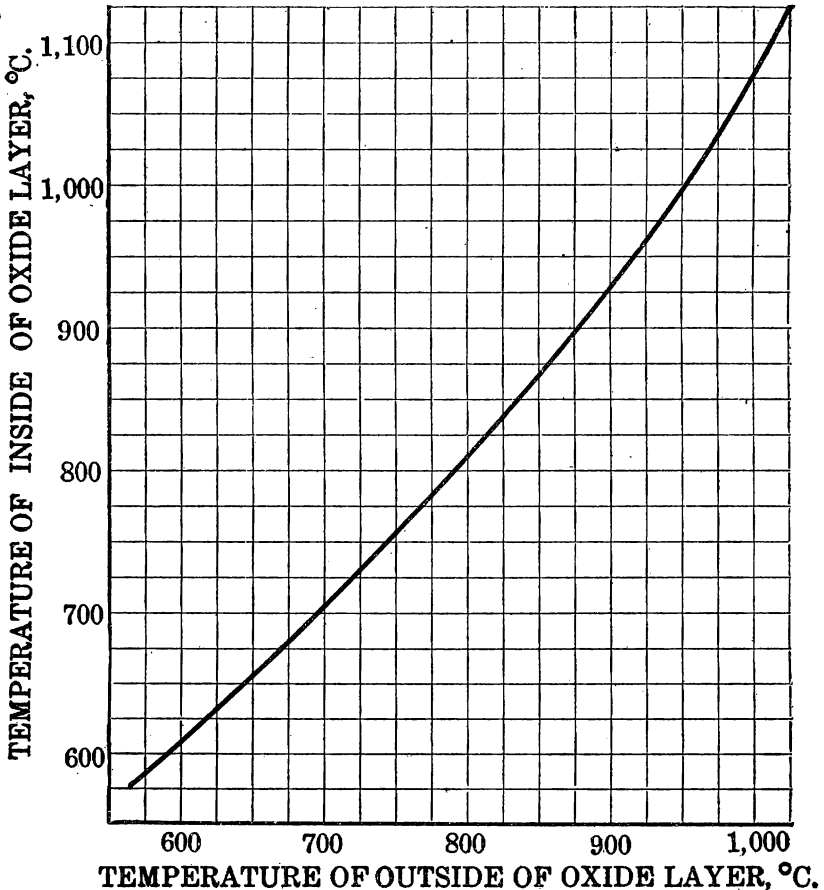


FIG. 19.—True temperature of iron under a layer of oxide (roll scale) for use with optical pyrometer

temperature of the outside of the layer in comparison with the true temperature of the inside of the layer is given in Figure 19. This plot assumes reasonable uniformity in the characteristics of the layer, an assumption known to be substantially incorrect. Therefore the curve is of only relative importance, although it should have some practical value.

SPECIFIC HEAT

The specific heat of magnetite has been measured from liquid-air temperatures to 792° C. The low-temperature data are from two dif-

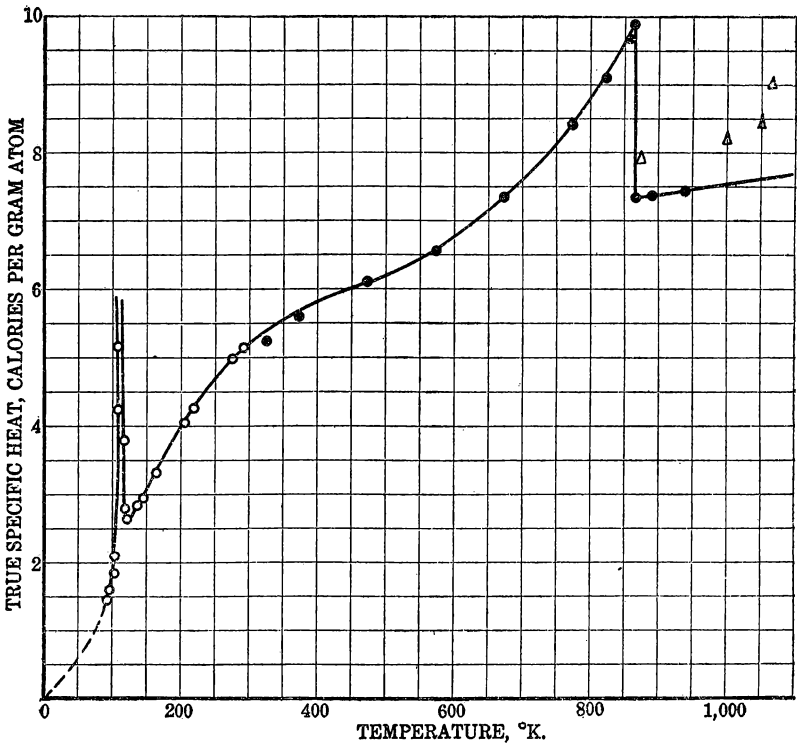


FIG. 20.—True specific heat of magnetite: ○, Data of Millar and Parks and Kelley; ●, data of Weiss, Piccard, and Carrard; Δ, data of Weiss and Beck

ferent observers working on the same sample of magnetite, a sample of very pure mineral from Mineville, N. Y.²⁸ Both used the aneroid calorimeter,

Regnault²⁹ is included. For the higher temperatures two sets of data (by the method of mixtures) are available, one by Weiss and Beck³⁰ and the other by Weiss, Piccard, and Carrard,³¹ the second set being made with improved calorimetry and better materials than were used for the first. All these data are included with the Parks and Kelley and Millar data in a large-scale plot which is reproduced in essential details in Figure 20. Weiss, Piccard, and Carrard used a sample of natural magnetite from Traverselle (Piedmont), and also an artificial preparation from the Griesheim Electron Co.

TABLE 9.—*Magnetite, true specific heat.*

Temperature		True specific heat		Authority and material
° C.	° K.	Calories per gram	Calories per gram-atom	
-186.6	86.5	-----	1.45	Millar. Natural mineral.
-180.7	92.4	-----	1.615	
-175.7	97.4	-----	1.685	
-172.3	100.8	-----	1.81	
-167.7	105.4	-----	2.10	
-159.4	113.7	-----	4.29	
-157.9	115.2	-----	5.18	
-156.0	117.1	-----	4.22	
-155.1	118.0	-----	3.78	
-153.1	121.0	-----	2.77	
-150.1	123.0	-----	2.64	
-143.6	129.5	-----	2.62	
-140.1	133.0	-----	2.635	
-136.1	137.0	-----	2.82	
-127.3	145.8	-----	2.945	
-109.9	163.2	-----	3.335	
-100.1	173.0	-----	3.555	
-95.4	177.7	-----	3.632	
-89.3	183.8	-----	3.818	
-66.6	206.5	-----	4.022	
-60.9	212.2	-----	4.095	
-54.7	218.4	-----	4.240	
+3.2	276.3	0.1513	5.00	Parks and Kelley. Natural mineral.
+5.6	278.7	.1525	5.04	
+19.0	292.1	.1558	5.15	Regnault.
+21.9	295.0	.1570	5.19	
62.0	335.1	.1678	5.55	Weiss, Piccard, and Carrard. Artificial mineral.
50.0	323.0	.159	5.26	
100.0	373.0	.170	5.63	
200.0	473.0	.185	6.12	
300.0	573.0	.199	6.59	
400.0	573.0	.222	7.35	
500.0	773.0	.255	8.44	
550.0	823.0	.277	9.17	
585.0	858.0	.295	9.76	
593.5	866.5	.300	9.93	
593.5	866.5	.221	7.32	Weiss, Piccard, and Carrard. Natural mineral.
625.0	898.0	.223	7.38	
670.0	943.0	.226	7.48	
500.0	773.0	.259	8.57	
550.0	823.0	.281	9.31	
585.0	858.0	.299	9.90	
585.0	858.0	.2255	7.45	
625.0	898.0	.229	7.58	
670.0	943.0	.232	7.63	
703.6	977.0	.2405	7.96	
725.6	999.0	.2493	8.25	Weiss and Beck. Natural mineral.
748.2	1,021.0	.2561	8.48	
791.8	1,065.0	.2743	9.09	

²⁹ Regnault, V., Sur la chaleur spécifique des corps simples et des corps composés: Ann. chim. phys., t. 1, 1841, p. 129.

³⁰ See footnote 16, p. 62.

³¹ See footnote 70, p. 36.

It will be noticed that the three points at the highest temperature are not allowed to influence the specific heat curve. These three points of Weiss and Beck are the only ones available at the high temperatures given and are part of the earlier work of Weiss's laboratory, which was later replaced by the much more careful work of Weiss, Piccard, and Carrard.

In the table of data the specific heats are given both for 1 gram of magnetite and for 1 mean gram-atom (one-seventh of the molecular weight of Fe_3O_4 , there being 7 atoms in a molecule). The mean gram-atom is 33.1 times as great as the gram.

The most striking thing about the specific heat plot is the two peaks, one at -156°C . and the other at 593°C . The latter is approached much more gradually as the temperature is raised but falls off very precipitately after the peak is passed. This shape of specific heat curve is common to ferromagnetic materials as they pass their Curie points and become paramagnetic. Although some authorities believe these peaks are discontinuities in specific heat, it seems more probable that the tip of the peak is the point at which in a magnetization-temperature curve the ferromagnetism is being lost most rapidly before the point is reached where only paramagnetism remains. These points are marked by arrows on Figure 17, which gives the magnetic data of Weiss and Beck already mentioned. Arrow *A* shows the point where the peak in specific heat should be observed and arrow *B* the true Curie point where ferromagnetism vanishes (if such a point can be said actually to exist—there may be a range of temperature in place of a sharp point).

The exact temperature of the Curie point for magnetite varies according to the material and method used and the observers. Table 10 below summarizes the situation:

TABLE 10.—*Variation of Curie point for magnetite*

Curie point	Observers	Method	Material
$^\circ \text{C}$.			
535	Curie.....	Magnetometric.....	Mineral.
580	Weiss and Beck.....	Calorimetric.....	Do.
588	do.....	Magnetometric.....	Do.
593.5	Weiss, Piccard, and Carrard.....	Calorimetric.....	Artificial.
585	do.....	do.....	Mineral.
550	Veil.....	Electric conduct.....	Artificial.
690	Honda and Sone.....	Magnetometric.....	Do.
570	Huggett and Chaudron.....	do.....	Do.

The mean is at about 580°C . and will be accepted here, although the Curie point will probably be observed at higher and higher temperatures as the sensitivity of measurement increases.

ENTROPY

The absolute entropy of a solid crystalline substance at any temperature is given by the integral, between absolute zero and that temperature, of the mathematical product of the molecular specific heat and the derivative of the natural logarithm of the temperature:

$$S = \int_0^T C_p d \ln T = 2.303 \int_0^T C_p d \log T.$$

Therefore, by plotting the molecular specific heat against the common logarithm of the absolute temperature, extrapolating the curve to absolute zero temperature, and then taking the area under the curve from zero to the temperature in question, the area is proportional to the entropy, and by multiplying by 2.303 (the conversion factor for converting common to natural logarithms) the absolute entropy is thus derived. Table 11 gives the values of the absolute

TABLE 11.—*Entropy of magnetite*

Temperature		Entropies, calories per degree			
° C.	° K.	3 Fe	+2O ₂	=Fe ₃ O ₄	ΔS
25	298	20.6	96.0	35.1	-81.5
100	373	24.7	98.0	43.8	-78.9
200	473	29.3	100.2	53.2	-76.3
300	573	31.6	102.0	61.9	-71.7
400	673	37.3	103.7	69.9	-71.1
500	773	40.7	104.9	77.5	-68.1
585	858	43.7	105.8	84.1	-65.4
700	973	47.6	107.2	90.9	-63.9
800	1,073	52.2	108.0	96.5	-63.7

entropy S as derived from the above molecular specific heat data (seven times the specific heat per mean gram atom) and similar data for metallic iron and oxygen, so that it is possible thus to estimate the change in entropy, ΔS , which takes place when 1 molecule of Fe₃O₄ forms from its elements. These entropies of formation, ΔS , are likewise tabulated. They are principally of value in calculating the free energy of formation which will be discussed later.

The value of the entropy at 298° K. (25° C.) is 35.1 calories per degree per mol. This is based on the specific heat measurements near room temperature of Parks and Kelley. Millar has more recently repeated his work, carrying his measurements to this temperature in a more carefully designed calorimeter, and has recalculated the entropy at 298° K. as 34.69. The difference can be subtracted from all the higher temperature data in the table, but Millar's correction was made too late to be incorporated throughout this paper.

HEAT OF FORMATION

The heat liberated when 3 atoms of iron combine with 2 molecules of gaseous oxygen to form magnetite according to the equation $3\text{Fe} + 2\text{O}_2 = \text{Fe}_3\text{O}_4$ has been determined calorimetrically by a number of experimenters and derived from thermodynamic data by several others. Unfortunately, the data vary considerably and need considerable discussion before one is justified in choosing them for precise calculations. Those regarded as the best are by Mixer,³² Ruff and Gersten,³³ Berthelot,³⁴ and Le Chatelier.³⁵

Other values have been published by Baur and Glaessner,³⁶ Wöhler and Günther,³⁷ Yermilov,³⁸ and Treadwell.³⁹ These values are summarized in Table 12.

TABLE 12.—*Heat of formation of magnetite*

Value, calories	Author	Method
265,700.....	Mixer.....	Sodium peroxide combustion, Fe, FeO, Fe ₃ O ₄ .
265,200.....	Ruff and Gersten.....	Oxygen-bomb combustion.
267,100±200.....	do.....	Do.
270,800.....	Berthelot.....	Dissolve Fe ₃ O ₄ in HCl in calorimeter.
268,800.....	Le Chatelier.....	Oxygen-bomb combustion.
267,380 (490° C.).....	Baur and Glaessner.....	Thermodynamic calculation, equilibria.
264,800.....	Wöhler and Günther.....	Do.
274,600.....	Yermilov.....	Oxygen-bomb combustion.
274,200 (1,000° C.).....	Treadwell.....	Oxide electrode potential.
266,980.....	Eastman and Evans.....	Thermodynamic calculation CO equilibria.
258,600.....	do.....	Thermodynamic calculation H ₂ equilibria.

The Berthelot value, although determined in 1881, is the one most frequently chosen by authorities. Redetermination by calorimetric methods of less doubtful precision is seriously needed. The values in Table 12 are discussed individually in the following pages.

MIXTER'S VALUE

Mixer developed a sodium peroxide combustion calorimeter, and some of the heats of formation determined in it have proved quite accurate and comparable with other precise determinations. Other

³² Mixer, W. G., Heat of Formation of Oxides and Sulphides of Iron, Zinc, and Cadmium: *Am. Jour. Sci.*, vol. 36, 1913, pp. 55-69.

³³ Ruff, O., and Gersten, E., Über das Triferro-Carbide (Zementit) Fe₃C: *Ber. Deut. chem. Gesell.*, Jahrg. 46, 1913, pp. 394-400.

³⁴ Berthelot, M., Sur l'oxyde du fer magnétique: *Ann. chim. phys.*, t. 13, 1881, p. 119.

³⁵ See footnote 67, p. 33.

³⁶ Baur, E., and Glaessner, A., Gleichgewichte der Eisenoxyde mit Kohlenoxyd und Kohlensäure: *Ztschr. physik. Chem.*, Jahrg. 43, 1903, p. 354.

³⁷ Wöhler, L., and Günther, R., Das Wasserdampfgleichgewicht über Eisen, Wolfram und deren Oxyden: *Ztschr. Elektrochem.*, Jahrg. 29, 1923, pp. 276-285.

³⁸ Yermilov, Y., or Jermilov, J., Heat of Formation of Iron-Carbon Alloys: *Jour. Russian Met. Gesell.*, vol. 4, 1911, pp. 357-365. Original not consulted. Abstract in Ruff and Gersten reference (see footnote 33, above), and in *Chem. Abs.*, vol. 6, 1912, p. 2387.

³⁹ Treadwell, W. D., Über den Sauerstoffdruck einiger Oxyde und die Kohle-Sauerstoffkette bei hoherer Temperature: *Ztschr. Elektrochem.*, Jahrg. 22, 1916, pp. 414-442.

of Mixer's values have suffered through unknown causes. For compounds of iron there is possible uncertainty, due to the occasional formation of sodium ferrites and ferrates. Mixer made corrections for this and also analyzed his products before and after combustion to make every correction possible for impurities and unreacted material. He used metallic iron, ferrous oxide (made by heating ferrous oxalate in a stream of nitrogen at red heat and then raising its temperature to 900° C. and containing 16.27 per cent of free iron), and magnetite (made by burning iron in oxygen). Pure ferrous oxide is a difficult material to prepare, but by his method of preparation the mixture of metallic iron and ferrous oxide probably contained very little magnetite, provided the sample was cooled rapidly from 900° C. to room temperature (a point not specified by Mixer). Since ferrous oxide and metallic iron are mutually soluble to a small extent only, there is fair probability that Mixer's sample of ferrous oxide could give a good calorimetric value. The uncertainty of the exact condition of the end product (ferrites, etc.) applies to all of the iron compounds examined by Mixer and probably obviates consideration of most of his experiments. As his value for heat of formation of magnetite is referred to the heat of formation of ferrous oxide, the above is important. The purity of the sample of magnetite prepared by oxygen combustion of metallic iron could easily be questioned. However, Mixer analyzed his products, and may have repeated his experiments until he obtained a magnetite preparation that contained small enough amounts of free ferrous oxide or ferric oxide to give a good value. That point is in doubt. He also tried a sample of "fused" magnetite and obtained a value of 265,200 calories, which is 500 calories lower than the one given in the table; he calls the difference "heat of polymerization," although it probably approaches the magnitude of his experimental error. In general, Mixer's value is probably good.

RUFF AND GERSTEN'S VALUES

Ruff and Gersten, using an oxygen-bomb calorimeter and burning iron, ferrous oxide, and magnetite, improved upon the Le Chatelier experiments. They found that ferrous oxide burned largely to magnetite. Sputtering and the resultant partial combustion of the sputtered particles which stuck to the cold walls of the calorimeter caused trouble. These investigators used three samples of ferrous oxide made by the Le Chatelier method of heating equal quantities of ferrous carbonate and ferrous oxalate in equal volumes of hydrogen and water vapor at bright red heat. The product always contained both magnetite and free carbon, the latter in small amounts but the former in amounts varying from 44 to 20 per cent. Since

magnetite and ferrous oxide are quite soluble in each other, it seems probable that Ruff and Gersten have obtained values that suffer from an unknown heat of solution of these constituents in each other. They repeated their work and published a second value for magnetite, 267,100 calories \pm 200 calories, whereas their first published figure was 265,200 calories. This variation is not surprising in view of the variation of their heats of combustion as measured. There were four combustions, two on the purest sample, and the heats of combustion per gram in the four tests were 330.3, 417.0, 452.4, and 395.1, the latter two representing duplicates. The average of these used for calculation was 398.7 ± 25 . The Ruff and Gersten data, especially the corrected datum, do not therefore inspire the confidence that the Mixer value does.

BERTHELOT'S VALUE

The Berthelot value of 270,800 calories succeeded an earlier value of 267,400 calories. Magnetite was dissolved by hydrochloric acid in the Berthelot calorimeter and the heat of solution compared with that of metallic iron. This method is fundamentally sound, and for that reason the Berthelot value is the one almost invariably accepted. However, not much was known about the characteristics of magnetite in 1881, and calorimetry has advanced considerably since then. Much greater precision is now possible, and the uncertainty of other data make a check of this one imperative.

BAUR AND GLAESSNER'S VALUE

The Baur and Glaessner calculation was made from their data on the equilibrium $\text{FeO} + \text{CO} = \text{Fe} + \text{CO}_2$ and the equilibrium $\text{Fe}_3\text{O}_4 + \text{CO} = 3\text{FeO} + \text{CO}_2$ by the accepted thermodynamic methods. The Baur and Glaessner equilibrium data are now known to have been considerably in error. Their datum should therefore be discarded.

WÖHLER AND GÜNTHER'S VALUE

The Wöhler and Günther datum is based on their own values for equilibrium constants of the same reactions, and since their equilibrium work compares well with the best equilibrium data their value is probably good. It is quite close to that of Mixer.

YERMILOV'S VALUE

The Yermilov datum was obtained in precisely the same manner as the Ruff and Gersten data, and its disagreement with the original Ruff and Gersten datum caused their second piece of work. Ruff and Gersten point out the use by Yermilov of an unsatisfactory

thermal value for the heat of formation of FeO and other defects in his work. The Yermilov datum is therefore probably not as good as that of Ruff and Gersten.

TREADWELL'S VALUE

The Treadwell datum is based on the use of an oxide cell consisting of molten silver kept saturated with oxygen and an electrolyte of silica glass dipped into the silver electrode; the cell contained the various oxides of iron moistened with molten borax, into which iron or platinum wires dipped, as the case demanded. The change in potential over a small temperature range was measured and used for calculating the heat of reaction. The value is high even at 1,000° C., and by using rough values of the specific heats of the substances involved one can calculate that the value of the heat of formation at 25° C., the determination by other authors, is 288,430 calories. Evidently Treadwell's oxide electrodes gave different potentials than they would have if all sources of error could have been removed, a highly probable explanation when one studies minutely the details of his experiments and remembers the properties of ferrous oxide and magnetite.

EASTMAN AND EVANS'S VALUES

The two Eastman and Evans⁴⁰ data are derived from equilibrium data on hydrogen reduction and on carbon monoxide reduction of various oxides of iron. Combining the equilibrium equations with those for the thermal dissociation of water vapor and of carbon dioxide, as accepted by Lewis and Randall,⁴¹ one gets equilibrium equations for the dissociation or formation of magnetite from its elements, one equation derived from hydrogen-reduction and water-vapor dissociation data and the other from carbon monoxide and carbon dioxide dissociation data. Then, by use of the relationship $\Delta F = -RT \ln K$, where ΔF is the free energy change, R the gas constant, T the absolute temperature, and K the equilibrium constant, the free energy change due to the formation of magnetite from its elements is obtained and this is expressed in the generalized empirical form, $\Delta F = \Delta H_0 - \Delta\gamma_0 T \ln T - 1/2\Delta\gamma_1 T^2 - 1/6\Delta\gamma_2 T^3 + IT$. From this equation the values in the constants of an expression giving the heat of reaction as a function of temperature can be picked:

$$\Delta H = \Delta H_0 + \Delta\gamma_0 T + 1/2\Delta\gamma_1 T^2 + 1/3\Delta\gamma_1 T^3,$$

where H_0 is the hypothetical heat of reaction at absolute zero.

⁴⁰ Eastman, E. C., and Evans, R. M., *Equilibria Involving Oxides of Iron*: Jour. Am. Chem. Soc., vol. 46, 1924, pp. 888-903.

⁴¹ Lewis, G. N., and Randall, M., *Thermodynamics and the Free Energy of Chemical Substances*: New York, 1923.

These two equations deduced from the Eastman and Evans data are:

$$\Delta H = -264,630 - 11.00T + 0.0112T^2 - 0.00000248T^3.$$

(from carbon reduction)

$$\Delta H = -256,377 - 3.76T - 0.006594T^2 + 0.00000296T^3.$$

(from hydrogen reduction)

The two values of ΔH_{298} are $-266,980$ calories and $-258,000$ calories, respectively. The second is so low as to be doubtful, although the equilibria measured were probably as precise as have yet been determined. Calculating backward from the free energy to heat of formation data, including specific heat terms, is not as precise as determining the heat of formation at some one temperature, including the specific heat data, and deriving the free-energy equation therefrom.

SUMMARY

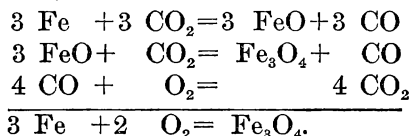
Ignoring the Treadwell and the Baur and Glaessner values, the average of the remaining values is $266,887$ calories per mol. This is very close to the value of Mixter, which is regarded as the best one, and the latter is therefore chosen as the heat of formation of magnetite at room temperature. Expressing this in chemical symbols, Fe_3O_4 , $\Delta H_{298} = -265,700$ calories, the negative sign indicating negative heat absorption (heat evolution).

The peak between 110° and 125° K. was taken by heating the magnetite through very small temperature intervals and is reproducible at each temperature, showing that some internal change takes place in this temperature range, the amount of change being a very definite function of the absolute temperature. The latent heat of this change can not be charged to any definite temperature but is a distributed latent heat, and the temperatures at which the change begins and ends are indefinite. The lower edge of the peak is not 110° K., and the upper edge is not 125° K., but these are temperatures somewhere near those at which the unknown effect is making itself quite evident. The total heat necessary to pass from magnetite at 110° K. to magnetite at 125° K., made up of the ordinary sensible heat plus the added energy necessary for the unknown transition, was measured by Millar as 361.4 calories per mol. This figure is probably low, because not quite all of the departure of the specific heat curve from the normal specific heat curve could be measured—nor could it be, because the normal specific heat curve is not known. Probably the actual curve is too high throughout its entire length as compared to what it would be if magnetite behaved as a simple substance.

FREE ENERGY

The change in free energy accompanying the formation of 1 mol of magnetite from its elements can now be calculated from several different sets of data. By use of the equation $\Delta F = \Delta H - T\Delta S$ one may make what is called a "third law" calculation (based on the third law of thermodynamics), using the above-determined value of the heat of formation and of the entropy of formation. This has been done, and the resulting values for a series of temperatures for which data exist are given in Table 13. Several extrapolated values are inclosed in parentheses. The standard free energy at 25° C. by the third law calculation is $\Delta F_{298} = -241,550$ calories. Parks and Kelley used this method, but with the Berthelot value of ΔH , making their value greater than the above by the difference between 271,000 and 265,700 calories.

Calculating from equilibrium data of Eastman and Evans, two courses are open. One may use the CO reduction equilibria or the hydrogen equilibria, both of which have been so critically summarized by Eastman and Evans. For instance, adding the equations



Adding the corresponding equations for the free energy changes of each of these reactions written as functions of the temperature and using equilibrium data of Eastman and Evans for the iron reduction and of Lewis and Randall⁴² for the CO combustion, an equation representing the free energy of formation of magnetite can be deduced and reads as follows:

$$\Delta F^\circ = -264,630 + 11T \ln T - 0.112 T^2 + 0.00000124 T^3 + 11.347T.$$

Values for various temperatures are calculated from this equation and included in Table 13 for comparison with the values deduced by the help of the third law of thermodynamics. As can be seen, the third law derivation gives the smaller value at 298° K. while the CO reduction equilibrium data give the lower value at 1,273° K. Figure 21 is a plot showing the various data. The two derivations agree exactly at about 500° C.

Similar derivations by means of hydrogen-reduction equilibria, together with the equilibrium data derived from the high-temperature dissociation of water vapor, result in the following equation for Fe_3O_4 :

⁴² See footnote 41, p. 75.

$\Delta F^\circ = -256,320 + 3.76T \ln T + 0.0066 T^2 - 0.00000148 T^3 + 40.56 T$. Values for the same series of temperatures as the above are likewise given in Table 13 and plotted in Figure 21. These values are uniformly lower than the ones derived from the CO-reduction data. Eastman and Evans have pointed out the discrepancy and have sought to explain by it discrepancies in the water-gas equilibrium constants, $\text{H}_2\text{O} + \text{CO} = \text{H}_2 + \text{CO}_2$, which should be derivable from the above data.

The failure of the hydrogen-reduction data to check the CO-reduction data and to allow derivation of water-gas reaction equilibrium

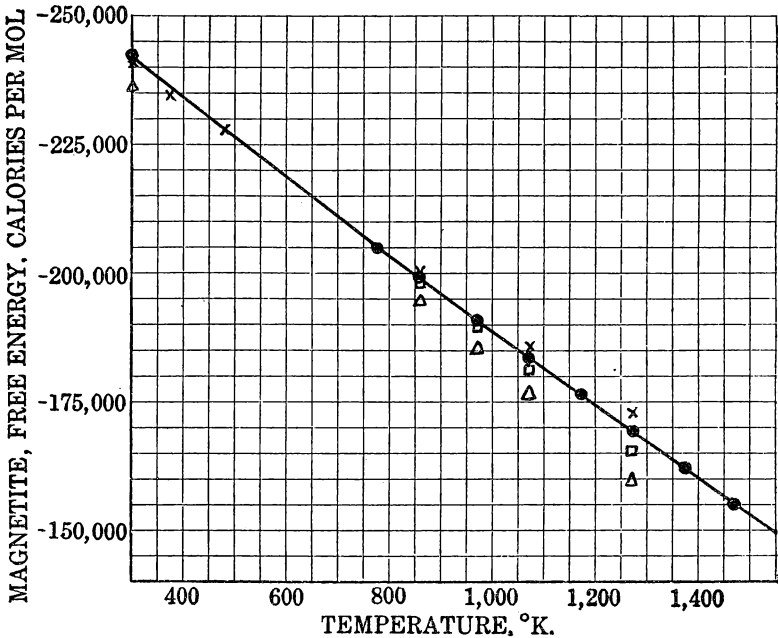


FIG. 21.—Free energy of magnetite: ●, Best values; ×, third law derivation; □, CO reduction equilibria; Δ, H₂ reduction equilibria

constants which check the observed constants shows that one of the three sets of data is affected by some undetermined factor. The only check obtained is that of the third law free energy of magnetite with the free energy as deduced from the CO-reduction data. As the three sets of equilibrium data in question are the harmonized results of many observers, lack of mutual consistency is probably not due to ordinary errors that enter in one or the other sets of determinations. For the present the best that can be done is to take the average of the third law and the CO-reduction data as the tentatively accepted values of free energy of magnetite. These aver-

ages are given in Table 13. They can be expressed with reasonable accuracy by the empirical equation:

$$F_{\text{Fe}_3\text{O}_4}, \Delta F^\circ = -269,246 - 8.1425T \ln T + 0.000341 T^2 + 136.332 T,$$

which will be accepted as representing the best data available. Values extrapolated to three higher temperatures by this equation are included in the table and extrapolation is indicated by parentheses. This equation corresponds to a value of the heat of formation of $-266,856$ calories at 25°C ., which is $1,156$ calories greater than the Mixer value chosen as the best and only 31 calories less than the above-calculated weighted average of the various determinations on heat of formation. This shows that the values of free energy of magnetite so far available are only approximate, and more careful thermal work on heat of formation and high-temperature specific heats must be done before values of undisputed precision can be obtained.

TABLE 13.—Free energy of magnetite

Temperature		Free energy, calories			
$^\circ \text{C}$.	$^\circ \text{K}$.	By third law	CO equilibrium	H ₂ equilibrium	Best value
25	298	-241,550	-243,512	-236,875	-242,531
100	373	-235,415			
200	473	-227,800			
300	573	-220,100			
400	673	-212,980			
500	773	-205,787	-205,433		-205,610
585	858	-200,010	-198,546	-194,892	-199,278
700	973	-192,580	-189,340	-185,451	-190,960
800	1,073	-185,880	-181,595	-176,873	-183,738
900	1,173	(-180,200)	-173,790	-168,873	-176,995
1,000	1,273	(-173,300)	-165,543	-159,946	-169,421
1,100	1,373				(-162,195)
1,200	1,473				(-155,141)
1,300	1,573				(-148,163)

IRON-OXYGEN COMPLEXES INTERMEDIATE BETWEEN MAGNETITE AND FERROUS OXIDE

Magnetite and ferrous oxide both crystallize in the regular system and might naturally be expected to form solid solutions. That they have been found to do so constitutes their principal point of interest. However, they have not been found soluble in each other in all proportions at temperatures below 1,175° C. Instead, solid magnetite can dissolve a certain amount of ferrous oxide, and ferrous oxide can dissolve a certain amount of magnetite. The evidence is largely qualitative and needs careful review.

SURFACE COATINGS ON METALLIC IRON

At high temperatures iron—in an atmosphere of air, oxygen, steam, or carbon dioxide—becomes coated with a layer of oxides with the highest stage of oxidation on the outer layer and the lowest on the inner layer. In air and oxygen the outer layer is Fe_2O_3 , but in steam or carbon dioxide the outer layer has the composition of Fe_3O_4 , as might be expected from the equilibrium diagrams. The actual junction between the oxide layers and metal is not sharp; but oxides form first in the metal along the grain boundaries, thus penetrating ahead of the general zone of oxidation, and these films of oxide grow and take in the grains of iron.⁴³ Possibly the first thing that happens in the surface layers of metal is the formation of a solid solution of ferrous oxide in iron; as more oxygen enters the solubility of FeO in Fe is exceeded, and it begins to precipitate in the grain boundaries where the microscopists have observed it. The remaining oxide grows on these nuclei. To cause oxygen to migrate inward an oxygen gradient must be set up within the oxide layers, and this is easily possible, due to the mutual solubility of FeO and Fe_3O_4 in each other; the FeO layer next to the metal dissolves Fe_3O_4 from the outer layers, and on contact of the Fe_3O_4 with the metal it is reduced to FeO and thereby oxidizes more metal.

⁴³ Stead, J. E., Solid Solution of Oxygen in Iron: Jour. Iron and Steel Inst., vol. 103, 1921, p. 271; Carpenter, H. C. H., and Elam, O. F., The Effect of Oxidizing Gases at Low Pressures on Heated Iron: Jour. Iron and Steel Inst., vol. 105, 1922, p. 83; Pilling, N. B., and Bedworth, R. E., The Oxidation of Metals at High Temperatures: Jour. Inst. Metals, vol. 29, 1923, p. 529.

WORK OF MOSANDER

Long ago Mosander⁴⁴ analyzed the various coatings of iron scale and found the innermost layer next the iron to be approximately of the composition $6\text{FeO}\cdot\text{Fe}_2\text{O}_3$ or $5\text{FeO}\cdot\text{Fe}_3\text{O}_4$, with increasing amounts of ferric iron in the outer layers. Whether compounds of these formulas exist is doubtful, and the ratios of ferric and ferrous iron in the various layers would doubtless vary with the oxygen gradient applied. Commonly, this iron scale is called roll scale, since it is found in greatest quantities in the roll scale formed in the steel rolling mills, and it is thought to approximate magnetite in composition. The above statements show that this conception is in error. The scale is magnetic and contains magnetite but is usually deficient in oxygen.

X-RAY INVESTIGATIONS OF BOZORTH

An X-ray examination of a special coating of iron oxides has been made by Bozorth⁴⁵ of the Bell Telephone laboratory. He applied the Barth protective coating,⁴⁶ which is obtained by use of steam on iron surfaces at 730°C . for several successive 1-hour treatments with intermediate cooling in air. The oxide layer so formed was examined by the powder method and by reflection of X rays at different angles of incidence and of various degrees of hardness. Preparations of pure ferric oxide and magnetite were used for comparison. The layer was found to consist of the three oxides in the following sequence and thickness: Fe_2O_3 , 0.2 micron; Fe_3O_4 , 2.0 microns; FeO , 97.8 microns; total, 100.1 microns.

No evidence of the presence of solid solutions of FeO and Fe_3O_4 was obtained, because the better photographs were too sharp to be consistent with a variation in atomic spacing greater than 0.5 per cent. It was acknowledged as barely possible that such solid solutions do exist and that the atomic spacing remains within that variation. A faint line, at first thought to be due to magnetite, was noticed on the reflection pattern of the inside surface of the FeO layer but was thought due to oxidation subsequent to removal from the iron. This negative evidence from the powerful X-ray method is disconcerting, but it must be remembered that failure of the X rays to show FeO in the Fe_3O_4 layer or Fe_3O_4 in the FeO layer parallels other instances, such as their failure to show Fe_3C in steel specimens, although the Fe_3C areas and crystals are plainly visible under the

⁴⁴ Mosander, C. G., —————: *Ann. Phys.*, vol. 6, 1826, p. 35; quoted by Evans, U. R., *Metals and Metallic Compounds*: London, 1923, pp. 28-40.

⁴⁵ See footnote 92, p. 55.

⁴⁶ Barth, F. S., —————: *Jour. Soc. Arts*, vol. 25, 1877, p. 254, and vol. 27, 1879, p. 390; Bower, G., —————: *Trans. Soc. Eng.*, vol. 23, 1883, p. 59.

microscope, behave differently on etching, and are otherwise known to be present.

X-RAY INVESTIGATIONS OF GROEBLER AND OBERHOFFER

A third piece of work on iron oxides done with X rays was that of Groebler and Oberhoffer,⁴⁷ who prepared a series of iron-oxygen mixtures by holding a small sample of ferric oxide at 800° C. in a combustion tube with a stream of gas of definite composition passing over it until constant weight was attained. The CO content of the gas used was gradually increased by steps, with the result that a reduction isotherm similar to those described in the next few pages was obtained, the analysis of the solid being plotted against the gas analysis. Twelve preparations made in this way were examined by the Debye-Scherrer powder method; for the Fe_3O_4 -FeO mixtures at least 5 per cent of FeO could dissolve in the Fe_3O_4 , as shown by the displaced magnetite lines and the absence of FeO lines. When lines of free FeO appeared and when the composition reached 61 per cent of FeO with 39 per cent of magnetite the spectrum of the latter vanished. Thereafter, only the spectrum of FeO was observed until the sample had been reduced to the point where free Fe began to appear. As ferrous oxide can take up 39 per cent of magnetite into its own lattice, Groebler and Oberhoffer see the probability that the extra oxygen of the magnetite must be distributed in haphazard fashion through the FeO lattice, and they call these excess atoms of oxygen "vagabond oxygen atoms" because they have no regularly appointed places.

WORK OF MERWIN AND FEDOTJEFF

The microscope has not been used much on mixtures of Fe_3O_4 and FeO, as they are both black solids tending to crystallize in octahedrons and are too opaque to allow measurement of optical properties. Their great difference toward solvents should allow etching of FeO in the presence of Fe_3O_4 on a polished surface, thus giving a method of distinguishing the two. H. E. Merwin,⁴⁸ of the Geophysical Laboratory, has a special method. A polished surface is prepared, heated to about redness, and cooled. Part of the FeO splits into magnetite and metallic iron, leaving a dull matte surface, while the original polished surface of magnetite remains unaffected.

The structure of the surface coating of oxide on iron has also been studied by Fedotjeff⁴⁹ recently, using steam as the oxidizing agent at

⁴⁷ Groebler, H., and Oberhoffer, P., Beiträge zur Untersuchung der Oxyde des Eisens, besonders des Eisenoxyduls: Stahl u. Eisen, Jahrg. 47, 1927, pp. 1984-1988.

⁴⁸ See footnote 3, p. 58.

⁴⁹ Fedotjeff, P. (The Mechanism of Oxidation of Iron by Steam, Carbon Dioxide, and Air at High Temperatures): Jour. Russ. Phys. Chem. Soc., vol. 58, 1926, pp. 222-228. Also in Ztschr. anorg. Chem., Jahrg. 157, 1926, p. 165.

1,000° to 1,100° C. He was able to distinguish octahedral crystals with deep etch figures but was unable to distinguish any layers, such as might be expected from the limited miscibility of Fe_3O_4 and FeO . Apparently the layer of oxide scale was optically homogeneous, although chemical tests showed it to be richer in FeO next to the metal.

MELTING POINTS

The melting points of intermediate mixtures of FeO and Fe_3O_4 are not known. FeO melts at 1,380° C. and Fe_3O_4 at 1,580° C., but the intermediate region remains to be explored. Heating and cooling curves of intermediate preparations should be instructive. A mixture of the two containing 4 per cent of FeO and 96 per cent of Fe_3O_4 was observed by Ruer and Nakamoto⁵⁰ to begin to melt at slightly over 1,550° C. in a platinum boat, but the melt was not completed. No other data are to be found.

Wyckoff and Crittenden (see section on "Ferrous oxide"), in preparing ferrous oxide, melted magnetite and iron together in the open air by resistance heating between iron electrodes. Numerous other experimenters have tried the same thing, and none of them have been able to reduce completely the ferric oxide in the magnetite, the final product always being between magnetite and FeO in composition with about 75 to 82 per cent of FeO , depending on the relative effectiveness of excluding air from the surface of the melt and possibly on the low activity of ferric oxide when highly diluted with FeO . The best sample of Wyckoff and Crittenden, although indicating the presence of unreduced Fe_2O_3 by chemical analysis, was nonmagnetic and on examination by X-rays showed no lines due to magnetite. The investigators erroneously concluded that their sample was pure FeO and that the chemical methods of analysis were at fault. The refutation of their claim is given in the section dealing with ferrous oxide.

MAGNETIZATION

That a mixture of FeO and Fe_3O_4 can be nonferromagnetic was discovered by Hilpert and Beyer,⁵¹ who examined the magnetic characteristics of a series of mixtures of Fe_3O_4 and FeO . They used pure ferric oxide as raw material and reduced it in a stream of hydrogen and water vapor at 400° to 1,100° C. No crystal structure could be detected in the black masses. With increasing FeO content the ease of dissolution in acids increased. The magnetic suscepti-

⁵⁰ Ruer, R., and Nakamoto, M., Über Eisen und Kupferoxyde: Rec. trav. chim., vol. 42, 1923, pp. 675-682.

⁵¹ See footnote 96, p. 56.

bility was approximated by placing a sample of the unknown material in the core of a transformer with a ballistic galvanometer in the secondary. The readings of the galvanometer were then proportional to the susceptibility. These readings are plotted as a function of the analysis of the sample in Figure 22, the abscissas being corrected to read the free FeO over that necessary to form Fe_3O_4 with the ferric iron in the samples, whereas Hilpert and Beyer's original plot used the total FeO. Unfortunately, they did not prepare enough samples with zero to 25 per cent of free FeO, and the exact course of the curve through that interval is not known. It might follow the dotted line in place of the straight line between the two points drawn, although this is less probable if solid solution is involved.

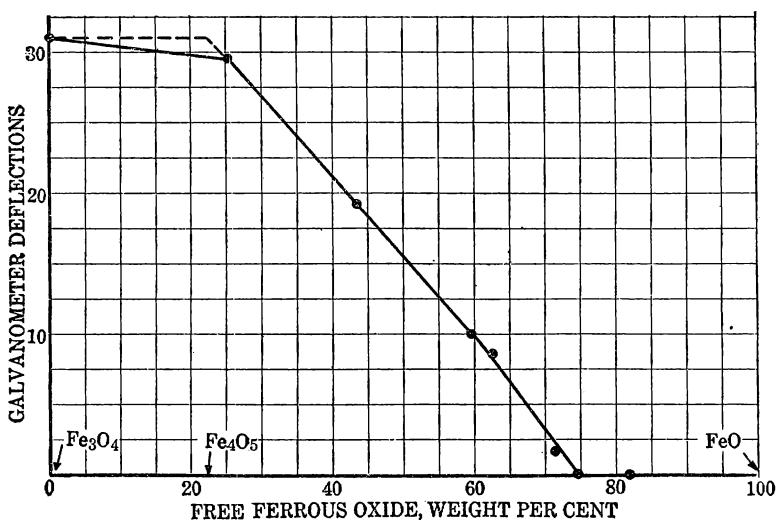


FIG. 22.—Magnetic characteristics in Fe_3O_4 — FeO system; magnetic susceptibility indicated by galvanometer deflections of magnetometer (Hilpert and Beyer)

The drop of magnetization to zero at 74 per cent of FeO (83 per cent of total FeO) is the most noticeable thing about the plot. All samples with more FeO were not ferromagnetic. Evidently at this point any magnetite in the preparation is in solid solution in the excess FeO and loses its ferromagnetism on passing into such solid solution. This and the failure of three experimenters with X-ray spectrographs to discover Fe_3O_4 lines forces the conclusion that magnetite is no longer magnetite when in solid solution in FeO. Evidently the ferric iron, whether present as ferric oxide or as a ferrous ferrite, when dispersed in a solid solvent of FeO, is either noncrystalline and hence incapable of giving an X-ray spectrogram or assumes the space lattice and atomic spacing of the FeO. The disappearance of magnetism leads us to suspect that the magnetism

of Fe_3O_4 is due to its molecular arrangement and that when this arrangement is destroyed by solution in a solvent the magnetism is destroyed. Other evidence to be discussed later prompts the feeling that ferrous oxide which is nonmagnetic can absorb magnetite in solution to the point of saturation and that as soon as free magnetite is present a magnetic effect can be detected. A product containing 74 per cent of FeO may therefore be assumed to represent a saturated solid solution of Fe_3O_4 in FeO formed probably at $1,000^\circ \text{C}$., although the difference in solubility between room temperature and $1,000^\circ \text{C}$. makes the exact temperature uncertain.

The kink in the Hilpert and Beyer curve at 61 per cent of FeO may have no significance, yet a product consisting of 61 per cent by weight of FeO and 39 per cent of Fe_3O_4 corresponds almost exactly to the formula $6\text{FeO}\cdot\text{Fe}_2\text{O}_3$. This agreement may be fortuitous, but it encourages more research.

The change in direction of the Hilpert and Beyer curve at 20 to 25 per cent of FeO can in a similar manner be interpreted as at the point where Fe_3O_4 is saturated with FeO in solid solution, and any further addition of FeO to the system displaces a corresponding amount of the magnetic component. If the dotted line in Figure 22 is correct, this point falls at 21.5 per cent of FeO and the solid solutions of FeO in Fe_3O_4 have the same magnetic susceptibility as pure Fe_3O_4 . This could be interpreted as meaning that when FeO dissolves in Fe_3O_4 it becomes ferromagnetic through assuming the space lattice of magnetite. On the other hand, the compound $2\text{FeO}\cdot\text{Fe}_2\text{O}_3$ would fall at the point for 23.6 per cent of FeO on our curve, which is very nearly at the kink in our extrapolated curve. In this connection Borchers⁵² states that magnetite and other ferrous ferrites are present in copper mattes and that the reducing action of the FeS and Cu_2S in the matte is enough to reduce these ferrous ferrites only as far as the compound $2\text{FeO}\cdot\text{Fe}_2\text{O}_3$. The whole subject merits investigation.

Another interesting research on magnetic properties of the $\text{FeO}\text{--}\text{Fe}_3\text{O}_4$ complexes is that by Huggett and Chaudron.⁵³ They prepared a series of products from Fe_2O_3 to Fe in composition by partial reduction with hydrogen, followed by 30 hours homogenizing at 650°C . to allow all of the solid solutions to reach homogeneity by diffusion. These products were then placed in weighed amounts in a magnetometer, heated up, and then cooled, the variation in their ferromagnetism with the temperature being noted. The products containing FeO on approaching 300°C . began to split into Fe_3O_4

⁵² Borchers, W., Kupfer: Halle, Germany, 1915.

⁵³ Huggett, J., and Chaudron, G., *Températures de transformations magnétiques dans le système fer-sesquioxyde de fer*: *Compt. rend.*, t. 184, 1927, pp. 199–201.

and Fe, as expected; at 575° C. another magnetic anomaly was passed due to the Curie point of magnetite, and at about 600° C. the components of the ferrous oxide recombined, so that with disappearance of iron to form FeO another magnetic anomaly was noticed. Figure 23 is a plot showing the temperatures at which the magnetic anomalies were observed as a function of the chemical analysis expressed as percentage reduction from Fe_2O_3 to Fe. Pure FeO began to decompose at 260° C. during heating, but dilution with magnetite raised the temperature to 300° C. with a product (27 per cent of reduction)

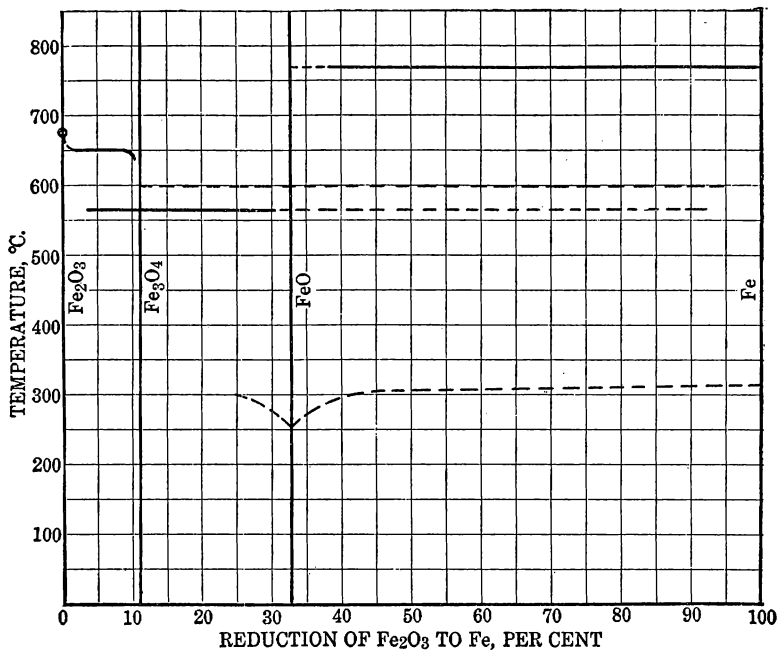


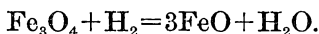
FIG. 23.—Magnetism-temperature anomalies in the Fe— Fe_2O_3 system. Solid lines, magnetic inversions of the ferromagnetics indicated; dotted lines, magnetic anomalies due to splitting or reforming of FeO

containing 31 per cent of Fe_3O_4 , which is nearly the solubility of Fe_3O_4 in FeO at 700° C. Beyond this point the rapid changes in magnetic susceptibility of magnetite masked the anomaly due to FeO, hence with samples richer in magnetite the effect was lost. We may take this figure as another rough measure of the solubility of magnetite in ferrous oxide.

REDUCTION-EQUILIBRIUM DIAGRAMS

Numerous experimenters have studied the gaseous reduction of Fe_3O_4 to FeO or the reverse oxidation process, and the attainment of equilibrium has been difficult and uncertain, due to the whim-

sicalities of the solid products. These have caused wide variation in the gas analyses at equilibrium. The work of producing CO_2 with CO as the reducing gas until equilibrium between the CO and CO_2 is reached is good but complicated by tendency of the CO to dissociate in the presence of an iron catalyst and by the compound Fe_3C forming. Therefore, reduction equilibria obtained by the use of hydrogen are regarded as most reliable. Most of the important work with hydrogen has been critically reviewed by Eastman and Evans,⁵⁴ whose summary of the better value is given in Figure 24, these values being the equilibrium constants, $k = (\text{H}_2\text{O})/(\text{H}_2)$ for the reversible equation:



In the curve the logarithms of these equilibrium constants are plotted against the reciprocals of the absolute temperatures, because such a plot should approximate a straight line if the solids are pure crystalline substances that do not dissolve in each other. The actual curve departs considerably from a straight line at the higher temperatures, the dotted line in Figure 24 being a straight line extrapolated from the lower temperature values. This departure from a straight line means either that there are big differences in the specific heats of the reacting substances or else that the solids dissolve in each other. The latter is known to be true, whereas specific heat data on the two solids are very meager, and the curvature is greater than that usually due to specific heat differences. One may conclude that the magnetite and ferrous oxide must be dissolving in each other in increasing proportions as the temperature rises, probably forming pairs of conjugate solutions at each temperature, and at a high enough temperature they doubtless dissolve in each other in all proportions. This critical temperature is unknown. It is probably high enough that all components are liquid.

SOLUBILITIES FROM REDUCTION ISOTHERMS

DISCUSSION OF FIGURE 25

Four investigators, Eastman and Evans,⁵⁵ Matsubara,⁵⁶ Groebler and Oberhoffer,⁵⁷ and Schenck⁵⁸ have collected reduction isotherms for the iron-oxygen system. Starting with Fe_2O_3 , they added suc-

⁵⁴ See footnote 40, p. 75.

⁵⁵ Work cited.

⁵⁶ See footnote 86, p. 52.

⁵⁷ See footnote 47, p. 83.

⁵⁸ Schenck, R., Eisen, Kohlenstoff, und Sauerstoff in ihren wechselseitigen Beziehungen: Stahl u. Eisen, Jahrg. 46, 1926, pp. 655-682.

cessive small amounts of reducing gas, waiting for equilibrium between each addition and analyzing the gas and solid, with the temperature constant until the analysis of solid and gas had been

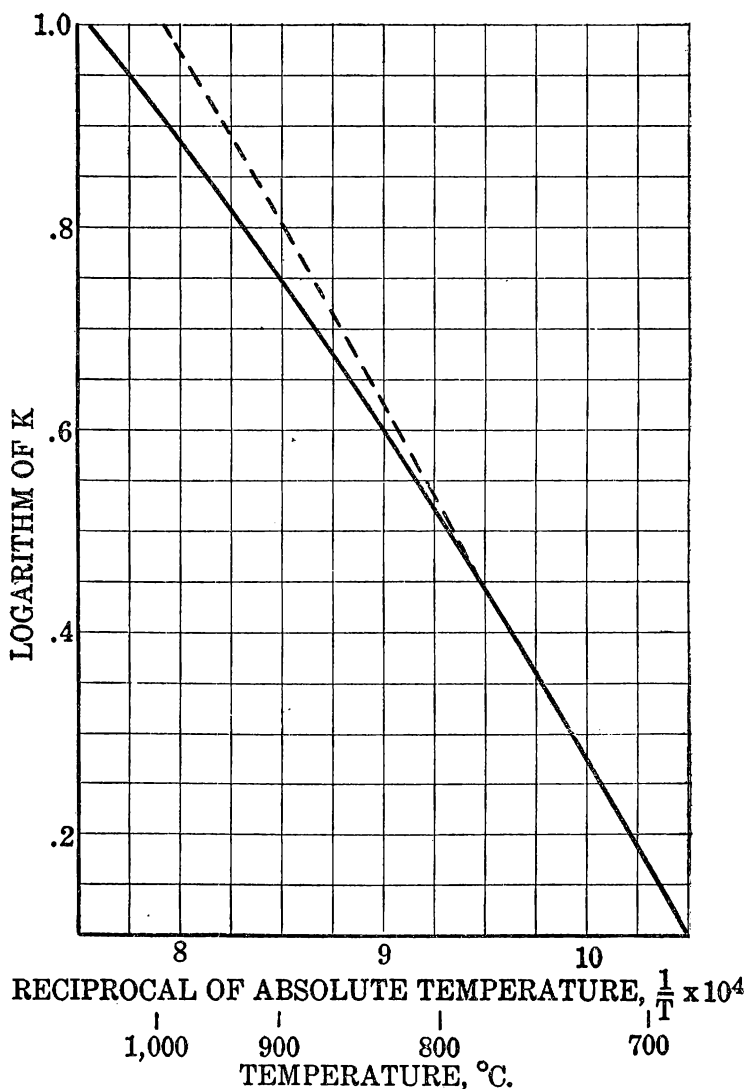


FIG. 24.—Equilibrium constants of system $\text{FeO} : \text{Fe}_2\text{O}_3 : \text{H}_2 : \text{H}_2\text{O}$ (Eastman)

followed from Fe_2O_3 to Fe. One of the isotherms (that of Eastman and Evans) was with hydrogen at 772°C . and was followed in both reducing and oxidizing directions. Six others, three by Matsubara and three by Schenck, were collected, using CO as the gas. Some of

them are plotted in Figure 25; no two were at the same temperature, and the temperatures used were from 700° to 1,175° C.

The sharp changes in direction of these isotherms are important. The horizontal lines represent equilibrium between pairs of phases of approximately constant composition, whether pure compounds or solid solutions. The portions curving away from horizontal are obtained when the relative amount of one phase or another is small. Between Fe_3O_4 and FeO the isotherms show a horizontal portion which does not quite reach Fe_3O_4 or FeO but is cut off by sloping

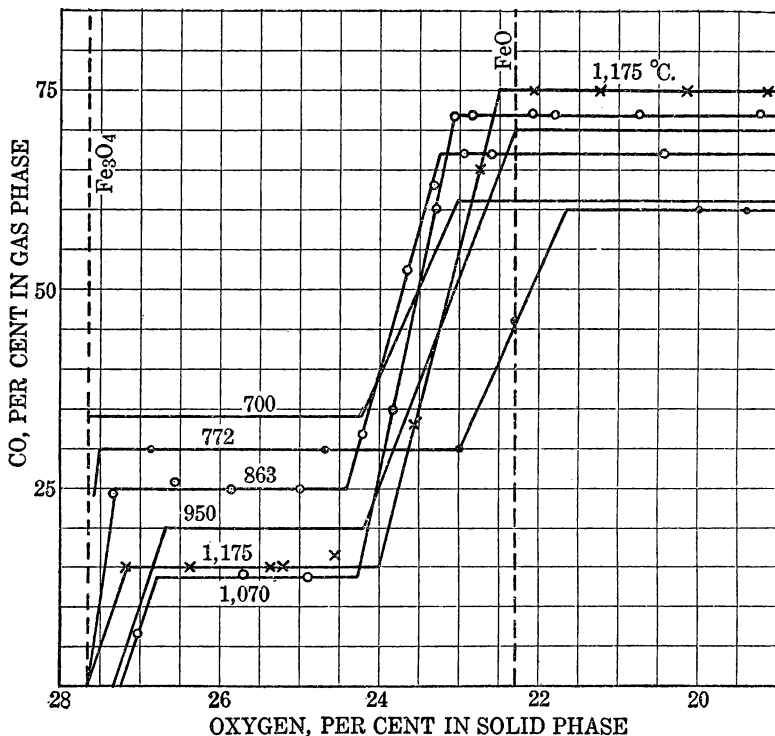


FIG. 25.—Gas-reduction isotherms at slow rate (Eastman, Matsubara, and Schenck)

portions of the curve. In this case, on the side next to FeO the change in direction is at the point where all of the free Fe_3O_4 is exhausted, and only a solid solution of Fe_3O_4 in FeO is left in equilibrium with the gas; and then for every decrease in the amount of dissolved Fe_3O_4 , gas of increased reducing power is necessary until all of the Fe_3O_4 is gone. Similarly, on the sloping branch of the curve next to the composition of Fe_3O_4 , the FeO dissolves in the Fe_3O_4 in solid solution, as Fe_3O_4 is reduced to FeO , reducing the activity of the Fe_3O_4 and requiring gas of higher reducing power for the next step until enough FeO has been formed to saturate the Fe_3O_4 . Afterwards the curve runs horizontally, excess FeO merely

dissolving Fe_3O_4 to form a saturated solution of Fe_3O_4 in FeO . The horizontal part of the curve is therefore actually one of equilibrium between two saturated solutions, one mainly made up of magnetite and the other of FeO . The ends of the horizontal portions of the curves give us directly the analyses of the saturated solutions. Using the isotherms of Figure 25 for this purpose, the solubilities of FeO in Fe_3O_4 and of Fe_3O_4 in FeO have been calculated and are tabulated in Table 14. The scattered determinations of Hilpert and Beyer and of Huggett and Chaudron are also included.

TABLE 14.—*Analyses of conjugate solutions of Fe_3O_4 and FeO*

[Approximations only]

Temperature, °C.	Fe_3O_4 in FeO	FeO in Fe_3O_4	Authority
	<i>Per cent</i>	<i>Per cent</i>	
300	+31	-----	Huggett and Chaudron.
700	35	0	Schenk.
772	32	6.35	Eastman and Evans.
800	32	.75	Schenk.
800	39	5.00	Groebler and Oberhoffer.
863	38	6.35	Matsubara.
950	28	19.0(?)	Schenk.
1,000	26	21.5(?)	Hilpert and Beyer.
1,070	51(?)	15.7	Matsubara.
1,175	26	6.35	Do.

DISCUSSION OF FIGURE 26

The sequences of figures in these columns are rather poor and give us a criterion to judge the precision of the work represented by the isotherms. Most of the isotherms were probably taken too rapidly and failed to reach equilibrium, especially at the points where sharp changes in direction take place. The columns of figures probably give at best only a rough idea of the magnitude of the solubility of one constituent in the other, and precise values are not available. They are plotted in Figure 26. In drawing curves determined by the points, exact positions can be changed considerably. The solid curve for the Fe_3O_4 phase is drawn to represent the points best, and yet the writer feels that the dotted branch is probably nearer its true course and that the conjugate solutions will blend into one at some point not far above the melting point of FeO (1,380° C.).

This poor agreement of data in Table 14 and Figure 26 calls for somewhat more critical examination of the isotherms in Figure 25. The sloping parts of the curves corresponding to reduction of the solutions of Fe_3O_4 in FeO to FeO (mixtures with between 24 and 22.3 per cent of oxygen) should not reach a horizontal portion at a higher concentration of reducing gas until all of the Fe_3O_4 is reduced. Actually, all but two of them do reach a new horizontal

portion, showing that the gases which are in equilibrium with the surfaces of the particles have evidently not had time to reduce the magnetite in their cores, and consequently that the gross composition of the mass is still intermediate between FeO and Fe_3O_4 . The

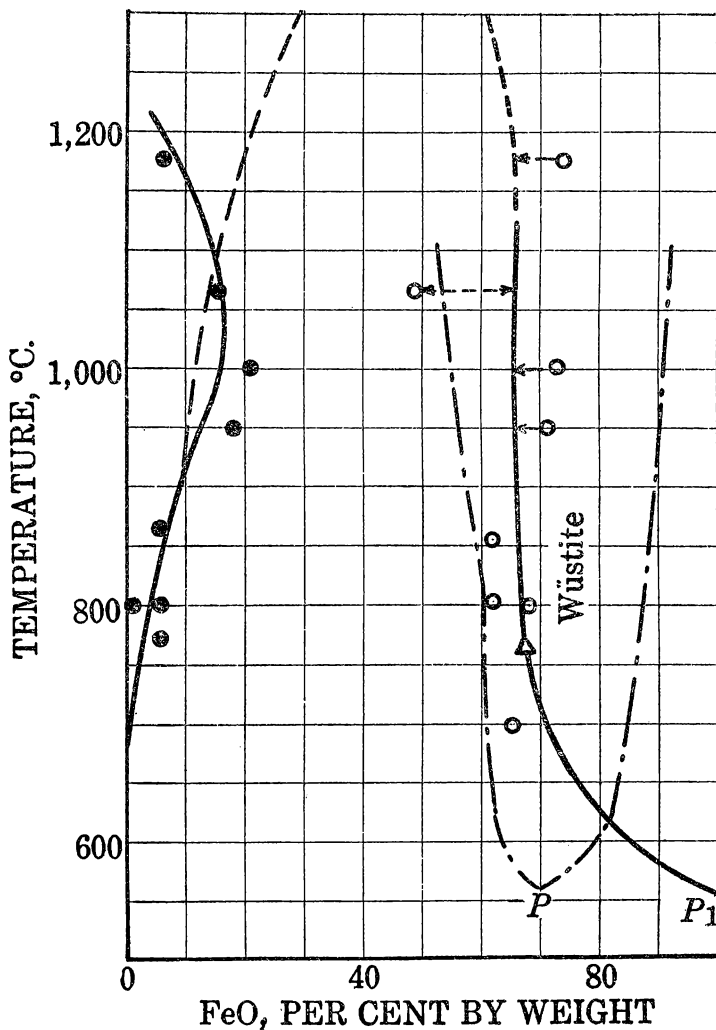


FIG. 26.—System Fe_3O_4 — FeO conjugate solid solutions. Solid lines, best average solubilities; dot-and-dash lines, Schenck's wüstite boundary

great variations in apparent solubility of Fe_3O_4 in FeO are due to the fortuitous differences in properties of the materials produced by reduction. If they are open and porous and are not allowed to sinter, they approach nearer true equilibrium in the time allowed; but if any combination of circumstances causes effective burial of unreduced Fe_3O_4 in FeO , the gases will reach equilibrium with the

FeO on the surfaces of the particles and the interiors will remain unreduced except after exceedingly long contact. An almost prohibitive amount of time is needed for following a reduction isotherm completely from the composition of Fe_2O_3 to Fe with perfect attainment of equilibrium after each slight new addition of reducing gas. Only the water-vapor oxidation isotherm of Eastman and Evans (772° C.) seems at all probable, and even it has irregularities that are hard to explain. The 950° C. CO-reduction isotherm of Schenck also changes its direction exactly at the composition of FeO and is probably a reasonably good curve, although he discards it and uses the 700° and 800° C. isotherms in a subsequent paper. The practical conclusion is that the data of Table 14 and Figure 26 are only loose approximations.

WÜSTITE FIELD

Shortly after Figure 25 had been prepared Schenck and Dingmann⁵⁹ published five new reduction isotherms, in all of which the horizontal between magnetite and FeO began at the composition of magnetite, with no indication of solid solutions of FeO in the magnetite. This fact contradicts the other isotherm data and indicates that Schenck, who says nothing about it in his article, was interested mainly in the inclined portion of the curve, which occurs later in the isotherm (the solid solutions of Fe_3O_4 in FeO) and probably hurried the work until the gas analyses showed he was on the desired horizontal part; or he may have arbitrarily drawn the horizontal back to the composition of Fe_3O_4 . To say the least, this new work contradicts all previous isotherms and solubility data derived from other sources. Therefore, the solubility curve for FeO dissolved in Fe_3O_4 , as given in Figure 26, although poorly determined, is regarded as valid. Schenck's second series of reduction isotherms was used mainly to study the inclined portion between 22 and 24 per cent of oxygen, commented on above. This region of solid solutions he wishes to name "wüstite." From the inclined portion to the left of FeO on these isotherms he derives the edges of the stability field of wüstite, which are included as dot-and-dash lines in Figure 26. Wüstite should lose its identity at 570° C., where FeO splits into magnetite and iron. The left side of the wüstite field seems to be nothing but the solubility curve of Fe_3O_4 in FeO, determined from the previous isotherms and other data. The agreement is as good as in the previous data. The right side requires more consideration.

For the inclined portion of the isotherm to reach the second horizontal before the composition of FeO is reached on a reduction iso-

⁵⁹ Schenck, R., and Dingmann, Th., Gleichgewichtsuntersuchungen über die Reduktions-Oxydations- und Kohlensvorgänge beim Eisen. III; Ztschr. anorg. allgem. Chem., Jahrg. 166, 1927, pp. 113-154.

therm means nothing more than that unreduced cores of oxide particles are present, probably due to conducting the work in too great a hurry. The oxidation isotherm of Eastman and Evans prepared from the opposite direction shows that the inclined portion intersects the horizontal between the compositions of FeO and Fe and that the intersection has nothing to do with Fe_3O_4 . One therefore feels constrained to reject Schenck's right boundary of the wüstite area and to move it so that the point *P* falls at 100 per cent of FeO and the remainder of the right boundary falls in the field between FeO and Fe and therefore not in Figure 26. The left boundary of the wüstite area need not be shifted any farther to the right than the datum of Eastman and Evans, represented by a triangle in the diagram. This point, approached by oxidation of iron, agrees reasonably well with most of the other points approached through reduction. The corrected left boundary of the wüstite area is therefore indicated by a solid line, which includes all the previous work and is properly weighted for the second Schenck publication. Schenck's proposal to use the name "wüstite" for these particular solid solutions, including those on the opposite side of the 100 per cent of FeO line, is acceptable.

At higher temperatures the two conjugate solid solutions of FeO and Fe_3O_4 should approach each other, so that in the molten state unlimited miscibility would prevail between these two materials of cubic crystallization.

ADJUSTMENTS

An interesting corollary of these solubilities is suggested by Ferguson.⁶⁰ Ferrous oxide is known to be metastable below about 570° C. This point should be affected, probably lowered, by the solution of Fe_3O_4 in FeO, and the lowering would be proportional to the amount of Fe_3O_4 dissolved. Ferguson therefore expects to find that the true critical point below which FeO is metastable is higher than 570° C. All of the determinations in which the 570° point has been involved have been made in the presence of plenty of Fe_3O_4 . Ferguson's own work has shown that he could lower the temperature of an FeO product containing excess Fe_3O_4 to 526° C. before dissociation took place, and he had to reheat it above 600° C. before the resulting Fe_3O_4 and Fe recombined. Of course this is not proof of his hypothesis, as few such transformations take place until the actual critical temperature has been passed; some driving force is necessary to cause the expected changes. One may, however, look for pure FeO, when prepared, to exhibit a different critical temperature.

⁶⁰ Ferguson, J. B., Oxides of Iron: Jour. Washington Acad. Sci., vol. 13, 1923, pp. 275-281.

FERROUS OXIDE

CHARACTERISTICS

Ferrous oxide, FeO , is the least known of the oxides of iron, because it is metastable at ordinary temperatures, and therefore most of the methods by which it is prepared fail to yield a pure product. Only two or three experimenters have ever produced it in a state approximating purity and collected enough evidence to make convincing their claims to having done so. Even those who used X-ray diffraction patterns have apparently believed that their product was purer than they could prove.

The color of the purest preparations has always been black, resembling magnetite, Fe_2O_4 , and distinguishable from magnetite under the microscope only by a special method developed by H. E. Merwin of the Geophysical Laboratory. He prepares a polished section of a fused specimen containing both FeO and Fe_3O_4 ; and when heated to red heat the polished magnetite surface is unaffected while the ferrous oxide surface assumes a matte appearance, due to conversion of the ferrous oxide into a mixture of iron and magnetite.

The crystal system of ferrous oxide is cubic. Work by Wyckoff and Crittenden, using X-ray diffraction patterns produced from the powder of a sample containing nearly 80 per cent of FeO , 20 per cent of Fe_3O_4 , and 0.54 per cent of Fe , showed that the unit cube contained 4 molecules of FeO with an edge length, $a=4.2944 \text{ \AA}$. This measurement probably is a trifle long, as the work of these investigators on preparations with different amounts of magnetite showed that its presence, probably in solid solution, increased the length of the edge.

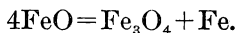
The density of a sample of ferrous oxide prepared by Hilpert and Beyer⁶¹ and containing 97.83 per cent of FeO was measured and found to be 5.9 grams per cubic centimeter. Wyckoff and Crittenden calculated from their edge length of the unit cube of FeO that its density would be 5.99, whereas the observed density of their impure sample was 5.7. Taking into account that their sample contained about 20.3 per cent of Fe_3O_4 , which has a density of only about 5.18, and assuming Hilpert and Beyer's observation as correct for FeO , one can calculate that the specific gravity of the Wyckoff and Crittenden sample is 5.72, which agrees very well with their observa-

⁶¹ See footnote 96, p. 56.

tion of 5.7. The Hilpert and Beyer observation of 5.9 can then be corrected for its 2.13 per cent of Fe_3O_4 , giving 5.92 as the corrected specific gravity of pure FeO , which agrees with the calculated figure, 5.99, derived from the X-ray data, as well as derived data usually do.

FIELD OF STABILITY

As mentioned above, FeO is metastable at ordinary temperatures. It is stable only above about 570°C ., and below that can split into two products according to the reaction:



The invariant or triple point is given as 570° by Chaudron⁶² and by Wöhler and Günther⁶³; it is placed at 565° by Eastman⁶⁴ after a critical thermodynamic analysis of existing data, at 570° by Eastman and Evans⁶⁵ after studying the hydrogen reduction system, at 578° by Ferguson⁶⁶ through interpolation from direct observations, and at 535° by Tigerschiöld⁶⁷ through thermodynamic calculations. An acceptable mean is 570°C . Many other authors have contributed to the qualitative evidence culminating in the above references, but these are quantitative.

On the reduction-equilibrium diagrams for both hydrogen and carbon monoxide used as reducing agents, ferrous oxide can be produced only at temperatures above this invariant point, 570°C . whereas below that temperature ferrous oxide is metastable with respect to $\text{Fe} + \text{Fe}_3\text{O}_4$, and instead of reducing Fe_3O_4 to FeO at these lower temperatures the tendency is to reduce Fe_3O_4 direct to Fe without any intermediate FeO step. Therefore, nearly all of the literature on ferrous oxide, written before 1920, or before this fact was definitely known, needs to be regarded very critically; and the various fanciful explanations as to the reasons for difficulty in preparing FeO free of magnetite and metallic iron should be disregarded. Some of the older methods may have actually produced it in an unknown condition of purity but need critical repetition now.

In the complete phase diagram (fig. 102) of the iron-oxygen system, given in one of the final sections of this paper, the stability field of FeO is shown. As will be explained there, it can not crystallize in a pure condition from a melt, loses its identity at its melting

⁶² Chaudron, G., Étude des réactions réversibles de l'hydrogène et de l'oxyde de carbone sur les oxydes métalliques: *Ann. chim.*, t. 16, 1921, pp. 271-281.

⁶³ See footnote 37, p. 72.

⁶⁴ See footnote 69, p. 35.

⁶⁵ See footnote 40, p. 75.

⁶⁶ See footnote 69, p. 35.

⁶⁷ Tigerschiöld, Magnus, Järnets Oxider Från Termodynamisk Synpunkt: Avtryck ur Jernkontorets Annaler För Ar, 1923, pp. 67-105.

point, 1,378° C., and is metastable below 570° C., where it splits into iron and magnetite.

SPLITTING AND RECOMBINATION OF FERROUS OXIDE

The reaction of the dissociation of ferrous oxide written above is reversible, and according to two of the above observers the magnetite and iron will recombine almost completely if the mass is heated above 570° C.

The work of Ferguson on one of his best ferrous oxide preparations is plotted in Figure 27. Part of the material was held at unspecified temperature between 570° and 300° for an unspecified period of time, to cause the ferrous oxide to split completely into Fe and Fe_3O_4 . This sample was divided and portions of it heated five

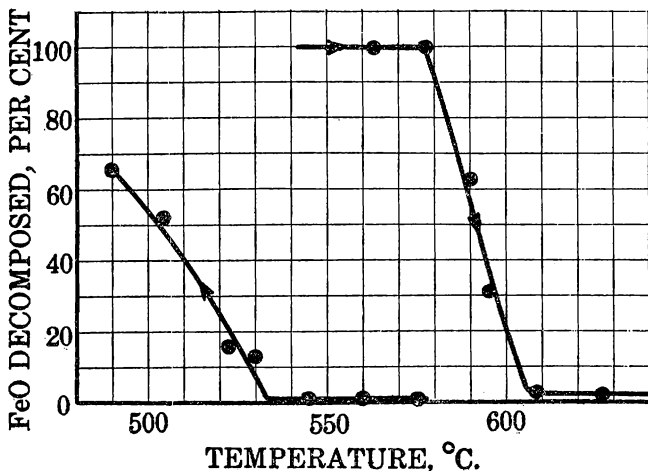


FIG. 27.—Splitting and recombination of FeO (Ferguson)

hours each at different temperatures, giving the curve at the right in Figure 27. Recombination set in at 577° and was complete at 607° C. if a 5-hour interval were used. Doubtless a long enough heating at lower temperatures would bring about the same result. The left curve of Figure 27 shows the effect of 5-hour periods of heating on the original ferrous oxide preparation; it did not split any in a 5-hour interval until the temperature was as low as 536° C., and then it broke up in increasing proportions until at 480° C. a 65 per cent decomposition was attained. These curves are derived from Ferguson's data, which show that apparently the FeO must be supercooled some distance below the supposed invariant point, 570°, before enough driving force becomes available to make the rigid solid rearrange into magnetite and iron, and the rate of conversion then increases with lowering temperatures.

More complete data are given by Chaudron and Forestier⁶⁸ and are plotted in Figure 28. The curve marked "Hours" was for samples of pure FeO heated for successive time intervals at 445° C. and analyzed for metallic iron, ferrous iron, and ferric iron after each interval. In eight hours only about 78 per cent decomposition of the FeO took place. They chose 12-hour intervals for comparison, and in the other curve of Figure 27 the results of heating samples for 12 hours at various temperatures are given. A maximum of 80 per cent decomposition in 12 hours is recorded, and below 300° C. practically no decomposition took place in that time.

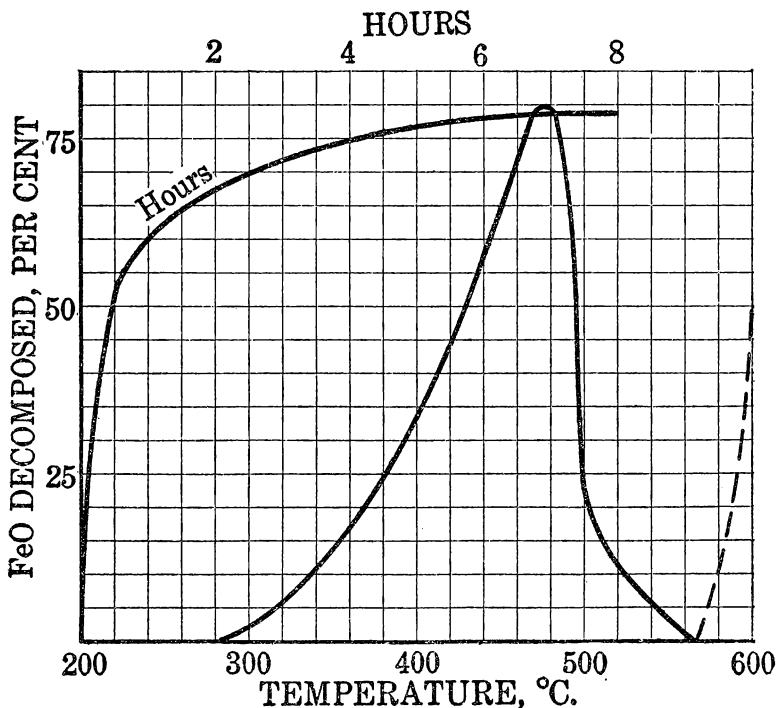


FIG. 28.—Splitting and recombination of FeO (Chaudron and Forestier)

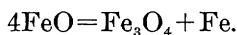
One sample was reheated for 24 hours at 600°, and at the end of that time only slightly over 50 per cent of the ferrous oxide had been remade from its decomposition products. At 590° only 24 per cent of reconstituted ferrous oxide was formed in 24 hours. The dotted curve in Figure 28 from Chaudron's work is evidently intended to show these facts but does so erroneously.

The failure of Chaudron and Forestier to cause magnetite and iron to recombine completely to form FeO at practically the same tem-

⁶⁸ Chaudron, G., and Forestier, H., Étude de la décomposition du protoxyde de fer. Anomalies de dilatation corrélatives de son instabilité: *Compt. rend.*, t. 178, 1924, pp. 2173-2176.

perature as that used by Ferguson, who claims almost complete recombination in five hours, is disconcerting. As will be pointed out later, the point is exceedingly important and needs further check. If Ferguson is correct, one might hope to produce ferrous oxide at high temperatures by the action of magnetite on iron. Only one piece of qualitative evidence supports Ferguson in his claim for almost complete reaction (about 1 per cent of metallic iron left in his best samples). That was in the original work by Chaudron,⁶⁹ which encouraged the work by Chaudron and Forestier and also that by Ferguson, discussed above. The work was only qualitative in character. Ferrous oxide heated in a closed tube for two hours at 440° became magnetic and precipitated copper from copper sulphate solution. Also, on metallographic examination of polished surfaces this product showed lamellæ of metallic iron which turned brown when touched with copper sulphate solution. When reheated for four hours at 600° in a sealed tube the material lost its magnetism and its ability to precipitate copper, indicating complete recombination. Evidently something further needs to be learned about the effect of previous history on the activity of these various ferrous oxide preparations.

Chaudron and Forestier measured the rate of decomposition of FeO at 445°, and their results can be given in the mathematical expression $dx/dt = k(100-x)^4$ where x represents the percentage decomposed in time t expressed in hours and k is a constant. It is an interesting fact that the rate is proportional to the fourth power of the concentration of undecomposed FeO, which might be connected with the fact that 4 molecules of FeO must decompose simultaneously in order that the reaction can take place as written,



Reactions of such high order are not common, but in this case the unit crystal cube contains 4 FeO molecules, and it is conceivable that the conditions indicated are true.

Ferguson advances the hypothesis that the invariant point at 570° is shifted to lower temperatures when much magnetite is in solid solution in the FeO, the new invariant point being between FeO-Fe₃O₄ solid solution, Fe₃O₄, Fe, and gas. This might account for the discordance of various experimenters' results at temperatures in this region. Although ferrous oxide and magnetite form solid solutions in each other to at least some extent, there is no other evidence to support the hypothesis.

The practical conclusion of this work is that pure ferrous oxide prepared at high temperatures can be brought safely to room tem-

⁶⁹ See footnote 62, p. 96.

peratures without appreciable decomposition, provided it is cooled rapidly from 570° to 300° C. At room temperature it keeps indefinitely if protected from the atmosphere.

ANALYSIS OF MIXTURES OF FeO, Fe₃O₄, AND Fe

One difficulty with earlier experimenters on FeO has been their failure to test the product for purity. Most of the recent work has used some variation of the copper sulphate solution method of removing metallic iron from the samples analyzed. Copper sulphate affects the metallic iron only, taking it into solution and leaving unaffected the ferrous oxide and magnetite. This was used as the basis of a method of analysis by Williams and Anderson,⁷⁰ later improved by Sims and Larsen.⁷¹ The latter remove metallic iron from the sample by use of copper sulphate solution, dissolve out the precipitated metallic copper with alkaline cyanide solution, then dissolve the residue in hydrochloric acid, titrating for ferrous iron, and finally reduce the solution to titrate for total iron, estimating ferric iron by difference.

Research on the analysis and preparation of FeO mixtures was carried out recently by Groebler and Oberhoffer.⁷² They found that when treating a mixture of Fe, FeO, and Fe₃O₄ the removal of metallic iron by chlorine, bromine, KI solution of iodine, and ferric chloride solutions were all unsuccessful, due either to incomplete action on the metallic iron or to attack of FeO by the gas or solution. They also condemned the Sims and Larsen method because it gave higher values of metallic Fe than their own modification of the mercuric chloride method about to be described. As a precipitate of mercurous chloride forms when mercuric chloride solution is used to remove metallic iron this method has value for analytical purposes only and not for the preparation of pure FeO free of Fe. The work of several previous investigators leads to the conclusion that the increasing hydrolysis of mercuric chloride by rise of temperature makes temperature an important point to watch when the iron is being dissolved out, as the acid produced by hydrolysis attacks FeO. The best compromise method found was to use 0.5 gram of the product to be analyzed, placed in a beaker with 3 grams of HgCl₂ and 75 c. c. of water, heated with shaking to incipient boiling temperature, and then cooled immediately. The volume can then be increased to 150 c. c. with water and the product filtered away from the residue of iron oxides and Hg₂Cl₂. The volume of each 50 c. c. of filtrate could be

⁷⁰ Williams, C. E., and Anderson, Arvid, The Determination of Metallic Iron in Sponge Iron: *Ind. and Eng. Chem.*, vol. 14, 1922, p. 1057.

⁷¹ Sims, C. E., and Larsen, B. M., Determination of Ferrous Iron in Materials Containing Metallic Iron: *Ind. and Eng. Chem.*, vol. 17, 1925, p. 86.

⁷² See footnote 47, p. 83.

increased to 100 c. c. with water, 5 c. c. of HCl, and 40 c. c. of manganous sulphate-phosphoric acid titrating mixture added, and the mixture titrated with potassium permanganate.

Ferrous iron from ferrous oxide, magnetite, and metallic iron was determined on a separate sample. Separate tests were made to prove that the hydrogen resulting from the action of the hydrochloric acid on metallic iron did not reduce the ferric chloride resulting from dissolution of the magnetite.

The ferric iron content of this solution could be determined by the difference between the ferrous iron and total iron or by reaction with KI solution producing ferrous chloride and free iodine, which could be determined with thiosulphate.

PREPARATION OF PURE FeO

The above preliminary discussion has been necessary to show the difficulties encountered in preparing pure FeO. One of the favorite early methods of preparing so-called FeO was to ignite ferrous oxalate. The usual end product was a material undoubtedly containing FeO but also containing metallic iron, magnetite, and carbon, usually as carbide. The proportions of carbon dioxide and carbon monoxide resulting from decompositions of the oxalate were not in accordance with those in the equilibrium diagrams involving FeO, Fe, Fe₃O₄, CO, and CO₂, and an adjustment usually took place in the solid and gas phases to approach nearer these equilibria, with the resulting production of some other solid substance in addition to FeO. Even the few early experimenters who managed to get a product consisting mostly of iron and oxygen in the proper gross ratio usually found, if they investigated at all, that the product was not entirely FeO. In addition, nearly all of the earlier workers violated the temperature-stability principles already enumerated, and products prepared above 570° C. were frequently degraded by too slow cooling through the range 570° to 300° C. For instance, the product prepared by Hilpert and Beyer was nearly 98 per cent pure but would probably have been purer had it been cooled more rapidly from 1,100°, the temperature where it was made, to room temperature (the report of the work states that it required over one hour to cool the sample in the furnace to room temperature).

WORK OF WÖHLER, BALZ, AND GÜNTHER

No samples of FeO approaching a condition of purity satisfactory to a chemist were prepared until 1921, when Wöhler and Balz,⁷⁸

⁷⁸ Wöhler, Lothar, and Balz, O., Die Bestimmung der Wertigkeitsskale von Eisen, Kobalt, Nickel, Kupfer, Mangan, Zinn, und Wolfram mit Hilfe ihres Wasserdampfgleichgewichtes, und der Dissoziations-druck der Oxyde dieser Metalle: *Ztschr. Elektrochem.*, Jahrg. 27, 1921, pp. 406-419.

and shortly thereafter, Wöhler and Günther,⁷⁴ made them. Wöhler and Balz treated finely divided iron with steam at high temperatures, and Wöhler and Günther reduced the ferric oxide with a stream of hydrogen and water vapor at temperatures and ratios such that ferric oxide was reduced to magnetite and the magnetite to FeO without the gas being sufficiently reducing to convert any FeO into iron. The equilibrium diagrams of hydrogen, iron, and oxygen prepared by Eastman and Evans⁷⁵ can be consulted for the proper gas mixtures to use at various temperatures above 570°. Wöhler and Günther bubbled hydrogen through water at 74.1° to 77.5° C. to saturate it, and for 0.1 gram of Fe₂O₃ they passed 1 liter of the mixture per hour per square centimeter cross section of combustion tube. In 12 hours a product analyzing 99.9 per cent of FeO was prepared. Reducing these figures to H₂O:H₂ ratios, at 700° C., the ratio was 0.58 and at 800° it was 0.71 for the production of exceptionally pure products. These products were cooled rapidly through the temperature range where there was danger of decomposition. No other method of preparing pure FeO has been reported with data enough to prove the purity of the product.

The material prepared in this manner was only half converted to magnetite and iron when heated in vacuo for three days at 550° C. It could therefore be used successfully for scientific work at all temperatures as long as it was not exposed for more than a few minutes to temperatures of 450° to 550° C.

WORK OF OTHER INVESTIGATORS

Groeble and Oberhoffer tried the Hilpert and Beyer method thinking that it might be of value for the preparation of a large quantity of FeO of good purity. At about 800° C., using a gas consisting of 66 per cent of CO and 34 per cent of CO₂, a 1-gram charge on a boat in a combustion tube could be reduced to a product which was 99.3 per cent pure. With 6-gram charges the best product obtained contained 95 per cent of FeO and had both magnetite and metallic iron as impurities. This latter charge required nearly 10 hours for preparation. The investigators concluded that small temperature variations are fatal and that the material must all be held at the same temperature. Small samples of shallow depth at one point in a combustion tube meet these conditions, but large ones do not.

In order not to be dependent on gas composition and constant temperature, Groeble and Oberhoffer also tried gas reduction with slightly more CO than necessary to reduce the last traces of magne-

⁷⁴ See footnote 37, p. 72.

⁷⁵ See footnote 40, p. 75.

tite and thereby produce a certain amount of metallic iron which should be capable of removal by solvents. The various solvents were discussed in connection with the analysis of mixtures containing FeO above, but the present reviewer could find no reason why a method which would dissolve the iron and a little FeO (admittedly of no value for analytical purposes) should not be satisfactory, provided the residue was pure FeO and not too much of it was lost by solution in the Fe solvent. All of these methods are condemned by Groebler and Oberhoffer with the bare statement that no solvent left better than a 95 per cent of FeO product. Seemingly, the method is worth further research. These investigators quite correctly carried on their work in a combustion tube, one end of which was water-cooled for withdrawal and rapid cooling of the boat after reduction to FeO had been completed. It is difficult to understand why they abandoned hydrogen as a reducing agent and substituted carbon monoxide, with attendant risk of partial carburization of their product.

Schenck⁷⁶ reports preparing a sample of FeO by treating Fe₂O₃ at 800° C. with a mixture of 66.66 per cent of CO and 33.33 per cent of CO₂, which he reports is the equilibrium ratio between FeO and Fe at that temperature. His product contained 0.1 per cent of Fe in excess of the theoretical ratio, and it was feebly magnetic. No mention is made of analyzing it for metallic Fe, magnetite, or carbon. Lacking such confirmatory data, Schenck's claim to preparation of high-purity FeO is not regarded as established.

Whether FeO can be made by dehydration of ferrous hydroxide at ordinary temperatures is not mentioned in the literature. Joannis⁷⁷ gives directions for preparing the dry Fe(OH)₂, which may be of value in this connection. A solution of a ferrous salt can be precipitated with caustic potash (ammonia is unsuitable on account of adsorption and later bad effect during drying) with all air excluded. Washing must be done rapidly with boiling water under a nitrogen atmosphere and with rigid exclusion of oxygen from the white precipitate. Boiling water acts slowly on ferrous hydroxide, with the production of hydrogen and magnetite. Therefore, after rapid washing and settling, the water is displaced by ether and the ether removed by gentle warming in vacuo, leaving a dry precipitate. Once dry, Fe(OH)₂ is light green, the color probably being connected with slight oxidation. It must be kept out of contact with air, as it oxidizes rapidly. Whether or not it can be dehydrated in vacuo over a desiccant is unknown.

⁷⁶ See footnote 58, p. 88.

⁷⁷ Joannis, M., Fremy's Encyclopedie chimique; III, Metaux: 9th ed., Paris, 1884.

PREPARATION OF FeO BY REDUCING MAGNETITE WITH IRON

The samples of ferrous oxide used by Wyckoff and Crittenden were prepared at the Fixed Nitrogen Research Laboratory in Washington by burning armco iron rods in an atmosphere of oxygen, allowing the molten iron oxide product to drop into a receptacle at the bottom. This material formed the basis of a series of iron oxide catalysts for ammonia production and was also used as a raw material for the production of ferrous oxide. It contained mostly magnetite with some ferrous oxide and some iron metal. It was broken up, mixed with more armco iron, and heated by resistance between two water-cooled iron electrodes, forming a puddle of the reaction product in the midst of unmelted raw materials and thus avoiding contamination with everything except the gases of the atmosphere. The product was broken up and remelted in an effort to make it thoroughly homogeneous and to encourage the reversible reaction $\text{Fe}_3\text{O}_4 + \text{Fe} = 4 \text{FeO}$ to proceed to completion and yield molten FeO of high purity. The material produced contained excess metallic iron which had to be separated by a strong electromagnet and the least magnetic portion of which was regarded as ferrous oxide. It was practically nonferromagnetic but contained 0.54 per cent of metallic iron which could not be separated. This product was that used by them for getting the X-ray diffraction spectrum of FeO mentioned above. On chemical analysis by the Sims and Larsen method it gave the following:

<i>Analyses of product</i>		Per cent
Material		
Free Fe.....	-----	0.54
Ferrous Fe.....	-----	65.84
Ferric Fe.....	-----	9.80
Total Fe.....	-----	76.18
<i>Calculated to oxides</i>		Per cent
Material		
Free iron.....	-----	0.54
FeO.....	-----	78.40
Fe ₃ O ₄	-----	20.32
Total.....	-----	99.26

Because of the lack of spectral lines ascribable to free iron and magnetite in their X-ray diffraction patterns and unknown difficulties in the analytical method, Wyckoff and Crittenden felt that these analyses were probably unreliable, especially as the product apparently contained enough magnetite to react strongly if free, under the electromagnet. No further evidence was collected to see just wherein the difficulty lay.

WORK OF MILLAR

At the Pacific Experiment Station of the Bureau of Mines, R. W. Millar (results unpublished) worked with some of the same material, a gift from the Fixed Nitrogen Laboratory. He purified it further by magnetic separation and obtained a sample with the following analysis, using the same analytical method:

<i>Analyses of sample</i>	
Material	Per cent
Free Fe.....	0.80
Ferrous Fe.....	68.46
Ferric Fe.....	7.98
Total Fe.....	77.24
<i>Recalculated</i>	
Material	Per cent
Free Fe.....	0.80
FeO.....	82.95
Fe ₃ O ₄	16.54
Total.....	100.29

Another sample was reduced by hydrogen, and the residual iron was 77.22 per cent of the original, which agreed nicely with the total Fe determination by titration and showed that the failure to add to exactly 100 per cent was probably connected with minor inaccuracies in the Sims and Larsen method; the result also showed that the Sims and Larsen method was probably not far from the truth. The oxygen content determined by hydrogen reduction indicates an intermediate analysis between FeO and Fe₃O₄. Removal of free iron by the use of a suitable CuSO₄ solution before determination of ferrous and ferric oxide iron left a product that colored the acid yellow the minute the sample was introduced into it, even though special precautions had been taken to exclude atmospheric oxygen. The ferric iron content was therefore real, and ferric oxide in the iron-oxygen product is not present as a magnetic form of magnetite. The ferric oxide of magnetite may be in the FeO:Fe₃O₄ solid solution as ferric oxide dispersed through ferrous oxide, but this is not probable. Why the X-ray spectograph does not show magnetite is difficult to explain.

WORK OF GROEBLER AND OBERHOFFER AND OF HILPERT AND BEYER

Groebler and Oberhoffer radiographed a series of reduction specimens of various iron-oxygen ratios between Fe₂O₃ and Fe. In the range between magnetite and ferrous oxide they likewise found that when the composition approaches 61 per cent of FeO and 39 per cent of magnetite the X-ray spectrum of the latter vanished.

Their hypothesis is that the magnetite, a material with a cubic lattice, tends to take on the cubic lattice of FeO at this dilution and the extra oxygen atoms exist in the haphazard positions in the interstices between the other Fe and O atoms. They call these oxygen atoms that fail to produce spectra "vagabond atoms."

Hilpert and Beyer, in the work already quoted, prepared a series of partly reduced products intermediate between magnetite and ferrous oxide and determined their magnetic susceptibility. Their results constitute some of the earliest reliable evidence of the existence of solid solutions of the two oxides. Figure 22 shows the galvanometer deflections of their ballistic galvanometer as plotted against the total percentage of FeO in their product. The galvanometer deflection becomes zero when the amount of FeO in the product reaches 82 per cent, the remainder being calculated as Fe_2O_3 , corresponding to 74 per cent of free FeO and 26 per cent of Fe_3O_4 or to $\text{Fe}_2\text{O}_3 \cdot 10\text{FeO}$, if such a compound existed. This analysis resembles that obtained by Wyckoff and Crittenden. As a further check on the magnetic method used, Hilpert and Beyer mixed finely powdered magnetite with nine times its weight of kaolin, which was tested and gave a galvanometer deflection of 2.9, or about what would be expected if the magnetite functioned as magnetite. Fine division lessens the deflection but is apparently not responsible for the present case of complete loss of susceptibility. The inevitable conclusion is that the magnetite has entered the material in some intermediate compound or solid solution and has lost its identity.

This remarkable result must be considered in connection with the fact that Wyckoff and Crittenden had repeatedly melted their iron-oxygen complex in contact with molten iron (under air, it is true), and its ferric oxide content had not been completely reduced to ferrous iron. Evidently the activity of the ferric oxide in the fusion is insufficient to cause reaction with free iron in the time allowed, at the melting temperature of iron. The method is therefore not adapted to the production of pure ferrous oxide.

WORK OF OTHER INVESTIGATORS

Three other investigators have obtained results parallel with the above. J. H. Whiteley,⁷⁸ of Saltburn, England, heated to 1,300° to 1,400° C. a mixture of ferric oxide and electrolytic iron strips packed in a hole in a block of armco iron which was tightly plugged. The reaction product had usually fused, at least in part, but it was never completely reduced to FeO, and the best product contained 8 per cent of Fe_2O_3 (equivalent to 11.5 per cent of Fe_3O_4). However, his

⁷⁸ Whiteley, J. H., Cupric Etching Effects Produced by Phosphorus and Oxygen in Iron: Jour. Iron and Steel Inst., vol. 103, 1921, pp. 277-289.

big block of metal may have been cooled too slowly through the critical range and suffered some splitting into Fe_3O_4 and Fe.

A similar attempt was made by Tritton and Hanson,⁷⁹ working under W. Rosenhain at the National Physical Laboratory, Teddington, England. Electrolytic iron was melted under ferric oxide in a high-frequency induction furnace in a magnesia crucible with specially glazed MgO lining, in the expectation that the molten iron would reduce the molten oxide to FeO, in order to determine the solubility of FeO in molten iron. The iron layer contained 0.21 per cent of oxygen, probably present as FeO, and the oxide layer had the following analysis:

<i>Analysis of oxide layer</i>		Per cent
Material		
Free Fe		0.99
Total FeO		80.6
Fe_2O_3		14.0
SiO_24
MgO		3.0
 <i>Recalculated</i> 		
Material		Per cent
Free Fe		1.03
FeO		77.1
Fe_2O_3		21.05
Total		99.18

The incompleteness of the reduction is notable, but in this case quick melting and cooling were necessary to avoid profound attack on the silica protecting tubes of the thermocouples and of the magnesia pot. Evidently too little time was allowed for the reactions to go as far as they might have done. Also, the solubility of oxide in the metal as measured was probably low, due to lack of time and to the presence of a large amount of some other oxide than FeO. No mention is made as to whether the free iron in the oxide layer was present in large or small units, but part was probably present in true solution.

More recent melts by Herty,⁸⁰ made in the same manner in a much larger induction furnace and kept molten for some time, gave molten oxides, two of which were analyzed with the following results:

Analyses of oxides

Material	Per cent	Per cent
FeO	75.0	83.3
Fe_2O_3	15.0	12.5
SiO_2	2.2	1.7
MgO	6.8	3.2

⁷⁹ Tritton, F. S., and Hanson, D. J., *Ferrous Alloys Research. Iron and Oxygen: Iron and Steel Inst.*, vol. 110, 1924, pp. 85-143.

⁸⁰ Herty, C. H., and others, *The Physical Chemistry of Steel Making: Carnegie Inst. of Technol., Bull. 34, 1927, 69 pp.*

By comparison it can be seen that one was less and the other slightly more reduced than the Tritton and Hanson oxide. Had the melts been conducted under an atmosphere of nitrogen or in vacuo, the FeO would have been reoxidized less by air, and it is conceivable that a reasonably complete reduction might have been obtained.

However, to date no method of mixing metallic iron and ferric oxide or magnetite, solid or liquid, has been devised under which even approximately complete reduction of the higher oxides to FeO would take place. Only the work of Ferguson on recombination of molecularly dispersed Fe_3O_4 and Fe, formed by spontaneous decomposition of FeO below 625°C ., has thus far claimed success, and it needs further check to adjust the apparent contradictions.

At this point it would be well to glance at the above-mentioned iron-oxygen temperature-composition phase diagram of Benedicks and Löfqvist (fig. 102), which, if correct, shows that a sample of pure FeO after melting would, on freezing, crystallize out metallic iron until a eutectic point was reached having about 24 per cent of oxygen instead of the desired 22.28 per cent. Quick cooling of a molten sample of about the correct composition, if conducted from about $1,500^\circ\text{C}$. to below $1,370^\circ\text{C}$. with enough rapidity, should leave a product from which metallic iron has not had the opportunity to separate and which should be in the stability field of Schenck's "wüstite" previously mentioned. However, it is still doubtful whether molten pure iron has sufficient reducing power to reduce the last traces of magnetite in a liquid magnetite-ferrous oxide mixture.

MISCIBILITY OF FeO AND Fe_3O_4

We have already seen that FeO and Fe_3O_4 are not miscible in all proportions but that each dissolves a considerable amount of the other, and we should expect them to become miscible in all proportions at higher temperatures, probably where one or both of them can exist in a molten condition.

MISCIBILITY OF FeO AND Fe

The work of Tritton and Hanson and of Herty and others quoted above constitutes nearly all of the available data on the solubility of metallic iron in ferrous oxide, except the unreliable reduction and oxidation isotherms discussed on page 107. This subject is discussed in the following section.

MELTING POINT

Tritton and Hanson took cooling curves on their iron melts saturated with iron oxide and observed a kink at $1,369^\circ\text{C}$., while on

heating it occurred at $1,371^{\circ}$ C. They therefore conclude that $1,370^{\circ}$ C. is the melting point of FeO. Schönert⁸¹ in criticizing their iron-oxygen phase diagram, showed that this temperature was doubtless that of the eutectic (see fig. 31) between Fe and FeO solutions, and the true melting point of pure FeO would probably be $1,380^{\circ}$ C.

Groebler and Oberhoffer worked with a series of samples of different purities and extrapolated to the melting point of the pure material. Their samples were made into little briquets around a platinum wire and hung in an electrically heated vacuum furnace with a glass window for sighting an optical pyrometer on the pendent briquet. When the briquet deformed and dropped off the corrected temperature readings were made and plotted against the percentage of FeO in the sample. Samples with 76 to 95.5 per cent of FeO were melted, and extrapolation to 100 per cent gave $1,377^{\circ}$ C., a remarkably close check on the value of Tritton and Hanson. Their exact data were not given but would be useful if published.

STABILITY IN AIR

Ferrous oxide preparations in finely divided form gradually oxidize at room temperature, but no observations have been reported on the action of the fused specimens. On heating to 200° or 250° C. FeO begins to oxidize rapidly and even glows in air. Carbon dioxide is supposed to be taken up with avidity,⁸² and the solubility in water is quoted by Thorpe as 1 part in 150,000. The hydrated oxide is known to all chemists as a white precipitate, which turns green quickly and absorbs oxygen from the air with great avidity, the final oxidation product depending upon the conditions of the solution in which the oxidation takes place.

HEAT OF FORMATION

Nearly all of the determinations of the heat of formation of ferrous oxide have been made from improperly prepared samples containing metallic iron, magnetite, and even carbon. Mixer and Ruff and Gersten show by their reports that these factors were taken into account and proper corrections made. Their reports are tabulated in Table 15.

⁸¹ Schönert, K., *Das Eisen-Oxygen System*: Ztschr. anorg. u. allgem. Chem., Jahrg. 154, 1926, pp. 220-225.

⁸² Thorpe, Sir E., *Dictionary of Applied Chemistry*: New York, Vol. III, 1922, p. 677.

TABLE 15.—Heat of formation of ferrous oxide in calories per gram-molecule

Heat of formation	Observer	Heat of formation	Observer
-68,300.....	Thomsen. ¹	-66,600 at 1,000° C.....	Treadwell. ⁶
-64,600.....	Le Chatelier. ²	-68,600 at 25° C.....	Treadwell. ⁷
-60,400+1,800.....	Ruff and Gersten. ³	-66,300.....	Tigerschiöld. ⁸
-64,300.....	Mixter. ⁴	-63,350.....	Wöhler and Günther. ⁹
-66,713.....	Yermilov. ⁵		

¹ Thermochemistry, New York, 1908.

² Le Chatelier, H., Sur chaleur de formation de quelques composés du fer: Compt. rend., t. 120, 1895, p. 623.

³ See footnote 33, p. 72.

⁴ See footnote 32, p. 72.

⁵ See footnote 38, p. 72.

⁶ See footnote 39, p. 72.

⁷ Calculated from 1,000° datum.

⁸ See footnote 67, p. 96.

⁹ See footnote 37, p. 72.

The Treadwell datum was calculated from cell measurements at 1,000° C. in a fused electrolyte. The data of Tigerschiöld and of Wöhler and Günther were calculated thermodynamically from the equilibrium data for the equation, $\text{FeO} + \text{H}_2 = \text{Fe} + \text{H}_2\text{O}$. Equilibrium data at the temperature range 700° to 1,000° C. undoubtedly suffer from the fact that the FeO and Fe are mutually soluble to at least a slight extent, and the heats therefore correspond to the conversion of a solid solution of FeO saturated with metallic iron into a solution of metallic iron saturated with FeO.

From the standpoint of science, a sample of ferrous oxide of greater purity should be prepared and its heat of formation determined by modern methods of calorimetry.

The weighted average chosen from the above table is:

$$\text{FeO}, \Delta H_{298} = -63,825 \text{ calories.}$$

FREE ENERGY

The free energy of formation of FeO can be derived from the existing data on two reactions. From the equilibrium constants of the reaction $\text{Fe} + \text{H}_2\text{O} = \text{FeO} + \text{H}_2$, as measured by Eastman and Evans, which agree very closely with those of Wöhler and Günther, one may derive immediately an expression for the free energy change of the reaction by use of the expression $\Delta F = -RT \ln K$. The equilibrium data of Eastman and Evans are summed up in the expression $\log K = 840/T - 0.632$, which gives directly the expressions $\Delta F = 2.895T - 3,850$. If one adds to the reaction $\text{Fe} + \text{H}_2\text{O} = \text{FeO} + \text{H}_2$ the other reaction equation for the formation of water vapor, $\text{H}_2 + \frac{1}{2}\text{O}_2 = \text{H}_2\text{O}(g)$, for which the free energy equation given by Lewis and Randall⁸³ is $\Delta F = -57,500 + 0.94 T \ln T + 0.00165 T^2 - 0.00000037T^3 + 3.93T$, the sum is the new reaction, $\text{Fe} + \frac{1}{2}\text{O}_2 = \text{FeO}$, and the sum of the two free energy expressions gives the free energy

⁸³ See footnote 41, p. 75.

equation for this new reaction, $\Delta F = -61,250 + 0.94 T \ln T + 0.00165 T^2 - 0.00000037 T^3 + 6.82 T$.

Since the heat of formation is expressed for ordinary temperatures and since $25^\circ \text{C.} = 298^\circ \text{K.}$ the free energy expression for 298°K. will be $\Delta F^\circ_{298} = -57,472$ calories, the free energy of formation of FeO at room temperatures.

This empirical equation for the free energy of ferrous oxide can be compared with earlier calculations of Eastman⁸⁴ which are not based on as sound data as were available for derivation of this equation. Eastman calculated the free energy at $1,000^\circ \text{C.}$ as $-43,255$ calories, while the equation above gives $-42,083$ calories.

SPECIFIC HEAT

No reliable data whatever are available on the specific heat of ferrous oxide above or at room temperature. From room temperature down to below the boiling point of liquid air Millar has determined the specific heat of the sample containing 82.96 per cent of FeO , 14.54 per cent of Fe_3O_4 , and 2.5 per cent of free iron. He worked with a very precise aneroid calorimeter, and while his data are good, they are difficult to use, as the sample was far from pure, consisted of a solid solution of magnetite in ferrous oxide, and differed quite markedly in heat content from magnetite. Inasmuch as the applicability of Raoult's solution law to this particular solid solution is not known, calculation of the partial molal specific heat of the FeO in the mixture would be fruitless. Therefore, Millar's data, collected in the Pacific Experiment Station of the Bureau of Mines, are presented in Table 16 as a matter of record and for purposes of comparison when better preparations have been made and tested. They are also plotted in Figure 29 and are of interest, due to the presence of a hump of unexplained origin that occurs at a different temperature from the humps in the specific heat curve of magnetite in the section on "Magnetite."

TABLE 16.—Heat capacity per gram—impure FeO sample (Millar)

$T, ^\circ \text{K.}$	C_p	$T, ^\circ \text{K.}$	C_p	$T, ^\circ \text{K.}$	C_p	$T, ^\circ \text{K.}$	C_p
70.7	0.04588	118.2	0.10350	185.7	0.19130	241.3	0.16390
74.3	.05055	121.6	.10750	189.5	.18580	242.5	.16280
77.5	.05500	125.4	.11150	194.1	.17500	245.5	.16420
81.0	.05920	129.5	.11575	198.8	.16825	260.0	.16840
85.5	.06395	149.3	.14080	203.3	.16280	261.0	.16280
88.5	.06800	150.6	.13970	204.9	.16700	264.7	.17200
90.2	.07020	155.3	.14625	209.3	.16310	270.4	.15980
93.0	.07310	159.5	.15130	212.8	.16280	270.7	.16620
96.4	.07760	163.4	.15570	216.5	.16140	274.6	.16730
99.8	.08170	168.0	.16130	217.9	.16320	279.8	.16810
103.4	.08590	177.8	.18120	219.9	.16220	296.2	.17760
107.1	.09030	181.0	.18920	230.5	.16370	301.8	.17480
113.0	.09720	183.2	.19290	236.5	.16480		

⁸⁴ See footnote 69, p. 35.

ENTROPY

The direct calculation of entropy from low-temperature specific heat data is desirable in order to check calculations by thermodynamic equations based on other thermal data. No one has ever prepared a pure enough sample of FeO to make the measurements of low-temperature specific heats worth while. As soon as this has been done it will be well to check these measurements against the following estimate made from the heat of formation and the free energy.

Using the fundamental expression $\Delta F = \Delta H - T\Delta S$, and solving from data presented in the preceding pages for the entropy at

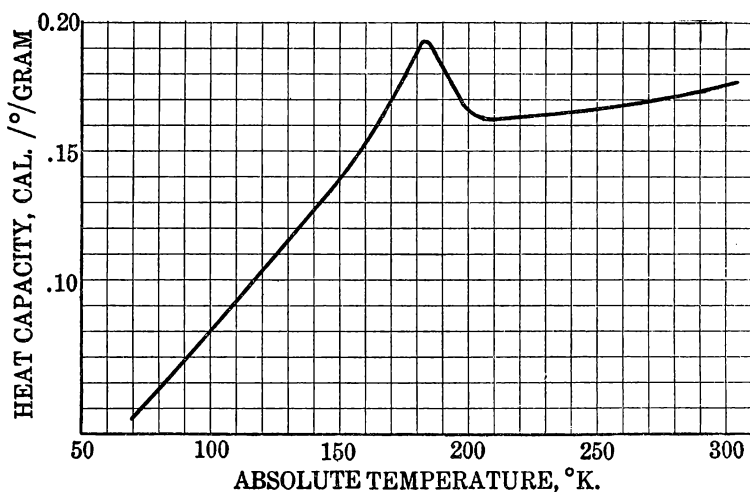


FIG. 29.—Specific heat of ferrous oxide (83 per cent) (Millar)

298° K., $\Delta S = (\Delta H - \Delta F) / T = (-63,825 + 57,472) / 298 = -21.3$ entropy units for the reaction $\text{Fe} + \frac{1}{2}\text{O}_2 = \text{FeO}$. The entropies of pure iron and of oxygen are available in Lewis and Randall's work and are:

$$\text{Fe}, S_{298} = 6.71; \frac{1}{2}\text{O}_2, S_{298} = 24.0.$$

Since the entropy of formation is -21.3 calories per degree, we can now solve for the absolute entropy of FeO at 298° K. $(6.71 + 24.0) - 21.3 = 9.41$ calories per degree. If the more recent value of 24.6 for the entropy of oxygen obtained by Millar and Sullivan⁸⁵ is used, the corrected value of the entropy of ferrous oxide at 289° K. is 10.01 entropy units.

⁸⁵ Millar, R. W., and Sullivan, J. D., Thermodynamic Properties of Oxygen and Nitrogen: Tech. Paper 424, Bureau of Mines, 1928, 20 pp.

DISSOCIATION PRESSURE

No one has ever been able to observe experimentally the dissociation pressure of ferrous oxide. It can, however, be calculated by thermodynamic means. We have the free energy expression for the reaction $\text{Fe} + \frac{1}{2}\text{O}_2 = \text{FeO}$. By altering the algebraic signs of this reaction (thereby reversing it) and of its corresponding free energy expression and multiplying by 2 in each case, $2\text{FeO} = 2\text{Fe} + \text{O}_2$, $\log k = \log P = -\Delta F/4.5787 T$.

$$\Delta F = -12.64 T + 122,500 - 1.88 T \ln T - 0.0033 T^2 + 0.00000074 T^3.$$

$$\log P = 2.76 - 26750/T + 0.946 \log T + 0.00072 T^2 - 0.0000001616T^2.$$

From this equation the dissociation pressure of ferrous oxide at its melting point is about 10^{-11} atmospheres (beyond possibility of direct measurement), is not much greater at the melting point of iron, and approaches 1 atmosphere only above $4,000^\circ \text{K}$. Extrapolation to such high temperatures from an empirical equation derived from data collected between 700°K . and $1,400^\circ \text{K}$. is not justified and means nothing. All that is gained by the calculations above is a conception of the extremely low dissociation pressure of ferrous oxide under ordinary conditions. Extrapolating downward to room temperature, the dissociation pressure at 25°C . (298°K .) is in the order of 10^{-42} atmosphere, such a small number that if expressed kinetically one can say that at any one instant only 1 molecule of FeO in every 1,000,000,000,000,000 tons is dissociated into iron and oxygen. As the industrial products approaching FeO in composition at ordinary temperatures are almost vanishingly small in tonnage over the whole world, dissociated ferrous oxide is nonexistent.

SUPPLEMENTARY NOTE

Following preparation of the above manuscript, C. Travis Anderson of the Pacific Experiment Station of the Bureau of Mines sought to prepare pure FeO by repeatedly melting magnetite in contact with pure iron, but obtained instead a melt of constant composition melting at $1,428^\circ \text{C}$. and containing 1.83 per cent free iron, 14.2 per cent magnetite, and 83.9 per cent FeO. Apparently an equilibrium is reached in which metallic iron, magnetite, and ferrous oxide participate. Assuming this was true in both his own case and also for the work of Tritton and Hanson the free energy change of the reaction $\text{Fe}_3\text{O}_4 + \text{Fe} = 4\text{FeO}$ should be equal to zero, and this fact can be used for calculating the free energy of ferrous oxide from that of magnetite. This calculation gave free energy values in reasonable accord

with the data above presented at both the 1,428° C. temperature of Anderson and the 1,540° C. temperature of Tritton and Hanson. The data also showed that the equilibrium allowed increasing percentages of FeO in the equilibrium mixture, the lower the temperature. However, below 1,380° C., the melting point of FeO, reaction would be almost impossible on account of the solid condition of the various reactants, and therefore this method of preparing pure ferrous oxide seems doomed to failure.

IRON-OXYGEN COMPLEXES HAVING LESS OXYGEN THAN FeO

The compounds Fe_2O , Fe_3O , and Fe_4O have all been reported to exist, but the evidence for all but Fe_3O has been almost totally lacking, and for Fe_3O it is far from conclusive, as will be seen below. Certain limited ranges of miscibility of FeO and Fe, both molten and solid, are known and will be reviewed, but they are not wide enough to account for the above three supposed suboxides, whose formulas can not fall within the known composition ranges of the solid solutions of Fe in FeO and FeO in Fe.

Joannis,⁸⁶ reviewing the early literature, quotes Marchand⁸⁷ to the effect that when iron is heated in the flame of the oxyhydrogen blowpipe it burns to give a compound which is not Fe_3O_4 but is a black fusible mass, somewhat malleable, which dissolves in HCl with evolution of hydrogen and has a constant composition of 6.79 per cent of oxygen corresponding approximately to Fe_4O (the formula demands 7.14 per cent of oxygen). Presumably the temperature of the oxyhydrogen flame was over $2,000^\circ\text{C}$., and an excess of hydrogen was used to exclude air. It will be shown below that at the melting point of iron ($1,535^\circ\text{C}$.) it can dissolve enough FeO so that the mass contains 0.21 per cent of oxygen. The work of Herty shows that this solubility increases with temperature, although not rapidly enough to lead one to expect 6.79 per cent at $2,000^\circ$ to $2,100^\circ\text{C}$. Marchand was probably mistaken about his product being of constant composition, but it was probably the solution of ferrous oxide in molten iron, possibly with an excess of FeO.

Later, Dusart⁸⁸ reported the suboxide Fe_2O , produced by reduction of ferric oxide with hydrogen. A preparation corresponding to this formula was taken from the reaction tube and thought to be homogeneous and definite. No one has yet been able to check this observation.

However, the limited solubility of ferrous oxide in metallic iron and of iron in ferrous oxide can not be disputed, even though the evidence of suboxides is too meager to be accepted.

Tritton and Hanson⁸⁹ have determined the solubility, at the melting point of iron, of ferrous oxide in iron and of iron in molten

⁸⁶ Joannis, M., *Fremy's Encyclopedie chimique*, III, Metaux, 9e cahier : Paris, 1884.

⁸⁷ Marchand, R. F., Ueber eine Verbindung des Eisenoxyduls mit metallischem Eisen : *Jour. prakt. Chem.*, Bd. 18, 1839, p. 184.

⁸⁸ Dusart, — : *Repertoire de chimie appliquee* : vol. 3, 1861, p. 357, quoted by Joannis ; "Sur le fer reduit par l'hydrogene."

⁸⁹ See footnote 79, p. 107.

ferrous oxide. Electrolytic iron was melted in air in an induction furnace and pure ferric oxide placed on top to be reduced to "FeO" by the iron. The iron oxide was reduced to only 80.6 per cent of FeO, and the remainder was made up of ferric oxide; 3 per cent of MgO and 0.99 per cent of free iron, most of which was presumably in solution in the molten FeO 1,528 C., were taken up from the

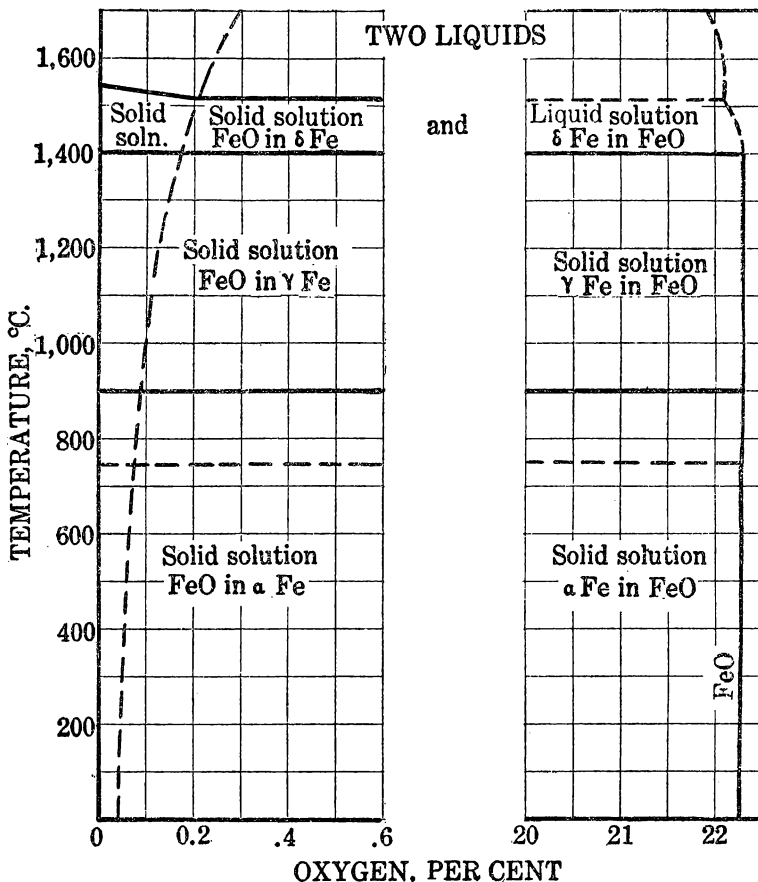


FIG. 30.—System Fe—FeO (Tritton and Hanson)

crucible. The figure for solubility of Fe in FeO would probably be slightly modified if pure FeO were used instead of the impure product. Tritton and Hanson sketched in the skeleton (acknowledged incomplete) of a phase diagram for the system FeO—Fe from their observations (see fig. 30). They took cooling curves and heating curves and examined the metal layer metallographically, thereby determining the solid solubility of FeO in Fe as 0.05 per cent of oxy-

gen (0.22 per cent of FeO at 25°C .) as compared to 0.21 per cent of oxygen (or 0.94 per cent of FeO) at the melting point of iron. Unfortunately these investigators did not study their FeO slag layer where similar cooling curves and metallographic study should be very illuminating, as much as their metal. Their paper is filled with valuable details of their technique.

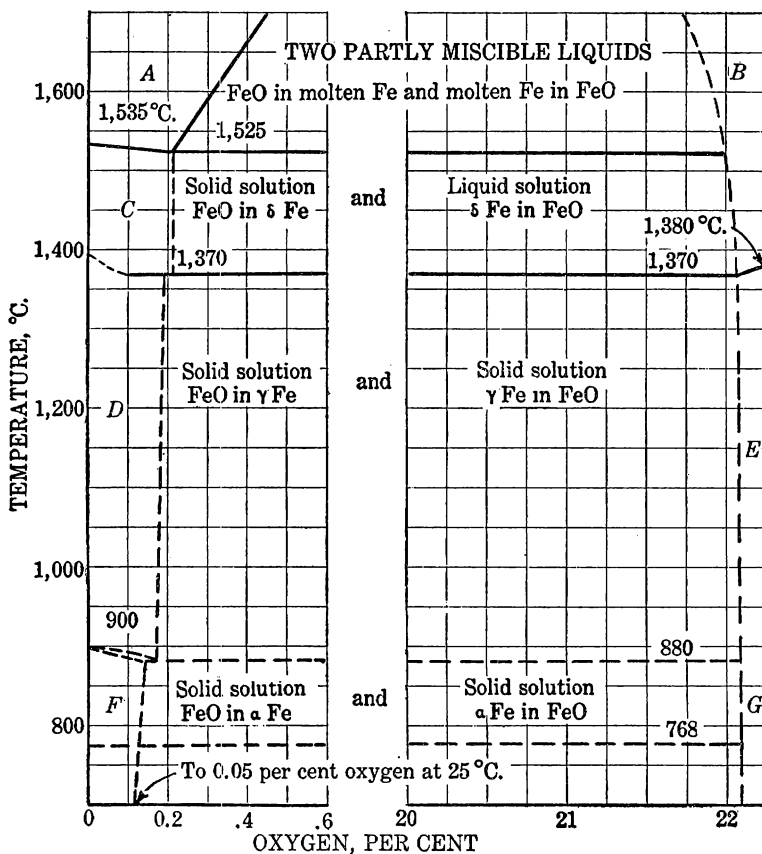


FIG. 31.—System $\text{Fe}-\text{FeO}$, modified (after Schönert). Areas *A*, *C*, *D*, and *F*, solutions of FeO in molten Fe , δ Fe , γ Fe , and α Fe ; areas *B*, *E*, and *G*, solutions of molten and δ Fe in FeO , γ Fe in FeO , and α Fe in FeO , respectively

The Tritton and Hanson phase diagram has not satisfied Schönert,⁹⁰ who has reviewed it critically in the light of certain previous work and gives his corrected phase diagram in Figure 31. Schönert differentiated between α and β Fe and included a eutectoid point at the A_2 transformation temperature, but the writer has ignored it in reproducing Schönert's diagram. Otherwise Figure 31 is drawn as Schönert recommended, based on the following data.

⁹⁰ See footnote 81, p. 109.

Oxygen as a cause of red-shortness in steel was first studied by Ledebur,⁹¹ who found a maximum content of 0.24 per cent of oxygen in liquid steel. Tritton and Hanson's figure of 0.21 per cent is undoubtedly more precise. Wimmer⁹² added ferric oxide to a very clean surface of molten metal having an analysis of 0.05 per cent of C, no Si, 0.38 per cent of Mn, 0.045 per cent of P, and 0.035 per cent of S, heated it 40° to 50° above its melting point, and found that 0.20 per cent of oxygen was taken into solution. This figure checks Tritton and Hanson very well. Recent unpublished work by C. H. Herty at the Pittsburgh Experiment Station of the Bureau of Mines involved melting electrolytic iron in a magnesia-lined crucible with ferric oxide melted on the surface of the metal and thereby reduced to FeO(?), after the manner of Tritton and Hanson. The metal at its melting point took up 0.21 per cent of oxygen, checking Tritton and Hanson. The solubility at higher temperatures was also determined and is plotted in Figure 32 and included in Schönert's diagram, Figure 31. His results between 1,535° and 1,750° C. are best expressed by a linear equation, Oxygen=0.0014-1.92. Wimmer also examined his products microscopically and estimated the solid solubility of ferrous oxide in α iron such that it contained 0.035 per cent of oxygen as contrasted to the 0.055 per cent determination of Tritton and Hanson. The solubility in β iron (?) was estimated at 0.13 per cent and supported by the fact that a eutectic structure was visible first at 0.13 per cent of oxygen. The solid solubility in γ iron varies from 0.15 to 0.19 per cent. The metallographically observable effect of the dissolved oxide was to cause greater crystal grains of ferrite. Other obvious changes of the phase diagram made by Schönert appear in his diagram (fig. 31).

Part of Schönert's diagram was based on the metallographic work of Herbert Monden,⁹³ who studied basic open-hearth steel and the effect of oxygen content on its rolling characteristics, especially red-shortness. He concluded that at about 900° to 1,000° C. part of the free iron oxide seen in his photomicrographs must have gone into solution in γ iron.

⁹¹ Ledebur, A., Das "Verbrennen" des Eisens und Stahls: Stahl u. Eisen, Jahrg. 3, 1883, p. 502; Prof. J. O. Arnolds und R. A. Hadfields Untersuchungen über den Einfluss der Bestandtheile des Eisens auf seine Eigenschaften: Stahl u. Eisen, Jahrg. 14, 1894, pp. 477-480 and 523-528.

⁹² Wimmer, A. Ueber den Einfluss des Sauerstoffs auf die physikalischen und technischen Eigenschaften des Flusseisens: Stahl u. Eisen, Jahrg. 45, 1925, pp. 73-79.

⁹³ Monden, Herbert, Beitrag zur Metallurgie des basischen Seimens-Martin-Verfahrens und zur Frage des Einflusses des Sauerstoffgehaltes auf die mechanischen Eigenschaften des Flusseisens, insbesondere des Rotbruches: Stahl u. Eisen, Jahrg. 43, 1923, pp. 745-752, 782-788.

Other metallographic studies of oxygen-bearing steel have been made by Stead,⁹⁴ who has drawn the following conclusions: Iron when heated in air or oxidizing gases takes up oxygen, which passes into solid solution, but when supersaturated the excess falls out of the solution, especially in patches along grain boundaries, which may eventually join and form continuous weak layers. This accounts for

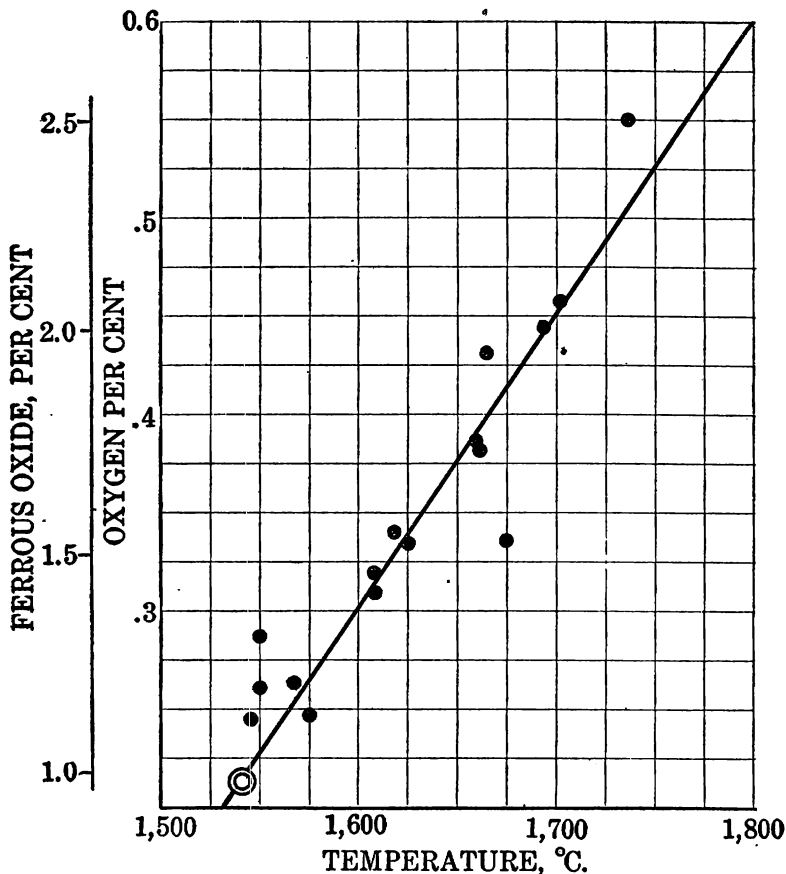


FIG. 32.—Solubility of FeO in molten iron (Herty)

the red-shortness. Stead's results were obtained by etching with alcoholic cupric chloride solutions which deposit copper more easily on iron than on its oxide alloy.

Earlier work supporting the above conclusions, but not so informative or so accurate, was done by Pickard⁹⁵ and by Austin.⁹⁶ P.

⁹⁴ Stead, J. E., Solid Solution of Oxygen in Iron: Proc. Iron and Steel Inst., vol. 103, 1926, pp. 271-275.

⁹⁵ Pickard, J. A., Oxygen Content of Iron and Steel: Iron Age, vol. 98, 1916, pp. 184-186.

⁹⁶ Austin, Wesley, The Influence of Oxygen on Some Properties of Pure Iron: Engineering, vol. 100, 1915, pp. 455-456.

Oberhoffer⁹⁷ has reviewed the effect of oxygen on iron and steel and compared the hydrogen reduction-determination method of oxygen of Goerens⁹⁸ with the bromine methods of Wüst and Kirpach.⁹⁹

At the other side of the diagram about the only estimate on the solubility of free iron in ferrous oxide is the analysis of Tritton and Hanson, giving 0.99 per cent of free Fe in their molten "ferrous oxide" layer, and this figure is used in the phase diagrams.

As can be seen from Schönert's diagram, only the two edges of the field have been explored properly, and the diagram does not exclude the possibility of existence of intermediate suboxides like Fe_2O , Fe_3O , and Fe_4O . In fact, little enough is known about FeO . The diagram suggests that above the melting point of iron where there is increasing solubility of FeO in Fe and probably of Fe in FeO two series of conjugate solutions are formed, and with rising temperature they approach each other in composition. At some temperature they should reach a critical point above which they are miscible in all proportions. This critical temperature is probably well above $2,000^\circ\text{C}$. and should form an interesting objective to be studied by the physical chemist.

While the precision of all the above data leaves much to be desired, it is probably satisfactory enough for the solubility of the liquid and gives at least a bird's-eye view of the probable solid solubility of ferrous oxide in solid iron. However, in studying the solids contradictory phenomena have been observed by Matsubara¹ and by Eastman² in their reduction "isotherm." Their isotherms have received further confirmation from Schenck.³ The three isotherms of Schenck, obtained by reducing ferric oxide with successive small additions of carbon monoxide in a reaction tube held at constant temperature, with periodic analyses of the gas phase and systematic calculation of the oxygen content of the solid phase from the change in analysis of the gases and their amounts removed, are given in Figure 33. As can be seen, during the stage of reduction of FeO to Fe the percentage of CO in the total oxides of carbon remained constant till toward the end, but during the removal of the last portions of oxygen a higher relative CO content was necessary. For the 700° and 800°C . isotherms of Schenck this corresponded to the last atom of oxygen out of nine, or, in weight per

⁹⁷ Oberhoffer, P., *Oxygen im Eisen: Stahl u. Eisen*, Jahrg. 45, 1925, pp. 1341-1348.

⁹⁸ Goerens, P., *Über die Gase aus technischen Eisensorten: Metallurgie*, Jahrg. 7, 1910, pp. 384-395.

⁹⁹ Wüst, F., and Kirpach, N., *Estimation of Slag in Steel: Mitt. Kaiser Wilhelm Inst.*, Jahrg. 1, 1920, pp. 31-38.

¹ Matsubara, A., *Chemical Equilibrium Between Iron, Carbon, and Oxygen: Trans. Am. Inst. Min. and Met. Eng.*, vol. 67, 1922, pp. 3-55.

² See footnote 40, p. 75.

³ See footnote 58, p. 88.

cents, to a solid product containing 4.56 per cent of oxygen (20.5 per cent of FeO and 79.5 per cent of Fe) or less. In the 950° C. isotherm the effect was noticeable for the last third of the total oxygen of the original ferric oxide, or, in weight per cents, to solid

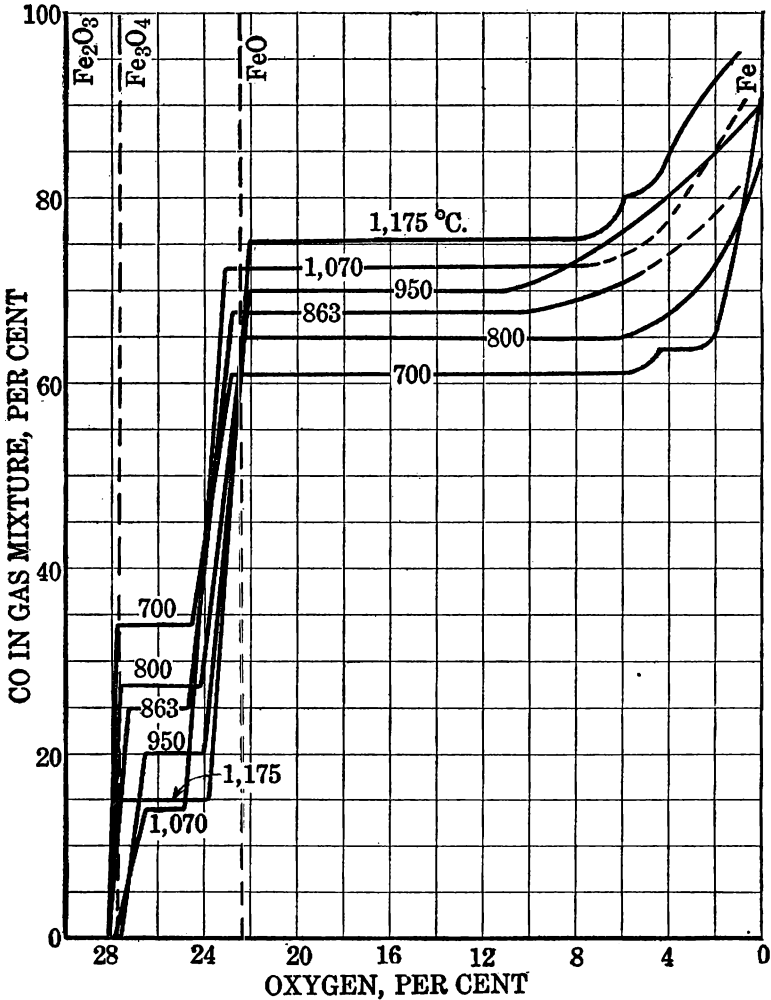


FIG. 33.—Isothermal slow reduction of Fe₂O₃ with CO (Matsubara, 1175, 1070, and 863° C.; Schenck, 950, 800, and 700° C.)

with up to 10 per cent of oxygen (44.9 per cent FeO and 55.1 per cent of Fe). The peculiar pause in the 700° C. isotherm is noteworthy.

Matsubara, who likewise used CO as reducing agent in a similar experiment, plotted isotherms for 863°, 1,070°, and 1,175° C. which are reproduced in Figure 33; and in all cases the increased CO con-

centration necessary for reduction was noticed when the solid had been reduced to 8 per cent of oxygen (35.6 per cent of FeO and 64.4 per cent of Fe). Due to the possible complications caused by carburization of the iron by CO in the above curves, the single isotherm of Eastman and Evans (fig. 34), obtained by oxidation of iron with water vapor, thus avoiding formation of carbides, is of interest because it affords a reasonable check. It was carried out at 772° C., and the same effect was noticed when the solid had been oxidized to about 6 per cent of oxygen (26.9 per cent of FeO and 73.1 per cent of Fe).

The hydrogen-water vapor oxidation isotherm of Eastman and Evans as drawn by them adheres to their observed points well, and the points showed good agreement except just where the isotherm

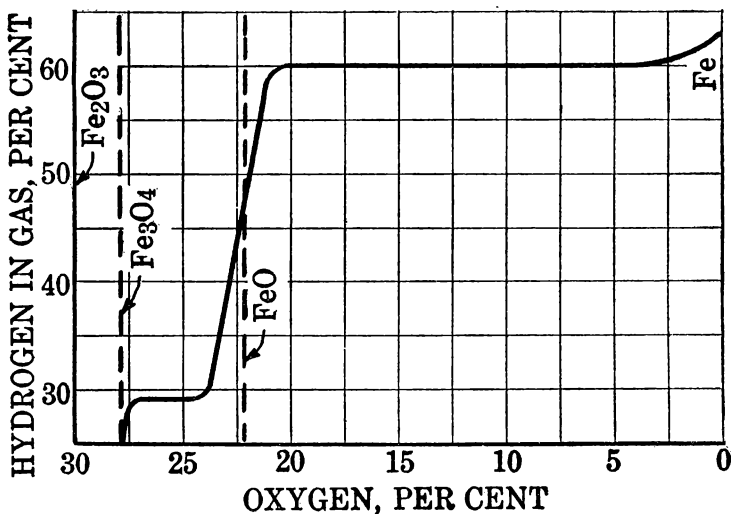


Fig. 34.—Isothermal oxidation of iron by water vapor at 772° C. (Eastman and Evans)

passed the composition of FeO. Here they chose to draw their curve to one side of most of their points and farther into the field toward Fe than any other investigators have observed. This indicates a solid solution having less oxygen than FeO (probably of Fe in FeO) and departing more from the composition of FeO at this temperature than would be expected from the six CO reduction isotherms. The hydrogen curve in Figure 34 adheres to the original points of Eastman and Evans better than their own curve, especially at the point near the composition of FeO.

At this point their curve indicates considerable solubility of metallic iron in FeO, which is not in agreement with other observers. Probably the oxidation of Fe to FeO was almost complete, but the last traces of Fe were buried under an impervious layer of FeO.

The X-ray spectrograms of Groebler and Oberhoffer⁴ of a series of products from along a reduction isotherm show very little displacement of the FeO lines by Fe at this point of the isotherm, indicating the probability of low solubility of Fe in FeO.

Both Matsubara and Eastman ascribe this effect of lessened activity to the disappearance of the pure FeO phase and to the fact that the remaining FeO in the sample exists in solid solution in the iron and will therefore be more difficult to reduce to metal as it becomes more dilute, due to reduction. However, the amount of oxygen which must be assumed to be present is so great in comparison with the apparent solubility of oxygen in any of the solid forms of iron as shown in Figure 30 or 31 that something must be wrong. Several possible explanations can be considered.

1. To be sure, the solid-solubility determinations with from 0.035 per cent of oxygen at 25° C. to as high as 0.19 per cent at 1,525° C., depending on temperature and polymorphic form of iron considered, were obtained by Tritton and Hanson and others by cooling curves on melts, and it may well be that at lower temperatures iron-oxygen complexes which are not stable at higher temperatures and would therefore be absent in chilled melts can form. Complexes carrying iron, carbon, and oxygen at the lower temperatures are definitely known to exist, as will be pointed out later. The work of Eastman and Evans with hydrogen and water vapor probably eliminates the necessity of suspecting the isotherms of Schenck and of Matsubara to be affected by the presence of carbon in the solid phase. However, the work of the three sets of investigators is not in good agreement on the exact oxygen content of the solid at which this effect is first noticed, as shown above, varying from 3.5 to 10 per cent of oxygen.

2. The fact that Eastman and Evans noticed a lessened activity of FeO near the iron edge of the diagram (fig. 34), when oxidizing iron to FeO by means of water vapor-hydrogen mixtures, makes it unnecessary to disbelieve the reality of the effect noticed in the CO reduction isotherms of Matsubara and of Schenck (fig. 33). If reduction isotherms only were available for study, one could claim that too little time had elapsed for the cores of the individual iron oxide particles to be reduced to metal and that the gas was in equilibrium only with the surface of the particles. The oxidation isotherm of Eastman and Evans shows the lowering of activity only in preparations containing less than 4 per cent of oxygen (18 per cent of FeO), and in this case the presence of cores of FeO coated over by metallic iron is impossible. The time necessary for reaching apparent equilibrium after new gas was introduced differed. Mat-

⁴ See footnote 47, p. 83.

subara stated that at 850° C., with CO reduction, he needed 14 to 20 hour intervals and at 1,100° C. about 2 hours; Schenck reported "suitable time intervals," and Eastman and Evans at 772° C. with a water vapor-hydrogen mixture for oxidation reported 30 to 45 minutes. The conclusion is that at 772° C. at least 18 per cent of FeO must dissolve in Fe, as shown by Eastman and Evans.

3. Pure, finely divided metallic iron resulting from low-temperature reduction is known to stick, sinter, or weld⁵ together at temperatures above about 600° C. This might easily account for the entrapping of unreduced oxides in the reduction isotherms, but it can not account for the Eastman and Evans oxidation isotherm. More oxidation isotherms are needed, so that the average solid compositions at changes in direction of the isotherms could be determined more precisely.

4. When a small amount of one phase is distributed in thin films over the other, gases of different analysis from the equilibrium gases are sometimes obtained. Richardson, Vibrans, and Bell,⁶ when studying the steam-iron process of making hydrogen found a higher conversion of steam to hydrogen and of reducing gases to oxidized gases at the beginning of each period of operation in the laboratory than is shown by equilibrium data. Also, Pease and Cook,⁷ when studying the reduction of nickelous oxide to metal by hydrogen, found similar effects and therefore feel that the free energies of formation of thin films of oxide on metal and of metal on oxide are higher than those of the oxide and metal, respectively, in the massive state. Whether an iron product containing up to 18 per cent of FeO can be regarded as containing the latter only in thin films is questionable, and the solid-solution theory is more tenable.

5. The matter can not be dropped without some consideration of an alternative hypothesis. Ferguson⁸ points out that the effects can be explained by assuming "two different forms of ferrous oxide." If the two forms of ferrous oxide were polymorphic, and one of high activity and the other of low activity, and both miscible in each other in all proportions (two different crystalline forms are usually not miscible in all proportions), a gradually descending curve of the type shown in Figure 33 for the two higher temperatures would be observed. However, this gradual slope should be succeeded by another horizontal portion of the line when the most highly active form

⁵ Hofman, Konrad, The Advantages of Smelting Fine-Grained Ores in the Blast Furnace: Trans. Am. Electrochem. Soc., vol. 51, 1927, p. 91.

⁶ Richardson, A. S., Vibrans, F. C., and Bell, W. P., Equilibrium in the Reduction of Iron Oxides and in the Oxidation of Iron by Steam: Science, vol. 56, 1922, p. 27.

⁷ Pease, R. N., and Cook, R. S., Equilibrium in the Reaction, $\text{NiO} + \text{H}_2 = \text{Ni} + \text{H}_2\text{O}$; The Free Energy of Nickelous Oxide: Jour. Am. Chem. Soc., vol. 48, 1926, pp. 1199-1206.

⁸ Ferguson, J. B., Equilibria in Systems Involving Ferrous Oxide: Trans. Faraday Soc., vol. 21, 1925, pp. 240-242.

of ferrous oxide had been completely reduced and only the form of lower activity remained. Four out of six isotherms in Figure 33 go directly to the composition of pure iron with no such jogs. Unless some way can be worked out for meeting this objection, Ferguson's hypothesis will be difficult to maintain. However, it is interesting to notice that in the Schenck isotherm for 700° in Figure 33, there is a short flat place of the type needed to substantiate Ferguson's hypothesis. It begins at a composition of the solid phase corresponding to Fe_6O and ends at what corresponds to Fe_{12}O . However, this isotherm is at a low enough temperature to allow considerable carburization as well as deoxidation by CO , and the flat step in the line may be connected with the carburization factor. Furthermore, the last 1.5 per cent of oxygen in the solid is still to be removed after this flat place is passed, and there is still the same difficulty of explaining the shape of the isotherm from that point on.

Scattered earlier observations by Schenck lend support to his claim that below 700°C . at least one oxygenated iron phase of unknown (at that time) composition can be formed, except that it contains very little carbon. When a mixture of 75 $\text{CO} + 25 \text{CO}_2$ at $\frac{1}{3}$ atmosphere total pressure was streamed over ferric oxide at 700° the end product contained 91.87 per cent of free Fe and 8.04 per cent of FeO (with about 0.07 per cent of C), corresponding to 1.776 per cent of oxygen in the solid phase. When iron is precipitated (presumably as hydroxide) on magnesia and then reduced by a 50:50 mixture of CO and CO_2 at 650°C . a brown pyrophoric powder is obtained which on standing in an evacuated tube seems to decompose and turn dark and contains 92 per cent of Fe and 8 per cent of oxygen, or is approximately Fe_3O .⁹

Schenck in 1926 has summarized all his information in an equilibrium diagram reproduced in part in Figure 35, giving gas analyses for equilibrium conditions at various temperatures. Four lines corresponding to successive apparent equilibria were observed. Lines 1 and 2 correspond well with the equilibrium data of others on the $\text{Fe}_3\text{O}_4 : \text{FeO}$ equilibrium and the $\text{FeO} : \text{Fe}$ equilibrium, respectively. However, lines 3 and 4 seem to involve also oxygen-bearing solid phases, and they show no shift in position with change in pressure, which means that the number of gas molecules does not change during the unknown reactions to which they correspond. The latter, then, can hardly represent carburization reactions, all of which seemingly involve reactions that are affected by change in pressure. Much work needs to be done in identifying the solid phases involved.

⁹ Schenck, R., Die Bedeutung des physikalischen Chemie für die Metallurgie des Eisens: Stahl u. Eisen, Jahrg. 43, 1923, pp. 65-69, 153-156.

In the succeeding year Schenck¹⁰ was able to report that his lines 3 and 4 were due to disturbing influences of the magnesia, silica, or porcelain apparatus on the solid phases. Magnesia was found to take up ferrous oxide into a solid solution, and in some of his work Schenck had been measuring the equilibria of the gases in contact with this solution instead of with pure ferrous oxide. There should be a whole series of lines in the diagram at higher and higher CO content as higher and higher MgO content in the FeO phase is attained. The solution of MgO in FeO would quite naturally lower

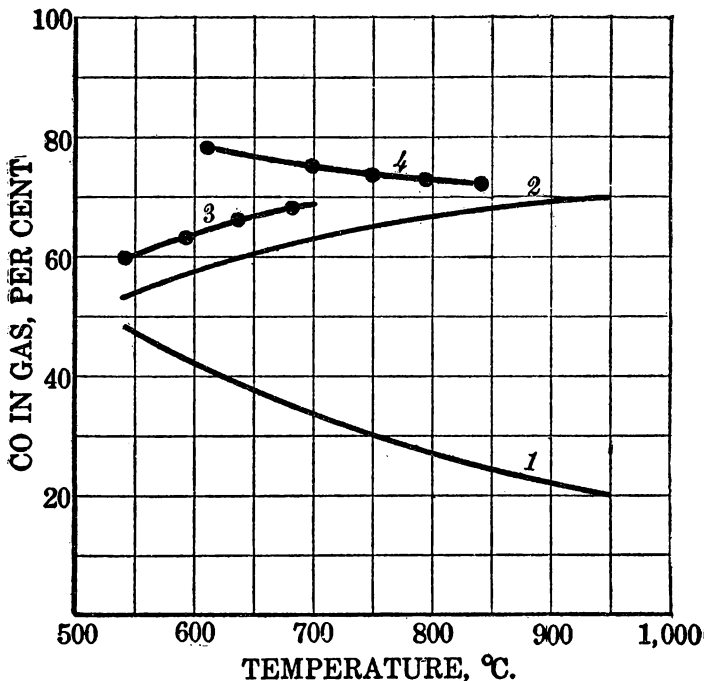


FIG. 35.—Equilibrium data of Schenck at 1 atmosphere and 0.33 atmosphere total pressure with mixtures of CO and CO₂ acting on iron oxide systems

the activity of the latter. Schenck also found that there was an area on the diagram, which will be discussed in a later section, where iron containing dissolved FeO could be in equilibrium with the gases, and he named this oxygen-bearing metallic iron phase, "oxyferrite." This phase is the one found in all the isotherms above discussed at the inclined portion approaching 100 per cent of Fe.

METALLIC IRON PHASE CONTAINING CARBON AND OXYGEN

The above problem has been complicated unnecessarily by the fact that most of the work has been done with gases containing CO and

¹⁰ See footnote 59, p. 93.

CO₂, which were shown by Terres and Pongracz¹¹ to give a metallic iron phase containing both oxygen and carbon. It is highly desirable to repeat most of the CO:CO₂ work with mixtures of hydrogen and water vapor in order to remove the carbon complications, and the work should be done from both the oxidizing and the reducing side as one approaches any definite equilibrium.

Matsubara has shown definitely that carbon monoxide can act on iron at moderate temperature with simultaneous production of Fe₃C and FeO and also inferred from certain of his data that the oxygen-bearing iron and the carburized iron could dissolve each other to a certain extent. Such phases, containing both iron carbide and ferrous oxide when heated to the melting point of iron, eliminate more of the oxygen and carbon as CO which boils out, as is well known in the open-hearth steel processes. As Matsubara points out, "the existence of oxygen-bearing carboniferous iron is not altogether imaginary." Caron¹² showed the existence of oxygen in carburized iron resulting from the action of CO on pure sponge iron at moderate temperatures. Grüner¹³ obtained the same result when he used iron wire, and even thick iron blocks were treated by Giolitti and Carnevali,¹⁴ with the formation of thick crusts of oxidized iron and a core of carburized iron. Goerens¹⁵ and more recently Jordan and Eckman¹⁶ have heated "deoxidized" steels in vacuo and obtained several times their own volume of oxides of carbon, hydrogen, and water vapor. The thought immediately occurs that these are merely dissolved gases, but the quantities of oxygen involved at lower temperatures are very much greater. Matsubara passed CO over reduced iron in a tube at 550° C. and got a small amount of iron-bearing distillate containing carbon. Presumably he had formed a carbonyl, at least temporarily, but in connection with the preceding paragraphs the thought occurs that possibly iron carbonyls, which are normally supposed to be unstable except at lower temperatures, could be dissolved in iron and thereby retain their stability at higher temperatures and constitute in part at least the oxygen-iron-carbon complex that seems to exist in iron samples after proper CO treatment, even up to rather high temperatures.

¹¹ Terres, E., and Pongracz, A., Beiträge zur Kenntnis der Reaktionen beim Hochofengleichgewichts: Ztschr. Elektrochem., Jahrg. 25, 1919, pp. 386-407.

¹² Caron, H. M., De la cementation du fer par l'oxyde de carbone: Compt. rend., t. 59, 1864, pp. 333-336.

¹³ Grüner, L., Rapport sur un mémoire de M. Grüner relatif à l'action de l'oxyde de carbone sur le fer et ses oxydes: Compt. rend., t. 74, 1872, p. 226.

¹⁴ Giolitti, F., and Carnevali, F., On Case-Hardening by Means of Compressed Gases: Jour. Iron and Steel Inst., vol. 84, 1911, p. 331.

¹⁵ Goerens, P., ———: Mitt. Eisenhüttenmann. Inst. König. Tech. Hochschule, Aachen, 1910.

¹⁶ Jordan, L., and Eckman, J. R., Gases in Metals; II, The Determination of Oxygen and Hydrogen in Metals by Fusion in Vacuum: U. S. Bureau of Standards Sci. Paper 514, 1925, 38 pp.

The above paragraphs should be regarded as more stimulating to research than they are informative. The whole subject needs an immense amount of work.

SUMMARY

To summarize, one of the most uncertain parts of the iron-oxygen system is that between the composition of ferrous oxide and metallic iron, where certain evidence indicates the probability of at least limited miscibility of these constituents and other evidence points toward the existence of either solid solutions of greater miscibility than that indicated by the other group of evidence or of suboxides. The confusion of evidence is complicated by the fact that much of the work has been done in the presence of the oxides of carbon, with the possibility of the formation of carbides in the solid phases or even of absorption of carbonyls, resulting in complex solid phases containing oxygen and carbon in undetermined association. For molten mixtures the data are more exact, and the nature of the material better understood.

THE SYSTEM IRON

INTRODUCTION

The system iron is an unusually complicated one because it has so many polymorphic and other changes. Although a great deal is known about the physical properties of the alloys of iron truly pure iron has been very little studied, and the physical data dealing with it are none too complete.

Not until the past few years has it been possible to obtain definite incontrovertible evidence of the difference between the various solid forms of iron and that new evidence has been obtained by using X rays to determine the crystal systems to which iron at various temperatures alters.

ATOMIC WEIGHT

The atomic weight of iron, on the basis that the weight of oxygen is 16, is 55.86; that is, a gram-atom of metallic iron weighs 55.86 grams. Dividing by 6.061 times 10^{23} , the number of actual atoms in a gram-atom, the weight of a single atom of iron is found to be 9.22 times 10^{-23} grams. The fact that iron does not have an atomic weight which is an even multiple of 1 seems to be due to the fact that it is isotopic, being made up of at least two different isotopes. Aston¹⁷ using the accelerated cathode ray method of analyzing vapors, familiar to physicists, has estimated that iron is made up of about 20 atoms with a weight of 56 for every atom of a weight 54. This check on the observed atomic weight is reasonably good. No other means of separating the two isotopes has yet been applied to iron. The two isotopes are otherwise so identical in physical and chemical characteristics that ordinary means do not separate them.

CRYSTAL SYSTEM

The earlier metallographers, working with iron-carbon alloys containing silicon and manganese, deduced by various methods the probability of existence of several kinds of iron. These were named α , β , γ and δ iron, and numerous workers have sought to establish the existence of even more forms and the transformation temperatures where one alters to the next. However, X-ray spectrographic

¹⁷ Aston, F. W., *The Mass-Spectra of Chemical Elements; Part VI, Accelerated Anode Rays Continued*: Philo. Mag., vol. 49, 1925, pp. 1191-1201.

data have narrowed the field down to three— α , γ , and δ —and even point out the fact that the α and δ varieties are identical in crystal structure, leaving only the α and γ fundamental structures.

The metallographers have had means of distinguishing between the various kinds of iron that have appeared under their microscopes and call the phase that approaches pure iron in composition "ferrite." Ferrite is not necessarily pure iron, as it is really capable of dissolving other elements like carbon and silicon to a certain extent, but to the metallographer it is essentially pure iron and appears as a homogeneous mass. The α ferrite is the form stable at ordinary temperatures, whereas γ or even δ ferrites are stable only at higher temperatures and are observed at room temperature only when specially treated and quenched. However, they are all distinguishable by the metallographer.

In pure iron the α form is stable up to 906° C., above which the γ form appears and is stable up to $1,400^{\circ}$ C., above which the δ form replaces it in turn and is stable to the melting point, $1,537^{\circ}$ C. Rosenhain and Humfrey,¹⁸ working with a specimen of nearly pure iron containing 0.029 per cent of carbon, 0.118 per cent of silicon, and 0.014 per cent of manganese, found that a polished surface on which the crystal structure was visible could be heated in vacuo without tarnishing and found that there were three different temperature regions in which the crystal structure of the material appeared different. These varieties correspond to the α , γ , and δ forms of iron. When one end of a specimen was heated and the other kept cold and simultaneously subjected to strain the rod was noticed again to be divided into zones. The α iron became weaker and softer with increased temperatures. In the temperature range formerly attributed to β iron (and now known to be merely α iron above its magnetic inversion temperature) the specimen was stronger and harder, and finally in the γ range the material developed crystalline structure more sharply, with some reduction in strength and stiffness.

STRENGTHS OF IRON AT DIFFERENT TEMPERATURES

An extremely interesting experiment on the relative strengths of iron at different temperatures was performed by Sauveur,¹⁹ who placed bars of electrolytic iron, armco iron, and various steels in an electrically heated tube furnace, leaving the two cold ends of the bars sticking out. Twisting and tensile stresses applied to these protruding ends cause deformation of the bars in greatest amounts

¹⁸ Rosenhain, W., and Humfrey, J. C. W., The Crystalline Structure of Iron at High Temperature: Proc. Roy. Soc. London (A), vol. 83, 1909-10, pp. 200-209.

¹⁹ Sauveur, Albert, What is Steel: Trans. Am. Inst. Min. and Met. Eng., vol. 70, 1924, pp. 3-24.

at their weakest points. In the twisting tests with pure iron at moderate temperatures the samples always twisted most and finally broke in the center, the hottest portion. However, when the temperature of the center of the bar was above and that of the ends below the A_3 point the greatest twist took place at the two points along the rods which were at the A_3 temperature. The same was true of the tensile tests. Seemingly, iron is more plastic while passing through the A_3 transformation (α to γ iron, or the reverse).

Later, the Rosenhain and Humfrey experiment was improved on by Wever and Giani,²⁰ who heated one end of a polished thin strip of electrolytic iron in vacuo in the same manner and called their experiment "heat etching." The temperature zones were much sharper and showed δ iron in fairly coarse crystals, succeeded below 1,400° C. by γ iron in finer grains and below 906° C. by α iron in crystals considerably larger than the γ iron but somewhat smaller than the δ iron. Wever has also used X rays to determine the crystal systems of the various forms of iron, but the original determinative work was done by predecessors.

X-RAY SPECTROGRAPHIC WORK

The first important X-ray spectrographic work was that of Hull,²¹ who found that at ordinary temperatures iron (α) forms a body-centered cubic space lattice of atoms. This finding was confirmed by Westgren,²² who extended the investigation to higher temperatures and showed the same lattice up to 906° C., thereby including the 768° to 906° C. range formerly considered to belong to β iron. It was also shown that δ iron whose stability range is 1,499° to 1,537° C., has the same structure. In other words, α , β , and δ irons have identical crystallographic structure. Spheres packed in this manner (assuming for convenience that atoms occupy spherical spaces) are illustrated in Figure 36, which was plotted by F. B. Foley. The crystal "unit cubes" are described as body centered, contain 2 atoms, and have an edge length of 2.86 Ångstrom units (2.860×10^{-8} cm.) as determined by Hull. Wever's measurements give 2.85 Å. as the edge length, while Westgren's measurements give 2.87 Å., and the most recent work by Osawa²³ gives 2.865 Å. at room temperature (15° C.). The edge length of the unit cell increases with temperature as iron expands on heating. Westgren's data show that it is 2.90 Å. at 800° to

²⁰ Wever, F., and Giani, P., *Zur Thermodynamik der Umwandlungen des Eisens*: Mitt. Kaiser Wilhelm Inst. Eisenforschungen Dusseldorf, Jahrg. 7, 1925, p. 59.

²¹ Hull, A. W., *The Crystal Structure of Iron*: Phys. Rev., vol. 9, 1917, p. 84.

²² Westgren, Arne, *Röntgen Spectrographic Investigations of Iron and Steel*: Jour. Iron and Steel Inst., vol. 103, 1921, pp. 303-337.

²³ Osawa, Atomi, *On the Relation Between the Lattice Constant and the Density of Iron-Nickel Alloys*: Jour. Iron and Steel Inst., vol. 113, 1926, pp. 447-456.

830° C., and the edge length of δ iron unit cube at 1,425° C. is 2.93 Å.

The lattice of γ iron is a face-centered cube whose length at 1,100° C. is 3.63 Å and at 1,400° C. is 3.68 Å. It contains 4 atoms. Foley's representative packing of spheres in this kind of lattice is shown in Figure 37.

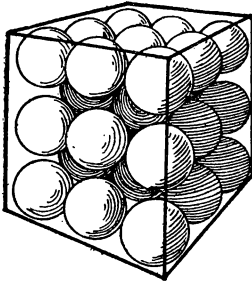


FIG. 36.—Body-centered cubic packing, alpha iron

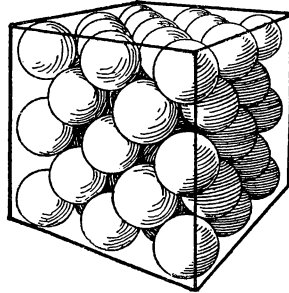


FIG. 37.—Face-centered cubic packing, gamma iron

This work was further extended by Westgren and Phragmen²⁴ and by Westgren and Lindh²⁵ and applied to steels, thereby providing for the first time definite direct evidence of the conditions of existence of iron in its various alloys. The X-ray methods of crystallography are now quite reliable and far surpass most previous work in their fundamental implications.

A summary of the X-ray data made by Sato,²⁶ is tabulated here-with and also plotted in Figure 38.

TABLE 17.—Summary of X-ray data on crystallography

Temperature, °C.	Edge-unit cube, Å.	Temperature, °C.	Edge-unit cube, Å.
20	$a_{\alpha}=2.86$	1,000	$a_{\gamma}=3.65$
800	2.89	1,100	3.66
1,450	2.93	1,425	3.68

ALLOTROPY AND POLYMORPHISM OF IRON

More discussion has probably raged about the various forms of iron than about any other elements, because the transitions from one

²⁴ Westgren, A., and Phragmen, G., X-Ray Studies of the Crystal Structure of Steel: Jour. Iron and Steel Inst., vol. 105, 1922, pp. 241-273.

²⁵ Westgren, A., and Lindh, A. E., Zum Kristallbau des Eisens and Stahls: Ztschr. physik. Chem., Jahrg. 98, 1921, pp. 181-210.

²⁶ Sato, K., Dilatometric Investigation of the A_3 and A_4 Transformations in Pure Iron: Sci. Rep. Tohoku Univ., 1st ser., vol. 14, 1925, pp. 513-527.

form to another have not all conformed to the usually accepted ideas of just what allotropy is. As above noted, the various forms of iron were originally discovered in connection with the heating and cooling curves so commonly used by metallographers in studying alloys. A change in direction of a heating or cooling curve at some temperature means evolution or absorption of heat in the metal, due to some change taking place in it at that temperature. These transition temperatures, commonly called critical temperatures or critical points, have received serial numbers in the case of the iron alloys and of iron itself. Thus, A_1 is associated with changes in iron carbide, and A_2 is a strange point where heat is evolved on cooling, where

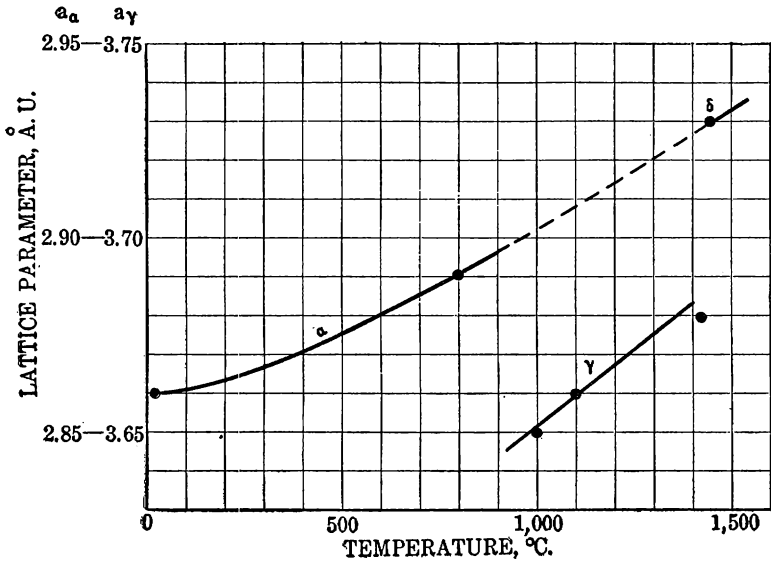


FIG. 38.—Lattice constant of iron (edge of unit cube in Ångstrom units)

the previously feebly magnetic hot iron begins to take on ferromagnetism, where also the temperature coefficient of electrical resistance is thought to change suddenly, and where the thermoelectric power is likewise suddenly changed. However, A_2 does not appear to be a sharp point in the temperature scale, but rather a transition taking place in a range of temperature and therefore difficult to make fit any ordinary definition of allotropy. It was formerly called the transformation point between α and β iron, but with the disproof of β iron as a definite crystallographic entity the question naturally came up as to whether A_2 was an allotropic transformation at all.

The word allotropy originated with Berzelius²⁷ in 1841 to denote elements appearing in various states distinguished by different

²⁷ Quoted from Copisarow, Maurice, Allotropy: Jour. Am. Chem. Soc., vol. 43, 1921, pp. 1870-1888.

physical properties. The definition is a loose one. Ostwald and Nernst used it in connection with energy changes in elements. Polymorphism was supposed to apply to compounds of elements in a similar sense. Other writers have insisted that allotropy applies to discontinuous changes in form, phase, and properties.

Allotropy has caused so much discussion through these disagreements of definition that it now appears expedient to drop it altogether and use another word which is not in such bad repute—polymorphism. The word "polymorphism" can apply as well to elements as to compounds. Wever and Gianì²⁸ define a phase change as characterized by a discontinuous change in suitable physical properties but not necessarily by all physical properties of the substances involved. They also define a polymorphic change or transformation as applying to crystalline material and characterized by a discontinuous change in the space lattice which is now capable of experimental realization without much difficulty. A change in crystalline form is usually accompanied by changes in physical properties, so a polymorphic change is practically always a phase change, but the question might be debated whether a phase change is always a polymorphic change.

On the above basis of polymorphism it is certain that there are only two forms of solid iron, α (including β and δ) and γ , corresponding to the above-described crystallography. However, β iron, which might be defined as nonmagnetic α iron, has enough difference in physical properties and energy content to deserve recognition, even though no satisfactory word or definition expresses the difference.

Better understanding of the differences between these forms of iron will be acquired as one reads the later sections of this paper dealing with the transformation points, their determination, and the amounts of energy associated with each.

PYROPHORIC IRON

When iron is reduced from its oxide at low temperatures and remains in a fine fluffy powder it is frequently pyrophoric. In other words, it ignites easily, even spontaneously, in air and is reoxidized. This extremely active form of iron will doubtless find increasing use as a catalyst or for other purposes where a large surface of iron is needed. Presumably the low-temperature reduction (usually with hydrogen) goes on at such a low temperature that only the skeleton framework of iron atoms remains where the iron oxide was before, and thermal motion of the atoms is too slight or too sluggish to

²⁸ See footnote 20, p. 131.

cause crystallization into the denser, more compact form of iron supposed to be stable at that temperature. In other words, pyrophoric iron is probably, at least in part, in the "colloidal" state.

Iron reduced from oxides by hydrogen at 370° to 530° C. is pyrophoric according to Tammann and Nikitn,²⁹ while above 530° C. it is not. By more careful manipulation Smits and Wallagh³⁰ report iron reduced at as high a temperature as 600° C. as being pyrophoric, with decreasing activity up to 710° C., above which the products were nonpyrophoric. Their heating period was one hour, and extremely dry hydrogen was used.

An X-ray spectrogram of pyrophoric iron would doubtless show at least some crystalline material present (α iron), and the samples of decreasing activity should show a sharper and sharper spectrum due to increasing size of crystalline iron.

TRANSFORMATION POINTS

As mentioned above, the temperatures at which the various polymorphic forms of iron transform into each other are known as critical points or temperatures, or, in the language of the physical chemist, as transformation temperatures. A brief tabulation of the recognized points with their approximate temperatures and a definition of each will serve as an introduction.

A_0 . 210° C.—This point is found only in iron-carbon alloys and is the temperature above which the compound Fe_3C is nonmagnetic. Such a point is found for all ferromagnetic substances and is named the Curie point, after its discoverer.

A_1 . 725° (*and up*).—Temperature of the iron-carbon eutectoid.

A_2 . 768°+.—A point found in pure iron and its alloys, being the Curie point of iron and formerly called the transformation from α to β iron, although β iron is now called nonmagnetic or paramagnetic α iron.

A_3 . 906° C.—A true polymorphic transition temperature of pure iron from the α to the γ form or vice versa; also noticed in iron alloys but displaced by other elements, some raising and some lowering it.

A_4 . 1,400° C.—A true polymorphic transition between γ and δ iron, also noticed in iron alloys and displaced by other elements dissolved in the iron.

Melting point, 1,537° C.; *boiling point*, 3,235° C.—In addition to these points, many others have been discussed, based on variations

²⁹ Tammann, G., and Nikitn, N., Pyrophorität von Metallpulvern: Ztschr. anorg. allgem. Chem., Jahrg. 135, 1924, pp. 201-204.

³⁰ Smits, A., and Wallagh, G., The Pyrophoric Phenomenon in Iron: Rec. trav. chim., vol. 44, 1925, pp. 130-131.

of physical properties which were difficult to explain otherwise, but in most instances they have not much foundation. Because a curve representing some physical property happens to change direction or pass through a maximum or a minimum is not sufficient evidence to justify claim of the existence of a transformation point. These will be discussed further along in this paper.

The accepted transformation points vary somewhat according to the conditions under which they are observed. When observed during heating of a specimen of iron each will have the letter "c" inserted, indicating the French word "chauffage," meaning "heating." Thus, A_2c_2 is the A_2 point as observed during heating. Likewise, the use of the letter "r" in the same position means "recalcescence" or "reheating" on a cooling curve. The A_3 point is a selected mean between the ordinarily observed A_3c_3 and A_3r_3 points, as there seems to be some lag in the actual transformation, and on a heating curve the specimen must in many cases be heated some distance past the expected temperature A_3 before A_3c_3 actually appears. Likewise, on cooling, the temperature of the material must usually be lowered somewhat beyond that expected. The faster the rate of heating or cooling the greater the difference between observed and expected temperatures. Part of the discrepancy is doubtless connected with difficulty in getting exact representative temperatures, and part may be a true expression of the inertia of the atoms of iron in rearranging themselves in the new crystal lattice, so that one may have to get some distance away from the true transformation temperature before there is sufficient driving force to cause the transformation to take place.

HEATING AND COOLING CURVES

For detecting transition points thermal methods of analysis, as used in metallography, have been most popular, as might be guessed from the last paragraph. An example of an ordinary cooling curve for electrolytic iron is given in Figure 39, which is taken from Ruer and Bode.³¹ It is also accompanied by part of a heating curve for the same sample. As noticed, the temperature of the sample stayed constant at 888° C. for nearly 50 seconds, and the sample then continued its regular cooling. This "constant" temperature during radiation of heat is due to an evolution of heat in the sample. The transition from γ to paramagnetic α iron at this temperature is accompanied by evolution of heat and during the reverse process by absorption of heat. The heat of transition has been accurately

³¹ Ruer, R., and Bode, K., Die magnetischen Umwandlungen der ferromagnetischen Metalle: Stahl u. Eisen, Jahrg. 45, 1925, pp. 1184-1189.

measured and will be discussed below. Likewise, when $768^{\circ}\text{C}.$ was reached another jog in the curve took place, due to transition of paramagnetic α iron into ferromagnetic α iron. This period of time was much shorter, and the heat evolved was evidently about one-sixth of the heat at $888^{\circ}\text{C}.$ These two points on the cooling curve are, respectively, the A_{r_3} and A_{r_2} points. On heating a sample similar discontinuities are observed, as mentioned above. The heating curve shown in Figure 39 shows a jog at 768° , although not all observers have been able to detect A_{c_2} so distinctly as the Ruer and Bode curve shows, and many entirely fail to detect it.

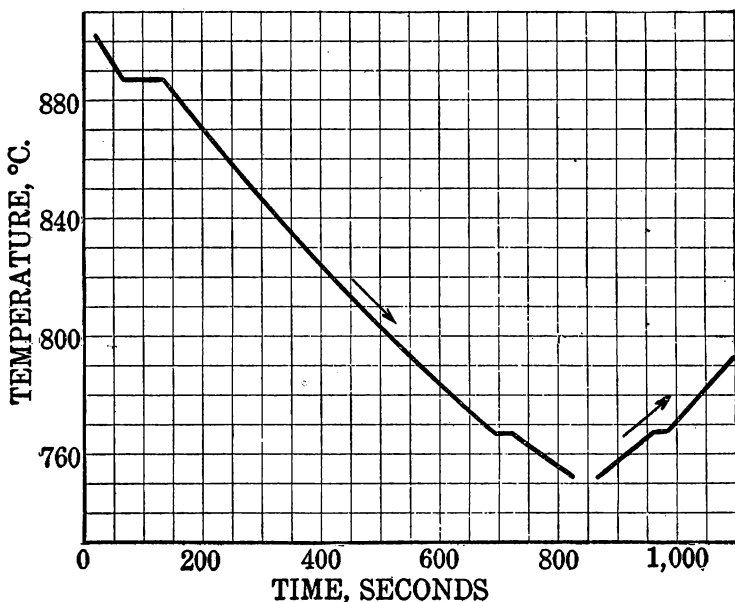


FIG. 39.—Cooling and heating curves of electrolytic iron (Ruer and Bode)

A more sensitive type of heating and cooling curves is obtained on heating an unknown sample together with a known sample of a standard substance like platinum, which has no transitions. If a thermocouple is placed in each and a galvanometer connected to record the difference in temperature between the unknown and the known materials, a much greater change in direction of heating and cooling curves is recorded; the method is therefore much more sensitive. When coupled with a recording instrument it has been a well-used instrument in the hands of steel metallurgists. In Figure 40 is a differential heating and cooling curve of a sample of electrolytic iron as observed by F. Wever.³² On the heating curve the A_{c_2} point

³² Wever, F., Über die Natur der magnetischen Umrwandlung des Eisens: Ztschr. anorg. u. allgem. Chem., Jahrg. 162, 1927, pp. 193–202.

is indicated by the sharp change of direction at 768° C. and the A_{c_3} point at 906° C. The sample was not heated highly enough to reach the A_4 point. On cooling, the A_{r_3} and A_{r_2} points fell at lower temperatures than the corresponding points on a heating curve, as would be expected, although by judicious choice in shape and size of specimens and cooling rates it has been found that A_{r_2} will occur at practically the same identical temperature as A_{c_2} , whereas the A_{r_3} point is always at a lower temperature than A_{c_3} .

Other physical properties than the heat content can be investigated as a function of temperature in locating the transition temperatures; in fact, it is these transitions from one form to another that

explain the changes in physical properties. Therefore, the following catalogue of physical properties of iron also helps determine the transition temperatures and leads to a final choice of the most probable temperature to choose as representing the A_2 , A_3 , and A_4 points.

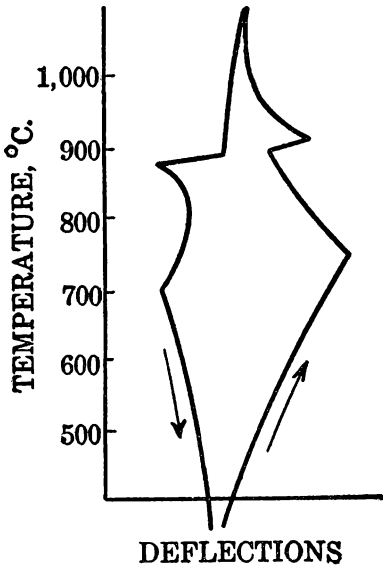


FIG. 40.—Differential cooling and heating curves, electrolytic iron (Wever)

A_2 TRANSFORMATION RANGE

This transition, the Curie point of pure iron, which has already been described as the magnetic transition, above which iron is paramagnetic and below which it is ferromagnetic, has been the subject of extended dispute. Not until the X-ray spectographic methods had shown that the paramagnetic α (formerly called β) iron was identical in crystal structure with ferromagnetic α iron was the exact nature of the transition understood. It is not polymorphic, but the magnetic change is the most prominent, and the other physical properties which are also altered with temperature are nearly all directly connected with the magnetic change. Most physical properties do not change at A_2 . The properties which are altered are heat content (with its concomitant, specific heat), electrical resistance, thermoelectric power, and a slight change in dimensions (dilatation), possibly associated with magnetostriction.

The most notable thing about the change has just been mentioned. It is strictly reversible, being observed at the same temperature in a

given instrument, no matter what the rate of heating or cooling, being therefore a function only of temperature. One can not superheat ferromagnetic α iron nor undercool paramagnetic α iron. Apparently, with rising temperature the ultimate magnetic particles of a sample of ferromagnetic α iron, even though in a strong magnetic field, acquire more and more violent thermal motion, which tends to destroy their magnetic orientations as imposed by the magnetic field. The most rapid loss in magnetic permeability or susceptibility is noted at about 768° C. and with it the greatest change in specific heat. This accounts for the apparent heat of transition. Seemingly energy must be expended in destroying orientation of the molecular atomic (?) magnets, and the specific heat is therefore made up of an ordinary "thermal motion" term plus a "magnetic" component. However, as will be seen shortly, the loss of magnetism is gradual; with it the change in specific heat is gradual, and the apparent "jogs" in heating or cooling curves like Figures 39 or 40 are not sharp. The physical changes are distributed over a temperature range and do not occur at a sharp point. Although most of the ferromagnetism is lost by the time 768° C. is reached, the last remaining traces detectible with apparatus now available die out at about 791° C. With increasing sensitiveness in measurements probably even higher temperatures will be set as the upper end of the magnetic transition range. The lower end is probably much below room temperature. The change probably takes place at all temperatures, with a maximum at A_2 . It has never been determined.

The fact that the principal physical properties altered at A^2 are magnetic properties, thermoelectric power and (possibly) electrical resistivity, has led Van Liempt and Geiss³³ to suggest that the changes in the solid lattice are not atomic but electronic at A_2 . This has caused Wever³⁴ to study the K - emission spectra, and to date he announces that no difference in the electron configurations of the outer shell of magnetic and nonmagnetic iron atoms has been found. So the question remains open.

A_2 BY HEATING AND COOLING CURVES

Since the greatest thermal effect of the A_2 transition occurs at about 768° and the treatment of steel is primarily heat treatment, this value has been chosen for practical purposes. Using electrolytic iron for the determination, the most careful work has been

³³ Geiss, M., and van Liempt, J. A. M., ————: Ztschr. Metallkunde, Jahrg. 18, 1926, p. 216.

³⁴ Wever, F., Über die Röntgen-Emissionsspektren der Eisenmodifikationen: Naturwissenschaft., Jahrg. 14, 1926, p. 1217.

done by Burgess,³⁵ who finds 768° C., by Ruer and Goerens,³⁶ who finds 769° C., and by Ruer and Bode,³⁷ who finds 768° C. The heating and cooling curves of Ruer and Bode have already been discussed. (See fig. 39.)

Previous thermal history seems to affect the position of the A_2 point as determined by thermal methods. Sauveur,³⁸ using Burgess's electrolytic iron in a recording differential instrument, noticed on the first heating to 1,000° C. that A_{c_2} occurred at 725° C. and A_{r_2} at 769° C. On the eighth heating A_{c_2} was at 769°, on the ninth at 781°, on the tenth at 783°, and on the eleventh at 783° C. The A_{c_3} point was also observed, first at 850° C. and finally at 919° C., which is somewhat higher than usually observed. Whether or not his pyrometer was registering correctly or his heating and cooling apparatus working at too high a rate of speed, the above comparative figures undoubtedly show a drift in the A_2 point as determined by previous heatings and coolings, the effect being gradual raising of the point to a constant temperature.

A_2 BY CALORIMETRIC METHODS

A number of experimenters have measured the heat capacities of iron and its alloys in various types of calorimeters at a series of temperatures, and the discontinuities in their heat-capacity curves and the derived specific heat curves are noted for the different transition points. They have been listed in Table 18. The details of this work will be discussed under the heading "Specific heat" below, together with references. A column is also included, showing the value of the true specific heat at the peak of the change for each experimenter, which serves to show that by magnification of error the absolute values of the specific heat at the transition are doubtful, although the position of the peak is definite. All the better calorimetric results were compared and replotted, and an average was included in the table. This average shows that the discontinuity in heat content and specific heat falls at 781° C., where the true specific heat at constant pressure has a value of 17.55 calories per gram-atom.

³⁵ Burgess, G. K., and Scott, H., Thermoelectric Measurement of the Critical Ranges of Pure Iron: U. S. Bureau of Standards Bull., vol. 14, 1918, p. 15.

Burgess, G. K., and Crowe, J. J., Critical Ranges A_2 and A_3 of Pure Iron: U. S. Bureau of Standards Bull. 213, 1914, 56 pp.

Berliner, J. F. T., Preparation and Properties of Pure Iron Alloys: U. S. Bureau of Standards Sci. Paper 484, 1924, pp. 347-356.

³⁶ Ruer, R., and Goerens, P., —————: Ferrum, vol. 13, 1916, pp. 1-6.

³⁷ See footnote 31, p. 136.

³⁸ Sauveur, Albert, The Allotropic Transformation of Iron: Engineering, vol. 96, 1913, p. 353.

TABLE 18.— A_2 transition by calorimetric methods

Authorities	Date	Material	A_2 ° C.	C_p peak
Weiss and Beck	1908	Nail iron	753	17.64
Wüst, Meuthen, and Dürer	1918	Electrolytic	755	21.00
Weiss, Piccard, and Carrard	1916	do	784	17.03
Do	1916	Swedish	784	17.26
Oberhoffer and Grosse (original)	1926	Electrolytic	785	14.55
Oberhoffer and Grosse (replotted)	1926	do	785	27.90
Umino (extrapolated from steels)	1926	Steels	825	14.53
Umino (armco iron)	1926	Armco iron	820	19.00
Ralston average from replots	1927	Pure iron	781	17.55

 A_2 BY MAGNETIC METHODS

With rise in temperature the magnetic susceptibility or magnetic permeability of iron rises at first in weak magnetic fields and then falls off, while in strong fields it falls off continuously. A great number of papers on magnetic theory have emanated from the laboratories of Pierre Weiss (Zurich, Switzerland) and Kotaro Honda (Sendai, Japan). They agree that with iron the magnetic effect falls off very rapidly at about 768° C., but Honda points out that it does not reach an apparent constant amount until about 790° C. is passed; and if the apparatus is sufficiently sensitive, further decrease is noted up to a sharp break at the A_3 point, beyond which it is constant until the A_4 point is reached, where a sharp rise is noted and then a gradual drop with further rise of temperature. A magnetization curve for strong fields, plotted by Honda,³⁹ is given in Figure 41 and in weaker fields at higher temperatures with a more sensitive instrument in Figure 42. These two curves illustrate well what has just been said. In Figure 42 the dotted line shows that the magnetic susceptibility of δ iron seems to be a continuation of that β (paramagnetic α) iron, lending support to the X-ray data which indicate that α , β , and δ irons are crystallographically identical, while γ iron belongs to a different system.

The original discoverer of the magnetic "inversion" of iron was Curie,⁴⁰ who placed it at 753° C. The same temperature was later noted by Weiss and Beck⁴¹ in their magnetometer. Weiss⁴² also independently observed 756° C. However, the Honda laboratory did more precise work than that of Weiss, and its higher temperature

³⁹ Honda, K., Nature of the A_2 Transformation in Iron: Tohoku Univ., 1st ser., vol. 4, 1915, pp. 169–214.

⁴⁰ Curie, P., Propriétés magnetiques des corps à diverses temperatures: Ann. chim. phys., vol. 5, 1895, pp. 289–405.

⁴¹ Weiss, P., and Beck, P. N., Chaleur spécifique et champ moléculaire des substances ferromagnétiques: Arch. sci. phys. nat., iv, vol. 25, 1908, pp. 529–548.

⁴² Weiss, P., Sur la théorie des propriétés magnétiques du fer au delà de la temperature de transformation: Compt. rend., t. 144, 1907, pp. 25–28.

data seem much more acceptable. Honda and Ogura⁴³ determined the point to be at 796° C. Ishiwara⁴⁴ found that with pure iron the

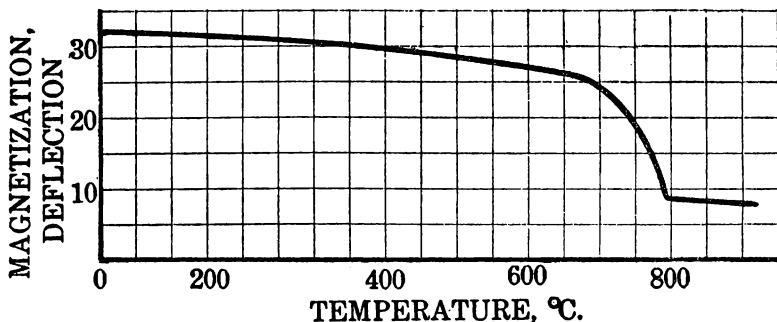


FIG. 41.—Magnetic susceptibility v. temperature; large units (Honda)

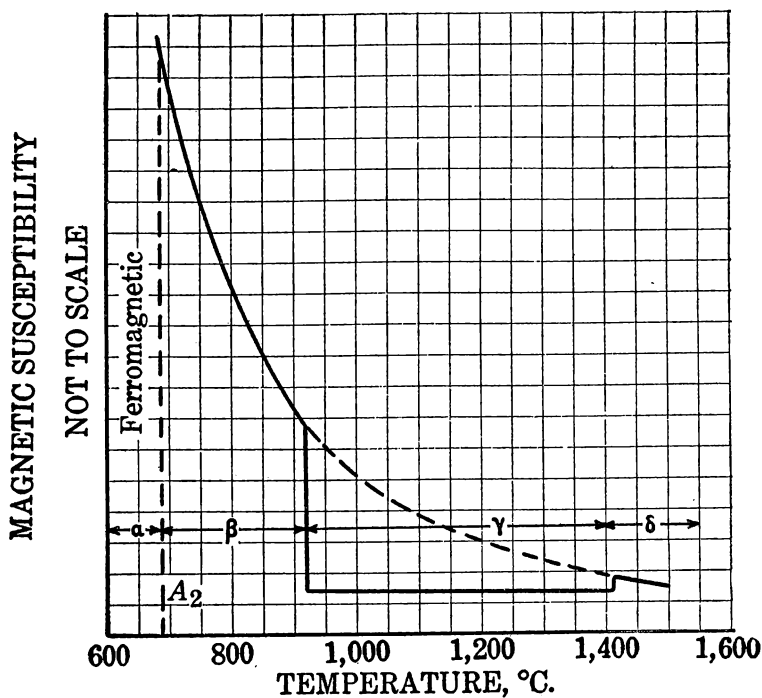


FIG. 42.—Magnetic susceptibility v. temperature; magnified vertical scale (Honda)

Curie point occurred at 800° C. but was lowered to 790° C. with low-carbon steels and to 780° C. for the high-carbon steels and cast iron.

⁴³ Honda, K., and Ogura, Y., Über die Beziehung zwischen den Änderungen der Magnetisierung und des elektrischen Widerstands in Eisen, Stahl, und Nickel bei hohen Temperaturen: Tohoku Univ. Sci. Repts., vol. 3, 1914, pp. 113–125.

⁴⁴ Ishiwara, T., The Magnetic Determinations of the A_0 , A_1 , A_2 , and A_3 Points in Steels Containing Carbon up to 4.8 Per Cent: Proc. Phys.-Math. Soc. Japan, vol. 3, No. 2, 1920, p. 91.

However, Honda⁴⁵ has recently objected on the grounds of a series of magnetization-temperature curves which he presents. He states that for pure iron the Curie point is at 790° C., but in the carbon alloys a point at 770° C. is usually observed and is called the A_2 point. He says this is the Curie point of austenite (solid solution of carbon in γ iron) and not of pure γ iron, and that carbon does not lower the temperature of the A_2 point. If a sufficiently sensitive magnetometer were used to detect small amounts of pure iron in the presence of austenite he anticipates that it would show changes at both 770° and 790° C. He therefore proposes calling the Curie point of austenite the A'_2 point, thus showing its near relationship to the A_2 point of pure iron.

One can only conclude that in spite of the immense amount of work that has been done there are still uncertainties about the nature of the A_2 range or Curie point in iron.

If one plots the reciprocal of the magnetic susceptibility of a ferromagnetic substance as a function of temperature, the result is frequently a straight or nearly straight line. This result encouraged Weiss in his early work to develop a theory of magnetism and to define a unit of magnetism called the magneton. Without attempting to go into the theory of magnetism at this point, suffice it to say that Weiss and Foex⁴⁶ plotted their magnetic data as shown in Figure 43, and as their plot showed a slight kink at 830° C. they deduced that there were two forms of β iron (at their time the nature of β iron was not understood), one with 12 and the other with 10 (Weiss) magnetons per gram-atom of iron, and each with its straight line in the diagram. These forms they named β_1 and β_2 . However, more careful work by Terry⁴⁷ showed that in the β range there were not two straight lines as found by Weiss and Foex, but one line, which curved considerably, and in the γ region Curie's law was not even obeyed approximately. A good sample of Burgess's electrolytic iron melting at 1,530° C. was used, and so much care was taken with the measurements that it is impossible to avoid feeling that Terry was right.

A₂ BY THERMOELECTRIC METHODS

Many experimenters have used iron with either platinum or copper wires in the form of thermocouples and have sought thereby to determine the critical points of iron. However, most of the work

⁴⁵ Honda, K., On the A_2 Line in the Equilibrium Diagram of the Iron-Carbon System: Tohoku Univ. Sci. Repts., vol. 15, 1926, pp. 247-250.

⁴⁶ Weiss, P., and Foex, G., L'aimantation des corps ferromagnetiques au-dessus du point de Curie: Arch. sci. phys. nat., vol. 31, 1911, pp. 5-19, 89-117.

⁴⁷ Terry, E. M., The Magnetic Properties of Iron, Nickel, and Cobalt above the Curie Point and Keesom's Theory of Magnetization: Phys. Rev., vol. 9, 1917, pp. 394-413.

previous to 1905 was with samples of iron that were insufficiently pure. Moreover, the methods of preparing the couples and observing their electromotive force were not above criticism. A review of the subject is given by Burgess and Scott, who are quoted below. Not until the work of Broniewski in 1913 was anything done worth consideration. Broniewski and Belloc⁴⁸ found that the plot of thermoelectric power v. temperature showed a slight discontinuity, which was attributed to A_2 , at about 795° C. The precise work of

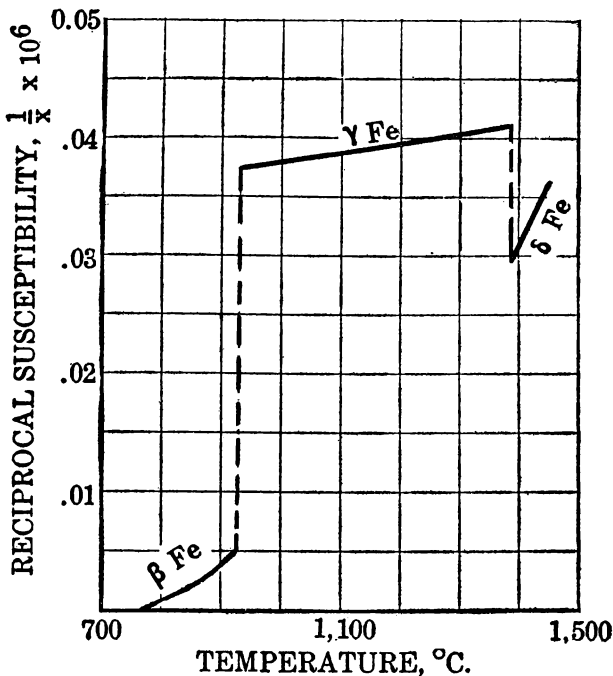


FIG. 43.—Iron: Reciprocal susceptibility v. temperature (Weiss and Foex)

Burgess and Scott⁴⁹ showed that there was undoubtedly a change in direction of the electromotive force curve at about 768° C., the temperature previously observed by the Bureau of Standards by thermal means. The iron sample used was electrolytic, and platinum was used for reference. After heating, the electromotive force rose with some wavering, but a clearly marked small deflection took place at 768° C. However, all the heating curves went through a maximum with a rather sharp drop beyond about 780° C., the latter being a much more strongly marked point. On cooling, the curves did

⁴⁸ Broniewski, W., Sur la thermo-électricité des aciers: *Compt. rend.*, t. 156, 1913, pp. 699, 1983.

⁴⁹ See footnote 35, p. 140.

not retrace themselves, but there was more or less of a continuous drop from the A_3 temperature, with a slight kink in the line at 768°C . In three out of six curves another wobble which is unexplained was noticed at about 880°C . It seems probable that the real A_2 point, as revealed by thermoelectric means, is one at 780° , while the small kinks at 768° were due to the maximum heat absorption or evolution known to take place at that temperature. One of the thermoelectric curves is shown in Figure 48, which is discussed later.

Similar studies of steel wires were made by Berliner⁵⁰ in the same laboratory. The A_2 kink was observed at 768°C in all steels up to those with 0.45 per cent of carbon but was obscured by more carbon. This latter phenomenon is due to the fact that the A_3 point is lowered by the presence of carbon in the iron, and with over 0.50 per cent of carbon the A_3 point is at a lower temperature than 768°C .

One of the great causes of error in testing iron wires for various physical properties at elevated temperatures is the chemical alteration that takes place, especially if the iron is heated in a gas. The work of Burgess and Scott, and also of Berliner, was done with iron wires in vacuo. Berliner had difficulty with decarbonization of his steel wires, but with pure iron wire the minimum alteration takes place under these conditions.

A_2 BY ELECTRICAL RESISTANCE METHODS

Electrical resistances of iron and its alloys have been measured by a long series of experimenters, because much can be learned about the metallographic condition of the alloys in this way. Unfortunately, the purity of most of the samples used and the temperature control during experiments were questionable up to about 1912, when supplies of good electrolytic iron, melted in vacuo without contamination, began to become available. Some of the experimenters observe a definite kink in their temperature-resistance curves at the A_2 temperature, although the most precise work, that of Burgess and Kellberg, does not show a kink. The work of Honda and Ogura is shown in Figure 44, which gives the electrical resistance in ohms of a Kahlbaum iron wire sample of the dimensions 0.71 millimeter times 122 centimeters. The curve shows a decided change in direction at 798°C ., which was interpreted as the A_2 point.⁵¹

Burgess and Kellberg⁵² used iron wire of 0.2 millimeter diameter and unspecified length, wound as a resistance thermometer, in com-

⁵⁰ See footnote 35, p. 140.

⁵¹ See footnote 43, p. 142.

⁵² Burgess, G. K., and Kellberg, I. N., *Electrical Resistance and Critical Ranges of Pure Iron*: Bull. U. S. Bureau of Standards, vol. 11, 1915, pp. 457-470.

parison with a platinum-wire resistance thermometer of similar dimensions. They estimate their precision as 1,000 times that of Honda and Ogura. Their temperature-resistance curve, shown in

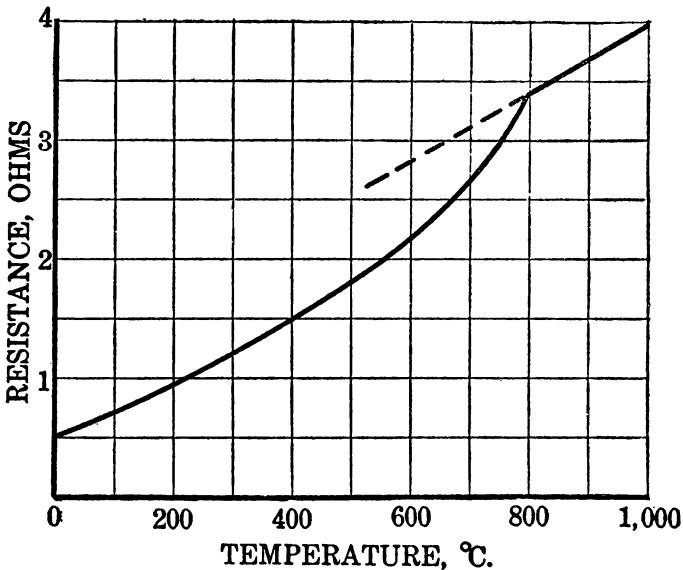


FIG. 44.—Electrical resistance of Kahlbaum iron (Honda and Ogura)

Figure 55 and discussed later, shows no hint of A_2 except that the greatest change in resistance per degree is taking place at this tem-

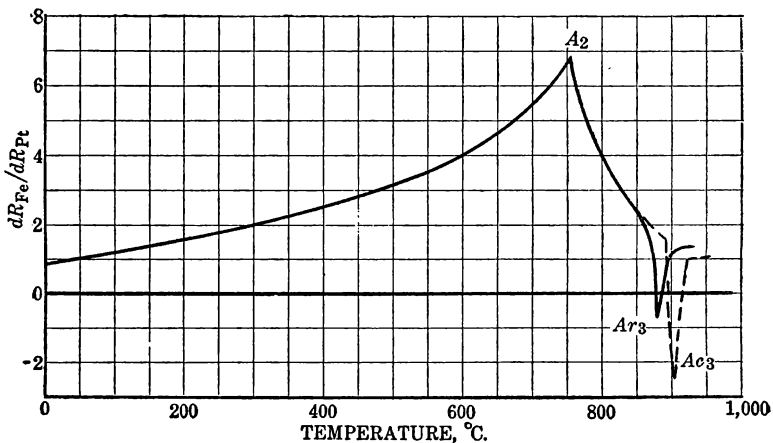


FIG. 45.—Increase of resistance of iron compared to platinum (Burgess and Kellberg)

perature. On plotting the change in resistance of iron as compared to the change in platinum as a function of temperature, they obtained the curve given in Figure 45, which gives a decided cusp at

757° C. and is taken by them as the A_2 point by this method. Possibly the difference between the Burgess and Kellberg results and those of Honda and Ogura is in the magnetic field in which the experiments were carried out. The mere fact that Burgess and Kellberg get a cusp at 757° C. in their differential coefficient curve does not establish any physical difference between the iron above and below 757° C. Being the plot of a differential coefficient, it means that the resultant of the curves from which it is derived goes through a point of inflection at 757° C. The platinum resistance-temperature curve is quite regular at this temperature, while the iron curve exhibits the anticipated inflection. Rarely is a point of inflection in any such curve of physical properties regarded as having much significance. The present reviewer is inclined to accept the high precision of the work of Burgess and Kellberg but to reject their differential curve in Figure 45 as not having any physical significance. To date no satisfactory resistance data have been presented which show the existence of the A_2 point. Possibly magnetic orientation of the ultimate magnetic units of metallic iron does not affect electrical conductivity. Study of the effect of a magnetic field on resistance of iron at various temperatures would probably be worth while.

A_2 BY DILATOMETER

The other remaining bit of evidence of the existence of the A_2 point is that obtained by dilatometric means, which has been done by Benedicks,⁵⁸ whose dilatometric measurements have been recognized as precise but whose temperature measurements and control have been severely criticized. He compared a bar of iron with a bar of gold in length. The differential dilatometric measurements are plotted in Figure 46, which shows a slight deflection at 760° to 775° C., interpreted as possibly indicating the A_2 point or range. This deflection was only 0.003 of the deflection noted at the A_3 point and may be purely illusory. Another slight change in direction was noted at 830° C. and was thought to coincide with the magnetic anomaly observed by Weiss and Foex, which was discussed above. Due to the slight effect at the place where A_2 was expected, Benedicks made measurements of magnetostriction (change in dimensions on magnetization) at various temperatures and found the maximum effect at 500° to 550° C., the fractional change in length being fourteen times greater there than at room temperature and falling off with further rise of temperature without apparently permitting any conclusion about the condition at 768° C. It is reasonable to believe that a slight change in length could be expected when the material passed

⁵⁸ Benedicks, C., The Allotropy of Iron in Ferromagnetic Mixtures; the Dilatation of Pure Iron: Jour. Iron and Steel Inst., vol. 89, 1914, pp. 407-459.

from the ferromagnetic range into the paramagnetic range and at that point all magnetic orientation would be destroyed. Therefore, while magnetostriction might account for the slight observed dilatation at the A_2 temperature, the evidence so far collected is too uncertain to be relied on.

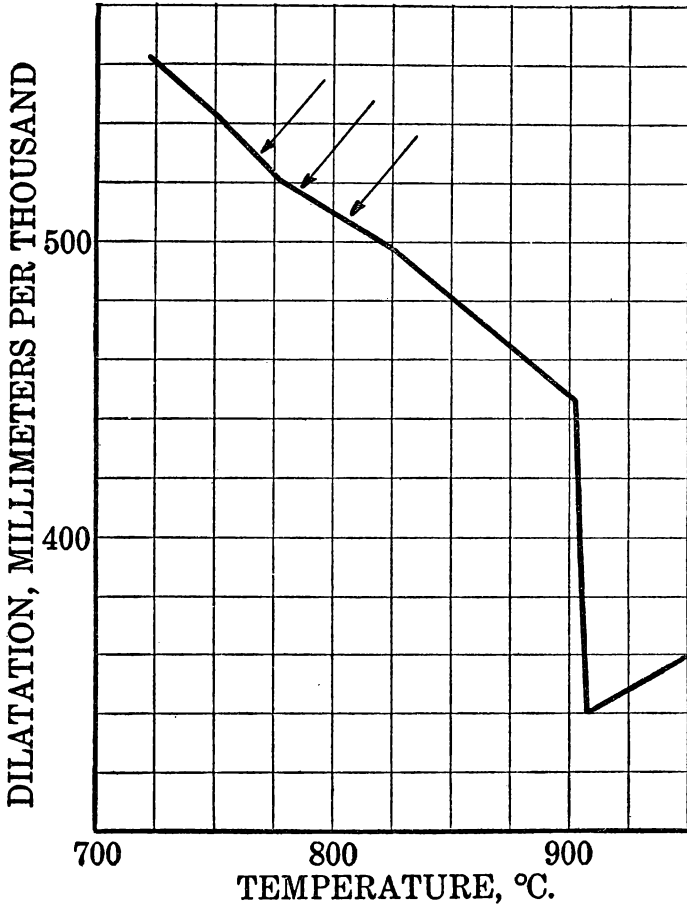


FIG. 46.—Differential dilatation iron-gold (Benedicks)

A_3 TRANSFORMATION RANGE

This temperature, the mean between A_c_3 (heating) and A_r_3 (cooling), is the one above which iron exists in the γ modification and below which it exists in the α modification. Nearly all important physical properties change at this point, and a large heat change is also noticed. The same critical point is observed in most iron alloys, the temperature being lowered by the presence of dissolved carbon in iron and either raised or lowered by other elements. In

steel treatment this is one of the most important points from the standpoint of alteration of physical properties, because of the profound recrystallization that takes place in passing the point and the great changes in the amount of dissolved carbon held in the solid iron. This transformation is not instantaneous, hence the apparent temperature at which it is observed varies with the heating or cooling rate of the specimen being examined. It also seems to suffer some lag, and a specimen must be superheated above the expected temperature before anything happens, or in cooling the specimen must be undercooled considerably before enough driving force is developed to bring about the change. That is why the average of A_{c_3} and A_{r_3} is used in determining the position of A_3 . For the most precise work one needs to know the exact values of A_{c_3} or A_{r_3} and the time allowed.

A_3 BY THERMAL METHODS

Hundreds of determinations of the location of the A_3 point by heating or cooling curves, differential or inverse rate, are available, but only a few need to be discussed. The Ruer and Bode cooling curve in Figure 39 places A_{r_3} at 888° C. Honda and Takagi⁵⁴ have placed A_{c_3} at 916° C. and A_{r_3} at 890° C. for a sample of pure electrolytic iron. Most of the previous work had suffered owing to the impurity of the iron specimens used, the effect of carbon being to lower the temperature of the A_3 point. The Honda and Takagi data are representative of the temperatures that may be expected with ordinary rates of heating or cooling. However, their work was done on the identical specimens that were previously used by Burgess and Crowe,⁵⁵ who tried several different rates of heating or cooling and then extrapolated to zero rate. Their corrected figures for zero rate are $A_{c_3}=909\pm 1^\circ$ C. and $A_{r_3}=898\pm 2^\circ$ C., and their arithmetic mean is $A_3=903.5^\circ$ C. These figures are accepted herewith as being some of the best available.

A_3 FROM SPECIFIC HEAT CURVES

A series of investigators have measured the heat capacity of iron and its alloys as a function of temperature, using the method of mixtures. The heated specimen has to be heated above the transformation point A_{c_3} before the specific heat curve is affected, therefore this method is regarded as determining the location of A_{c_3} . Usually the samples are held at the desired temperature for some time before being dropped into the calorimeter, in order to obtain uniform temperature, therefore the A_3 point as determined from specific heat

⁵⁴ Honda, K., and Takagi, H., Magnetic Study of the A_3 Transformation in Pure Iron: Tohoku Univ. Sci. Repts., vol. 4, 1915, pp. 261-269.

⁵⁵ See footnote 35, p. 140.

curves corresponds very nearly to zero heating rate. Table 19 gives the principal observers and their observed values of A_3 temperature.

TABLE 19.—Values of A_3 temperature

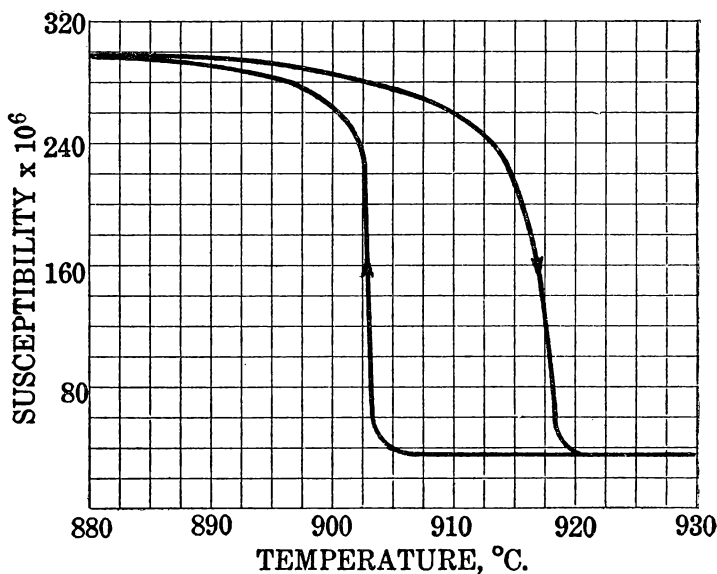
Observers	Date	Electrolytic iron, A_3 , °C.
Wüst, Meuthen, and Dürrer ¹	1918	919
Oberhoffer and Grosse ²	1927	906
Umino ³	1926	906

¹ Wüst, W., Meuthen, A., and Dürrer, R., ———: Verein Deut. Ing. Forschungs Arbeiten, 1918, No. 204.

² Oberhoffer, P., and Grosse, W., Die spezifische Wärme des Eisens: Stahl u. Eisen, Jahrg. 47, 1927, pp. 576-582.

³ Umino, S., On the Latent Heat of Fusion of Several Metals and Their Specific Heats at High Temperature: Tohoku Univ. Sci. Repts. vol. 15, 1926, p. 597.

The Umino value above was assumed from previous work, as none of the points on the specific heat curve were sufficiently close to the A_3 point to fix it definitely. None of the values is regarded as precise.

FIG. 47.—Magnetic changes at A_3 point (Terry)

A_3 BY MAGNETIC METHODS

A very sharp change in direction of the magnetic susceptibility temperature curve takes place at the A_3 point (see fig. 43), and the lag noticed in the thermal experiments is not so noticeable. Several competent investigators have contributed curves. That of Terry ⁵⁶ is reproduced in Figure 47. Although the slope of the heating curve

⁵⁶ See footnote 47, p. 143.

leaves the exact location of A_3 in doubt, there is no doubt about A_3 . Similar curves have been obtained by Honda and Takagi⁵⁷ (see fig. 42), and by Ishiwara,⁵⁸ except that between 880° and 990° C. their slope is not so flat. The data of these three investigators are summarized in Table 20.

TABLE 20.— A_3 point by magnetic methods, electrolytic sample

Observer	Date	A_3 , ° C.	A_3 , ° C.
Honda and Takagi.....	1915	911	898
Do.....	1915	908	889
Ishiwara.....	1917-18	898	890
Terry.....	1917	918	903

Terry checked his thermometric scale against the melting point of gold (1,062° C.), and his iron sample melted at 1,530° C., showing that it was fairly pure. Honda's work was also known to be good, although the low temperatures recorded on his second sample above reported suggest some contamination (probably of carbon), and the low values of Ishiwara are especially suggestive of impurities. However, allowing equal weight to all determinations, the arithmetic mean of these two used for determining the A_3 point is 902° C.

A_3 BY THERMOELECTRIC METHODS

The work of Burgess and Scott, mentioned above, on pure iron wire used against platinum as a thermoelectric reference standard is summarized in Figure 48. A discontinuity at the A_3 point is noticed and A_3 is at a higher temperature than A_3 . Their work shows that the A_3 transition begins at 906° C. on heating and continues to 912°, while the A_3 transition begins at 900° C. on cooling and is complete at 896° C. The later work of Berliner, also mentioned above, confirmed these temperatures. The specimens, being in the form of thin wire, can hardly be said to suffer from lag of temperature distribution, and the precision of temperature measurement is well within the ranges noted above. Evidently, therefore, the transition is subject to hysteresis and requires some superheating or supercooling, as the case may be, before it becomes effective. It will also be remembered that the readings of a thermocouple are not instantaneous.

⁵⁷ See footnote 54, p. 149.

⁵⁸ Ishiwara, T., Magnetic Investigations of the A_3 and A_4 Transformations in Iron and Steel: Tohoku Univ. Sci. Repts., vol. 6, 1917-1918, pp. 134-138.

A_3 BY ELECTRICAL RESISTANCE METHODS

The change in electrical resistance of iron at the A_3 point is only slight in comparison with the change of many other physical properties. However, owing to the high precision possible in such electrical measurements, Burgess and Kellberg⁵⁰ were able to show a marked loop at A_3 when plotting resistance on a large scale. The portion of their work adjacent to A_3 is given in Figure 49. This shows A_{c_3} beginning at about 900° C. and continuing to 911° C., while A_{r_3} begins at about 887° C. and is finished at 872° C. The medial line of the "hysteresis" loop is at about 893.5° C. Here

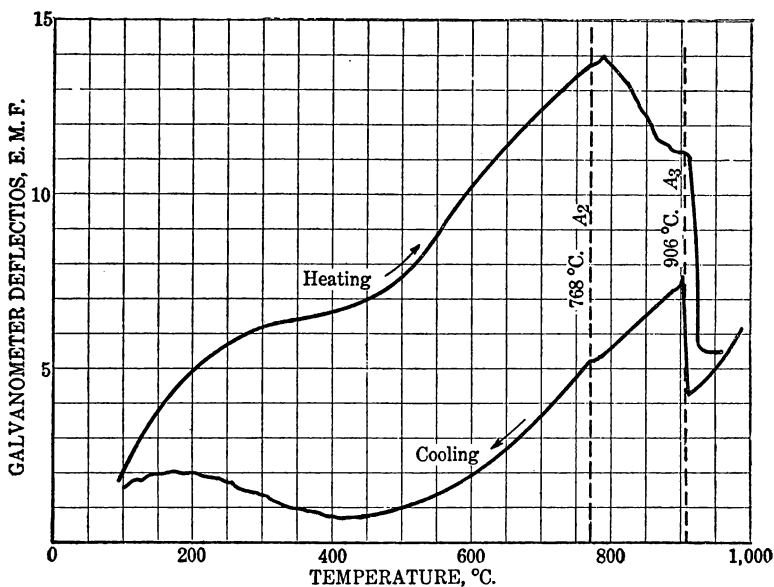


FIG. 48.—Thermoelectric power of iron against platinum (Burgess and Scott)

again the fine wire probably suffered only a small temperature lag, and yet the temperature range through which the change takes place is apparent. The location of the A_{c_3} and A_{r_3} points as a function of the electrical resistance is also shown well in Figure 45.

 A_3 BY DILATOMETER

The dilatometric work of Benedicks, mentioned in discussion of the A_2 point above and plotted in Figure 46, showed a marked change in dimensions at A_3 . Only a heating curve was observed, and the location of A_{c_3} was about 903° to 906° C. As mentioned above, Burgess has criticized the thermometric measurements severely, although the length measurements were sufficiently precise.

⁵⁰ See footnote 52, p. 145.

A permanent lengthening of samples heated through the A_3 point and cooled again is reported by Benedicks. Evidently the profound recrystallization taking place at this point relieves certain strains on heating, and on cooling a sample does not return entirely to its original dimensions.

The difference between beginning and ending temperatures of the A_3 transformation, as shown in the curves of nearly all physical properties, are usually passed over by experimenters as being connected with imperfections of the apparatus and methods used. However, Honda and Miura⁶⁰ have found in the iron-nickel system that

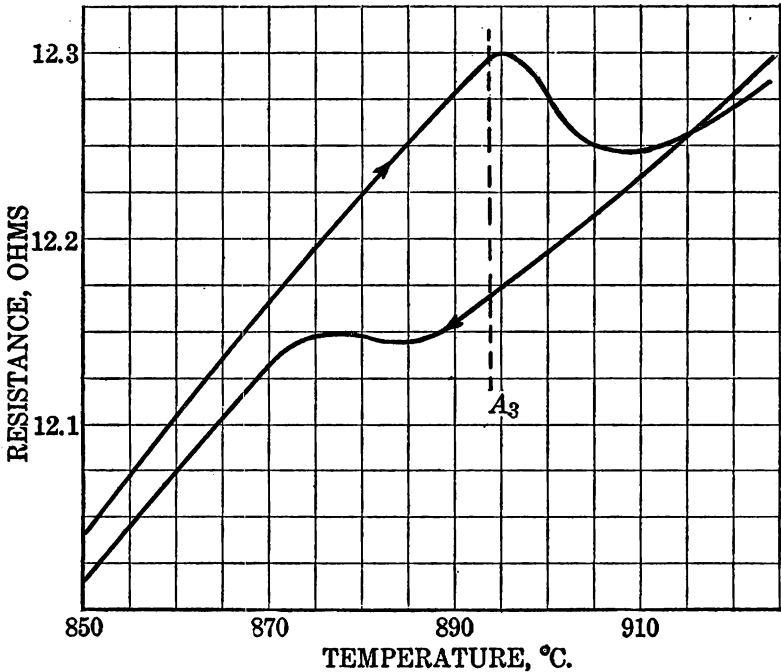


FIG. 49.— A_3 point by electrical resistance (Burgess and Kellberg)

the difference between the beginning and ending temperatures of the A_3 transformation is real and is increased by alloying the iron with nickel. With a heating or cooling rate of 2° C. per minute they find in armco iron that A_{c_3} begins at 860° C. and ends at 905° C., while A_{r_3} begins at 889° C. and ends at 850° C. In Figure 50, *A*, are given the temperatures of beginning and endings of the A_{c_3} point and in Figure 50, *B*, are the same temperatures for the A_{r_3} transition. Evidently the upper curve can be regarded as a "liquidus" curve and the lower as a "solidus" curve. This conclusion is based upon calcu-

⁶⁰ Honda, K., and Miura, S., On the Determination of the Heterogeneous Field in the Iron-Nickel System: Preprint, Sept., 1927, meeting Am. Soc. Steel Treating.

lation of the depression of the transformation point as a function of the differences in concentration of nickel in the solidus and liquidus and the heat of transformation. Fair agreement is shown between the calculated and observed lowering at several different temperatures. However, the liquidus and solidus should meet at the point of the diagram for the pure substance, and although armco iron is not exactly chemically pure iron it is nearly so. The principal value of the Honda and Miura work is to point out that the A_3 transformation in iron alloys takes place through a range of temperature and should not be regarded as a point.

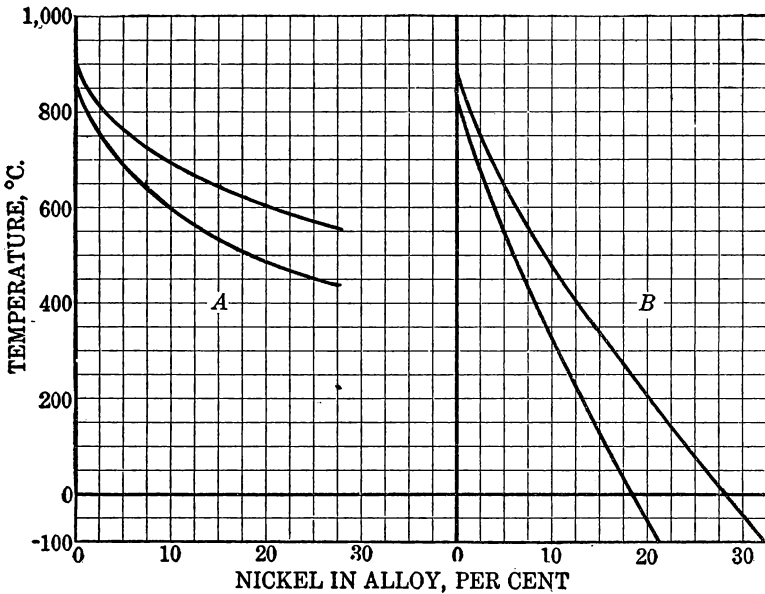


FIG. 50.—Upper and lower limits of A_3 transformation range, Fe-Ni alloys (Honda and Miura)

OTHER CHANGES AT A_3 POINT

Although the primary change at the A_3 point is from α to γ iron, or vice versa, nearly all other physical properties change. Alpha iron is an entirely different substance from γ iron, and while the two substances can not be expected to have as marked differences in characteristics as iron and copper each has its own distinct character. The solubility of carbon in γ iron is much greater than in α iron, as will be seen later. The twisting experiment of Sauveur, mentioned above, showed qualitatively that iron in the transition stage is more plastic than either α or γ iron. Every physical property can be expected to show some differences in the two ranges.

A₄ TRANSFORMATION RANGE

At about 1,400° C. γ iron, on heating, is transformed back to the same type of space lattice as α iron. Above this transition temperature such α iron is usually called δ iron, although as far as known it is identical with α iron. In fact, such elements as chromium added in increasing amounts lower the A_4 transformation temperature and raise the A_3 temperature until they become identical, and the formation of γ iron is entirely suppressed, so that one passes continuously from the field of temperature in which α iron is supposed to be stable up to the range of temperature where δ iron is stable. The transformation of α to γ iron at A_3 , followed by reverse transformation at A_4 , is quite anomalous, but not thermodynamically inconsistent, as will be seen later on.

The A_4 transformation has been studied mainly by thermal and magnetic methods. It was first discovered by Ball,⁶¹ whose findings were confirmed by Osmond,⁶² both placing it at about 1,300° C. by thermal means. Curie⁶³ later noticed it by magnetic means and similarly placed it at about 1,300° C. The samples of all investigators were impure, which alters the temperature of the A_4 transition; probably their thermometry was also deficient.

The more up-to-date thermal and magnetic determinations are summarized in Table 21.

TABLE 21.—*Thermal and magnetic determinations*

Observers	Date	A_4 , °C.
Thermal methods:		
Gontermann ¹	1908	1,411
Ruer and Kaneko ²	1914	1,420
Ruer and Klesper ³	1914	1,401
Hanson and Freeman ⁴	1923	1,400
Magnetic method:		
Weiss and Foex ⁵	1911	1,395
Ishiwara ⁶	1917	1,390
Terry ⁷	1917	1,406

¹ Gontermann, W., Über einige Eisen-Silicium-Kohlenstofflegierungen: Ztschr. anorg. Chem., Jahrg. 59, 1908, p. 378.

² Ruer, R., and Kaneko, K., ———: Ferrum, vol. 11, 1914.

³ Ruer, R., and Klesper, R., ———: Ferrum, vol. 11, 1914, pp. 258-261.

⁴ Hanson, D., and Freeman, J. R., The Constitution of the Alloys of Iron and Nickel: Jour. Iron and Steel Inst., vol. 107, 1923, pp. 301-314.

⁵ See footnote 46, p. 143.

⁶ See footnote 58, p. 151.

⁷ See footnote 47, p. 143.

The Weiss and Foex magnetic data are plotted in Figure 43. Ishiwara, whose work was discussed in connection with the A_3 point, studied very slow passage through the A_4 point in order to determine

⁶¹ Ball, E. J., On the Changes in Iron Produced by Thermal Treatment: Jour. Iron and Steel Inst., vol. 1, 1890, p. 85.

⁶² Osmond, F., Discussion: Jour. Iron and Steel Inst., vol. 1, 1890, p. 102.

⁶³ Curie, P., "Oeuvres": Paris, 1895, p. 289.

if the A_{c_4} and A_{r_4} points might not be identical in temperature, but he found, as did also Terry, that they were not. This is shown in Figure 51, *A*, which gives the Ishiwara data at the A_4 point and shows that with his rates of heating and cooling the A_{c_4} point occurs at $1,395.5^\circ\text{C}$. and the A_{r_4} point at $1,386^\circ\text{C}$. For comparison, the data of Terry are shown in Figure 51, *B*, where no such great difference between A_{c_4} and A_{r_4} is discernible. Difficulties in such high-temperature measurements make it remarkable that agreement between observers is as good as it is. The work of Ruer and Klesper and of Terry seems to be the most consistent and best described, and the average of their two data would place the A_4 point at $1,403.5^\circ\text{C}$.

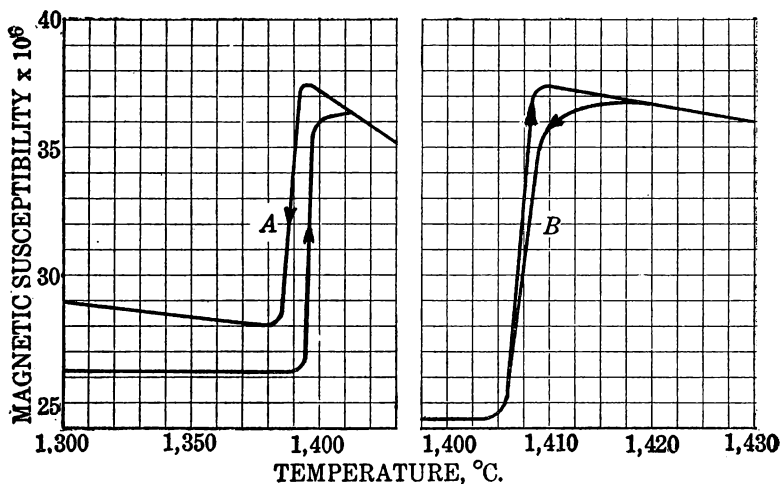


FIG. 51.—Magnetic susceptibility near A_4 point: *A*, Ishiwara; *B*, Terry

Other physical properties probably vary just as much in passing the A_4 point as the A_3 point, as they are so similar. However, less work has been done in this temperature range. In every case it is expected that the physical properties of δ iron will prove to be extrapolations of those of α iron, as has been found in the magnetic work of Weiss and Foex and Honda and in the specific heat work of several investigators.

When determining the specific heat of iron through a range of temperatures Wüst, Meuthen, and Dürer determined A_4 to be at $1,404.5^\circ$, while Oberhoffer and Grosse found it at $1,401^\circ\text{C}$. Their method is not capable of as great precision in locating the point as the magnetic or thermal curves, but the agreement is good. Further reference to their work (under the heading "Specific heat") should be made. Oberhoffer and Grosse find that the curve of total

heat content v. temperature for δ iron is a continuation of that of α iron. (See fig. 68.)

MELTING POINT

In Europe the melting-point determination of iron which has been assumed to be the best is that of Ruer and his coworkers,⁶⁴ 1,528° C. In the United States the best accepted melting point is that determined by Burgess and Waltenberg,⁶⁵ of the United States Bureau of Standards. Their temperature scale rested on the assumption that palladium melts at 1,549° C.; therefore the melting point of electrolytic iron as determined by them was 1,533° ± 1° C. As the melting point of palladium is now corrected to 1,553° C ± 1° C. their melting point of iron should be corrected to 1,537° C. According to a letter from Burgess under date of August 1, 1927, recent work of the Bureau of Standards on a somewhat less pure sample of iron has shown a melting point of 1,535° C. However, for the present it seems well to accept the corrected careful determination of Burgess and Waltenberg; that is, 1,537° C.

The more important melting-point determinations of the past few years are listed in Table 22.

TABLE 22.—Melting point of iron

Authority	Material	Date	Melting point, °C.
Saklatwalla ¹	Electrolytic	1908	1,510
Gwyer ²	Flusseisen	1908	1,515
Sahmen ³	do.	1908	1,532
Ruer and Klesper ⁴	Electrolytic	1913	1,528
Ruer and Goerens ⁵	do.	1916	1,528
Terry ⁶	do.	1917	1,530
Hanson and Freeman ⁷	Armco iron	1923	1,530
Burgess and Waltenberg ⁸	do.	1913	1,533
Burgess and Waltenberg ⁹	Armco iron (corrected)	1927	1,537

¹ Saklatwalla, B., "Eisen und Phosphor, die Konstitution ihrer Verbindungen": Metallurgie, Jahrg. 5, 1908, p. 331.

² Gwyer, Alfred, G. C., "Über die Legierungen des Aluminiums mit Kupfer, Eisen, Nickel, Kobalt, Blei, und Cadmium": Ztschr. anorg. Chem., Jahrg. 57, 1908, pp. 113-153.

³ Sahmen, R., "Über die Legierungen des Kupfers mit Kobalt, Eisen, Mangan, und Magnesium": Ztschr. anorg. Chem.; Jahrg. 57, 1908, pp. 1-33.

⁴ See footnote 3, Table 21, p. 155; and footnote 64, this page.

⁵ See footnote 64, this page.

⁶ See footnote 47, p. 143.

⁷ See footnote 4, Table 21, p. 155.

⁸ See footnote 65, this page.

⁹ Letter from G. S. Burgess, Aug. 1, 1927.

BOILING POINT AND VAPOR PRESSURE

Only a few data are available on the boiling point and vapor pressures of iron. Volatilization of iron has been detected in vacuo at as

⁶⁴ Ruer, R., and Klesper, R., —————: Ferrum, vol. 10, 1913, p. 257.

Ruer, R., and Goerens, P., —————: Ferrum, vol. 13, 1916, pp. 1-6.

⁶⁵ Burgess, G. K., and Waltenberg, R. G., Melting Points of the Refractory Elements; I, Elements of Atomic Weight from 48 to 59: Jour. Washington Acad. Sci., vol. 88, 1913, pp. 371-378.

low as 755° C. by Knocke.⁶⁶ It is stated to have a vapor pressure of 760 millimeters at 2,450° C. (optical) by Greenwood.⁶⁷ His temperature scale is based on the melting point of palladium as 1,551° C. and iridium 2,006° C. This boiling point is believed to be considerably in error, as it does not agree with the data of Ruff and Bormann,⁶⁸ which are described below.

Ruff and Bormann have determined that iron has a vapor pressure of 36 millimeters at 2,450° C. (optical). Using this datum, Millar⁶⁹ has calculated, by the help of the Sackur and Tetrode equations, the vapor pressures of iron at other temperatures, which are given in Table 23, from which we see that his calculated boiling point for iron is 3,235° C.

TABLE 23.—*Vapor pressures of iron (Millar)*

Tem- perature, ° C.	Vapor pressure, milli- meters Hg	Tem- perature, ° C.	Vapor pressure, milli- meters Hg
1,655	0.1	2,670	100
1,900	1	2,930	300
2,225	10	3,097	500
2,450	36	3,235	760
2,520	50		

¹ Boiling point.

Jones, Langmuir, and Mackay,⁷⁰ using the rate of evaporation of iron from a glowing filament in vacuo, at various temperatures, have been able to calculate by a formula of their own the vapor pressures of iron, which are given in Table 24. When these are extrapolated to 1 atmosphere the boiling point of iron is at 3,475° K.=2,202° C. This is in very good agreement with the datum of Millar given above.

The two data of Millar and of Jones, Langmuir, and Mackay may therefore be averaged, giving a final value of 3,218° C. for the boiling point of iron.

⁶⁶ Knocke, A., Über Verdampfung von schwerflüchtigen Metallen, insbesondere von Platin und Eisen, in evakuierten Glasgefäßen: Ber. Deut. chem. Gesell., Jahrg. 42, 1909, p. 206.

⁶⁷ Greenwood, H. C., An Approximate Determination of the Boiling Points of Metals: Chem. News, vol. 100, 1909, pp. 39-42, 49-50.

⁶⁸ Ruff, Otto, and Bormann, Walter, Arbeiten im Gebiete hoher Temperaturen; VII, Eisen und Kohlenstoff: Ztschr. anorg. Chem., Jahrg. 88, 1914, pp. 397-409.

⁶⁹ Millar, R. W., Vapor Pressures of Some Liquid and Solid Metals: Ind. and Eng. Chem., vol. 17, 1925, p. 34.

⁷⁰ Jones, H. A., Langmuir, I., and Mackay, G. M. J., The Rates of Evaporation and the Vapor Pressures of Tungsten, Molybdenum, Platinum, Nickel, Iron, Copper, and Silver: Phys. Rev., vol. 30, 1927, pp. 201-214.

TABLE 24.—Vapor pressures of iron (Jones, Langmuir, and Mackay)

Temperature, ° C.	Vapor pressure, milli- meters Hg	Temperature, ° C.	Vapor pressure, milli- meters Hg
1, 427	0.0076	2, 527	83
1, 527	.023	2, 727	165
1, 727	.22	2, 927	345
1, 927	1.2	3, 127	631
2, 127	7.5	3, 202	760
2, 327	26		

OTHER SUPPOSED POINTS

The literature is full of references in which other points of discontinuity or sudden change of physical properties are recorded. In many cases their discoverers seriously propose them as possible critical points in iron. As X-ray spectrographs have been taken at only a few temperatures, it is impossible to rule out most of these supposed critical points, yet we know that the α iron lattice is found at room temperature, at 800° C., and at 1,425° C., while the γ iron lattice is found from 920° to 1,400° C., and no other arrangement of iron atoms has been observed. Probably some of the supposed points are due to undetermined impurities, but in many cases very pure iron has been used for experiments which, nevertheless, show apparent discontinuities in certain physical properties of iron.

370° C. POINT

At 370° C., using electrolytic iron, Sirovich⁷¹ found a distinct break in a dilatometric curve, using either molten tin or paraffin as confining liquid. The same results were obtained with a sample of armco iron, the volume suddenly increasing at 370° C., but with a low-carbon iron containing 0.49 per cent of manganese the break was scarcely detectable. Sirovich suggests that previous workers have failed to find this point because of the presence of manganese or similarly acting impurities in their samples. He did considerable work on a series of steel samples and decided that there are two kinds of α iron, which he designated α_1 and α_2 . The first is stable below 370°, is hard and magnetically resistant, and will dissolve carbon, while the second is stable above 370° C., is relatively soft and magnetic, and does not dissolve carbon in the solid state. All of this work was done with heating curves only.

⁷¹ Sirovich, G., La trasformazione polimorfica del ferro a 370° e la possibilita di soluzione della cementite nel ferro α : Gazz. chim. Ital., vol. 53, 1923, pp. 674-688.

The Bureau of Standards⁷² undertook to check the existence of Sirovich's 370° point by heating curves and X-ray patterns. A slight irregularity in the heating curve (heat evolution) could be detected, best shown in iron of appreciable oxide content which had been reduced by hydrogen at high temperatures. On such a reduced specimen the X rays showed a finer grain than in ordinary iron, and it was thought the apparent "point" is due to recrystallization of the near-amorphous metal at 370° C.

The work of Thompson and Goffey, discussed below, also shows an apparent minimum in torsional elastic limit at about 370° C. and a peak in electrical conductivity curves at about 350° C. However, they had peaks or minima in their curves at so many temperatures that this can hardly be regarded as very positive confirmation.

830° C. POINT

The 830° C. point found by Benedicks in a dilatometric curve, above mentioned, and thought by him to support the Weiss and Foex 830° C. magnetic point, also mentioned above, has been given little credence. Benedicks's dilatometric curve showed such a slight deflection that it might mean nothing, and the Weiss and Foex work has since been proved defective. However, in the specific heat work on iron to be discussed below, Umino located the A_2 point at 820° and at 825° C. in two different series of specific heat curves, whereas most observers have found it at slightly below 800° C. It is possible that with sufficiently sensitive apparatus or proper treatment the A_2 point can actually be observed at this temperature. Perrier and Wolfers, in work to be discussed below, found among other numerous strange points one at 800° to 830° by a method of comparison of specific heat of iron with that of a standard substance. They suggest that this is the $\beta_1 \beta_2$ point of Weiss and Foex, but again it is necessary to point out that it is probably only the A_2 point observed at a somewhat higher temperature than usual. Finally, Broniewski⁷³, in plotting the electrical resistance of electrolytic iron as a function of temperature (see fig. 52), found a change in direction at a little below 850° C. It will be noticed in his curve that there was also a slight change in direction at 750° C. and a near-discontinuity at 950° C., neither of which is in quite the right place to be called, respectively, A_2 and A_3 .

The thermoelectric power of iron against other metals is likely to be an unreliable index of transformation points because of the possi-

⁷² Iron Age, Low-Temperature Transformation of Iron: Vol. 117, 1926, p. 1720.

⁷³ Broniewski, W., Sur les points critiques du fer: Compt. rend., t. 156, 1913, pp. 699-702.

bilities of alloying or other contamination. However, Borelius⁷⁴ has compared the potential of an unheated specimen of pure iron with that of one which has just previously been heated to definite temperatures and then cooled to the temperature of the unheated reference specimen. The potential curve as a function of the temperature of heating is very irregular, but he deduced a generalization that the absolute temperature of the n^{th} "transition" can be ap-

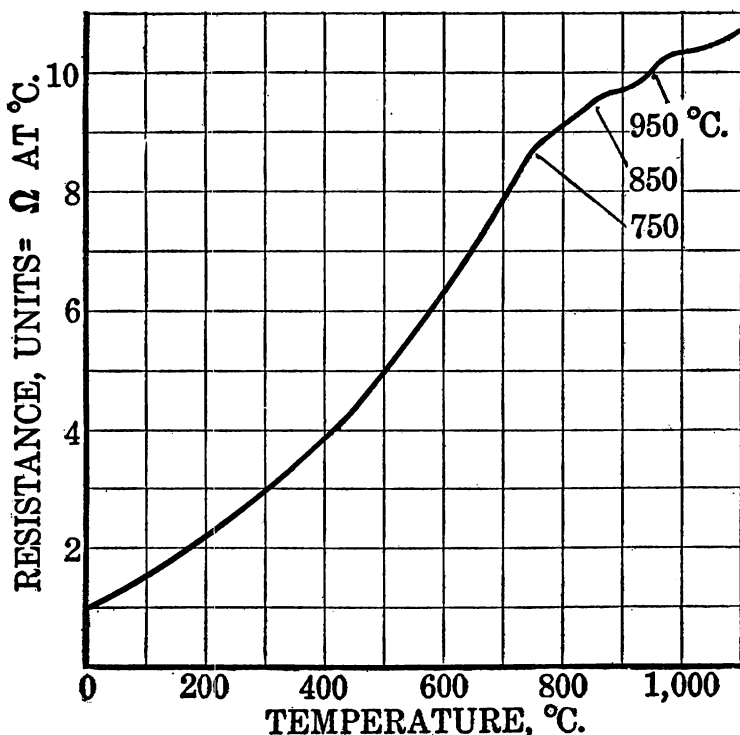


FIG. 52.—Electrical resistance of electrolytic iron (Broniewski); units of resistance=resistance at 0° C.

proximated by the formula $T_n = 97n$, and that the β - γ transformation comes when $n=12$. Borelius attempted to connect these phenomena by use of the quantum theory, and each new transformation was connected with another quantum either absorbed or radiated.

⁷⁴ Borelius, G., and Gunneson, F., Über eine neue Art von Umwandlungen in Eisen, IV: Ann. Physik, Jahrg. 67, 1922, pp. 227-235.

Borelius, G., Über eine neue Art von Umwandlungen in Eisen, V: Ann. Physik, Jahrg. 67, 1922, pp. 236-252.

Heraeus, W., Die Abhängigkeit der thermoelektrischen Kraft des Eisens von seiner Struktur: Ann. Physik, Jahrg. 73, 1924, p. 554.

Borelius, G., Bemerkungen zu einer Arbeit von W. Heraeus über die Abhängigkeit der thermoelektrischen Kraft des Eisens von seiner Struktur: Ann. Physik, Jahrg. 74, 1924, p. 757.

However, Heraeus repeated the work and showed that the method was extremely liable to error and therefore quite uncertain, and the many supposed transitions improbable.

THOMPSON AND GOFFEY POINTS

Using the torsional elastic limit of rods as a property to be measured at different temperatures, Thompson and Goffey⁷⁵ found, contrary to previous investigators, that it was a very sensitive indicator of transformations in the solid. Electrolytic iron gave the curve reproduced in Figure 53, every one of whose peaks or valleys corresponded to kinks in the electrical resistivity-temperature curves which were prepared simultaneously from the same specimens.

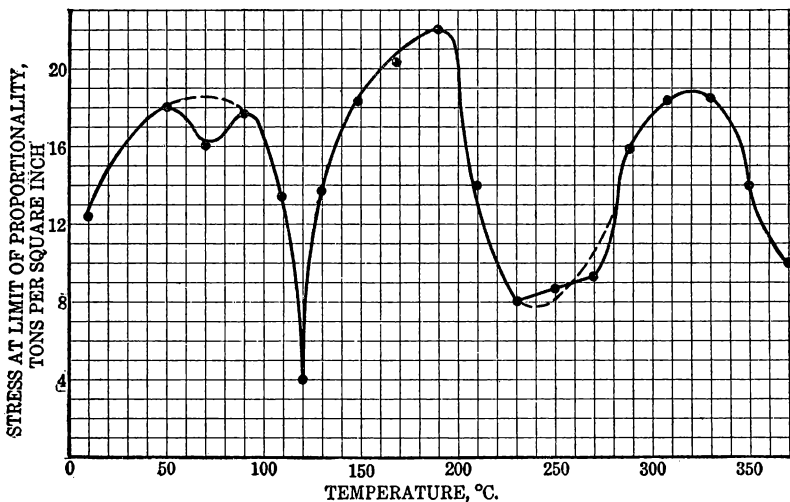


Fig. 53.—Torsional elastic limit v. temperature (Thompson and Goffey)

While the point at 70° may not be placed accurately and the points at 50° and 90° C., respectively, may therefore not be real, there are apparently important changes at about 70°, 120°, 200°, 240°, and 320° C., with indications that another valley was being approached at 370° C. The dotted curves in Figure 53 were not plotted by Thompson and Goffey but are what are thought justified by their data in the eyes of the present reviewer. Each point on the diagram is the average of four determinations. Just what these points are is a matter of conjecture, as the few data so far obtained by X-ray methods indicate no major changes in atomic lattice, but it is reasonable to sup-

⁷⁵ Thompson, F. C., and Goffey, A., Changes in Iron and Steel Below 400° C.: Jour. Iron and Steel Inst., vol. 107, 1923, pp. 465-490.

pose that in a material on the borderland between two stable states abnormal elastic limits could be expected.

That the Thompson and Goffey points are not purely illusory is shown by the work of Ishimoto⁷⁶ on the internal friction of "pure iron." Tuning forks and torsion pendulums were investigated, and the number of vibrations necessary to produce a certain degree of damping were recorded at various temperatures, both on an ascending and on a descending heating curve. The Ishimoto curves are reproduced in Figure 54. An important minimum at 65° C., corre-

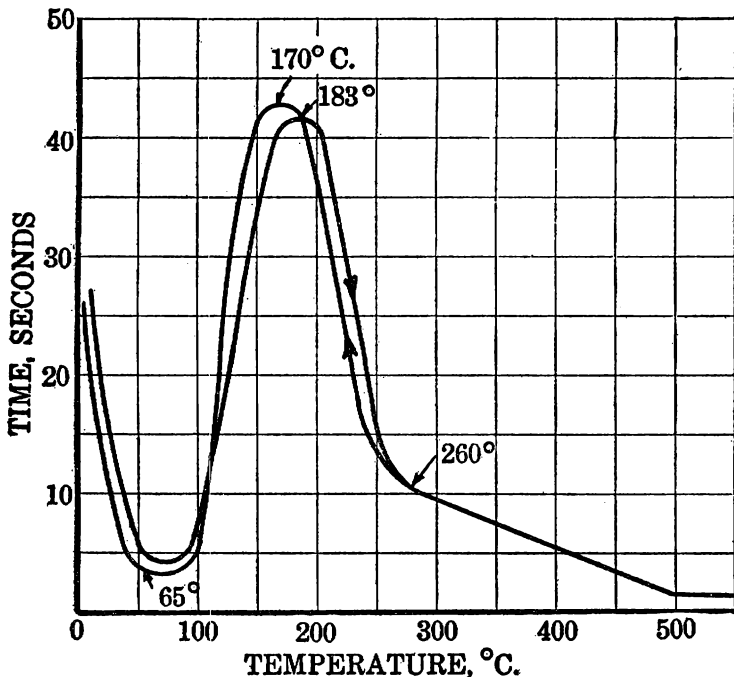


FIG. 54.—Pure iron: Inner friction v. temperature (Ishimoto)

sponding to the 70° C. point of Thompson and Goffey, is noted on both ascending and descending curves. Maxima at 183° C., on ascending and at 170° C. on descending curves are also to be noted, possibly corresponding to the 200° C. point of Thompson and Goffey; finally, at 260° C., anomalous changes cease up to 500° C. The Thompson and Goffey points could be interpreted as also showing a minimum at 260° C. instead of 240° C. if the position of the 250° C. point in their diagram were to be ignored. Ishimoto found the curves of Brinell hardness practically parallel to those of internal friction.

⁷⁶ Ishimoto, Mishio, Investigation of Metals with Regard to their Internal Friction: Proc. Math.-Phys. Soc. Japan, vol. 1, 1919, pp. 267-276.

OTHER INVESTIGATIONS

That the mechanical properties of iron, as functions of the temperature, are useful for investigating the inner condition of the solids, can not be denied, but up to date the properties have been investigated too cursorily to allow very important conclusions to be drawn.

The heat capacity of a substance should change fairly regularly with temperature, but at transitions irregular changes should be noted, the energy of transformation being superimposed on the energy involved in change of temperature. Perrier and Wolfers⁷⁷ have developed a method of comparing the temperature of one sample of a substance with that of another sample, both being heated or cooled but so arranged that one lags behind the other in the process. A sensitive differential thermocouple records approximately constant differences in temperature as long as the substance in question is not passing through transitions, but one sample reaches the transition temperature before the other, and immediately the reading of the differential thermocouple is altered. Perrier and Wolfers's heating and cooling curves for iron show plainly the A_2 and A_3 points, but many other irregularities as yet unexplained were also noticed.

In connection with these low-temperature points, recent work of Deardon and Benedicks⁷⁸ with a recording magnetometer has shown a slight kink due to increased magnetization at 250° C. when electrolytic iron is heated. Quenching electrolytic iron from 910° C. gives a sample which on heating in the magnetometer gives a slight increase in slope of the magnetization-temperature curve at 225° C. and another further increase in slope at 345° C., the cause of the quenching effects being unexplained. For comparison, a series of steels was investigated, but all their changes of direction in the magnetization curves were in the opposite direction (decrease in slope), and the above effects were therefore thought not due to carbon. The 250° C. point may have some connection with the 260° C. point of Ishimoto and the 240° C. point of Thompson and Goffey.

About all that can be concluded about these low-temperature points is that iron is capable of numerous thermal and physical anomalies which have as yet been only imperfectly investigated and which might prove a fertile field for research.

MAGNETISM OF IRON

The magnetic properties of iron and its alloys constitute a field of study which can hardly even be reviewed here. An attempt to

⁷⁷ Perrier, Albert, and Wolfers, F., Méthode sensible d'analyse thermique et les transformations du quartz, du fer, et du nickel: Arch. sci. phys. nat., t. 2, 1920, pp. 372-381.

⁷⁸ Deardon, W. H., and Benedicks, C., Magnetic Changes in Iron and Steel Below 400° C.: Jour. Iron and Steel Inst., vol. 113, 1926, pp. 393-416.

define the terms used in magnetic theory—magneton, permeability, susceptibility, saturation, retentivity, reluctance, remanance, and others—would take up too much space. Extremely small amounts of impurities have been found to influence magnetic properties profoundly, and therefore little is known about the properties of truly pure iron. From the standpoint of the iron metallurgist extensive literature under the names of Pierre Weiss, Kotaro Honda, and Niels Bohr must be read to gain a conception of this important field of science. The A_2 point, where transition from ferromagnetic iron to paramagnetic iron occurs when the temperature is raised, is by far the most important magnetic datum to the physical metallurgist; it has already been discussed.

The intensity of magnetization of iron when magnetically saturated (incapable of stronger magnetization) has been measured by Weiss⁷⁹ as 1,731 gauss (measured in 1908) and later corrected to 1,706 gauss at ordinary temperatures. Darrow,⁸⁰ who has written an exceedingly readable review of ferromagnetism, quotes 1,706 gauss at 20°C. and 1,742 gauss at 20°K. He also gives 19,000 as the value of the permeability of electrolytic iron, although the permeability is so greatly affected by small amounts of impurities that this is probably not a very reliable datum.

The saturation intensities at a series of temperatures have been measured by Dussler and Gerlach,⁸¹ who find that with rising temperature the saturation intensity falls off. In a single crystal in the tetragonal direction at 20° C. saturation was reached at about 150 gauss; at 629° C., 4.5 gauss; at 680° C., 3.5 gauss; and at 739° C., 2.5 gauss.

The magnetostriction of iron has been investigated by Benedicks.⁸² Magnetostriction is the change in dimensions of a substance on magnetization and in crystals has been shown to be a vectorial quantity varying with the crystallographic axes. However, in a large sample of iron containing crystals oriented in all directions the changes in length noticed are probably mean values. The magnetostriction of Benedicks's samples went through a maximum at 500° to 550° C. and at that point was fourteen times as great as at room temperature. Above 550° C. it fell off, and not much change was noticed at the Curie or A_2 point. In view of the fact that the magnetization is fading rapidly long before the A_2 point is reached, and the A_2 point is merely the apparent temperature where the last

⁷⁹ Weiss, P., *Mesure de l'intensité d'aimantation à saturation en valeur absolue*: Jour. phys., t. 9, 1910, pp. 373-393.

⁸⁰ Darrow, K. K., *Ferromagnetism*: Bell System Tech. Jour., vol. 6, 1927, pp. 295-366.

⁸¹ Dussler, E., and Gerlach, W., *Eiseneinkristalle*; III, Mitteilung; *Die Magnetisierung in verschiedenen Kristallrichtungen*: Ztschr. Physik, Jahrg. 44, 1927, pp. 279-285.

⁸² See footnote 53, p. 147.

measurable traces of ferromagnetism disappear, these observations are to be expected. However, experiments with a dilatometer show a marked contraction at the Curie point, which might or might not be associated with magnetostriction.

The magnetization phenomena have in general been some of the most useful ones for studying the major transformations in iron, and as shown in Figure 42 with rise of temperature magnetization of iron falls off slowly to a sudden drop at the A_2 point with further slow fall or rise of temperature and an extremely sharp drop at the A_3 point, after which it decreases only a small amount until the A_4 point is reached, where there is a discontinuous increase and then a slow fall to the melting point of iron. No data on molten iron have been collected.

ELECTRICAL RESISTANCE

Numerous measurements of the electrical resistance and its reciprocal, the conductivity, of iron have been made, but only the more reliable ones will be reviewed here. Some data have already been given in this paper. In Figure 44 a curve of Honda and Ogura for the relative resistances of a sample of iron wire measured by them is given. Insufficient points were taken, so that there was an apparent discontinuity in the curve at the A_2 temperature, and this same mistake has been committed by a number of other experimenters. Although the electrical properties of iron undoubtedly change at the A_2 point, as revealed by Figure 45, which is the result of the work of Burgess and Kellberg, the sharp change in direction shown in the Honda and Ogura curve is not true, but if the measurements are taken at sufficiently close temperatures, no "point" is indicated. The work of Burgess and Kellberg, when plotted as a function of resistance versus temperature in the same manner as the Honda and Ogura curve, gives the solid line in Figure 55. Burgess and Kellberg took observations at every 2° or 3° of temperature both on a slowly rising and a slowly falling temperature curve, finding that the two did not quite coincide, especially at the A_3 temperature. The enlarged scale plot of the curves near the A_3 point is given in Figure 49. The Broniewski curve given in Figure 52 probably suffers from the same difficulties as the Honda and Ogura curve, as the description of Broniewski's work does not show the apparent precision of the Burgess and Kellberg work. In Figure 55 the circles also are data from Meyer⁸³ to show the degree of agreement of his work with that of Burgess and Kellberg and also to illustrate the point that the marked difference in slope of his data might have justified the as-

⁸³ Meyer, A. R., —————: Verhand. Deut. phys. Gesell., Jahrg. 13, 1911, p. 680.

sumption that a change in direction of the electrical resistance curve took place near 768°C ., an intersection which is actually obtained by drawing a straight line to the left from his two highest temperature points and extending the curve up from his lower temperature points. The work of Burgess and Kellberg definitely showed that there is no sharp change in direction at this A_2 point, but the resistance of nonmagnetic α iron is apparently a continuous function of

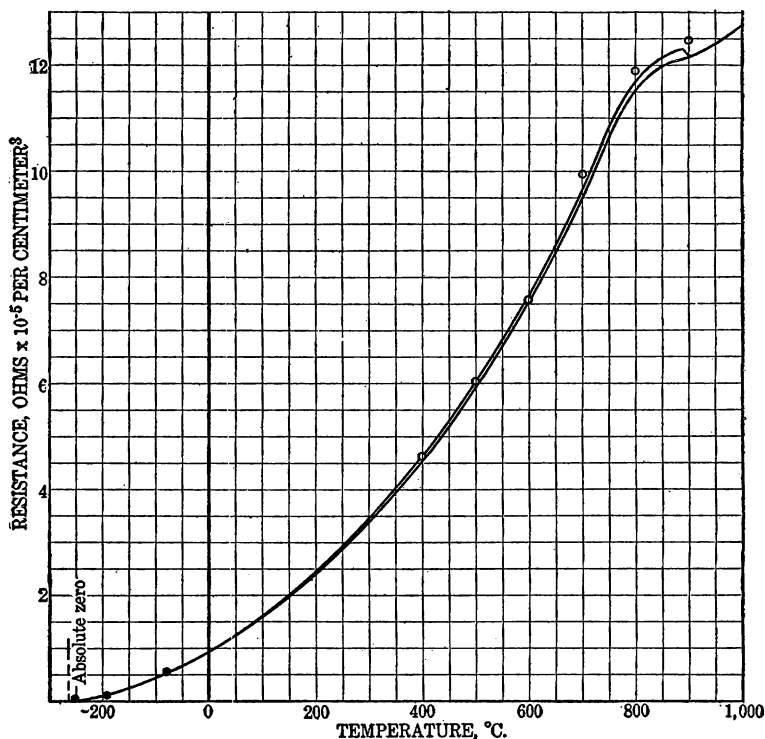


Fig. 55.—Electrical resistance of iron (Burgess and Kellberg): ●, points by Holborn; ○, points by A. R. Meyer

the resistance of the magnetic variety, and no sharp change can be proved. For purposes of comparison the data of several other investigators are placed in corresponding columns of Table 25. These include the work of Holborn⁸⁴ and Nicolai.⁸⁵ The work of Holborn at lower temperatures is indicated by dots in Figure 55 and indicates that iron approaches zero resistance at -253°C . or 20°K .

⁸⁴ Holborn, L., Über die Abhängigkeit des Widerstandes reiner Metalle von der Temperatur: *Ann. Phys.*, Jahrg. 59, 1919, p. 145; *Ztschr. Physik*, Jahrg. 8, 1921, p. 58.

⁸⁵ Nicolai, Guido, Über den elektrischen Widerstand der Metalle zwischen sehr hohen und sehr tiefen Temperaturen: *Phys. Ztschr.*, Jahrg. 9, 1908, p. 367.

TABLE 25.—*Electrical resistivity of iron; ohms* $\times 10^{-5}$ *per cubic centimeter*

Temperature, ° C.	Burgess and Kellberg	Holborn		Nicolai	Meyer	
		No. 1	No. 2		No. 1	No. 2
—253			0.0113			
—192		0.1003	.0878	0.237		
—78		.5800	.5794	.691		
0	0.9713	1.0000	1.0000	1.000	1.000	1.000
+100	1.5880	1.6572	1.6476	1.557	1.657	1.608
200		2.4726		2.24	2.435	2.472
300	3.40	3.4897	3.4738	3.069	3.418	3.569
400	4.61	4.6536		4.058	4.622	4.998
500	6.05	6.041			6.065	6.518
600	7.61				7.600	8.315
700	9.51				9.94	10.80
750	10.67					
800	11.60				11.88	12.40
900	12.16				12.61	12.67
950	12.24					
1,000	12.41					12.80

One thing that is noticed from the tabulated data is that at temperatures between the ice point and room temperature the resistance is almost exactly 10 microhms per cubic centimeter, Burgess and Kellberg measuring 9.713 microhms at 0° C. All the other work tabulated refers the resistance of iron at other temperatures to that at 0° C. as the unit.

One datum frequently found in the literature relating to the effect of temperature on resistance of iron is the “temperature coefficient of resistance,” by which is understood the proportionate increase in resistance, say, between 0° and 100° C., $\alpha = (R_{100} - R_0) / 100R_0$. From Figure 54 one can see that the temperature coefficient of resistance varies with the temperature. A series of its values from different observers, using the above formula for calculation, is as follows:

TABLE 26.—*Temperature coefficient of resistance*

Observer	Coefficient $\times 16^3$	Observer	Coefficient $\times 16^3$
Burgess and Kellberg ¹	635	Bridgman ⁴	621
Dewar and Flemming ²	625	Holborn ⁵	657
Nicolai ³	557	Meyer ⁶	657

¹ See footnote 52, p. 145.

² Dewar, James, and Flemming, J. A., The Electrical Resistance of Metals and Alloys at Temperatures Approaching the Absolute Zero: Phil. Mag., vol. 36, 1893, p. 271.

³ See footnote 85, p. 167.

⁴ Bridgman, P. W., The Electrical Resistance of Metals Under Pressure: Proc. Am. Acad. Sci., vol. 52, 1917, p. 571; vol. 56, 1921, p. 61.

⁵ See footnote 84, p. 167.

⁶ See footnote 83, p. 166.

Although the precision of electrical measurements is such that many significant figures can be measured it will be noticed in Table 25 that the work of Burgess and Kellberg, while regarded

as the most precise, is not reported beyond the second decimal place by the present writer. The disagreement of the various observers and different samples of "pure" iron is such that greater precision in stating the results is in general not justified. Small amounts of impurities have such profound effects on electrical resistance that endless care is necessary to prepare a pure sample of iron and to prove that it was pure. The proof of the purity of the samples used is largely lacking in all cases.

Not only has the effect of temperature on the resistance of iron been measured, but also the effect of pressure. Bridgman⁸⁶ has published 24.1×10^{-7} as the value of the change $(1/R)(dR/dP)$ due to pressure change. This is related to the change in conductivity and compressibility through the equation $(1/R)(dR/dP) = ((1/C)(dC/dP) + (1/3V)(dV/dP))$, in which C is the conductivity, V the volume, and R the resistance; and the expression (dV/dP) is the compressibility. Beckmann⁸⁷ has published 27.4×10^{-4} at 0° C. as the value of the relative change in conductivity, $(1/C)(dC/dP)$, due to pressure. The compressibility, as mentioned later on, is 0.60×10^{-6} . The values do not check well in the above equation.

THERMOELECTRIC PHENOMENA OF IRON

Although the literature on this subject is fairly voluminous, it is equally unsatisfactory for the reason that slight contaminations of the iron-metal junctions have such profound effects. The most acceptable data are those of Burgess and Scott, which have already been discussed and plotted in Figure 47. They used the thermoelectric power against platinum for the purpose of locating the critical points in iron. Further elaboration of the method was made by Berliner,⁸⁸ who did not report his data in a form that can be used for estimates of the thermoelectric forces, but they were nevertheless used for detection of the critical changes in iron. The electromotive forces observed when iron contacts platinum at various temperatures are given by Broniewski,⁸⁹ whose curve is given in Figure 56 in comparison with the data on copper-iron couples. Although the curve shows several changes in direction of curvature, the only apparent sharp change in direction was observed at $1,020^\circ$ C., about 100° higher than would be expected for the A_3 point. As Broniewski does not describe his apparatus with any minuteness, it is possible that his temperature scale was in error or that his methods were

⁸⁶ See footnote 4. Table 26, p. 168.

⁸⁷ Beckmann, B., Über den Einfluss von Druck auf die elektrische Leitfähigkeit der reinen Metalle nach einer Theorie von E. Grüneisen: Phys. Ztschr., Jahrg. 16, 1915, p. 59; vol. 18, 1917, p. 507.

⁸⁸ See footnote 35, p. 140.

⁸⁹ See footnote 48, p. 144.

faulty. The curve therefore serves to show in general the shape of the platinum-iron thermoelectric curve. Another curve comparing platinum and iron with a platinum-platinum rhodium thermocouple and plotting ratios of the E. M. F.'s measured is given in Figure 57, which is plotted by W. Schneider.⁹⁰ In place of the usual temperature scale Schneider merely plotted the electromotive force of the usual platinum-platinum 10 per cent rhodium thermocouple and noted the corresponding temperatures on his graph. The Curie point

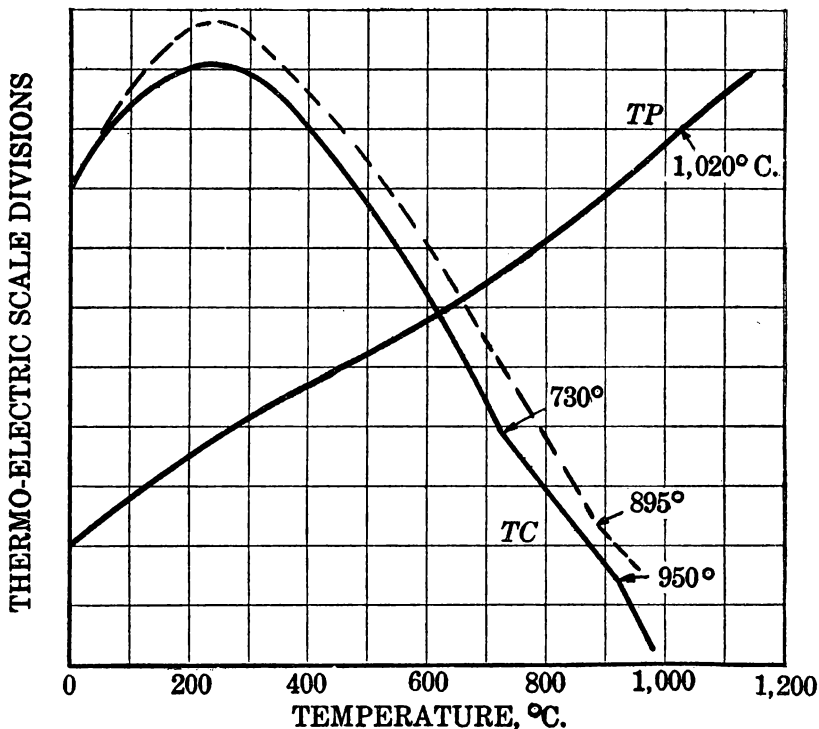


FIG. 56.—Thermoelectric power of electrolytic iron (Broniewski and Harrison): *TP*, iron-platinum, 1 division, 2 mv.; *TC*, iron-copper, 1 division, 0.5 mv.; dotted curve, iron-copper (Harrison)

appears at 769° C., the A_3 point at 909° C., the A_2 point at 898° C., and the A_1 point at 1,403° C.

The thermoelectric force of the iron-copper couple is also given by Broniewski in Figure 56. It has the usual parabolic shape up to the temperature where the magnetic changes become prominent and a change in direction is noted at 730° C. instead of the 769° observed by Schneider, lending further doubt as to the precision of

⁹⁰ Schneider, W., From Dissertation; quoted by P. Oberhoffer in *Das technische Eisen*: 2d ed., Berlin, 1925, p. 14.

Broniewski's temperature measurements. A second change in direction is noticed at 950° C. Here again temperatures seem to be unsatisfactory. For comparison, earlier careful work by Harrison⁹¹ on impure samples is shown in the dotted line of Figure 56, in which a discontinuity was noticed at 859°, which is much nearer the A_3

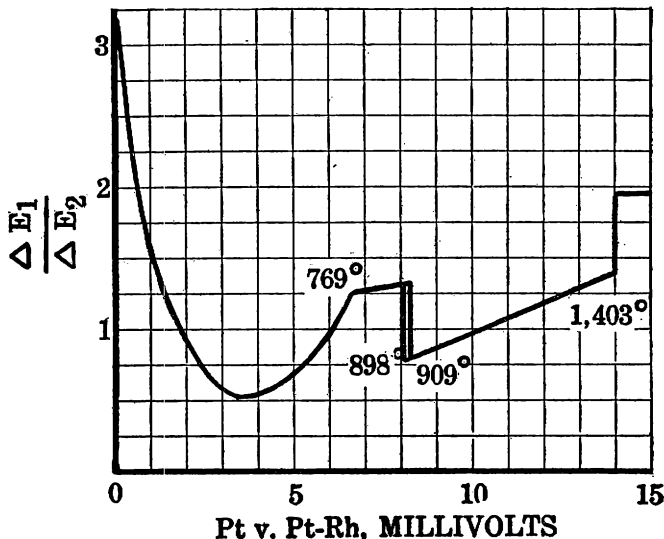


FIG. 57.—Thermoelectric power of platinum v. iron (Schneider)

point as now known, but was left unexplained by Harrison at that date (1902).

For iron-nickel thermocouples Harrison published the following determinations:

°C.	Milli-volts	°C.	Milli-volts
-191.2	-5.111	200	6.160
0	0	500	11.807
+100	+3.130	700	15.010

THERMAL CONDUCTIVITY

Numerous data on the technical varieties of iron and its alloys but very few on the pure material are available. The best are those of Honda and Simidzu⁹² on Swedish iron of low carbon content.

⁹¹ Harrison, E. P., On the Variation with Temperature of the Thermoelectromotive Force and the Electrical Resistance of Nickel, Iron, and Copper Between the Temperatures of -200° and +1,050°: *Phil. Mag.*, vol. 3, 1902, pp. 177-195.

⁹² Honda, K., and Simidzu, T., On the Thermal and Electrical Conductivities of Carbon Steels at High Temperatures: *Tohoku Univ. Sci. Repts.*, vol. 6, 1917, p. 219.

They are tabulated below, being expressed in calories per square centimeter per second per degree centigrade:

TABLE 27.—Data on thermal conductivity

Temperature, °C.	Thermal conductivity	Temperature, °C.	Thermal conductivity
0	(0.134)	500	0.097
100	.131	600	.087
200	.124	700	.080
300	.116	800	.077
400	.106	900	(.078)

SPECIFIC VOLUME AND DENSITY

These two reciprocal properties have been measured by numerous investigators, but the purity of the materials used has only been satisfactory in a few cases. The determinations of density, in grams per cubic centimeter, have been tabulated in Table 28 for the more important references, together with the specific volumes in cubic centimeters per gram. These are for pure iron, usually electrolytic iron. Those of Cross and Hill are based on vacuum-fused electrolytic iron, presumably as free of dissolved gases as is possible, therefore their determinations are probably the better. Nevertheless, the work of Kaya on single crystals of iron may be given some consideration, as single crystals give no possibility of interspaces between microcrystals. The densities of iron at other temperatures and pressures than normal are discussed under compressibility and thermal dilatation below.

TABLE 28.—Determinations of density and specific volume

Product	Observers	Density	Sp. Vol.
Electrolytic iron, vacuum fused.....	Cross and Hill ¹	7.8685	0.12709
Do.....	do. ¹	7.867	.12711
Pure iron, 775° annealed.....	do. ¹	7.8547	.12731
Pure iron, annealed.....	Andrew and Honeyman ²	7.864	.12716
Pure iron.....	Kaye and Laby ³	7.86	.12723
Do.....	Benedicks ⁴	7.85	.12739
Pure iron, annealed.....	Levin and Dornhecker ⁵	7.871	.12705
Single crystal.....	Kaya ⁶	7.8701	.12706

¹ Cross, H. C., and Hill, E. E., Density of Hot-Rolled and Heat-Treated Carbon Steels: U. S. Bureau of Standards, Sci. Papers, vol. 22, No. 562, 1925, pp. 451-466.

² Andrew, J., and Honeyman, A. J. K., Specific Volume of Steels: Carnegie Schol. Mem., Jour. Iron and Steel Inst., vol. 13, 1924, p. 253.

³ Kaye, G. W. C., and Laby, T. H., Physical and Chemical Constants: New York, 4th ed. 1921, p. 22.

⁴ Benedicks, C., Recherches physiques et physico-chimiques sur l'acier au carbone: Jour. Iron and Steel Inst., vol. 77, 1908, II, p. 222.

⁵ Levin, M., and Dornhecker, K., Über das spezifische Volumen und über die Härte von Eisen-Kohlenstofflegierungen: Ferrum, Jahrg. 11, 1913-14, p. 321.

⁶ Kaya, Seiji, On the Density of Single Crystals of Iron: Kinzoku no Kenkyu, vol. 4, 1928, pp. 81-82.

COMPRESSIBILITY

The effect of pressure on volume of iron has been measured in the laboratories at Harvard several times. The first publication by

Richards, Brink, and Bonnet⁹³ gave 0.40 times 10^{-6} as the compressibility, but more recent work by workers in the same laboratory, reviewed by Mehl and Mair,⁹⁵ corrects this figure to 0.60 times 10^{-6} , which applies to α iron. Mehl and Mair have also measured the compressibility of invar, an alloy of iron, with 36.27 per cent of nickel, and calculated the compressibility of the iron in the alloy, as iron in invar exists in the γ form. The calculation leads to 0.85 times 10^{-6} , if the assumptions of the calculation are valid ones, indicating that γ iron is much more compressible than α iron.

Iron and steel, when put under strain, usually lose density. Lowry and Parker⁹⁵ have found that the density of iron filings is 0.49 per cent less than that of the iron from which they were made. Kahlbaum and Sturm⁹⁶ made a careful comparison of hard-drawn with soft steel wires and found a maximum reduction of 0.25 per cent in the density of the hard drawn. Landon⁹⁷ twisted a bar of wrought iron containing 0.58 per cent of carbon through various angles per unit length of the iron and measured the density of the mid portions of the bars. The results are tabulated below and are somewhat greater than those observed for a sample of armco iron. The change in density was thought due to formation of amorphous material with a lower density than the crystalline.

TABLE 29.—*Change of density of iron under strain*

Angle of twist per unit length	Density at 0° C., grams per cubic centimeter	Decrease in density
°	7.7149	
70.5	7.6678	0.047
150	7.6136	.101
225	7.5802	.135
262	7.5757	.139

The work of Ishigaki⁹⁸ illustrates quite vividly how the density of a sample of iron or steel is a function of its previous history. Using armco iron, he subjected samples to tensile stress, to compres-

⁹³ Richards, T. W., Brink, F. N., and Bonnet, F., *The Compressibilities of the Elements and Their Periodic Relations*: Carnegie Inst. Washington, Pub. 76, May, 1907.

⁹⁴ Mehl, R. F., and Mair, B. J., *Chemical Affinity in Metallic Alloys, Especially Solid Solutions; A Study in Compressibility*: Jour. Am. Chem. Soc., vol. 50, 1928, pp. 55-73.

⁹⁵ Lowry, T. M., and Parker, R. G., *Properties of Cold-Worked Metals; Part 1, The Density of Metallic Filings*: Jour. Chem. Soc. London, 1915ii, p. 1010.

⁹⁶ Kahlbaum, G. W. A., and Sturm, E., *Über die Veränderlichkeit des spezifischen Gewichtes*: Ztschr. anorg. Chem., vol. 46, 1905, pp. 217-310.

⁹⁷ Landon, J. W., *Change of Density of Iron Due to Overstrain*: Jour. Iron and Steel Inst., vol. 107, 1923i, pp. 455-463.

⁹⁸ Ishigaki, T., *On the Change in the Hardness and the Density in Iron and Steel Caused by Cold Working*: Tohoku Univ. Sci. Repts., vol. 15, 1926, pp. 777-794.

sion, and to hammering. In all cases the density decreased more or less in proportion to the stress applied. All density determinations were referred to water at 4° C. When annealed at various temperatures and then cooled to room temperature for a density determination the samples had to be heated to about 700° C. before their density began to return to normal, and annealing at 1,000° C. allowed them to recover their density almost completely, probably owing to acceleration of the molecular motion until the material assumed the densest possible packing once more. Although it is not surprising to have tensile stress decrease the density of iron, it is decidedly anomalous to have hammering or compression cause decrease of

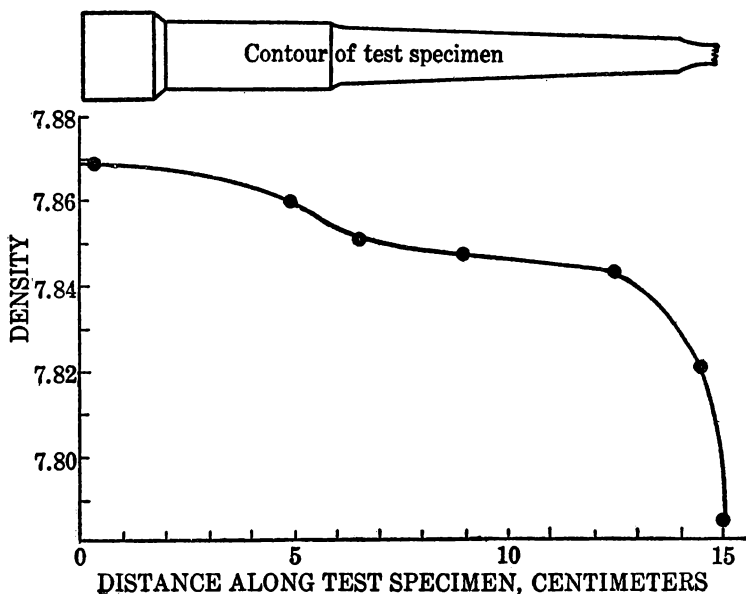


FIG. 58.—Density of armco iron after tensile test

density of the sample after release of the applied stress. The effect of tensile stress is illustrated in Figure 58, which gives the shape of the tensile-stress specimen from the lug to the point of breakage, and plotted below are the densities of the sections of this piece, which were sawed out and tested. The density at the point of rupture was the least. The density changes during annealing of a hammered specimen are shown in Figure 59. The density of the original specimen was about 7.862 and after hammering was 7.855. The recovery during annealing did not commence till nearly 700° C. was reached. In fact, at 500° an apparent further decrease in density took place and can not be explained. The same anomaly was shown in the compressed sample and with several of the tensile specimens.

THERMAL DILATATION

The changes in dimensions of iron resulting from change of temperature have been studied by several investigators. The results of Benedicks, as plotted in Figure 46, are described in connection with the A_2 point above. His results were merely the differential dilatation of iron compared to gold and were used for finding transition temperatures in iron. An absolute dilatation curve over a wide range of temperatures is given by Broniewski,⁹⁹ whose curve is given in Figure 60. It suffers from the same difficulties that other work by

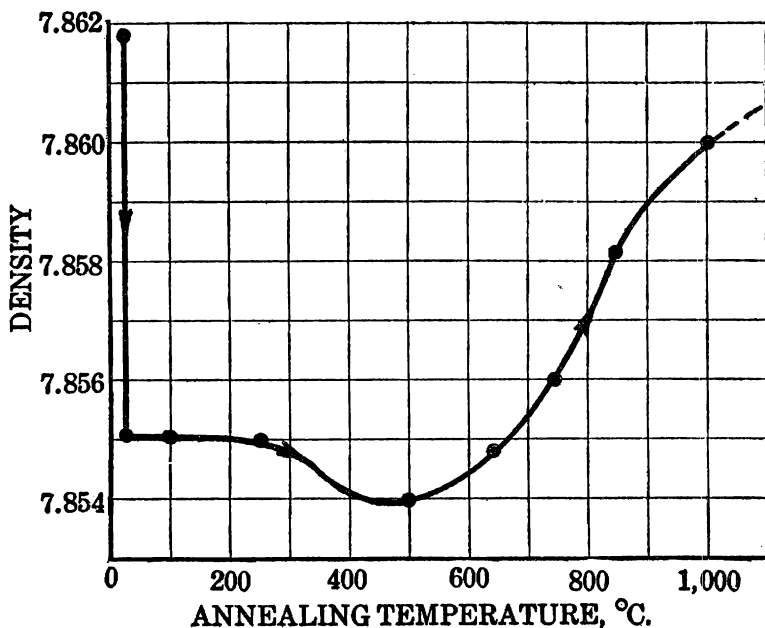


FIG. 59.—Change in density on annealing hammered armco iron (Ishigaki)

the same author does—the thermometry was either incorrect or the work was done so rapidly in heating that the A_3 point apparently occurs at above 950°C . More accurate work has been published by Sato¹ for the range 500° to $1,500^\circ\text{C}$., and his curve is given in Figure 61. His specimen of electrolytic iron was 700 millimeters long, and the deflections plotted in the above curve are one thousand two hundred times the actual change in length in millimeters. Therefore, the length of his specimen at any temperature is 700 millimeters $+1/1,200$ the deflection in the above curve. At the A_3 point the dilatation was negative, the “expansion” being -0.200 millimeter, so

⁹⁹ See footnote 48, p. 144.

¹ Sato, Seikichi, Dilatometric Investigation of the A_3 and A_4 Transformations in Pure Iron: Tohoku Univ. Sci. Repts., vol. 14, 1925, pp. 513-527.

that the linear fractional expansion on passing through the A_3 point is $\Delta L/L = -0.00282$, therefore the volume fractional expansion is three

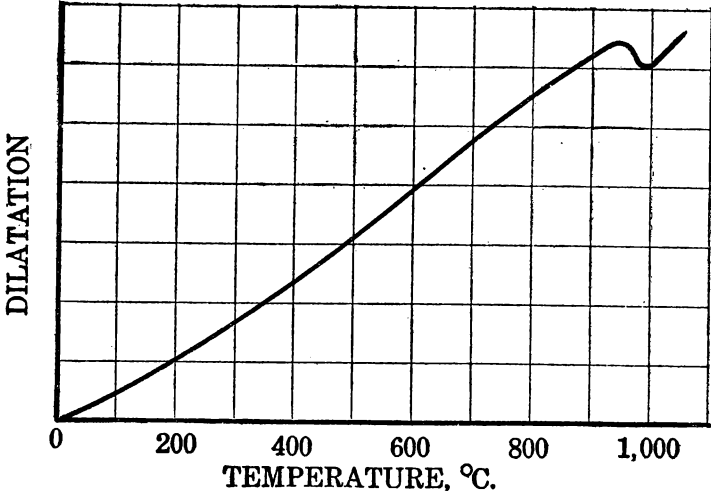


FIG. 60.—Dilatation of electrolytic iron (Broniewski); 1 division equals 0.002 elongation above 0° C.

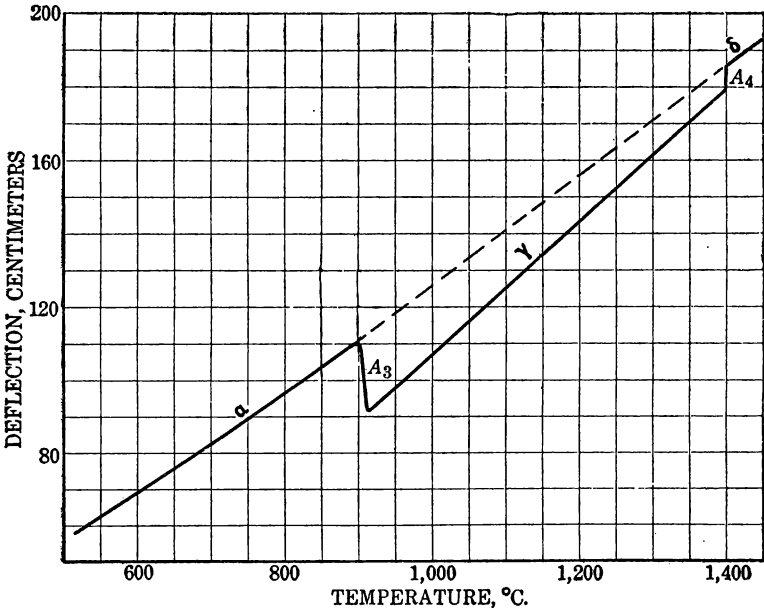


FIG. 61.—Dilatation of electrolytic iron (Sato)

times this, or $\Delta V/V = -0.00846$. In the same manner at the A_4 point the material underwent a positive expansion such that $\Delta L/L = 0.000851$ or $\Delta V/V = +0.002553$ or 0.2553 per cent increase in volume.

All of these figures refer to γ iron just before its transition to α iron. An interesting thing about the plot is that the deflections for the δ iron range of temperatures are a continuation of the deflections for the α iron range of temperatures. The work is also consistent in that the A_3 and A_4 transformations occur at temperatures consistent with other approved work on iron.

From the dilatation curve of Benedicks (fig. 46) the linear change at the A_3 point is 0.082 per cent; the volume change is 0.25 per cent, which we see is much smaller than the Sato figure of 0.846 per cent quoted above. Both the work of Benedicks and of Sato is so described as to give the impression of great precision, and yet these two data differ by a factor of over 3. More work needs to be done on volume changes in pure iron.

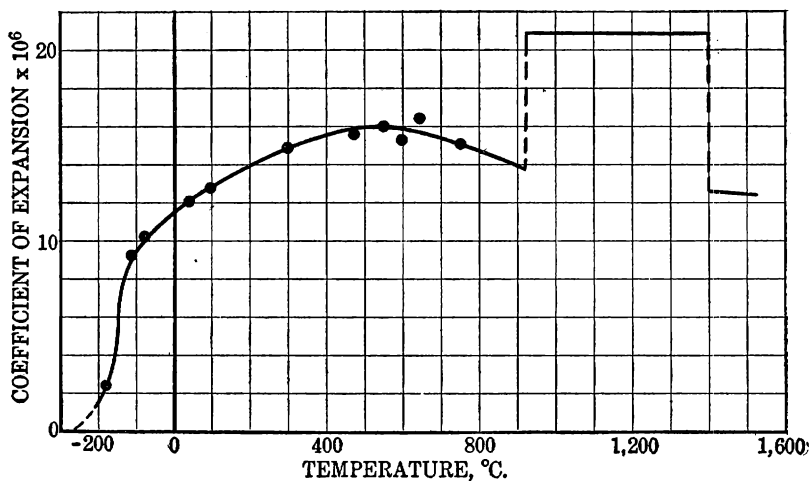


FIG. 62.—Coefficient of thermal expansion

EXPANSION COEFFICIENTS OF GAMMA AND DELTA IRON

These data make it possible to estimate the approximate thermal coefficient of expansion of γ and of δ iron and to correlate them with previous data on the coefficients for α iron over a wide range of temperatures. The data are contained in Table 30 and are plotted in Figure 62. At the absolute zero of temperature there should be no thermal coefficient of expansion, and the coefficient should rise with temperature. The decrease beyond about 500° C. may be correlated with the rapid fall in magnetizability at that temperature, as magnetostriction should fall off with decreased magnetizability. The discontinuity at the A_3 and A_4 points is to be expected. A constant coefficient for either γ or δ iron is probably only an approximation, and the coefficient may actually vary somewhat with temperature.

The datum for δ iron was calculated directly from the data plotted by Sato (0.0000125) and is in poor agreement with his own statement that the coefficient for δ iron is 0.000016. If the coefficient did not pass through a maximum at 500° and then fall off slightly, as shown in the figures of Le Chatelier and Honda, the figure calculated and stated by Sato would be an exact continuation of the α iron range. However, the calculation of 0.0000125, mentioned above, seems also to be reasonably near an extrapolation of the existing data. The subject needs further study.

TABLE 30.—*Thermal coefficients of expansion, system iron*

Temperatures, °C.	Coefficients of expansion		Authority	Reference
	Integral	Differential		
40.....		0.00001210	Fizeau.....	Compt. rend., t. 68, 1869, p. 1125.
50.....		.00041228do.....do.....
-103-25.....	0.00001092	.0000093	Zakrzewski.....	Fortschr. Phys., Jahrg. 48, 1892, p. 238.
-78-25.....	.00001110	.0000103do.....	Do.
+25-100.....	.00001252	.0000131do.....	Do.
-180-20.....	.00000930	.0000025	Le Chatelier.....	Compt. rend., t. 129, 1899, p. 331.
0-100.....	.000011	.0000130do.....	Do.
500-600.....	.000016	.0000150do.....	Do.
600-700.....	.0000165	.0000165do.....	Do.
700-800.....	.000015	.000015do.....	Do.
100.....		.000013	Honda.....	Tohoku Univ., Sci. Repts., vol. 6, 1917, p. 203.
300.....		.0000149do.....	Do.
500.....		.0000158do.....	Do.
600.....		.0000154do.....	Do.
906-1,400.....		.00002112	Sato.....	Tohoku Univ., Sci. Repts., vol. 14, 1925, p. 513.
1,400-1,535.....		.0000125do.....do.....

The accuracy of the expansion coefficients listed in Table 30 can be tested by using them to calculate the specific gravities of iron at higher temperatures and comparing them with the observations and calculations from other methods. Using the above data to calculate the increase in volume of a unit volume of iron for every 100° C. and interpolating to the transition points of iron, the calculated specific gravities given in Table 31 were derived. The Sato data on expansions at the A_3 and A_4 points were used in this calculation and also the Honda and Endo² estimate of the volume decrease during freezing of pure iron. Honda and Endo had observed experimentally the volume change on freezing of a series of iron-carbon alloys and had extrapolated to the probable volume change of pure iron, 3.6 per cent. The resulting estimate of the specific gravity of iron just above its melting point (1,535° C.) is 7.0995, which carries all the errors of determination of the expansion coefficients and of the volume changes at the above-mentioned transition points and the melting point. The figure may be compared with the datum of

² Honda, K., and Endo, H., On the Volume Change in Cast Iron During Solidification, with a Criticism of the Double Diagram of the System Iron-Carbon: Tohoku Univ. Sci. Repts., vol. 16, 1927, pp. 9-25.

Benedicks, Berlin, and Phragmen,³ $6.92+0.07$, and with the earlier data of Roberts and Wrightson,⁴ who report the specific gravity to be 6.95 just below the melting point and 6.88 just above it. However, the most recent determinations on molten iron—namely, 7.45 and 7.38, an average of 7.41 at $1,530^{\circ}$ (?)—are by Berlin,⁵ who also observed a density of molten iron at $1,670^{\circ}$ C. of 6.95 and 6.94, or an average figure of 6.945 grams per cubic centimeter. His figures on molten iron were obtained in the apparatus previously used by Benedicks, Wrightson, and himself. However, the unusually high specific gravities for molten iron make one wonder whether the improvements he introduced also brought in some new undetermined disturbing factor. The question of the exact density of molten iron and of the δ and γ forms therefore remains open.

TABLE 31.—*Specific gravity of iron as a function of temperature*

Form of iron	Temperature, ° C.	Specific gravity calculations		
		Expansion	X ray	Observed
α	20		7.8404	7.8685
α	906	7.5706	7.55	
γ	906	7.6327		
γ	1,400	7.4077		
δ	1,400	7.3900	7.32	
δ	1,535	7.3550	7.25	
Molten.....	1,535	7.0995		6.92-7.41
Do.....	1,670			6.94

A few more data are available on the density of γ iron. Osawa, in the work mentioned above, studied a series of iron-nickel alloys in which the iron was present as γ iron at room temperature and calculated the density of γ iron at 20° by extrapolation to the composition of pure iron to be 8.008. Accepting this datum and using Sato's thermal coefficient of expansion, we can calculate from this that the density of γ iron at 906° C. should be 7.58, as compared to 7.6327 in the above calculation.

EFFECT OF EXTREMELY LOW TEMPERATURES

One other interesting item about the density of pure iron in its relation to temperature changes is the observation by Osawa⁶ that a sample of armco iron with a density of 7.8787 grams per cubic centimeter, at 20° C., after being dipped into liquid air (about -185° C.)

³ Benedicks, C., Berlin, D. W., and Phragmen, G., Density of Liquid Iron: Carnegie Schol. Mem., Iron and Steel Inst., vol. 13, 1924, pp. 129-174.

⁴ Roberts, W. C., and Wrightson, T., De la densité de certains métaux de l'état liquidé: Ann. chim. phys., ser. 5, t. 30, 1883, p. 274.

⁵ Berlin, D. W., Some Determinations of the Specific Gravity of Iron and Low-Carbon Steel in a Molten Condition: Carnegie Schol. Mem., Iron and Steel Inst., vol. 15, 1926, pp. 1-15.

⁶ See footnote 23, p. 131.

and brought back to room temperature, showed a density of 7.8795, whereas his X-ray lattice measurement called for a calculated density of 7.8820 at 20° C. Evidently iron can be caused to become more compact by taking it to extremely low temperatures and thereby to eliminate at least some of the void space doubtless present in iron cooled from high temperatures to the room temperature.

For general calculation purposes the average volume changes of iron can now be summarized in the following Table 32:

TABLE 32.—Average volume changes in iron with temperature

Form of iron	Temperature range, ° C.	Change in volume per unit volume
α	0- 906	0.00014 per ° C.
α - γ change.....	906	- .00846 = $\Delta V/V$.
γ	906- 1,400	.000021 per ° C.
γ - δ change.....	1,400	+ .002553 = $\Delta V/V$.
δ	1,400- 1,535	.0000125 per ° C.
Melting expansion.....	1,535	+ .036 = $\Delta V/V$.
Molten.....	1,535-+1,670	.000483 per ° C.(?)

CHANGE OF TRANSFORMATION TEMPERATURE WITH PRESSURE

The A_3 and A_4 transformation temperatures can be either raised or lowered by proper manipulation. Most of the other elements added to the iron to alloy with it either raise or lower each of these transformation points, the elements which raise A_3 usually lowering A_4 , and those which lower A_3 raising A_4 . The individual elements and their effects will be discussed below.

Pressure is also another controllable variable which affects the transformation points and the melting point. In general, any physical transformation which takes place in a system and is accompanied by a volume change will be affected by changes in pressure. When the volume change is positive with rising temperature the effect of increased pressure is to make the change more difficult, and one must raise the system to a higher temperature before the transformation takes place. The reverse condition is exemplified by ice, which contracts on melting, and if the pressure on the system is increased the ice melts at a lower temperature than under normal pressures. Very little study has been given to effects of pressure on the melting point of iron or on the A_3 and A_4 transitions. One can say immediately, however, that increased pressure should lower the A_3 point and raise the A_4 and melting points of iron. Any volume change at the A_2 point is so small that pressure variations are likely to have very little effect on it.

The classical thermodynamic equation of Clausius-Clapeyron can be used for calculation of the change in a transition temperature with pressure. The equation reads $dT/dP = T(\Delta V)/(\Delta H)$, in which dT

is the change in absolute temperature of the transition point, dP is the differential of pressure (in atmospheres), ΔV the change in volume (in cubic centimeters) of 1 mol of the substance when passing through the transition point, and ΔH the change in heat content of 1 mol of the substance during the change, expressed in cubic centimeter-atmospheres. One calorie is equivalent to 41.2711 cubic centimeter-atmospheres. The equation can also be written $dT/dP = \Delta V/\Delta S$, in which ΔS is the change in entropy of 1 mol of the substance on passing through the transition point. One needs to know the change in volume and the heat of transition (or the entropy change) in order to calculate the desired change in the temperature of the transition point with pressure. These thermal data are given in a later section and, used in conjunction with the volume changes tabulated in the preceding section, give the figures desired. In Table 33 are assembled the data and resulting calculated alterations of the A_3 , A_4 , and melting points of pure iron when the pressure on the system is increased from 1 to 2 atmospheres.

TABLE 33.—Change in transition temperatures with pressure

Point	T , °K.	ΔH , calories	ΔV , cubic centimeter	dP , atmosphere	dT , °/atmosphere
A_3	1, 179	370	-0.0625	1	-0.00482
A_4	1, 673	140	+ .0192	1	+ .00557
Melting.....	1, 808	3, 640	+ .2735	1	.00330

Although the changes in heat and volume of these three critical points in iron are quite different, the amounts by which their temperatures are altered by pressure change are all in the same range of magnitude. The change in the melting point of ice is 0.0075° per atmosphere, which compares very well with the above magnitudes.

To raise the melting point of iron by 1° a pressure of $1/0.0033 = 300$ atmospheres must therefore be applied. Similarly, by melting iron in vacuo its melting point is lowered 0.0033° C.

Also, the A_3 point is lowered and the A_4 point raised by pressure, which amounts to saying that γ iron has a longer temperature range of stability under pressure. This fits in qualitatively with the fact that γ iron is more dense than α or δ iron at the same temperature.

The A_3 point is lowered 1° C. by the application of 208 atmospheres, according to the above data. For comparison, in 1916 Thompson⁷ calculated that this point would be lowered 1° C. by the application of a pressure of 1 ton per square inch (136 atmos-

⁷ Thompson, F. C., The Allotropy of Iron: Trans. Faraday Soc., vol. 11, 1916, pp. 134-140.

pheres). He used a value for the heat change which was too low and also used the volume change shown on the dilatation curve of Benedicks, given earlier in this paper, which is probably as good as that used in the above table. The relatively poor agreement illustrates how much precise work is needed on the changes in heat and volume at the transformation points.

EFFECT OF ALLOYING ELEMENTS ON TRANSITIONS

The whole heat treatment of steels is based on the fact that carbon and other elements alloyed with iron raise or lower the transition points and melting point and thereby make possible imposing a wide variety of properties on iron. The subject is a large one and is

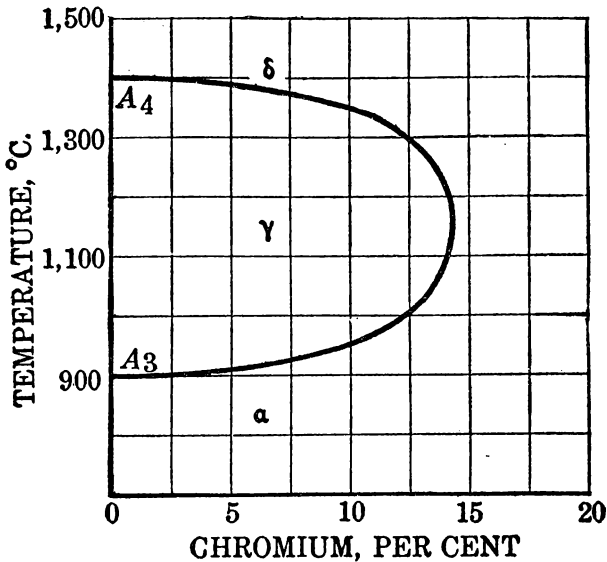


FIG. 63.—Effect of chromium on A_3 and A_4 transitions

adequately dealt with in any text on alloy steels. The iron-carbon alloys are dealt with to some extent in another section of this publication. Only a brief abstract can be given here of the effects of various elements on iron.

The melting point of iron is lowered by the addition of most elements, in accordance with the usual rules of physical chemistry regarding melting points. Where it is raised the iron almost invariably forms a long series of liquid and solid solutions with the alloying element.

The most interesting part about the iron alloys is the change in the A_3 and A_4 transformation temperatures by addition of the alloying elements. The effect of chromium on these two points is shown in Figure 63. The A_4 point is lowered and the A_3 point raised by

increasing additions of chromium, approaching each other, until at 14 per cent chromium they meet at about 1,075° C. With further additions of chromium there are no critical points in the alloy and one passes continuously from α iron on heating to δ iron, with which it is crystallographically and otherwise identical. In other words, transition from α or δ to γ iron is entirely suppressed. The temperature-composition field of stability of γ iron is therefore inclosed within the loop marked in the diagram, and only the body-centered cubic crystals can form outside it.

A similar effect is produced on the A_3 and A_4 transitions by silicon, aluminum, tin, vanadium, tungsten, molybdenum, and phosphorus. It requires 6 per cent of tungsten, 1.85 per cent of silicon, 2 per cent of tin, or 2.5 per cent of vanadium to reach the composition where γ iron is suppressed.

The reverse effect is exerted by carbon, copper, and nickel. Cobalt raises A_3 slightly and A_4 markedly, being the only element whose presence does not produce opposite effects on the two points. The A_4 point is raised from 1,400° to 1,470° C. by 6 per cent of copper, to 1502° C. by 3.2 per cent of nickel, to 1,486° C. by 0.38 per cent of carbon, to 1,477° C. by 8 per cent of copper, and to 1,492° C. by 22 per cent of cobalt. The A_3 point is lowered to 730° C. by 0.9 per cent of carbon, to room temperature by about 36 per cent of nickel, and to 833° C. by 3 per cent of copper. This means that the stability field of γ iron is enlarged instead of decreased by the addition of this group of elements. Although the effect of a light atomic weight element like carbon is great in comparison to the heavier ones, when calculated to the effect, atom for atom, there is not great difference between elements.

The A_2 point has not been very well studied from the standpoint of effects of alloys. It is lowered from 780° to 690° C. by 21 per cent of titanium, is lowered slightly by the presence of nitrogen, is lowered by chromium nickel and carbon, and is raised by cobalt, but in general few quantitative data are available.

MECHANICAL AND PHYSICAL PROPERTIES

The mechanical properties of pure iron were not known until recently. It was known to be quite ductile and soft, resembling copper. The tensile strength as a function of temperature has not been worked out on absolutely pure metal, but part of the temperature range is available on 0.1 per cent of carbon steel, from the work of Rosenhain and Humfrey.⁸ It is plotted in Figure 64 for samples that were previously heated above the A_3 point and then cooled to the tempera-

⁸ Rosenhain, Walter, and Humfrey, J. C. W., The Tenacity, Deformation, and Fracture of Soft Steel at High Temperatures: Jour. Iron and Steel Inst., vol. 87, 1913i, p. 219.

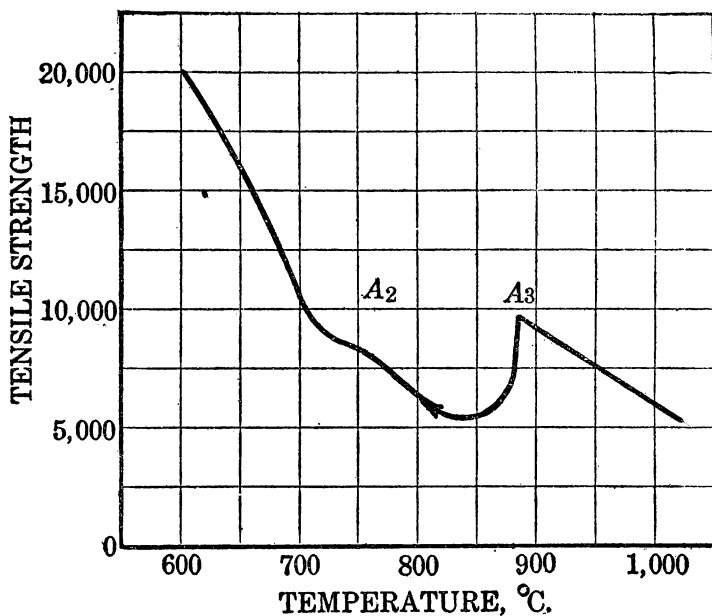


FIG. 64.—Tensile strength of iron as a function of temperature

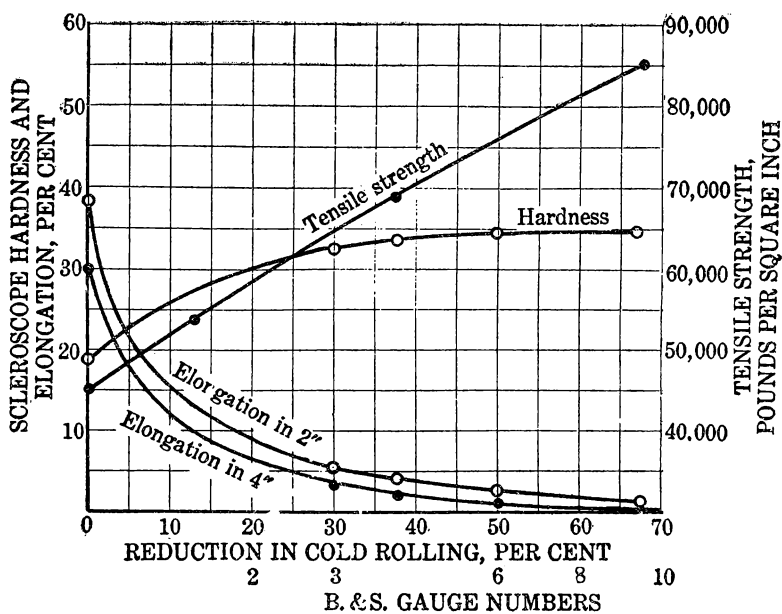


FIG. 65.—Physical properties of cold-rolled electrolytic iron

ture of the test. The A_3 and A_2 points are plainly visible in this series of tests, although, as expected, the material was markedly weakened when near the A_3 transition point, where transformation from one crystal form to another was in process and the material in a disorganized condition.

The physical properties of electrolytic iron, after heating to remove hydrogen and melting into test bars, followed by rolling down to various sizes, are given by Stoughton,⁹ and a copy of his diagram is given in Figure 65. As would be expected, the tensile strength and the hardness increase with cold-rolling, while the elongation decreases. The diagram is entered more as a matter of record of actual properties to be expected than to show anything unusual.

EMISSIVITY OF IRON

By measuring the apparent temperature in comparison with the true black body temperature of iron surfaces Bidwell¹⁰ has found that the relative emissivity of bright clean iron radiating freely into air varied from as low as 28 per cent at 700° C. through 30 per cent at 1,300° C. to 48 per cent at 1,700° C. His apparatus was rather complicated, and the metal was probably saturated with carbon, due to being heated by hot carbon electrodes. More recent work by Moller, Miething, and Schmick¹¹ at 700° to 1,100° C. has shown that the relative emissivity (degree of blackness) is 43.5 per cent for polished iron, whereas an oxidized surface showed an emissivity of 80 per cent that of a black body. Burgess and Foote,¹² working in the temperature range 700° to 1,100° C., found that an oxidized surface of iron had a relative emissivity of 85 to 80 per cent. Evidently, then, optical and total radiation pyrometric readings on bright iron surfaces require very large corrections. The corrections necessary for optical and for total radiation pyrometers, for both bright and oxidized surfaces of iron, as calculated from the results of all these authors, are compared in Figure 66. Although the two curves for optical pyrometers on oxidized surfaces parallel each other nicely and differ only about 10° in their correction, the large correction of Moller, Miething, and Schmick's carefully controlled optical work on bright iron does not agree very well with the less precise and doubtful data of Bidwell. On that account the data of the latter are represented only by points in circles on the diagram.

⁹ Stoughton, Bradley, *Electrolytic Iron a Commercial Product*: Chem. and Met. Eng., vol. 26, 1922, pp. 128-131.

¹⁰ Bidwell, C. C., *Comparison of Actual and Black Body Temperatures*: Phys. Rev., vol. 3, 1914, pp. 439-449.

¹¹ Moller, M., Miething, H., and Schmick, H., ———: *Ztschr. tech. Phys.*, Jahrg. 12, 1925, pp. 644-650.

¹² Burgess, G. K., and Foote, P. D., *Emissivity of Metals and Oxides*; IV. *Iron Oxide*: U. S. Bureau of Standards Sci. Papers, vol. 12, 1915-16, pp. 83-89.

The two total radiation curves on oxidized surfaces are at about the same magnitudes but have opposite slopes and promise to depart from each other radically at higher temperatures.

From the diagram it may be concluded that corrections for optical pyrometers sighted on oxidized surfaces have been worked out satisfactorily within 10° at about $1,000^\circ$ C., while on bright iron surfaces

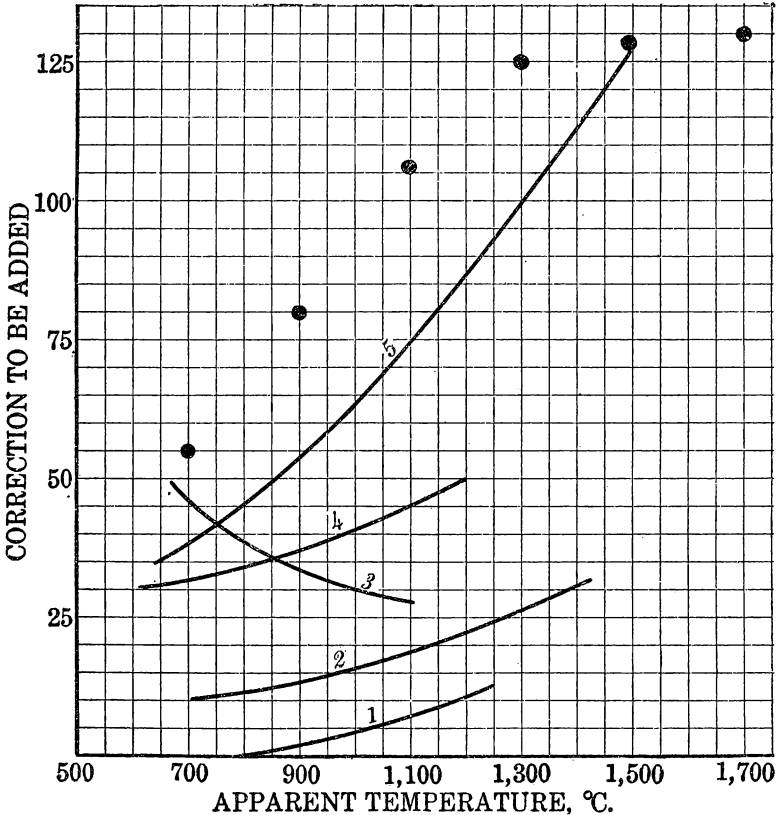


FIG. 66.—Pyrometric corrections for iron surfaces: 1, Burgess and Foote optical pyrometer, oxidized iron; 2, Moller, Miething, and Schmick, optical pyrometer, oxidized iron surface; 3, Moller and others, total radiation pyrometer, oxidized iron; 4, Burgess and Foote, total radiation, oxidized; 5, Moller and others, optical pyrometer, polished iron; circles, Bidwell, optical pyrometer, polished iron

the different experimenters differ by about 20° on the correction to be added, whereas for total radiation pyrometers the data are conflicting.

SPECIFIC HEAT AND TOTAL HEAT

The heat capacity of iron and its alloys has been the subject of very much experimentation, and yet such great discrepancies exist between even the best work that the whole matter is rather disappointing. To detail the reasons for discarding the work of numerous

experimenters would be beyond the compass of this report. Suffice it to say that after comparisons and study of nearly all the available data, the work of six experimenters has been chosen for averaging, in order that a determination could be made of the entropy of iron at various temperatures.

The best and most complete work at low temperatures has been done by Rodebush and Michalek,¹³ who used an aneroid calorimeter of good design. They also review previous low-temperature work with part of which their own work is in good agreement. Their data are incorporated in Table 34, in which are given the absolute temperatures, beginning with 72.86° K. and rising to room temperature. The heat capacity per gram atom is used in obtaining the atomic entropy at each of the temperatures of importance, and at room temperature the true heat capacity per gram is also given. Total heats at these low temperatures are not derived, as such data are commonly used only in making heat balances at elevated temperatures. This work was done on pure chemically prepared "iron by hydrogen."

For temperatures above room temperature the work of five experimenters, representing the best that is available, is summarized in Table 35. The specific heats are also plotted in Figure 67, including data from the lowest to the highest temperatures yet attained.

EARLY CALORIMETRIC INVESTIGATIONS

The work of Weiss and Beck¹⁴ was one of the earliest pieces of precise calorimetry to be carried out on iron. A soft steel called "nail iron" was used. The metal, without any protection, was heated electrically and dropped into a method-of-mixture calorimeter, and the metal doubtless oxidized somewhat on contact with the water. The object of the work was to determine the heat changes through the range in which iron is losing its magnetization. The result was to find that, different from most substances, the specific heat as the substance approached the Curie point increased to a maximum followed by a precipitous drop to a low value characteristic of paramagnetic substances. Evidently the magnetic transition A_2 is associated with an energy change manifested by this excess specific heat over the specific heat normally expected. This excess falls off with diminishing temperatures below the Curie point but is probably sensible even at room temperatures and thereby alters the shape of the specific heat curve from that of a normal substance and likewise the shape of the total heat-temperature curve.

¹³ Rodebush, W. H., and Michalek, J. C., The Atomic Heat Capacities of Iron and Nickel at Low Temperatures: Jour. Am. Chem. Soc., vol. 47, 1925, pp. 2117-2121.

¹⁴ Weiss, P., and Beck, P. N., Chaleur spécifique et champ moléculaire des substances ferro-magnétiques: Arch. sci. phys. nat., vol. iv 25, 1908, pp. 529-548.

The importance of the above result caused Weiss, Piccard, and Carrard¹⁵ to repeat the work in a more exactly designed calorimeter and with as many precautions as possible to eliminate error. Two different samples of electrolytic iron were employed, one of which was gold plated to prevent action of water. The same type of calorimeter, using the method of mixtures but with many new devices, was used.

About the same time the laboratory of Wüst¹⁶ was determining the specific heats of a long series of metals, including iron. The

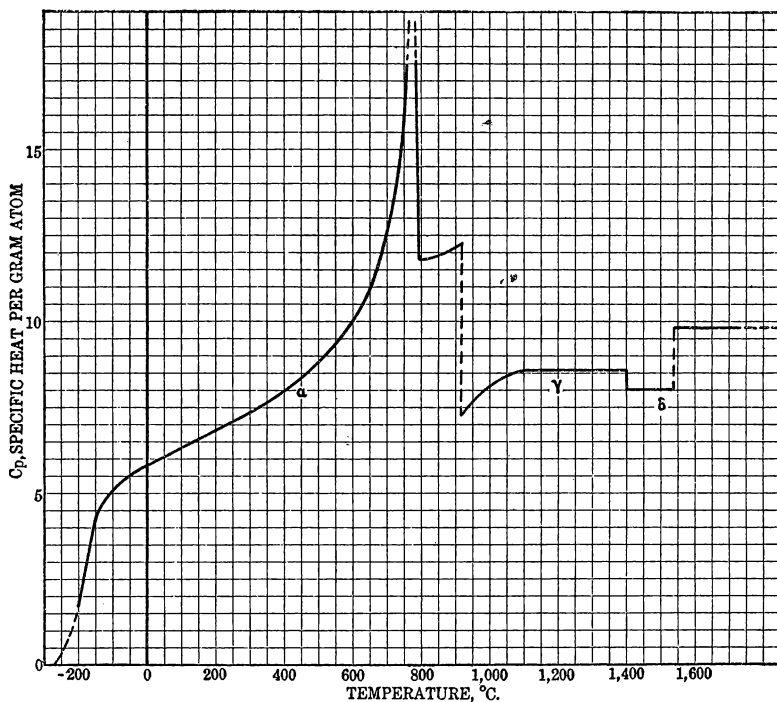


FIG. 67.—Specific heat of iron

vacuum ice calorimeter of Oberhoffer was used, and the iron was inclosed in fused-silica capsules for protection from gases and water, the heat capacity of silica glass having been determined previously. The final specific heat curve published by Wüst did not show the same magnetic component of specific heat that had been indicated by the two papers of Weiss and coworkers. However, the present

¹⁵ Weiss, P., Piccard, A., and Carrard, A., *Calorimétrie des substances ferro-magnétiques*: Arch. sci. phys. nat., vol. 42, 1916, pp. 378–401, and vol. 43, 1917, pp. 22–52, 113–130, 199–216.

¹⁶ Wüst, F., Meuthen, A., and Durrer, R. ———: Ver. Deut. Ing. Forschung., 1918, No. 204; also *Ztschr. Instrumentenkunde*, vol. 39, 1919, pp. 294–295.

writer, on going to Wüst's original data and plotting the total heat content at each temperature and deriving therefrom the specific heats, found that the same type of specific heat curve obtained by Weiss and Wüst had merely smoothed his results to eliminate or average the apparent deviation. The work of Wüst carried the specific heat work to above the melting point of iron and gave an opportunity to determine the heat change at the A_3 , A_4 and melting points of iron in addition to that of the magnetic change.

The work was repeated by Oberhoffer and Grosse¹⁷ because they were also dissatisfied with the shape of Wüst's true specific heat curve, and their results justified the above criticism. They likewise used the vacuum ice calorimeter with electrolytic iron and carried the work up into the field of molten iron.

Finally, Umino¹⁸ published three series of specific heat measurements, one of which was on armco iron, another on a series of carbon steels of widely varying content from which extrapolation to the heat contents of pure iron was possible, and the third on electrolytic iron.

SUMMARY OF WORK

Taking the total heat content determined by each of these five investigators, plotted as a function of temperature, the average heat content at a series of representative temperatures was calculated, and the slope of this curve is the true specific heat at the temperature where the slope is taken. The data, as assembled in this fashion, are contained in Table 35. (The "mean specific heat" is the total heat at a definite temperature divided by the temperature.) The true specific heat was derived in calories per gram and also in calories per gram-atom (55.84 grams). The temperatures are given in the table on centigrade and on absolute scales, and also the common logarithm and the natural logarithm of the absolute temperature were included for the purpose of calculating the entropy, to be discussed later. The critical points, as observed by the various authors, also varied somewhat in temperatures, but again averages were taken and the discontinuity in the total heat-temperature curve was the heat of transition at each of these temperatures.

¹⁷ Oberhoffer, P., and Grosse, W., Die spezifische Wärme des Eisens: Stahl. u. Eisen, Jahrg. 47, 1927, pp. 576-582.

¹⁸ Umino, S., On the Latent Heat of Fusion of Several Metals and Their Specific Heats at High Temperatures, and On the Specific Heat of Carbon Steels: Tohoku Univ. Sci. Repts., vol. 15, 1926, pp. 597 and 331-369; On the Heat of the A_2 and A_3 Transitions in Carbon Steels: Tohoku Univ. Sci. Repts., vol. 16, 1927, pp. 1009-1010.

TABLE 34.—Heat capacity of iron at low temperatures (Rodebush and Michalek)

[Values in parentheses are interpolations]

Temperature, ° K.	Log T	True C_p per gram atom	Entropy
72.86	1.863	1.82	0.95
75.64		1.98	
77.85		2.05	
(80.00)	1.9035	(2.19)	
80.17		2.21	
82.43		2.42	
84.55		2.46	
86.53		2.54	
88.51		2.68	
(90.00)	1.954	(2.73)	1.43
90.37		2.74	
196.44	2.294	5.38	
197.58		5.43	
198.04		5.45	
(200.00)	2.302	5.48	4.71
273.1	2.437	5.84	6.36
(298.1)			6.87

TABLE 35.—Total heat, heat capacity, and entropy of pure iron

[Total heats determined by five best authors averaged and specific heat derived from average curve, then plotted and values of true specific heat per gram atom plotted and smoothed-curve values taken between 0 and 180° C. Entropy derived by usual $\ln T-C_p$ plot with planimeter]

Temperature				Total heat (mean), grams	True specific heat		Entropy, calories per gram atom
° C.	° K.	Log T	$\ln T$		Gram	Atom	
0	273.1	2.437	5.610	0	0.104	5.81	6.36
25	298.1	2.4745	5.700			5.93	6.87
100	373	2.572	5.925	11.17	.120	6.27	8.24
200	473	2.675	6.161	23.25	.124	6.79	9.78
300	573	2.758	6.355	36.04	.132	7.39	10.55
400	673	2.828	6.520	50.28	.147	8.08	12.45
500	773	2.889	6.658	65.8	.1635	8.87	13.57
600	873	2.942	6.780	82.6	.178	9.96	14.74
700	973	2.988	6.882	100.77	.228	12.64	15.88
720	993	2.996	6.900	105.5	.247	13.85	16.00
740	1,013	3.006	6.920	110.8	.285	15.85	16.40
760	1,033	3.014	6.940	117.0	.300	17.05	16.71
780	1,053	3.0223	6.960	123.0	.314	17.65	17.14
790	1,063	3.0265	6.970	125.3	.311	11.76	17.27
800	1,073	3.030	6.980	125.2	.312	11.77	17.41
850	1,123	3.0505	7.025	137.6	.312	11.89	17.89
900	1,173	3.069	7.070	146.9	.220	12.29	18.48
906	1,179	3.072	7.080	152.2		12.34	18.63
906	1,179	3.072	7.080	156.6	.128	7.15	18.86
950	1,223	3.088	7.116	161.0	.135	7.54	19.04
1,000	1,273	3.105	7.155	168.0	.146	8.16	19.39
1,100	1,373	3.138	7.230	183.0	.154	8.61	20.08
1,200	1,473	3.168	7.300	198.4	.154	8.61	20.68
1,300	1,573	3.197	7.368	213.8	.154	8.61	21.11
1,400	1,673	3.2235	7.420	229.6	.154	8.61	21.71
1,400	1,673	3.2235	7.420	231.3	.143	7.99	21.77
1,450	1,723	3.2362	7.455	240.7	.143	7.99	21.99
1,500	1,773	3.249	7.480	250.2	.143	7.99	22.25
1,535	1,808	3.257	7.500	252.3	.143	7.99	22.41
1,535	1,808	3.257	7.500	317.2	.176	9.83	24.00
1,550	1,823	3.261	7.510	319.8	.176	9.83	24.10
1,600	1,873	3.2725	7.540	328.6	.176	9.83	24.39

781°. At point A_2 ; no heat; over range; 335 calories per atom.906°. At point A_3 ; 4.9 calories per gram; 273.6 calories per atom.1,400°. At point A_4 ; 1.7 calories per gram; 94.9 calories per atom.

1,535°. At melting point; 64.9 calories per gram; 3,625 calories per atom.

The data in Tables 34 and 35 are plotted in Figure 67. It is extrapolated to zero specific heat at absolute zero (this is the third law of thermodynamics) and shows the specific heat rising until toward

room temperature the curve tends to turn off toward a horizontal asymptote, as most normal substances do. However, from here up to the magnetic transition the magnetic component of the specific heat is becoming noticeable, bending the true specific heat curve upward instead of downward until a peak is reached where the magnetic change is the most rapid with rise of temperature. After the A_2 or Curie point is passed the specific heat of paramagnetic α iron is constant (probably along the above-mentioned horizontal asymptote), until at the A_3 point α iron is abruptly converted into γ iron, which has its own specific heat, also a constant value at these temperatures. After the A_4 point is passed and the iron is now δ iron the specific heat has discontinuously changed to a new constant value. If δ iron is merely high-temperature α iron, it should have approximately the same specific heat. Only the Oberhoffer and Grosse observations show this, and they started out with the preconceived idea that this would be so. However, the data at these high temperatures are quite widely divergent, and it is not surprising to find poor agreement in an average figure. Lastly, after passing the melting point the heat capacity of molten iron was a constant for all three observers of this range of temperatures, and their results are reasonably good checks on each other.

The peak and quick drop in the specific heat curve at the A_2 point seem to be the cause of the apparent heat effect in the heating and cooling curves, and the wide discrepancy in the estimates of the "heat effect" at this point is probably coincident with the precision of the instruments used. No real "heat of transition" is involved.

HEATS OF TRANSITION

The total heat curves used for derivation of the specific heats also show the heats of transition. By this means the various experimenters have estimated the heats of all the transitions. They are tabulated successively and discussed.

TABLE 36.—Heat effect at A_2 point or magnetic transition (Curie point)

Observer	Per gram	Per gram atom	Temperature, °C.
Osmond ¹	1.3
Stansfield ²	1.0	55.84
Pionchon ³	5.3
Meuthen ⁴	5.6
Wüst ⁵	6.56	755
Umino ⁶	3.65	795
Selected.....	3.65

¹ Osmond, M., Sur les phénomènes qui se produisent pendant le chauffage et le refroidissement de l'acier fondu: *Compt. rend.*, t. 103, 1886, p. 743.

² Stansfield, Alfred, The Present Position of the Solution Theory of Carburized Iron: *Jour. Iron and Steel Inst.*, vol. 11, 1899, p. 169.

³ Pionchon, M., Recherches calorimétriques sur les chaleurs spécifiques et les changements d'état aux températures élevées: *Compt. rend.*, t. 103, 1886, p. 1122.

⁴ Meuthen, A., ———: *Ferrum*, Jahrg. 10, 1912, p. 1.

⁵ See footnote 16, p. 188.

⁶ See footnote 18, p. 189.

As just mentioned, the total heat curve shows no discontinuity at all but only a change in direction at the A_2 point, and this means merely a change in specific heat but not a real heat of transition. Therefore, the heats estimated from cooling curves and heating curves are merely the magnetic component of the specific heat integrated over a more or less wide range of temperature, according to the sensitiveness of the instrument used. The true heat of transition at the A_2 point is therefore zero, unless we look on the heat accompanying the magnetic changes as a distributed (over a temperature range) latent heat. This latter idea is quite permissible, although not in common acceptance.

TABLE 37.—*Heat effect at A_2 point*

Observer	Calories per gram	Calories per gram-atom	Temperature, °C.	Date
Osmond.....	3.8	212	-----	1886
Stansfield.....	2.86	160	-----	1899
Meuthen.....	5-6	310	-----	1912
Wüst.....	6.56	356	919	1918
Oberhoffer.....	6.765	377	906	1927
Umino (1).....	3.1	173	-----	1926
Umino (2).....	5.35	-----	920	1927
Selected.....	4.9	273.6	906	1928

The A_3 point is a true transition, and there is no doubt that heat is absorbed or liberated as iron is being heated or cooled, respectively. The Umino datum is much lower than the other two "good" ones but has been allowed to have its effect on the average. The average is really derived from the average heat-content curve.

TABLE 38.—*Heat effect at A_4 point*

Observer	Calories per gram	Calories per gram-atom	Temperature, °C.	Date
Wüst.....	1.94	108	1,404.5	1918
Umino.....	3.00	168	1,399	1926
Oberhoffer.....	2.53	141	1,401	1927
Selected.....	1.7	94.9	1,400	1928

The A_4 point is also a true transition, and all the total heat-temperature curves have discontinuities corresponding to the heat of transition. The replotted average data of all the best observers did not give an average of their observations but a datum which was lower and which showed therefore that they had all smoothed their results to some extent.

TABLE 39.—*Heat of fusion*

Observer	Calories per gram	Calories per gram atom	Temperature, ° C.	Date
Brisker.....	31.6	1,765	1,500	1908
Brisker, corrected.....	57.50	3,210	1,535	1908
Wüst.....	49.35	2,755	1,528	1918
Umino.....	68.3	3,820	1,535	1926
Oberhoffer and Grosse.....	64.36	3,600	1,528	1927
Selected average.....	64.9	3,625	1,535	1928

The data on the heat of fusion of pure iron are none too concordant. The selected average given in our table is that resulting from plotting of the heat contents of the three reliable observers in this field, Wüst, Umino, and Oberhoffer and Grosse. As usual, the personal equations involved in their interpretation of their own data were ignored, and the data were used as collected. The datum of Wüst, therefore, did not lower the selected average in the proportion that it might if Wüst's smoothed curve had been used. For comparison, the calculated datum of Brisker¹⁹ is tabulated. He used the van't Hoff equation for lowering the freezing point of substances by solutes and chose the data on iron and carbon, the alloy containing 4.3 per cent C, freezing at 1,130° C. The melting point of iron was assumed to be 1,500° C. and the molecular weight of carbon 24. This gave the result tabulated, 31.6 calories per gram, which was in fair agreement with the observed heats on white and gray cast iron (the available data at that time). Probably the reason the molecular weight of carbon was chosen as 24 was to make the result come out in better agreement with the (poor) data—Brisker does not state. However, assuming the carbon to be present only as the element and to possess an effective "molecular weight" of 12, taking the melting point of pure iron as 1,535° C., the corrected calculation gives 57.5 calories, which is in much better agreement with the more recently observed data on pure iron as above tabulated. Whether the carbon exists in molten iron as free elemental carbon, as a molecule of carbon with more than 1 atom, as the molecule Fe_3C (which crystallizes at lower temperatures), or otherwise is not known. However, either C or Fe_3C is most probable.

To test the value of the van't Hoff equation in making such calculations as the above, the data available in International Critical Tables on other iron alloys were used in precisely the same manner for calculating the heat of fusion of pure iron. The gold alloys gave a value of 110 calories, the tin alloys 112 calories, the titanium alloys

¹⁹ Brisker, Carl, Die latente Schmelzwärme des reinen Eisens: Metallurgie, Jahrg. 5, 1908, pp. 183-184.

97 calories, boron alloys 56 calories, arsenic 51 calories, and phosphorus 44 calories. The equation is therefore evidently not very reliable.

LATENT HEAT OF EVAPORATION

No direct measurements of the latent heat of evaporation of iron are available. It must be calculated from other data on vaporization. This has been done by Jones, Langmuir, and Mackay, whose data on vapor pressure are given earlier in this paper. Langmuir worked out a relationship connecting the rates of evaporation of iron filaments with the Clausius-Clapeyron equation, assuming the validity of the third law of thermodynamics and using the Sackur and Tetrode relations familiar to physical chemists. His final equation calls for only the rate of evaporation at a definite temperature in order to derive the theoretical heat of evaporation at absolute zero, and from four different temperatures good agreement on the calculated values of this hypothetical latent heat are obtained, averaging 89,027 calories per gram-atom= L_0 . Using the vapor-pressure data of Greenwood and of Mack, Osterhof, and Kraner, discussed above, the calculated latent heats at various temperatures are:

TABLE 40.—*Latent heat of evaporation of iron*

Observer	Temperature ° K.	L_T , calories per gram atom	L_0 , calories
Greenwood.....	2,925	94,300	96,975
Do.....	2,723	88,900	91,575
Mack and others.....	2,723	71,400	74,075

Although the data are not very concordant and apply to evaporation at a relatively low temperature and pressure, the Greenwood data seem to coincide better with the Langmuir data, and using them to extrapolate to the boiling point of iron the indications are that at the boiling point, 3,218° C., the latent heat of evaporation of iron is of the approximate magnitude—100,000 calories per gram atom.

As a rough check on this datum, one may use Trouton's rule that the entropy of vaporization of unassociated liquids is a constant approximately equal to 22. At the boiling point of iron on the absolute scale, 3,491° K., this corresponds to about 77,000 calories for the heat of vaporization—a reasonable check.

TOTAL HEAT OF IRON

Enough data have been assembled for drawing the complete total heat-temperature curve of pure iron, acknowledging that above

1,000° C. it is subject to considerable revision. The total heats up to 1,600° C. have already been tabulated in Table 35, being referred to 0° C., which for practical purposes is also the total heat above room temperature. A gram of iron requires 252.3 calories to bring it to the melting temperature, 317.2 calories to produce 1 gram of molten iron from cold iron, 613.6 calories to produce liquid iron at its boiling point, and 2,403.6 calories to produce 1 gram of iron gas at

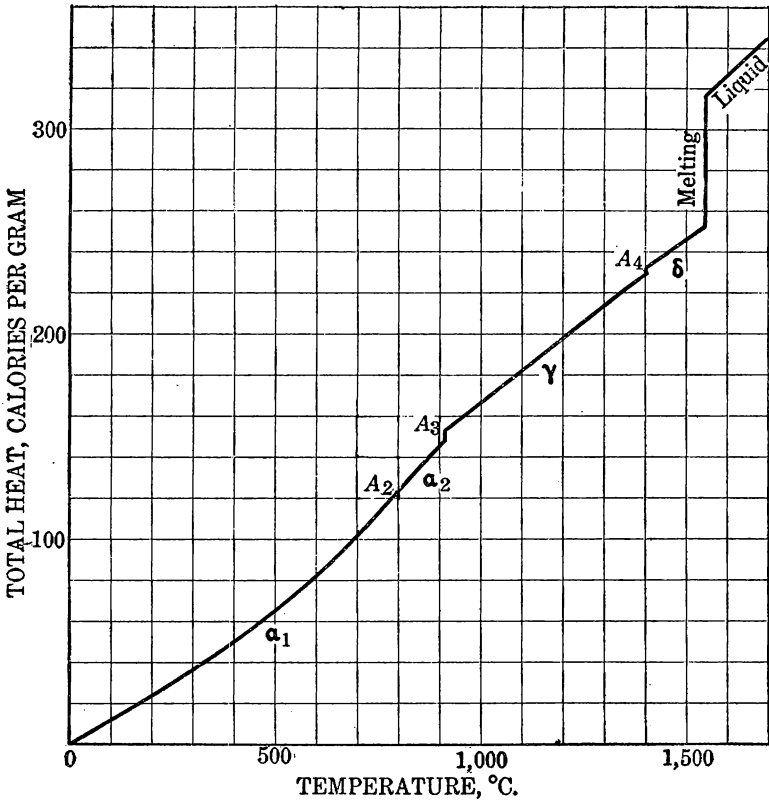


FIG. 68.—Total heat-temperature curve for iron

its boiling point. These two later data are obtained by assuming the specific heat of molten iron is constant and is 0.176 calorie per gram.

The total heat curve up to 1,600° C. is given in Figure 68 for purposes of discussion. This is made up from the average total heats of Table 35. By its help the comparative magnitudes of the A_2 , A_3 , A_4 , and melting points in conjunction with the amounts of heat necessary to change the temperature of iron can be visualized. The portion for magnetic α iron is not a straight line but a curve of increasing slope, which culminates at A_2 . In this range we have already explained that the total heat involved in heating the sample

is probably made up of the energy necessary to change the temperature of α iron plus the energy necessary to cause increasing randomness in the orientation of the ultimate magnetic particles. This second component should end at A_2 . Above A_2 α iron, provided no other magnetic or other effects intervene, might be expected to have a relatively constant specific heat. Oberhoffer pointed out in connection with his specific heat work that a constant specific heat requires that the total heat-temperature curve be straight and should pass through the origin, because, thermodynamically, specific heat is the first derivative of the total heat-temperature curve, $C_p = dH/dT$. The line in our figure for nonmagnetic α iron, between A_2 and A_3 , does not pass through the origin if extrapolated downward but has a higher slope than that required to make it pass through the origin. It is well at this point to mention that Oberhoffer is correct in his statement that a straight line in the total heat curve means a constant specific heat for the temperature range in which the total heat curve is straight, but he is incorrect in requiring it to pass through the origin of coordinates. If the energy required to raise the temperature of iron over a straight portion of the total heat curve were required exclusively for increasing the thermal motion of the atoms or groups of atoms in the space lattice, Oberhoffer's criterion about the straight line passing through the origin would be correct. However, energy involved in increasing the distance between atoms in the lattice, in overcoming their tendency to orient magnetically, and in causing electrons to leave their orbits and assume new orbits or to be emitted as free electrons, and energy used up in a number of other conceivable ways is undoubtedly superposed on the purely "thermal" energy and causes the total heat curves to depart from the slope expected of them. Even in Oberhoffer's total heat curve the slope of the γ iron total heat curve (between A_3 and A_4) was too low to allow it to pass through the origin, and this is true of our own average total heat curve. This means that less than the expected amount of heat is necessary to raise the temperature of γ iron. The explanation is totally beyond us at present.

The safest conclusion from these facts is that iron is an extremely complicated substance, as evidenced primarily in the thousands of lines in its spectrum, and that we should not expect its total heat-temperature curve to conform to that expected of simple substances. In fact, more careful calorimetry is likely to turn up even more interesting departures from the thermal properties of a simple substance.

ENTROPY OF IRON

As mentioned above, the entropy of iron at various temperatures was derived from the specific heat-temperature data and the values

were included in Table 35. The third law of thermodynamics is implied in these derivations of the absolute entropy, and therefore the entropy is zero at the absolute zero. The entropy values were derived by plotting the true atomic specific heats (specific heat per gram atom) against the natural logarithms of the absolute temperatures (this distorts the diagram of Figure 67, exaggerating the scale to the left, since the logarithm of zero is minus infinity) and estimating the areas under the curve by use of a planimeter up

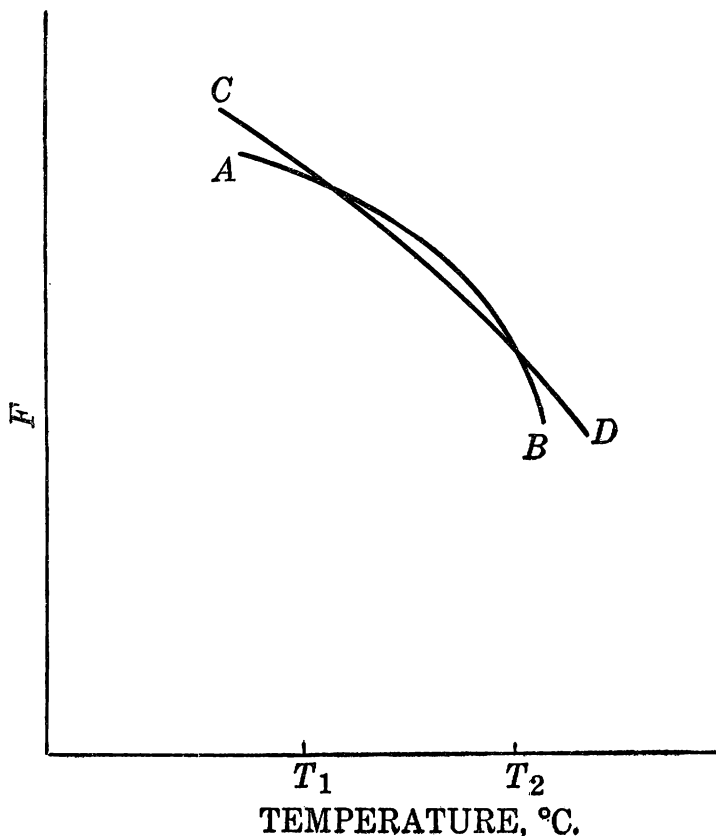


FIG. 69.—Free energy of alpha and delta forms of iron as a function of temperature

to the desired temperature in each case. Such an area is a mathematical expression of entropy. The values of entropy up to room temperature were calculated by Rodebush and Michalek and those above room temperature by the present writer, based on the figures of specific heat derived from his average heat-content curve.

ALLOTROPY AND THERMODYNAMICS OF IRON

A very suggestive discussion of how it can be that α and δ iron can have identical crystallographic and phase properties and be

separated in the temperature scale by γ iron has been presented by Bredemeier²⁰. His view is that if we could plot the thermodynamic potential or free energy of the one crystallographic form as a function of temperature and compare it to the similar plot for the other form, the two curves would look like those in Figure 69. The curve ab would be the isobaric curve of thermodynamic potential of $\alpha=\delta$ iron. Curve cd is the same for γ iron; their intersections at $T_1=906^\circ$ C. and $T_2=1,400^\circ$ C. are the transformation points; the form of iron with the lowest potential is the most stable. We therefore find γ iron most stable between 906° and $1,400^\circ$ C.

It must be remembered that the thermodynamic potential can be expressed as a function of energy and entropy, $F=E-TS+vp$, and thermodynamics tells us that the entropy S is the first derivative of the free energy, $S=dF/dT$, while the second derivative, $d^2F/dT^2=-C_p/T$, is a function of the specific heat. Comparing the slopes, dF/dT of the curves at 906° and $1,400^\circ$ C., it is seen that at 906° C. the entropy of α iron is greater than that of γ iron, while at $1,400^\circ$ C. the entropy of γ iron is greater than that of δ iron. With this and the first equation of this paragraph in mind, the energy contents of the various forms at the two temperatures can be compared and the discovery made that in passing from α to γ iron or from γ to δ iron the heat of transformation is positive (absorption of heat).

Finally, comparing the curvatures of the two lines, it can be seen that the curvature, d^2F/dT^2 , of γ iron is less than that of the α - δ line, pointing to a lower specific heat for γ iron. Unfortunately, our specific heat curve does not show this, for, while it gives the specific heat of γ iron lower than that of α iron, it is higher than that of δ iron. While the original data of Wüst did show the specific heat of γ iron lower than that of both α and δ irons, the process of averaging total heat data of the three workers in this field brought about the curve which has been chosen. Bredemeier's thermodynamic picture therefore gives us a valuable criticism of the thermal data as we have presented them and shows that further work on the thermal properties of pure iron at temperatures above $1,000^\circ$ C. is needed. His qualitative picture also gives glimpses of the reasons for the strange behavior of the various forms of iron.

²⁰ Bredemeier, H., Beitrag zur Polymorphie des Eisens: Ztschr. anorg. allgem. Chem., Jahrg. 151, 1926, pp. 109-112.

THE SYSTEM IRON-CARBON

During the reduction of iron ore with carbon and in the working of steel baths it is not sufficient to know the equilibria between the various iron-oxygen phases, because the iron tends to combine with carbon before all the oxygen is gone, and there are equilibria between these various carbon and oxygen bearing phases. Before they can be dealt with it is necessary, therefore, to consider the iron-carbon diagram briefly and to discuss especially the properties of the carbide, Fe_3C . The following discussion is not intended to be exhaustive from the standpoint of the metallographer or the steel metallurgist but is intended to present a reasonable discussion of the scientific data so far accumulated.

The iron-carbon diagram presented in Figure 70 is the result of so much work by hundreds of authors that references to sources of information are hardly necessary. It is the standard diagram in use by steel metallurgists and is revised as far as possible up to date. The solid phases involved in the diagram are discussed in the following pages, under both the metallographic names and the scientific names.

All iron-carbon alloys on cooling at usual air-cooling rates result in mixtures of nearly pure iron (ferrite) and iron carbide, Fe_3C (cementite). The structure under the microscope reveals that during cooling the metal had passed through a number of transitions, and the metallographers have given the names defined below to these transition mixtures. Even the diagram can not show all the structures that result.

The diagram is further complicated by the fact that cementite, Fe_3C , is an endothermic, metastable compound, at least in certain temperature ranges, and that very slow heating and cooling cause the cementite to be replaced by graphite. The dotted lines in Figure 70 show the equilibria between the liquid and solid solutions of this so-called "stable" system as compared to the usual "metastable" cementite system. The relations of the stable to the metastable system have not been worked out satisfactorily as yet.

The alloys are divided into two grand classes—steels and cast irons. As can be seen from the ranges indicated at the top of the diagram, the steels include alloys up to about 1.7 per cent of C; there is then a transition zone which may be regarded as either steel or cast iron, and cast irons begin at about 2.2 per cent of C and go

as high as 6 per cent of C, the upper limit being more or less indefinite but not quite reaching the composition of Fe_3C , which is 6.67 per cent of C. Each grand division is subdivided by metallographers into hypoeutectoid and hypereutectoid steels and hypoeutectic and

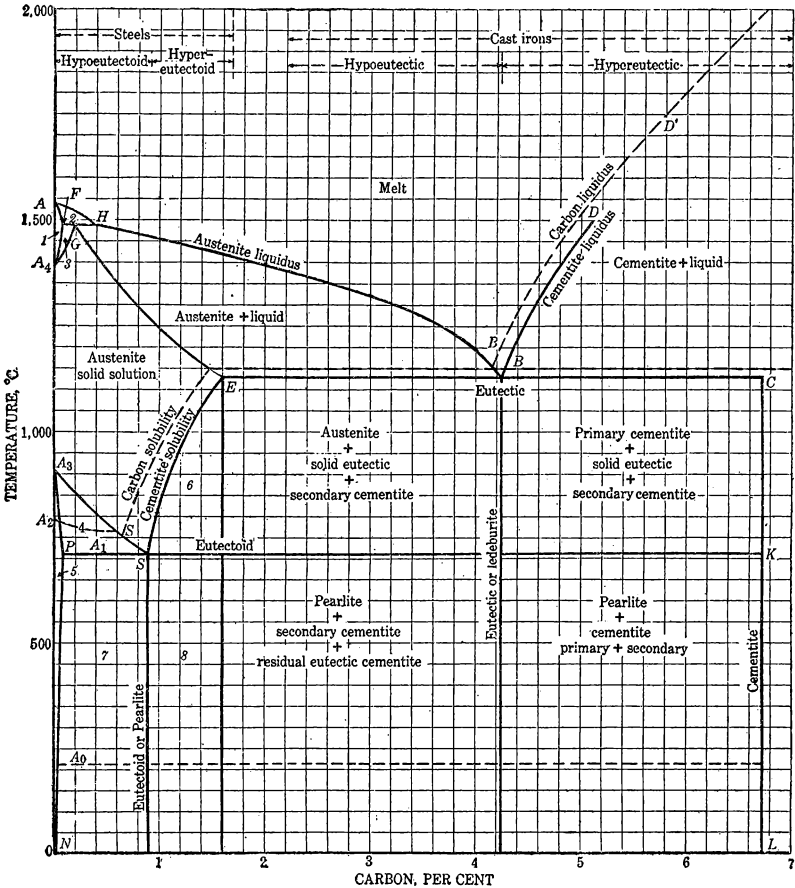


Fig. 70.—Iron-carbon temperature-composition phase diagram: Area 1, δ ferrite, maximum solubility of carbon 0.07 per cent; area 2, δ ferrite + melt; area 3, δ ferrite + austenite; area 4, α ferrite + austenite; area 5, α ferrite, maximum solubility of carbon 0.034 per cent; area 6, austenite + proeutectoid cementite; area 7, proeutectoid α ferrite + pearlite; area 8, proeutectoid cementite + pearlite. Point A_0 , temperature of magnetic transformation of Fe_3C , 210° C.; point A_1 , temperature of eutectoid (splitting of solid austenite into α ferrite and cementite), 720° C.; point A_2 , temperature of magnetic transformation of α ferrite, 795° C.; point A_3 , temperature of transformation of γ ferrite to α ferrite, 906° C.; point A_4 , temperature of transformation of δ ferrite to γ ferrite, 1,400° C.; point A , melting point of pure iron, 1,535° C.; point N , solubility of carbon (as cementite) at room temperature, 0.003 per cent C

hypereutectic cast irons, respectively, thus distinguishing between the groups in which one or the other metallographic constituent crystallizes out first.

The next logical step is to define the constituents which can be observed on polished surfaces of iron-carbon alloys by the help of

the microscope and also of certain other solid phases known to exist as transitory stages.

CONSTITUENTS ON SURFACE OF IRON-CARBON ALLOYS

DELTA FERRITE

This substance, which is the first constituent to crystallize from melts lower in carbon than point H in the diagram, is merely δ iron containing a small amount of dissolved carbon, the maximum amount of carbon being 0.07 per cent (see point F'). It is quite unfortunate that the metallographers have chosen to use the name ferrite for the metallic iron when chemists already have the same word to define a compound in which Fe_2O_3 exists in the acid radical. Delta ferrite is the single constituent in field 1 of the iron-carbon diagram. In field 2 it is the δ iron crystal in equilibrium with the melt from which it has crystallized, and in field 3 it is in equilibrium with the solid solution of iron and carbon known as austenite, which will be defined below. The A_4 point of pure iron is shown on the diagram and is raised by the solution of carbon in δ iron along the line between A_4 and the point F , which is at $1,486^\circ \text{C}$. (the peritectic temperature).

AUSTENITE

The solid solution of carbon in γ iron, austenite, has the stability field just below that of δ ferrite in the diagram. An alloy of composition intermediate between A and G , on cooling below G ($1,486^\circ \text{C}$), splits into δ ferrite crystals of the compositions along line A_4F and austenite solid solution of compositions along the line A_4G , and as the mixture is cooled nearer and nearer to $1,400^\circ \text{C}$. more and more of the δ ferrite is converted into γ iron, which passes into the austenite solid solution. Austenite, when examined by the X-ray spectrographic methods, shows the space lattice of γ iron, and the carbon in the mixture creates no lines in the spectrum, indicating thereby that it is present either in random positions scattered through the iron lattice or else that it displaces random iron atoms in the lattice. The latter possibility has been disproved²¹ by comparing the observed specific volumes of the actual steels with those calculated, on the assumption that the carbon displaces iron atoms in the γ iron lattice or that it exists in the interstices between the iron atoms in the lattice. The latter hypothesis fits the facts better.

Whether the carbon is present in austenite as such or as the compound Fe_3C (cementite) is a moot question, as there are good but inconclusive arguments on both sides. Certainly cementite is the

²¹ Wever, F., and Rütten, P., Zur Kenntnis des Mischkristalles Gamma Eisen-Kohlenstoff; *Mittel. Kaiser Wilhelm Inst. Eisenforschung*, Jahrg. 6, 1924, pp. 1-6.

material which crystallizes out of the austenite solid solution when it is further chilled, but that is not proof that it existed in any appreciable concentration before it crystallized. Carbon diffuses through austenite with quite an appreciable rate, and it is difficult to conceive of the large Fe_3C molecules being able to diffuse through the γ iron lattice, whereas the small carbon atoms should be easily able to do it. However, the carbon atoms which diffuse may result from a small percentage dissociation of Fe_3C , which could carry the major portion of the carbon in the austenite. Whether there is any difference between a solid solution of Fe_3C in γ iron and a solid solution of carbon in γ iron no one knows. A few authorities favor the view that the two solid solutions are actually different and give a special name to the carbon solid solution.

BOYDENITE

Boydenite is the name proposed for the solid solution of carbon in γ iron from which carbon (graphite) would crystallize on slow cooling.²² Its proponents presuppose a difference in the solid solutions from which the cementite of graphite, respectively, crystallize. It is supposed to be γ iron in which a carbon atom replaces one of the iron atoms in the face-centered cubic lattice, whereas in austenite the carbon atoms are in interstices of the lattice.

They present evidence that there is some apparent difference in the density of austenite and boydenite. Until more conclusive evidence can be marshaled the writer is inclined to accept boydenite only as a name that could be used, if found necessary, to define the supposed different kind of solid solution.

CEMENTITE

Cementite is the definite compound, Fe_3C , which is the usual form in which carbon crystallizes from most of the iron-carbon alloys. It forms a eutectic with austenite, freezing at about $1,130^\circ$ C. For alloys richer in carbon than the point *B*, the eutectic, cementite is the primary constituent to crystallize on cooling a melt. On cooling any alloy with more carbon than the point *S*, below $1,130^\circ$ C., cementite also tends to crystallize out along the line *ES*, coming out of the austenite solid solution until the point *S* is reached. Its properties will be discussed at length later. Cementite is one of the crystals formed at the eutectoid temperature, 720° C., the eutectoid being the point where the last remaining solid solution disappears with separation of two kinds of crystals just as a eutectic

²² Schwartz, H. A., Evidences Concerning the Location of the Carbon Atom in Boydenite: Trans. Am. Soc. Steel Treating, vol. 11, 1927, pp. 277-283.

forms from a liquid solution. Cementite can therefore form as primary crystals from a rich carbon melt, as eutectic from freezing any iron-carbon melt, as secondary crystals coming from the austenite solid solution, and as eutectoid cementite. All of these are recognized by the metallographer.

LEDEBURITE

The eutectic between cementite and austenite, having the composition 4.25 per cent of C, is sometimes called ledeburite. Its structure is recognizable in spite of the fact that the austenite on cooling splits further into ferrite and cementite. However, it is more commonly recognized in alloyed steels containing elements which render austenite stable down to room temperatures. Manganese and nickel steels are two commonly used alloy steels in which this is possible.

PEARLITE

Pearlite is the composition of the eutectoid alloys, 0.9 per cent of C, named for its pearly appearance in polished sections under the microscope. It is commonly resolved under high magnifications into alternating leaves of cementite and α ferrite, giving a structure that resembles fingerprints. It is the most pronounced and most unmistakable constituent viewed by the metallographer. As mentioned below, if the cooling of the steel has been more rapid than normal, the size of the grains in the pearlite decreases until they are beyond the resolving powers of the microscope, and the constituent then has other names—martensite, troostite, and sorbite. By cooling through the range 700° to 300° C. in three to four seconds, Matsushita²³ has shown that these transformations are entirely prevented, but at still lower temperatures, 200° to 100° C., formation of martensite begins.

ALPHA FERRITE

The form of iron ordinarily seen by the average person is α ferrite. Absolutely pure α iron is a rare material. However, the solubility of carbon (presumably as Fe_3C) in α iron is very low at room temperatures, being about 0.003 per cent, and the maximum solubility is encountered at the A_1 point, 726° C., and is about 0.034 per cent of C. The stability field of α ferrite is numbered 5 in the iron-carbon diagram. It is the constituent which crystallizes simultaneously with cementite in the eutectoid. Also, during cooling of any austenite with less carbon than 0.9 per cent (point S), α ferrite crystallizes out

²³ Matsushita, T., Some Investigation on the Quenching of Carbon Steels: Tohoku Univ. Sci. Repts., vol. 12, 1923, pp. 7-25.

as primary crystals until the eutectoid temperature is reached. The line from A_3 to S is the line for this primary crystallization and corresponds to the A_3 point of pure iron, since the change is from a contaminated γ iron at higher temperatures to nearly pure α iron at these temperatures. Field 4 in the diagram is the one where α ferrite is crystallizing from and in equilibrium with austenite. The composition of the α ferrite crystals formed during this process follows line A_3P , while that of the austenite in equilibrium, as just mentioned, follows the line A_3S .

MARTENSITE

Martensite is an indefinite intermediate product which is quite characteristic in its metallographic appearance but has been the subject of an immense amount of controversy when its exact definition is attempted. It usually consists of needlelike structures under the microscope, which are apparently partly altered material formed on the two sides of the incipient octahedral cleavage planes in austenite. It is formed by suddenly quenching an austenitic steel. When a quenched steel containing martensite is reheated it is altered first into troostite, then into sorbite, and finally into pearlite. Martensitic steels are extremely hard.

Slowly cooled steels are soft and have no martensite; quenched steels are hard and have martensite. It is therefore quite natural to ascribe hardness to martensite. However, modern ideas on hardness do not accord with such a simple explanation, and the theories of the mechanism by which martensitic steels can be so hard are very numerous. The slip-interference theory of hardness developed by Jeffries and other American metallurgists seems to have the best foundation. This theory assumes that well-crystallized material can be deformed by slippage of the various planes of atoms over each other in the crystals, but if other atoms of different diameters enter the crystal lattice and tend to deform the planes slippage is hindered and greater hardness of the gross structure results. Bain²⁴ has put in words the reason for the hardness of martensite in the light of this theory: "In martensite there is a vast amount of very poorly crystallized material having warped planes and such imperfections." More recently Jeffries²⁵ has pointed out that carbon plays three rôles in hardening a freshly quenched carbon steel. It assists in lowering the temperature of the allotropic modification, it assists in producing smaller α iron solid solution grains (experimentally determined), and it hardens by its actual presence in the solid solution.

²⁴ Bain, E. C., The Nature of Martensite: Trans. Am. Inst. Min. and Met. Eng., vol. 70, 1924, pp. 25-46.

²⁵ Jeffries, Zay., A Contribution to the Theory of Hardening and the Constitution of Steel: Trans. Am. Soc. Steel Treating, vol. 13, 1928, pp. 369-407.

In all the controversy over the nature of martensite the most convincing arguments have come in a long series of papers from the research institute at the Tohoku University in Sendai, Japan, directed by K. Honda. He uses the hypothesis that martensite, being the first stage in transition from the solution of carbon in γ iron to the α iron form, is merely a solid solution of carbon in α iron. Although the solubility of carbon in α iron is very low, nevertheless the quick cooling of the specimens could amount to the freezing or forming of a supersaturated solution. One might point toward glasses as supercooled solutions, and possibly some of the material in martensitic steel is in the form of a glass, but X-ray patterns of α iron and also lines of γ iron can be obtained from it, as though a certain amount of austenite had been supercooled.²⁶ Austenitic specimens at room temperature have been further converted into martensite by tensile stress²⁷ and by hammering.²⁸ Plunging into liquid air creates sufficient stress to accomplish the same result²⁹ and is probably the most thorough method of approaching completion in the decomposition of austenite.

Freshly formed martensite hardens on standing several hours at room temperature or on standing a few minutes at 100° C. Apparently a temperature slightly below 0° C. is necessary to preserve fresh martensite and prevent its alteration into aged martensite and troostite, which will be defined below. This means that room temperature is near the limit which will permit diffusion of carbon in steel, and at temperatures below it any supercooled austenite can be held indefinitely in frozen condition. The principal evidence that little carbide is present in fresh martensite is based on volume changes. The change from γ to α iron is accompanied by expansion, while formation of Fe_3C is accompanied by contraction of volume. When martensite forms the expansion accompanying it, as pointed out by Jeffries,³⁰ shows that the principal change is from γ to α iron. Later, during reheating (tempering) of quenched steels contractions commensurate with the appearance of carbide in the microstructure take place. The γ iron supercooled solution is unstable but at room temperature only slowly changes to α iron solid solution, and the α iron solid solution is supersaturated with respect to either carbon

²⁶ Heindlhofer, K., and Wright, F. L., Density and X-Ray Spectrum of Hardened Ball Steel Tempered at Various Temperatures: *Trans. Am. Soc. Steel Treating*, vol. 7, 1925, p. 34.

²⁷ Dowell, R. L., and Harder, O. E., The Decomposition of the Austenitic Structure in Steels; III. Effect of Drawing or Tempering on Decomposition of Austenite; IV. Effect of Stress on the Decomposition of Austenite: *Trans. Am. Soc. Steel Treating*, vol. 11, 1927, pp. 781-790.

²⁸ Honda, K., and Iwase, K., On the Transformation of Retained Austenite into Martensite by Stress: *Trans. Am. Soc. Steel Treating*, vol. 11, 1927, pp. 399-406.

²⁹ Schroeter, Kurt, Über die Umwandlung des Austenite in Martensit durch flüssige Luft: *Ztschr. anorg. allgem. Chem.*, Jahrg. 169, 1928, pp. 157-160.

³⁰ See footnote 25, p. 204.

or cementite; but the thermal agitation is too low to permit of its splitting spontaneously into its constituents otherwise than very slowly. Whether on splitting it precipitates carbon or cementite is a very difficult question to answer. The first product of such splitting is called troostite.

TROOSTITE

Under the microscope troostite is difficult to identify, as it is so nearly optically homogeneous. It has commonly been regarded as the next step in the decomposition of martensite and to be identical with pearlite, into which it alters by standing at high enough temperature for a few minutes, recrystallization presumably taking place. However, recent work under Honda³¹ has brought out evidence leading to the belief that troostite formed by tempering an austenitic steel for 20 minutes at 100° to 300° C., and again cooling is really made up of α iron in which elemental carbon has precipitated in practically atomic dispersion. Tempering of quenched steels is the common method of producing troostite.

SORBITE

Sorbite has long been regarded as ultramicroscopically fine-grained pearlite. It is formed by tempering quenched (martensitic) steels at 300° to 400° C. for 20 minutes and cooling. The work of Matsushita and Nagasawa quoted above points toward its consisting of iron and cementite in high dispersion. Heating troostite to this higher temperature, they say, gives the free carbon sufficient activity to combine with iron and form FeC_3 . A mixture of troostite and sorbite formed by tempering between 300° and 400° C. is sometimes called osmondite.

Further heating of troostite or sorbite at 450° to 500° C. forms granular pearlite, the end product of the transition from austenite, probably through coagulation and growth of the small crystals of α ferrite and cementite. The cementite forms in spheroidal grains under these conditions. The sorbitic steels are the most easily dissolved in dilute sulphuric acid of all the quenched or tempered products.

This rather long series of definitions has been necessary in order that the energy changes in steel, of interest to the physical chemist, can be properly understood. However, before we can proceed, certain proposals on interpretation of the tempering and quenching phenomena, different from the interpretation involved in the above definitions, must be considered.

³¹ Matsushita, T., and Nagasawa, K., On the Mechanism of Tempering of Steels: Tohoku Univ. Sci. Repts., vol. 16, 1927, pp. 901-913.

EPSILON AND ETA PHASES OF HANEMANN

When martensite was studied microscopically, Hanemann⁸² inspected the tempered structures and found that the martensite was not homogeneous. A part of the martensite, he thought, had one carbon content and the other part had another carbon content. Moreover, the martensite needles which lie in an austenite ground-mass apparently have a carbon content different from the austenite. In slowly cooled steels and hardened steels with definite carbon content the crystal structure changes, due, according to Hanemann, to a change in the type of phases whose limiting carbon contents lie at 0.1, 0.9, and 1.4 per cent. These phenomena he explains by assuming the existence in quenched carbon steels of a second metastable system in the temperature interval below 720° C., which is blank in Figure 70. This second metastable system proposed by Hanemann is given in Figure 71, which might have been included in Figure 70 if Hanemann's theory were better established.

An epsilon (ϵ) form of iron is assumed to exist in quenched steels below 685° C., but the presence of increasing amounts of carbon depresses the ϵ field, giving rise to a duplex field of ϵ and γ phases. (See fig. 71.) At 350° and below a peritectic equilibrium is encountered between the ϵ phase with 0.1 per cent of C and γ iron with 1.4 per cent of C (at 350°), and giving rise to a new phase, the eta (η) phase, with 0.9 per cent of carbon. The homogeneous state of the ϵ phase is to the left of TU_1 , and the homogeneous state of the η phase is inside of V_1V_2 . In hardened steel with less than 0.1 per cent of C the microstructure is homogeneous in agreement with the diagram. Between 0.1 and 0.9 per cent of C it is heterogeneous, with increasing amounts of the η phase, until at 0.9 per cent the structure is again homogeneous, and only the η phase can be seen. From 0.9 to 1.4 per cent of C increasing amounts of γ phase (austenite) are noted in addition to the η . With a carbon content greater than 1.4 per cent, the field of the ϵ phase is not even touched, and the occasional observation of unconverted ϵ phase in the 0.9 to 1.4 per cent C field is no longer possible. As all steels on quenching have to enter the η - γ area, η iron (martensite needles) will always be found in quenched austenite. The η phase is considered to be the carrier of the martensite hardness, the hardness of the steel then increasing with amount of η phase. The η phase is also assumed to have higher specific volume than the others, in order to conform to the changes in specific volume observed in hardened steels.

Hanemann also prepared X-ray spectrographs of his samples of steel, and the lines from the martensite showed such width that one

⁸² Hanemann, H., Über die Härtung des Stahles; Stahl u. Eisen, Jahrg. 46, 1926, pp. 1585-1587.

can only conclude that it is present in very small crystals. This agrees with the idea that the "needles" of martensite seen in the microscope are not single crystals but zones of alteration of austenite, the zones being made up of crystals too small to be seen in the microscope. Of course, using Hanemann's nomenclature, the crystals of η phase must be very minute. Also, the interference lines of the

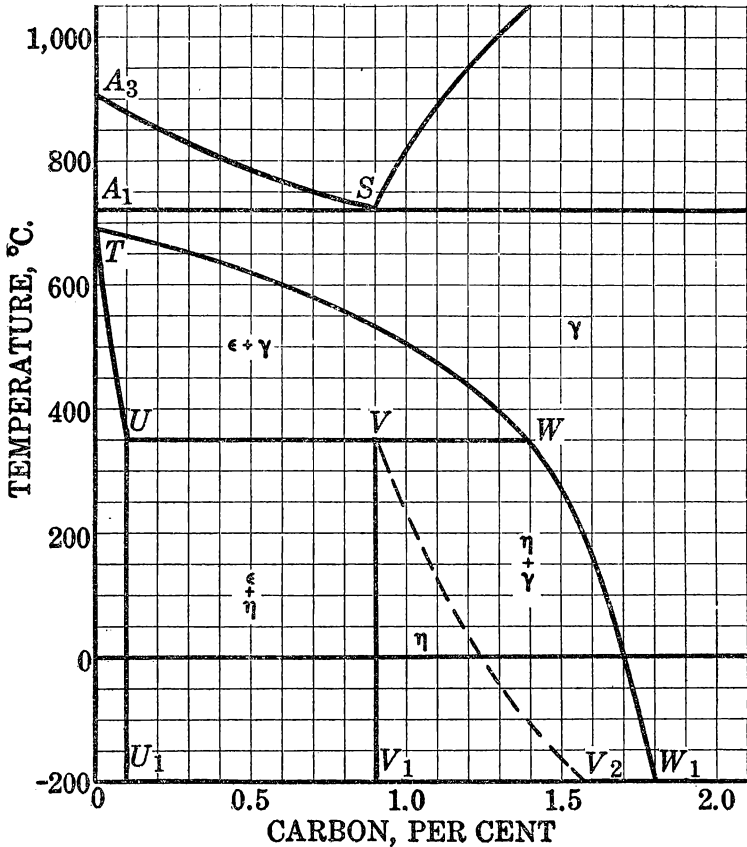


FIG. 71.—Hanemann's proposed addition to iron-carbon diagram

ϵ and η phases were almost identical, although Hanemann concludes that the widened lines are probably pairs of lines, one set due to ϵ and the other to η phase. This latter assumption is very questionable. The X-ray work of Heindlhofer and Wright³³ showed that the martensite lines fell in almost the same position as the α iron lines, except that they were very slightly displaced and the peaks of intensity were not so sharp. Probably Hanemann's ϵ phase is nothing more than α ferrite. He claims his investigation shows that

³³ See footnote 26, p. 205.

on tempering martensite it passes through two phases into ferrite, one at least of which he calls the zeta (ζ) state. His new nomenclature for troostite and sorbite, unaccompanied by any better interpretation than that of Honda advanced above, does not give the reader much satisfaction. Nevertheless the η phase is accepted by several recent German authors³⁴ as that formed when martensite is annealed at 235° C., and is probably best still called troostite.

Although Hanemann's diagram is an attempt to express the known relationships between metallographically visible phases of undetermined true composition, his renaming them has not contributed to clarifying the subject. Nevertheless, his diagram may yet prove to be quite useful and valuable.

DEFINITIONS

Cast iron.—Arbitrarily cast iron is defined as any alloy of iron and carbon with over 2.2 per cent of carbon.

White cast iron.—This is an alloy of iron and carbon which may have other elements present, but it is white by virtue of the fact that it has been produced by chilling quickly from the molten state, so that all of its carbon remains combined as Fe_3C (combined carbon). The alloy is brittle and hard.

Gray cast iron.—While this alloy might be identical in chemical composition with white iron, it has usually been made by cooling slowly enough so that part of the cementite originally crystallizing has had opportunity to split into iron and carbon, the latter being deposited in the form of graphite, which causes the gray color. The graphite also weakens the structure and makes the iron soft. Silicon dissolved in the cast iron increases the ease with which the carbon can be thrown out of solution. If enough silicon is present, it seems to replace carbon in the cementite, and it is difficult to chill such iron rapidly enough to keep the carbon in "combined" form instead of "free." On reheating white iron to temperatures between 800° and 1,100° C. graphitization sets in and proceeds slowly.

Malleable cast iron.—This is an alloy which has about the same analysis as white iron and has been originally cast as white iron. When reheated above the cementite-solubility curve and held for a period of time the cementite slowly decomposes and liberates carbon, which is much more finely disseminated than the graphite precipitated in gray iron; consequently the structure is not weakened to the same extent.

Graphite.—Graphite is the form of carbon deposited from molten cast iron on slow cooling. If enough silicon is present in the cast

³⁴ Trager, L., Die Vorgänge beim Anlassen gehärteter Stähle: Ztschr. Ver. Deut. Ing., Jahrg. 71, 1927, pp. 891-894.

iron, the graphite will also separate on more rapid cooling. Chill casting of cast iron results in white iron with no graphite and all the carbon "combined" as cementite.

Temper carbon.—Temper carbon is also graphite but is different in metallographic appearance, due to its origin. It forms, due to the splitting of cementite, during annealing of solid cast iron and is therefore usually very finely disseminated.

Graphitization of cast irons.—This has come to be a very important heat treatment, and the amount of malleable iron in use is quite large. A great amount of literature has been written discussing evidence as to whether temper carbon comes direct from cementite or from austenite, into which the cementite has dissolved before the carbon deposition can take place. Saito and Sawamura³⁵ distinguish between graphitization in the first stage and the second stage. The first stage is graphitization from free cementite above the A_1 point (726°C). The second stage is graphitization of eutectoid cementite and hypereutectoid cementite at temperatures below the A_1 point (see the iron-carbon diagram). As will be shown later, graphitization is accompanied by increase in volume. The more rapid the cooling rate of the original chilled casting the more easily is a cast iron graphitized during annealing.

Solubility of graphite in molten iron.—The iron-carbon diagram given in this chapter is not extended to include the higher temperatures. Ruer and Biren³⁶ have determined the solubility of graphite up to above $2,500^\circ\text{C}$. Their data are given in the table below. The samples were poured into a metal pipe and thereby chilled very rapidly. Samples of the metal were treated with nitric acid for determination of graphite in the usual way. The conclusion was reached that the graphite eutectic is at $1,152^\circ\text{C}$. for 4.25 per cent of C and the cementite eutectic at $1,145^\circ$ with 4.30 per cent of C. Although the very existence of two separate eutectics is now in doubt, these higher temperature solubility determinations are of interest because some of the alloys poured had more carbon than corresponds to pure cementite (6.67 per cent of C). On examination they all showed graphite, cementite, and some austenite, with no other crystalline substance. Evidently the diagram has been correctly drawn in showing no conditions under which a solid sample consisting exclusively of cementite could be prepared. Table 41 shows weight per cent of carbon at various temperatures.

³⁵ Saito, D., and Sawamura, H., A New Phenomenon Concerning the Graphitization of White Cast Iron and Its Application to the Manufacture of Black Heart Malleable Castings: College Eng. Kyoto Univ. Memoirs, vol. 5, 1927, pp. 1-59.

³⁶ Ruer, R., and Biren, J., Über die Löslichkeit des Graphits in geschmolzenem Eisen: Ztschr. anorg. allgem. Chem., Jahrg. 113, 1920, pp. 98-112.

TABLE 41.—Weight per cent of carbon at various temperatures

Temperature, ° C.	Weight, per cent of carbon	Temperature, ° C.	Weight, per cent of carbon
1,152	4.25	1,900	6.37
1,200	4.37	2,000	6.78
1,300	4.60	2,100	7.28
1,400	4.85	2,200	7.72
1,500	5.10	2,300	8.26
1,600	5.37	2,400	8.88
1,700	5.67	2,500	9.54
1,800	6.00		

CRITICAL POINTS IN IRON-CARBON ALLOYS

Polymorphic and other transformations take place in iron-carbon alloys in the same way that they do in pure iron. The A_2 , A_3 , and A_4 points of iron are found in the carbon alloys, although the first two are lowered in temperature by the addition of carbon and finally merge with the A_1 point to be described below. The individual transitions will be discussed separately.

Melting point.—The melting point of iron is lowered by alloying with carbon, as can be seen from the iron-carbon phase diagram. The eutectic with cementite is the lowest melting point of any of the iron-carbon alloys and occurs at $1,135^\circ$ C. Cementite itself does not exhibit a definite melting point but seems to decompose, giving a liquid lower in carbon than cementite, and graphite is the other product.

A_4 point.—The A_4 point of pure Fe is raised from $1,400$ to $1,486^\circ$ C.⁸⁷ by the presence of only 0.07 per cent of carbon (point F in the iron-carbon diagram). In other words, in this range of temperatures the field of stability of δ iron is encroached on by that of γ iron. The only iron-carbon alloys which can exhibit the A_4 point of iron are those with less carbon than point G in the iron-carbon diagram (fig. 70), about 0.38 per cent of C, according to Honda.⁸⁸

The peritectic point (G) of δ iron is at 0.18 per cent of carbon.

A_3 point.—Almost invariably when the addition of an element raises the A_4 point the A_3 point is lowered (and vice versa), and this is true for the carbon alloys. The iron-carbon diagram (fig. 70) shows the lowering suffered by the A_3 point as carbon is added to pure iron, the line A_3S being the one to indicate the point at which γ iron in the alloys is converted to α iron. The point S is the eutectoid between α iron and cementite. For alloys higher in carbon than the point S the A_3 point is coincident with the eutectoid or A_1 point.

⁸⁷ Tamura, Seiichi, Notes on Pseudo-Twinning in Ferrite, and on the Solubility of Carbon in Alpha Iron at the A_1 Point: Jour. Iron and Steel Inst., vol. 115, 1927, pp. 747-753.

⁸⁸ Honda, K., Constitutional Diagram of the Iron-Carbon System; Recent Investigations: Jour. Iron and Steel Inst., vol. 105, 1922, pp. 381-392.

This transition between the alloys containing α iron and those containing γ iron is of profound significance in the metallurgy of steel. However, it is not the purpose of this chapter to discuss the iron-carbon diagram from the standpoint of the steel metallurgist but rather from the standpoint of the physical chemist.

A₂ point.—The magnetic transition of pure iron is somewhat lowered by small amounts of carbon, dropping from 780° to 790° C. down to about 768° C. or even lower. With growing carbon content it is almost completely obscured, so that with steels of over 0.5 per cent of C it is nearly lost and is of no importance for the higher carbon alloys.³⁹

A₁ point.—The *A₁* point is the eutectoid temperature of the iron-carbon diagram, being the point at which the last remaining austenite (solid solution of cementite in γ iron) decomposes into pearlite during cooling, or the point where during heating cementite begins to redissolve in iron. Being connected with the properties of a solid solution, its temperature is not a sharp point and suffers considerable thermal lag. Although it is given as 715° C. in the iron-carbon diagram, it should be at about 726° C., according to some of the recent more precise work. The *A_{r1}* point occurs at various temperatures down to 700° or even 570° C., according to the rate of cooling, and the *A_{c1}* point at as high as 760° C., according to the rate of heating, the displacement upward being due to the fact that the crystallization during cooling has caused quite profound segregation in some cases. Rapid cooling through this point is the proper manipulation for production of martensite instead of pearlite, as described in earlier paragraphs. Theoretically the line *PK* should be horizontal, although it actually seems to rise with increasing carbon content, the rise being as much as 20° C., but is possibly associated with the presence of silicon as an impurity, silicon being known to raise this point. Manganese lowers the temperature of this point. It is here that α iron has its greatest dissolving power for carbon, being about 0.034 per cent, according to Tamura.⁴⁰ However, at this temperature γ iron can dissolve 0.9 per cent of carbon. Honda⁴¹ has shown that the *A₁* transformation of high-carbon steels on cooling takes place in two stages during rapid quenching, and with sufficiently rapid quenching the second stage can be entirely suppressed, so that the metal reaches room temperature in a "frozen" labile condition. The first stage seems to be conversion of γ to α

³⁹ Honda, K., On the *A₂* Line in the Equilibrium Diagram of the Iron-Carbon System: Tohoku Univ. Sci. Repts., vol. 15, 1926, pp. 247-250.

⁴⁰ See footnote 37, p. 211.

⁴¹ Honda, K., Stepped *A₁* Transformation in Carbon Steel: Jour. Iron and Steel Inst., vol. 105, 1922, pp. 393-407; also Sci. Rept. Tohoku Univ., vol. 8, 1919, p. 181; On the Formation of Martensite in Carbon Steels: Tohoku Univ. Sci. Repts., vol. 14, 1925, pp. 165-172.

iron, a thing very difficult to suppress by quenching and impossible to suppress in pure iron. The second stage consists of the separation of the carbon from the supersaturated solution in α iron, as discussed under the heading of martensite above. This result could be expected from the iron-carbon diagram, which shows the A_3 or γ - α transformation at a higher temperature than the A_1 or cementite (or carbon) precipitation, but for carbon contents of over 0.9 per cent, for which the A_3 and A_1 transformations are supposed to be merged, this result could not be predicted.

DISCUSSION

The above discussion deals with the so-called metastable iron-carbon system in which cementite is the form in which the carbon crystallizes during cooling. The A_{c_1} point in the stable system, in which the carbon appears as graphite, has been shown by Ruer⁴² to be at about 12° C. higher temperature than that of the metastable system (see iron-carbon diagram). Ruer places A_{c_1} (stable) at 733° C. and A_{c_1} (metastable) at 721° C.

As can be seen, the exact placement of the theoretically best average temperature for A_1 is a matter of choice, there being such great thermal hysteresis. However, Takahashi,⁴³ using a method of forming carburized iron by reaction with mixtures of CO and CO₂ at different temperatures, accompanied by microscopic examination, found that in his specimens pearlite was visible, below 726.5° C. and free cementite was visible above that temperature. This method of determining the point is a totally independent one and, provided the temperature scale used by Takahashi was accurate, could easily be the most reliable datum. However, some of Takahashi's data do not agree well with other data against which they can be checked, and on that account the datum needs further confirmation.

The A_1 change is one of the most complex in the whole system and needs much further work done on it. The confusion of nomenclature and interpretation of phenomena associated with this change is appalling. Matsushita,⁴⁴ by publishing a paper, started a series

⁴² Ruer, R., *Nachweis der Wärmetönung des Eisen-Kohlenstoff-Eutektoides*: Stahl u. Eisen, Jahrg. 46, 1926, pp. 918-920.

⁴³ Takahashi, Genske, *On the Equilibrium Between Austenite and the Carbon Oxides*: Tohoku Univ. Sci. Repts., vol. 15, 1926, pp. 157-175.

⁴⁴ Matsushita, T., *On the Slow Contraction of Hardened Carbon Steels*: Tohoku Univ. Sci. Repts., vol. 7, 1918, p. 43.

Honda, K., and Kikuta, T., *Stepped A_1 Transformation in Carbon Steel*: Jour. Iron and Steel Inst., vol. 105, 1922, pp. 393-407.

Jones, H. A., *The A_1 Range in Alloy Steels*: Jour. Iron and Steel Inst., vol. 107, 1923, pp. 439-451.

Scott, H., *Effect of Rate of Temperature Change on the Transformations in Alloy Steels*: U. S. Bureau of Standards Sci. Papers, vol. 15, 1919-20, pp. 91-100.

Honda, K., *On the Nature of Martensite Crystals*: Trans. Am. Soc. Steel Treating, Preprint, October, 1928.

of experimenters collecting evidence on the possibility of the A_1 transformation splitting into two, as mentioned above, and the probability of the existence of two kinds of martensite, to be called α and β martensite. The α form was supposed to be more easily etched, and during slow heating it tempered into β at 130° C. while the β form decomposed on heating through the range 200° to 280° C. Supercooled austenite has since been found to be stable up to higher temperatures than martensite. Also, the definitions of troostite and sorbite given above reflect the more modern theory of what happens at these various tempering temperatures. The most recent work of Honda indicates that the basis of the changes in the range 300° to 400° C. is the travel of carbon atoms through the strained lattice to the grain boundaries where cementite builds up. His studies of the two forms of martensite and the sorbitic steels are supported by new X-ray data showing α martensite to have a body centered tetragonal lattice while β martensite has a body centered cubic lattice. Austenite has a face centered cubic lattice.

In spite of this the evidence of Honda and Kikuta should be reviewed. Although Ar_1 occurs at 726° C. under sufficiently slow cooling, it is evidently a change demanding considerable time for rearrangement of the atoms in the iron-carbon structure and can be lowered in temperature by more rapid cooling, finally apparently splitting into two steps called A'_1 and A''_1 , or merely A' and A'' . The first was never observed below about 570° C. and the other never above 360° C. but as low as 200° C. More recent work points to the probability that while Ar_1 can be lowered to 570° C. or lower by rapid cooling, with faster cooling some of the austenite is supercooled and, instead of altering into pearlite for all temperatures below 360° C., it is altered into martensite in increasing proportions as the temperature is lowered. For each quenching temperature below about 100° C. there seems to be a definite amount of austenite converted into martensite, even down to the temperature of liquid air, as will be shown later in this section. Honda's great service in this period of uncertainty and conflicting theories has been to show that the A_1 transformation is a complex one in which not only the γ iron lattice alters to α iron, but in the latter the solubility of carbide (Fe_3C) is lower and that by rapid enough cooling supersaturated α solid solutions are obtained.

The great difficulty in study of these quenched products has been the definition and identification of the solid phases produced. Fair agreement on their metallographic names has been reached, but that is merely giving names to certain optical and other appearances and does not show the true physicochemical condition of each phase.

The A_0 point.—The A_0 point was overlooked by the early experimenters, whose “critical points” on cooling and heating curves were named numerically so that the subnumber applied to this transition when later discovered had of necessity to be zero. It is a point occurring only in iron-carbon alloys and not in pure iron, is the magnetic transition of cementite, and has been found similar in nearly all respects to the magnetic transition in pure iron, A_2 . It begins on a cooling curve at about 215° to 200° C. and extends downward about 50° to 60°. In a heating curve it ends at 215° C. Heat is liberated in this range during cooling and is absorbed during heating. Above 215° it is only paramagnetic. No change in crystal lattice takes place at this point.⁴⁵

The apparent thermal effect at A_0 , like the thermal effect at A_2 in pure iron, is evidently the integrated magnetic component of the specific heat, although it could seemingly be observed at different temperatures, according to the rate of heating or cooling. Morris and Scott,⁴⁶ working with a pearlite steel and with a high-carbon steel, found A_{c_0} occurred at 191° to 207° C., according to the heating rate and the carbon content, high heating rate and carbon content both raising the thermal point. In like manner A_{r_0} was raised by carbon content and lowered by cooling rate, although in this case the variations were between the limits 199° and 205° C.

The electrical resistance was used by Iitake⁴⁷ to locate the A_0 points of a series of carbon steels, and A_{c_0} was observed from 195° to 212° C., while A_{r_0} was observed at 192° to 200° C. These values agree better with the thermal measurements than with the magnetic measurements, just as was the case with the A_2 point in iron.

The A_0 point is lowered to room temperature by 0.5 per cent of boron or by 10 per cent of manganese, according to Tammann and Ewig.⁴⁸ These are substances which dissolve in the carbide, whereas substances which dissolve in iron alone, like gold, do not affect the A_0 point of steels.

CEMENTITE

From what has just been said, it can be seen that, while martensite is one of the most important constituents of steel from the metallographic-metallurgical standpoint, the chemical compound which is

⁴⁵ Wever, Franz, ————: *Mittel. Kaiser-Wilhelm Inst. Eisenforschung*, Jahrg. 4, 1922, pp. 67–80.

⁴⁶ Morris, M. G., and Scott, H., *Similarity of the Magnetic Change in Cementite and Ferrite*: *Chem. and Met. Eng.*, vol. 22, 1920, pp. 1069–1070.

⁴⁷ Iitake, Iitiro, *A Study of Cementite Transformation and of the Equilibrium Diagram of the System of Iron-Carbon by Means of Electrical Resistance Measurements*: *Tohoku Univ. Sci. Repts.*, vol. 7, 1918, pp. 167–175.

⁴⁸ Tammann, G., and Ewig, K., *Zur Kenntnis des Eisencarbids*: *Ztschr. anorg. allgem. Chem.*, Jahrg. 167, 1927, pp. 385–400.

at the bottom of the whole puzzle is the hard, brittle constituent cementite (Fe_3C) present in the steel. It is thought to be metastable with respect to iron and graphite but is nevertheless the constituent usually appearing in steels. A discussion of the properties of cementite itself is therefore in order.

Although a piece of iron can be "cemented" by treatment at proper temperatures (500° to $1,100^\circ$ C.) with either methane or carbon monoxide gases, according to the reaction, $3\text{Fe} + 2\text{CO} = \text{Fe}_3\text{C} + \text{CO}_2$, it is difficult to convert the iron completely into cementite, and the latter is therefore rarely seen in a pure state.

PREPARATION

The usual method of preparation is to treat samples of steels, preferably of eutectoid or hypereutectoid composition, which have been cooled sufficiently slowly, so that all the iron carbide could form large crystals and all the free iron be present as ferrite. On treatment with a large excess of dilute hydrochloric acid the ferrite goes into solution much more rapidly than the cementite, so that after standing at room temperature for as much as several weeks the residue contains only cementite. Tammann and Ewig⁴⁹ used a pearlitic steel containing 0.91 per cent of C and treated it for 8 to 10 days with 2N-HCl under a CO_2 atmosphere. The residual powder was washed with alcohol and dried at about 100° C. in an atmosphere of CO_2 . No precautions are mentioned about frequent changing of the acid, but attention must be called to the statement by Schenck and Stenkhoff⁵⁰ that when cementite is treated with acid solutions containing ferrous salts it yields graphite and hydrogen instead of hydrocarbons. Most of their work was done with sulphuric acid, and a temperature of 60° C. was used. In effect, their work tends to point out the danger of forming carbon which will remain in the residue with the cementite and contaminate it. On that account it is probably best to renew the acid in the solution used for preparation of Fe_3C , in order that the ferrous salt content could not rise to a dangerous percentage. Brodie, Jennings, and Hayes⁵¹ have made pearlitic steel by fusion of the theoretical amounts of armco iron and carbon and cooled them from 850° C. at the rate of 6° per hour, giving an almost perfect pearlite alloy of eutectoid composition. This was made into anodes and placed in a 5 per cent HCl electrolyte with platinum cathodes; a current density of 0.005 to 0.01 ampere per square centimeter was used. The electrolyte was changed every 12

⁴⁹ See footnote 48, p. 215.

⁵⁰ Schenck, R., and Stenkhoff, R., Über die Saurezerlegung des Eisencarbids: Ztschr. anorg. u. allgem. Chem., Jahrg. 161, 1927, pp. 287-303.

⁵¹ Brodie, G. H., Jennings, W. H., and Hayes, Anson, Heat of Formation of Cementite: Trans. Am. Soc. Steel Treating, vol. 10, 1926, pp. 615-629.

hours, and the anode slime of cementite was scraped off every day, washed in alcohol and then in ether, and then dried in vacuo. The product had the composition 93.33 per cent of Fe and 6.67 per cent of C, which is practically the theoretical composition of Fe_3C . Tammann and Ewig state that cementite has a galvanic potential only 0.032 volt nobler than iron. It can not therefore be expected to remain unattacked by acid in the alloy but should be dissolved less rapidly than the iron.

Another method of preparation employed by Ruff and Gersten⁵² was to melt crude cast iron, containing 4.13 per cent of carbon, 0.2 per cent of phosphorus, 0.15 per cent of manganese, 0.074 per cent of silica, 0.006 per cent of sulphur, and 0.005 per cent of copper, under excess carbon to saturate it completely with carbon; it was then suddenly quenched. The product was leached for four weeks with normal acetic acid, then broken up and treated with 0.2 normal HCl; the final residue was shaken with acetylene bromide, which on account of its high specific gravity floats off silica, graphite, and other impurities of low specific gravity, leaving a slime which was washed with alcohol and ether and when dried gave a bronze to yellow powder with 6.69 per cent of C and 93.28 per cent of Fe.

CRYSTAL SYSTEM

By X-ray analysis Wever⁵³ has shown that the various forms of cementite met in the iron-carbon diagram are not distinguishable from each other by their crystal lattices, and that Fe_3C crystallizes in a rhombic structure with edge lengths, $a=4.481$, $b=5.034$, and $c=6.70$ Ångstrom units. No change in structure is suffered on passing through the magnetic transition temperature at 215°C ., the lattice merely expanding slightly with temperature, as would be expected (thermal expansion).

The X-ray data of Westgren and Phragmen⁵⁴ are very similar. They report the elementary parallelepiped to have the dimensions, $a=4.53$, $b=5.22$, and $c=6.77$ Ångstrom units, and to contain 4 molecules of Fe_3C , in good agreement with Wever.

DENSITY

From the dimensions of the crystal lattice Wever calculates that pure cementite would have a density of 7.82 grams per cubic centimeter, while Westgren and Phragmen calculate 7.68. With these densities of cementite calculated from the densities of steels in which

⁵² Ruff, O., and Gersten, E., Über das Triferro-carbid (Zementit) Fe_3C : Ber. deut. chem. Gesell., Jahrg. 45, 1912, pp. 63-72.

⁵³ See footnote 45, p. 215.

⁵⁴ Westgren, Arne, and Phragmen, Gösta, X-Ray Studies on the Crystal Structure of Steel: Jour. Iron and Steel Inst., vol. 109, 1924, p. 159.

it is present in known amounts can be compared. For instance, in pearlitic carbon steels (0.9 per cent of C), which consist of 13.5 per cent of Fe_3C and 86.5 per cent of Fe, if the density of the steel sample and of the pure iron is known, one can calculate the density of the cementite by subtraction. Thus, Cross and Hill⁵⁵ give the densities of a series of well-annealed carbon steels, in which the cementite and ferrite were present in well-defined large plates as pearlite, from which the density of pearlite is interpolated to be 7.8296 grams per cubic centimeter at 20° C. Taking the density of ferrite as 7,864, the density of pure cementite is calculated to be 7.63.

Ishigaki⁵⁶ has listed the results of all previous investigators and has himself redetermined the density of cementite by extrapolating the density concentration curves of a series of annealed steels and cast irons to the concentration of cementite, using hot forged and annealed specimens to eliminate intercrystalline cracks. His figure is 7.662.

International Critical Tables (first edition, 1926) gives a figure—7.4—from Ruff and Gersten's direct determination of Fe_3C powder (7.396), which seems to be entirely out of line with all other carefully determined estimates; therefore even the first decimal point is indicated as uncertain. This value has been disregarded, because calculations from precise determinations on steels are possible.

If graphite and iron combined to form Fe_3C with simple addition of their atomic volumes, by assuming graphite to have a density of 2.255 (International Critical Tables), we find that the density of the cementite would be 6.743. The formation of the Fe_3C molecule, therefore, involves a considerable decrease in volume, being 12 per cent or 3.1937 cubic centimeters per gram molecule.

The various values of density and specific volume of cementite are given in Table 42.

TABLE 42.—*Density and specific volume of cementite*

Authority	Specific gravity	Specific volume		Reference
		Per gram	Per molecule	
Benedicks.....	7. 74	0. 12920	23. 1940	Thesis, Upsala, 1904, 45 pp.
Levin and Dornhecker....	7. 59	. 13175	23. 6518	Ferrum, Jahrg. 11, 1914, p. 321.
Ruff and Gersten.....	7. 396	. 13557	24. 3375	Ber. Deut. chem. Gesell., Jahrg. 46, 1913, pp. 394-400.
Wever.....	7. 82	. 12788	22. 9570	See footnote 45, p. 215.
Westgren and Phragmen.	7. 680	. 13020	23. 3735	Jour. Iron & Steel Inst., vol. 109, 1924, p. 167.
Andrew and Honeyman.	7. 66	. 13055	23. 4364	Carnegie Schol. Mem., vol. 13, 1924, p. 13.
Takahashi.....	7. 662	. 13051	23. 4292	See footnote 43, p. 213.
Selected datum.....	7. 67	. 13038	23. 4058	

⁵⁵ Cross, H. C., and Hill, E. E., Density of Hot-Rolled and Heat-Treated Carbon Steels: U. S. Bureau of Standards Sci. Papers No. 562, vol. 22, 1927, pp. 451-466.

⁵⁶ See footnote 98, p. 173.

ACTION TOWARD REAGENTS

The chemistry of cementite has not received much attention. The studies of Schenck and Stenkhoff, above mentioned, have determined the conditions under which it generates hydrocarbons and those under which carbon is deposited. Presumably it will also precipitate metallic copper from copper sulphate solutions. There is also recorded the fact, mentioned by Tammann, that cementite is 0.032 volt nobler than iron toward iron sulphate solutions. The metallographers have developed etching solutions for recognizing cementite, and one of the common methods of recognition is to note that cementite is darkened by boiling sodium picrate solution and not by alcoholic nitric acid, and that Stead's reagent does not precipitate copper on it.

CEMENTITE AT VARIOUS TEMPERATURES

As far as can be proved, cementite is metastable at all temperatures, being endothermic and possessing positive free energy. Therefore, although it appears stable at room temperature, with rising temperature it begins to decompose into carbon (graphite) and ferrite (if below the A_1 point), or graphite and austenite (if above the A_1 point). This graphitizing of cast iron is an important industrial operation in the production of malleable cast iron, as described earlier in this section. The rate of decomposition is rather slow even above 900° C., which is the common lowest temperature of commercially rapid graphitization, and yet the articles being graphitized must not be heated above the eutectic point, 1,135° C. Therefore, this slow decomposition of cementite in commercial practice calls for two to five day periods of time. One thing which hinders it is the fact that an expansion in volume must take place when it decomposes into its elements, and in a rigid matrix of iron there is too little room for the reaction to go on. While the commercial annealing temperature is above 900° C., graphitization of cementite can be observed in the laboratory at as low as 700° C.

If the cementite particles are near the surface of a piece of iron or steel, where they can expand during splitting, they do so. For instance, R. Ruer⁵⁷ reports heating a piece of white iron to 1,140° C. and finding only the exterior graphitized. When the matrix of iron is entirely dissolved away the cementite on heating begins to decompose at a much lower temperature, being noticeable at 500° C. Tammann and Ewig⁵⁸ sealed cementite powder in glass tubes to prevent access of air and heated them for 2-hour intervals at 300°, 400°, and 500° C., then cooled and tested for magnetization to determine the amount of splitting. The 300° and 400° samples were unaltered. The

⁵⁷ See footnote 42, p. 213.

⁵⁸ See footnote 48, p. 215.

500° C. sample had lost about two-thirds of its 200° to 215° C. magnetic change, while five hours' heating seemed to have completely decomposed it. During heating it was noticed that when it decomposed the cementite powder gave off gases (100 c. c. per gram of Fe_3C) containing about 15 per cent of CO_2 , 33 per cent of CO , 40 per cent of H_2 , 8 per cent of N_2 , 3 per cent of CH_4 , and minor amounts of unsaturated hydrocarbons. Since cementite in steels does not evolve gas, it is supposed that these gases result from action of water remaining from the solution in which the iron was dissolved away from the cementite grains, or the gases were formed by action of the acid during preparation of the powder and then adsorbed. The cementite made from steel annealed 24 hours at 700° C. by Schenck and Dingmann was much more stable and gave off only 2.3 c. c. of gases on heating through the same range. It could also be heated for long periods to 800° C. without much decomposition. (See footnote 59, p. 98.)

CURIE OR MAGNETIC TRANSITION POINT

As mentioned in connection with steels, cementite has a Curie point at which temperature the ferromagnetism is lost, and the material above that point is only paramagnetic. This temperature, the A_0 temperature of steels, is at about 215° to 220° C. The amount of the magnetic change at this point is a good index of the amount of cementite present in a steel. A quenched steel consisting of martensite and austenite shows no A_0 point, but on tempering the A_0 magnetic change becomes more pronounced. On long heating at slightly higher temperatures with gradual graphitization the amount of magnetic change at 215° again decreases. The work of Tammann and Ewig on steels showed that the same magnetic change took place whether the cementite was formed during ordinary slow cooling with formation of lamellar pearlite or during tempering and formation of granular or spheroidal cementite—for a definite carbon content (cementite content) the magnetic effect was the same.

The cementite magnetic transformation, like that in iron, takes place over quite a range of temperature, and on cooling the apparent evolution of heat can be detected over the whole range. Honda and Takagi⁵⁹ publish a differential cooling curve of a steel in which the apparent heat evolution begins at 215° and is ended at about 175° C. One of the temperature-magnetization curves of these investigators is given in Figure 72, from which it can be seen that the magnetization of cementite is much less than that of metallic iron.

⁵⁹ Honda, K., and Takagi, H., The Magnetic Transformation of Cementite: Tohoku Univ. Sci. Repts., vol. 4, 1915, pp. 161-168.

Magnetic saturation of cementite is reached at $4\pi J=12,350$ gauss, according to F. Stablein and K. Schroeter (*Ztschr. ausg. u. allgem. Chem.*, Jahrg. 174, 1928, pp. 193-215).

CEMENTITE IN MOLTEN IRON

Cementite is credited with being the compound of carbon which is the first to separate from a melt, and opinions differ as to whether graphite is ever the primary carbon compound separating from a molten steel or hypoeutectic cast iron. Such a competent observer as Honda⁶⁰ states that graphite does not form directly from any

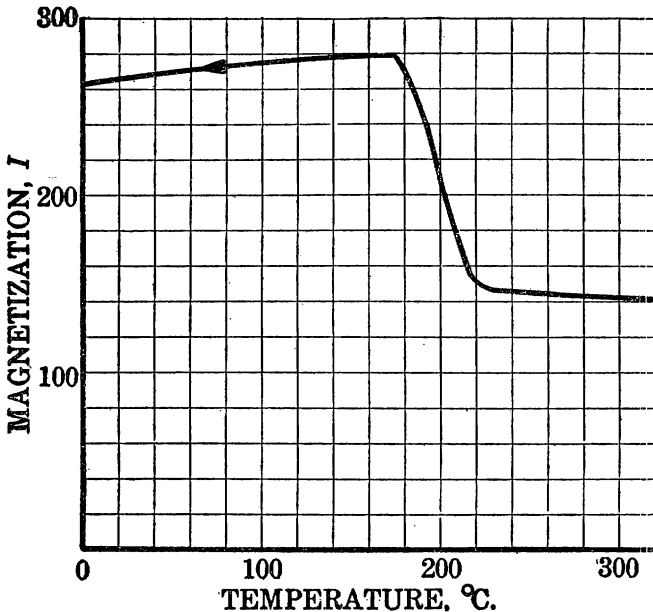


FIG. 72.—Magnetization curve of a steel near A₀.

melt, as proved by a careful series of quenching experiments, but graphitization takes place in the range 1,135° to 1,050° C. He feels therefore that the double diagram above the eutectic temperature is incorrect and that the carbon is all in solution as cementite. No satisfactory thermal data are available to judge the possible existence of a field of stability for cementite, but in the solid states the free energy is always positive, and qualitatively it can be said that it increases in positive value with rising temperature, meaning thereby that the stability of the cementite with respect to carbon decreases. The magnetic susceptibility of the molten alloys remains constant for 200° C. above the melting point, which is as far as has been

⁶⁰ See footnote 38, p. 211.

observed, indicating that if the carbon is present as cementite there is no dissociation of the cementite through that range. The melting of pure cementite has never been observed.

INTERFACIAL TENSION BETWEEN CEMENTITE AND FERRITE

This datum has been approximated by Thompson,⁶¹ who attempted to determine the change in solubility of cementite in ferrite as a function of fineness of division of the cementite particles by conductivity methods. Identical samples of steel wire were heat treated, one being slowly annealed to give coarse cementite and the other quenched and tempered at 500° C. to give fine-grained granular cementite. The calculation, based on reasonable but unsafe assumptions and approximations, gave the value 1,350 dynes per centimeter, which can be compared with 72 dynes for the surface tension of water in air at normal temperatures.

SPECIFIC RESISTANCE

Recent work by Masumoto⁶² on a series of carbon steels and cast irons has given their specific resistance over a wide range of composition, and it has been extrapolated to the composition of pure cementite and found to be 14.0×10^{-5} ohms per cubic centimeter at 34.0° C., compared to that of pure iron, which is determined from the same series by extrapolation to be 1.044 times 10^{-5} ohms.

These data can be compared with a similar set of measurements by Stablein,⁶³ who worked on a series of pure carbon steels and obtained 1.000×10^{-5} ohms (10 microhms) for pure iron and 7 microhms instead of 14 for pure cementite. The data on iron check well but are quite conflicting on cementite and require further elucidation. The long extrapolation probably is the principal difficulty. Also, considering the wide variety of forms of the carbon in steels and the variation in crystal size and shape of the ferrite and cementite in steels according to the previous heat treatment, this variation in the apparent resistance of the cementite is not surprising.

THERMAL CONDUCTIVITY

Masumoto also determined the thermal conductivity of his series of steels at the same temperature and found on extrapolation that the conductivity of pure cementite would be 0.017 gram calorie per

⁶¹ Thompson, F. C., The Interfacial Tension Between Carbide of Iron and Iron: *Trans. Faraday Soc.*, vol. 17, 1922, pp. 391-392.

⁶² Masumoto, H., Electric and Thermal Conductivities of Carbon Steel and Cast Iron: *Tohoku Univ. Sci. Repts.*, vol. 16, 1927, pp. 417-435.

⁶³ Stablein, F., Über den Einfluss des gebundenen Kohlenstoffs auf den spezifischen Widerstand des Eisens: *Ztschr. Phys.*, Jahrg. 20, 1923-24, pp. 209-228.

degree per centimeter per second, as compared to 0.1741 calorie for pure iron at 34° C.

MAGNETIC SUSCEPTIBILITY

Working with a series of carbon steels at high temperatures in a similar manner, Honda and Endo⁶⁴ extrapolated to the magnetic susceptibility of pure cementite at a series of temperatures, which when plotted are a straight line. The four data are:

Temperature, ° C.	Susceptibility
800	24.3×10^{-6}
900	24.0×10^{-6}
1,000	23.7×10^{-6}
1,100	23.5×10^{-6}

HEAT CAPACITY

No direct determinations of the specific heat of cementite at any temperature seem to be available. As shown above, pure powdered cementite can not be heated above 400° C. without decomposition, but the specific heats up even that far would be very useful. Umino⁶⁵ has observed the heat contents of a whole series of carbon steels (commercial) containing up to 2.84 per cent of carbon and has extrapolated thence to the composition of cementite, 6.67 per cent of C, in order to get the specific heat of pure cementite. His tabulated total heats and true specific heat are given in Table 43.

However, believing that the long extrapolation involved in Umino's calculations was likely to lead to inaccuracies, the writer carried out another series of calculations based on Umino's data. Up to the A_1 point, 720° C., the heat contents of carbon steels which have been slowly cooled should consist of two portions, the heat due to the ferrite (iron) and the heat due to the cementite, which being confined in the iron matrix does not dissociate during heating under these conditions. From the total heat at any temperature for 1 gram of steel one may subtract the total heat of the calculated content of ferrite, leaving the total heat of the cementite. This method of subtraction was used on the total heats for three of Umino's steels, the ones containing respectively 1.575, 0.994, and 0.795 per cent of carbon. The total heats of these three steels at 700° C., for instance, averaged 113.13 calories per gram above 0° C., and the maximum deviation from the mean was about 1 calorie.

⁶⁴ Honda, K., and Endo, H., The Magnetic Susceptibility of the Iron-Carbon Alloys at High Temperatures and the Equilibrium Diagram of the System: Tohoku Univ. Sci. Repts., vol. 16, 1927, pp. 627-637.

⁶⁵ Umino, S., On the Specific Heat of Carbon Steels: Tohoku Univ. Sci. Repts., vol. 15, 1926, pp. 331-369.

Using the total heats of cementite calculated from Umino's three steels by the method of subtraction, the true specific heats, derived by taking the slopes of the total heat curves at each temperature reported, are reported in Table 43 and plotted in Figure 73. Umino's results are likewise reported for comparison. The advantage of using the subtraction method is that it shows a "hump" in the true specific heat curve at the magnetic transition temperature, whereas Umino's original work did not. Such a hump is expected at a magnetic transition.

TABLE 43.—*Thermal data for cementite*

[Calculated from total heats of annealed steels (Umino): 1. By extrapolation to analysis of cementite (Umino). 2. By subtraction of total heat of iron (Ralston). (Figures in parentheses by extrapolation from adjacent portions of curve)]

Temperature		Total heat		True specific heat			Relative entropy
° C.	$\ln T$	Extrapolation	Subtraction	Extrapolation	Subtraction	Per mol	
0	5.61	0	0	(0.1475)	(0.1500)	26.9	0
100	5.92	14.80	15.00	.1480	.1500	26.9	5.79
200	6.17	29.70	28.76	.1495	.2867	51.5	12.92
220	6.22	-----	38.50	.1497	.5600	100.4	-----
			31.5	-----	.1000	17.9	16.90
300	6.35	44.70	46.56	.1525	.1175	21.1	18.94
400	6.52	60.20	59.66	.1575	.1350	24.2	23.40
500	6.66	76.20	73.23	.1660	.1650	29.6	27.2
600	6.78	93.42	92.66	.1785	.2000	35.9	31.01
700	6.89	112.03	113.13	.1925	.2100	37.7	34.8
720	6.91	-----	(118.2)	.1955	.2167	38.9	35.68
800	6.98	131.92	179.90	.2100	-----	-----	-----
900	7.03	153.90	165.82	.2264	-----	-----	-----

These average total heats were plotted, and the plot showed two branches, the two lower points (100° and 200° C.) falling on one branch and out of line with the curve for the points for 300° C. and above. This result was ascribed to the magnetic transformation at 220° C., so both lines were extended to that temperature. Of course, the magnetic transformation is known to extend downward over a considerable temperature range, but if all the change could be concentrated into an instantaneous one at 220° C., the two heat contents given in the tables at 220° C. (31.5 and 38.5 calories, respectively) would show a difference of 7 calories (per gram of cementite) due to the magnetic transformation.

A more accurate way of calculating the "magnetic component" of the specific heat—in other words, to calculate the "distributed latent heat" of the magnetic transformation—is to plot the true specific heat as a function of temperature and take the area between the observed curve and the estimated normal curve, if the magnetic component were not superposed on the ordinary specific heat. Although too few data were available to do so with accuracy in this case, it was nevertheless attempted, assuming the magnetic component to become appreciable at about 190° C.; the result was 8 calories.

In a more recent publication, Umino⁶⁶ has studied three carbon steels of 0.57, 0.94, and 1.16 per cent of carbon, respectively, determining their total heats more precisely at short intervals from room temperature up to 300° C. and calculating the true specific heats for purposes of obtaining the area between the observed curve and the estimated "normal" curve. This gave results of 0.86, 1.38, and 1.63 calories, which are nearly proportional to the three above carbon contents and when referred to 1 gram of pure cementite would

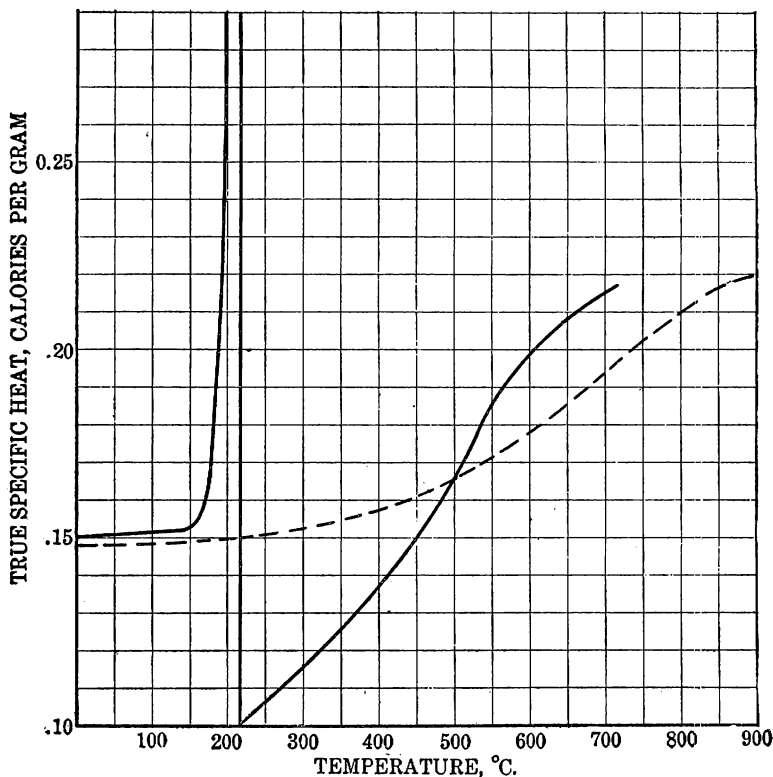


FIG. 73.—True specific heat of cementite. Solid line, Ralston calculation; dotted line, Umino calculation

amount to 9.72 calories. This result compares favorably with the above two rough estimates of 7 and 8 calories, respectively, per gram of cementite. Referred to 1 mol of cementite, it amounts to 1,742 calories as the total extra energy necessary to heat cementite from room temperature through the A_0 point (220° C.). If desired, it can be called the energy necessary to demagnetize the steel.

The total heats for 800° and 900° C. in the table are seen to be quite out of line with the other data. Those obtained by extrapola-

⁶⁶ Umino, S., On the Latent Heat of Fusion and the Heat of Transformation of Some Metals: Tohoku Univ. Sci. Repts., vol. 16, 1927, pp. 775-798.

tion by Umino encouraged him to calculate the specific heat from them, but those obtained by the more accurate subtraction method give a higher apparent total heat at 800° than at 900° C. This is undoubtedly due to the fact that above 720° C. the cementite of the steels goes back into solid solution (austenite) during heating, and the rapid quenching in Umino's calorimeter produced a sample with some undercooled austenite and a great deal of martensite. If the transformation from austenite into its various transformation products is suppressed, the corresponding heat of transformation will fail to appear, which probably explains the above anomaly where the sample quenched from 900° C. actually gave up less heat to the water of the calorimeter, because the more drastic the quenching the greater the amount of retained austenite in a steel. On account of the A_1 transformation, therefore, no final calculations were made with any data higher than 720° C.

ENTROPY

As the low-temperature specific heat data on cementite have never been collected, it is impossible to obtain the absolute entropy of cementite at room temperature. However, if the above specific heat data are used, the relative entropies of cementite at temperatures up to 720° C. have been calculated and are referred to the ice point, 0° C. (273.1° K.). These data are given in the last column of Table 43. The relative entropy at 220° C. is 16.90 and at 720° is 35.68 calories per degree per mol above the entropy at 0° C.

HEAT OF FORMATION

Serious disagreement has existed in the literature on the heat of formation of Fe_3C , and only recently have determinations been made which have helped dissipate the reasonable indecision of those who have tried to choose a reliable value. The most successful work has been done by preparing pure cementite and burning it in a combustion bomb calorimeter. Dissolution of Fe_3C in solvents seems to have been disappointing, due to formation of hydrocarbons by acids in the solvents, the hydrocarbons being formed in unknown ratios and quantities and part of the carbon of the Fe_3C being left as graphite. The third method which has been used has been to determine the equilibrium constant of the reaction $3\text{Fe} + 2\text{CO} = \text{Fe}_3\text{C} + \text{CO}_2$, at temperatures high enough to give a reasonable rate of reaction and yet not high enough to cause solution of the cementite in γ iron (above 720° C.), and thence calculate the heat of formation thermodynamically.

In Table 44 are tabulated the various observations, and following is a discussion of each. The conventions favored by Lewis and

TABLE 44.—Heat of formation of cementite

[Heat absorption indicated by + sign; heat evolution indicated by - sign]

Authority	Heat, calories		Temperature, ° C.	Date
	Per mol	Per gram		
Combustion determinations:				
Ruff and Gersten.....	+15,100	+84.0	17	1911
Yermilov.....	-2,270	-12.6	17	1911
Ruff and Gersten.....	+15,300	+85.25	17	1913
Ruff and Gersten (recalculated).....	+14,330	+79.8	17	1926
Brodie, Jennings, and Hayes.....	+13,580	+75.6	25	1926
From equilibrium data:				
Schenck, Semiller, and Falcke.....	-8,940	-49.7	650	1907
Schenck.....	+15,405	+85.9	650	1927
Maxwell and Hayes.....	+19,163	+106.8	650	1926
Do.....	+19,161	+106.8	700	1926
From dissolution in CuCl ₂ solution: Campbell.....	-8,494	-47.2	15	1901
Selected values.....	+13,580	+75.6	25	-----
	+15,400	+85.7	700	-----

Randall, that heat absorption will be called positive and heat evolution negative, have been adopted.

Work of Ruff and Gersten and others.—The first combustion calorimetry on iron carbide was that of Ruff and Gersten,⁶⁷ who prepared pure iron carbide and burned it in an enamel-lined Berthelot bomb with compressed oxygen. The products of combustion were assumed to be mixtures of FeO and Fe₃O₄, and the values for the heats of formation of these two oxides chosen in making the calculation influenced the result, +15,100 calories. This work has been criticized by Hayes (see below), who fails to understand how spattering of the charge and slagging of the materials of the calorimeter by the ferrous oxide formed were avoided. Nevertheless, recalculation of Ruff and Gersten's results with more recently accepted values for the heats of formation of the iron oxides gives Hayes a value of +14,330 calories from the original Ruff and Gersten data. Ruff and Gersten⁶⁸ themselves, on learning of simultaneously determined results of Yermilov in Russia, redetermined some of the iron oxides heat of formation and recalculated their own results in 1913 to +15,300 calories per mol, but this can be discarded in favor of Hayes's recalculation.

Yermilov⁶⁹ likewise burned pure cementite in a Berthelot bomb but apparently was unable to obtain the precision obtained by Ruff and Gersten. He states that, according to his results, the carbide is slightly exothermic in its heat of formation, -2,270 calories, but that the uncertainties of his work are at least this great, and there-

⁶⁷ Ruff, O., and Gersten, E., Über Triferrocarbid (Zementit) Fe₃C: Ber. Deut. chem. Gesell., Jahrg. 45, 1911, pp. 63-72.

⁶⁸ See footnote 67.

⁶⁹ Yermilov, Y., Heat of Formation of Iron-Carbon Alloys (original in Russian): Jour. Russ. Met. Ges., vol. 4, 1911, pp. 357-365; not available, but abstracts in Chem. Abst., vol. 6, 1912, p. 2387.

fore it may have a zero heat. The heat of formation of FeO was taken as 66,713, and that of magnetite as 274,660 calories, determined in the same calorimeter, but the latter heat, especially, is many thousands of calories higher than the work of most other authors. Yermilov's datum is therefore regarded as of little value.

The most painstaking work is that of Brodie, Jennings, and Hayes,⁷⁰ who burned pure cementite powder in an Emerson oxygen bomb calorimeter with many precautions to prevent dusting and chilling of unburned carbide on the walls and slagging of the materials of the calorimeter by ferrous oxide. A thin layer was spread out over a magnesia tray under an inverted alundum crucible. The product of combustion differed from that of Ruff and Gersten, being red dust of ferric oxide and a certain amount of black magnetic oxide material which was found to have a slight excess of ferric oxide. The heats of formation of the iron oxides used in calculation were ferrous oxide, -63,560; magnetite, -267,400, and ferric oxide, -194,340 calories. This gave a heat of formation of +13,580 calories for cementite. This determination is accepted herewith as the most reliable datum yet available for room temperature.

Thermodynamic calculations.—Thermodynamic calculations of the heat of formation rest on the determination of equilibria in the reversible reactions which can be added to give the equation $3\text{Fe} + \text{C} = \text{Fe}_3\text{C}$. For instance, the equilibria in the reactions $3\text{Fe} + 2\text{CO} = \text{Fe}_3\text{C} + \text{CO}_2$, and $\text{C} + \text{CO}_2 = 2\text{CO}$, which add to give the desired reaction above, have been measured by numerous experimenters. Denoting the equilibrium constant by K , a plot of the natural logarithms of K at various temperatures against the reciprocal of the absolute temperatures in each of the equations gives a nearly straight line whose slope at any desired temperature is the heat of reaction at that temperature and, adding the two heats of reaction, gives the heat of reaction in formation of Fe_3C from its elements. In this manner Schenck, Semiller, and Falcke⁷¹ calculated the heat of formation to be -8,940 calories at 650° to 700° but later abandoned this value. They had chosen from a great mass of available equilibrium data those which would give a calculated heat of formation in agreement with the previous estimate of Campbell. Also, insufficient care was given to assuring the absence of free carbon in their solid phases. However, in a later paper, Schenck,⁷² using more reliable

⁷⁰ See footnote 51, p. 216.

⁷¹ Schenck, R., Semiller, H., and Falcke, V., Experimentelle Studien über die Reduktion und die Carbidbildung beim Eisen: Ber. Deut. chem. Gesell., Jahrg. 40, 1907, pp. 1704-1725.

⁷² Schenck, R., Gleichgewichtsuntersuchungen über die Reduktions-, Oxydations und Kohlungsvorgänge beim Eisen; IV: Ztschr. anorg. allgem. Chem., Jahrg. 164, 1927, pp. 145-185.

equilibrium data, recalculated the heat of formation of Fe_3C to be +15,405 calories at 525° to 720° C. As pointed out by Maurer and Bishof,⁷³ Schenck was again choosing from his data those which afforded the best agreement with the published datum of Ruff and Gersten, with which he wished to check. They calculated the heats of formation from the other recently published data in Schenck's paper and found values from +24,000 to -30,000 calories. In justice to Schenck, they pointed out in addition that most of these widely varying data come from observations at temperatures above 700° C., where the presence of cementite in the solid material is doubtful, except where conditions assuring the saturation of austenite with cementite and the presence of excess free cementite can be guaranteed. Below 700° C. the published datum of Schenck is probably the best choice and can be accepted.

The most carefully described work on carburization equilibria, according to the above equations, is that of Maxwell and Hayes, described later under the discussion on the free energy of formation of Fe_3C . Using the thermodynamic relations of the free energy change to the heat of formation $d(\Delta F)/dT = (\Delta F - \Delta H)/T$, and making the assumption that the first member of this equation was constant over the short temperature interval 650° to 700° C., they calculated the heats of formation of cementite at 650° and 700° C. to be, respectively, +19,163 and +19,161 calories. These data are probably as reliable as any.

Dissolution in solvents.—Calorimetric work by dissolution of cementite in solvents has been performed only by Campbell,⁷⁴ who used a slightly acid solution of ammonium or potassium cupric chlorides. The reaction is supposed to be $\text{Fe}_3\text{C} + 6\text{CuCl}_2 = 3\text{FeCl}_2 + 3\text{Cu}_2\text{Cl}_2 + \text{C}$. Neutral solution failed to attack Fe_3C rapidly enough. Previous reviewers have always pointed toward the probable evolution of hydrocarbons due to action of the acid and the uncertainty of the residual graphite containing all the original carbon. Brodie, Jennings, and Hayes tested the solution and found no evolution of hydrocarbons, but they report the residual carbon weighed 50 per cent too much and contained iron. The Campbell datum, -8,494 calories, is entirely out of accord with all other reliable work and is therefore thought untrustworthy.

⁷³ Maurer, Ed., and Bishof, W., Gleichgewichts Untersuchungen über die Reduktions- und Kohlungsvorgänge beim Eisen: Stahl u. Eisen, Jahrg. 48, 1928, pp. 15-21.

⁷⁴ Campbell, E. D., The Heat of Formation of Carbides and Silicates of Iron: Jour. Iron and Steel Inst., vol. 59, 1901, pp. 211-226.

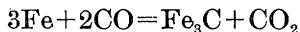
TABLE 45.—Cementite, change in heat of formation with temperature

Temperature, ° C.	$C_p \text{ Fe}_3$	$C_p \text{ C}$	ΣC_p	$C_p \text{ Fe}_3\text{C}$	ΔC_p	$\Delta H_2 - \Delta H_1$	ΔH_T
25	18.46	2.30	20.76	26.90	+6.14	0	+13,580
100	19.29	2.70	21.99	26.90	+4.91	+432	+14,012
200	20.43	3.23	23.66	51.50	+27.84	+780	+14,360
220	20.73	3.33	24.06	{ 100.4 17.9	{ +76.5 -6.16	+2,825	+16,405
300	21.93	3.75	25.68	21.1	-4.58		
400	23.97	4.25	28.22	24.2	-4.02	+2,000	+15,580
500	26.46	4.71	31.17	29.6	-1.57	+1,880	+15,460
600	29.73	5.15	34.88	35.9	+1.0	+1,880	+15,460
700	35.19	5.54	40.73	37.7	-3.0	+1,830	+15,410
720	37.41	5.61	43.02	38.9	-4.1	+1,800	+15,380

Derived specific heat.—Some means of comparing the combustion data with the equilibrium calculations directly at the same temperature is desirable. It can be done by the use of the derived specific heat of cementite given earlier. The thermodynamic definition of specific heat is that it is the differential with respect to temperature of the total heat content of a unit of substance. Therefore, in a chemical reaction $d\Delta H/dT = \Delta C_p$. By integrating between the temperature limits T_1 and T_2 we get $\Delta H_2 - \Delta H_1 = \int_{T_1}^{T_2} \Delta C_p dT$. By tabulating the true specific heats (molal) of cementite, iron, and carbon it is possible to get values of the change in specific heat of the system ΔC_p due to the formation of cementite from its elements. This was done (see Table 45) and the values plotted as a function of temperature in order that the integration could be done graphically by taking the area under the curve between 25° C. and the desired temperature. This tabulation shows that the change in the heat of reaction due to raising the temperature from 25° to 700° C. is 1,830 calories greater heat absorption. Therefore, if the Brodie, Jennings, and Hayes datum of +13,580 calories at 25° C. is taken as the best available one, the calculated heat of reaction at 700° C. would be +13,580 + 1,830 = +15,410 calories. This compares most favorably with the most recent Schenck datum, at 650° to 700°, +15,405 calories, and not so well with the Maxwell and Hayes datum of +19,161 calories at the same temperature. In the above calculation the data of Umino on pure iron and carbon were used because the above specific heat data on cementite had been derived from his observations, and his other data should therefore be more logically comparable.

FREE ENERGY

Only one experimenter has published data on the free energy of cementite. Maxwell and Hayes⁷⁵ sought to measure the equilibria in the reaction



directly and from them to calculate the corresponding free energy change by the simple relation $\Delta F = -RT \ln K$, in which R is the gas constant (1.98 calories per mol) and T the absolute temperature. This, taken in conjunction with the existing data on the reaction $\text{C} + \text{CO}_2 = 2\text{CO}$, allowed calculation of the free energy change in the reaction $3\text{Fe} + \text{C} = \text{Fe}_3\text{C}$ by simply adding the above equations and their corresponding free energy changes. The equilibrium constant desired was measured by treating a pearlite steel with a mixture of CO and CO₂ at constant temperature until the gas analysis became constant. A pearlite steel consists of the two desired phases, Fe and Fe₃C, at all temperatures below the A_1 point, 720° C. If these can be brought into equilibrium with the gases, the equilibrium constant is then the ratio of the partial pressures of CO₂ and CO. They were successful in attaining constant ratios at two temperatures, 650° and 700° C. There was some tendency for Fe₃C to split and give carbon, and it was therefore necessary to examine the steel turnings after every experiment to determine the presence of any free carbon microscopically. Whenever carbon was noticed the equilibrium content of CO measured in the gas was also lower by nearly 10 per cent.

Their values for the gas compositions at 650° and 700° C., were, respectively, 35.58 per cent of CO₂ (the remainder CO) and 25.27 per cent of CO₂. From these values, using the data by Rhead and Wheeler on the producer gas reaction, $\text{C} + \text{CO}_2 = 2\text{CO}$, mentioned above, the calculated free energies for cementite were: $\Delta F_{973} = +3,138$ calories at 650° C., $\Delta F_{973} = +3,281$ calories at 700° C. (973° K.).

Having both the free energy of cementite and its heat of formation at 700° C., by use of the equation $\Delta F = \Delta H - T\Delta S$ it can be calculated that the entropy of formation of cementite at 700° C. is $\Delta S_{973} = +13.5$. The absolute entropies of iron (3×15.88) and of carbon (5.6) at this temperature are known, and the absolute entropy of cementite at 700° C. can then be calculated as:

$$S_{973} = 3 \times 15.88 + 5.6 + 13.5 = 66.74.$$

⁷⁵ Maxwell, H. L., and Hayes, Anson, The Free Energy and Heat of Formation of Iron Carbide for the Temperature Interval, 650° to 700°: Jour. Am. Chem. Soc., vol. 48, 1926, pp. 584-593.

From the specific heat tables it is found that the relative entropy of cementite at 700° C. compared to cementite at 25° C. is 34.8 calories per degree per mol. Therefore the absolute entropy of cementite at 25° C. (298° K.) is $66.74 - 34.8 = 31.94$ entropy units. Having the heat of formation of cementite at 298° K., the use of the above equation may be reversed and the free energy at 298° calculated as:

$$F_{298} = \Delta H - T\Delta S = 13,580 - 198 \times 10.3 = +10,590 \text{ calories.}$$

This calculation is based on a number of shaky approximations, but they are the only available data and give us a tentative value for the free energy of cementite under standard conditions.

IDENTIFICATION OF QUENCHED PHASES

As mentioned earlier in this chapter, much of the difficulty in interpretation of the various metallographic constituents visible in quenched steels has been associated with the failure to obtain definite physicochemical data and descriptions of them. Martensite, troostite, and sorbite are still more or less mysteries. Only in the last few years has enough definite evidence been accumulating to help clear away the cloud of uncertainties, misconceptions, and false theories. The use of the X ray to determine the atomic crystal pattern has been one of the powerful tools. For instance, Zorning⁷⁶ found by that method that ordinary "martensite" contains both α and γ iron, but only α iron was visible in troostite, sorbite, and pearlite X-ray patterns. This merely adds confirmation to the growing weight of evidence that martensite produced by quenching austenite to room temperature is not completely converted and needs quenching to lower temperatures to convert more supercooled austenite into martensite (supercooled γ iron solid solution into super-saturated α iron solid solution of Fe_3C). As previously mentioned, the carbon atoms leave no trace in the austenite and martensite X-ray patterns and seem to be present in the interstices between the iron atoms in unknown association. Some of the best physical evidence has been recently collected by determining specific volumes and will now be discussed.

SPECIFIC VOLUMES AND DENSITIES OF IRON-CARBON SYSTEM

Literally thousands of data on densities of various iron and steel products are available, but the most systematic and precise are those

⁷⁶ Zorning, —, —————: Army Ordnance, vol. 4, 1923, p. 77.

of Cross and Hill, Honda,⁷⁷ Tammann and Schiel,⁷⁸ Levin and Dornhecker,⁷⁹ and Andrew Honeyman.⁸⁰

The specific volume, or its reciprocal, the specific gravity, of a sample of steel is very largely a matter of its previous history. As has been seen in previous pages, the percentages of ferrite, cementite, austenite, and martensite in a sample vary with the heat treatment. Therefore, in order that the following discussion can be more easily understood it is well to give some of the mean values of the specific volume and specific gravity at room temperature of the above constituents before their derivation and measurement are described.

Mean values of constituents of steel

	Specific volume	Specific gravity
Iron.....	0. 1271	7. 864
Cementite.....	. 13038	7. 670
Pearlite.....	. 12856	7. 778
Austenite ¹ 1275	7. 843
Martensite ¹ 1310	7. 633
α martensite ¹ 1319	7. 581
β martensite ¹ 1282	7. 800

¹ 0.9 per cent of C.

From these figures, which agree well with calculations from X-ray parameters, it is seen that, if a steel is in austenitic condition, its conversion to martensite involves an expansion in volume. This gives one reason why the center of a quenched steel does not show as much martensite as the exterior, because the center portions are confined in the iron lattice and do not have the opportunity to go through the necessary expansion. The quenched austenite has been found more stable at room temperature and up to 200° C. than the martensite, so such a sample can be tempered up to 200°, thereby converting the martensite needles into troostite. If the sample is then cooled to liquid-air temperatures, needles of martensite appear in the center of the specimens and the ground mass of unaltered austenite throughout the specimen, according to Tammann and Schiel. The transition from martensite to pearlite involves a decrease in volume, although pearlite is less dense than austenite.

The data are now at hand for understanding the volume changes of a steel sample during tempering. The steel is assumed to exist in

⁷⁷ See footnotes 55 and 44, pp. 218 and 213.

⁷⁸ Tammann, G., and Schiel, E., Die Umwandlung des Austenits und Martensits in gehärteten Stählen: Ztschr. anorg. allgem. Chem., Jahrg. 157, 1926, pp. 1-21.

⁷⁹ Levin, M., and Dornhecker, K., Über das spezifischen Volumen und über die Harte von Eisen-Kohlenstofflegierungen: Ferrum, Jahrg. 11, 1913-14, p. 321.

⁸⁰ Andrew, J. H., and Honeyman, A. J. K., Specific Volume of Steels: Carnegie Schol. Mem., Jour. Iron and Steel Inst., vol. 13, 1924, p. 253.

the water-quenched condition, which means that it contains some unaltered austenite and a great deal of martensite. Tammann and Schiel have shown by other simultaneous evidence that on tempering martensite alters to troostite and sorbite (these investigators call it pearlite on the assumption that troostite, sorbite, and pearlite are all the same phase in different states of subdivision), with increase in volume, the main change beginning at about 100° C. and being nearly complete at 200° C. Austenite begins to be converted into sorbite at about 250° C. On further heating (300° to 500° C.) the specific volume decreases, according to Tammann and Schiel, due to collapse of the "distended pearlite" into normal pearlite. Any austenite converted at or below 250° C. gives this "distended pearlite" (troostite), and any converted above about 250° C. gives pearlite (sorbite) of the usual density.

The figures quoted above on the specific volumes of pure austenite and martensite were derived by Tammann and Schiel by extrapolating the volumes of a series of specimens after altering their martensite or austenite contents through heat treatment. The Honda data on α and β martensite are from X-ray measurements.

An ordinary sample of water-quenched steel, called martensite by most experimenters, was shown by Tammann and Schiel, through their specific-volume measurements, to contain only about 50 per cent of martensite, and the remainder was a matrix of supercooled austenite. When the steel was quenched to liquid-air temperatures the specific volume approached 0.12965, which indicates about 80 per cent of martensite. By repeated cooling and warming back to room temperature it was possible finally to work the specific volume of the sample up to 0.1303, compared to the calculated volume of pure martensite of 0.1310. Therefore, even quenching in liquid air did not completely eliminate austenite. As the samples were cooled to successively lower temperatures they each time approached a limiting specific volume corresponding to a definite ratio of austenite to α martensite. The principal value of this work is to show that most of the calorimetric work on steels to be reported below has been done on steels that were only partly converted into the constituents they were supposed to contain.

A piece of steel rod 10 millimeters in diameter and containing 1.72 per cent of C was heated to the austenitic temperature range and then quenched in water. Its specific volume showed there must be considerable austenite present. Placing it in a lathe, turning off successive layers, and measuring the volumes of the residual core after each cut and then calculating the austenite content of each layer, it was found that the outer layer must have contained about 10 per cent of austenite, while the layer 3 millimeters beneath the

surface had 60 per cent. This agreed with the qualitative appearance of a polished section.

Tammann and Schiel claim that their "distended pearlite" at 100° to 300° C. is distended, due to the fact that it has less specific volume than the martensite from which it was derived, yet there is not sufficient mobility of the solid at these temperatures to let it contract and fill all the voids that tend to form. Tempered steels, therefore, usually have high specific volume. Pearlite formed by slow cooling of austenite has the specific volume 0.12856 quoted above, but the "distended pearlite" of Tammann and Schiel has a specific volume of 0.1303. It is called pearlite because it is stained by a 5 per cent alcoholic solution of picric acid, which is supposed to stain only pearlite. One might easily ask whether this distended pearlite is not sorbite or troostite and the 0.1303 specific volume corresponding to it a real volume, not due to distension of the pearlite lattice as a result of its rigidity.

An excellent summary of the specific volumes and densities of steels is given by Cross and Hill,⁸¹ who concluded that with annealed steels (pearlitic) the density up to at least 1.4 per cent of carbon can be represented by the linear equation, density = 7.860 - 0.04 per cent of C. All quenched specimens showed lower density and had to be tempered to 600° C. before their density approached that of the annealed steels.

The specific volumes of the martensite and austenite steels have been calculated from X-ray data and agree well with the above values assumed. The principal investigators have been Wever and Rütten,⁸² Westgren and Phragmen,⁸³ Heindlhofer and Wright.⁸⁴ All the available X-ray data up to 1926 have been summed up by Fink and Campbell.⁸⁵

VOLUME CHANGE AT A₀ POINT

At the magnetic transition of cementite a slight increase in volume has been detected by Tammann and Ewig,⁸⁶ who placed some pure cementite powder in a glass dilatometer filled with mercury and found a change of 0.0714 cubic millimeter per gram of carbide (0.13038 c. c.) or 5.48 cubic millimeters per cubic centimeter (0.548

⁸¹ See footnote 55, p. 218.

⁸² See footnote 21, p. 201.

⁸³ Westgren, A., and Phragmen, G. *Zum Kristallbau des Eisens und Stahls II: Ztschr. phys. Chem.*, vol. 102, 1922, pp. 1-25.

⁸⁴ Heindlhofer, K., and Wright, F. L., *Tempering Phenomena of Austenite: Trans. Am. Soc. Steel Treating*, vol. 7, 1925, p. 34.

⁸⁵ Fink, W. L., and Campbell, E. D., *Influence of Heat Treatment and Carbon Content on the Structure of Pure Iron-Carbon Alloys: Trans. Am. Soc. Steel Treating*, vol. 9, 1926, pp. 717-755.

⁸⁶ See footnote 48, p. 215.

per cent). From a piece of cast iron placed in the dilatometer, a volume increase was calculated at A_0 corresponding to 0.0705 cubic millimeter per gram of Fe_3C .

VOLUME CHANGE AT EUTECTIC

One of the useful properties of gray cast iron has been its volume expansion at the freezing point. Sauerwald and Wecker⁸⁷ and Sauerwald and Widawski⁸⁸ report that white iron increased in volume on melting, while gray iron decreased, and the two liquids differed in specific volume by only 1 per cent. Their data are for white iron, before melting, $V_s=0.139$ and after melting 0.1418, while for gray iron, before melting $V_s=0.1449$ and after melting 0.1433. The gray-iron sample was lower in carbon and contained 2.76 per cent of silicon to cause precipitation of carbon. Their data include specific volumes of the two solid samples as far down as 700°C . and for the liquid samples up to $1,300^\circ\text{C}$. At 700°C . the specific volume of white iron was 0.1340 and of gray iron 0.1456, while at $1,200^\circ\text{C}$. the two molten samples, respectively, showed 0.1429 and 0.1447.

A more extensive study of the change in volume during solidification of cast iron has been made by Honda and Endo.⁸⁹ They found that when the total carbon content is kept constant and the silicon contents diminish the amount of precipitated graphite diminished simultaneously; the increase in volume diminished as well, becoming zero at 0.38 per cent of Si, 2.06 per cent of graphite, and 4.1 per cent of total carbon. By extrapolation they figured that when no graphite is precipitated and the iron is 100 per cent white iron the contraction during solidification was 3.6 per cent. A diagram with these results is given in Figure 74, which is a function of the volume change as related to the graphite liberated during freezing.

PRESSURE AND THE IRON-CARBON DIAGRAM

By means of the Clausius-Clapeyron equation it is possible to calculate the effect of pressure on the melting point of iron or its alloys. The equation may be used in the form $dP/dT=L/T\cdot\Delta V$, where dP/dT is the change in pressure necessary to alter the melting point 1 unit

⁸⁷ Sauerwald, F., and Wecker, J., Über die Volumenänderung beim Schmelzen des Roheisens; Dichtemessungen bei hohen Temperaturen VI: Ztschr. anorg. allgem. Chem., Jahrg. 149, 1925, pp. 273-282.

⁸⁸ Sauerwald, F., and Widawski, E., Über die Dichte und Ausdehnung des weissen und grauen Roheisens im flüssigen und festen Zustande: Ztschr. anorg. allgem. Chem., Jahrg. 155, 1926, pp. 1-12.

⁸⁹ See footnote 2, p. 178.

in temperature, L is the latent heat of fusion, and ΔV is the change in volume on fusion. White iron expands about 0.0020 of its volume on melting, while gray iron contracts 0.0014. The heat of fusion of white iron is given later in this chapter as about 46.8 calories per gram, which, expressed in mechanical units, is about 2,300 kilogram calories per gram. All the necessary data for calculating the effect of pressure on the melting point of white iron are now available and

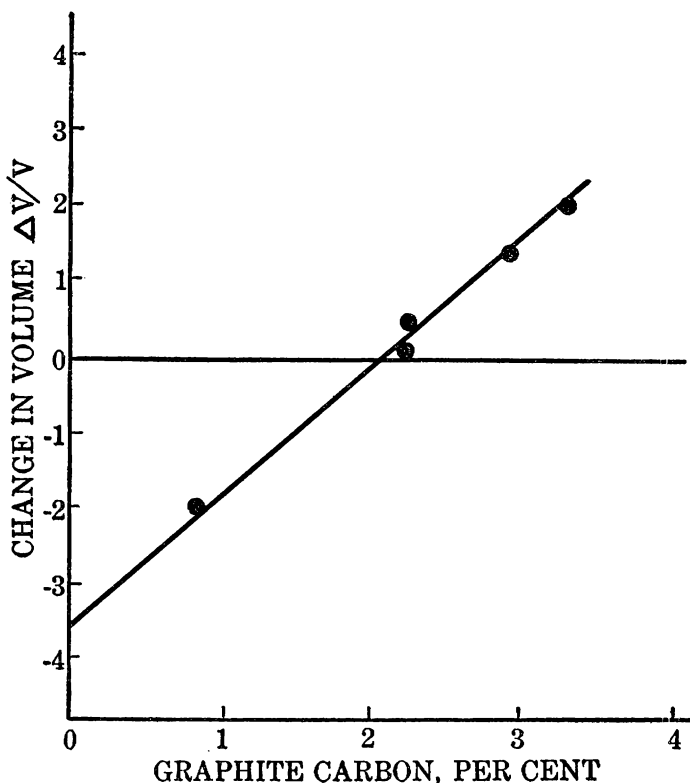


FIG. 74.—Proportionate change in volume during freezing of cast iron with 4.1 per cent of total carbon (Honda and Endo)

the answer is that it requires a pressure of 812 kilograms per square centimeter to raise the melting point 1° . The heat of fusion of gray iron is not known but is presumably different by the heat of formation of cementite, which is an endothermic compound involving nearly 90 calories per gram of Fe_3C at $1,135^\circ \text{C}$. Referred to 1 gram of cast iron of 4.25 per cent of carbon if completely graphitized, this is an endothermic heat of nearly 60 calories to be added to the above 46.8 calories. Using these data, it is found that a pressure of 2,640 kilograms per square centimeter (roughly, 2,640 atmospheres)

is required to lower the melting point of gray iron 1°. This change is not a very great one from a practical standpoint. Nevertheless, Scheil⁹⁰ has drawn up a hypothetical composition-temperature-pressure diagram for the iron-carbon system which is based on such data as are available and indicates that at very high pressures cementite should be stable. Due to the impracticability of attaining the conditions forecast, the diagram will not be reproduced here. Principal interest is in the fact that the melting point of white iron should be raised by pressure and that of gray iron should be lowered.

HEAT CONTENT OF STEELS

Although many data are available in literature relating to the heat content of various steels, the principal systematic work has been done by three observers, Meuthen,⁹¹ Yamada,⁹² and Umino.⁹³ All of them have worked with calorimeters into which heated samples of steels were quenched under various conditions. The heat content of a definite steel at a definite temperature is a function of its previous history, and therefore it is difficult to tabulate it. A thin sample plunged into the water of a method-of-mixtures calorimeter will be more severely quenched and converted into martensite (if quenched from above the A_1 temperature) than a thick piece of the same composition. Some of the total heat data of Meuthen are given in Figure 75. If the sample is covered with a thin coating of nonconducting material so that it cools more slowly in the calorimeter, a different amount of martensite is formed than for a bare sample. Therefore the data of Umino given in Figure 76 represent merely Umino's peculiar conditions. These data are for mean specific heats (total heat divided by temperature range through which sample was quenched). Up to the A_1 temperature, 720° C., the steels all have a reasonably reproducible heat content, which is a function of the amount of carbon present. Above that the apparent total heat on quenching is a function of the proportion in which the austenite of the samples is converted into martensite, troostite, sorbite, or pearlite.

The energy changes connected with all these structural changes are not known, but the step from austenite to martensite and from martensite to pearlite has been worked out with fair agreement between experimenters. These are summarized in Figure 77, which deals principally with the quenching of steels from the austenite range to room temperature.

⁹⁰ Scheil, E., Zur Frage der Stabilität des Eisencarbids bei höherem Druck: *Ztschr. anorg. allgem. Chem.*, Jahrg. 158, 1926, p. 175.

⁹¹ See footnote 4, Table 36, p. 191.

⁹² Yamada, N., Heat of Transformation of Austenite to Martensite and of Martensite to Pearlite: *Jour. Iron and Steel Inst.*, vol. 105, 1922, pp. 409-427; also *Tohoku Univ. Sci. Repts.*, vol. 10, 1921, pp. 453-470.

⁹³ See footnote 65, p. 223.

RESULTS OF RAPID QUENCHING

Rapid quenching, in order to gain the maximum amount of martensite and yet leave no undecomposed austenite, gives the energy due to the normal heat capacity plus the energy involved in passing

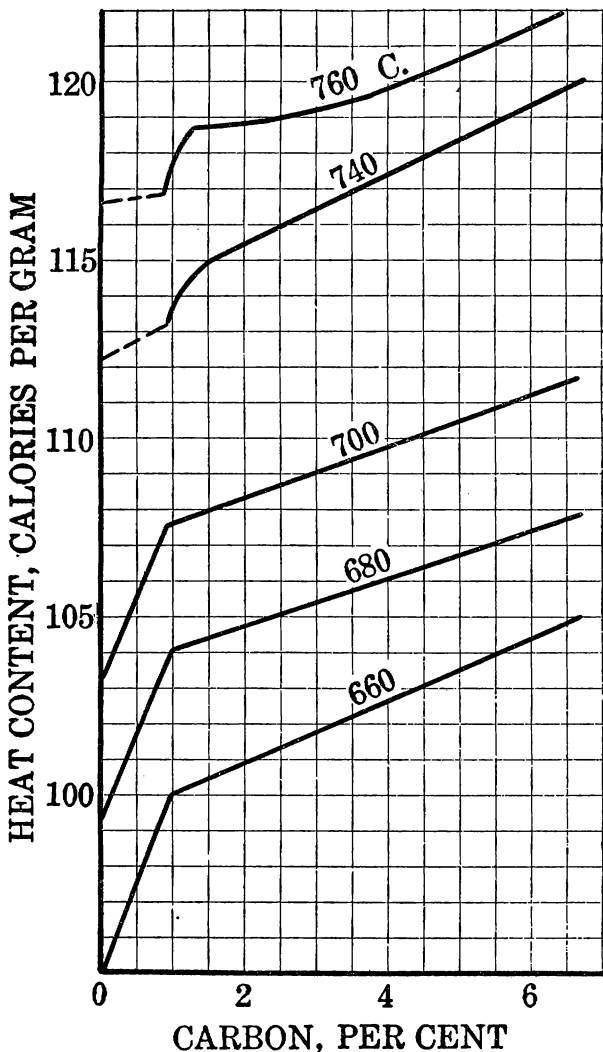


FIG. 75.—Total heats of steels (Meuthen)

from austenite across the A_1 line (see the iron-carbon diagram) to martensite. If the martensite were allowed to pass into pearlite, further heat could be developed, but this first step is a definite one, and the heats associated with it in a series of carbon steels are shown by the line marked "austenite-martensite" in Figure 77.

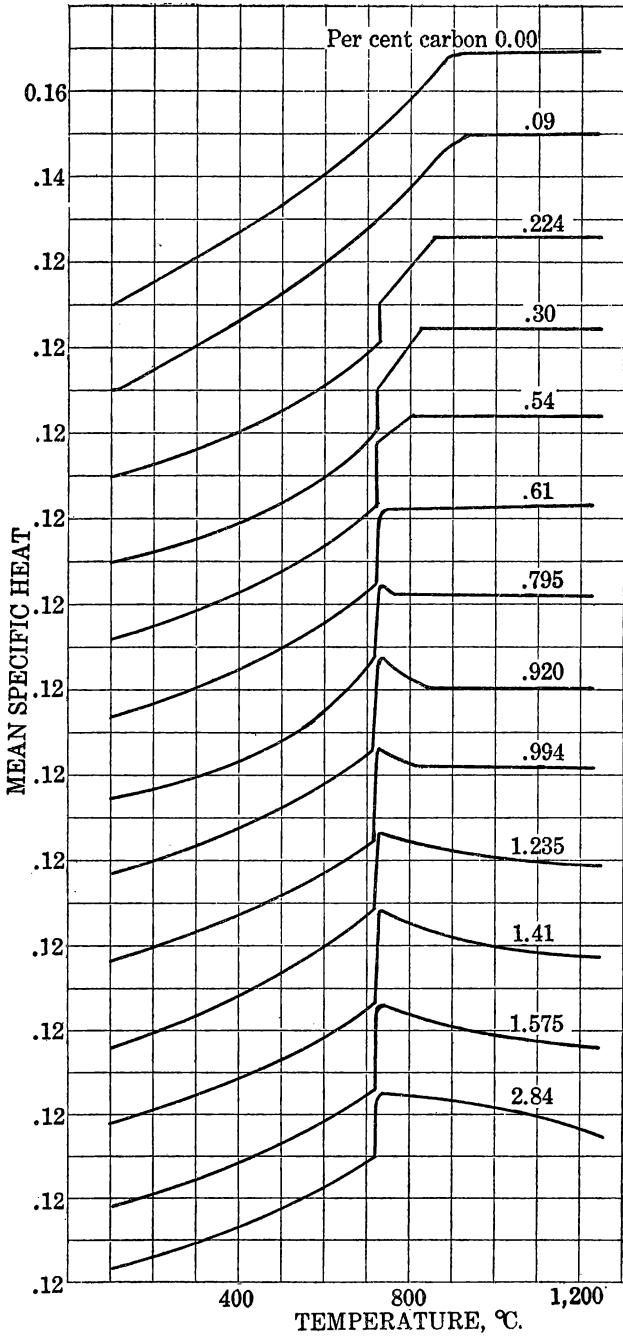


FIG. 76.—Mean specific heats of steels (Umino)

(The solid line represents the observations of Yamada and the dotted those of Umino, the two experimenters showing good agreement.) This line was derived by subtracting the martensite-pearlite

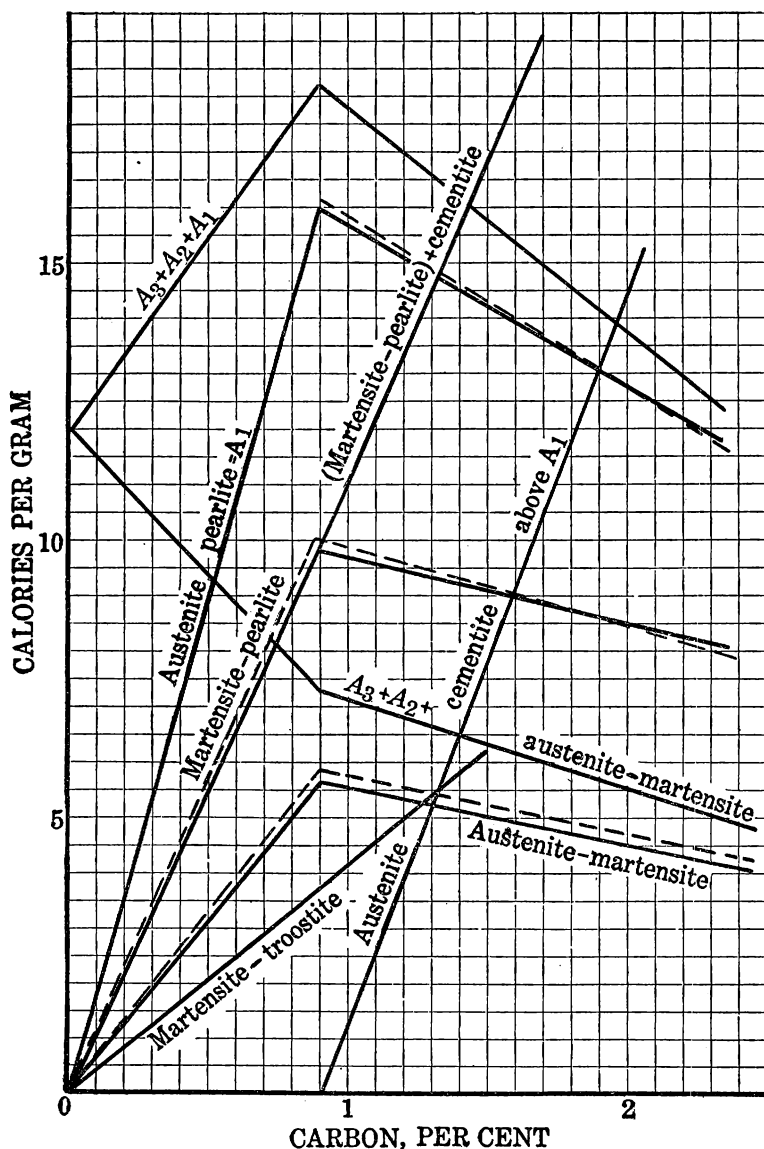


FIG. 77.—Heat changes in steels

curve from the A_1 or austenite-pearlite curve. Yamada obtained the martensite-pearlite heats by quenching pairs of samples from the austenite field in the iron-carbon diagram, then tempering one each

at 500° C., and keeping the others in the martensite condition. He built a calorimeter for operation at 350° to 400° C. and dropped into it the two series of quenched and tempered steels to be warmed up to 350° C. from room temperature. With the tempered specimens, which were in the pearlite condition, nothing but the normal heat capacity was needed, but with the martensitic samples which begin to temper at about 100° C. and become sorbitic by the time 350° C. is reached the heat corresponding to the change was liberated. The differences between the two were the martensite-pearlite heats, except that above the eutectoid composition the martensitic samples also contained austenite from which the excess cementite over the eutectoid composition had not crystallized. These data are represented by the martensite-pearlite lines in Figure 77, the two lines meeting at the eutectoid composition and reaching a maximum heat evolution there. The hypereutectoid samples on the martensite-pearlite curve were quenched from temperatures below the cementite-solubility line of the iron-carbon diagram, while the hypereutectoid samples which were quenched from within the austenite field form a continuation upward of the hypoeutectoid martensite-pearlite line. The difference between the results on these hypereutectoid samples is interpreted as the heat of precipitation of cementite from austenite and is plotted as a straight line which passes through the two differences as ordinates and cuts the zero axis at the composition of pearlite, showing that the difference is a function of the excess cementite over the pearlite ratio. This line is called the "cementite from austenite above A_1 " line on the diagram.

In the temperature range from A_3 down to A_1 the total heat curves are very steep and even discontinuous. By plotting these on a large scale the heat involved in passing through them was obtained by both Yamada and Umino and called the "austenite-martensite" heats plus the A_3 heat (and the A_2 heat). The A_3 heat is obtained by Yamada by extrapolating to zero carbon and proves to be 12 calories per gram. For the hypereutectoid steels it corresponds to the transformation austenite-martensite alone. Umino also covered some of his specimens with asbestos paper and repeated the determinations, the rate of cooling of the samples in the calorimeter being sufficiently retarded to give him pearlite instead of martensite, and he was able to plot the austenite-pearlite curve direct to compare with the previously observed data on this " A_1 " heat by Meuthen. Their work checked beautifully. The Yamada total heats on $A_3 + A_2 +$ austenite-pearlite were obtained by addition and are also plotted, although the plot of these sums is erratic. On extrapolation to zero they likewise give a (doubtful) check of 12 calories per gram of pure iron for $A_3 + A_2$.

The austenite-martensite heats of all experimenters were then obtained by subtracting from the austenite-pearlite heats the previously observed martensite-pearlite heats.

The most prominent point in these curves is the eutectoid point, 0.9 per cent of C, also called the pearlite point because on cooling a steel from the austenite range only one thermal anomaly is observed and because the structure under the microscope shows 100 per cent of pearlite (the eutectoid being ferrite and cementite). Therefore at this temperature austenite splits uniformly to give α iron and cementite from the α iron supersaturated solid solution plus the A_3 transformation heat. However, the data were so collected that the γ - α iron transition has already taken place, and as measured the change represented the heat corresponding to austenite-martensite. The points fell along a straight line up to the composition of pearlite for all the hypoeutectoid steels, and therefore the heat evolved here is proportional to the carbon or possibly the cementite content. Yamada's work showed it to be 75.3 calories per gram of Fe_3C and Umino's gave 75.9 calories. This is the heat of precipitation of cementite from solution in α iron or the heat of solution of cementite into α iron. From the austenite-pearlite curve it is also seen that the heat of precipitation of cementite from the γ iron solution is 118.5 calories per gram of Fe_3C according to Meuthen and 120 calories according to Umino.

PRECIPITATION OF CEMENTITE IN HYPEREUTECTOID STEELS

The Yamada data on the precipitation of cementite in hypereutectoid steels above the A_1 point in similar fashion show that 83.6 calories per gram are involved. This amount is intermediate between the figures on precipitation from α iron and from γ iron as given above and is consistent with the probability that in quenching these hypereutectoid steels from temperatures intermediate between A_1 and the cementite-solubility line part of the austenite survived in the quenched samples and part was converted to martensite. It must also be called to mind that according to the most recent theories, which were not in circulation at the time the work here described was done, martensite represents α iron containing carbon in solid solution in indefinite relation; on mild tempering the first change is to α iron and atomically dispersed carbon (troostite), which on further tempering forms cementite (sorbite). On still further tempering the cementite in the latter crystallizes to microscopically visible pieces in pearlite. With one exception the heat effects of these latter changes have not yet been measured and are probably involved as a total sum now expressed by the difference between the austenite-martensite and the austenite-pearlite heats.

RESULTS OF TEMPERING MARTENSITE TO 200° C.

The heat change on tempering martensite in a 200° C. calorimeter in place of the 400° C. calorimeter of Yamada was measured by Kawakami.⁹⁴ Tempering martensite to 200° C. usually gives troostite, although Kawakami is one of those who believe that there are two forms of martensite, α and β , and that heating to 200° C. decomposes only the α form, leaving the β intact, while heating to 370° C. is necessary to decompose the β form. Whether or not his hypothesis and nomenclature are accepted, or the conversion to troostite is assumed, the heat effect was measured similarly to the Yamada martensite-pearlite heats and is plotted in Figure 77 under the label "Martensite-troostite." As can be seen, the heat effect on tempering eutectoid steel at 200° C. is 3.7 calories liberated per gram. If the definition of troostite proposed in this chapter is accepted—that is, the conversion of supersaturated solid solution of cementite in α iron into atomically dispersed carbon in α iron—the heat effect referred to 1 gram of carbon is 410 calories (or 4,920 calories per gram atom). If, on the other hand, the actual mechanism is the precipitation of Fe_3C from supersaturated solid solution in α iron, the heat effect referred to 1 gram of cementite is 27.4 calories, or 4,920 calories per mol of Fe_3C .

HEAT CHANGES AT PEARLITE COMPOSITION

As all iron-carbon alloys contain austenite above the A_1 temperature, the heat changes at the pearlite composition (0.9 per cent of C) are of importance, and from the work above discussed Table 46 has been prepared, summarizing all the known information. In it the observed metallographic changes are tabulated, together with the hypothetical chemical changes that accompany them.

TABLE 46.—Heat changes at pearlite composition

Metallographic change	Hypothetical chemical change	Heat liberated, calories		
		Per gram of pearlite	Per gram of Fe_3C	Per molecule of Fe_3C
Austenite→martensite	γFe —solution→ αFe —solution.....	5.9	43.8	7,870
Martensite→troostite.....	αFe —solution→ $\alpha\text{Fe}+\text{C}$	3.7	27.4	4,920
Troostite→pearlite.....	$\alpha\text{Fe}+\text{C}$ → $\alpha\text{Fe}+\text{Fe}_3\text{C}$	6.2	46.0	8,260
Martensite→pearlite.....	αFe —solution→ $\alpha\text{Fe}+\text{Fe}_3\text{C}$	9.9	73.4	13,170
Austenite→pearlite.....	γFe —solution→ $\alpha\text{Fe}+\text{Fe}_3\text{C}$	15.8	117.2	21,040

If the only change from austenite to martensite, in accordance with theory, is the conversion of γ iron to α iron, the heat involved

⁹⁴ Kawakami, M., Determination of Precipitation of Cementite from Alpha and Beta Martensites: Tohoku Univ. Sci. Repts., vol. 14, 1925, pp. 559-568.

should be comparable to the γ - α transition heat. Taking the eutectoid point in the heat diagram, the eutectoid consists of 0.8636 grams of Fe and 0.1344 grams of Fe_3C per gram of sample, and the heat involved in the austenite-martensite change as shown on the diagram is 5.8 calories. Referring all this heat to the iron in the specimen, it is 6.72 calories per gram of Fe. This can be compared with the various values of the γ - α transition given in an earlier chapter, Oberhoffer having observed 6.765 calories and Wüst 6.56 calories per gram of Fe, while the selected average of all experimenters is 4.9 calories. The work of Oberhoffer and of Wüst is known to be good, and their values may be better than the selected average. Furthermore, as will soon be pointed out, probably none of the samples used in the above calorimetry were completely converted from austenite to martensite during quenching, therefore not all the expected heat of conversion of γ to α iron was liberated. The above can therefore be taken only as a doubtful check.

HEAT CONTENTS AT A_1 , A_2 , AND A_3 POINTS

Umino⁹⁵ has also calculated the A_1 , A_2 , and A_3 heats in a series of four carbon steels and in electrolytic iron. He measured their total heat contents over short temperature intervals up to 950° C. and found that it took the samples near the transformation temperatures as much as 30 minutes to bring them to a constant total heat content. After taking precautions to age the samples properly at these temperatures he got very good results. In electrolytic iron A_2 took place at 795° C., but in the 0.77 per cent C steel it took place at 780° C., to which level it had already dropped in the 0.27 and 0.35 per cent C steels. The values of A_1 , A_2 , and A_3 are tabulated in Table 47, and when plotted (see fig. 78) the values of A_3 fell on a straight line.

TABLE 47.—Heats of A_3 and A_2 transitions in steels, in calories

Specimens	A_1	A_2	A_3	Specimens	A_1	A_2	A_3
Electrolytic iron.....	0.00	3.63	5.35	0.270 per cent C steel.....	4.70	3.36	3.66
0.040 per cent C steel.....	.67	3.55	5.00	0.350 per cent C steel.....	6.00	3.23	3.50
0.135 per cent C steel.....	2.40	3.50	4.48	0.770 per cent C steel.....	13.60	3.18	.80

Meuthen obtained for pure iron $A_2=5.60$ calories and $A_3=3.0$ calories, almost the reverse of the Umino results. Some interest attaches to the fact that Umino, by his calorimetric method, followed the A_2 transformation out to the composition of 0.770 per cent of C, whereas most experimenters observing cooling curves

⁹⁵ See footnote 18, p. 189.

are unable to detect any cooling curve deflection at the A_2 point beyond about 0.40 per cent of C. Umino obtained the A_2 "heat of transformation" by plotting the true specific heats of the steels involved as a function of temperature, showing the well-known hump at the magnetic transition temperature (A_2) and taking the area between this and the normal curve, as he did with cementite. This heat of transformation is therefore one distributed over a considerable range of temperature. Umino found effects of the magnetic component of specific heat as much as 130° C. below the A_2 "point," and the probability is that there is a slight disturbance for several

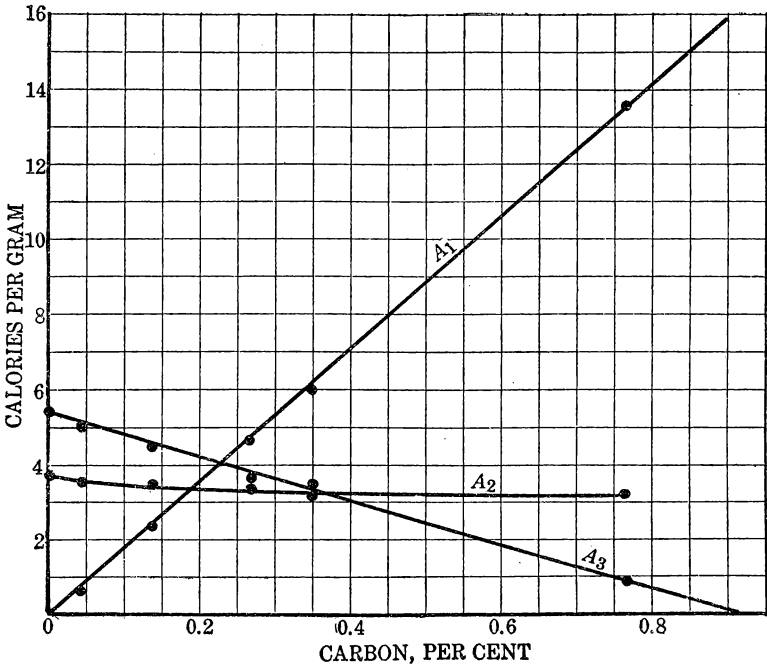


FIG. 78.—Heats of A_1 , A_2 , and A_3 transformations (Umino)

hundred degrees lower, although the total energy involved is small at these lower temperatures.

Looking at Figure 78, it is interesting to note that the extrapolation of the A_3 values to the composition of pearlite (0.9 per cent of carbon) gives zero heat change due to A_3 and that A_1 amounts to 15.95 calories, in good agreement with the previous work of Umino, Meuthen, and Yamada.

One might very pertinently ask why the A_2 heat would not be added to the A_1 heat at the pearlite composition and elsewhere. The answer is that it is not a discontinuity in the total heat curve but only a change in direction and is included only in the specific

heat curves which, by definition, are the first differentials of the total heat curves. With Umino's 0.77 per cent C steel the A_2 point was at a temperature higher than the A_3 point, according to the iron-carbon diagram, because the A_3 - S line in that diagram crosses the A_2 temperature line at about 0.6 per cent C content. There is therefore some doubt as to the validity of his interpretation of his specific heat curves for the higher carbon samples. The portion of the A_2 transformation of α iron which would fall above the A_3 - S line may be included in the austenite-pearlite transition and added to A_1 , and the true A_1 heat should be diminished by just that much. The whole matter needs further attention from investigators.

UNCERTAINTY OF HEATS AT A_1

The above data on the heats involved in the series of steps between austenite and pearlite (the reverse change from pearlite to austenite is presumably one merely of preliminary transformation of α to γ iron followed by solution of cementite in the γ iron and has never been segregated into two steps experimentally) at the A_1 point are given for what they are worth. Careful study has revealed many discrepancies and contradictions, and they are almost certainly open to early revision. The studies of Tammann and Schiel on the specific volume of steels and of austenite, martensite, and pearlite show that the ordinary quenched steels called martensite by the men who have done calorimetric work contain supercooled austenite which needs to be reheated above 200° C. to cause it to convert into martensite or one of its decomposition products. Only by cooling to liquid-air temperatures can most of the austenite be converted to martensite; therefore the samples used for the above calorimetric work consisted of unknown mixtures of martensite and austenite, and the heat changes ascribed to them actually apply only to portions of the samples. As a result, the heat changes ascribed to conversion of martensite to troostite are probably too low. The change from martensite to pearlite is also too low. This means that the change from austenite to martensite is also too low.

The whole investigation needs repetition, with samples carefully quenched in liquid air or even liquid hydrogen and manipulated until their specific volumes show they have approached the composition of martensite as nearly as they can.

OTHER THERMAL DATA IN IRON-CARBON SYSTEM

The heat of fusion of none of the iron-carbon alloys except the eutectic (4.25 per cent of C) is unique. Umino⁹⁶ has determined the

⁹⁶ See footnote 18, p. 189.

heat of fusion of two different samples of eutectic cast iron at two different times and finds, respectively, 47 and 46.63 calories per gram, presumably for white cast iron. He compares this with the earlier datum of Schmidt,⁹⁷ who observed 59 calories per gram for a sample with 4.35 per cent of C. These samples, on chilling as quickly as they do in a calorimeter, give white iron. No reliable data are available about gray iron except the gray irons which contain enough silicon to throw the carbon out of the solution in spite of quick cooling, and they do not enter in the present considerations.

The A_0 point has also been investigated by Umino for three carbon steels. He plotted their specific heats as functions of temperature, getting the familiar hump due to the magnetic transition and estimated the departure from the normal heat capacity. The integration of the area between the observed and the theoretical curve gave areas proportional to the carbon content and amounting to 9.72 calories per gram of cementite.

All the important thermal data at unique points are summarized in Table 48.

TABLE 48.—*Summary transition heats at unique points in Fe-C system*

Point	Heat of transition, calories			Temperature, °C.
	Per gram of alloy	Per gram of Fe	Per gram of Fe ₃ C	
Pure iron, freezing point.....	64.9	64.9	-----	1,535
Eutectic, freezing point.....	46.8	-----	-----	1,135
Pure iron, A_3 point.....	4.9	4.9	-----	906
Pearlite, from austenite.....	15.8	-----	117.4	720
Pearlite, from martensite.....	9.9	-----	73.6	720
Martensite, from austenite.....	5.9	-----	43.9	720
Cementite, Curie point.....	-----	-----	9.72	220-150

⁹⁷ Schmidt, W., Die spezifische und Erstarrungs-Wärme des geschmolzenen Roheisens: Metallurgie, Jahrg. 7, 1910, p. 164.

OTHER EQUILIBRIA INVOLVING IRON CARBIDE

In the iron blast furnace the chemical reduction of the oxides to metal is all that is desired, but in practice reduction actually proceeds further and the metal is in part carburized. The usual product of the blast furnace, pig iron or cast iron, contains up to 4.5 per cent of carbon, which on cooling crystallizes as the carbide cementite (Fe_3C) unless enough silicon has also been reduced to throw the carbon out of solution as graphite.

The equilibria involving formation or decomposition of iron products carrying carbon are therefore of interest. These reactions are called carburization and decarburization, respectively. One would think that after the great amount of work spent in studying these reactions the system would be well understood, but the fact is that the puzzle is just beginning to be solved.

The principal difficulty in the past has been due to the assumption of simpler conditions than actually existed, which has led to endless confusion. In nearly all the literature available the assumption is made that the following pure phases are present: Ferrite, ferrous oxide, magnetite, cementite, and one series of iron-carbon solid solutions called austenite, whose field of stability is given in the iron-carbon diagram of the previous section.

As a matter of fact, two of these supposed pure substances are solid solutions. The ferrite can dissolve ferrous oxide, giving a series of solutions which Schenck⁹⁸ has named oxyferrite, while the ferrous oxide phase never actually has the composition of FeO but is part of a series of solid solutions of FeO and Fe_3O_4 , with FeO as the preponderating constituent and similar to the iron-carbon series called austenite. This series of solid solutions, approximating FeO at higher temperatures, is named *wüstite* by Schenck.

With three series of solid solutions to handle it is little wonder that the observations of gas-equilibrium constants from different experiments should vary so grievously, because each experimenter assumed that the constants measured were between certain pure phases. Actually the various experimenters have been dealing with solutions of varying concentrations, and instead of having bivariant equilibria they have been working with trivariant equilibria. Expressed graph-

⁹⁸ Schenck, R., and Dingmann, Th., Gleichgewichtsuntersuchungen über die Reduktions-, Oxydations und Kohlunsvorgänge beim Eisen. III: Ztschr. anorg. allgem. Chem., Jahrg. 166, 1927, pp. 113-154.

ically, they have thought they were dealing with equilibria represented by lines in space but have actually been dealing with equilibria represented by surfaces or fields.

Most of the older literature must therefore be abandoned and consideration given only to the few recent researches which have taken proper account of the existence of these solid solutions.

As pointed out by Schenck, the exact conditions for participation of carbon in any of the equilibria are uncertain. In nearly all work in which carbon is introduced the phases cementite, austenite, and a third called oxyaustenite by him appear. This happens even at temperatures above 720° C., at which cementite is supposed to be metastable with respect to iron and carbon. The oxyaustenite just mentioned is a solid solution of carbon in γ iron, which also contains ferrous oxide in solution.

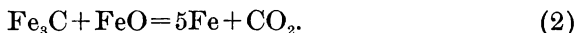
OXYAUSTENITE

For austenite to be capable of dissolving ferrous oxide and for oxygen and carbon thus to exist simultaneously without interaction in a γ iron solid solution appear at first somewhat anomalous. However, if the reaction

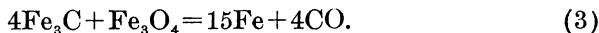


is reversible, it must have an equilibrium pressure of CO at each temperature. Actually, iron does react with carbon monoxide with formation of an oxygenated 'austenite at temperatures above 720° to 906° C., depending on the carbon content. Cementite and ferrous oxide (or more correctly, wüstite) form at temperatures below that, although it is possible that an oxycementite can also form.

It will be recalled that ferrous oxide is metastable below 570° C.; therefore the reaction below that temperature is the formation of magnetite in place of wüstite. Carbon dioxide reacts somewhat similarly; and the reversible reaction could be:



The corresponding reactions for temperatures below 570° C. are:



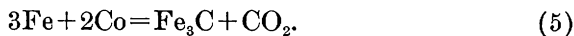
It must be made plain that in the first two reactions at temperatures above 720° C. the action is supposed to take place between the gas and a homogeneous solid phase called oxyaustenite, whereas below that temperature practically all the carbide and probably the oxide are precipitated out of the excess α iron. γ iron seems to be a much

better solvent than α iron. The equilibrium constant for each of these four reactions would be the pressure of the gas involved. Actually, at equilibrium both CO and CO₂ are present, their ratio depending in the case of oxyaustenite on the ratio of carbide to oxide in the oxyaustenite. The analysis of the solid phase at any one temperature depends upon the total pressure of gas applied, and by increasing gas pressure more oxides of carbon are absorbed until the solid composition has increased enough in carbon and oxygen content to be in equilibrium with the gas. Conversely, if one heats a definite sample of oxyaustenite in a closed space oxides of carbon will be evolved until they are under enough pressure to reach equilibrium with the solid.

If a continuous large supply of gas high in CO is used, presumably the oxide content of oxyaustenite would be gradually reduced and the composition of the solid approach that of normal carbide austenite. No one has determined the gas concentration at which the oxide content of austenite becomes negligible. Therefore in an equilibrium diagram involving the oxides of carbon the stability field of oxyaustenite must include also the field of normal carbide austenite.

WORK OF SCHENCK

The boundaries of the oxyaustenite stability field (see figs. 79 and 83) contiguous to the fields for cementite, oxyferrite, and wüstite have been determined independently by Schenck,⁹⁹ by Johansson and von Seth,¹ and by Takahashi.² The work of Schenck has been the most thorough in depicting the boundaries, whereas the work of the two others has been best in determining the CO:CO₂ ratios of gas in equilibrium with each analysis of austenite. Both of the latter reported their work as dealing with the simple carburization and decarburization reaction of normal austenite, the chemical reaction being



The Fe₃C is understood to be in solid solution in excess Fe.

Schenck's diagram, given in Figure 79, shows that oxyaustenite has a stability field extending indefinitely to high temperatures (presumably to the melting point) and narrowing at lower temperatures till it finally ends at 540° C. This latter is quite surprising,

⁹⁹ Schenck, R., Gleichgewichtsuntersuchungen über die Reduktions-, Oxydations und Kohlungsvorgänge beim Eisen. V: Ztschr. anorg. u. allgem. Chem., Jahrg. 167, 1927, pp. 315-328.

¹ Johansson, A., and von Seth, R., The Carburization and Decarburization of Iron and Some Investigations on the Surface Decarburization of Steels: Jour. Iron and Steel Inst., vol. 114, 1926ii, pp. 295-357.

² See footnote 43, p. 213.

because normal austenite is not stable below 720° C. The unknown possibility of the existence of an oxycementite, mentioned above, immediately suggests itself, and one wonders if it would be just as plausible to interpret the long, narrow strip of oxyaustenite in the diagram below 720° C. as that constituent. Alternatively one could assume the existence of an oxycarbide at these lower temperatures.

WORK OF OTHER INVESTIGATORS

For comparison, the data of Johansson and von Seth, and also of Takahashi, are plotted in Figure 83, which is an enlargement of the

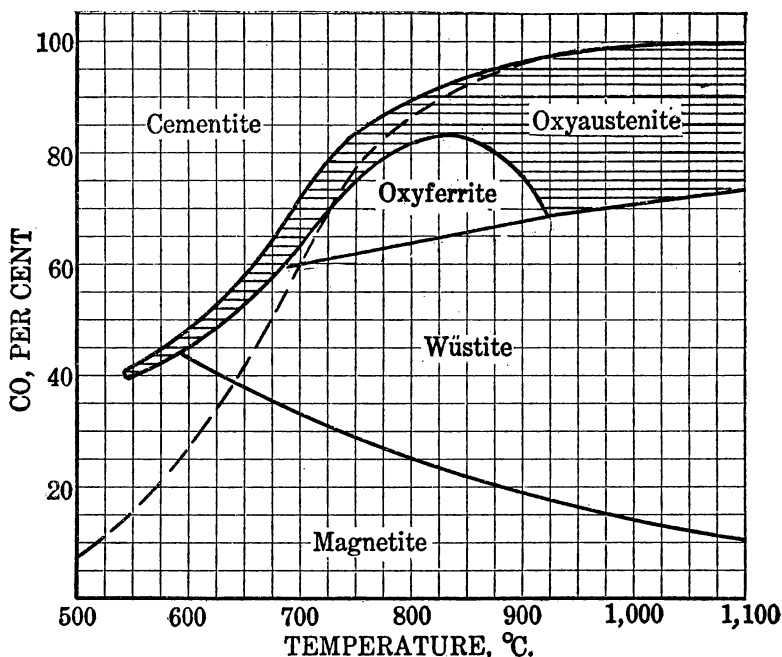


FIG. 79.—Iron-oxygen-carbon reduction system, 1 atmosphere (Schenck). Broken line for $C + CO_2 = 2CO$

oxyaustenite area of Figure 79. Takahashi's work very definitely placed the lower limit of austenite (he calls it austenite but it might have been oxyaustenite) at 725° C. \pm 1.5°. On the other hand, the work of Johansson and Von Seth was of such a nature that their observation at 710° C., the lowest temperature used by them, indicated, contrary to ideas of solubility of carbon in α iron, there was considerable carbon in the iron. This could be interpreted as being associated with the presence of oxyaustenite or oxycementite. However, A_1 can occur at even lower temperatures and A_c , up to 740° C., and this observation at only 10° below the average position of A_1 might be reasonably expected. Possibly Schenck's observations are

correct, and the addition of iron oxide to austenite lowers the A_1 point. Iron-carbon alloys melted in air, as compared to the same alloys melted in vacuo, have been shown by Reed³ to exhibit a lower A_3 point, and the effect may also extend to the A_1 point.

OXYFERRITE-OXYAUSTENITE EQUILIBRIUM

From the data in Figure 83 it can be seen that the agreement is none too good between the three experimenters on the positions of

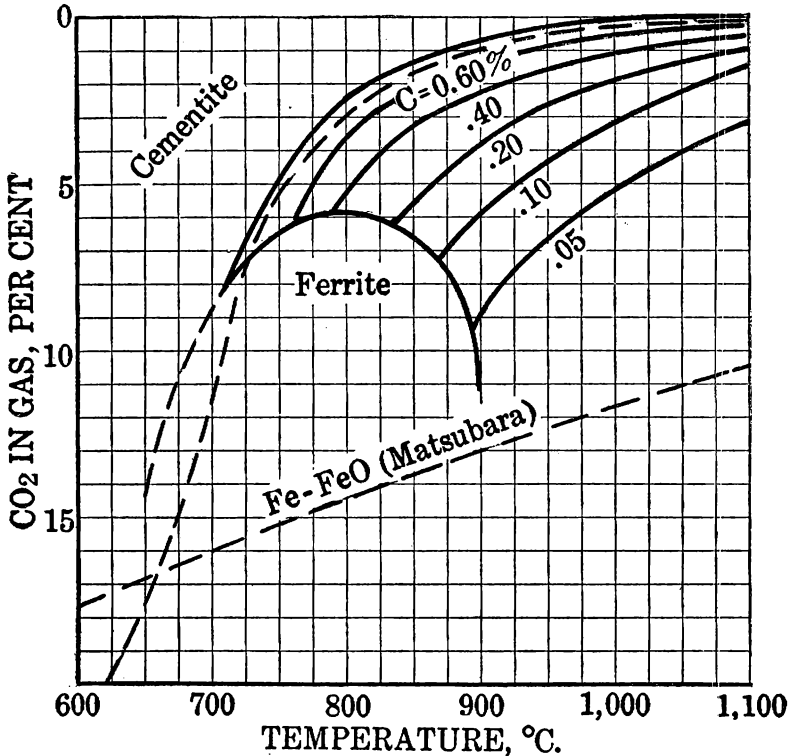


FIG. 80.—Carburization of iron v. temperature; pressure, 0.4 atmosphere $\text{CO}_2 + \text{CO}$. Lines of equal carbon content in austenite (Johansson and von Seth)

the equilibrium line between oxycerrite and oxyaustenite. The data are for 1 atmosphere total pressure of the oxides of carbon. Figure 80 contains the Johansson and von Seth data for 0.4 atmosphere total pressure, which are of greater industrial importance, because blast-furnace gas consists of about 60 per cent of nitrogen and the remainder oxides of carbon.

³ Reed, E. L., An Investigation of the Properties of Iron-Carbon Alloys: Carnegie Schol. Memoirs, Jour. Iron and Steel Inst., vol. 14, 1925, pp. 91-130.

EFFECT OF PRESSURE ON CARBURIZATION EQUILIBRIA

This last sentence brings to mind only one instance of the effect of pressure on the carburization equilibria. In all the equations, like equations (1) to (5), corresponding to these equilibria, there is a different number of molecules of gas on the two sides of the equation. This means that the ratio of CO to CO₂ changes with change in pressure. It will be recalled that when a reaction takes place with increase in volume increase in pressure tends to drive back the equilibrium, and therefore at a higher pressure a higher proportionate amount of the final product of reaction must be present. The producer-gas reaction



also suffers the same change. While the 1-atmosphere isobars are included in the diagram of Figure 79, there is greater interest in their position under conditions in the iron blast furnace, as shown in Figure 80, where 0.4 atmosphere pressure of CO + CO₂ is assumed, the remainder being nitrogen. Air enters the bottom of the blast furnace at a total pressure of 1.8 to 2 atmospheres, is converted almost instantly into a mixture of 60 per cent of nitrogen and 40 per cent of CO, and passes up the stack with decreasing pressure and increasing CO₂ content until it reaches the top at about 1 atmosphere pressure.

CEMENTITE IN HIGH-TEMPERATURE EQUILIBRIA

Throughout the work of all the experimenters little is said about the fact that they are ostensibly measuring equilibria at temperatures where cementite is supposed to be quite unstable. Free cementite in powdered form decomposes in a short time at all temperatures above 500° C., and some of Schenck's so-called equilibrium experiments involving long periods of time used a mixture of powdered cementite and iron oxides as a starting point. The very reasonable doubt therefore arises as to how many of the equilibria measured actually involved some form of cementite. One sees quite clearly that in all future gas equilibrium work involving the carbide the final solid product attained at equilibrium should be analyzed for free and combined carbon and for oxygen. Johansson and von Seth did this. Only when the absence of free carbon shows that the gas analyses are not connected with the producer-gas reaction can some of these higher temperature equilibria be taken as dealing with Fe₃C. It will be noted in the diagram of Figure 79 that Schenck's equilibria between oxaustenite and cementite call for higher CO contents of the gas than does the producer-gas reaction. Schenck ascribes this to the

fact that cementite is metastable with respect to carbon and iron and hence should have a higher carbon pressure and therefore a higher CO concentration in equilibrium with it. This consideration is in agreement with the observations of Maxwell and Hayes,⁴ who investigated the equilibrium involved in equation (5) at 650° and 700° C. and observed that whenever carbon started to form in their preparations the CO content in the gas fell.

EQUILIBRIUM BETWEEN AUSTENITE AND CARBON OXIDES

DISCUSSION OF FIGURE 81

The work by Takahashi mentioned above involved treating sheets of electrolytic iron 0.4 millimeter thick with mixtures of CO and

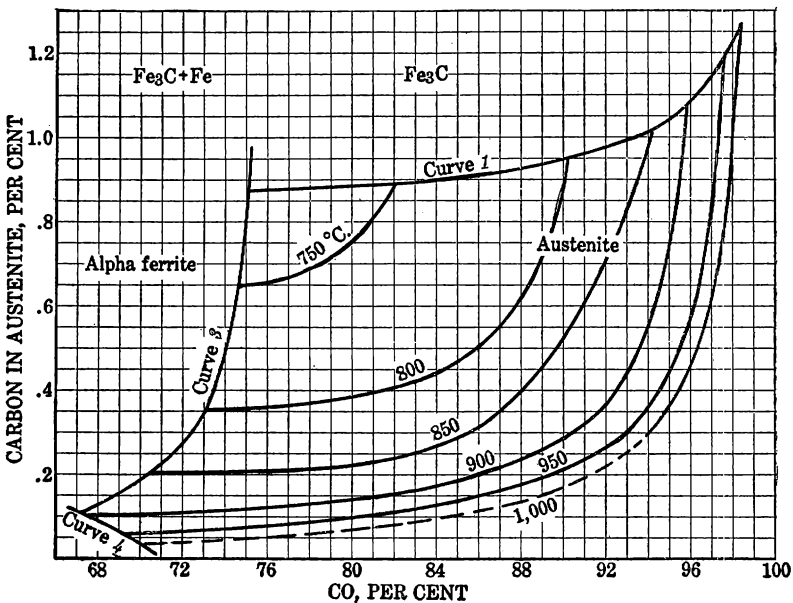


FIG. 81.—Isotherms in austenite stability field (Takahashi)

CO₂ passed over them in a combustion-tube furnace at constant temperature at such a rate that the gas was displaced every 1.5 minutes. The sheets were held until reaction was complete and equilibrium established, then withdrawn; cross sections were cut, examined metallographically for homogeneity, and finally analyzed for carbon. The oxygen content was not determined, and on that account it is uncertain whether the solid phase dealt with was austenite or oxy-austenite. In Figure 81 the carbon contents of the solid materials as a function of the CO:CO₂ ratios are given as isothermals. These isothermals terminated at one end against curve 1, the curve repre-

⁴ See footnote 75, p. 231.

senting equilibrium between austenite and cementite (detected metallographically), and at the other end in the equilibrium line (curve 3) between austenite and α ferrite. In the lower left corner they also terminated against the line (curve 4) for the oxidation of iron to FeO, or wüstite, the latter having its stability field in this corner of the diagram. One must recall that the ordinates of this diagram apply only to the austenite field and not to the areas outside, and on that account all that is known of the Fe_3C , Fe, and wüstite fields is the equilibrium conditions at their edges. In the upper left corner of Takahashi's austenite area, which represents temperatures below the A_1 point (the intersection of curves 1 and 3), a mixture of cementite and α ferrite is stable. The Johansson and von Seth diagram, which is similar to the Takahashi one but does not coincide with it, is definitely known to be oxygen free.

The 800° C. isothermal may be followed in order to illustrate the utility of the diagram. With a gas mixture containing less than 73 per cent of CO (the sum of CO and CO_2 percentages is assumed to be 100 per cent and 1 atmosphere) ferrite would not be carburized. The diagram as prepared can not express the fact that if iron is heated at 800° C. in a gas stream containing less than 64.5 per cent of CO it will be oxidized to FeO by the CO_2 in the mixture, but it does claim that α iron can not be carburized with a gas stream containing less than 73 per cent of CO. With gas containing 73 per cent the metal is carburized and reaches equilibrium when it contains 0.35 per cent of carbon. Raising the CO content of the gas raises the carbon content of the material according to the 800° C. isotherm of the diagram, until with a gas containing 90.2 per cent of CO the austenite will be saturated with carbon and free cementite will begin to appear. Further carburization should form Fe_3C , and austenite would disappear. This ends the isotherm. Conversely, if one had a steel of over 0.35 per cent C. content and it were held at 800° C. in a stream of 73 per cent CO gas it would be decarburized down to 0.35 per cent of C. Just a slight drop in the CO concentration would then completely decarburize the steel, leaving α iron. Curve 3, therefore, corresponds to the separation of α iron from austenite, which is line A_3S in the iron-carbon diagram. Curve 1 is that where cementite and austenite are in equilibrium and therefore corresponds to the cementite solubility line, ES , in the iron-carbon diagram.

DISCUSSION OF FIGURES 82 AND 83

The data of Figure 81 are presented in a somewhat more useful form in Figure 82, which shows definitely the position of the A_1 point below which austenite is not stable. For purposes of comparison with Johansson and Seth, the data are presented in still another

form in Figure 83, which is a plot of gas composition versus temperature, across which are drawn curves (solid lines) of equal carbon content in the austenite stability field. As mentioned earlier, the oxyaustenite stability field should include the austenite field, and therefore there is uncertainty as to whether Takahashi's isotherms represent austenite or oxyaustenite. Schwartz,⁵ in discussing Takahashi's work, is of the opinion that Takahashi's equilibrium line between cementite and austenite is actually the one between cementite and oxyaustenite, previously misinterpreted by both Schenck and Matsubara.⁶

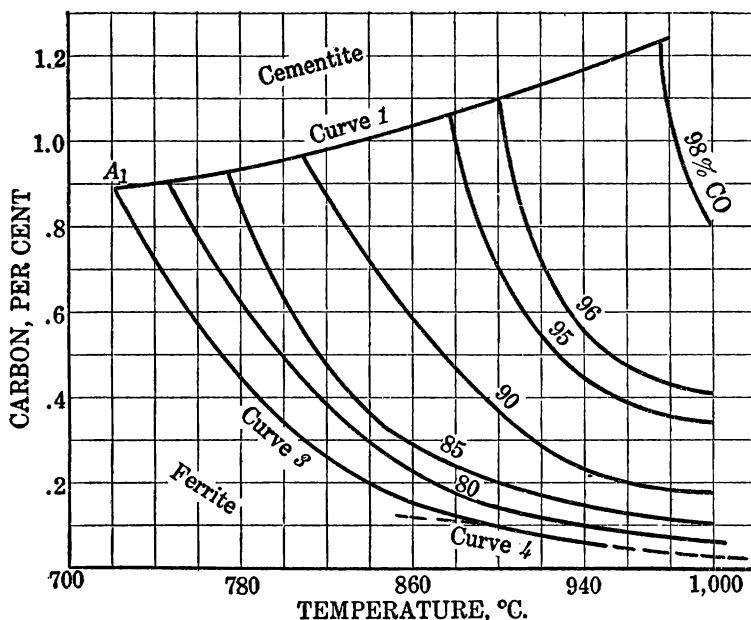


Fig. 82.—Lines of constant gas composition in equilibrium with austenite (Takahashi)

WORK OF JOHANSSON AND VON SETH AND OF TAKAHASHI

The work of Johansson and von Seth was so conducted that this uncertainty as to whether oxyaustenite or austenite is present is considerably reduced. Their lines of equal austenitic carbon across the field in Figure 83 (represented by dotted lines) give reasonable checks with the work of Takahashi at the lower temperatures but depart markedly from Takahashi's lines (represented by full lines) at slightly higher temperatures. The deviations seem to be more

⁵ Schwartz, H. A., Discussion of paper by W. P. Sykes on Carburizing Iron by Mixtures of Hydrogen and Methane: *Trans. Am. Soc. Steel Treating*, vol. 12, 1927, pp. 737-758.

⁶ Matsubara, A., Chemical Equilibrium Between Iron, Carbon, and Oxygen: *Trans. Am. Inst. Min. and Met. Eng.*, vol. 68, 1922, pp. 3-55.

than is possible for identical materials, because for a given carbon composition and temperature the gas in equilibrium contains about 4 per cent more CO in Takahashi's work than in that of Johansson and von Seth. Stated in another manner, for a given carbon composition and a given gas composition the Takahashi temperatures are 25° to 50° C. lower than those of the other experimenters. The same

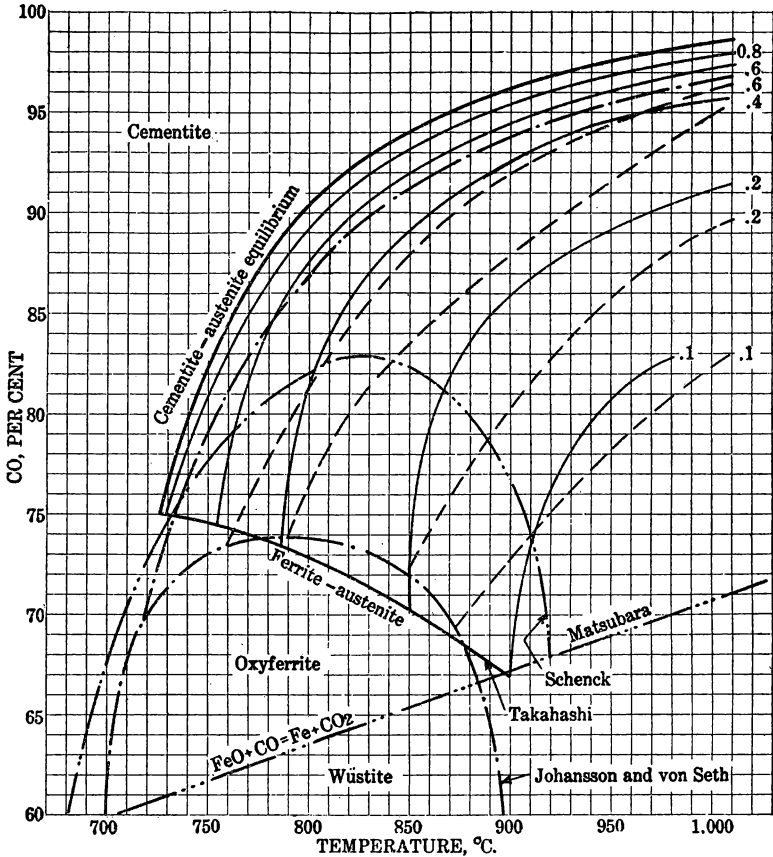


FIG. 83.—Trivariant equilibria of austenite. Solid lines, lines of equal carbon (Takahashi); broken lines, lines of equal carbon (Johansson and von Seth); heavy lines, boundaries of austenite and oxyferrite fields, including oxyferrite (Schenck)

applies to the cementite-austenite equilibrium lines bounding the left edge of the austenite field.

The method used by Johansson and von Seth is of interest. They placed small samples of carbon steel of definite carbon contents in a combustion-tube furnace and passed different mixtures of CO and CO₂ over them, determining by change in weight and by metallographic examination the gas mixture which was neutral and neither carburized nor decarburized them (reduced or oxidized). This null

method assured the composition of the solid phase, a thing no previous experimenter has been able to do. All their work was done with gas mixtures containing 60 per cent of nitrogen, so that the sum of the two carbon oxides was only 0.4 atmosphere. The results are given in Figure 80, and the data given in Figure 83 have been recalculated from them so that the sum of the pressures of the carbon oxides is 1 atmosphere, in order that they might be compared more exactly with the work of Takahashi.

The equilibrium line between austenite and ferrite, according to Takahashi, starts at the A_3 point of pure iron and rises to higher CO percentages with lower temperatures to meet the supposed cementite-austenite line at a temperature of 725°C ., corresponding to A_1 with a gas containing 75 per cent of CO. According to Johansson and von Seth, it starts at the A_3 point in temperature (but far down into the wüstite field of stability), rises with lower temperatures, crossing the equilibrium line separating wüstite from ferrite and passing through a maximum CO percentage, and then with still lower temperatures intersects the cementite-austenite line at the A_1 temperature, which in their diagram falls at 720°C . with a gas containing 70 per cent of CO. The Schenck line, taken from Figure 79, starts at $A_3=920^\circ\text{C}$. and passes with a shape similar to that of Johansson and von Seth through a maximum CO concentration much higher than the latter observed, intersecting once more the wüstite-ferrite line at 675°C . and 58 per cent of CO (fig. 79) and not the cementite line.

Which of these lines is correct is very difficult to decide. This Schenck line meets the objections of Schwartz (Schenck's earlier work did not) by not intersecting the cementite line at all. On the other hand, it represents apparent equilibria between two phases whose precise analysis is still uncertain. The other two experimenters have curves which check each other reasonably, although one fails to contain a maximum and the other is known to represent oxygen-free solid phases. Since Takahashi's curve at the lowest temperatures represents extrapolations it can be disregarded at its lower temperature intersection. The Johansson and von Seth work at low temperatures is founded on too few points to be conclusive as to the exact shape and the points of intersection, but it does represent the true austenite equilibria, and these may be different from the oxy-austenite equilibria. Therefore, until better data at the lower temperatures are available, Schenck's data on oxyaustenite will have to be accepted. For the equilibria within the austenite area, representing austenite of various degrees of saturation with carbon, the Johansson and von Seth data are the safest to accept for pure austenite, and presumably the Takahashi data are the best for the oxyaustenite field.

VARIATIONS WITH TEMPERATURE

One important conclusion is that when FeO is reduced to Fe at any temperature above about 906° C., the A_3 point, the resulting metal will always be somewhat carburized, and carbon-free metal can be produced by use of CO only at temperatures lower than that.

Another thing that will be noticed from the diagrams is the fact that at the higher temperatures, 1,000° C. or above, although a carbon-free iron can not be produced, the carbon content is low, unless gas compositions very high in CO are used. On that account the spongy iron resulting from action of the hot bosh gas on iron ore in the high levels of the blast furnace is usually a low-carbon metal, because the gas passing over it has enough CO₂ to prevent heavy carburization.

In the temperature range below 720° C. Schenck has been the most prolific experimenter, and his equilibrium diagram given in Figure 79 is the result of a tremendous amount of work with about 25 students, extending over about 25 years. His diagram must be accepted until something better is presented. Schenck has written profusely and has repeatedly changed his ideas as he has accumulated data and experience. At present the only place where fault might be found is with the downward extension of the oxyaustenite area, on which comment was made above and which might prove to be a stability field for an oxycementite.

CARBON PRESSURES OF CARBON AND CEMENTITE

The work of Johansson and von Seth was further elaborated by them through study of the relative carbon pressures of pure carbon and of cementite. Considering equation (5) the equilibrium constant is usually written on the basis of the only gases present being CO and CO₂. If carbon vapor is also regarded as being present from the Fe₃C, the equilibrium constant involving the partial pressures of these three gases would be written $K_5 = C_5 \times \frac{CO_2}{(CO)^2}$. Equation (6) written in the reverse direction, would give the same volatile products with CO₂ and CO in the same ratio and would have the same equation for the equilibrium constant, except that the vapor pressure of pure carbon would be involved. The two carbon pressures are therefore in the same ratio as the two equilibrium constants, if carbon pressures were excluded. This ratio of the carbon pressures of cementite to the carbon pressure of pure carbon, $C_5 : C_6 :: K_5 : K_6$, was plotted by them against the carbon content of a series of iron-carbon alloys, as calculated from their austenite-equilibrium

curves and from the Rhead and Wheeler,⁷ data on the equilibrium constants of the producer-gas reaction, equation (6).

DISCUSSION OF FIGURE 84

This method of calculation gives only the ratios of the two carbon pressures but not their absolute values, which at the temperatures of the experiments are extremely small. Present interest is not in their absolute magnitudes but in the conditions under which the

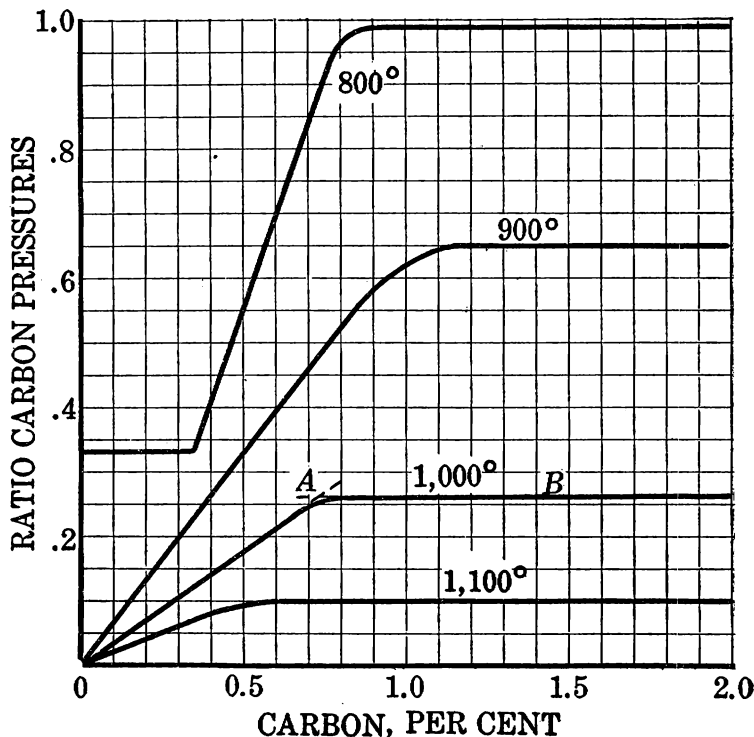


Fig. 84.—Ratio of carbon pressures, austenite to carbon (Johansson and von Seth)

carbon pressure of cementite or austenite equals or exceeds that of pure carbon. The data are given in Figure 84. In studying this graph the first thing to remember is that the carbon pressure of pure carbon at a given temperature is a constant, while that of austenite varies with the carbon content because a solid solution is being tested. The 800° C. isotherm is interesting when compared with the iron-carbon diagram. Starting with a steel of almost no carbon content at 800° C., treatment with CO:CO₂ mixtures pro-

⁷ Rhead, T. F. E., and Wheeler, R. V., The Effect of Temperature on the Equilibrium $2\text{CO} = \text{CO}_2 + \text{C}$: Jour. Chem. Soc. London, vol. 97, 1910, pp. 2178-2189.

duces an austenite whose carbon pressure is 0.33 that of carbon and is in equilibrium with the gas and the other solid phase. By referring to the iron-carbon diagram it is found that this horizontal portion of the 900° isotherm is obtained, while the stability field of α iron is crossed in equilibrium with austenite of 0.35 per cent C content. When all the α iron has been converted to austenite of this content the ratio of the carbon pressures can increase as the carbon content of the austenite increases. On the iron-carbon diagram the stability field of austenite is now being crossed. This inclined portion of the 800° C. isotherm is almost a straight line; consequently the carbon pressure of an austenite solid solution seems to follow the same law as the osmotic pressure of an ordinary solution.

When the second horizontal portion of the curve is reached the iron-carbon diagram indicates that the austenite is saturated with cementite, and the horizontal portion of the curve corresponds to the carbon pressure of cementite, which, like the carbon pressure of pure carbon, is constant; and the only thing that is happening as steels of higher carbon content are approached is the conversion of saturated austenite into cementite. If this were being done with a CO:CO₂ gas mixture, the chemical reaction could be written: Austenite + CO = Fe₃C + CO₂. From the iron-carbon diagram it is noted that the apparent horizontal portion corresponding to Fe₃C is not all horizontal but (see the 1,000° C. isotherm) really becomes horizontal only at point *b*, while the bend over at *a* is a gradual, almost asymptotic, approach to the horizontal, ending at *b*. It is seen in Figure 84 that the carbon pressure of cementite does not increase with temperature as rapidly as that of austenite and consequently the higher the temperature the lower the carbon content of austenite, where its carbon pressure approaches that of pure cementite.

The three isotherms above the A_3 temperature of iron are entirely in the austenite field of the iron-carbon diagram and have no horizontal portion at the left side of the figure to correspond to α iron.

DISCUSSION OF FIGURE 85

Using all the preceding data, Johansson and Von Seth prepared Figure 85, which shows the ratio of carbon pressures of austenite to carbon as a function of temperature and with lines of equal carbon content crossing the austenite field. Below the line corresponding to the ratio 1.0 the carbon pressure of cementite and of austenite is less than that of pure carbon; above it the reverse is true. It may, therefore, be said that an atmosphere of CO and CO₂ in equilibrium with elementary carbon is unable to carburize iron until a temperature corresponding to the point *A* (735° C.) is reached, and at that point the austenite formed would have about 0.7 per cent of carbon.

With rising temperature and the carbon pressures of the two phases kept the same by allowing sufficient time for equilibrium to be reached the austenite field is crossed to point *B* (790° C.), where the austenite is now saturated with carbon. The iron-carbon diagram shows that this austenite would contain about 1 per cent of carbon, and free cementite would begin to form. Below 735° C. (follow line *AC* upward) decarburization would take place, even in an atmosphere of pure CO, because the latter would split to form carbon and CO₂, and the CO₂ would return to the austenite to react once more with carbon vapor and form CO. Of course, the mechanism of de-

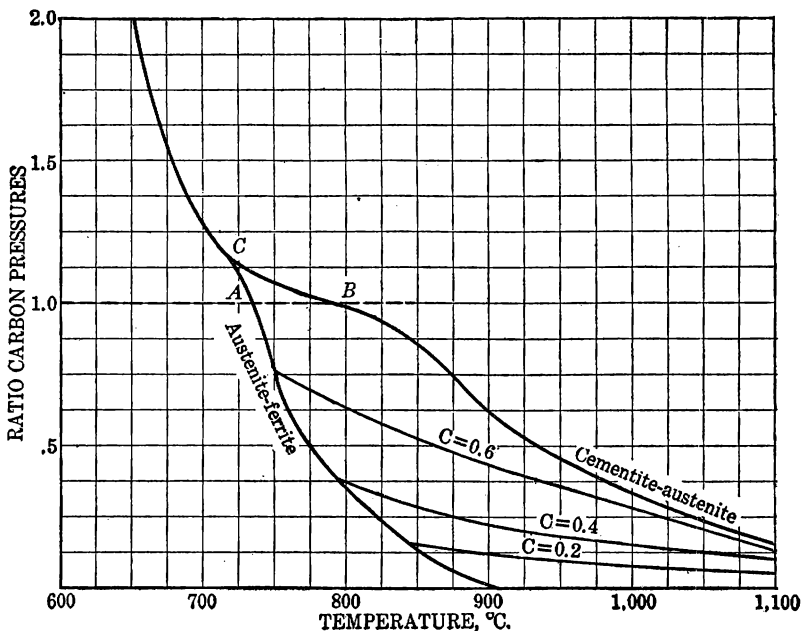


FIG 85.—Ratio of carbon pressures v. temperature (Johansson and von Seth)

carburization by the gases need not be invoked in this case, because even in a vacuum at a temperature below 735° C. austenite or cementite would evaporate carbon, which would condense on the solid carbon, the solid carbon acting as a reservoir for catching carbon vapor.

The physical significance of the points *A* and *B* can be interpreted in another way. They are the temperatures at which the equilibrium line for the producer-gas reaction, $C + CO_2 = 2CO$, crosses (see fig. 79) the lines for the ferrite-austenite and the austenite-cementite equilibria. Schenck's diagram in Figure 79 does not show the latter intersection and according to the Johansson and von Seth viewpoint is thereby incorrect. Schenck has always insisted that cementite has

a greater carbon pressure than carbon, in order that the cementite could be metastable throughout the whole temperature range of the iron-carbon diagram. The data now under discussion demand the interpretation that the carbon pressure of cementite be lower than that of pure carbon at temperatures above 790° C.

The point *C* is the eutectoid temperature, the point where austenite, cementite, and ferrite can be in equilibrium and the system contain 0.9 per cent carbon. Steels with more than 0.9 per cent of C would give lines of equal carbon content intersecting line *CB*. This diagram shows that point *C* has a higher carbon pressure from the cementite and austenite than has pure carbon, and with lowering temperature along the cementite-ferrite equilibrium line the ratio increases. Physically these facts mean that a mixture of cementite and ferrite can not be in equilibrium in a system in which pure carbon is also present. While they can be in equilibrium with a gas phase containing CO and CO₂, any catalyst which causes the CO to split, as it can do in this temperature range, will cause deposition of elemental carbon and destruction of the cementite-ferrite equilibrium, with formation of pure iron in place of cementite. Iron itself happens to be a catalyst for the splitting of CO, and on that account it is difficult to attain the cementite-ferrite equilibrium with gases in this temperature range.

At the lower temperatures one is also likely to encounter equations (1), (2), (3), and (4), taking place in the reverse sense to that in which they are written. If such a solid solution as oxycementite or an intermolecular compound of Fe₃C and FeO, which we could call an oxycarbide, can form, further equilibrium curves would be drawn in the diagram and Schenck's low-temperature oxyaustenite would be explained. The system is still full of contradictions and needs more work.

CARBON-OXYGEN-IRON EQUILIBRIA IN LIQUID STEEL

A very good piece of work on the equilibria of iron, oxygen, and carbon in the liquid state and of the compositions of low-carbon steels has been done by Herty and his coworkers.⁸ They first determined the solubility of ferrous oxide in molten pure iron at a series of temperatures. These determinations are given in an earlier section of this paper. They then determined that in the ordinary basic open-hearth furnace the amount of ferrous oxide dissolved by the metal is proportional to the ferrous oxide in the slag floating on top of it, all iron present being calculated to FeO. They then made slag

⁸ Herty, C. H., jr., *The Physical Chemistry of Steel Making: The Solubility of Iron Oxide in Iron*: Bull. 34, Mining and Metallurgical Investigations, Carnegie Institute of Technology, 1927, Pittsburgh.

analyses and found the carbon contents for a series of heats in a basic open-hearth furnace and obtained the data presented in Table 49.

TABLE 49.—*Results of Herty and coworkers*

Temperature, °C.	Molecular fraction FeO	Distribution ratio	O ₂ in metal, per cent	C in metal, per cent	K _c	1/T times 10 ³	Log K _c
1,524.....	0.041	5.30	0.0077	1.27	102	55.7	2.008
1,526.....	.206	4.03	.0512	.16	122	54.6	2.086
1,592.....	.199	3.43	.0580	.10	172	53.7	2.235
1,605.....	.202	3.22	.0627	.084	190	53.3	2.278
1,660.....	.209	2.56	.0815	.056	219	51.7	2.340

The calculation of the equilibrium constant, $K_c=1:(C)(O_2)$, is based on the following considerations: The carbon and ferrous oxide dissolved in the molten iron react during the "boil" in an open-hearth furnace to give bubbles of carbon monoxide, which rise and escape. Presumably a small amount of carbon dioxide is also present, but no reliable data are available, and a sufficiently accurate solution of the problem can be obtained on the assumption that the gas evolved is 100 per cent CO. The reversible chemical reaction involved is presumably



In this reaction the equilibrium constant would be the ratio of the product of the activities of the substances produced to that of the activities of the reactants, and the activities have to assumed to be proportional to the concentrations. The iron is present in overwhelming proportion and its concentration is changed so little throughout all the considerations of importance to this question that it can be assumed to be constant and equal to 1.0. The variation of solubility of CO in the metal under various conditions is also unknown but is probably likewise a constant, and it must be in equilibrium with CO gas under slightly greater than atmospheric pressure, so its activity can likewise be assumed to be 1.0. Whereas the complete equilibrium constant would have been written

$$k = (CO)(Fe) : (C)(O_2)$$

these simplifying assumptions reduce it to $k=1:(C)(O_2)$, which are the values incorporated in the table.

DISCUSSION OF FIGURE 86

These values have been plotted in the regular $\log k$ v. $\frac{1}{T}$ chart in Figure 86, the best representative line through the points being used. This gives a chart of value for interpolation or extrapolation.

DISCUSSION OF FIGURES 87 AND 88

Having these data, a series of representative open-hearth heats were carefully sampled, both metal and slag being analyzed and the data reduced to carbon in the metal as a function of oxygen in the metal at three different temperatures, shown in Figure 87. The same data were used to plot the carbon in the metal as a function of the ferrous oxide in the slag (see fig. 88) after the metal and slag have reached approximate equilibrium and the boil has died down. These two charts are of great practical interest. They show

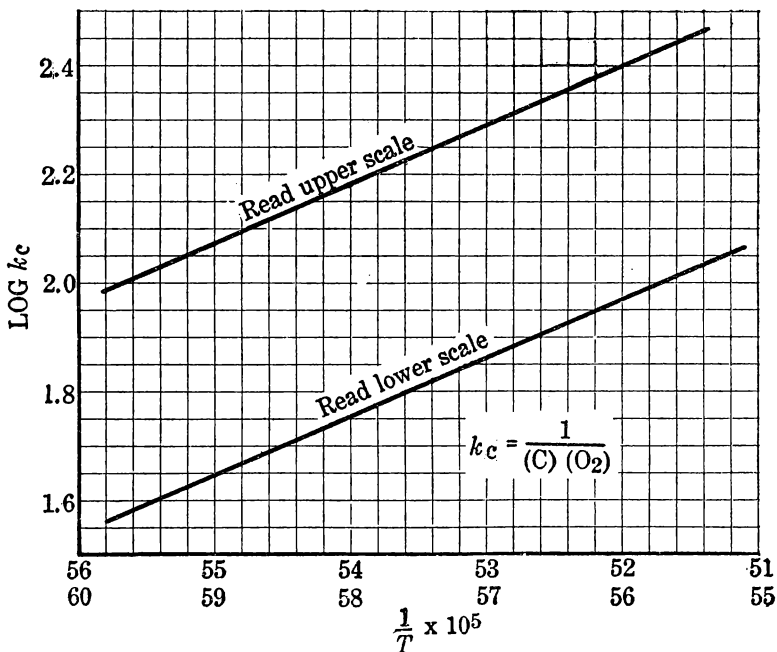


FIG. 86.—Equilibrium constants in carbon-oxygen-liquid iron (Herty and others)

that in working any open-hearth charge the decarburization of the metal, which takes place on interaction with the slag, which in turn is oxidized by the gases of the furnace, can not proceed to completion. It stops when the equilibrium ratio of carbon to oxygen (ferrous oxide) is reached at the temperature in question. To get a low carbon percentage in the metal the oxygen percentage must be run up, which in turn means allowing the heat to oxidize until there is a high FeO content in the slag. In like manner if a low oxygen content of the metal is desired a high carbon percentage must be kept and the action of the bath stopped earlier. If the bath is allowed to work until a low carbon content is reached and the excess

oxide in the metal reduced by a more powerful reducing agent like manganese, silicon, or aluminum, the bath then has the power of taking up more carbon without exceeding the equilibrium ratio and the result is cessation of all CO formation, bubbling or boiling

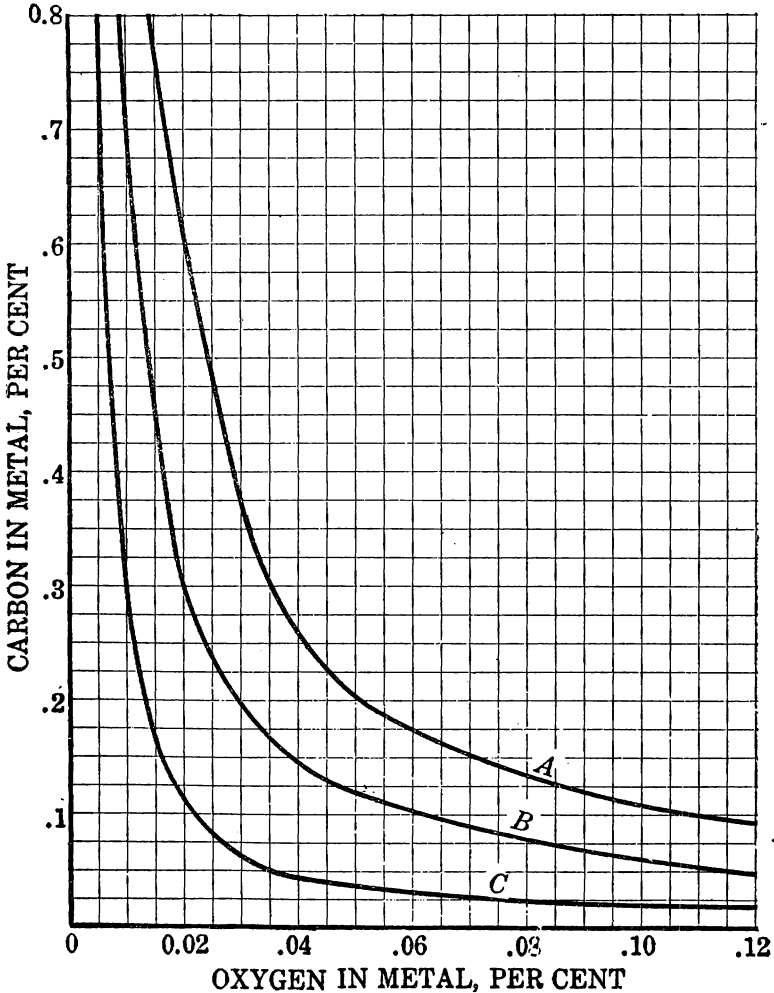


Fig. 87.—Equilibrium concentrations of carbon and oxygen in liquid iron at various temperatures (Herty and others): A, 1,512° C. (2,750° F.); B, 1,595° C. (2,900° F.); C, 1,650° C. (3,000° F.)

stops, and the steel has been “killed.” Study of these diagrams will allow many other practical deductions.

Nothing has been done on the oxygen content of cast iron, but if the above equilibrium constant is accurate enough and no other com-

plications arise from the assumptions which were made in deriving it, extrapolations to the carbon contents of cast irons are valid. How-

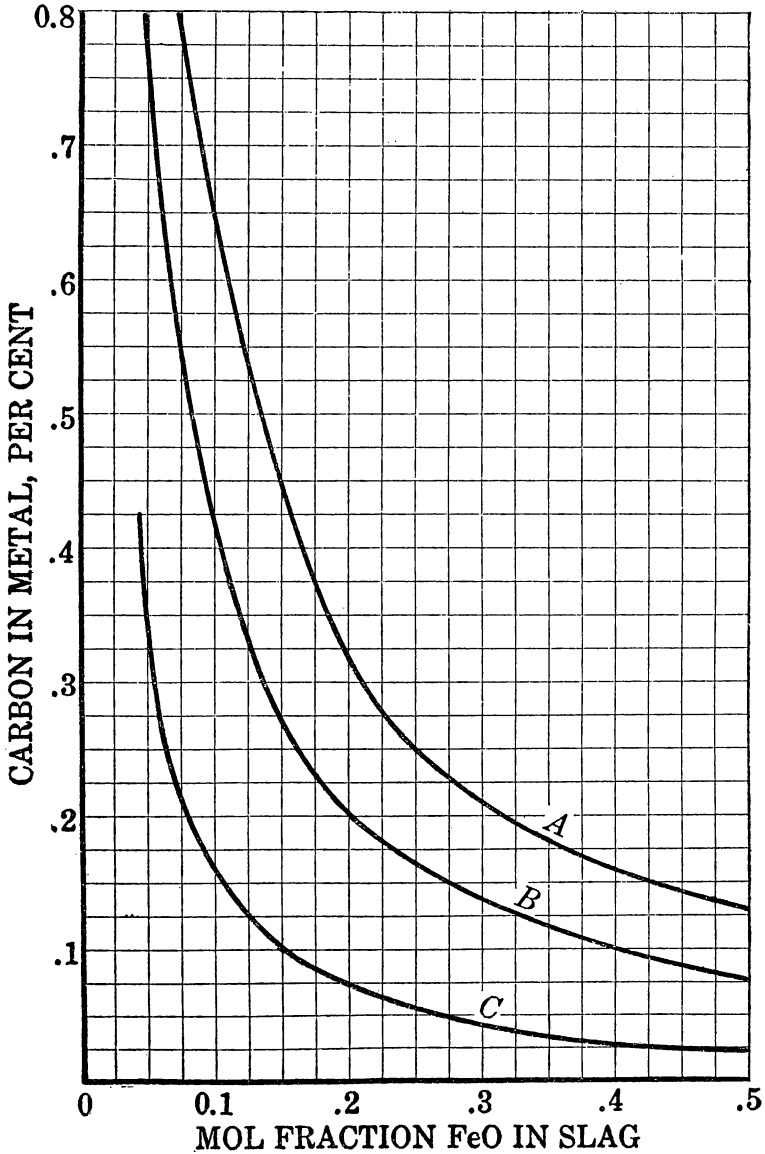


FIG. 88.—Relation between carbon in metal and FeO in slag; basic open hearth (Herty and others): A, 1,512° C. (2,750° F.); B, 1,567° C. (2,800° F.); C, 1,622° C. (2,960° F.)

ever, until actual experimental work has been done sole reliance should not be placed upon them.

DETERMINATION OF OXYGEN IN IRON AND STEEL

Oxygen is the sole element, known to enter steel or iron in appreciable and measurable quantities, which has been almost totally neglected until recently, except for occasional lone voices raised in the wilderness. The reason has lain in the difficulty of determining the oxygen content directly, and on that account little has been known about its effects on steels or on the iron-carbon system in general. The problem so appealed to Oberhoffer, of the Technische Hochschule in Aachen, Germany, that he spent many years in developing a satisfactory method for general analytical purposes and then applying it to a series of different commercial products. His work has been published in a long series of papers but was summed up after his recent death by some of his coworkers.⁹ His "hot-extraction" method involves melting in vacuo the sample to be analyzed with some Swedish iron as a carrier of carbon, collecting the carbon monoxide and carbon dioxide formed, and determining thereby the oxygen evolved. The iron-carbon alloy used to supply carbon must have been melted previously in vacuo and all traces of oxygen boiled out, and the sample so manipulated in the laboratory that it does not have opportunity to oxidize. This work is done in a special porcelain combustion tube with a porcelain boat, all designed to withstand vacuum at the melting temperatures of iron. A determination occupies 1 to 1.5 hours. Whether all the oxygen in the steel is evolved by this method is not known, but apparently all the oxygen present as FeO, most of that present as MnO, and probably a great deal of that present as SiO₂ and Al₂O₃ are evolved. Several hundred samples from different commercial products have been studied this way and the results reviewed in the above paper, but the method has not yet been applied by any of the investigators for purely scientific purposes, such as the study of oxyferrite, oxyaustenite, and other oxygenated phases in the iron system.

Apparently the time is ripe to use this analytical method in repeating much of the equilibrium work, making analyses for carbon and oxygen in some of the solid products whose composition now involves too much conjecture.

SCHENCK'S SPACE MODEL

Although Figure 79 gives the relations in the iron-carbon-oxygen system at 1 atmosphere, according to Schenck's interpretation of the

⁹ Oberhoffer, P., Hessenbruch, W., and Esser, H., Die Rolle des Sauerstoffes für die Metallurgie und die Qualität des Stahls: Ztschr. Ver. deut. Ing., Jahrg. 71, 1927, pp. 1569-1576.

equilibria which he measured, it is impossible to express in a single-plane diagram the pressure-composition-temperature relations. Schenck therefore represents the system in a space model, nine cross sections of which he has given, and which are reproduced in Figures 89 to 97. The bivariant equilibria which are not affected by pressure are represented by straight lines on these pressure-composition curves. Those equilibria which are affected by pressure are represented by curved lines. The producer-gas equilibrium is shown by dotted lines

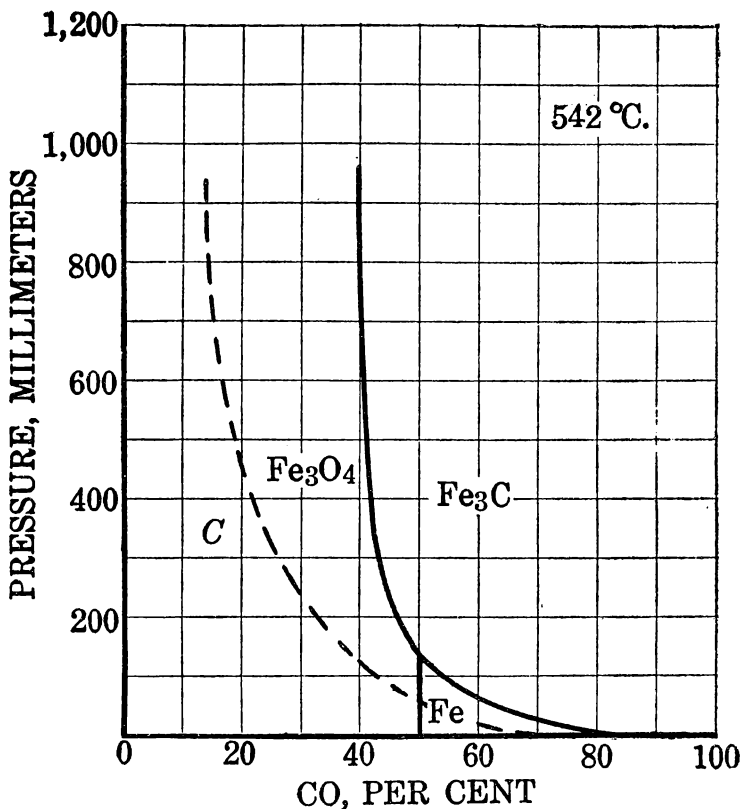


FIG. 89.—Schenck's space model of the iron-carbon-oxygen system

on all these figures. The following scheme of numbering of the various bivariant equilibria was used:

- 1 Bivariant equilibrium, Fe_3O_4 -wüstite-gas.
- 2 Bivariant equilibrium, wüstite-oxyferrite-gas.
- 3 Bivariant equilibrium, Fe_3C -oxyaustenite-gas.
- 4 Bivariant equilibrium, wüstite-oxyaustenite-gas.
- 5 Bivariant equilibrium, oxyferrite-oxyaustenite-gas.
- C Bivariant equilibrium, $2\text{CO}=\text{C}+\text{CO}_2$.

The various stability fields are designated, the wüstite by a *W* and the oxyferrite and oxyaustenite by *Fe* and *A*, respectively. All of

these data apply to the pure system iron-oxygen-carbon. If silica, magnesia, or a similar material which dissolves or combines with FeO is present, the above diagrams are profoundly modified. Schenck publishes two that are not reproduced here, with the plea that for complete understanding of the oxidation-reduction systems involved separate complete researches will have to be made in the presence of each of these constituents. In similar fashion any con-

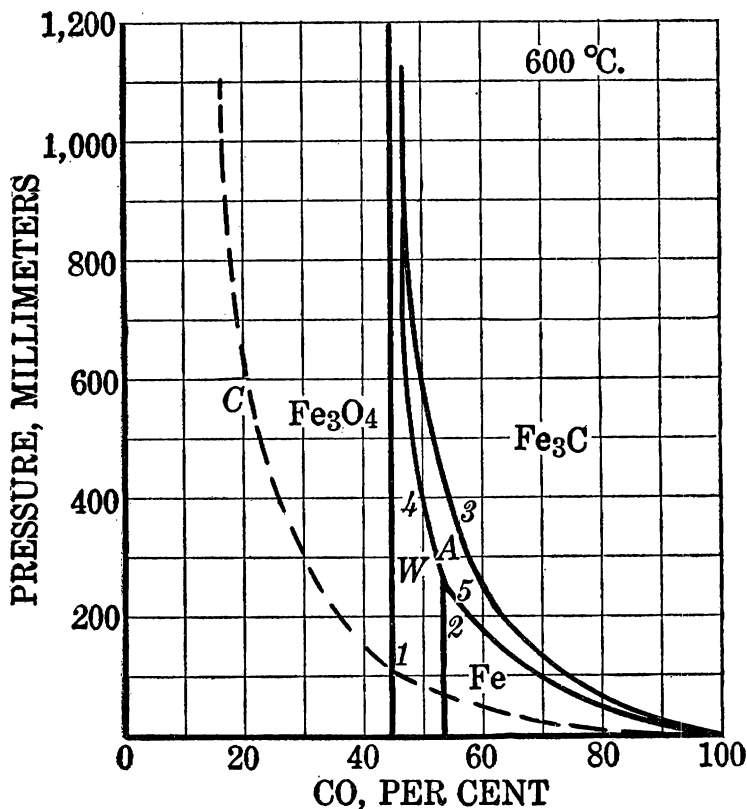


FIG. 90.—Schenck's space model of the iron-carbon-oxygen system

stituent that can combine with or dissolve iron metal will modify the system. Evidently a great deal of work still needs to be done to get a complete physicochemical picture of what goes on in the iron blast furnace.

CARBURIZATION EQUILIBRIA INVOLVING METHANE

When iron is heated in hydrocarbons like methane it is carburized and hydrogen is liberated; likewise, when iron-carbon alloys are heated in hydrogen they are decarburized. This suggests immediately that the tangle of oxygenated phases that result from the study

of carbon oxides on iron and iron-carbon-oxygen products might be unscrambled by studying the equilibria between iron-carbon alloys and mixtures of methane and hydrogen, oxygen being excluded thereby. Schenck¹⁰ has attempted this, but his results to date are somewhat sketchy and contradictory. He determined the equilibria at various temperatures of the equation:

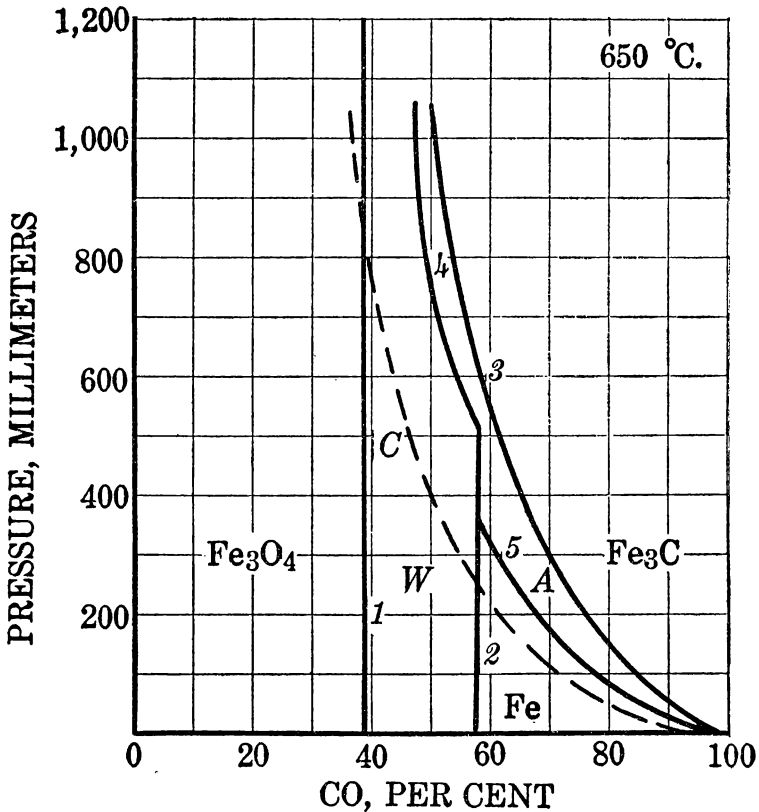
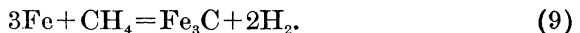


FIG. 91.—Schenck's space model of the iron-carbon-oxygen system

Both iron and cobalt were tested as catalysts and gave results that were in fair agreement, tabulated in Table 50. The equilibria were also studied for the equation:



These data are likewise tabulated in Table 50.

¹⁰ Schenck, R., Gleichgewichtsuntersuchungen über die Reduktions- Oxydations- und Kohlunsvorgänge beim Eisen; I: Ztschr. anorg. u. allgem. Chem. Jahrg. 164. 1927, pp. 145-185.

TABLE 50.—Equilibria of methane and of iron and methane at various temperatures

Temperature, °C.	$\text{CH}_4 = \text{C} + 2\text{H}_2$		$3\text{Fe} + \text{CH}_4 = \text{Fe}_3\text{C} + 2\text{H}_2$		Temperature, °C.	$\text{CH}_4 = \text{C} + 2\text{H}_2$		$3\text{Fe} + \text{CH}_4 = \text{Fe}_3\text{C} + 2\text{H}_2$	
	CH_4 , per cent	H_2 , per cent	CH_4 , per cent	H_2 , per cent		CH_4 , per cent	H_2 , per cent	CH_4 , per cent	H_2 , per cent
310	99.20	0.80	-----	-----	640	23.31	76.69	36.15	63.85
360	95.60	4.40	98.30	1.70	680	16.83	83.18	22.70	77.30
445	77.00	23.00	95.70	4.30	700	14.19	85.81	17.50	82.50
480	63.97	36.03	88.32	11.68	710	13.00	87.00	15.23	84.77
510	-----	-----	93.00	8.00	720	11.95	88.05	12.07	87.93
580	36.65	63.35	59.80	40.20	740	10.90	89.10	-----	-----

They apply to 1 atmosphere total pressure. Both of the above equations have a different number of molecules of gas on the two sides of the equation and therefore are affected by pressure.

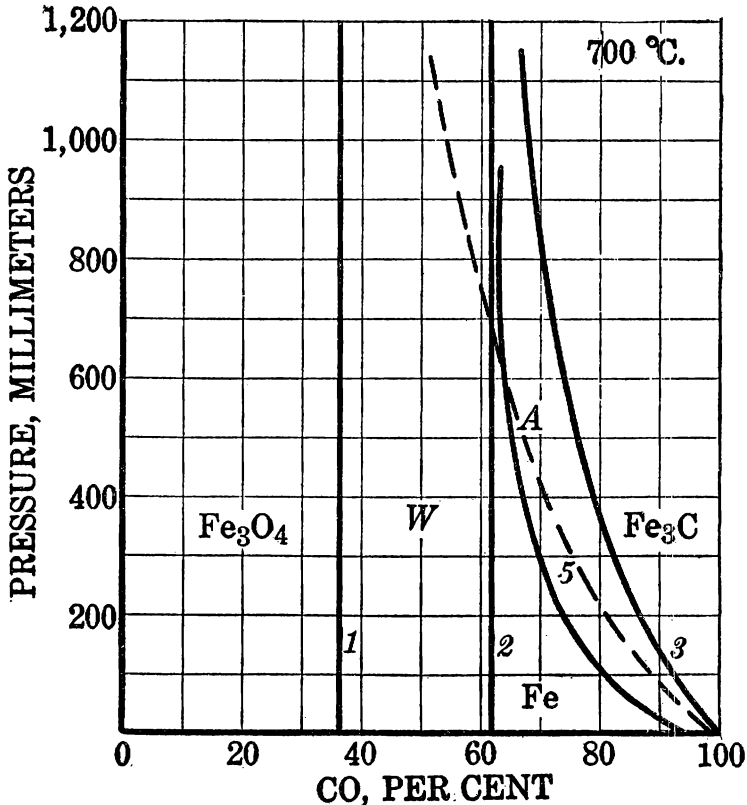


FIG. 92.—Schenck's space model of the iron-carbon-oxygen system

DISCUSSION OF FIGURE 98

The methane equilibrium results above were plotted in Figure 98 to compare them more definitely. The two curves intersect at 720° C.,

but all experience with the two systems leads us to expect that above the A_1 point there will be a widening into an area in which austenite is stable and that various hydrogen-methane mixtures will be capable of existing in equilibrium with various carbon contents of austenite, just as was true for the $\text{CO}-\text{CO}_2$ gas equilibria. Schenck therefore calculates that at point P_1 the iron-carburization equilibrium, if so manipulated that saturated austenite was maintained, would continue on past some point m , as indicated by the heavy line. Actually

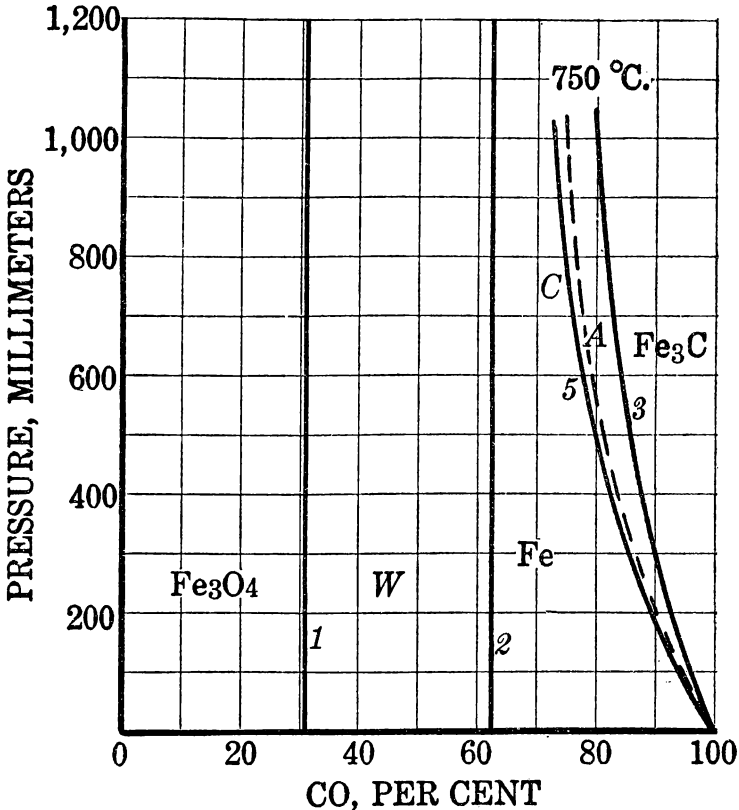


FIG. 93.—Schenck's space model of the iron-carbon-oxygen system

it swings over to point P_2 and if continued would follow the heavy line there indicated, after crossing the methane dissociation equilibrium line at P_2 . The point P_2 at 720°C . Schenck considers the eutectoid point for the stable system iron-carbon, and the point P_1 at 695°C . he considers the eutectoid point for the metastable system iron-cementite. This hypothesis is open to debate but in the absence of enough data can be conveniently left out of discussion for the present. All the curves for equilibria involving iron should approach zero methane in the gas as the A_3 point, 906°C ., is approached.

If Schenck's interpretation of the points P_1 and P_2 is correct, below P_2 it should not be possible to obtain direct cementation of iron by elemental carbon under a methane-hydrogen atmosphere, but by methane only. The reason is that at these temperatures less methane than can exist in equilibrium with carbon and hydrogen is present, and methane forms from carbon and hydrogen, while iron keeps on absorbing carbon from methane and producing hydrogen. Above

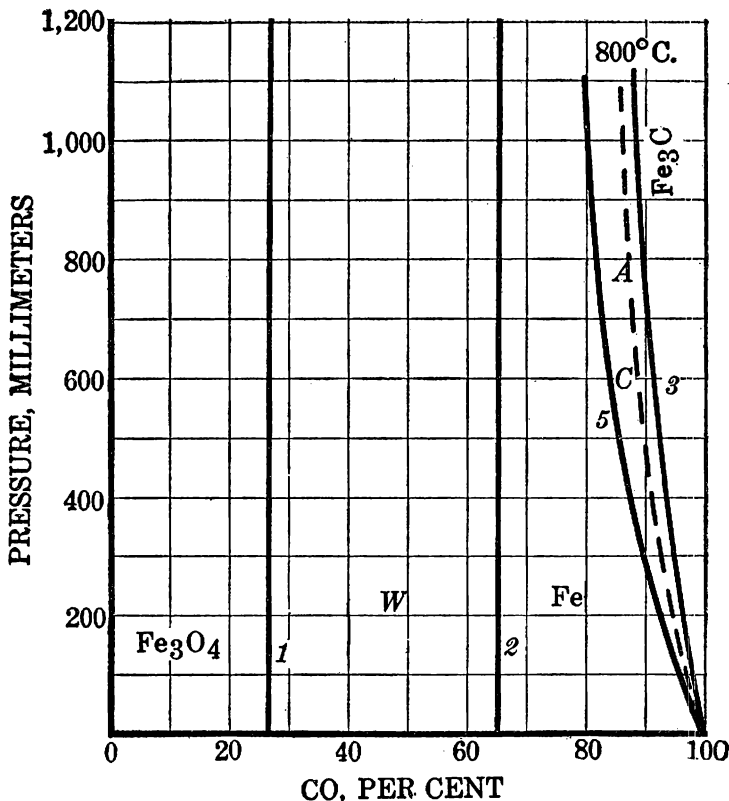
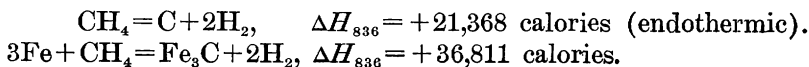


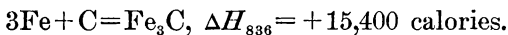
FIG. 94.—Schenck's space model of the iron-carbon-oxygen system

point P_2 is the only condition where it should be possible to make metallic iron absorb carbon direct from elemental carbon.

Using these data, in particular those for 445° and 680° C., Schenck made use of the van't Hoff isochore to calculate the heats of the reactions assumed for the above equilibria, with the following results, which apply to the mean temperature, 563° C. (836° K.):



By subtraction the equation for the formation of cementite is evolved:



This figure compares favorably with other thermal data about cementite. However, as Maurer and Bishof¹¹ point out, this favorable comparison can be obtained only with the lower temperature data, and at temperatures above 700° C. the calculated heats of reaction

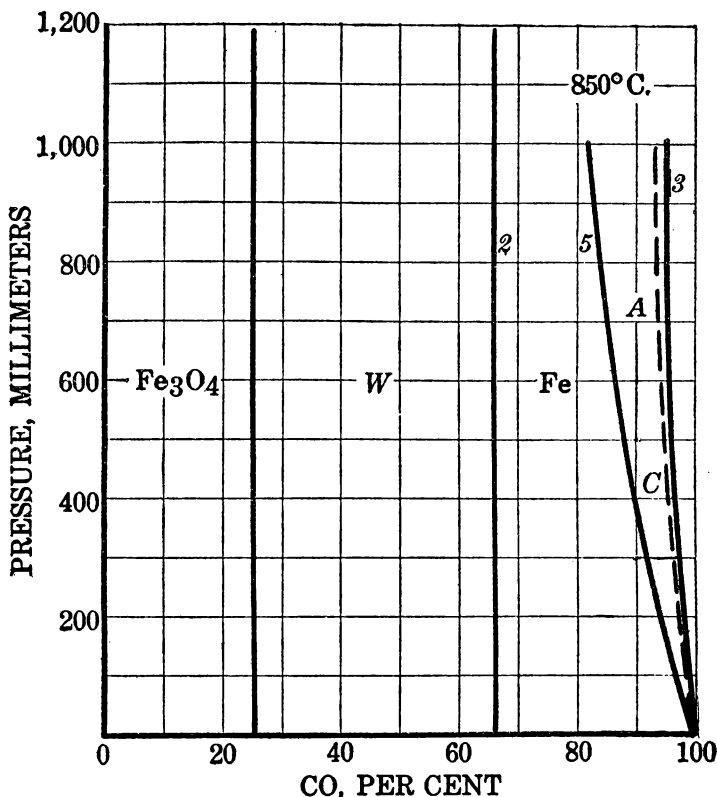


FIG. 95.—Schenck's space model of the iron-carbon-oxygen system

for both of the above equations are quite erratic. For the methane dissociation equilibrium they calculate from Schenck's data that whereas the heat of reaction just below 700° C. is about 21,368 calories, as above quoted, just above that temperature the data are fairly consistent in pointing toward a value about 4,000 calories higher. They ascribe this fact to the formation below 700° C. of amorphous carbon and above 700° C. to a form of carbon more re-

¹¹ Maurer, E., and Bishof, W., Gleichgewichtsuntersuchungen über die Reduktions- Oxydations- und Kohlungsvorgänge beim Eisen: Stahl. u. Eisen, Jahrg. 48, 1928, pp. 15-21.

sembling graphite. Alternatively, it must be remembered that an iron catalyst was used for the methane equilibrium, and the erratic behavior above 700°C . may be connected with the catalyst and not with the form of carbon. Whatever the cause, the data above 700°C . are too unsafe to allow any conclusions.

Using Schenck's methane data and their own $\text{CO}-\text{CO}_2$ data, Johansson and von Seth calculated a diagram for methane similar to that in Figure 83, giving the gas analyses (methane and hydrogen) in

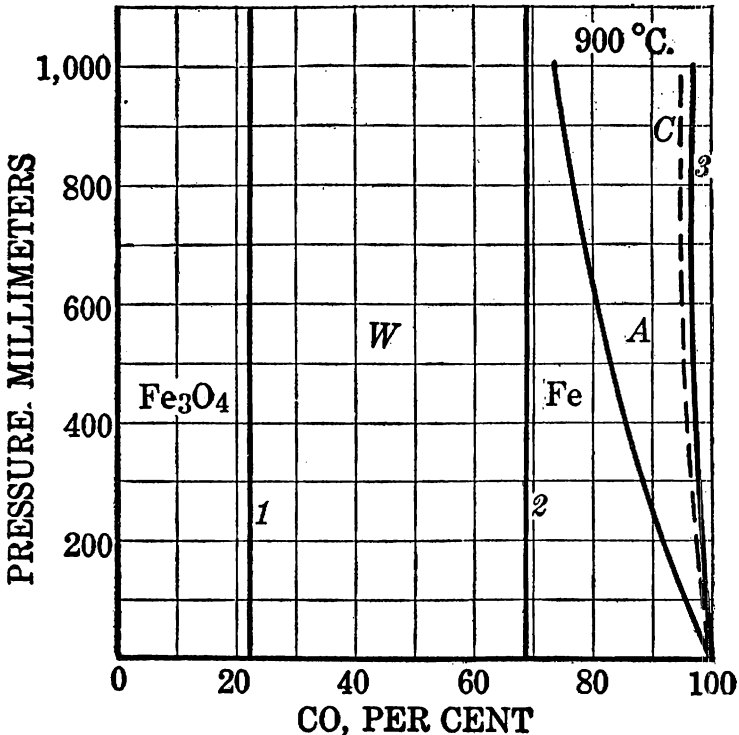


FIG. 96.—Schenck's space model of the iron-carbon-oxygen system

equilibrium over austenites of different concentrations at various temperatures. As there is so much doubt about the $\text{CO}-\text{CO}_2$ equilibria, their diagram has only passing interest and awaits experimental confirmation.

Higher temperature data involving iron, methane, and hydrogen are very scattered. Hydrogen has long been known as a good decarburizing gas; moreover, it has been known qualitatively that methane and other hydrocarbons would carburize iron. At the higher temperatures very little methane can exist, as shown by the equilibrium

data for the methane dissociation equation at higher temperatures, derived from the data of Pring and Fairlie,¹² quoted in Table 51.

TABLE 51.—Equilibrium data for methane dissociation at high temperatures

Temperature, °C.	CH ₄ = C + 2H ₂		Temperature, °C.	CH ₄ = C + 2H ₂	
	CH ₄ , per cent	H ₂ , per cent		CH ₄ , per cent	H ₂ , per cent
700	15.0	85.0	1,000	1.02	98.98
750	10.0	90.0	1,100	.485	99.515
800	5.50	95.0	1,200	.255	99.745
850	3.45	96.55	1,300	.145	99.855
900	2.30	97.60	1,400	.08	99.92
950	1.53	98.47			

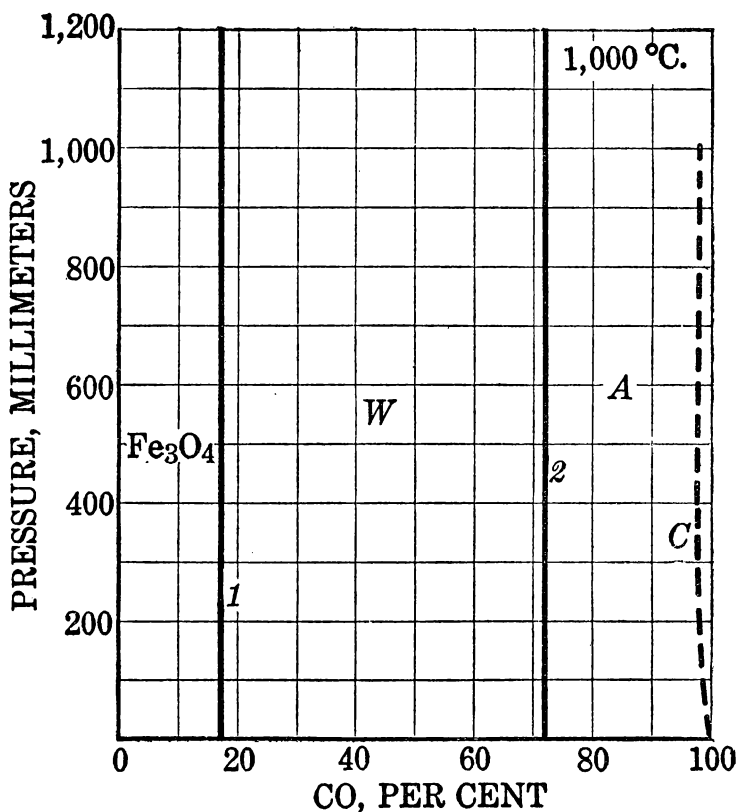


FIG. 97.—Schenck's space model of the iron-carbon-oxygen system

On this account, in decarburizing with hydrogen at high temperatures a great excess must be used. Conversely, when carburizing with methane nearly all of its available carbon can be absorbed.

¹² Pring, J. N., and Fairlie, D. M., The Methane Equilibrium: Jour. Chem. Soc. London, vol. 101, 1912, pp. 91-103.

DISCUSSION OF FIGURE 99

A few experiments on the methane-hydrogen equilibrium with iron-carbon alloys in the temperature range of austenite stability have been made by Sykes.¹³ He used the null method of Johansson and von Seth, determining by many trials at each temperature the mixture of CH_4 and H_2 that was neutral to a given steel. He used a mixture of hydrogen and natural gas, the latter as a source of methane. It actually contained ethane in addition to 77 to 82 per cent of methane and was calculated by Sykes to be equivalent to 80

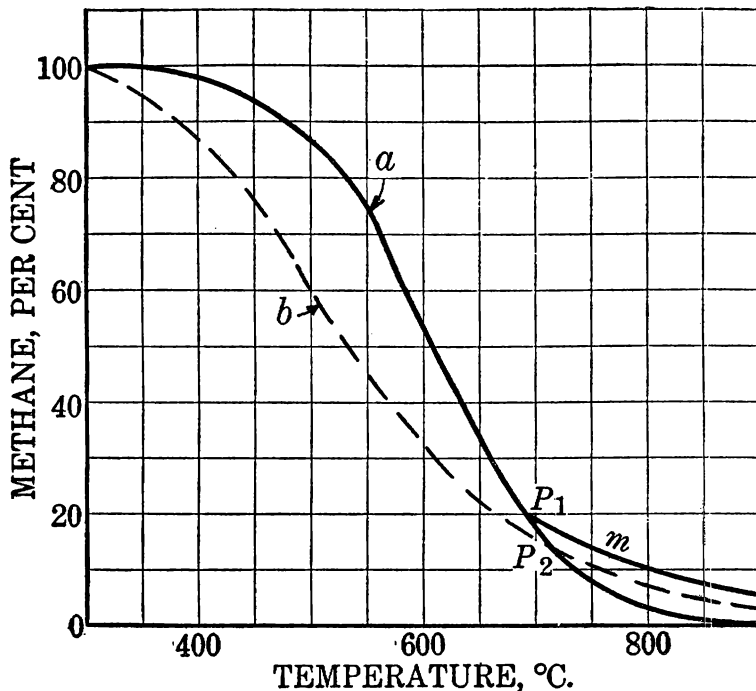


FIG. 98.—Equilibria for methane (Schenck): *a*, equilibrium, $3\text{Fe} + \text{CH}_4 = \text{Fe}_3\text{C} + 2\text{H}_2$; *b* equilibrium, $\text{CH}_4 = \text{C} + 2\text{H}_2$

per cent of CH_4 . The ethane content was 12 to 17 per cent, and the remaining constituents are not mentioned. Therefore, Sykes's results can be taken only in a qualitative way. Figure 99 gives his results for gas mixtures neutral to three different steels, with carbon contents, respectively, of 0.95 to 0.59, and 0.18 per cent in curves *a*, *b*, and *c*. The abscissas are given as per cent natural gas and should be divided by 1.3 to give the approximate methane percentage. The steel with 0.18 per cent of carbon received the most attention.

¹³ Sykes, W. P., Carburizing Iron by Mixtures of Hydrogen and Methane: *Trans. Am. Soc. Steel Treating*, vol. 12, 1927, pp. 737-758.

Whereas it had been expected that curve *c* at higher temperatures would continue toward *d*, it actually turned up to higher methane percentages, and this behavior was checked by that of the higher carbon steels as far as their curves were followed. No explanation

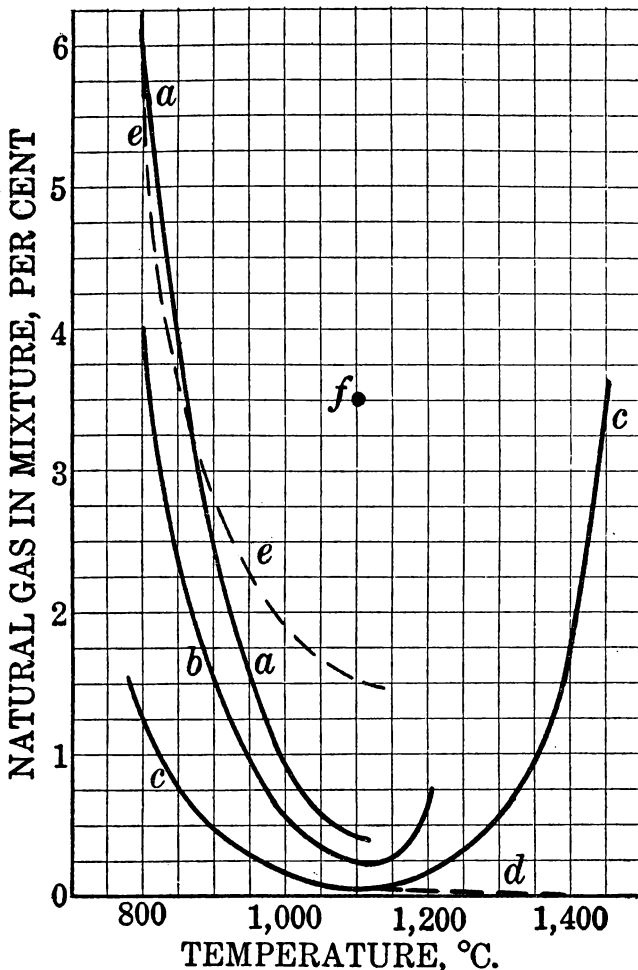


FIG. 99.—Equilibria for methane-hydrogen-steel (Sykes): *a*, 0.95 per cent carbon steel; *b*, 0.59 per cent carbon steel; *c*, 0.18 per cent carbon steel; *d*, anticipated extrapolation of carbon; *e*, 0.18 per cent carbon steel, gas with 0.6 per cent H_2O ; *f*, 0.18 per cent carbon steel, gas with 3.3 per cent H_2O .

is given or seems available. Of course, it must be remembered that in the temperature range above $1,135^{\circ}C.$ a portion of the steel is molten and approximates the eutectic composition, while the remainder should be austenite (see the iron-carbon diagram). The

increase in methane content required to keep the gas neutral is coincident with the appearance of the liquid phase.

Sykes tried the effect of small amounts of water vapor in his gas mixture, as it was known that hydrogen would decarburize steel much more rapidly if it were moist. Curve *e*, which must be compared with curve *c*, shows the effect of 0.6 per cent by volume of water vapor on the composition of the gas mixture neutral to 0.18 per cent C steel. Presumably the water vapor reacted with part of the methane, thereby removing it from the mixture, and the gas actually resulting differed from the synthetic mixture entering the apparatus. With a different rate of flow a different gas mixture might have been needed. Point *f* is for the same steel and shows the effect of adding 3.3 per cent of water vapor to the gas mixture.

These data are too scanty to allow determination of the total stability fields of the various concentrations of austenite, as was done by Takahashi and by Johansson and von Seth. Throughout the whole literature involving methane and iron only small amounts of rather disappointing data are available. In no case are there enough data to assist much in solving the problems of carburization and decarburization by CO-CO₂ mixtures.

MISSING EQUILIBRIA

The systems involving Fe and Fe₃C in contact with CO-CO₂ mixtures as gas probably contain more phases than have been identified. Cementite and ferrous oxide are both apparently soluble in γ iron to a considerable extent, forming a mixed material called oxyaustenite. If the iron-oxygen system were as well known as the iron-carbon system, one would probably find that ferrous oxide, like cementite, could lower (possibly raise) the A_3 transformation point and form solid solutions with γ iron, just as cementite can form the normal austenite solid solution. The stability field of the oxygen austenite in contact with gas could hardly be expected to coincide with that of the carbon or cementite austenite. The equilibria where these various unknown phases exist simultaneously with each other and with the known phases are known very imperfectly. Almost certainly the diagram of Schenck in Figure 79 will be corrected and elaborated.

The greatest need at present is to study carburization in an oxygen-free system, say with methane, and to work out the diagrams more completely, identifying and defining the solid phases that form. Second, the iron-oxygen system should be worked out, followed by a study of iron-oxygen reduction by means of hydrogen (carbon-

free system), in order that all three groups of results could finally be used to help interpret phenomena when iron is treated by gases containing CO and CO₂.

In this system, if iron is to be carburized by CO almost certainly the primary reaction is the splitting of CO according to the reaction, $2\text{CO}=\text{C}+\text{CO}_2$, the carbon combining with the iron to form solutions or carbide and the CO₂ remaining inactive due to dilution with CO, or reacting with iron to form FeO in case conditions are right. Pure iron dissolving an infinitesimal amount of C, Fe₃C, or of FeO so lowers the activity of the solute that its commonly known thermodynamic properties are of little value in predicting its behavior. Therefore, the first product of action of a small amount of CO on either α or γ iron is bound to be a solid solution of two or more of them in the iron, with the resulting disappearance of most of the CO. If one chooses a certain temperature on the iron-carbon diagram, starting with pure iron which is to react with small increments of CO and proceeding thence across the diagram, carburizing the iron, the complexities in possible solid phases and equilibria become so great that the task appears almost hopeless. More phase changes are called for than can possibly be found by taking a constant-temperature cross section of Schenck's diagram in Figure 79. The subject must, therefore, be left to future investigators with the injunction to use more rigorously the phase rule and the probabilities of existence of various solid phases.

IRON CARBONYLS

Since the presence of iron carbonyls has been suggested several times in the preceding pages as a possible explanation of the complexes of iron, carbon, and oxygen which formed under various conditions, it is well to review their properties briefly here.

Iron will unite directly with carbon monoxide to form three different carbonyls, which in the order of their importance and ease of preparation are: Ferropentacarbonyl, $\text{Fe}(\text{CO})_5$; diferrononacarbonyl, $\text{Fe}_2(\text{CO})_9$; and iron tetracarbonyl, $\text{Fe}(\text{CO})_4$. The latter two are crystalline solids under ordinary conditions, and the first is an amber liquid at room temperatures. When heated the two solid forms decompose, yielding the pentacarbonyl, iron, and CO.

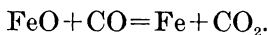
Although pentacarbonyl can be formed directly from iron under 1 atmosphere pressure at about 80°C ., the yield is low and is very much enhanced by increasing the pressure of the CO gas. The gas need not be pure, as water gas will react in the same way, and most of the common impurities of water gas, coke-oven gas, or coal gas do not show very bad effects. By using higher pressures higher temperatures may be used, and at 200°C . a pressure of 50 to 200 atmospheres will give a gas containing 2 to 8 per cent of the pentacarbonyl. Above 250°C . the tendency of CO to split into carbon and CO_2 is too great and makes the yield of $\text{Fe}(\text{CO})_5$ lower. Under ordinary atmospheric pressure heating above about 100°C . causes the pentacarbonyl to dissociate again into iron and carbon monoxide. These facts are at the basis of several patents for the production of pure iron.¹⁴

The most complete discussion of the iron carbonyls is that of Fieldner and Jones,¹⁵ to which those interested are referred. They state that the reaction $\text{Fe} + 5\text{CO} = \text{Fe}(\text{CO})_5$ takes place mainly in the temperature range 100 to 300°C ., and is reversed by increase in temperature and decrease in pressure. Toward 330°C . another reaction begins to be appreciable, $\text{Fe} + \text{CO} = \text{FeO} + \text{C}$, according to Sabatier

¹⁴ Johnson, J. Y., Für badische Anilin und Soda Fabrik: British Patent 256428, 1925; also, I. G. Farbenindustrie, A.-G.: British Patent 262938, Dec. 14, 1925.

¹⁵ Fieldner, A. C., and Jones, G. W., Iron Carbonyls; Their Physical and Chemical Properties: Am. Gas. Assoc. Monthly, vol. 6, 1924, pp. 439-447.

and Senderens,¹⁶ but this is improbable, as FeO is too unstable at 330° C., and if any oxide is formed it must be magnetite. The same authors also claim that above 400° C. a new reaction sets in:



This is the ordinary gas-reduction equation which has been dealt with in this report, but again Sabatier and Senderens were wrong on the composition of the oxide involved, as it is probably magnetite. The net result of these last two equations is the splitting of CO into C+CO₂. In fact, the basic reaction underlying both is probably 2CO=C+CO₂, which is known to be catalyzed at low temperatures by iron, and if the temperature is insufficient to cause the iron oxide to be reduced by CO, carbon monoxide might be split continuously until all the metallic iron had been oxidized by CO₂. This amounts to saying that at 330° to 400° C. the oxidation of finely divided iron by CO₂ is more rapid than the reduction of the resulting oxide by CO, whereas above 400° C. the two rates are nearer equal, so that equilibrium can be attained.

FORMATION OF CARBONYLS

The easiest conclusion that can be reached in consideration of these facts is that carbon monoxide can combine with metallic iron to form a pentacarbonyl, which is largely dissociated at all temperatures above 200° C., except under high pressures of CO. Of course, nothing is known of the solubility of ferropentacarbonyl in metallic iron, nor its stability while so dissolved, but any of it which does dissolve could easily be much more stable and might have some relation to the iron-carbon-oxygen solid complexes known to exist at temperatures up to 1,100° C. The carbonyls have been associated¹⁷ with the deposits of finely divided iron oxide found in the "down-comer" pipes that convey exit gas away from the top of an iron blast furnace, the theory being that small amounts of carbonyls formed in the furnace were dissociated and the iron oxidized and carried along as a fume (more finely divided than a dust).

Carbonyl forms when CO is compressed and stored in iron cylinders at ordinary pressures, an instance being given of a case where water gas (39 per cent of CO) stored under 8 atmospheres in a steel cylinder¹⁸ for a month gave a gas which on release car-

¹⁶ Sabatier, P., and Senderens, J. B., *Action de divers metaux divises sur l'oxyde de carbone*: Bull. soc. chim., t. 29, 1903, p. 294.

¹⁷ Mond, L., *Metallic Carbonyl*: Jour. Soc. Chem. Ind., vol. 11, 1892, p. 750.

¹⁸ Roscoe, H. E., and Scudder, F., *Notes of the Action of Water Gas on Iron*: Proc. Chem. Soc., vol. 7, 1891, p. 126.

ried 2.4 milligrams of Fe per liter. The gas industry has always suspected that some of the deposits in pipes and valves and on gas mantles originated in the formation of carbonyls.

PROPERTIES OF CARBONYLS

The above justifies the cataloguing in this paper of the more important properties of the three carbonyls, as reported by Mond and his coworkers¹⁹ and by Dewar and Jones²⁰ (see Table 52).

TABLE 52.—*Properties of iron carbonyls*

Property	Fe(CO) ₅	Fe ₂ (CO) ₉	Fe(CO) ₄
Room temperature.....	Yellow liquid.....	Hexagonal orange crystals.	Green prismatic crystals.
Specific gravity.....	{ 1.4937 at 0°/4°..... 1.4565 at 21.1°/4°..... 1.4330 at 40°/4°.....	2.085 at 18° C.....	1.996 at 18° C.
Melting point.....	19.5 to 20° C.....	Dissociates.....	Dissociates.
Boiling point.....	102° C. at 744 millimeters.do.....	Do.
Critical temperature.....	285 to 288° C.....do.....	Do.
Do.....	29.5 atmospheres (calculated).do.....	Do.
Latent heat of evaporation	39.45 calories/gram.....do.....	Do.
	° C. Mm.		
	{ 7.0 14.0..... 10.0 16.0..... 16.1 25.9.....	Unknown.....	Unknown.
Vapor pressure.....	{ 18.4 28.2..... 35.0 52.0..... 57.0 133.0..... 68.0 311.2.....do.....	Do. Do. Do. Do.
Soluble in.....	Ether, alcohol, mineral oil, benzene.	Pyridine.....	Toluene, petroleum, ether.
Effect of light:			
Liquid in dark.....	Stable.....do.....do.....
Liquid in light.....	Gives Fe ₂ (CO) ₉ +CO.....do.....do.....
Liquid in sun.....do.....do.....do.....
Solutions in light.....do.....do.....do.....
Effect of heat.....	At 180° C. splits to Fe+5CO.	At 100° C. gives Fe(CO) ₅ +Fe+CO.	At 140° C. gives Fe(CO) ₄ +Fe+CO.

Addition properties of the pentacarbonyl have recently been published by A. Mittasch (*Ztschr. angew. Chem. Jahrg. 41, 1928, pp. 827-833*). Its surface tension at 20° C. is 22 dynes per centimeter and its viscosity 0.0075 c. g. s. units. The heat of formation of the liquid is 54,200 calories, its heat of combustion 384,500 calories, and its latent heat of fusion 3,250 calories per mol (16.6 calories per gram). In alkaline solution it behaves as a powerful reducing and dechlorinating agent for organic compounds.

¹⁹ Mond, L., and Quincke, F., Note on a Volatile Compound of Iron with Carbon Monoxide: *Jour. Chem. Soc.*, vol. 59, 1891, p. 1090.

Mond, L., *Metallic Carbonyls*: *Jour. Soc. Chem. Ind.*, vol. 11, 1892, p. 750.

Mond, L., and Wallis, A., Some Researches on the Metallic Carbonyls: *Jour. Soc. Chem. Ind.*, vol. 40, 1921, p. 430-r.

²⁰ Dewar, J., and Jones, H. O., *Physical and Chemical Properties of Iron Carbonyls*: *Proc. Royal Soc.*, vol. 76-a, 1905, p. 558.

Further interest attaches itself to the pentacarbonyl, due to the fact that it has promise as an antiknock compound for use in motor fuels. Unfortunately, in light the solutions in organic solvents tend to decompose to give the diferrononacarbonyl and CO, but this defect can be overcome by adding a coloring substance or one capable of acting as a protective colloid.²¹ New publications on these compounds may therefore be expected, as considerable research and semicommercial development work has been done in Germany.

²¹ Badische Anilin und Soda Fabrik, Iron Carbonyl: British Patent 260639, 1925.

THE SYSTEM IRON-OXYGEN

The preceding sections have given details of many important portions of the system iron-oxygen, and it now remains to assemble the total system, as far as the materials with less oxygen than ferric oxide are concerned. For the metallurgy of iron no importance whatever can be attached to the pure oxygen end of the system, except possibly the thermodynamic properties of oxygen gas, which are of importance in deriving the thermodynamic properties of the iron oxides. These data on oxygen gas are available in such texts as that of Lewis and Randall²² and therefore need no discussion here. In like manner the thermodynamic properties of water, methane, carbon monoxide, and carbon dioxide gases are satisfactorily presented in such texts. The substances requiring present critical discussion are the oxides of iron and their intermediate complexes.

Many papers written on the system iron-oxygen have speculated on the form it should take but have lacked experimental data for most of their areas and have therefore been only of qualitative value, if any. The first experimenters to begin an approach toward actual facts which could be plotted intelligently were Sosman and Hostetter²³ on the mixtures between ferric oxide and magnetite, Kohlmeyer²⁴ on the mixtures between magnetite and ferrous oxide, and Tritton and Hanson²⁵ on the mixtures between ferrous oxide and metallic iron. All of this work has been reviewed critically in preceding sections, and what remains now is to combine it all.

DISCUSSION OF FIGURE 100

One of the principal difficulties has been the failure to understand the properties of ferrous oxide. Repeated attempts to prepare a pure specimen have met failure, and the reason was finally pointed out by the work of Schenck,²⁶ who found that between magnetite and ferrous oxide was a zone of solid solutions which he named wüstite.

²² Lewis, G. N., and Randall, M., *Thermodynamics and the Free Energy of Chemical Substances*: McGraw Hill Book Co., New York, 1923.

²³ Sosman, R. B., and Hostetter, J. C., *The Oxides of Iron, I. Solid Solution in the System Ferric Oxide-Magnetic Oxide*: Jour. Am. Chem. Soc., vol. 38, 1916, pp. 807-833.

²⁴ Kohlmeyer, E. J., *Über Bleioxyd und Eisenoxydulferrierte*: Metall. u. Erz., Jahrg. 1, 1913, pp. 447-462; *Versuche über das Schmelzen von Eisenoxyd*: Metallurgie, Jahrg. 6, 1909, pp. 323-325.

²⁵ Tritton, F. S., and Hanson, D. J., *Ferrous Alloys Research. Iron and Oxygen*: Iron and Steel Inst., vol. 110, 1924, pp. 85-143.

²⁶ Schenck, R., *Eisen, Kohlenstoff, und Sauerstoff in ihren wechselseitigen Beziehungen*: Stahl u. Eisen, Jahrg. 46, 1926, pp. 655-682.

His conception of the total system, exclusive of the mixtures intermediate between Fe_2O_3 and Fe_3O_4 , is included in Figure 100. This diagram shows the stability field of wüstite, which above 570°C . (Schenck says 560°C .) can exist as a homogeneous solid solution of variable composition. Another field of solid solutions capable of existing as a homogeneous phase is that of oxyferrite—iron with various concentrations of dissolved ferrous oxide or, more properly, wüstite. Any mixture intermediate between wüstite and oxyferrite can not exist at any of the temperatures plotted as a homogeneous single phase but splits into two solid solutions represented by the ends of the horizontal lines drawn between the oxyferrite and the wüstite fields. That at the oxyferrite side of the heterogeneous field is oxyferrite saturated with wüstite and that at the wüstite side of

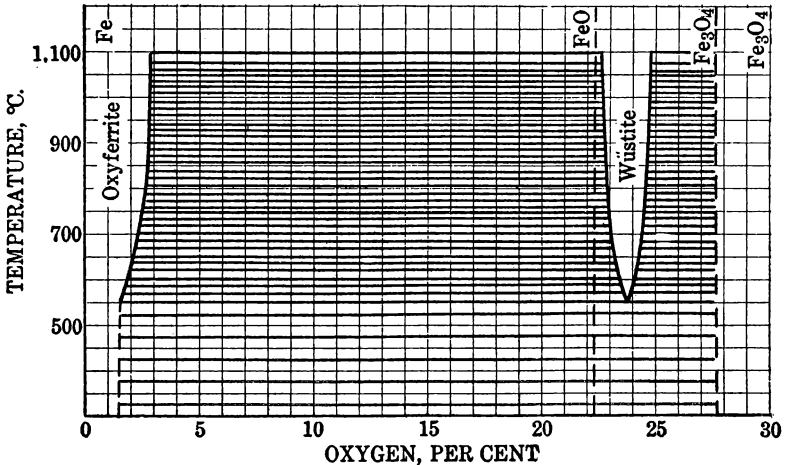


FIG. 100.—Iron-oxygen composition-temperature diagram (Schenck)

the field consists of wüstite saturated with oxyferrite or iron. Alteration in the gross over-all analysis of a sample in this field merely alters the relative amounts of the two solid solutions present. A mixture of the total oxygen-iron ratio corresponding to ferrous oxide is seen to be doomed to split into wüstite and oxyferrite and on chemical analysis will show the presence of at least small amounts of metallic iron and ferric iron (supposedly magnetite).

A similar heterogeneous field exists between wüstite and magnetite.

PLACING OF WÜSTITE AREA

The placing of the wüstite area adjacent to FeO but actually in the area between FeO and Fe_3O_4 requires rather careful scrutiny. Schenck found the boundaries of this area by means of a series of reduction isotherms, the details of which are given in part in Figure

25 of the section on "Complexes intermediate between magnetite and ferrous oxide." All of Schenck's isotherms were obtained by *reducing* ferric oxide at set temperatures with mixtures of carbon monoxide and carbon dioxide, periodically removing part of the gas and replacing it with carbon monoxide. The flat portions on his curves corresponded to the equilibrium between one phase of higher oxidation and that of next lower oxidation. Vertical portions or inclined portions of his curves came when one phase of an equilibrium was exhausted; therefore the gas mixture in equilibrium with the solid material could retain a greater amount of CO than before this solid of high oxygen composition had disappeared. Inclined portions of the isotherms are due to solid solutions, each ratio of solid constituents in the solution demanding a definite ratio of CO to CO₂ in the gas. Schenck was therefore always proceeding from left to right along his isotherms. However, one of the isotherms given in the diagram mentioned above is that of Eastman and Evans, who not only reduced ferric oxide isothermally with hydrogen but also oxidized iron with water vapor, and their averaged results (the 772° C. isotherm) do not show the inclined portion of their isotherm (wüstite) in the same relative position as does Schenck.

An explanation of this discrepancy could be found by assuming that the cores of some of Schenck's lumps of material remained unreduced or partly reduced and that the gas was approaching equilibrium with their shells only. Eastman and Evans, by oxidizing isothermally and averaging the results with isothermal reduction, placed their wüstite line where one would normally expect it—astride the portion on the diagram corresponding to FeO. If Schenck's position for the wüstite area is accepted, no one could possibly produce pure FeO by gas reduction or oxidation methods, and yet there are several reports that claim the accomplishment of this very thing. On that account the writer has seen fit in Figure 102, about to be described, to shift the position of the wüstite area to a point where it includes FeO.

Below 570° C. wüstite is metastable and all the mixtures intermediate between oxyferrite and magnetite split into these two constituents, producing a heterogeneous mixture.

DISCUSSION OF FIGURE 101

Schenck's diagram does not show any difference between the solubility of wüstite in γ and in α iron. It also does not extend below 570° C., at which point a different material, magnetite, is in solution in the oxyferrite, and the shape of the oxyferrite boundary ought to change to correspond. With the idea that the lower slope of the Schenck oxyferrite boundary between 570° and 800° C. might be associated with the properties of α iron, as compared to γ iron at the

higher temperatures, Schenck's original data were consulted and plotted on a large scale (see fig. 101), giving thereby seven data fixing the oxyferrite boundary. Instead of a single smooth curve, as plotted by Schenck, the three lower temperature data did not seem to be at all consistent with the four higher temperature ones. Although so few points are insufficient for drawing any safe con-

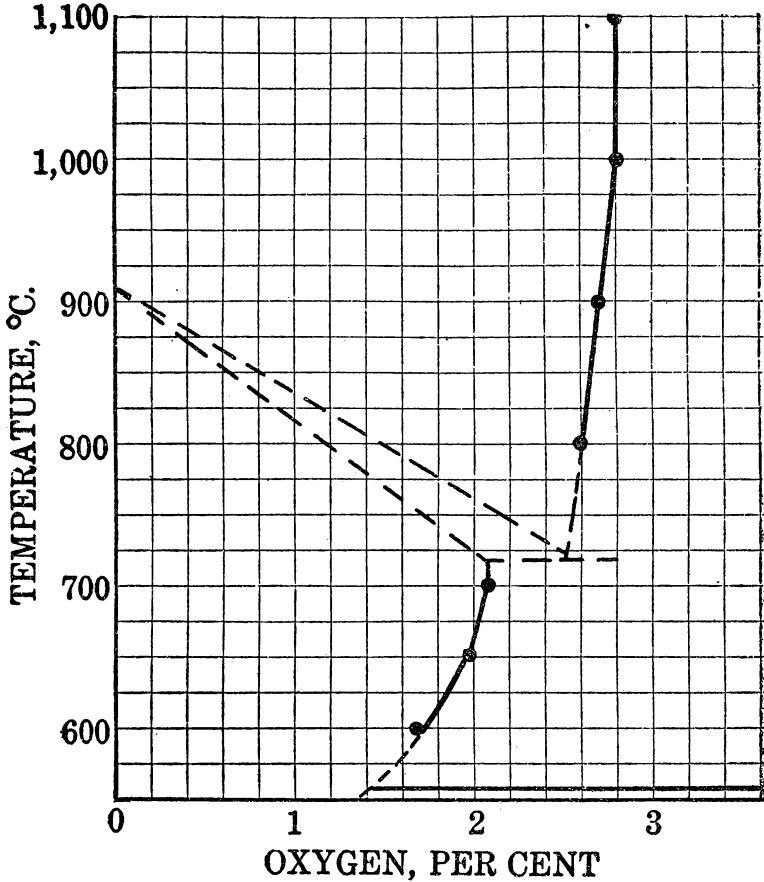


FIG. 101.—Possible interpretation of Schenck's oxyferrite

clusions, it is reasonable to suppose that these two apparently different curves are real, the lower being the solubility curve for FeO in α iron and the upper for FeO in γ iron. Another fixed point is the A_3 temperature of pure iron known to be lowered by the presence of many substances to a eutectoid point, as is the case with carbon. Such a eutectoid point has been sketched in with dotted lines, the exact temperature of the eutectoid being unknown, but somewhere in the range between 700° and 800° C.

Schenck's data on oxyferrite were determined by changes in direction of his reduction isotherms and may involve other phases than those assumed. They show many times greater solubility of wüstite in oxyferrite (FeO in Fe) than do the results of experimenters who have melted iron in contact with molten iron oxides and then chilled the samples of liquid and solid. In justice to Schenck it must be pointed out that the phase liquid iron, formed by melting δ iron (high-temperature α iron), is a different substance from γ or α iron and doubtless has its own peculiar dissolving power for materials approximating the analysis of FeO. This dissolving power is much lower than that indicated by Schenck's low-temperature forms of iron, and, naturally, samples cooled from high temperatures will therefore not contain amounts of FeO which would uphold Schenck's work. However, here again Schenck may have suffered from having cores of unreduced oxide coated over by shells of metallic iron during his isothermal slow reductions, although Eastman and Evans's oxidation isotherm gives him powerful support.

BENEDICKS AND LÖFQUIST'S TEMPERATURE-COMPOSITION DIAGRAM

The most complete and most recent diagram of the total system is that of Benedicks and Löfquist,²⁷ reproduced, with a few corrections, in Figure 102. The existence of a wüstite field is accepted from Schenck's work and its position shifted to FeO, but the high solubility of FeO in oxyferrite is not accepted, and other data are therefore substituted. The solubility of oxygen in solid α iron at room temperature has been determined by a number of observers, whose average is 0.05 per cent (0.227 per cent of FeO); Wimmer²⁸ found 0.035 per cent, while Oberhoffer, Schiffler, and Hessenbruch²⁹ found about 0.05 per cent. For γ iron the solubility of FeO is somewhat greater because there is a certain lowering of the A_3 point in oxidized iron, as was pointed out in an earlier chapter. Lowering of the A_3 point will be accompanied by raising of A_4 point of the iron.

The melting point of pure iron is lowered by presence of dissolved FeO, as determined by Tritton and Hanson, giving point B in the diagram. The solubility curve of FeO in molten Fe, line BD , is taken from the more recent work of Herty,^{29a} quoted in an earlier section, whereas Benedicks and Löfquist used the approximations of de Coussergues.³⁰

²⁷ Benedicks, C., and Löfquist, H., Über das System Eisen-Sauerstoff: Ztschr. Ver. Deut. Ing., Jahrg. 71, 1927, pp. 1576-1577.

²⁸ See footnote 92, p. 118.

²⁹ Oberhoffer, P., Schiffler, H. J., and Hessenbruch, W., Sauerstoff in Eisen und Stahl: Stahl u. Eisen, Jahrg. 47, 1927, p. 1540.

^{29a} See footnote 8, p. 264.

³⁰ de Coussergues, C., "Influence de la temperature dans la fabrication d'acier": Rev. Metal., t. 19, 1922, p. 639.

In the higher temperature ranges liquid Fe and liquid FeO are only partly miscible, the compositions of the two liquids being shown by the two lines extending upward and probably approaching each other at some point above 2,000° C., where they become miscible in all proportions. The freezing point of FeO is near 1,370° C., therefore the curve *CGM* extends down at least that far, the melting point of FeO seemingly being hidden and thereby forcing point *M* to fall to the right of the wüstite area and the latter to close at the melting point of FeO, at *T*. Tritton and Hanson on taking a cooling curve of

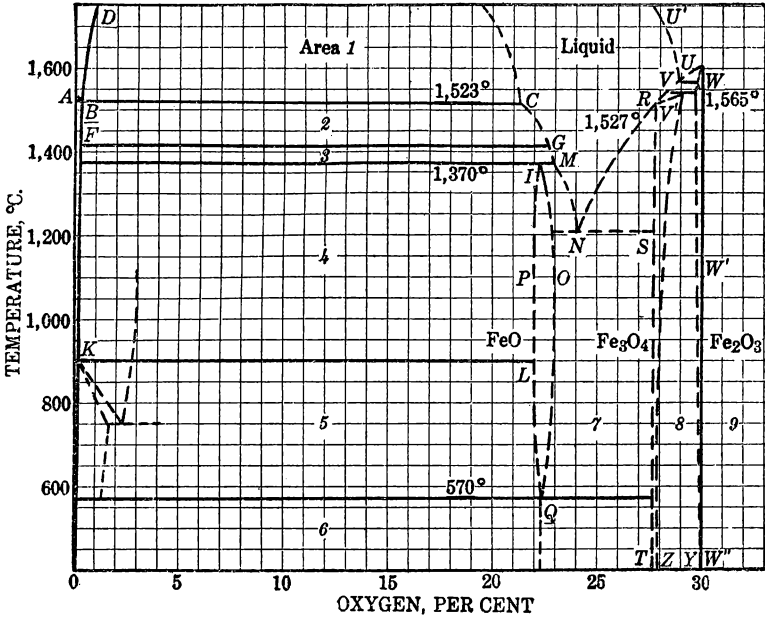


FIG. 102.—Composition-temperature phase diagram for iron-oxygen: Area 1, Liquid iron and liquid FeO conjugate solutions; 2, δ iron and liquid FeO; 3, γ iron and liquid FeO; 4, γ iron and solid FeO as wüstite; 5, α iron and solid FeO as wüstite; 6, α iron and solid magnetite; 7, magnetite and FeO as wüstite, solids; 8, magnetite and ferric oxide, solids; 9, solid Fe₂O₃ and oxygen gas

a molten “FeO” observed a weak A_4 point, indicating the presence of some metallic iron in accordance with the presence of an incongruous melting point. Another piece of evidence is the fact that pure FeO has never been obtained by cooling a melt, the products always having some magnetite and metallic iron.

Between FeO and Fe₃O₄ is a eutectic, *N*, observed by Oberhoffer and d’Huart³¹ and by others qualitatively. Its composition is not known exactly but must include about 24 per cent of oxygen at

³¹ Oberhoffer, P., and d’Huart, K., Beiträge zur Kenntnis oxydischer Schlackeneinschlüsse sowie der Desoxydationsvorgänge im Flusseisen: Stahl u. Eisen, Jahrg. 39, 1919, pp. 165 and 196.

1,200° C. Melting points of the series of mixtures between FeO and Fe₂O₃ are not in good agreement and need revision. The other principal source of information for the portion of the diagram was the work of Hilpert and Kohlmeier.³²

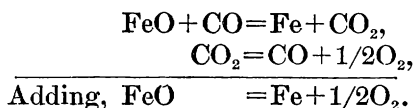
Between magnetite and ferric oxide a miscibility gap is assumed in spite of the excellent work of Sosman and Hostetter at two temperatures below the melting points. They had stated that there was a continuous series of solid solutions, although their oxygen-pressure isotherms were of such shape as to suggest that possibly there was limited miscibility at lower temperatures. However, the great difference in crystal structure of the two compounds led Benedicks and Löfquist to reject their conclusion of unlimited miscibility. None of the polymorphic forms of Fe₂O₃ or Fe₃O₄ are included in the diagram.

The Fe-FeO eutectoid, as deduced from Schenck's data and plotted in Figure 101, is dotted into Figure 102 for comparison with the accepted data.

Many of the curves sketched have a quantitative basis and are therefore given as solid lines, whereas others are only imperfectly determined or are even assumed and are therefore represented by dotted lines. The diagram shows that much important information remains to be collected.

SMITS AND BIJVOET'S PRESSURE-TEMPERATURE DIAGRAM

In 1919 Smits and Bijvoet³³ discussed from a theoretical standpoint the possible forms which the complete pressure-temperature phase diagram of the iron oxides would take. They found very few data actually available. All of the oxygen pressures that have been measured directly were those by Sosman and Hostetter, as discussed in the section on the system Fe₂O₃-Fe₃O₄. However, from the reduction equilibria of the oxides Fe₃O₄-FeO and FeO-Fe, together with the dissociation equilibria of either CO₂ or H₂O vapor, one can calculate the oxygen pressures of these oxides. The equilibria added together to get this result are:



When these equations are added the expressions for the equilibrium constants corresponding to them must be multiplied. The result is

³² Hilpert, S., and Kohlmeier, E. J., *Über Calciumferrit*: Ber. Deut. chem. Gesell., Jahrg. 42, 1909, p. 4581.

³³ Smits, A., and Bijvoet, J. M., *The System Iron-Oxygen*: Proc. Acad. Sci. Amsterdam, vol. 21, 1919, pp. 386-400.

that the equilibrium constant of the final equation is the oxygen pressure desired. Smits and Bijvoet calculated the oxygen pressures from equilibrium data available in their time, and the result resembled Figure 103. To avoid plotting ridiculously small numbers and to contract the plot the logarithms of oxygen pressures (in at-

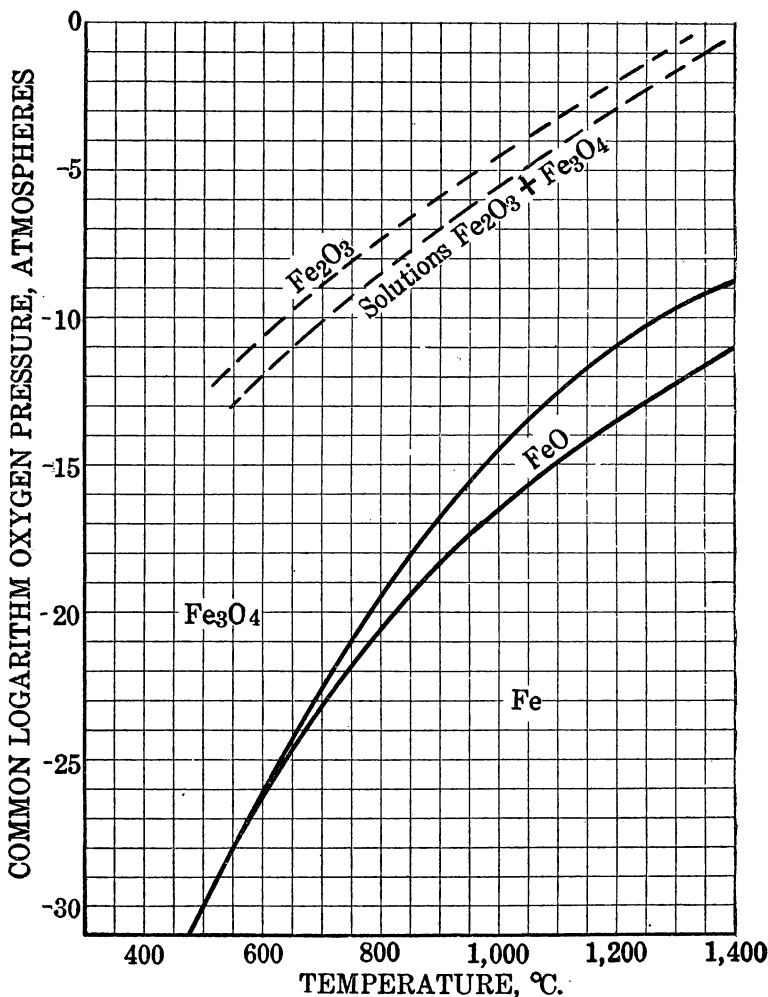


FIG. 103.—Pressure-temperature phase diagram for iron-oxygen

mospheres) are used. If the plot had been made against the reciprocal of absolute temperature instead of directly against centigrade temperature, the lines on the diagram would have approximated straight lines. The stability fields of pure Fe₂O₃, Fe₃O₄, FeO, and Fe are indicated according to the understanding of the system at that time. To this the writer has added the stability field of the solutions

of Fe_2O_3 and Fe_3O_4 in each other, as indicated by the work of Sosman and Hostetter. Part of the stability field of FeO should be occupied by solid solutions of FeO and Fe_3O_4 , but these are too imperfectly understood to make worth while the recalculation of data available.

Instead of using Smits and Bijvoet's actual calculated oxygen pressures in preparing Figure 103 the data of Wöhler and Günther³⁴ dealing with the hydrogen reduction system, which check very well with the work of Eastman and Evans, were used.

While it is known that the system is not as simple as that pictured by Smits and Bijvoet, too scanty quantitative information is available to make any reasonable completion of the picture possible.

PRESSURE-COMPOSITION PHASE DIAGRAM

From the temperature-composition and pressure-temperature diagrams it should be possible to derive the pressure-composition diagram. An idealized diagram is included by Smits and Bijvoet in their work, but it is too much a matter of conjecture to be worth reproduction in this paper.

³⁴ Wöhler, L., and Günther, R., Das Wasserdampfgleichgewicht über Eisen, Wolfram und deren Oxyden: Ztschr. Elektrochem., Jahrg. 29, 1923, pp. 276-285.

OXIDATION-REDUCTION SYSTEMS FOR IRON OXIDES

After the tremendous amounts of data that have been discussed in the previous sections, one would quite naturally expect that the equilibrium diagrams of the complete oxidation-reduction systems for the iron oxides, involving the oxides of carbon or involving hydrogen and water vapor, would be very well worked out. On the contrary, only diagrams full of disappointing approximations are possible. The complexity of the partial systems involved is responsible for this, and in general the work of the past can be called the pioneer work, making possible more precise work by scientists of the future. To date the systems can be said to be merely roughly blocked out. This viewpoint will be justified as one follows the series of reduction-oxidation diagrams in chronological sequence as set forth in the following paragraphs.

BAUR AND GLAESSNER'S DIAGRAM

One early classical attempt to formulate an equilibrium diagram involving magnetite, ferrous oxide, and iron in contact with carbon monoxide and carbon dioxide was that of Baur and Glaessner³⁵ in 1903. Their famous incorrect diagram, which has entered so many textbooks on metallurgy, is given in Figure 104. In the temperature range between 700° and 950° C. their equilibrium gas compositions were in reasonable agreement with more recent work, as can be seen by comparison with the following diagrams. At the lower temperatures they were completely in error, and in both cases their curves turned in the wrong direction.

The fact that the iron blast furnace operates with a mixture of CO and CO₂ as the active reducing agent for the ore passing through it has always inspired investigators to use these gases when investigating iron oxide reduction equilibria; therefore most of the published diagrams have dealt with the same system as that discussed by Baur and Glaessner. A number of other competent experimenters worked with the system, but the next outstanding contribution was that of Matsubara.³⁶

MATSUBARA'S DIAGRAM

By the time Matsubara published the results of his painstaking work it was well known that the low-temperature data of Baur

³⁵ Baur, E., and Glaessner, A., Gleichgewichte der Eisenoxyde mit Kohlenoxyd und Kohlensäure; *Zeit. physikalische Chemie*, vol. 43, 1903, pp. 354-368.

³⁶ See footnote 6, p. 257.

and Glaessner were incorrect. Matsubara's method of determining the equilibrium gases was to follow a reduction isotherm of the type so frequently discussed in preceding pages of this paper and

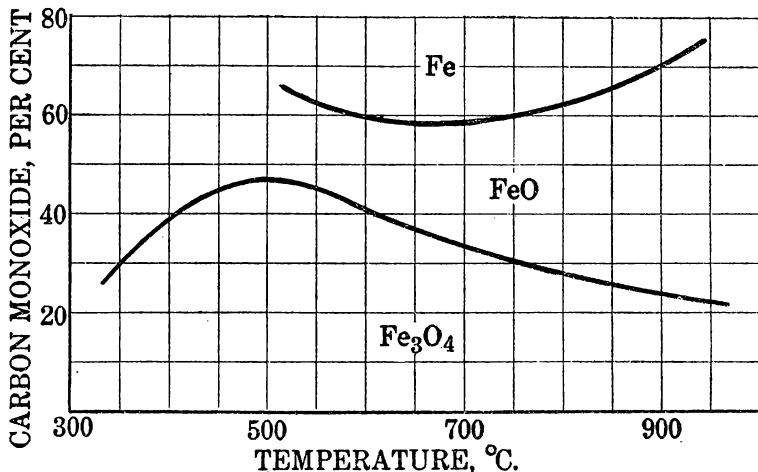


FIG. 104.—Equilibrium diagram of Baur and Glaessner

illustrated in Figure 25. The horizontal portions of these isotherms were almost certainly generated during the reduction of one solid

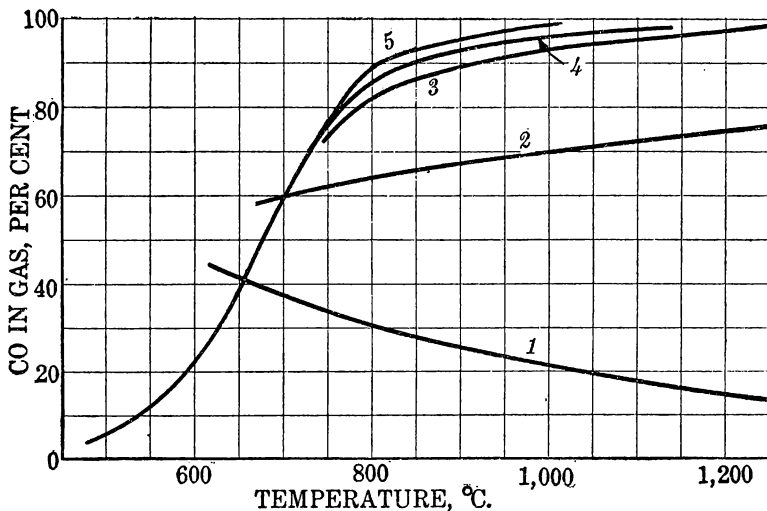


FIG. 105.—Equilibrium diagram of Matsubara, showing equilibria involving Fe_3C : 1, Equilibrium, $\text{Fe}_3\text{O}_4 + \text{CO} = 3\text{FeO} + \text{CO}_2$; 2, equilibrium, $\text{FeO} + \text{CO} = \text{Fe} + \text{CO}_2$; 3, equilibrium, $3\text{FeO} + 5\text{CO} = \text{Fe}_3\text{C} + 4\text{CO}_2$; 4, equilibrium, $3\text{Fe} + 2\text{CO} = \text{Fe}_3\text{C} + \text{CO}_2$; 5, equilibrium, $2\text{CO} = \text{C} + \text{CO}_2$

phase in equilibrium with a second solid phase and the gas. Matsubara's resulting equilibrium diagram, Figure 105, also contains the data, curve 5, for the producer-gas equilibrium, it being assumed

that both solid oxides of iron and solid carbon would be present in most of the commercial metallurgical apparatus, and therefore the equilibria involving both systems would be of interest. Matsubara obtained two other curves involving the carbide Fe_3C which are plotted in the diagram. He was uncertain about their correctness and admitted it but published such data as he had.

Curves 3 and 4 have since been shown by Schenck, by Johansson and von Seth, and others, to be involved in the trivariant field (austenite), and the other diagrams contain better placements for curve 4, whereas the equilibrium involved in curve 3 is probably

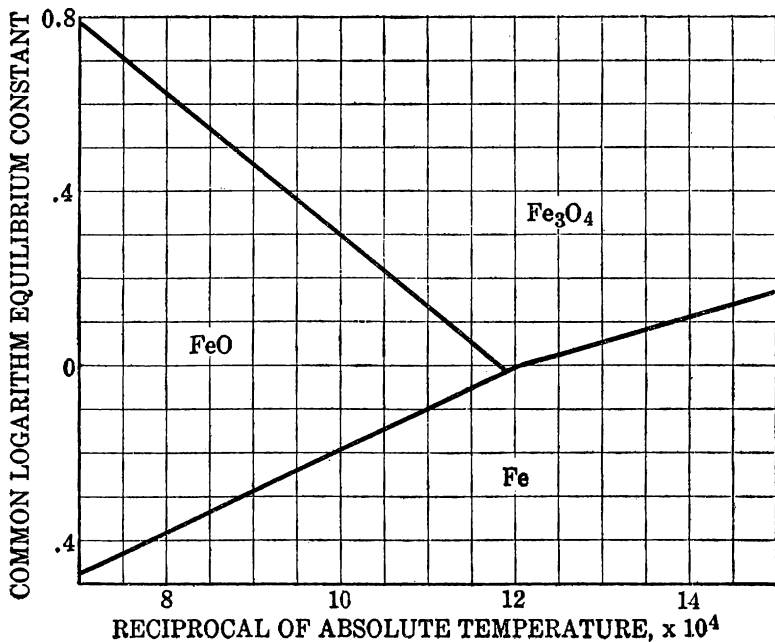


Fig. 106.—Reciprocal temperature v. logarithm constant, $k = \frac{\text{CO}_2}{\text{CO}}$. CO—CO₂ oxidation-reduction system, iron oxides (Eastman)

incompatible with the others, and its existence is doubtful. Matsubara's curves 1 and 2 are regarded as very precise, and no better work on these two equilibria has been published. These data, when plotted in a different fashion, logarithm of equilibrium constant $\left(\frac{\text{CO}_2}{\text{CO}}\right)$ against reciprocal of the absolute temperature, should give curves that depart very little from straight lines and are therefore of value for purposes of extrapolation. Eastman has prepared such a plot, which is given in Figure 106 and is on too small a scale to show the curvature of the lines involved. A third line at low temperatures, involving the equilibrium between Fe, Fe_3O_4 , and gas, is also plotted,

as it is derivable from the other two and tells what are equilibrium conditions, if attainable, at temperatures below 570°C ., the invariant point for the system or the critical splitting temperature of FeO . The fields of stability of Fe , FeO , and Fe_3O_4 are indicated and could also be indicated in Figure 105 as they were in Figure 104, except for the fact that Matsubara's work showed the probability of a series of solid solutions along the reduction isotherms at the points where the isotherms departed from a horizontal or a vertical position. Therefore Matsubara did not label his stability fields, although he was reasonably sure of the chemical reactions taking place in the equilibria represented by curves 1 and 2. He obtained good evidence of the existence of dissolved oxide and carbide in the supposed sta-

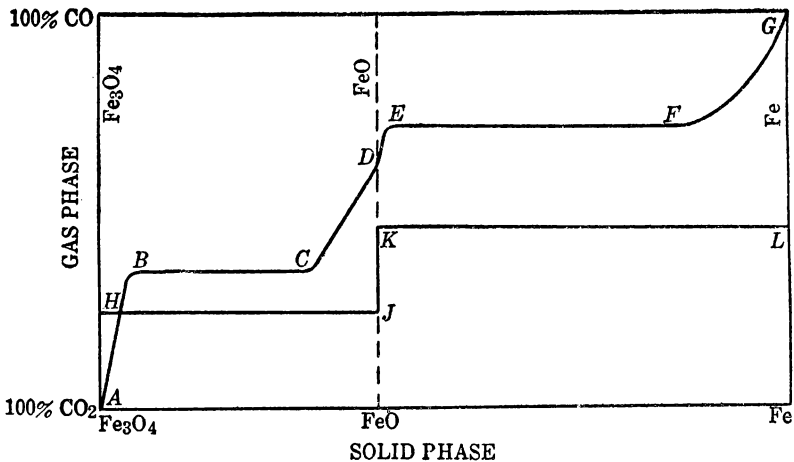


Fig. 107.—Ideal reduction-oxidation isotherms: *ABCDEF*G, solid solutions involved; *HJKL*, no solid solutions involved

bility field for iron. Eastman's plot, Figure 106, likewise did not venture to name the solids in the various fields, but the writer has introduced names purely for illustration of the inaccuracies which have pervaded the literature in the past.

IDEAL REDUCTION-OXIDATION ISOTHERM

The reduction isotherms reported in the literature have suffered from many limitations, especially those of time, and before quitting the subject it would probably be well to discuss a few ideal types. In Figure 107 the gas compositions are plotted vertically, the gas being assumed to be made up entirely of CO and CO_2 and to exist at 1 atmosphere total pressure. The horizontal scale includes the composition of the solid, starting at the left with pure Fe_3O_4 and passing through FeO near the center to Fe at the right, the variation being

in the oxygen content of the solid phase. If the three substances Fe_3O_4 , FeO , and Fe were mutually insoluble, the gas compositions in equilibrium with various mixtures of solids would be represented by the line $HJKL$, which has two horizontal and one vertical portion. Any solid intermediate in composition between H and J would consist in part of Fe_3O_4 and in part of FeO , and being in equilibrium with the gas the gas composition could not vary as long as some of each constituent was present. The point J would be that where the solid would consist of nearly all FeO and a vanishingly small amount of Fe_3O_4 . If a small amount of metallic iron were to be introduced at this point, the last trace of Fe_3O_4 would disappear, and the gas would assume the new composition represented by the point K , richer in CO and in equilibrium with FeO and a minute amount of metallic iron. All mixtures of FeO and Fe represented by the line KL would be in equilibrium at constant temperature with the same gas.

If one were to start with pure Fe_3O_4 in vacuo and add minute amounts of CO until the total pressure was 1 atmosphere and thereafter would continue to displace small amounts of the gas mixture with fresh CO , waiting in each instance until equilibrium was established, the composition of the gas and the solid at equilibrium would alter correspondingly along the line $AHJKL$, and finally after all the solid was reduced to Fe the gas would alter in composition from L to G , pure CO .

No substances are totally immiscible with each other, and the more usual type of curve is like $ABCDEFGG$. Here each of the three substances is assumed to be soluble to some extent in the others at the temperature involved. Starting with pure Fe_3O_4 at A , pure CO at first added is practically completely converted into CO_2 , and the first traces of Fe_3O_4 reduced to FeO dissolve in the excess of unreduced Fe_3O_4 , forming a solid solution. Further amounts of CO form more FeO , which dissolves in the Fe_3O_4 until the latter approaches saturation at point B . Only when this has been done will the gas composition approach a constant value during further reduction. As soon as too much FeO is produced to remain dissolved in Fe_3O_4 the excess crystallizes. Since Fe_3O_4 is assumed to be soluble in FeO , the new crystals produced will be FeO saturated with Fe_3O_4 and have the composition C instead of being pure FeO . Along the line BC saturated solution of FeO in Fe_3O_4 is in equilibrium with gas of constant composition and saturated solution of Fe_3O_4 in FeO . With advancing reduction more of solution B disappears and more of solution C forms until all of B is gone. It then takes gas stronger in CO to reduce the Fe_3O_4 remaining in the solid solution to FeO . The gas-solid composition therefore alters along the

line CD , the solid becoming more and more dilute in Fe_3O_4 and more nearly approaching the composition FeO at D .

During the whole course of the curve $ABCD$ the dominant chemical reaction has been $\text{Fe}_3\text{O}_4 + \text{CO} = 3\text{FeO} + \text{CO}_2$, but the magnetite existed first as pure material; then as a solvent in which FeO was dissolved, with increasing saturation, until no more FeO could be taken up; and next as a solute in a solvent of FeO , with increasing dilution, until the last traces of Fe_3O_4 disappeared at point D .

Taking up the study of FeO reduction at point D it can be reduced to Fe along the curve $DEFG$ in like manner, very nearly pure CO being necessary to reduce the last traces of FeO dissolved in Fe , the last FeO , therefore, having very low activity.

In most of the equilibria investigated experimentally enough of the solids of interest has been used so that the equilibria measured corresponded to the horizontals BC and EF . The positions of points along curves 1 and 2 in Matsubara's diagram (fig. 105) were determined in this way, and it was to Matsubara's credit to introduce the use of the reduction isotherm in determining the equilibrium constants and being able to form an idea of the actual solid phases present in the work of previous investigators.

SCHENCK'S DIAGRAM

The Schenck diagram (fig. 79) has already been discussed and should now be considered in greater detail. It is prepared in part by the use of isotherms like those of Matsubara, and in the mind of Schenck he was justified in calling the field between the curves 1 and 2 of Figure 105 "wüstite." Comparing with the ideal isotherm of Figure 107, one can see that wüstite must represent the part from C to E on each isotherm. Two series of solid solutions are represented in the wüstite field; below are the solutions of Fe_3O_4 in FeO , and above are the solutions of Fe in FeO . These may be one continuous series of solutions. Lines could be drawn across the wüstite field representing equal oxygen content in the solid in the same way that Takahashi and Johansson and von Seth drew lines of equal carbon content across the austenite or oxyaustenite field. A guess at the probable course of such lines has been introduced in Figure 108.

Schenck's diagram (fig. 79) is therefore not satisfying, and Figure 108 amounts to an amplification and a correction of it. It will be noticed that in Figure 108 the long strip of the oxyaustenite field which Schenck (see fig. 79) extended to unusually low temperatures has been eliminated, and the oxyaustenite field is drawn more in accordance with the ideas of Takahashi and von Seth.

Schenck's oxyferrite field is accepted, and its boundary is an average of those of Schenck and the other two investigators. The lines of equal carbon content are drawn in as light solid lines across the oxy-austenite field and are the averages of those of Takahashi and of Johansson and von Seth. The dotted lines across the wüstite field represent probable lines of equal oxygen content. Fe is probably not very soluble in FeO, and on that account the equal oxygen lines ought to be crowded together more toward the top of the wüstite area. Somewhere in the wüstite area should be a line representing conditions for formation of pure FeO, because by the time one

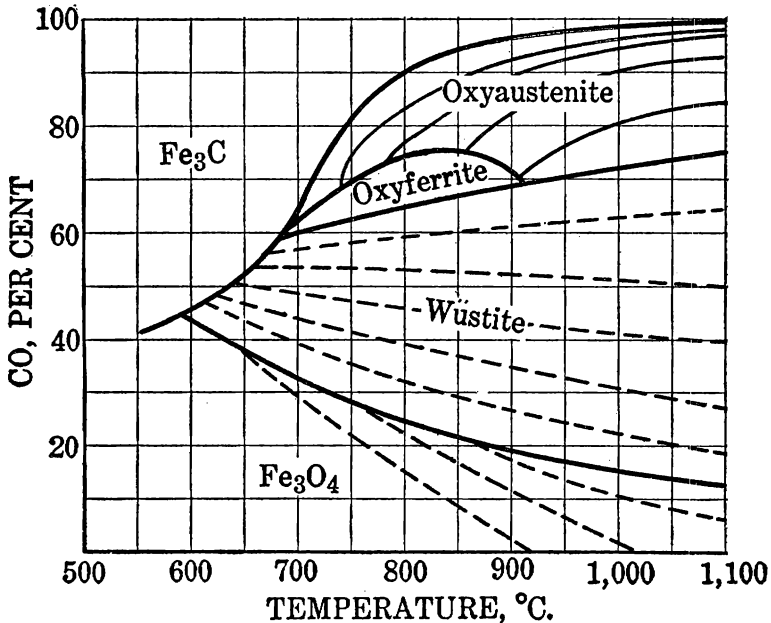


FIG. 108.—Equilibria between oxides of carbon and iron

reaches the upper boundary of the wüstite area the material is reduced beyond the pure FeO stage.

A number of lines of equal oxygen content are also dotted into the magnetite area, the last one representing the one where the last traces of FeO vanish, and to the left of it pure Fe₃O₄ can be stable in contact with the gases.

Above the wüstite area, in the oxyferrite and the oxyaustenite areas, Schenck was undoubtedly correct in claiming that oxygen-bearing phases were present—if the isotherm *DEFG* in Figure 107 represents the truth. Unfortunately for Schenck he was working with gases which also provided carbon to the iron and made his area above the wüstite unnecessarily complicated. The hydrogen reduc-

tion system will, therefore, carry considerable interest for us because complications due to carbon are eliminated.

HYDROGEN-REDUCTION SYSTEM

The work on equilibria of iron oxide systems with mixtures of hydrogen and water vapor has not been as complete as that with the oxides of carbon, but it has been well summed up by Eastman and Evans,³⁷ and their choice of the best data is plotted in the heavy lines of Figure 109. Here again are areas containing mainly Fe, FeO, and Fe₃O₄, but in all respects similar to the CO reduction system, except that carburized phases are absent. For comparison

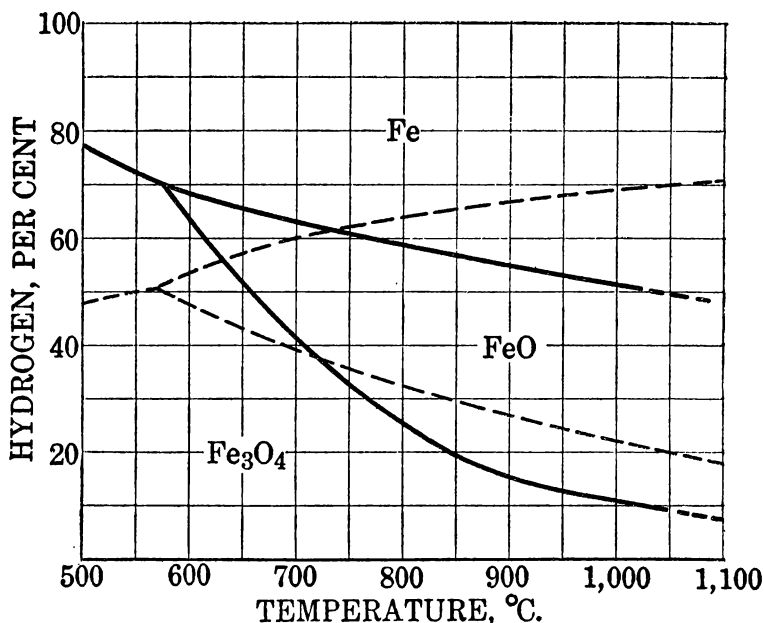


FIG. 109.—Hydrogen equilibria with iron oxides (after Eastman). Dotted lines, CO equilibria

the Matsubara data from Figure 105 are dotted in Figure 109. The obvious conclusion is that at low temperatures a much higher relative amount of hydrogen remains unutilized for reduction by the iron oxides, and hydrogen is, therefore, the poorer reducing agent at these temperatures. At about 735° C. the hydrogen and CO are equally good reducing agents, as their equilibrium lines cross at that temperature, and above this temperature hydrogen is the better reducing agent.

To forecast the probable results of future work with hydrogen and water vapor as the equilibrium gas mixture, Figure 110 has been

³⁷ Eastman, E. C., and Evans, R. M., Equilibria Involving Oxides of Iron: *Jour. Am. Chem. Soc.*, vol. 46, 1924, pp. 888-903.

prepared. Here, as in Figure 108, the wüstite area is divided by dotted lines of supposed equal oxygen content in the solid phase. The oxyferrite area is divided into two, one in which α iron is involved, below 906°C ., and the other in which γ iron is involved, above that temperature. Only above line ODE can pure iron exist, and it is assumed that the solution of FeO in Fe lowers the A_3 transition temperature to some extent. The magnetite field is also invaded in part by the lines showing various solutions of FeO in Fe_3O_4 , and pure Fe_3O_4 exists only to the left of line OA .

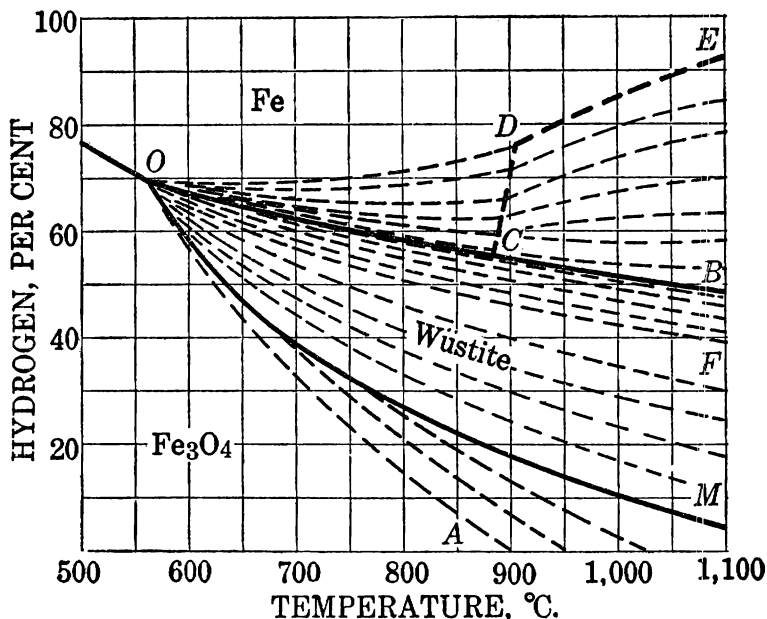


FIG. 110.—Hydrogen reduction-equilibrium diagram (corrected hypothetically). Pure Fe_3O_4 only in field to left of line OA ; pure Fe only in field above line ODE ; area MOB , wüstite, solutions in FeO of Fe_3O_4 and Fe ; line OF , pure FeO ; area COD , solid solutions of FeO in αFe ; area $CDEB$, solid solutions of FeO in γFe ; area MOA , solid solutions of FeO in Fe_3O_4

STABILITY FIELD FOR FERRIC OXIDE

In none of the diagrams presented in this chapter has a stability field for Fe_2O_3 been plotted. For practical purposes the reduction of ferric oxide to magnetite by carbon monoxide or hydrogen is considered irreversible, since the equilibrium mixture of gases contains only, say, 1 part of hydrogen or carbon monoxide per million. The line separating the magnetite field from the ferric oxide field is therefore practically coincident with the horizontal axis of coordinates and so closely spaced to it that it can not be shown graphically. It can therefore be said that the field of stability for ferric oxide is the horizontal axis of coordinates in the above diagrams.

TERNARY DIAGRAM, Fe-O-C

An attempt to combine all three binary equilibria and deduce in a qualitative way the form of the solid model of the system Fe-C-O as a function of temperature at constant pressure has been made by Iwase.³⁸ He has published a cross section of the triangular model which can be made, choosing as his temperature one at which the iron formed is in the γ form, Figure 111. Along each edge of the cross section he gives the characteristic points, not to scale, of each

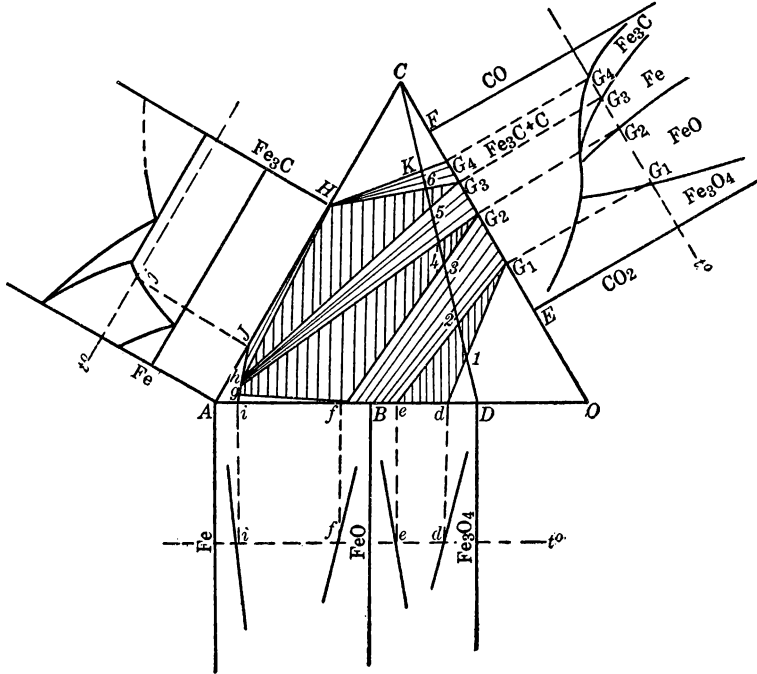
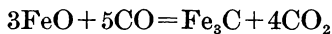


FIG. 111.—Isotherm in γ iron range for system carbon-iron-oxygen (Iwase). Cross sections of solid model (trilinear)

binary system involved. The iron-carbon diagram along the edge AC is simplified to leave out the δ iron area; the Matsubara reduction-equilibrium diagram along the CO edge shows the line for the equilibrium



omitted, as it is probably a hypothetical one. The diagram along the AO edge shows only the solids Fe, FeO, and Fe_3O_4 , and solid solutions of each are assumed in the adjacent ones. The projections of

³⁸ Iwase, K., Equilibrium Between Iron, Carbon, and Oxygen; Reduction of Iron Ores, Cementation, and Gas Occlusion of Iron and Steel: Tohoku Univ., Sci. Repts., 1st ser., vol. 15, 1926, pp. 511-529.

the important points at t° C. onto the edges of the triangle are indicated by dotted lines. A mixture of carbon and magnetite will lie along the line CD , depending on the proportions of the mixture, and on reacting it forms the solid and gaseous phases represented along the lower left and upper right edges of the diagram, respectively.

Iwase's discussion of the various uses of his diagram is too long to reproduce here, but it allows the deduction of no new facts and amounts to a convenient way of representing facts already expressed in other ways. The unhatched area near the A corner is the stability field of iron metal containing mainly dissolved carbon on the left portion and mainly dissolved FeO on the portion extending to f on the right. It is the so-called field of gas occlusion, which in treatment of Fe with CO produces a resulting product containing both C and O , and the gas has largely disappeared. The field G_3H h is the stability field for Fe_3C . A catalogue of the fields and the gas and solids in equilibrium in each is given in Table 53.

TABLE 53.—*Equilibrium fields in the system Fe-C-O*

Field	Gas phase	Solid phase in equilibrium
$Ajhg_i$	Fe (solid solutions).
fg	Fe (solution)+ FeO (wüstite).
Hjh	Fe (solution)+ Fe_3C .
HG_3G_3	G_3 to G_4	Fe_3C .
G_3de	G_1	FeO (solution)+ Fe_3O_4 (solution).
G_3fg	G_2	FeO (solution)+ Fe (solution).
G_3hH	G_3	Fe (solution)+ Fe_3C .
G_3efG_3	G_1 to G_2	FeO (wüstite).
G_3ghG_3	G_2 to G_3	Fe (solution or oxyaustenite).
CHG_4	G_4	$\text{Fe}_3\text{C}+\text{C}$ (?).

REINDERS'S TRIANGULAR DIAGRAMS

Another student of the system Fe-C-O who made early use of the triangular diagram and space model was Reinders,³⁹ in 1916, a time when reliable interpretations of the various complex systems were few. He likewise drew cross sections of the triangular model, one below 720° C., where austenite (he called it martensite) is unstable, another in the austenite temperature range, 880° to $1,100^\circ$ C., and a third between 720° and 880° C., where both α iron and austenite could enter the diagram. His diagrams were much less complete than those of Iwase but had the interesting value of being compared to a pressure-gas composition diagram and a gas composition-temperature diagram, respectively. From these he derived a pressure-temperature diagram, a portion of which was later corrected⁴⁰ and is given here-

³⁹ Reinders, W., The System Iron-Carbon-Oxygen (In English): Vers. Akad. Wetenschapen Amsterdam, vol. 25, 1916, pp. 10-24.

⁴⁰ Reinders, W., and van Groningen, P., Equilibria in the System Fe-Martensite-FeO-Gas: Rec. trav. chim., vol. 1921, pp. 701-706.

with as Figure 112 because of its interesting conclusion. The point O represents a quintuple point in the system, being the point of intersection of five monovariant equilibria between the five phases gas, carbon, α iron, FeO, and martensite (?), the solid solution of carbon in α iron. The quintuple point thus deduced is at 2,300-millimeter pressure and 740° C., and on the iron-carbon diagram represents the

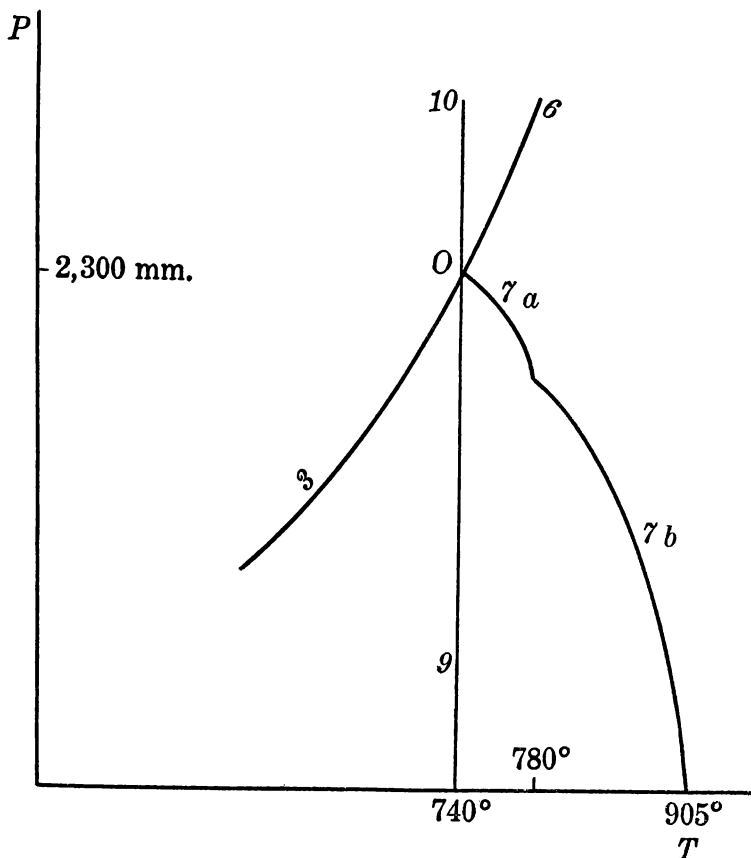


FIG. 112.—Portion of pressure-temperature diagram in α iron range (Reinders). Quintuple point, O , at 740° C. and 2,300 mm. pressure. Monovariant equilibria: 3, Carbon, α iron, gas; 6, solid solution of carbon in α iron, FeO, gas; 7, solid solution of carbon in α iron, FeO, gas; 9, solid solution of carbon in α iron, carbon, gas; 10, solid solution of carbon in α iron, FeO, and carbon

eutectoid between carbon and α iron, which is termed part of the so-called stable system of the iron-carbon diagram and has been found in no other way. If a solid solution splits directly into α iron and carbon it can be justly called martensite instead of the orthodox austenite, as Reinders has done.

Another interesting result of Reinders's diagrams is that by phase-rule considerations and the use of such meager data as were his at

that time he predicted the type of phase diagram containing an oxy-ferrite area which is now observed and plotted in Figure 108. His diagrams showed the transition from α to the supposed β iron at that time, and he made proper kinks in his various equilibrium curves for the corresponding A_2 point, but that in no wise affected the validity of most of his conclusions.

Before another attempt is made to prepare a solid three-component model of the reduction system, except for purposes of learning what data are missing, it is felt that a much greater amassing of precise information is advisable.

SUMMARY OF IMPORTANT THERMAL DATA

For convenience in use some of the more important thermal data have been assembled from the body of the text into Tables 54, 55, 56, and 57.

It must be pointed out that such data as free energies are presented as derived, and no attempt has been made to make them too consistent, because the causes of deviations from expected consistency are not known. The system is too complex to make safe any very deep-seated smoothing of curves or correction of data. They are, therefore, presented for what they are worth and with the statement that they are only of value for approximations and not for precise calculations. The heat-capacity data are probably the most precise of all.

The total heats above the freezing point of water are calculated both in calories per gram and in British thermal units per pound of material. Unfortunately, no data whatever are available for ferrous oxide.

In Table 55 the heats of the various transformations are estimated. For the magnetic transformations the heats are the "distributed" latent heats over the whole transformation range as nearly as can be estimated. The latent heat of melting the eutectic is referred to 1 mol of cementite, the eutectic consisting of 63.5 per cent by weight of Fe_3C . In like manner the latent heat of the eutectoid transformation from austenite to pearlite is referred to 1 mol of cementite, although part of the heat was undoubtedly due to transformation of γ to α iron.

TABLE 54.—Heats, entropies, and free energies (standard)

Substance	Heat of formation, ΔH_{298}	Free energy, ΔF_{298}	Entropy, ΔS_{298}	Absolute entropy, S_{298}
Fe_2O_3	-192,200	-173,050	-64.24	21.5
Fe_3O_4	-265,700	-242,531	-80.5	35.1
FeO	-63,713	-57,472	-21.3	9.41
Fe				6.87
Fe_3C	+13,580	+10,590	+10.03	31.94
C (graphite).....				1.3
$\frac{1}{2}\text{O}_2$				24.0

TABLE 55.—Important thermometric points in iron-oxygen-carbon system

Substance	Temperature, ° C.	ΔH	Nature of point	Authority
Fe ₂ O ₃	360	775	Transformation	Furnas.
	678	6,680	Transformation, polymorphic	Sosman.
	755-85	?	? (barely detectible)	Do.
	1,035+	?	Cooling curve anomalies	Kohlmeyer.
	1,400+	?	Sintering	Numerous.
Fe ₃ O ₄	1,455	?	1 atom dissociation pressure	Sosman and Hostetter.
	1,550+	?	Melting	Ruey and Nakamoto.
	-153	361.4	Peak in specific heat curve	Miller.
	1,600	2,191	Magnetic transformation	Weiss and Beck.
	2,550	?	Melting point	Kohlmeyer.
FeO	585	?	1 atom dissociation	Wöhler and Günther.
	-170	54	Peak in specific heat curve	Miller.
	570	?	Metastable below this	Chaudron, Eastman.
Fe	1,378	?	Melting point	Tritton and Hanson.
	790	335	Magnetic transformation	Numerous.
	906	274	Transformation No. A ₃	Do.
	1,400	95	Transformation No. A ₄	Do.
	1,537	3,625	Melting point	U. S. Bureau of Standards.
Fe ₃ C	3,218	79,000	Boiling point	Miller, Langmuir.
	220	1,745	Magnetic transformation	Numerous.
	720	21,000	Eutectoid temperature (steels)	Do.
	1,135	13,260	Eutectic temperature cast iron	Do.

TABLE 56.—Total heats above 0° C., calories per gram

Temperature, ° C.	Fe ₂ O ₃	Fe ₃ O ₄	Fe	Fe ₃ C	Temperature, ° C.	Fe ₂ O ₃	Fe ₃ O ₄	Fe	Fe ₃ C
0	0	0	0	0	900	-----	-----	146.9	153.90
100	16.0	15.9	11.17	15.0	1,000	-----	-----	168.0	-----
200	35.3	33.65	23.25	28.76	1,100	-----	-----	183.0	-----
300	56.9	52.85	36.04	46.56	1,200	-----	-----	198.4	-----
400	80.0	73.85	50.28	59.66	1,300	-----	-----	213.8	-----
500	108.0	97.55	65.8	73.23	1,400	-----	-----	229.6	-----
600	139.1	123.5	82.6	92.66	1,500	-----	-----	250.2	-----
700	173.3	146.5	100.77	113.13	1,535	-----	-----	252.3	-----
800	-----	171.0	125.2	131.92	1,600	-----	-----	328.6	-----

TABLE 57.—Total heats above freezing point of water (32° F.), in B. t. u. per pound

Temperature, ° F.	Fe ₂ O ₃	Fe ₃ O ₄	Fe	Fe ₃ C	Temperature, ° F.	Fe ₂ O ₃	Fe ₃ O ₄	Fe	Fe ₃ C
32	0	0	0	0	1,652	-----	-----	264.5	277.0
212	28.8	28.6	20.1	27.0	1,832	-----	-----	302.5	-----
392	63.6	60.6	41.8	51.7	2,012	-----	-----	330.0	-----
572	102.5	95.2	65.0	83.9	2,192	-----	-----	357.5	-----
752	144.1	133.0	90.6	103.8	2,372	-----	-----	385.0	-----
932	194.7	175.6	108.5	132.0	2,552	-----	-----	413.5	-----
1,112	250.8	222.5	148.7	166.8	2,732	-----	-----	451.0	-----
1,292	312.0	254.0	181.5	204.0	2,795	-----	-----	455.0	-----
1,472	-----	308.0	222.5	237.5	2,912	-----	-----	592.0	-----

INDEX OF AUTHORS

Page	Page
Abraham, Henri, and Planiol, Rene, investigations of.....	27
work cited.....	27
Abt, —, investigations of, curve showing.....	30
work cited.....	30
Albrecht, W., investigations of. <i>See</i> Wedekind, I. E., and.	
work cited.....	27
Anderson, Arvid, investigations of. <i>See</i> Williams, C. E., and.	
work cited.....	100
Anderson, C. T., investigations of.....	113
Andrew, J., and Honeyman, A. J. K., investigations of.....	233
tables showing.....	172, 218
work cited.....	172, 218, 233
Arctowski, H., investigations of.....	7
work cited.....	7
Aston, F. W., investigations of.....	129
work cited.....	129
Austin, Wesley, investigations of.....	119
work cited.....	119
Bäckström, H., investigations of.....	11, 13
work cited.....	11, 13
Bain, E. C., investigations of.....	204
work cited.....	204
Ball, E. J., investigations of.....	155
work cited.....	155
Balz, O., investigations of. <i>See</i> Wöhler, Lothar, and.	
work cited.....	101
Barth, F. S., investigations of.....	82
work cited.....	82
Baudisch, Oskar, and Welo, L. A., investigations of.....	56
investigations of. <i>See</i> Welo, L. A., and.	
work cited.....	27, 56
Baur, E., and Glaessner, A., investigations of.....	72, 74, 76, 297
curves showing.....	298
table showing.....	72
work cited.....	72, 297
Beck, P. N., investigations of. <i>See</i> Weiss, P., and.	
work cited.....	62, 69, 141, 187
Beckmann, B., investigations of.....	169
work cited.....	169
Bedworth, R. E., work cited.....	81
Bell, W. P., investigations of. <i>See</i> Richardson, A. S., Vibrans, F. C., and.	
work cited.....	124
Belloc, —, investigations of. <i>See</i> Breniewski, W., and.	
Benedicks, C., Berlin, D. W., and Phragmen, G., investigations of.....	179
investigations of.....	147,
152, 153, 160, 165, 172, 175, 177, 182	
curve showing.....	148
tables showing.....	172, 218
work cited.....	147, 164, 165, 172, 179, 218, 291
Berlin, D. W., investigations of.....	179
<i>See also</i> Benedicks, C., etc.	
work cited.....	179
Berliner, J. F. T., investigations of.....	145, 151, 169
work cited.....	140, 145, 169
Berthelot, M., investigations of.....	72, 74, 77
table showing.....	72
work cited.....	72
Berzelius, —, investigations of.....	133
Beyer, J., investigations of. <i>See</i> Hilpert, S., and.	
work cited.....	56, 84, 95
Bidwell, C. C., investigations of.....	14, 185
curves showing.....	14, 186
work cited.....	14, 185
Bijveet, J. M., investigations of. <i>See</i> Smits, A., and.	
work cited.....	293
Biren, J., investigations of. <i>See</i> Ruer, R., and.	
work cited.....	210
Bishop, W., investigations of. <i>See</i> Maurer, Ed., and.	
work cited.....	229, 276
Blanc, L., and Chaudron, G., investigations of.....	9, 21
work cited.....	9, 21
Bloxam, C. L., work cited.....	39
Bode, K., work cited.....	136, 140
Bohm, J., investigations of.....	6
work cited.....	6
Bohr, Niels, investigations of.....	165
Bonnet, F., investigations of. <i>See</i> Richards, T. W., Brink, F. N., and.	
work cited.....	173
Borchers, W., investigations of.....	86
work cited.....	86
Borelius, G., and Gunneson, F., investigations of.....	161
work cited.....	161
Bormann, Walter, investigations of. <i>See</i> Ruff, Otto, and.	
work cited.....	158
Bower, G., work cited.....	82
Bozorth, R. M., investigations of.....	55, 58, 82
work cited.....	55, 58, 82
Bredemeier, H., investigations of.....	198
work cited.....	198
Bridgman, P. W., investigations of.....	169
table showing.....	168
work cited.....	168, 169
Brink, F. M., investigations of. <i>See</i> Richards, T. W., etc.	
work cited.....	173
Brisker, Carl, investigations of.....	193
table showing.....	193
work cited.....	193
Broderick, T. M., investigations of.....	41
work cited.....	41

Page	Page
Brodie, G. H., Jennings, W. H., and Hayes, Anson, investigations of..... 216, 228, 230 table showing..... 226 work cited..... 216, 228	Copisarow, Maurice, work cited..... 133
Broniewski, W., and Belloc, —, investiga- tions of..... 144	Crittenden, E. G., investigations of. <i>See</i> Wyckoff, R. W. G., and. work cited..... 58, 83
investigations of..... 144, 160, 166, 169, 170, 171, 175 curves showing..... 170, 176 work cited..... 144, 160, 169, 175	Cross, H. C., and Hill, E. E., investigations of..... 172, 218, 233, 235 table showing..... 172
Brown, J. H., work cited..... 55	work cited..... 172, 218, 233, 235
Brown, S. L., and Shuddemagen, L. O., in- vestigations of..... 65, 66	Crowe, J. J., investigations of. <i>See</i> Burgess, G. K., and. work cited..... 140, 149
investigations of..... 60	Curie, P., investigations of..... 64, 155 table showing..... 70
work cited..... 60, 65	work cited..... 64, 141, 155
Bureau of Mines, data collected by..... 2 work of..... 105	Dana, E. S., investigations of..... 9 work cited..... 9, 54
Bureau of Standards, work of..... 144 table showing..... 312	d'Ans, J., investigations of. <i>See</i> Keppler, G., and. work cited..... 21
<i>See also</i> Burgess, G. K., and coworkers.	Darrow, K. K., investigations of..... 165 work cited..... 165
Burgess, G. K., and Crowe, J. J., investiga- tions of..... 140, 149	Deardon, W. H., and Benedicks, C., investi- gations of..... 164 work cited..... 164
and Foote, P. D., investigations of..... 66, 185 curves showing..... 186	des Cloiseaux, M., work cited..... 54
and Kellberg, I. N., investigations of..... 145, 147, 152, 166, 167, 168	de Senarmont, M. H., work cited..... 7
curves showing..... 146, 153, 167	Deville, H. St. C., method of..... 7
tables showing..... 168	Dewar, James, and Flemming, J. A., in- vestigations of, table showing..... 168 work cited..... 168, 285
and Scott, H., investigations of..... 140, 144, 145, 151, 169	d'Huart, K., investigations of. <i>See</i> Ober- hoffer, P., and. work cited..... 292
curves showing..... 152	Dingmann, Th., investigations of. <i>See</i> Schenck, R., and. work cited..... 93, 126, 249
and Waltenberg, R. G., investigations of... 157 table showing..... 157	Doelter, C., investigations of..... 20, 54 work cited..... 20, 54
investigations of..... 143, 152, 157	Dornhecker, K., investigations of. <i>See</i> Levin, M., and. work cited..... 172, 218, 233
work cited..... 66, 140, 144, 145, 152, 157, 168, 185	Dowell, R. L., work cited..... 205
Campbell, E. D., investigations of..... 228, 229 work cited..... 37, 229, 235	du Bois, H. E. J. G., investigations of..... 64, 65 table showing..... 65 work cited..... 64, 65
Carnegie Institution, Geophysical Labora- tory of, work of..... 2	Dürrer, R., investigations of. <i>See</i> Wüst, F., Meuthen, —, and. work cited..... 150, 188, 238
Carnevali, F., investigations of. <i>See</i> Giolitti, F., and. work cited..... 127	Dusart, —, investigations of..... 115 work cited..... 115
Caron, H. M., investigations of..... 127 work cited..... 127	Dussler, E., and Gerlach, W., investigations of..... 165 work cited..... 165
Carpenter, H. C. H., work cited..... 81	Eastman, E. D., and Evans, R. M., investi- gations of..... 75, 76, 77, 88, 93, 94, 96, 102, 110, 122, 124, 289, 291, 295, 304 curves showing..... 89, 90, 122 tables showing..... 72, 91
Carrard, A., investigations of. <i>See</i> Weiss, P., Piccard, A., and. work cited..... 36, 58, 69, 188	investigations of..... 35, 36, 96, 111, 120, 123, 299, 300 curves showing..... 299, 304 table showing..... 312 work cited..... 35, 75, 88, 96, 102, 111, 120, 304
Chaudron, G., and Forestier, H., investiga- tions of..... 6, 21, 98, 99	Eckman, J. R., investigations of. <i>See</i> Jordan, L., and. work cited..... 127
curves showing..... 98	Elam, O. F., work cited..... 81
investigations of..... 96	
table showing..... 312	
<i>See also</i> Blanc, L., and; Forestier, H., and; Huggett, J., and. work cited..... 6, 9, 21, 22, 25, 43, 65, 86, 96, 98, 99	
Chevallier, Raymond, investigations of... 27, 28, 29 work cited..... 27, 28	
Claasen, A. A., investigations of..... 58 work cited..... 58	
Compton, A. H., and Rogney, O., investiga- tions of..... 65 work cited..... 65	
Condrea, C., work cited..... 5	
Cook, R. S., investigations of. <i>See</i> Pease, R. N., and. work cited..... 124	

	Page		Page
Endo, H., investigations of. <i>See</i> Honda, K., and Endo, H.		Geiss, M., investigations of. <i>See</i> van Liempt, J. A. M.	
work cited.....	178, 223, 236	work cited.....	139
Esser, H., work cited.....	269	Gerlach, W., investigations of. <i>See</i> Dussler, E., and.	
Estelle, T. C., investigations of.....	8	work cited.....	165
work cited.....	8	Gersten, E., investigations of. <i>See</i> Ruff, O., and.	
Evans, R. M., investigations of. <i>See</i> Eastman, E. D., and.		work cited.....	72, 217, 218, 227
work cited.....	75, 88, 96, 102, 120, 304	Giani, P., investigations of. <i>See</i> Wever, F., and.	
Ewig, K., investigations of. <i>See</i> Tammann, G., and.		work cited.....	131, 134
work cited.....	215, 219, 235	Giolitti, F., and Carnevali, F., investigations of.....	127
Fairlie, D. M., investigations of. <i>See</i> Pring, J. N., and.		work cited.....	127
work cited.....	278	Glaessner, A., investigations of. <i>See</i> Baur, E.	
Falcke, V., investigations of. <i>See</i> Schenck, R. Semiller, H., and.		work cited.....	72, 297
work cited.....	228	Coerens, P., investigations of.....	120, 127
Fedotjeff, P., investigations of.....	83	<i>See also</i> Ruer, R., and.	
work cited.....	83	work cited.....	120, 127, 140, 157
Ferguson, J. B., investigations of.....	94,	Goffey, A., investigation of. <i>See</i> Thompson, F. C., and.	
96, 97, 99, 108, 124, 125		work cited.....	160
curves showing.....	97	Gontermann, W., investigations of table showing.....	155
work cited.....	94, 124	work cited.....	155
Fieldner, A. C., and Jones, G. W., investigations of.....	283	Gorget, A., investigations of.....	54
work cited.....	283	work cited.....	54
Fink, C. G., and Mantell, C. L., investigations of.....	15	Greenwood, H. C., investigations of.....	158, 194
work cited.....	15, 235	table showing.....	194
Fink, W. L., and Campbell, E. D., investigations of.....	235	work cited.....	158
work cited.....	235	Greulich, Erich, investigations of.....	7
Fixed Nitrogen Research Laboratory, work of.	104	work cited.....	7, 57
Fizeau, R., investigations of.....	11	Groeblor, H., and Oberhoffer, P., investigations of.....	83, 88, 100, 102, 105, 109, 123
table showing.....	178	table showing.....	91
work cited.....	11	work cited.....	83, 88, 100, 123
Flemming, J. A., investigations of. <i>See</i> Dewar, James, and.		Grosse, W., investigations of. <i>See</i> Oberhoffer, P., and.	
Foex, G., investigations of. <i>See</i> Weiss, P., and.		work cited.....	32, 150, 189
work cited.....	63, 143, 155	Grüner, L., investigations of.....	127
Foley, F. B., investigations of.....	131, 132	work cited.....	127
diagram illustrating.....	132	Gunneson, F., investigations of. <i>See</i> Borelius, G., and.	
Footo, P. D., investigations of. <i>See</i> Burgess, G. K., and.		work cited.....	161
work cited.....	66, 185	Günther, R., investigations of. <i>See</i> Wöhler, L., and.	
Forestier, H., and Chaudron, G., investigations of.....	22, 25	work cited.....	72, 96, 102, 295
curves showing.....	22	Gwyer, A. G. C., investigations of, table showing.....	157
investigations of. <i>See</i> Chaudron, G., and.		work cited.....	157
work cited.....	6, 21, 22, 25, 98	Hammick, D. L., work cited.....	8
Frebold, G., work cited.....	26	Hanemann, H., investigations of.....	207, 208, 209
Freeman, J. R., investigations of. <i>See</i> Hanson, D. J., and.		curve showing.....	208
work cited.....	155	work cited.....	207
Friend, J. N., investigations of.....	6, 16, 55	Hanson, D., and Freeman, J. R., investigations of. <i>See</i> Tritton, F. S., and.	
work cited.....	6, 16, 55	work cited.....	107, 115, 155, 157, 287
Furnas, C. C., investigations of.....	13, 21, 23, 31, 35	Harder, O. E., work cited.....	205
curves showing.....	14, 30	Harrison, E. P., investigations of.....	171
tables showing.....	14, 30, 312	curve showing.....	170
work cited.....	13, 21	table showing.....	171
Gay-Lussac, M., investigations of.....	7	work cited.....	171
work cited.....	7		

	Page		Page
Hayes, Anson, investigations of.....	227	Huggett, J., and Chaudron, G., investigations	
<i>See also</i> Brodie, G. H., Jennings, W. H.,		of.....	21, 43, 45, 64, 65, 86, 91
and Maxwell, H. L., and.		curves showing.....	22, 44
work cited.....	216, 228, 231, 255	table showing.....	70
Hedvall, J. A., investigations of.....	5	work cited.....	21, 43, 65, 86
work cited.....	5, 6	Hull, A. W., investigations of.....	131
Heindlhofer, K., and Wright, F. L., investiga-		work cited.....	131
tions of.....	208, 235	Hull, T. E., work cited.....	55
work cited.....	205, 208, 235	Humfrey, J. C. W., investigations of. <i>See</i>	
Heraeus, W., investigations of.....	162	Rosenhain, W., and.	
work cited.....	161	work cited.....	130, 183
Herty, C. H., investigations of.....	107,		
108, 118, 264, 291		Itake, Itiro, investigations of.....	215
curves showing.....	119, 266, 267, 268	work cited.....	215
table showing.....	265	Ishigaki, T., investigations of.....	173, 218
work cited.....	107, 115, 264, 291	work cited.....	173, 218
Hesemann, J., work cited.....	26	Ishimoto, Mishio, investigations of.....	163
Hessenbruch, W., work cited.....	269	curves showing.....	163
Hill, E. E., investigations of. <i>See</i> Cross, H.		work cited.....	163
C., and.		Ishiwara, T., investigations of.....	142, 151, 156
work cited.....	172, 218, 233, 235	curves showing.....	156
Hilpert, S., and Beyer, J., investigations of ..	56,	table showing.....	151, 155
84, 85, 86, 91, 95, 96, 102, 106		work cited.....	142, 151, 155
curve showing.....	85	Iwase, K., investigations of.....	306, 307
and Kohlmeyer, E. J., investigations of....	15,	curve showing.....	306
59, 293		work cited.....	205, 306
investigations of.....	29	Jeffries, Zay, investigations of.....	204, 205
work cited.....	15, 29, 56, 59, 84, 95, 293	work cited.....	204, 205
Hofman, Konrad, work cited.....	124	Jennings, W. H., investigations of. <i>See</i>	
Holborn, L., investigations of.....	167	Brodie, G. H., etc.	
curve showing.....	167	work cited.....	216, 228
table showing.....	168	Jermilof, J. <i>See</i> Yermilov, Y.	
work cited.....	167, 168	Joannis, M., investigations of.....	10, 103, 115
Holmquist, P. J., investigations of.....	20	work cited.....	10, 54, 103, 115
work cited.....	20	Johansson, A., and von Seth, R., investiga-	
Honda, K., and Endo, H., investigations		tions of.....	251, 252, 253, 254, 256, 257, 258,
of.....	178, 223, 236	259, 260, 262, 263, 277, 279, 281, 299, 302, 303	
curve showing.....	237	curves showing.....	261, 263
and Kikuta, T., investigations of.....	214	work cited.....	251
and Miura, S., investigations of.....	153, 154	Johnson, J. Y., work cited.....	233
curve showing.....	154	Joly, J., investigations of, curve showing....	30
and Ogura, Y., investigations of.....	142,	work cited.....	30
145, 146, 147, 166		Jones, G. W., investigations of. <i>See</i> Field-	
curve showing.....	145	ner, A. C., and.	
and Simidzu, T., investigations of.....	171	work cited.....	283
and Sone, T., investigations of.....	25, 64	Jones, H. A., Langmuir, I., and Mackay, G.	
curve showing.....	26	M. J., investigations of.....	158, 194
table showing.....	70	table showing.....	159
and Takagi, H., investigations of.....	149, 151, 220	work cited.....	158, 213
table showing.....	154	Jordan, L., and Eckman, J. R., investigations	
investigations of.....	178, 205, 211	of.....	127
table showing.....	178	work cited.....	127
investigations of.....	141,	Kahanowicz, M., investigations of.....	66
143, 156, 165, 206, 209, 212, 214, 233, 234		work cited.....	66
curves showing.....	142	Kahlbaum, G. W. A., and Sturm, E., investi-	
work cited.....	25, 64, 141, 142, 143, 145,	gations of.....	173
151, 153, 165, 171, 205, 211, 212, 213, 220, 223, 233		work cited.....	173
Honeyman, A. J. K., investigations of. <i>See</i>		Kaneko, K., investigations of. <i>See</i> Ruer, R.,	
Andrew, J., and.		and.	
work cited.....	172, 218, 233	work cited.....	155
Hostetter, J. C., investigations of. <i>See</i> Ses-		Kawakami, M., investigations of.....	244
man, R. B., and.		work cited.....	244
work cited.....	18, 21, 41, 45, 57, 287		

Page	Page		
Kaya, Seiji, investigations of.....	172	Lewis, G. N., and Randall, M., investigations of.....	32, 75, 77, 110, 112, 227, 287
table showing.....	172	work cited.....	31, 75, 77, 110, 287
work cited.....	172	Lindh, A. E., investigations of. <i>See</i> Westgren, A., and.	
Kaye, G. W. C., and Laby, T. H., investigations of table showing.....	172	work cited.....	132
work cited.....	172	Losana, L., investigations of.....	39
Kellberg, I. N., investigations of. <i>See</i> Burgess, G. K., and.		work cited.....	39
work cited.....	145, 152, 168	Lowry, T. M., and Parker, R. G., investigations of.....	173
Kelley, K. K., investigations of. <i>See</i> Parks, G. S., and.		work cited.....	173
work cited.....	29, 58, 68	Mack, —, Osterhof, —, and Kraner, —, investigations of.....	194
Keppler, G., and d'Ans, J., investigations of.....	21	table showing.....	194
work cited.....	21	Mackay, G. M. J., investigations of. <i>See</i> Jones, H. A., Langmuir, I., and.	
Kikuta, T., investigations of. <i>See</i> Honda, K., and.		work cited.....	158
work cited.....	213	Malfert, M. l'abbé, work cited.....	39
Kirpach, N., investigations of. <i>See</i> Wüst, F., and.		Mair, B. J., investigations of. <i>See</i> Mehl, R. F., and.	
work cited.....	120	work cited.....	173
Klesper, P., investigations of. <i>See</i> Ruer, R., and.		Mantell, C. L., investigations of. <i>See</i> Fink, C. G., and.	
work cited.....	155, 157	work cited.....	15
Klobie, E. A., investigations of. <i>See</i> van R Emmelen, J. M., and.		Marchand, R. F., investigations of.....	115
work cited.....	37	work cited.....	115
Knocke, A., investigations of.....	158	Masumoto, H., investigations of.....	222
work cited.....	158	work cited.....	222
Kohlmeyer, E. J., investigations of.....	9,	Matsubara, A., investigations of.....	52,
15, 23, 37, 42, 59, 287		88, 89, 91, 120, 121, 123, 127, 257, 297, 298,	
curves showing.....	43	299, 300, 302, 304, 306.	
table showing.....	312	curves showing.....	51, 90, 121, 298
<i>See also</i> Hilpert, S., and.		work cited.....	52, 88, 120, 257, 297
work cited.....	9, 15, 37, 42, 59, 287, 293	Matsushita, T., and Nagasawa, K., investigations of.....	206
Königsberger, J., and Reichenheim, O., investigations of.....	13	investigations of.....	203, 213
and Schilling, K., investigations of.....	58, 61	work cited.....	203, 206, 213
curves showing.....	60	Maurer, Ed., and Bischof, W., investigations of.....	229, 276
work cited.....	13, 60	work cited.....	229, 276
Kraner, —, investigations of. <i>See</i> Osterhof, —, Mack, —, and.		Maxwell, H. L., and Hayes, Anson, investigations of.....	226, 229, 230, 231, 255
Kuhlmann, F., investigations of.....	54	work cited.....	231, 255
Laby, T. H., investigations of. <i>See</i> Kaye, G. W. C., and.		Mehl, R. F., and Mair, B. J., investigations of.....	173
work cited.....	172	work cited.....	173
Landon, J. W., investigations of.....	173	Merwin, H. E., investigations of.....	83, 95
table showing.....	173	work cited.....	37
work cited.....	173	Meuthen, A., investigations of.....	191, 238, 242, 246
Langmuir, I., investigations of. <i>See</i> Jones, H. A., etc.		curve showing.....	239
table showing.....	312	<i>See also</i> Wüst, F.	
work cited.....	158	work cited.....	150, 188, 191, 238
Larsen, B. M., investigations of. <i>See</i> Sims, C. E., and.		Meyer, A. R., investigations of.....	166
work cited.....	100	curve showing.....	167
le Chatelier, H., investigations of.....	33, 35, 73, 178	table showing.....	168
tables showing.....	72, 110, 178	work cited.....	166, 168
work cited.....	33, 72	Michalek, J. C., investigations of. <i>See</i> Rodebush, W. H., and.	
Ledebur, A., investigations of.....	118	work cited.....	32, 187
work cited.....	118	Miething, H., investigations of. <i>See</i> Moller, M., etc.	
Levin, M., and Dornbecker, K., investigations of.....	233	work cited.....	185
tables showing.....	172, 218		
work cited.....	172, 218, 233		

	Page		Page
Millar, R. W., and Sullivan, J. D., investigations of.....	112	Pacific Experiment Station, work at.....	105, 111, 113
investigations of... 58, 64, 68, 69, 71, 105, 111, 112, 158		Parker, R. G., investigations of. <i>See</i> Lowry, T. M., and.	
curve showing.....	68	work cited.....	173
tables showing.....	69, 105, 158, 312	Parks, G. S., and Kelley, K. K., investigations of.....	29, 31, 36, 58, 64, 69, 71, 77
work cited.....	112, 158	curves showing.....	30, 68
Miura, S., investigations of. <i>See</i> Honda, K., and.		tables showing.....	34, 69
work cited.....	153	work cited.....	29, 58, 68
Mixter, W. G., investigations of.....	24,	Pease, R. N., and Cook, R. S., investigations of.....	124
tables showing.....	33, 35, 72, 73, 76, 109	work cited.....	124
work cited.....	72, 110	Perrier, Albert, and Wolfers, F., investigations of.....	160, 164
Moissan, H., investigations of.....	57	work cited.....	164
work cited.....	57	Phragmen, G., investigations of. <i>See</i> Benedicks, C., Berlin, D. W., and; Westgren, A., and.	
Moller, M., Miething, H., and Schmick, H., investigations of.....	185	work cited.....	132, 179, 217, 218, 235
curves showing.....	186	Piccard, A., investigations of. <i>See</i> Weiss, P., Piccard, A., and Carrard, A.	
work cited.....	185	work cited.....	36, 58, 69, 188
Mond, L., investigations of.....	285	Pickard, J. A., investigations of.....	119
work cited.....	284, 285	work cited.....	119
Monden, Herbert, investigations of.....	118	Pilling, N. B., work cited.....	81
work cited.....	118	Pionchon, M., investigations of, table showing.....	191
Morris, M. G., and Scott, H., investigations of.....	215	work cited.....	191
work cited.....	215	Pittsburgh Experiment Station, work at.....	118
Mosander, C. G., investigations of.....	55, 82	Planiol, Rene, investigations of. <i>See</i> Abraham, Henri, and.	
work cited.....	55, 82	work cited.....	27
Nagasawa, K., investigations of. <i>See</i> Matsu-shita, T., and.		Pongracz, A., investigations of. <i>See</i> Terres, E., and.	
work cited.....	206	work cited.....	127
Nakamoto, Mineru, investigations of. <i>See</i> Ruer, Rudolf, and.		Posnjak, E., investigations of. <i>See</i> Sosman, R. B., and.	
work cited.....	15, 18, 49, 84	work cited.....	24, 57
Nernst, —, investigations of. <i>See</i> Ostwald, W., and.		Pring, J. N., and Fairlie, D. M., investigations of.....	278
Nicolai, Guido, investigations of.....	167	work cited.....	278
table showing.....	168	Quincke, F., work cited.....	285
work cited.....	167, 168	Ralston, O. C., investigations of, curve showing.....	225
Nikitn, N., investigations of. <i>See</i> Tammann, G., and.		tables showing.....	141, 224
work cited.....	135	work cited.....	37
Oberhofer, P., and d'Huart, K., investigations of.....	292	Rammelsberg, —, investigations of.....	9
and Grosse, W., investigations of.....	32,	work cited.....	9
curve showing.....	141, 156, 189, 191, 193	Randall, M., work cited.....	31, 75, 77, 110, 287
tables showing.....	32	Reed, E. L., investigations of.....	253
investigations of.....	150, 193	work cited.....	253
<i>See also</i> Groebler, H., and.		Regnault, V., investigations of.....	69
work cited... 32, 83, 88, 100, 120, 123, 150, 189, 291, 292		curve showing.....	30
Oeberg, —, investigations of, curve showing.....	30	table showing.....	69
work cited.....	30	work cited.....	30, 69
Ogura, Y., investigations of. <i>See</i> Honda, K., and.		Reichenheim, O., investigations of. <i>See</i> Königsberger, H., and.	
work cited.....	142, 145	work cited.....	13
Osawa, Atemi, investigations of.....	131, 179	Reinders, W., investigations of.....	307, 308
work cited.....	131, 179	curves showing.....	308
Osmond, F., investigations of.....	155	work cited.....	307
table showing.....	191	Rhead, T. F. E., and Wheeler, R. V., investigations of.....	261
work cited.....	155, 191	work cited.....	261
Osterhof, —, investigations of. <i>See</i> Mack, —, and.			
Ostwald, W., and Nernst, —, investigations of.....	124		

Page	Page		
Richards, T. W., Brink, F. N., and Bonnet, F., investigations of.....	173	Sato, Seikichi, investigations of.....	175, 179
work cited.....	173	work cited.....	175
Richardson, A. S., Vibrans, F. C., and Bell, W. P., investigations of.....	124	Sauerwald, F., and Wecker, J., investigations of.....	236
work cited.....	124	and Widawski, E., investigations of.....	236
Roberts, W. C., and Wrightson, T., investigations of.....	179	work cited.....	236
work cited.....	179	Sauveur, Albert, investigations of.....	130, 140, 154
Rodebush, W. H., and Michalek, J. C., investigations of.....	32, 187, 197	work cited.....	130, 140
curve showing.....	32	Sawamura, H., investigations of. <i>See</i> Saito, D., and.	
table showing.....	190	work cited.....	210
work cited.....	32, 187	Scheets, F. H., work cited.....	5
Rogney, O., investigations of. <i>See</i> Compton, A. H., and.		Schenck, R., and Dingmann, Th., investigations of.....	93, 220, 249
work cited.....	65	and Stenkhoff, K., investigations of.....	216, 219
Roscoe, H. E., work cited.....	284	investigations of.....	88,
Rosenhain, W., and Humfrey, J. C. W., investigations of.....	130, 131	89, 93, 94, 103, 120, 121, 123, 124, 125, 126, 219,	
investigations of.....	107	228, 229, 230, 249, 250, 251, 252, 254, 257, 259,	
work cited.....	130, 183	260, 263, 264, 269, 270, 272, 274, 275, 277, 281,	
Ruer, R., and Biren, J., investigations of.....	210	282, 287, 288, 289, 290, 291, 293, 299, 302, 303.	
and Bode, K., investigations of.....	136, 137, 149	curves showing.....	90,
curve showing.....	137	92, 121, 126, 252, 258, 270, 271, 272, 273, 274,	
and Goerens, P., investigations of.....	140	275, 276, 277, 278, 279, 288, 290.	
table showing.....	157	tables showing.....	91, 226, 279, 288, 290
and Kaneko, K., investigations of, table showing.....	155	Semiller, H., and Falcke, V., investigations of.....	228
and Klesper, R., investigations of.....	156	table showing.....	226
tables showing.....	155, 157	work cited.....	88,
and Nakamoto, Minoru, investigations of.....	15,	93, 103, 120, 125, 126, 216, 228, 249, 251, 272, 287	
16, 17, 19, 20, 49, 50, 84		Schiel, E., investigations of.....	238
curves showing.....	18, 51	<i>See also</i> Tammann, G., and.	
tables showing.....	17, 312	work cited.....	233, 238
investigations of.....	213, 219	Schilling, K., investigations of. <i>See</i> Königberger, J., and.	
work cited.....	15, 18,	work cited.....	60
49, 84, 136, 140, 155, 157, 210, 213, 219		Schmick, H., investigations of. <i>See</i> Moller, M., Miething, H., and.	
Ruff, Otto, and Bormann, Walter, investigations of.....	158	work cited.....	185
Gersten E., investigations of.....	72,	Schmidt, W., investigations of.....	248
73, 74, 109, 217, 218, 227, 228, 229		work cited.....	248
tables showing.....	72, 110, 218, 226	Schneider, W., investigations of.....	170
work cited.....	72, 158, 217, 227	curve showing.....	171
Russel, A. S., investigations of.....	29	work cited.....	170
curve showing.....	30	Schönert, K., investigations of.....	109, 117, 118, 120
table showing.....	34	curve showing.....	117
Russel, A. S., work cited.....	29	work cited.....	109, 117
Rütten, P., investigations of. <i>See</i> Wever, F., and.		Schröder, H., investigations of.....	9
work cited.....	201, 235	work cited.....	9
Sabatier, P., and Senderens, J. B., investigations of.....	283, 284	Schroeter, Kurt, investigations of. <i>See</i> Stablein, F., and.	
work cited.....	284	work cited.....	205
Sahmen, R., investigations of, table showing.....	157	Schwartz, H. A., investigations of.....	257, 259
work cited.....	157	work cited.....	202, 257
Saito, D., and Sawamura, H., investigations of.....	210	Scott, H., investigations of. <i>See</i> Burgess, G. K., and; Morris, M. G., and.	
work cited.....	210	work cited.....	140, 144, 213, 215
Saklatwalla, B., investigations of, table showing.....	157	Scudder, F., work cited.....	284
work cited.....	157	Semiller, H., investigations of. <i>See</i> Schenck, R., etc.	
Sato, K., investigations of.....	132, 177, 178	work cited.....	228
curve showing.....	176	Senderens, J. B., investigations of. <i>See</i> Sabatier, P., and.	
tables showing.....	132, 178	work cited.....	284
work cited.....	132	Shuddemagen, L. O., investigations of. <i>See</i> Brown, S. L., and.	
		work cited.....	65

	Page		Page
Simidzu, T., investigations of. <i>See</i> Honda, K., and.		Terres, E., and Pangraz, A., investigations of.....	127
work cited.....	171	work cited.....	127
Sims, C. E., and Larsen, B. M., investigations of.....	100, 104, 105	Terry, E. M., investigation of.....	143, 150, 151, 156
work cited.....	100	curves showing.....	150, 156
Sirovich, G., investigations of.....	159, 160	tables showing.....	151, 155, 157
work cited.....	159	work cited.....	143, 150, 155, 157
Smith, E. A. C., work cited.....	59	Thompson, F. C., and Goffey, A., investigations of.....	160, 163, 164, 222
Smits, A., and Bijvoet, J. M., investigations of.....	293, 294, 295	curves showing.....	162
and Wallagh, G., investigations of.....	135	investigations of.....	181
work cited.....	135, 293	work cited.....	160, 181, 222
Sone, T., investigations of. <i>See</i> Honda, K., and.		Thompson, H. V., investigations of.....	56
work cited.....	25, 64	work cited.....	56
Sosman, R. B., and Hostetter, J. C., investigations of.....	16, 17, 19, 20, 21, 33, 41, 45, 48, 50, 52, 57, 287, 293, 295	Thomsen, —, investigations of, table showing.....	110
curves showing.....	18, 46, 48	Thorpe, E., investigations of.....	109
tables showing.....	17, 312	work cited.....	109
and Posnjak, E., investigations of.....	24, 27, 29	Tigerschiöld, Magnus, investigations of.....	19,
investigations of.....	21, 59	curves showing.....	33, 48, 96, 110
table showing.....	312	tables showing.....	17, 110
work cited.....	2, 18, 21, 24, 37, 41, 45, 57, 59, 287	work cited.....	19, 49, 96
work quoted.....	2	Trager, L., work cited.....	209
Stablein, F., and Schroeter, K., investigations of.....	221	Treadwell, W. D., investigations of.....	72, 75, 76, 110
investigations of.....	222	tables showing.....	72, 110
work cited.....	221, 222	work cited.....	72
Stanfield, Alfred, investigations of table showing.....	191	Tritton, F. S., and Hanson, D. J., investigations of.....	107, 108, 109, 113, 114, 115, 116, 117, 118, 120, 123, 287, 291, 292
work cited.....	191	curve showing.....	116
Stead, J. E., investigations of.....	119	table showing.....	312
work cited.....	81, 119	work cited.....	107, 115, 287
Stenkhoff, R., investigations of. <i>See</i> Schenck, R., and.		Umino, S., investigations of.....	150, 160, 189, 192, 223, 224, 226, 230, 238, 241, 242, 245, 246, 247, 248
work cited.....	216	curves showing.....	225, 240, 241, 246
Stoughton, Bradley, investigations of.....	185	table showing.....	141, 150, 191, 192, 224, 225
work cited.....	185	work cited.....	150, 189, 191, 225, 238, 245, 247
Sturm, E., investigations of. <i>See</i> Kahlbaum, G. W. A., and.		van Bemmelen, J. M., and Klobie, E. A., investigations of.....	37
work cited.....	173	work cited.....	37
Sullivan, J. D., investigations of. <i>See</i> Millar, R. W., and.		van Groningen, P., work cited.....	307
work cited.....	112	van Liempt, J. A. M., and Geiss, M., investigations of.....	139
Sykes, W. P., investigations of.....	279, 281	work cited.....	139
curve showing.....	280	Veil, S., investigations of.....	61
work cited.....	279	curves showing.....	61
Tainton, U. C., work of.....	38	table showing.....	70
Takagi, H., investigations of. <i>See</i> Honda, K., and.		work cited.....	61
work cited.....	149, 151, 220	Vibrans, F. C., investigations of. <i>See</i> Richardson, A. S., etc.	
Takahashi, Genske, investigations of.....	213, 251, 252, 255, 256, 257, 258, 259, 281, 302, 303	work cited.....	124
curves showing.....	255, 257, 258	von Seth, R., investigations of. <i>See</i> Johanson, A., and.	
table showing.....	218	work cited.....	251
work cited.....	213, 218, 251	Walden, P. T., investigations of.....	16, 18, 19, 20
Tammann, G., and Ewig, K., investigations of.....	215, 216, 219, 235	curve showing.....	18
and Nikitin, N., investigations of.....	135	table showing.....	17
and Schiel, E., investigations of.....	233, 234, 235, 247	work cited.....	18
investigations of.....	219	Wallagh, G., investigations of. <i>See</i> Smits, A., and.	
work cited.....	135, 215, 216, 219, 233, 235	work cited.....	185
Tamura, Seichi, investigations of.....	212	Wallis, A., work cited.....	285
work cited.....	211, 212		

	Page		Page
Waltenberg, R. G., investigations of. <i>See</i> Burgess, G. K., and.		Widawski, E., investigations of. <i>See</i> Sauerwald, F., and.	
work cited.....	157	work cited.....	236
Wecker, J., investigations of. <i>See</i> Sauerwald, F., and.		Williams, C. E., and Anderson, Arvid, investigations of.....	100
work cited.....	236	work cited.....	100
Wedekind, I. E., and Albrecht, W., investigations of.....	27	Wimmer, A., investigations of.....	118, 291
work cited.....	27	work cited.....	118, 291
Weintraub, E., investigations of.....	59, 60	Wöhler, L., and Balz, O., investigations of. 101, 102 and Günther, R., investigations of.....	72, 74, 96, 102, 110, 295
work cited.....	59	tables showing.....	72, 110, 312
Weiss, P., and Beck, P. N., investigations of. 62, 69, 70, 141, 187		work cited.....	5, 72, 96, 101, 102, 295
curves showing.....	62, 68	Wolfers, F., investigations of. <i>See</i> Perrier, Albert, and.	
tables showing.....	69, 70, 141, 312	work cited.....	164
and Foex, G., investigations of.....	63, 143, 147, 155, 156, 160	Wright, F. L., investigations of. <i>See</i> Heindlhofer, K., and.	
curves showing.....	63, 144	work cited.....	205, 208, 235
tables showing.....	63, 155	Wrightson, T., investigations of. <i>See</i> Roberts, W. C., and.	
investigations of.....	64, 65, 70, 141, 143, 165, 189	work cited.....	179
Piccard, A., and Carrard, A., investigations of.....	36, 58, 65, 70, 188	Wüst, F., and Kirpach, N., investigations of. 120 investigations of.....	198, 245
curve showing.....	68	table showing.....	191, 193
tables showing.....	69, 70, 141	Meuthen, A., and Dürrer, R., investigations of.....	156, 188, 189, 238
work cited.....	36, 58, 62, 63, 65, 69, 141, 143, 155, 165, 187, 188	tables showing.....	141, 150
Welo, L. A., and Baudisch, Oskar, investigations of.....	27, 29	work cited.....	120, 150, 188, 191, 193, 238
investigations of. <i>See</i> Baudisch, Oskar, and.		Wyckoff, R. W. G., and Crittenden, F. G., investigations of.....	84, 95, 104, 106
work cited.....	27, 56	investigations of.....	58
Westgren, A., and Lindh, A. E., investigations of.....	132	work cited.....	58, 83
and Phragmen, G., investigations of. 132, 217, 235		Yamada, N., investigations of.....	238, 241, 242, 243, 244, 246
table showing.....	218	curve showing.....	241
investigations of.....	131	work cited.....	238
work cited.....	131, 132, 217, 218, 235	Yernilov, Y., investigations of.....	72, 74, 227, 228
Wever, F., and Giani, P., investigations of. 131, 134 and Rütten, P., investigations of.....	201, 235	tables showing.....	72, 110, 226
investigations of.....	137, 139, 217	work cited.....	72, 227
curve showing.....	138	Yoe, J. H., investigations of.....	5
table showing.....	218	work cited.....	5
work cited... 131, 134, 137, 139, 201, 215, 217, 218, 235		Zakrzewski, —, investigations of, table showing.....	178
Wheeler, R. V., investigations of. <i>See</i> Rhead, T. F. E., and.		Zorning, —, investigations of.....	232
work cited.....	261	work cited.....	232
Whiteley, J. H., investigations of.....	106		
work cited.....	106		

INDEX OF SUBJECTS

	Page		Page
Alpha ferrite, characteristics of	203	Cementite, free energy of	231
Alpha ferrite and austenite, equilibrium between	255	table showing	311
curve showing	255	heat capacity of	223
Alpha iron, characteristics of	130	curves showing	225
crystal system of	131	table showing	224
diagram showing	132	heat of formation of	226
ferromagnetic, crystal system of	138	tables showing	227, 230, 311
free energy of	197	important thermometric points of, summary of, table showing	312
curve showing	197	in high-temperature equilibria, study of	254
paramagnetic, crystal system of	138	magnetic susceptibility of	223
solid solution of ferrous oxide in	118	precipitation of, in hypereutectoid steels	243
solid solution in ferrous oxide, curve showing	117	preparation of	216
specific gravity of, as function of temperature, table showing	179	quenched phases of, identification of	232
strength of	131	specific resistance of	222
Aluminum, effect of, on A_3 and A_4 transitions	183	thermal conductivity of	222
Austenite, characteristics of	201	Cementite and austenite, equilibrium between	257
Austenite and carbon oxides, equilibrium between	255	curves showing	257, 258
curves showing	255, 257	Cementite and ferrite, interfacial tension between	222
Austenite to carbon, ratio of carbon pressures of	261, 262	Cementite field, position of, in iron-oxygen-carbon reduction system, diagram showing	252
curves showing	261, 263	Chromium, effect of, on A_3 and A_4 transitions	182
Barium ferrate, characteristics of	39	curve showing	182
formation of	39	Clausius-Clapeyron equation, citation of	47, 180, 194, 236
Beta iron, crystal system of	131	Cobalt, effect of, on A_3 and A_4 transitions	183
solid solution of ferrous oxide in	118	Copper, effect of, on A_3 and A_4 transitions	183
<i>See also</i> Alpha iron, paramagnetic.		Cupric ferrite, disadvantages of, in hydrometallurgy	37
Boydénite, characteristics of	202	Curie point, definition of	29
Calcium ferrite, preparation of	37	Delta ferrite, characteristics of	201
Calcium ferrate, formation of	39	Delta iron, characteristics of	130
Carbon, carbon pressures of	260	crystal system of	131
curves showing	261	expansion coefficients of	177
effect of, on A_3 and A_4 transitions	183	free energy of	196
temper, definition of	210	curve showing	197
Carbon monoxide, as reducing agent	121	solid solution of ferrous oxide in, curve showing	117
effect on iron, at moderate temperatures	127	specific gravity of, as function of temperature, table showing	179
Carburization equilibria, effect of pressure on	254	strength of	131
curves showing	255	Diferro-nona-carbonyl, composition of	283
Cast iron, definition of	209	properties of	285
graphitization of	210	Dilatation, definition of	138
gray, definition of	209	differential, of iron and gold	148
malleable, definition of	209	Epsilon iron, determination of	207
white, definition of	209	curves showing	208
Cementite, action toward reagents	219	Equilibrium conditions, gas analyses for, curves showing	126
carbon pressures of	260	Eta iron, determination of	207
characteristics of	202	curves showing	208
condition of, at various temperatures	219	Ferrates, characteristics of	38
crystal system of	217	Ferric oxide, boiling point of	16
Curie point of	220	characteristics of	5
curve showing	221		
density of	217		
table showing	218		
entropy of	221		
table showing	316		

	Page		Page
Ferric oxide, chemical behavior of.....	7	Ferrites, characteristics of.....	37
crystal system of.....	20, 41	preparation of.....	37
Curie point of.....	21	Ferrite and austenite, equilibrium between..	257
density of, table showing.....	9	Ferropentacarbonyl, composition of.....	283
dissociation pressure of.....	16	properties of.....	285
curves showing.....	18	Ferrous ferrite. <i>See</i> Magnetite.	
table showing.....	17	Ferrous oxide, characteristics of.....	95
electrical conductivity of.....	12	dissociation pressure of.....	113
entropy of.....	31	entropy of.....	112
table showing.....	311	table showing.....	311
ferromagnetic, conversion to paramagnetic..	28	field of stability of.....	96
Curie point of.....	29	free energy of.....	110
occurrence of.....	26	table showing.....	311
preparation of.....	27	heat of formation of.....	109
free energy of.....	35	tables showing.....	110, 311
table showing.....	311	important thermometric points of, sum- mary of, table showing.....	312
glow effect of.....	24	melting point of.....	108
heat capacity of, table showing.....	34	mixtures of, with magnetite and iron, analyses of.....	100
heating of, behavior on.....	10	preparation of, by reducing magnetite with iron.....	104
heat of formation of.....	32	tables showing results of.....	104, 107
table showing.....	311	production of, in iron blast furnace.....	3
hydration of.....	8	pure, preparation of.....	101
important thermometric points of, sum- mary of, table showing.....	312	solubility of, in alpha iron.....	118
magnetic characteristics of.....	24	in metallic iron.....	116
properties of.....	25	in molten iron.....	119
magnetic susceptibility of, curve showing..	26	specific heat of.....	111
melting point of.....	15	curve showing.....	112
polymorphism of.....	20	table showing.....	111
preparation of.....	6	splitting and recombination of.....	97
production of, in iron blast furnace.....	3	curves showing.....	97, 98
reduction of, with carbon monoxide, curves showing.....	121	stability in air.....	109
sintering of.....	23	study of.....	95
solution of, in acids.....	8	Ferrous oxide and iron, miscibility of.....	108
specific gravity of.....	9	Ferrous oxide and magnetite, miscibility of..	108
specific heat of.....	29		
curve showing.....	30	Gamma iron, characteristics of.....	130
specific volume of.....	9	crystal system of.....	132
stability field for.....	305	diagram showing.....	132
study of.....	41	expansion coefficients of.....	177
thermal coefficient of expansion of.....	10	solid solution of ferrous oxide in.....	118
thermal conductivity of.....	13	curve showing.....	117
curves showing.....	14	specific gravity of, as function of tempera- ture, table showing.....	179
table showing.....	14	strength of.....	131
transition point of, lowering of, by alumi- num oxide.....	22	Gas analyses, for equilibrium conditions, curves showing.....	126
curve showing.....	22	Graphite, absolute entropy of, table showing..	311
by chromium oxide.....	22	definition of.....	209
curve showing.....	22	solubility of, in molten iron.....	210
by magnetite.....	22	table showing.....	211
curve showing.....	22		
Ferric oxide-magnetite system, derived ther- mal data on, curve showing.....	48	Hematite, electrical conductivity of.....	13
heating and cooling curves of.....	42	<i>See also</i> Ferric oxide.	
magnetic properties of.....	43	Hematite rods, resistance of, curve showing..	12
curves showing.....	44	table showing.....	11
optical properties of.....	52	Hydrogen-reduction system, equilibria of iron oxide systems with, curves showing..	304, 305
oxygen pressure of.....	45	discussion of.....	304
curves showing.....	46	Iron, A_2 transformation range of. <i>See</i> Iron, magnetic transition of.	
table showing.....	46	A_3 point of, heat effect at, table showing...	192
reduction isotherms of.....	52	magnetic changes at, curves showing....	150
curves showing.....	51	miscellaneous changes at.....	154
residues after heating, curve showing.....	51	A_3 temperature of, values of, table showing..	150
study of.....	41		
thermal points of, curves showing.....	43		
Ferric oxide-oxygen pressures, table showing..	17		

	Page		Page
Iron, A_3 transformation range of, by dilatometer.....	152	Iron, magnetic transmission of, by magnetic methods.....	141
by electrical resistance methods.....	152	curves showing.....	142, 144
curves illustrating.....	152	by thermoelectric methods.....	143
by magnetic methods.....	150	study of.....	138
electrolytic sample of, table showing....	151	magnetic transition point of, heat effect at, table showing.....	191
by thermal methods.....	149	magnetism of.....	164
by thermoelectric methods.....	151	melting point of.....	157
curves illustrating.....	152	table showing.....	157
from specific heat curves.....	149	metallic, containing carbon and oxygen, study of.....	126
study of.....	148	surface coatings on.....	81
upper and lower limits of, curves illustrating.....	154	oxidized, surface layer of, examination of ..	55
A_4 point of, heat effect at, table showing....	192	polymorphism of.....	132
magnetic susceptibility near, curves showing.....	156	production of, in iron blast furnace.....	3
A_4 transformation range of, by magnetic method, table showing.....	155	pure, Curie point of.....	138
by thermal methods, table showing.....	155	density of, effect of low temperatures on. table showing.....	179
study of.....	155	heat of fusion of.....	193
allotropy of.....	132	table showing.....	193
atomic weight of.....	129	inner friction v. temperature of, curves illustrating.....	163
boiling point of.....	157	mechanical properties of.....	183
table showing.....	158	curve showing.....	184
characteristics of, at various temperatures ..	159	physical properties of.....	185
compressibility of.....	172	curve showing.....	185
crystal system of.....	129	pyrophoric, characteristics of.....	134
Curie point of.....	29	solubility of, in ferrous oxide.....	116
density of.....	172	specific heat of.....	186
curves showing.....	174, 175	curve showing.....	188
diagram showing.....	174	specific volume of.....	172
table showing.....	172, 173	table showing.....	172
effect of alloying elements on transitions of.....	182	strength of, at different temperatures.....	130
curve showing.....	182	temperature coefficient of resistance of, table showing.....	168
electrical resistance of.....	166	tensile strength of, as function of temperature, curve showing.....	184
curves illustrating.....	167	thermal conductivity of.....	171
table illustrating.....	168	table showing.....	172
electrolytic, electrical resistance of, curve showing.....	101	total heat of.....	189, 194
thermal dilatation of.....	175	curve showing.....	195
curves showing.....	176	table showing.....	190
thermoelectric power of.....	169	transformation points of.....	135
curves illustrating.....	170, 171	transformation temperature of, change of, with pressure.....	180
torsional elastic limit of.....	162	table showing.....	182
curve illustrating.....	162	vapor pressure of.....	157
emissivity of.....	185	table showing.....	158
curves illustrating.....	186	X-ray spectrographic work on.....	131
table showing.....	190	curves showing.....	133
entropy of.....	196	table summarizing.....	132
table showing.....	311	Iron and gold, differential dilatation of, curve showing.....	148
heating and cooling curves of.....	136	Iron carbide, equilibria involving, study of ..	249
diagrams illustrating.....	137, 138	Iron-carbon alloys, A_1 point of.....	212
heats of transition of.....	191	A_2 point of.....	212
important thermometric points of, summary of, table showing.....	312	A_3 point of.....	211
isothermal oxidation of, by water vapor....	122	A_4 point of.....	211
curves showing.....	122	constituents on surface of.....	201
latent heat of evaporation of.....	194	melting point of.....	211
table showing.....	194	Iron-carbon-oxygen system, curves showing ..	252
lattice constant of, curves showing.....	133	equilibrium fields in, table showing.....	307
magnetic transition of, by calorimetric methods.....	140	space model of, cross sections of.....	270, 271, 272, 273, 274, 275, 276, 277, 278
by dilatometer.....	147	explanation of.....	270
curve showing.....	148	ternary diagrams of.....	306, 308
by electrical resistance methods.....	145	discussion of.....	306, 307
curves showing.....	146		
by heating and cooling curves.....	139		

	Page		Page
Iron-carbon system, densities of.....	232	Magnetite, important thermometric points	
eutectic of, volume change at.....	236	of, summary of, table showing.....	312
magnetic transition point of, volume change		magnetic properties of.....	62
at.....	235	magnetic susceptibility of, curves showing...	62, 63
melting point of, effect of pressure on.....	236	melting point of.....	59
curve showing.....	237	polymorphism of.....	58
miscellaneous thermal data on.....	247	preparation of.....	54
table showing.....	248	production of, in iron blast furnace.....	3
study of.....	199	specific heat of.....	68
temperature-phase diagram of.....	200	curve showing.....	68
Iron carbonyls, formation of.....	284	study of.....	53
properties of.....	285	temperature changes in, behavior under...	58
table showing.....	285	theoretical Curie point of, table showing...	63
study of.....	283	thermal electromotive force of.....	65
Iron ferrites, characteristics of.....	40	thermal emissivity of.....	66
Iron-ferrous oxide system, curves showing... 116, 117		weathering of.....	57
magnetism anomalies in.....	87	Magnetite and ferrous oxide, conjugate solu-	
Iron oxides, color of.....	5	tions of, analyses of.....	91
oxidation-reduction systems for.....	297	Magnetite field, position of, in iron-oxygen-	
diagrams illustrating.....	298,	carbon reduction system, diagram	
299, 300, 302, 304, 305, 306, 308		showing.....	252
discussion of.....	297, 300, 302, 304, 305, 306, 307	Martensite, characteristics of.....	204
reduction of, in blast furnace.....	3	tempering of, results of.....	244
X-ray examination of.....	82, 83	two forms of, existence of.....	214
Iron-oxygen complexes, intermediate between		Martite, characteristics of.....	41
magnetite and ferrous oxide, magneti-		density of.....	10
zation of.....	84	Metals, ferrites of.....	37
curve showing.....	85	Methane, carburization equilibria involving,	
melting points of.....	84	curves showing.....	270, 280
reduction-equilibrium diagrams for.....	87	discussion of.....	271
solubilities from reduction isotherms.....	88	tables showing.....	273, 278
curves showing.....	89, 90, 92	Molybdenum, effect of, on A_3 and A_4 transi-	
study of.....	81	tions.....	183
with less oxygen than ferrous oxide, study		Nickel, effect of, on A_3 and A_4 transitions....	183
of.....	115	Oxyaustenite, formation of, study of.....	250
Iron-oxygen system, composition-temperature		Oxyaustenite field, position of, in iron-oxygen-	
diagram of.....	288	carbon reduction system, diagram	
discussion of.....	287	showing.....	252
pressure-composition phase diagram of,		Oxyferrite field, in iron-oxygen composition-	
citation of.....	295	temperature diagram, position of....	288
study of.....	287	possible interpretation of, diagram show-	
temperature-composition diagram of.....	292, 294	ing.....	290
discussion of.....	291, 293	position of, in iron-oxygen-carbon reduc-	
Iron perferates, characteristics of.....	40	tion system, diagram showing.....	252
Iron scale, coatings of, composition of.....	82	Oxyferrite-oxyaustenite equilibrium, study	
Iron system, study of.....	129	of.....	253, 259
thermal expansion of, coefficient of, curve		curves illustrating.....	253, 258
showing.....	177	Oxygen, in iron and steel, determination of...	269
table showing.....	178	red-shortness in steel caused by.....	118
Iron tetracarbonyl, composition of.....	283	Pearlite, characteristics of.....	203
properties of.....	285	Pearlite composition, heat changes at.....	244
Ledeburite, characteristics of.....	203	table showing.....	244
Magnetite, characteristics of.....	53	Perferates, formation of.....	39
chemical properties of.....	57	Peroxyferrates. <i>See</i> Perferates.	
crystal system of.....	41, 57	Peroxyferrites. <i>See</i> Ferrates.	
Curie point of.....	29, 44, 70	Phosphorus, effect of, on A_3 and A_4 transi-	
dissociation pressure of.....	59	tions.....	183
electrical conductivity of.....	59	Pyrometers, sighted on surfaces of iron oxide,	
electrical resistance of, curves showing....	60, 61	corrections for, table showing.....	67
entropy of.....	71	Reduction equilibria, data on, importance	
tables showing.....	71, 311	of.....	3
free energy of.....	77	study of, scope of.....	1
curve showing.....	78	Roll scale, temperature of iron under, curve	
tables showing.....	79, 311	showing.....	67
heat of formation of.....	72		
table showing.....	311		

	Page		Page
Silicon, effect of, on A_3 and A_4 transitions . . .	183	Tin, effect of, on A_3 and A_4 transitions	183
Sodium perferate, characteristics of	39	Troostite, characteristics of	206
Sorbite, characteristics of	206	Tungsten, effect of, on A_3 and A_4 transitions . .	183
Steel, constituents of, mean values of, table showing	233	"Vagabond atoms," definition of	106
heat content of	238	Vanadium, effect of, on A_3 and A_4 transitions .	183
curves showing	239, 240	van't Hoff equation, use of	193
heats of various transitions of	245	van't Hoff isochore, use of	275
curves showing	246	Wüstite, definition of	249
table showing	245	Wüstite field, in iron-oxygen composition- temperature diagram, location of	288, 289
liquid, carbon-oxygen-iron equilibria in	264	position of, in iron-oxygen-carbon reduction system, diagram showing	252
curves showing	266, 267, 268	Zinc ferrite, decomposition of	38
table showing	265	disadvantages of, in hydrometallurgy	37
oxygen-bearing, metallographic studies of . .	119	formation of	38
rapid quenching of, results of	239		
curve showing	241		
Strontium ferrate, formation of	39		



